Analytical assessment of peptide-metal interactions and subsequent stability

Laura A. Byrne B.Sc. (Hons)

NUI MAYNOOTH

Ollscoil na hÉireann Má Nuad

A thesis submitted to the National University of Ireland
for the degree of Doctor of Philosophy (Ph.D.)

May 2010

Research Supervisors:	Dr. Richard Murphy Dr. Cathal Connolly Prof. Sean Doyle
Head of Department:	Prof. Kay Ohlendieck

Department of Biology
Faculty of Science
National University of Ireland
Maynooth,
Co. Kildare,
Ireland

Table of Contents

List of Figures

Chapter 1. Introduction

Chapter 3. Results and discussion

List of Tables

Declaration of Authorship

This thesis has not been submitted in whole or in part, to this or any other university, for any degree and is, except where otherwise stated the original work of the author.

Signed: _____

Laura Anne Byrne

Date: _____

Dedication

Acknowledgements

The help and guidance provided by my research supervisors is gratefully acknowledged. Thank you to Dr. Richard Murphy who, as my supervisor, provided valuable support and advice over the course of the project and during the proof-reading of this manuscript. I would also like to thank Dr. Cathal Connolly who, as my co-supervisor, provided encouragement throughout this project, excellent analytical advice and assistance with preparation of the final document.

I wish to express my sincere gratitude and appreciation to Prof. Michael Hynes for his continuous interest and support in the project and for sharing his expertise in relation to stability constants. The work of Prof. Peter Gans to effect Hyperquad software modifications is also greatly appreciated. Thank you also to Dr. Karina Horgan for advice over the duration of my project, to Nathan Harris of Ciphergen Biosystems for assistance during the MS/MS section of the project and to Prof. Sean Doyle for placing the facilities of N.U.I. Maynooth at my disposal.

My sincere thanks to Alltech Inc. for affording me the opportunity to pursue my Ph.D. studies in conjunction with my work and providing the funding and facilities to complete this research. I would like to express my gratitude to my fellow colleagues in Alltech Ireland, both past and present, for their support and assistance over the years and for making the lab such a great working environment.

A big thank you to my wonderful friends, in particular to Caoimhe, Claire and Julie who have been an incredible source of support and encouragement – I couldn't have done it without you. Thanks also to John, Mary and Mags for all the cards, good wishes and fond memories.

Last, but by no means least, a very special word of thanks to my family for your constant love, support and unwavering faith in me.

Abstract

The importance of trace minerals in livestock nutrition is widely recognised and one of the common methods of dietary supplementation is by inclusion of metal proteinates in feedstuffs. This work examined proteinate production methods in addition to assessing a variety of analytical techniques to compare and contrast metal proteinates. Furthermore, the development of reliable methods for quality control was also examined. Novel mass spectrometry methods combined with innovative analytical techniques were used to allow for the determination of batch consistency across the proteinate range (Cu, Fe, Mn and Zn). Together, these techniques were used to examine the size and distribution of peptides present in the metal chelates. In particular, emphasis was placed on peptide patterns that enabled the generation of mass spectrometry profiles characteristic of each of the proteinates. Results indicated that profiles selective to specific hydrolysis procedures could be obtained and enabled further progression of this method to qualitatively detect metal proteinates in premix and feed samples. Successful detection of metal proteinates was achieved in premix samples but low concentrations of the proteinates and the effect of other feed components hindered qualitative detection in feed.

A technique based on the combined use of potentiometric titration and ion-selective electrodes in conjunction with computer simulations was employed to model speciation of Cu(II) complexes in solution with a selection of ligands with the aim of understanding the extent of binding and stability of the complexes formed. Formation constants obtained from the literature as well as those obtained from studies in this work were compared and excellent agreement was observed between the computer model and experimental results in the majority of cases. The study was extended to include larger peptides and polypeptides and stability constants for a range of species were obtained. Furthermore, the stability of a selection of proteinates was investigated over a wide pH range using potentiometric methods and results indicated that the hydrolysis procedure, the peptide sequence and the extent of chelation played a significant role in the stability of the proteinates.

Abbreviations

AAFCO	American Association of Feed Control Officials
AAS	Atomic Absorption Spectrometry
ABTS	2-2'-azino-bis 3-ethylbenzthiazoline-6-sulfonic acid
ACTH	Adrenocorticotrophic Hormone
a_{H+}	Hydrogen ion activity
AOAC	Association of Official Analytical Chemists
ATR	Attenuated Total Reflectance
β_{ML}	Cumulative stability constant for a complex ML with respect to the concentration of the free metal ion, $[M^{n+}]$
BSA	Bovine Serum Albumin
BSE	Bovine Spongiform Encephalopathy
CHCA	alpha-cyano-4-hydroxycinnamic acid
CHN analysis	Carbon, Hydrogen and Nitrogen analysis
CM10	Weak cation exchange array
COMICS	Concentration Of Metal Ions and Complexing Species.
Da	Dalton
DNA	Deoxyribonucleic Acid
DTT	Dithiothreitol
E	Electrode potential
E^0	Standard electrode potential
EAM	Energy Absorbing Matrix
EDTA	ethylenediaminetetraacteic acid
EDDS	ethylenediamine-N,N'-disuccinic acid
ELISA	Enzyme Linked Immunosorbent Assay
EMF	electromotive force
ESI-MS	Electrospray Ionisation Mass Spectrometry
E.U.	European Union
FAAS	Flame Atomic Absorption Spectrometry
FAN	Free α-Amino Nitrogen
FAO	Food and Agricultural Organisation of the United Nations

FTIR	Fourier Transform InfraRed Spectroscopy
$[H^+]$	Hydrogen ion concentration
IMAC	Immobilised Metal Affinity Capture
ISD	In-source decay
ISE	Ion Selective Electrode
K_{ML}	Stepwise stability constant for a complex ML with respect to the concentration of the free metal ion, $[M^{n+}]$.
K_w	autoionisation constant of water
KLH	Keyhole Limpet Hemocyanin
[L]	Concentration of ligand L not bound to metal ion
LOD	Limit of detection
$[M^{n+}]$	Concentration of free metal ion of M
MALDI-ToF-MS	Matrix-Assisted Laser-Desorption/Ionization Time-of-Flight Mass Spectrometry
ML	Complex between metal ion M and ligand L
M:L	Metal:Ligand ratio
MS/MS	Tandem Mass Spectrometry
m/z	mass-to-charge ratio
NIST	National Institute of Standards and Technology
NP20	Normal Phase array
NPN	non-protein nitrogen
NTA	nitrilotriacetic acid
pCu	$-\log_{10}$ of Cu
pH	$-\log_{10}$ of the hydrogen ion activity
pI	Isoelectric point
pK_a	$-\log_{10}$ of the acid dissociation constant
pK_w	$-\log_{10}$ of the water ion product, K_w
QqToF	a triple-quadrupole mass spectrometer with a time-of-flight mass spectrometer replacing the third quadrupole
SDS-PAGE	Sodium Dodecyl Sulphate-Polyacrylamide Gel Electrophoresis

SELDI-ToF-MS	Surface-Enhanced Laser-Desorption/Ionization Time-of-Flight Mass Spectrometry
SPA	Sinapinic acid
Std. dev.	Standard deviation
TFA	trifluoroacetic acid
UV-vis	ultraviolet-visible spectrometry
v/v	Volume per volume
w/w	Weight per weight

1. Introduction

1.1 General introduction

Demand for livestock products has increased markedly due to population growth and projections from the Food and Agriculture Organisation of the United Nations (FAO) suggest that global meat production and consumption will rise from 233 million tonnes in 2000 to 300 million tonnes by 2020 (FAO, 2002). Furthermore, it is estimated that egg production will increase by 30 percent and milk consumption will increase from 568 to 700 million tonnes over the same period (FAO, 2002). Genetic progress in relation to animal husbandry has provided higher-producing and more rapidly growing stock in an attempt to meet such demands. Such genetically superior livestock require more exacting formulation and feeding management regimes to obtain optimum results. Furthermore, nutritional stress points are more easily reached in such livestock, where deficiencies or imbalances in the diet affect performance and health (Jacques *et al.*, 1991; Rompala *et al.*, 1995). Health concerns are universal in production across all livestock and avian species. Decreased performance in sick animals, medication cost and death loss can rapidly reduce profitability in an operation.

Approximately 30 elements are believed to be essential to animal or plant life at either bulk or trace levels and these can be divided into four major categories (Roat-Malone, 2007):

- Bulk elements (H, C, N, O, P, S)
- Macrominerals and ions (Na, K, Mg, Ca, Cl, PO_4^{3-}, SO_4^{2-})
- Trace elements (Fe, Zn, Cu)
- Ultra-trace elements comprised of metals (Mn, Mo, Co, Cr, V, Ni, Cd, Sn, Pb, Li) and non-metals (F, I, Se, Si, As, B).

Some of the trace elements listed are known for their toxicity but such concerns usually originated in geographic areas where gross excesses or deficiencies existed (Mertz, 1977). Elements previously known only for their toxicity have essential

functions in animals and man. Examples of such include: molybdenum, selenium, chromium, fluorine (Underwood, 1971) and even elements such as lead (Schwarz, 1974) and arsenic (Nielsen *et al.*, 1975).

Minerals that are required in relatively large amounts are referred to as macrominerals. Trace elements (or microminerals) may be defined generally as those which occur, or are required, at relatively low concentrations in living tissues. The role of trace minerals in animal nutrition is an area of interest for producers, feed manufacturers, veterinarians and scientists. Adequate trace mineral intake and absorption is required for a variety of metabolic functions including immune response to pathogenic challenge, reproduction and growth. Deficiencies are known to limit livestock production through dysfunctions in animal metabolism. Many of these deficiencies are marginal, resulting in unrecognised disorders that reduce animal performance and profitability (Bull, 1999).

Confusion can exist regarding terms such as mineral and element which are used interchangeably in nutrition and feeding. In practical nutrition, the term “mineral” is generally used to denote all the mineral inorganic elements. However, not all the elements are minerals (i.e., carbon, hydrogen, oxygen and nitrogen), and minerals frequently found as salts (e.g., carbonates, oxides and sulphates) can be a combination of different inorganic elements (McDowell, 2003). Very few authors tend to differentiate the two terms and the term “mineral” is commonly used in reference to all macro and micro elements.

Supplementing diets with trace elements is common practice as it is assumed that diets may not always contain adequate amounts of mineral to meet animal requirements due to more aggressive agronomic practices or because the minerals in feed ingredients may not be in a form that is biologically available to the animals. Interest in mineral supplementation has increased due to awareness of animal nutritionists with regard to the roles of trace minerals in maintaining adequate immune response, disease and stress resistance, nutrient partitioning, reproduction, liveweight gain and feed efficiency (Vandergrift, 1992). The small amounts of trace elements required and their comparatively low expense belie their importance in normal metabolism, disease resistance and reproductive function. As animal trace mineral status declines, immunity

and enzyme functions are compromised first, followed by a reduction in maximum growth and fertility, and finally normal growth and fertility decrease prior to evidence of clinical deficiency (Figure 1.1).

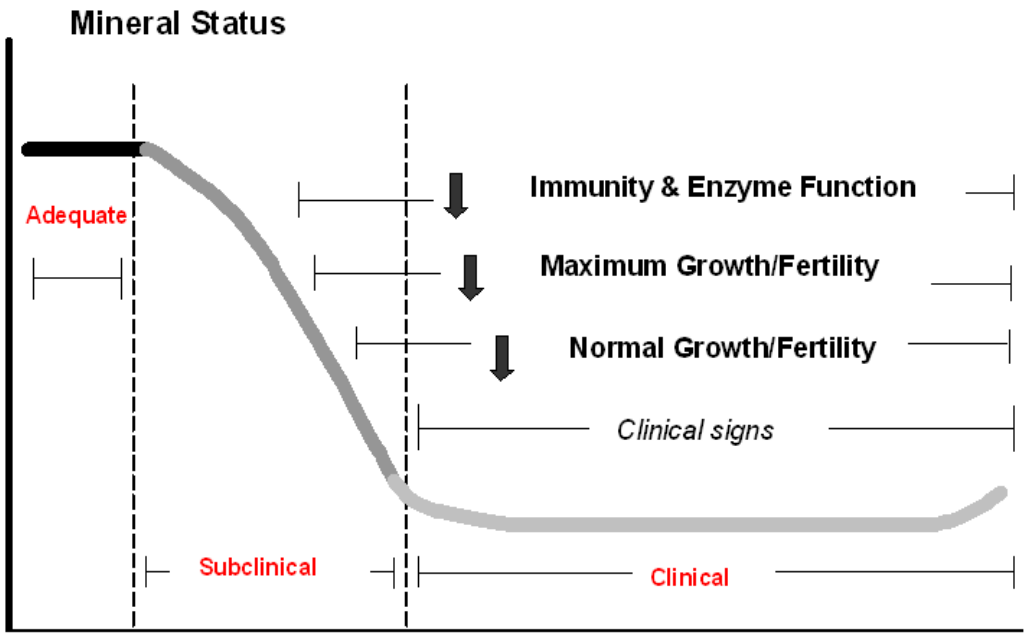

Adapted from Fraker, 1983.

Figure 1.1 Effect of declining trace mineral status on animal performance

Dietary supplementation of trace minerals can be in the form of inorganic salts such as sulphates, oxides and chlorides or an organic form in which the mineral is bound to an organic ligand such as an amino acid or peptide, resulting in a mineral complex or chelate. Considerable interest has been expressed in the optimum form of trace mineral supplementation. Various forms of organic trace mineral supplements can command higher prices than inorganic forms of the same mineral based on the apparent superiority of the organic form (Patton, 1990; Vandergrift, 1992). However, animal production industries are driven to reduce their production costs and the largest contributor to cost is feed, which accounts for more than 50 % (Wilson *et al.*, 2003). The ability to reduce feed costs without suppressing productivity, or increasing the efficiency of feed utilisation without drastically increasing cost would be readily embraced by these industries (Wilson *et al.*, 2003). Recent progress relating to developments in analytical

instrumentation and methodology can enable identification and comparison of nutritional supplements available in the marketplace. This allows informed decisions to be made regarding the choice of nutritional supplement to use and its effectiveness on a cost-benefit basis. Environmental concerns are also an important factor. Maximising feed utilisation would lead to a reduction in minerals excreted thereby reducing the environmental impact.

Public concerns relating to food safety have also come to the forefront in recent years. Issues such as bovine spongiform encephalopathy (BSE), dioxin contamination, outbreaks of food borne bacterial infection, microbial resistance to antibiotics and growing concern about veterinary drug residues have lead to close scrutiny of the industry (FAO, 2002). Effective quality control measures and the development of methods to detect, identify, characterise and differentiate products can instil confidence in particular products. Furthermore, there is an increasing need for clarity in relation to products available in the market due to the fact that feedstuffs used in animal diets have variable composition and this variability can lead to uncertainty in final diet composition (Green *et al.*, 2008).

1.2 Trace minerals in animal nutrition

A trace element is considered essential if it meets the following criteria (Florence, 1989; Roat-Malone, 2007):

- A physiological deficiency appears when the element is removed from the diet.
- The deficiency is relieved by the addition of that element to the diet.
- A specific biological function is associated with the element.

Trace mineral functions can be described by four broad categories (Underwood *et al.*, 1999): structural, physiological, catalytic and regulatory. Structural function refers to minerals forming structural components of body organs and tissue. Physiological function occurs when minerals in body fluids and tissues act as electrolytes to maintain osmotic pressure, acid-base balance and membrane permeability. Catalytic function refers to the catalytic role of metalloenzymes in enzyme and hormone systems. Trace elements serve as a structural component of metalloenzymes and their removal has a detrimental effect on metal enzyme activity. Furthermore, minerals have been found to regulate cell replication and differentiation.

Subclinical trace mineral deficiencies occur frequently and currently represent a bigger problem than acute mineral deficiencies due to the absence of specific symptoms. In the case of farm animals, this is manifested in the form of reduced growth and reproduction rates, decreased feed efficiency and a depressed immune system. The end result is inefficient production and lower profitability. As a result, trace element nutrition has become important in modern agricultural practices and the provision of essential minerals at the correct inclusion rates and in the correct form is imperative.

Table 1.1 illustrates some of the effects of trace mineral deficiencies. Although not an exhaustive list or species specific, it provides a clear indication of the importance of trace minerals in the diet.

Table 1.1 Some general effects of trace mineral deficiencies in animals

Copper	Reduced growth rate, anaemia, abnormal skeletal development, nerve disorders, lameness, swelling of joints, diarrhoea, weak/broken bones, cardiovascular disorders, reproductive failure, keratinisation failure in hair, fur or wool
Iron	Nutritional anaemia (low red blood cell count), paleness of mucous membrane, changes to skin, hair condition, diarrhoea/scours, fatigue, retarded growth in foetus and youngstock, poor growth, reduced appetite, increased susceptibility to disease
Manganese	Impaired fat and carbohydrate metabolism, affects membrane integrity, poor growth, skeletal abnormalities, shortening and bowing of joints, reproductive failure, nervous disorders, reduced vitamin K-induced clotting response
Zinc	Reduced growth rates, poor skin condition, loss of appetite, bone problems, poor hair formation, delays healing wounds, poor testicular development, impairment of glucose tolerance, depleted immune system, reduced conception rate, offspring malformations and behavioural issues

Information obtained from The Minerals Directory (Ewing and Charlton, 2007)

In addition to the importance of trace mineral inclusion in the diet, the form in which the trace mineral is included also plays an important role and had been discussed in a significant number of publications (Cao *et al.*, 2002; Spears, 2003; Veum *et al.*, 2004; Li *et al.*, 2005; Ao *et al.*, 2006 ; Nollet *et al.*, 2007; Lamb *et al.*, 2008; Leeson *et al.*, 2008). Studies in a number of species have shown that the absorption of trace metals is influenced by many factors including their chemical form, valence state and relative concentrations of competing metals which may be present. There are many interactions between different metals and some of these interactions occur due to inorganic trace minerals dissociating after digestion into free ions which are very reactive. This process can reduce the bioavailability of the metal to the animal. Organic trace mineral forms

have received considerable attention due to their apparent effectiveness at increasing metal status in an animal.

1.3 Bioavailability

Bioavailability may be defined as the proportion of an ingested mineral that is absorbed, transported to its site of action and converted to the physiologically active species (O'Dell, 1983). The mucosal layer surrounding the lumen of the gastrointestinal tract regulates the type and amount of nutrients which are absorbed. This is a protective mechanism that keeps potentially harmful substances from entering the body (Rompala *et al.*, 1995). A host of intrinsic and extrinsic factors are known to affect the bioavailability of dietary trace elements including animal species, interaction with other minerals and dietary nutrients, physiological state, chemical form and solubility of the mineral element (Ammerman *et al.*, 1995). Most researchers have agreed that the absorption rate of minerals from organic trace minerals can be substantially greater than those from inorganic forms (Kincaid *et al.*, 1986; Wedekind *et al.*, 1992; Ward *et al.*, 1996; Predieri *et al.*, 2005).

Further examples of data confirming the advantages of organic forms of supplementation include a publication which indicated that the utilisation of organic copper from a copper proteinate or copper lysine was higher than that of inorganic copper sulphate when fed to rats in the presence and absence of elemental Zn or Fe (Du *et al.*, 1996). The data suggest that, unlike inorganic copper, organic Cu chelates exhibit absorption and excretion mechanisms that do not interfere with Fe. The copper proteinate examined also achieved higher liver Zn, suggesting less interference at gut absorption sites in comparison with the other forms of copper. Another trial compared a Zn proteinate, a Zn polysaccharide complex and inorganic zinc oxide in bull beef cattle, and concluded that the organic forms resulted in improvement in hoof claw quality (Kessler *et al.*, 2003). Research into the bioavailability of Cu and Zn proteinates in sheep compared with the inorganic sulphate forms suggested proteinates were more readily absorbed and more easily deposited in key tissues compared with inorganic

forms and increases in plasma concentrations of both metals were observed (Ryan *et al.*, 2002). Finally, a review article of the role of minerals in fertility and reproductive diseases of dairy cattle suggested that organic forms of zinc are better than inorganic sources and consequently may provide greater benefit in disease prevention particularly in relation to mastitis and lameness (Wilde, 2006).

Inorganic mineral forms such as oxides, sulphates, chlorides and carbonates exhibit lower solubility and therefore have lower bioavailability compared to organic mineral forms. However, they are still the most widely used forms in animal nutrition. Cupric oxide (CuO) is particularly insoluble and so net absorption from CuO is thought to be minimal (Baker. D.H. *et al.*, 1991). When inorganic mineral forms enter stomach acid, the mineral is released as a free metal ion e.g. Cu^{2+}, Mn^{2+}. When stomach acid is neutralised in the intestine, the free metal often forms insoluble complexes that cannot be absorbed and are excreted. This raises environmental issues due to increased metal concentrations in soil which can potentially contaminate ground water supplies (Nollet *et al.*, 2007). Based on the assumption that organic mineral complexes have higher availability, it is assumed that a lower concentration of these minerals would be required in the diet than inorganic forms and would be assimilated more effectively therefore alleviating environmental concerns. In a trial carried out in 2004, 50 ppm Cu in the form of organic Cu decreased copper excretion by 77 % compared with feeding 250 ppm Cu as $CuSO_4$ for growth promotion indicating increased absorption of the organic form (Veum *et al.*, 2004).

Concern about possible detrimental effects of excess supplementation with trace minerals on the environment or human and animal health caused the European Union to issue new legislation relating to a reduction in permitted feed concentrations of several trace metals (Co, Cu, Fe, Mn and Zn) (E.U., 2003a). Fortunately, research in trace element nutrition has led to the development of more bioavailable organic minerals, including trace minerals in the form of chelates. Chelates allow a lower supplementation rate of trace minerals with an equivalent or improved effect on animal health, growth and productivity.

1.4 Inorganic versus organic trace minerals

Inorganic trace minerals are ingested and solubilised by digestive fluids in the gut. It is believed that dissociated metal ions move through the digestive system and can potentially bind to ligands. Many free metal ions do not find a ligand, and although some may be absorbed, others simply pass through the digestive system and are excreted. Antagonists in the diet, which bond to free metal ions, can make them unavailable for absorption. Examples of dietary antagonists include phytate, fibre and clay in addition to micro-flora in the rumen and digestive system which can deplete mineral levels. In addition, minerals can react with other minerals and examples of such include those of zinc with calcium and iron with copper. It is thought that only 5-10 % of dietary copper is absorbed by adult animals due to antagonistic factors in the diet (McDowell, 2003). The remaining 90-95% of the copper is excreted.

Supplementation of animal feed with organic trace minerals has been common practice for a number of years and represents a world market valued between 100 and 200 million Euros. Although inclusion of inorganic forms of trace minerals is common, recognition of the benefits of organic trace mineral supplementation has increased. For example, in 1999 approximately two percent of the German dairy herd was supplied with organic trace minerals, by 2004 this value had increase to approximately twenty percent (Schlegel, 2006).

Organic trace minerals differ from inorganic forms as a result of their chemical association with an organic ligand (Lamb *et al.*, 2008). Their characteristics are determined by the type of ligand used to bond with the metal. An organic trace mineral is less affected by the digestion process than an inorganic trace mineral and moves directly to the gut for absorption. This allows more metal to be absorbed and increases metal status within the animal more than inorganic trace minerals (Parks *et al.*, 1994).

1.4.1 Ligand sources

Ligands are organic compounds such as amino acids, peptides, polysaccharides and organic acids that bond to metal atoms and form a unique chemical structure. Organic trace minerals with different chemical structures have different chemical properties which greatly affect their bioavailability. Researchers have found that organic trace minerals are not equally stable at low pH, and therefore, some have a limited ability to increase the bioavailability of a given trace mineral (Cao *et al.*, 2000).

The interaction of a metal ion, M^{n+}, and a ligand, L, to form a metal complex is a particular case of general chemical equilibrium. The formation of the complexes can be described according to the Lewis acid-base theory, where an acid is the acceptor of electron pairs from a base. It is generally assumed that such coordinate bond formation takes place between a lone pair of electrons on the ligand donor atom (a Lewis base) and empty orbitals of suitable energy and symmetry on the metal acceptor ion (a Lewis acid). Binding can occur via oxygen, nitrogen or sulphur atoms as electron donors either by replacement of hydrogen ions or by coordination (Tables 1.2 and 1.3).

As their name suggests, amino acids are compounds that contain both an amino group and a carboxylic acid unit. A generalised structure for α-amino acids is shown in Figure 1.2, in which R represents any of the side chain constituents that are found in naturally occurring amino acids. Appendix 2 contains the full list of side chains of all the amino acids and their representative structures.

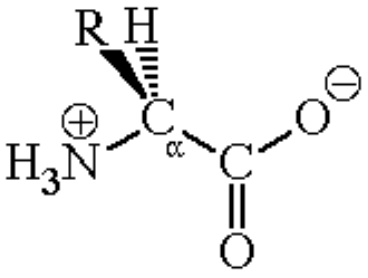

Figure 1.2 General schematic of an amino acid

The amino acids form stable complexes of varying degrees with many metals and for those not containing protonation sites in the side chain it is observed that the -NH_2 group is by far the most basic group. When amino acids are covalently linked together by amide bonds, the resulting molecules are called peptides or proteins. These peptide bonds are essentially planar and usually exist in the *trans* configuration (Figure 1.3)

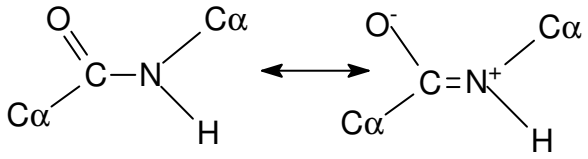

Figure 1.3 Stereochemistry of the peptide bond

Although both peptides and proteins are composed of amino acid residues, there is a subtle difference between these two types of molecule. Proteins are large molecules that usually contain at least 50 residues, polypeptides contain approximately 20 -50 residues and peptides are smaller molecules containing less than 20 residues (Bailey, 1990). The word protein is derived from the Greek *proteios*, meaning primary or foremost which is fitting since proteins are central to life process. There is a wide diversity of proteins due to the existence of a wide range of amino acid combinations.

Table 1.2 Groups interacting with metal ions after dissociation of a proton

Donor atom	Group	Example
Oxygen	-COOH	The carboxyl group which is present in a large number of metal ion chelating model compounds and in biological macromolecules such as proteins
	-OH (enolic or phenolic)	The enolic or phenolic hydroxyl group which is present in the amino acid tyrosine
	$-SO_3H$	The sulphur-containing group with oxygen as a donor atom is the sulphonic acid group present in heparin
	$-PO_3H_2$	The phosphorus-containing group with oxygen as a donor atom is the phosphate present for example in ATP, which readily binds Mg^{2+} and Ca^{2+}, in phospholipids, and in phosphorylated proteins such as phospholamban
Nitrogen	$-NH_2$ -NH-R	Functional groups containing nitrogen are the $–NH_2$ group, and the –NH-R group of secondary amines, in both of which one proton can be replaced by metal ions. The incorporation of Fe^{2+} into the heme moiety is one of the best-known examples of the latter case.
Sulphur	-SH	A functional group containing sulphur is the –SH group present for example in cysteine with a very high affinity to heavy metal ions such as Zn^{2+}, Cd^{2+} and Hg^{2+}.

Adapted from Wolf (1986)

Table 1.3 Groups interacting with metal ions by coordination

Donor atom	Group	Example
Oxygen	=O	Oxygen donor atoms are the oxygen atom of the carbonyl function, present in organic acids, amino acids and proteins, the alcoholic –OH function, for example, that of the amino acid threonine, and the ether –O- atom.
	-OH	
	-O-	
Nitrogen	$-NH_2$	Groups with nitrogen atoms are primarily the NH_2 group of amino acids and of proteins containing diaminomonocarboxylic acids like lysine. The =NH group of secondary amines and the –N= group of tertiary amines occur in the imidazole moiety of histidine.
	-NH-R	
	-N=	
Sulphur	-S-	A group with sulphur as a donor heteroatom occurs as a thioether group in methionine.

Adapted from Wolf (1986)

The strength of the ligand field at a metal centre is strongly dependent on the character of the ligand's electronic field and leads to the classification of ligands according to a "spectrochemical series" arranged in order from weak field (halides, sulphides, hydroxides) to strong field (cyanide and carbon monoxide):

$$I^- < Br^- < S^{2-} < Cl^- < NO_3^- < OH^- - RCOO^- < H_2O – RS^- < NH_3 – \text{imidazole} < \text{en}$$

(ethylenediamine or diaminoethane) < bpy (2, 2' – bipyridine < CN^- < CO

Improving absorption is a critical characteristic of an organic trace mineral and its molecular mass plays an important role as ligands of small molecular mass have higher absorption potential (Wedekind *et al.*, 1992). Research has shown that single amino acids, dipeptides and tripeptides are absorbed intact and can be found in the portal blood of animals (Koeln *et al.*, 1982) and that it is possible for the small intestine to absorb small peptides (Fricker *et al.*, 1991; Fricker *et al.*, 1992). Some research indicates peptides as large as 8 amino acids in length may be absorbed by the enterocyte without hydrolysis (Fricker *et al.*, 1991; Fricker *et al.*, 1992). Larger peptides and

proteins will be hydrolysed into small peptides and amino acids in the digestion process in order to be absorbed. In ruminant nutrition, research has shown that amino acid absorption from the rumen in the form of peptides is more important than absorption of free amino acids (Webb *et al.*, 1992; Webb *et al.*, 1993) as peptide absorption may constitute the primary source of absorbed amino acids.

1.5 Complexes and chelates

A metal complex consists of a central metal atom or ion surrounded by a set of ligands that have one or more atom(s) bearing lone pairs of electron(s). These "donor" atoms can bind electrostatically or covalently to the metal ion. In non-transition metal complexes, the binding is largely electrostatic, whereas covalent binding is prevalent in transition metal complexes. Ligands that contain only one donor atom are termed 'monodentate' ligands. Ligands that contain two or more donor atoms capable of bonding to a metal ion are termed polydentate ligands. When a ligand contains two or more donor centres which are able, sterically, to coordinate to the same metal ion, chelated complexes can form (Figure 1.4). Chelation is the ability of a ligand or chelating agent to form a complex containing a heterocyclic ring structure with a metal ion (Walker *et al.*, 1997). The bonds formed between the metal ion and the ligand form a ring structure, which binds the metal much like the pincers of a lobster. In fact, a chelate draws its name from the Greek '*chele*', meaning claw. Many chelates contain five or six membered rings.

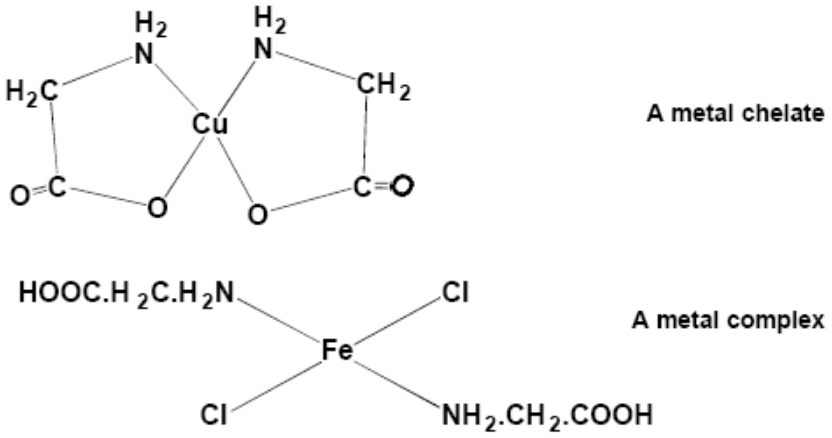

(Jondreville *et al.*, 2003)

Figure 1.4 Schematic diagrams of a metal chelate and a metal complex

An important feature of metal chelates is their high stability due to the conformation in which the metal atom is held by coordinating groups. Due to their ability to form fused chelate rings, polydentate ligands have larger formation constants (which refer to the strength of complexation between a ligand and a metal) compared to monodentate ligands (Pettit *et al*., 1977; Kozlowski *et al*., 1998). This so called chelate effect is mainly due to the more favourable entropy change that occurs during complex formation involving polydentate ligands.

Chelated metals have been proposed as superior alternatives to inorganic supplements as they are thought to overcome two of the major limitations of inorganic supplements – low bioavailability at low concentrations and biological toxicity at high levels. The increasing utilisation of these supplements centres around the theory that they are more bioavailable as a result of the stability of the complex which protects the metal from further reaction with antagonists that inhibit the absorption of the metal. Most chelates remain soluble throughout the changes in pH during digestion and are electrically neutral. The duodenal mucosa is negatively charged and as such a positively charged complex will stick to the mucosa instead of passing through. In deference to this, a negatively charged molecule would be repelled. The strength of the bond between the ligand and the metal on formation of a metal chelate can prevent dissociation and loss of mineral as it passes through the digestive system. In general, it has been assumed

that minerals dissociate from their organic or inorganic carriers in the intestinal lumen and are then absorbed via a passive and/or active route into enterocytes lining the gastrointestinal tract. Therefore, reported differences in the bioavailability of organic and inorganic minerals have been attributed to differences in dissociation rates of the mineral from the organic or inorganic substrate to which they are bound, or to differences in mineral-chelate solubility (Radcliffe *et al.*, 2007). However, very little is known with regard to the mechanisms by which minerals are absorbed and it is possible some organic minerals may be absorbed while still attached to organic carriers. A recent study examined the transport behaviour of copper glycinate complexes through the porcine gastrointestinal membrane and found such complexes penetrated the digestive membrane easily, whereas inorganic copper species apparently did not (Tastet *et al.*, 2009).

Trace minerals cannot form chelates with just any organic ligand. The ligand must be able to bind the metal at two points resulting in the formation of a heterocyclic ring. Amino acids and peptides form coordinate covalent bonds and make good chelating agents for nutritional purposes. Numerous investigations into the binding of amino acids and the formation of metal complexes and chelates have been described in the literature (Sharma *et al.*, 1971; Dembowski *et al.*, 1988; Hopgood *et al.*, 2002) and in most of the data the α-amine and carboxylate amino acid functional groups are used to chelate the metal. Working with peptides or proteins, these binding processes are not as relevant. C-terminal carboxylate and N-terminal amino groups of a protein will not chelate a metal. In typical peptide conformations, these two coordinative binding sites are too far away from each other to act as a chelating ligand (Kruppa *et al.*, 2006). In proteins, the metal binding sites may well occur within the side chains of the constituent amino acids since all but the terminal $-NH_2$ groups are bound up in peptide linkages. Therefore, a great deal of work has been done to investigate the role of the reactive groups in the side chains of amino acids. The additional side chain functionalities are essential for binding (Sanna *et al.*, 2001; Kruppa *et al.*, 2006). Only a relatively small number of the amino acid side chains are potential metal ligands. The ligand groups, which are commonly encountered, include the thiolate of cysteine (Cys), the imidazole of histidine (His), the carboxylates of glutamic acid (Glu) and aspartic acid (Asp) and

the phenolate of tyrosine (Tyr) (Figure 1.5). Less frequently, the thioether group of methionine (Met), the amino group of lysine (Lys), the guanidine group of arginine (Arg) and the amide groups of asparagine (Asn) and glutamine (Gln) are involved in metal binding. Metal ions can also bind to peptide bonds, through the carbonyl or the deprotonated amide nitrogen, and to the terminal amino and carboxyl groups of the protein (Crichton, 2008).

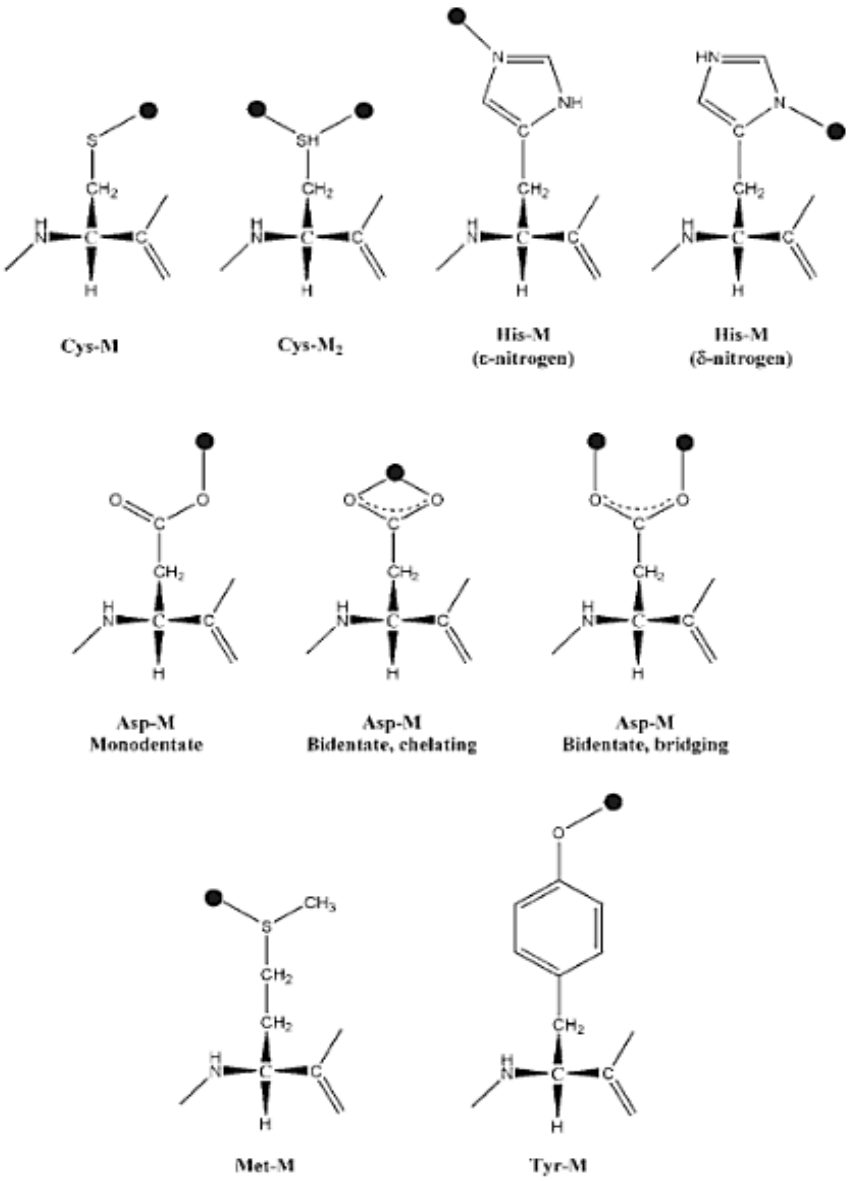

Adapted from Creichton (2008)

Figure 1.5 Selection of amino acid side-chain metal-ion binding modes (the metal ion is represented as a dark filled circle)

An example of one of the constituent amino acids having a coordinating centre in the side chain is glycyl-histidine, in which there is another potential binding centre in the molecule, the imidazole nitrogen. In neutral solutions glycyl-L-histidinate chelates Cu^{2+} as a tridentate ligand with three nitrogen donor atoms: amino, deprotonated peptide, and imidazole (Martin *et al.*, 1960; Aiba *et al.*, 1974; Sigel *et al.*, 1982)**.** Compared to Gly-Gly the imidazole nitrogen obtains the third coordination position from the less basic carboxylate group. This structure, originally deduced from potentiometric titrations, has been found in crystal structures of Cu^{2+} complexes of Gly-His, Gly-His-Gly, and Gly-His-Lys (Osterberg *et al.*, 1972; Sigel *et al.*, 1982). Similarly, in the case of a tripeptide containing an imidazole residue such as Gly-Gly-His, chelation to Cu^{2+} is as a quadridentate ligand with four nitrogen donor atoms: amino, two deprotonated peptide and imidazole (Figure 1.6).

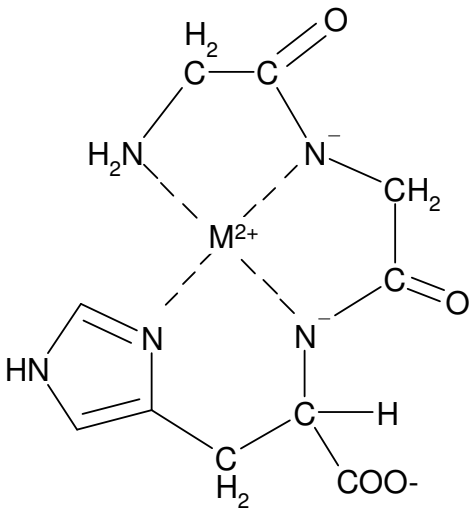

Adapted from Sigel (1982)

Figure 1.6 Chelate formed from Copper and the tripeptide Gly-Gly-His

The interactions between peptide residues may favour a particular peptide conformation, which in turn may have an essential impact on metal-peptide coordination equilibria, both in a thermodynamic and a structural sense. The formation of stable five-membered chelate rings is the driving force of the coordination process, lowering the pK_a value of the first amide nitrogen by as much as 10 log units (Sigel *et al.*, 1982).

Much of the chemistry of metal ions in solution depends on the formation and relative stability of their complexes with neutral or anionic ligands. The stability constant of a complex, which is the equilibrium constant for its formation from the component parts, gives an indication of how strongly the ligands coordinate to the metal. A relatively high stability constant indicates a stable complex or chelate in which the ligands are not displaced to any significant extent in solution. Chelation can protect the trace mineral in the metal proteinate from interaction with dietary antagonists and the metal may then be absorbed intact into the blood system by peptide or amino acid uptake pathways rather than the normal metal ion uptake mechanism (Hardy, 2003). The metal is not prone to the physico-chemical factors that can adversely affect efficient uptake of the "unprotected ions", as found with inorganic sources and the hypothesis is that this will increase net retention, minimise excretion and increase the amount that is biologically available for productive purposes (Hardy, 2003). It has been postulated that the small peptides/amino acids can increase incorporation into the target site aiding metabolic function (e.g. metallo-proteins in enzyme systems). However, in many cases the stability constants of complexes are quite low, which means they can be difficult to isolate and, in solution, there may be a mixture of complex species present. If the binding is weak, the metal-ligand complex may dissociate into its component parts and act in a similar manner to an inorganic metal salt. Factors such as the concentration of the metal and the ligand in solution, in addition to the ionic strength and the pH of the solution, will all play a role in determining the relative stability of complexes and chelates. Furthermore, individual properties of the metal ion such as ionic charge and electron affinity also play a role in conjunction with several ligand characteristics. Properties such as the basicity of the ligand, the number of metal-chelate rings per ligand, the size of the chelate ring, steric effects and resonance effects can all contribute to the stability of the complexes and chelates.

Metal - organic ligand combinations can result in the production of one of several classes of organic trace minerals, which are available in the animal feeding industry and include chelates, proteinates and complexes (AAFCO, 2000). Terminology in relation to organic mineral complexes is not standardised and terms such as chelate, complex and proteinate are incorrectly used interchangeably. Japan has a single

classification for mineral chelates called peptides. The United States has developed six classifications for organic trace mineral forms including chelate. Europe has a defined organic mineral classification called chelate but the definition differs to that of the United States chelate which can create confusion when comparing products (Scrimgeour *et al.*, 2004). A European chelate requires a specific chemical structure, specifies hydrolysed soy protein as the ligand, and requires a molecular mass less than 1500 Daltons (EU, 1970) whereas the Association of American Feed Control Officials (AAFCO) definition of a metal amino acid chelate does not require a specific chemical formula or type of protein and molecular size must be less than 800 Daltons (AAFCO, 2005).

The absence of standardised methods to chemically characterise mineral chelates and to relate those characteristics to *in vivo* bioavailability has been considered a major hurdle to the acceptance of these products (Leach *et al.*, 1997). The AAFCO definitions for organic mineral complexes outlined in Table 1.4 provide a comprehensive definition of the organic trace mineral categories and will be used throughout this study.

Table 1.4 AAFCO Definitions for Organic Mineral Complexes

Metal Amino Acid Complex	The product resulting from complexing a soluble metal salt with an amino acid (< 300 Da)
Metal (specific amino acid) Complex	The product resulting from complexing a soluble metal salt with a specific amino acid
Metal Amino Acid Chelate	The product resulting from the reaction of a metal ion from a soluble metal salt with amino acids with a mole ratio of one mole of metal to one to three (preferably two) moles of amino acids to form coordinate covalent bonds. The average weight of the hydrolysed amino acids must be approximately 150 Da and the resulting molecular weight of the chelate must not exceed 800 Da
Metal Proteinate	The product resulting from the chelation of a soluble salt with amino acids and/or partially hydrolysed protein.
Metal Polysaccharide Complex	The product resulting from complexing of a soluble salt with a polysaccharide solution declared as an ingredient as the specific metal complex i.e., copper polysaccharide complex

The AAFCO defines an amino acid metal chelate as " the product resulting from the reaction of a metal ion from a soluble metal salt with amino acids with a mole ratio of one mole of metal to one to three (preferably two) moles of amino acids to form coordinate covalent bonds". Since this definition does not consider the actual binding in the complex, it is possible that a complex considered a chelate by animal nutritionists might not be considered as such by a chemist. The defined categories (Table 1.4) should help to describe the identity of existing products in the market. However, since most available organic trace minerals have not had their chemical structure analysed fully or their chelation or degree of complexation, their categorisation remains somewhat theoretical (Guo *et al.*, 2001).

1.6 Methods of comparative analysis for metal proteinates

Commercial mineral supplements are frequently described as complexes, chelates or proteinates and not all products are equally effective. Based on the AAFCO definitions outlined in Table 1.4, the focus in this work was on metal proteinates. These are normally produced by first partially hydrolysing a protein source using enzymatic procedures. This results in the formation of a hydrolysate containing a mixture of amino acids and peptides of varying chain length. The average chain length will depend on a number of factors including the degree of hydrolysis. Reaction of a metal salt with the hydrolysate under the appropriate conditions results in the formation of complexes containing chelated metal ions.

In 1994, an analytical method was proposed which used the Kjeldahl method (Cohen, 1924) to determine the quantity of total nitrogen in the product (Parks *et al.*, 1994). Since nitrogen is an indicator of the presence of protein or amino acids, its presence in the compound may indicate the mineral was chelated. The problem with this theory lies in the fact that the Kjeldahl method does not distinguish between free nitrogen, nitrogenous organic filler, nitrogen in ligands or whether the ligands, if any, are amino acids, partially hydrolysed protein or intact protein. From an industrial perspective, more sophisticated methods of analysis were required to conclusively determine if a complex is in fact a chelate.

Techniques such as the Kjeldahl method and carbon, hydrogen and nitrogen (CHN) analysis can determine the amount of nitrogen present in a proteinate and may be used as a guide to select a ligand source based on possible chelation potential. However, it is necessary to apply additional analytical techniques to fully investigate chelation potential in addition to obtaining further characterisation information.

Free α-amino nitrogen (FAN) determines the presence of amino acids in a proteinate although limitations exist in relation to differentiating between other forms of FAN (ammonium ions and short chain peptides). Consequently, this method may only be used as an additional guide to indicate the effectiveness of a hydrolysis method and consequently chelation potential. An effective hydrolysis procedure is essential to metal proteinate production as it cleaves peptide bonds in the protein source thereby providing

amino acids and small peptides to which the metal ion can bind. The extent of hydrolysis however, will vary depending on the choice of enzyme used in the hydrolysis procedure in addition to hydrolysis conditions such as pH and temperature. The FAN assay can assess the effect of adjusting hydrolysis parameters in an attempt to improve current hydrolysis conditions with respect to FAN release and cost considerations. Once the proteinates are produced, whether under the conditions stated in this work, or by those suggested by an alternative manufacturer, further analytical techniques are still required to provide additional information on the proteinates including characterisation data which can enable effective comparison of various proteinates. Conditions and enzymes vary between manufacturers so analytical techniques which can compare and contrast the resultant proteinates formed from different hydrolysis procedures are required.

Characterisation of metal proteinates is required for a number of purposes. Firstly, from a quality control perspective, so that consistency between proteinate batches may be determined. The ability to monitor reproducibility and hence the consistency of a product is of great importance. Additionally, the ability to establish a method to differentiate products in the marketplace is required. Ideally, a method enabling comparative analysis of a selection of products with the ability to highlight differences between products should be established. A number of techniques were selected with the ability to meet these requirements and are described in detail in this section.

The ability to precisely and accurately measure the total metal concentration in proteinate samples is essential for a number of reasons. In the case of some metals, there is a fine line between essential and toxic levels and the ability to accurately determine the metal content is imperative from a safety perspective. E.U. regulations are also in place regarding accepted metal concentrations for human and animal consumption and it is therefore necessary to have an accepted method in place to confirm metal content in nutritional products. Flame atomic absorption spectrometry (FAAS) is commonly used to determine the metal content in samples and has few interferences, good sensitivity and precision and is relatively low cost (McDowell, 2003). The main drawbacks are limited linear calibration range and the fact that it is a single-element technique

(McDowell, 2003). Regarding metal proteinate analysis, these disadvantages are not major issues as the metal content of the proteinates falls within the linear calibration range in most cases. Furthermore, most proteinates produced as nutritional supplements contain specific individual metals (e.g. Cu proteinates, Fe proteinates etc.) and although other metals may be present at low concentrations in the proteinates, single-element analysis is sufficient for analysis. It can show consistency between batches, confirm if the metal content is close to what is stated and also determine if variation between batches is low.

Fourier Transform Infrared Spectroscopy (FTIR) can facilitate further metal proteinate characterisation and is an additional method to compare products. FTIR spectroscopy is a form of vibrational spectroscopy, and the FTIR spectrum reflects both molecular structure and the molecular environment. In this technique, the sample is irradiated with infrared radiation which stimulates vibrational motions of molecules. The molecule absorbs at frequencies corresponding to its molecular modes of vibration in the region of the electromagnetic spectrum between visible (red) and short waves (microwaves). These changes in vibrational motion produce bands in the vibrational spectrum and similar to a fingerprint, no two unique molecular structures produce the same infrared spectrum. This is useful for qualitative analysis such as aiding identification of unknown materials in addition to assessing the quality or consistency of products from a quality control perspective. Furthermore, potential complexation can be examined based on spectral analyses. When a metal ion forms a bond with a ligand, the vibrational frequencies of the functional groups involved in the bond formation will be altered such as those of the carboxylic oxygen and the nitrogen of the amino group. Application of this technique to commercially available proteinates allows a direct comparison of products and can provide further evidence of the extent (if any) of chelation. Advantages of FTIR include precision, sensitivity, accuracy and speed. Furthermore, it requires no external calibration, is a non-destructive technique and very small sample quantities are required for analysis. Limitations do exist however and one general limitation of infrared spectroscopy is that it cannot detect atoms or monatomic ions. Due to the fact that single atomic entities contain no chemical bonds and do not possess vibrational motion they do not absorb infrared radiation (Smith, 1996).

Furthermore, an element cannot be detected unless it is present as part of a molecule whose spectrum can be detected, noble gases such as helium and argon exist as individual substances and cannot be detected and homonuclear diatomic molecules such as N_2 and O_2 do not absorb infrared radiation due to their symmetry (Smith, 1996; Subramanian *et al.*, 2009). A specific limitation of FTIR spectrometers is the fact that it is a single beam technique which means the background spectrum (which measures the contribution of the instrument and the environment to the spectrum) is measured at a different point in time than the spectrum of the sample (Smith, 1996). Occasionally deviations may arise if the environment or something in the instrument changes between the time the background is analysed and the time the sample is analysed. Another limitation is the strong absorption band that appears in aqueous solutions that can mask certain important signals. However, this particular limitation was eliminated in this work by lyophilisation of all samples prior to FTIR assessment. Biological samples, including proteinates and feed samples, are complex mixtures and hence their FTIR spectra are complicated with overlapping peaks and signal masking (Subramanian *et al.*, 2009). In such cases it can be difficult to determine which bands are from which molecules in a sample unlike in the case of pure samples in which all bands can be assigned a specific structure. FTIR is an effective tool for detecting functional groups but by itself it cannot necessarily be used to elucidate the complete structure of an unknown molecule. However, use of this technique in conjunction with other techniques such as those selected in this work (SELDI-ToF-MS, amino acid profiling and potentiometry) can provide further information with respect to aiding characterisation and comparison of proteinates.

Amino acid profiling can enable differentiation between proteinate products in the marketplace as the technique can identify the amino acids present in the sample in addition to their percentage abundance.

A mass spectrometric technique that proves extremely useful as a complimentary technique to the other methods of assessment is Surface Enhanced Laser Desorption/Ionisation Time of Flight Mass Spectrometry (SELDI-ToF-MS). This method of analysis can be used to analyse peptide profiles for consistency between metal proteinate batches which is advantageous from a quality control perspective.

Furthermore, identification of new peptide peaks upon complex formation which may be indicative of peptide-metal adducts is possible. This technique, which is discussed in further detail (Section 1.6.1) due to its central role in this work, also provides a means to compare and contrast proteinate samples over a wide molecular mass range.

1.6.1 Surface Enhanced Laser Desorption/Ionisation Time of Flight Mass Spectrometry (SELDI-ToF-MS)

In the last two decades, mass spectrometry has become the method of choice for the characterisation of proteins and protein modifications (Burlingame *et al.*, 1996). This is, in large measure, due to the discovery of new ionisation techniques such as Electrospray Ionisation Mass Spectrometry (ESI-MS) (Fenn *et al.*, 1989), Matrix-Assisted Laser Desorption/ Ionisation Time of Flight Mass Spectrometry (MALDI-ToF-MS) (Karas *et al.*, 1988) and Surface-Enhanced Laser Desorption/ Ionisation Time of Flight Mass Spectrometry (SELDI-ToF-MS) (Hutchens *et al.*, 1993) which provide both the high sensitivity and extended mass range required for a detailed structural characterisation of covalently modified proteins. Although MALDI-ToF-MS often gives very good quantification (Oda *et al.*, 1999), factors such as variable crystallisation and laser ablation may lead to poor standard curves (Lill, 2003).

SELDI-ToF-MS can be considered an extension of the MALDI-ToF-MS method. In both cases, proteins to be analysed are co-crystallised with UV-absorbing compounds and vaporised by a pulsed-UV laser beam. Ionised proteins are then accelerated in an electric field, and the mass to charge ratios of the different protein ion species can be deduced from their velocity. The differences between SELDI-ToF-MS and MALDI-ToF-MS are in the construction of the sample targets, the design of the analyser and the software tools used to interpret the acquired data. In the SELDI-ToF-MS method, protein solutions are applied to the spots of ProteinChip Arrays which have been derivitised with planar chromatographic chemistries. The proteins actively interact with the chromatographic array surface, and become sequestered according to their surface interaction potential (Figure 1.7).

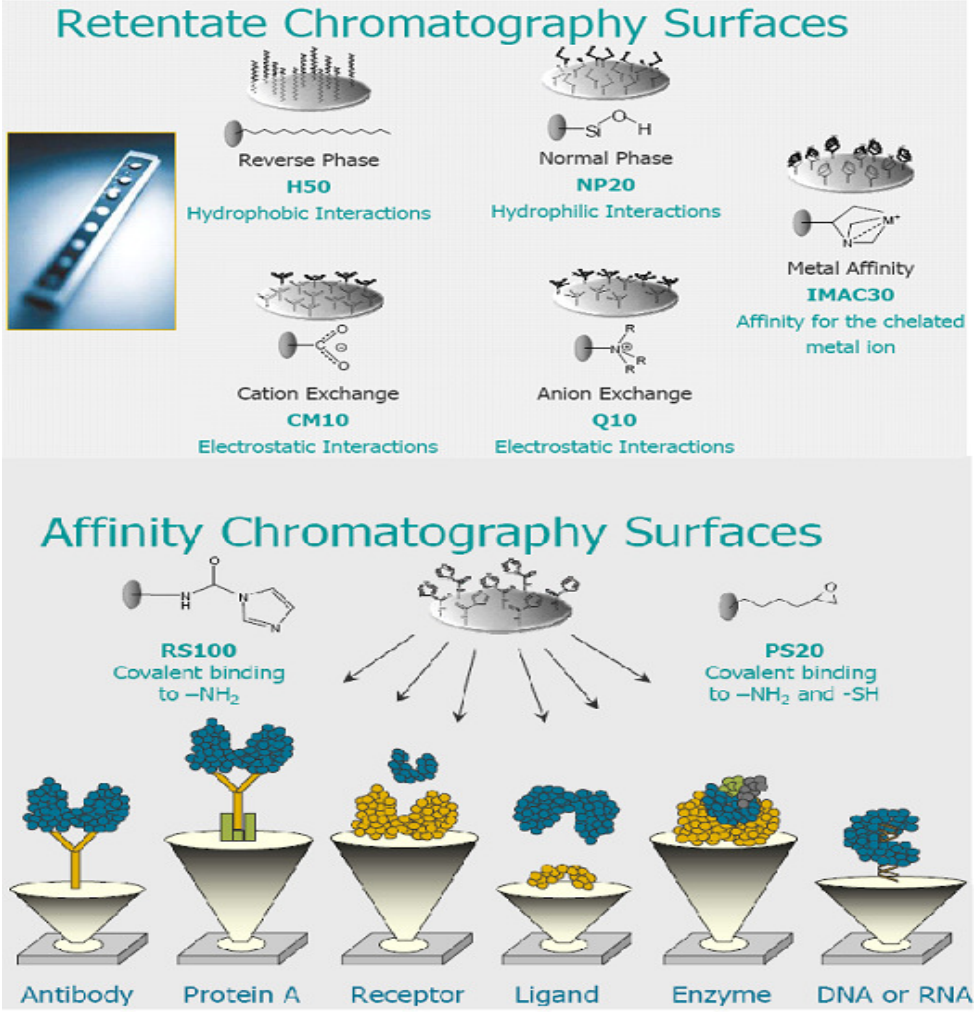

Adapted from Ciphergen Inc.

Figure 1.7 SELDI-ToF-MS chromatographic surface types

The SELDI-ToF-MS technology selects subgroups of peptides and proteins from a sample through their affinity for chromatographic surfaces, where different classes of peptides and proteins bind to chips with different coatings, e.g. cationic, anionic or hydrophobic. Even in the presence of elevated levels of other compounds in a biological sample, only those molecules whose properties match the binding characteristics of the surface are retained and all others are washed away by employing appropriate wash strategies after the desired analyte has been bound. After the binding phase of the sample to the surface, the unbound proteins are washed off while retained molecules are overlaid with an Energy-Absorbing Matrix (EAM). In the final step, mass spectra are recorded using a laser for the ionisation and a time of flight mass spectrometer for its

resolving power. Spectra of complex protein mixtures based on the mass-to-charge ratio of the proteins and on their binding affinity to the chip surface are produced.

Characterisation of proteins has become such a significant part of modern biology it has inspired a new discipline: proteomics. This can be defined as the classification of the protein complement expressed by the genome of an organism (Blackstock *et al*., 1999). Proteomics can play a pivotal role in mapping protein profiles in different sample groups, e.g. SELDI-ToF-MS protein profiles have been used to distinguish different pathologic states (Kozak *et al.*, 2003; Zhang *et al.*, 2004), to evaluate different experimental conditions (Boot *et al.*, 2004; Xiao *et al.*, 2004) and as a means for detecting early stages of cancer and other diseases (Wright Jr *et al.*, 1999; Clarke *et al.*, 2005; Solassol *et al.*, 2005; Xiao *et al.*, 2005). Technological developments have enabled rapid evolution in this field and one area of notable interest, based on the volume of publications, is biomarker discovery. Several definitions of biomarkers exist and one of the most commonly used general definitions refers to a biomarker as a characteristic that can be objectively measured and evaluated as an indicator of a physiological as well as a pathological process or pharmacological response to a therapeutic intervention (Jain, 2010). A biomarker (or marker peptide) can be defined in terms of this project as a peptide or group of peptides selective to a particular hydrolysis procedure used to identify a product, sample or aid characterisation.

In this body of work, SELDI-ToF-MS was used for a variety of purposes. Current protocols for enzymatic hydrolyses were re-examined with the intention of adapting the procedure with respect to lowering costs. Assessment of peptide patterns produced during temperature, pH and enzyme concentration profiling was carried out using SELDI-ToF-MS to determine the effect of altering the hydrolysis parameters on the resultant peptide profiles. The molecular mass of peptides available for chelation with trace elements was also established using SELDI-ToF-MS. Furthermore, marker peptides were identified which were specific to the hydrolysis procedure used in this work and consequently a method was established to compare proteinates based on their respective profiles. Additionally, this method provided a means to detect whether or not the products were included in feed components such as premix samples.

Advantages of SELDI-ToF-MS include high sensitivity and selectivity. Although mass spectrometry is a destructive technique most variants are very sensitive, requiring only micrograms or nanograms of sample for analysis. Furthermore, this method of analysis enables multiple protein analyses on a single experimental platform, combining selective protein capture with sensitive and quantitative mass spectrometric analysis. The experimentally measured mass of the captured molecules allows for the accurate detection of multiple variants of a given protein in a single assay (Rossi *et al.*, 2006). SELDI-ToF-MS can be used for high throughput analysis and can also be used for a wide range of applications such as protein profiling (clinical proteomics, drug effect studies, toxicology studies, pharmaco-kinetic studies), protein characterisation (peptide mapping, protein identification, analysis of post-translational modifications, epitope mapping, monitoring of purification process, sequencing) and interaction discovery (peptide or protein assay by antibody capture, screening of ligands, receptor-ligand interaction, protein-protein interaction, DNA-protein interaction) (Jourdain, 2004). Low molecular mass peptides can also be detected with greater ease than with other methods such as Sodium Dodecyl Sulfate Polyacrylamide Gel Electrophoresis (SDS-PAGE) which separates proteins by mass.

Disadvantages of SELDI-ToF-MS include spectral variability; formation of salt adducts and multiply charged ions, array surface variations and fluctuation in laser intensity and/or detector sensitivity (Dijkstra *et al.*, 2007). Sources of spectral variability such as matrix crystallisation, ion suppression and in-source decay occurring during mass spectra acquisition strongly influence the peak intensities. During the crystallisation process, a competition phenomenon can occur between proteins for crystal inclusion. Easily embedded proteins will be present at higher concentrations in the matrix and consequently more efficiently desorbed and ionized (Albrethsen *et al.*, 2006). During ionisation, analytes compete for protons that are transferred from matrix molecules. If a protonated analyte collides with an unprotonated one which has higher gas-phase basicity, it may pass its proton to the collision partner. Therefore, the presence of an analyte may reduce the signal intensity of another. This phenomenon is called “ion suppression effect” (Albrethsen *et al.*, 2006; Dijkstra *et al.*, 2007; Poon, 2007). Another source of variation is the fragmentation of proteins or peptides during the mass

spectrometric process. Fragmentation occurring before the field-free region is called in-source decay (ISD) and has been shown to give rise to consecutive series of c_n ions from peptides and small proteins (Lennon *et al.*, 1997; Ekblad *et al.*, 2007). Additionally, chemical reactions using energy from the laser may take place between sample protein molecules, matrix molecules or molecules from the washing buffers generating intermolecular complexes known as "ion clusters" (Dijkstra *et al.*, 2007). As protein binding onto chromatographic surfaces depends not only on its affinity and concentration, but also on the surface binding capacity, competition for binding sites is very complex (Piperno *et al.*, 2009). A highly abundant protein with low affinity for the chip surface and a low abundant protein with high affinity may give similar peak intensities in the SELDI-ToF-MS spectra. Protein steric hindrances can also affect the profile.

The majority of the aforementioned disadvantages can be addressed in a number of ways. A substantial reduction in sample complexity and the application of a rigorous standardisation program for the entire analytical process can alleviate the majority of issues. This involves optimised acquisition protocols (i.e. avoiding too high laser intensity), a fully operational and calibrated instrument and the use of suitable quality control samples, similar in nature and complexity to the studied samples.

SELDI-ToF-MS technology does not provide peptide/protein identification. In order to succeed in the identification by sequencing (Q-ToF, ToF-ToF, ion-trap) or peptide fingerprinting (MALDI-ToF), enrichment and purification of the biomarker of interest is often needed and can be time consuming. Recent developments allow direct sequencing of peptides < 6000 Da by means of a ProteinChip interface coupled to tandem mass spectrometer (Peng *et al.*, 2009). The ProteinChip arrays which are read on Bio-Rad's ToF mass spectrometers can also fit onto Applied Biosystems' QSTAR quadrupole ToF (Q-ToF) hybrid mass spectrometer via a special adaptor (Cottingham, 2003). Identifications can also be corroborated using antibody-based detection (i.e. Western blot or ELISA).

1.6.2 Tandem Mass Spectrometry (MS/MS)

Tandem mass spectrometry (MS/MS), the process of peptide ion fragmentation with subsequent mass/charge (*m/z*) measurement, is typically induced by isolating the protonated peptide *m/z* of interest and subjecting it to several hundred collisions with rare gas atoms (Hunt *et al.*, 1986) (Figure 1.8). This process, termed collision-activated dissociation (CAD), supplies sufficient internal energy to induce covalent bond breakage. In the gas phase, the amide bonds of the peptide backbone are typically the preferred sites of protonation. These protonated amide linkages are weakened and, upon collisional-activation, are favoured for cleavage to create a series of homologous product ions. The process aims to produce a collection of peptide fragment ions that differ in mass by a single amino acid, allowing one to read the amino acid sequence of the precursor peptide.

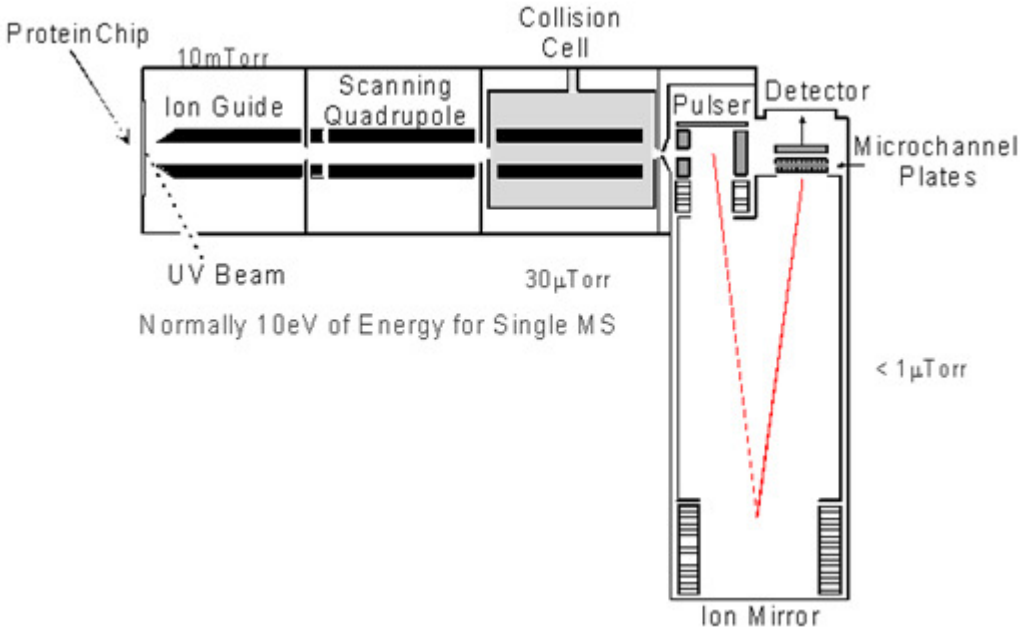

Adapted from Ciphergen Inc.

Figure 1.8 Schematic diagram of a Triple Quadrupole Time of Flight (QqToF) mass spectrometer used to obtain peptide sequences

In the context of this work, tandem mass spectrometry was selected to obtain the amino acid sequence of the marker peptides identified using SELDI-ToF-MS. As a

further developmental step, MS/MS was used to verify that the peptide sequence was consistent between proteinate batches and whether adjustments to the hydrolysis protocol resulted in differences in the peptide sequence.

As previously mentioned, the sequences obtained using MS/MS can be corroborated using antibody-based detection methods such as ELISA. The main purpose for selecting ELISA as an additional method was to determine if detection in-feed was feasible. As effective as the mass spectrometry methods were for initial characterisation and identification of peptide proteinates it was necessary to detect these products in premixes and feed.

1.6.3 Enzyme-Linked Immunosorbent Assay (ELISA)

An Enzyme-Linked Immunosorbent Assay, or ELISA, is a biochemical technique used mainly in immunology to detect the presence of an antibody or an antigen in a sample. ELISA has been used as a diagnostic tool in medicine and plant pathology, as well as a quality control check in various industries. The term Immunoassay describes a wide range of assays used to detect and quantitate antigens and antibodies. Antibodies are host proteins produced in response to the presence of a foreign molecule (antigen). The antigen antibody interaction is specific, which makes antibodies an important reagent for immunological research.

Performing an ELISA involves at least one antibody with specificity for a particular antigen. The sample with an unknown amount of antigen is immobilised on a solid support (usually a polystyrene microtitre plate) either non-specifically (via adsorption to the surface) or specifically (via capture by another antibody specific to the same antigen, in a "sandwich" ELISA). After the antigen is immobilised, the detection antibody is added which forms a complex with the antigen. The detection antibody can be covalently linked to an enzyme, or can itself be detected by a secondary antibody which is linked to an enzyme through bioconjugation. Between each step the plate is typically washed with a mild detergent solution to remove any proteins or antibodies that are not specifically bound. After the final wash step the plate is developed by

adding an enzymatic substrate to produce a visible signal, which indicates the quantity of antigen in the sample (Figure 1.9). Older ELISAs utilise chromogenic substrates, though newer assays employ fluorogenic substrates with much higher sensitivity.

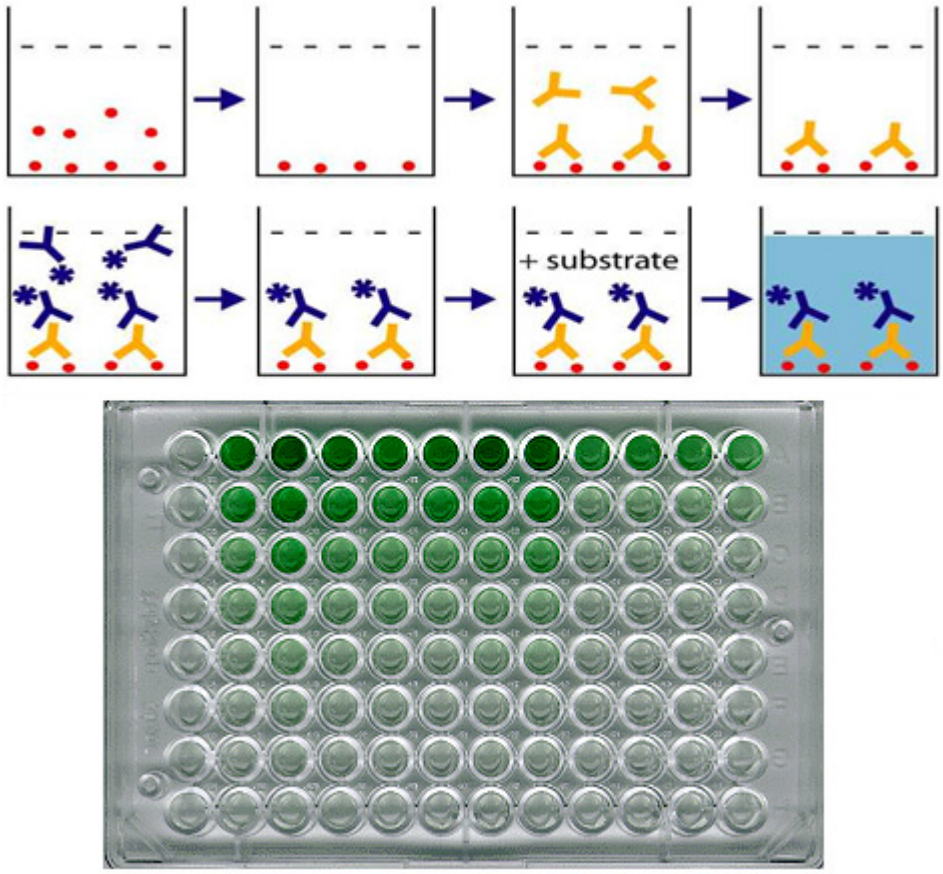

Figure 1.9 An example of a typical ELISA assay and corresponding 96-well plate. ● = antigen, Y = primary antibody specifically raised against the antigen, Y* = secondary antibody labelled with an enzyme. The colour observed in the 96-well plate is relative to the concentration of antigen contained in each of the wells.

Peptides longer than 20 residues in length are often more difficult to synthesize with high purity because there is greater potential for side reactions, and they are likely to contain deletion sequences. On the other hand, short peptides (< 10 amino acids) may generate antibodies that are so specific in their recognition that they cannot recognise the native protein or do so with low affinity. The typical length for generating anti-peptide antibodies is in the range of 10-20 residues. Peptide sequences of this length

minimise synthesis problems, are reasonably soluble in aqueous solution and may have some degree of secondary structure (Sigma, 2000).

The properties of antibodies are dependent on the primary sequence information. A good response to the desired peptide usually can be generated with careful selection of the sequence and coupling method. The advantage of anti-peptide antibodies is that they can be prepared immediately after determining the amino acid sequence of a protein and the particular regions of a protein can be targeted specifically for antibody production. The only disadvantage is that they might not recognise the native protein. Non-specific antibody cross reactivity can occur using enzyme linked imunosorbent assays.

The ELISA work in this project centred on the development of an ELISA assay to develop a synthetic peptide and monoclonal antibody to a specific target based on the peptide profile results obtained using SELDI-ToF-MS. Synthetic short peptides were used to generate protein-reactive antibodies. The advantage of immunising with synthetic peptides was that unlimited quantity of pure stable antigen could be used. This approach involved synthesising short peptide sequences, coupling them to a large carrier molecule, and immunising the animal of choice (mouse) with the peptide-carrier molecule.

1.6.4 Introduction to stability constants

Metal ion complex formation is among the prominent interactions in nature and metal complexation is of widespread interest. The strength of the complexation between organic ligands and metals is usually expressed in terms of a stability constant, also called an equilibrium, formation or binding constant. Stability constants characterise binding interaction between the analyte and the complexing agent and are of immense importance for a broad variety of technologies in biology and medicine (Samavat *et al.*, 2007). Accumulation, deposition and migration of heavy metals in soils has been a concern for a number of years and numerous publications have investigated the interactions of soil components such as humic and fulvic acids with metal ions (Takamatsu *et al.*, 1978; Saha *et al.*, 1985; Buffle *et al.*, 2002). The availability of

micronutrients to plants and microorganisms is a further area of interest. Knowledge of stability constants makes possible the prediction and estimation of binding behaviour of constituents (amino acids, peptides, proteins, drugs, antibiotics, enzymes, enantiomers) to their partners, and the finding of a suitable partner for the given analyte to form a stable complex (Stevenson *et al.*, 1991; Uselová-Vceláková *et al.*, 2007). Quantitative information concerning the products of acid-base, metal-ligand or enzyme-substrate interactions is invaluable in areas such as analytical chemistry, industrial process chemistry and biochemistry to name but a few. It has been suggested that a greater control of metal nutrition and physiology can be accomplished through a better understanding of coordination complexes formed by essential trace metals. The coordination of ligands to a metal ion may profoundly change the apparent properties of that ion. Its solubility may be dramatically increased or decreased in a particular solvent, the metal ion may be stabilised in unexpected oxidation states (as in oxyhemoglobin in which the iron is still iron(II) although it is bonded directly to O_2), or it may be permitted to pass through cell walls which are impervious to the simple hydrated metal ions (Pettit *et al.*, 1977).

The "stability of a complex in solution" refers to the degree of association between the two species involved in the state of equilibrium. Qualitatively, the greater the association, the greater the stability of the compound. The magnitude of the stability constant quantitatively expresses the stability. The development of the measurement of stability constants and their use paralleled the development of the instrumentation for their measurement. Potentiometric measurements were first used for the measurement of stability constants by Arrhenius, Ostwald and Nernst, who provided the basis for the introduction of electrodes responding reversibly and selectively to only one species present in solution (Martell *et al.*, 1996). The investigations of Bjerrum, Brønsted and McGuinness on activity coefficients and the development of the theory of strong electrolytes in solution by Debye and Hückel in 1923 (Bjerrum, 1908; Brønsted, 1922; Debye *et al*., 1923), formed the basis for exact studies of metal ions and of anions in solution (Martell *et al.*, 1996). Improved methods for stability constant measurement and calculation have been developed since then and complex systems can now be assessed without approximations.

There are a number of notations used for stability constants and confusion has arisen due to variations in the usage of terms. As far back as the 1950s, deviations in the usage of stability constant terms were observed (Irving *et al.*, 1953) and to avoid further confusion it is necessary to fully describe the terms used in this work and their use (Table 1.5).

Table 1.5 Stability constant terminology

Symbol	Definition
$\mathbf{M^{n+}}$	Metal ion
L	Organic Ligand
ML	Complex between metal ion M and ligand L
$\mathbf{[M^{n+}]}$	Molar concentration of free metal ion of M
[L]	Molar concentration of ligand L not bound to the metal ion
$\mathbf{K_{ML}}$	Stepwise stability constant for complex ML with respect to the concentration of free metal ion, [M]
β	Cumulative stability constant
$\mathbf{a_{H+}}$	Hydrogen ion activity
$\mathbf{[H^+]}$	Hydrogen ion concentration
γ	Activity coefficient
$\mathbf{K_w}$	Autoionisation constant of water
μ	Ionic strength of a solution

Metal ions such as Cu^{2+}, Zn^{2+}, Ni^{2+}, and Co^{2+}, generally react with water to form octahedral aquo-complexes of the formula $M(H_2O)_6^{2+}$. The addition of another ligand, L^- to such solutions results in the competition of L^- for coordination sites occupied by H_2O and can be described as:

$$M(H_2O)_6^{2+} + L^- \leftrightarrow M\,(H_2O)_5\,(L)^+ + H_2O \qquad (\mathbf{1.1})$$

The equilibrium expression can be written as:

$$K = \frac{[M(H_2O)_5(L)^+][H_2O]}{[M(H_2O)_6{}^{2+}][L^-]} \qquad (\mathbf{1.2})$$

However, concentration of H_2O in dilute solutions is virtually the same regardless of the position of the equilibrium so $[H_2O]$ in the equilibrium expression is effectively a constant and is included in the equilibrium constant:

$$K_1 = \frac{[M(H_2O)_5(L)^+]}{[M(H_2O)_6{}^{2+}][L^-]} \quad (\mathbf{1.3})$$

As H_2O always occupies coordination sites in the complex not filled by L^-, the H_2O ligands are usually omitted from the complex formula in both the equilibrium reaction and the associated equilibrium constant expression. Thus,

$$M^{2+} + L^- \leftrightarrow ML^+ \quad (\mathbf{1.4})$$

$$K_1 = \frac{[ML^+]}{[M^{2+}][L^-]} \quad (\mathbf{1.5})$$

The constant, K_1, is called an equilibrium constant.

The existence of six coordination sites in many metal complexes means that L^- and H_2O compete for all six sites, and the following equilibria are possible:

$$M^{2+} + L^- \leftrightarrow ML^+ \qquad K_1 = \frac{[ML^+]}{[M^{2+}][L^-]} \quad (\mathbf{1.6})$$

$$ML^+ + L^- \leftrightarrow ML_2 \qquad K_2 = \frac{[ML_2]}{[ML^+][L^-]} \quad (\mathbf{1.7})$$

$$ML_2 + L^- \leftrightarrow ML_3^- \qquad K_3 = \frac{[ML_3^-]}{[ML_2][L^-]} \quad (\mathbf{1.8})$$

$$ML_3^- + L^- \leftrightarrow ML_4^{2-} \qquad K_4 = \frac{[ML_4^{2-}]}{[ML_3^-][L^-]} \quad (\mathbf{1.9})$$

$$ML_4^{2-} + L^- \leftrightarrow ML_5^{3-} \qquad K_5 = \frac{[ML_5^{3-}]}{[ML_4^{2-}][L^-]} \quad (\mathbf{1.10})$$

$$ML_5^{3-} + L^- \leftrightarrow ML_6^{4-} \qquad K_6 = \frac{[ML_6^{4-}]}{[ML_5^{3-}][L^-]} \qquad (\mathbf{1.11})$$

The equilibrium constants, K_1, $K_2 \ldots K_6$, in the series of equilibria are called *stepwise stability constants*. The equilibrium constants may also be expressed as overall or *cumulative stability constants*, β, which are simply products of the stepwise stability constants. Due to the large numbers involved, stability constants are usually expressed as log β_n (Angelici *et al.*, 1999).

The relationship between stepwise and cumulative formation constants is:

$$\beta_n = \prod_1^n K_n \qquad \text{e.g., } \beta_3 = K_1K_2K_3$$

Some of the above complexes may exist in *cis* and/or *trans* forms and these equilibrium expressions do not distinguish these isomeric forms. Thus they refer to the total concentration of both isomers. Usually, for anionic L^- groups, the introduction of six L^- ligands into the complex is prevented by the build up of negative charge on the complex (Angelici *et al.*, 1999). It should be noted that writing the equilibrium constant as a cumulative equilibrium constant does not indicate that two or more ligands are added simultaneously. All association reactions occur in a stepwise manner, although in a few cases the successive reactions overlap extensively (Angelici *et al.*, 1999).

Formation constant data is readily available from databases such as the IUPAC Stability Constants Database (SC-Database) and the NIST Critically Selected Stability Constants of Metal Complexes database. The SC-Database is a compilation of literature data, intended to direct the user to the original literature reference. It contains all significant stability constants and associated thermodynamic data published from 1887 to the present day. The NIST Critically Selected Stability Constants of Metal Complexes Database is a reference work covering large volumes of interactions for aqueous systems of organic and inorganic ligands with protons and various metal ions and has similar information as that contained in Martell and Smith's six-volume set (Martell *et al.*, 1974) but most of the data contained in the database has been updated and new material

added as further results have been published. The NIST database was employed to obtain the published values used for comparative purposes in this work.

1.6.5 Potentiometry

Potentiometric titration methods are relatively simple and effective ways to obtain metal-ion complex stability constants and acid dissociation constants and, under favourable conditions, the speciation of complex mixtures in solution can be estimated with fair confidence (Martell *et al.*, 1988). Of all methods used to determine stability constants, pH analysis with a glass electrode has been applied most extensively. The direct pH method is based on the fact that the potentiometric titration of solutions of a protonated ligand, alone and in the presence of a metal ion, through the stepwise addition of a strong base allows evaluation of the constants for the ligand deprotonation equilibrium and for the proton displacement equilibrium due to the metal ion competition (Beck, 1977). Although pH measurements have been used frequently to determine formation constants, there are a number of limitations to the method. At high pH, the concentration of the free ligand is almost independent of pH and, at low pH, the complexation is negligible owing to virtually complete protonation of the ligand (Eriks *et al.*, 1983).

A pH meter determines the EMF of the glass electrode relative to the standard calomel electrode and therefore a pH measurement determines the H^+ activity, a_{H+} , and not its concentration, $[H^+]$, in solution. To eliminate uncertainties arising from activity constant variations, it is common practice to keep activity coefficients constant by use of a background electrolyte (e.g., 0.10 M $NaNO_3$). Since the glass electrode measures hydrogen ion *activity*, i.e., $pH_{meas} = -\log(H^+) = -\log[H^+]\gamma_+$, it is necessary to convert activity to concentration in the calculations that follow.

The mean activity coefficient, $\gamma_\pm$, of the ions may be calculated from the Davies equation, an empirical extension of the Debye – Hückel limiting equation (Debye *et al*., 1923; Davies, 1962):

$$-\log \gamma_\pm = (0.5091|Z_1Z_2|\sqrt{\mu}) / (1+\sqrt{\mu}) \qquad (\mathbf{1.12})$$

where Z_1 and Z_2 are the charges of the ionic species in solution.

The ionic strength of the solution, μ, is given by the usual definition,

$$\mu = \frac{1}{2}\sum_i M_i Z_i^2 \quad (\mathbf{1.13})$$

where M_i is the molar concentration of the ion, I and Z_i is its charge.

By definition,

$$a_{H+} = \gamma_{\pm}[H^+] \quad (\mathbf{1.14})$$

Rearranging and substituting:

$$pH = -\log a_{H+} = -\log \gamma_{\pm}[H^+] = -\log \gamma_{\pm} - \log[H^+] \quad (\mathbf{1.15})$$

or

$$-\log[H^+] = pH + \log \gamma \quad (\mathbf{1.16})$$

$[OH^-]$ can be calculated by making use of the autoionisation constant of water, K_w:

$$K_w = [H^+][OH^-] = 10^{-14} \quad (\mathbf{1.17})$$

At a given pH the conditional constant or apparent stability constant β, so called because it is a constant valid for only a particular pH value, can be determined.
The development and application of ion selective electrodes (ISEs) for potentiometric use continues to be an interesting area of analytical research as they provide accurate, rapid, non-destructive and low cost methods of analysis (Escoda *et al.*, 1999; Gupta *et al.*, 2005). Ion-selective electrodes are electrochemical sensors that enable potentiometric determination of the activity of certain ions even in the presence of other ions. Response of these sensors towards charged species is provided by ion-selective membranes, which can be prepared from a variety of materials such as glass, solid crystalline, ceramic or polymers. Their selectivity can be achieved either by means of material structure or by doping the membrane with specific ion-selective complexing agents. Changes in the activity of the ion of interest cause changes of the membrane potential and is measured as ISE response against a reference electrode.

A Cu^{2+} combination ion selective electrode was selected for the ISE titrations carried out in this work to determine the degree of complexation of a particular ligand to Cu^{2+} (Figure 1.10). The reference system is contained in the same cylindrical body as

the sensor head in combination electrodes which produces a simple, compact unit for immersing in the test solution and minimises the effect of any stray electrostatic fields or heterogeneity in the test solution (Rundle, 2005). Use of this particular technique for other minerals of interest is problematic however, as efforts made so far for developing accurate iron, manganese and zinc-selective electrodes have not been very successful. Most of them have poor selectivity, sensitivity and stability, long response time and short lifetime (Gorton *et al.*, 1977; Fiedler-Linnersund *et al.*, 1979; Kojima *et al.*, 1994; Srivastava *et al.*, 1995; Singh *et al.*, 1997; Gupta *et al.*, 1998; Teixeira *et al.*, 1998; Shamsipur *et al.*, 1999; Fakhari *et al.*, 2000; Jain *et al.*, 2002; Gupta *et al.*, 2005). As a consequence, the focus of this section of the project was solely based on Cu^{2+} complexes. Provided suitable electrodes can be produced for the other metals of interest, the techniques described here should be easily applied to the complex formations of ligands with Zn^{2+}, Fe^{2+} and Mn^{2+}.

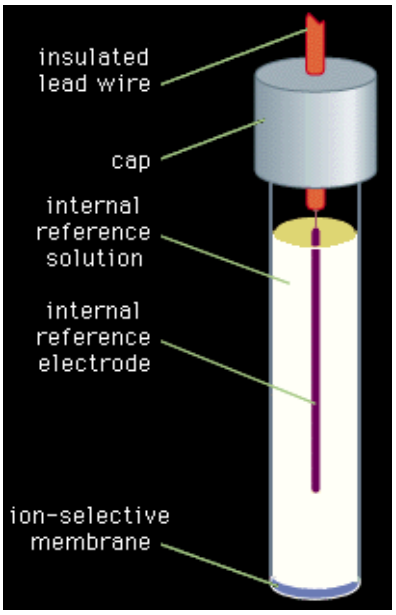

Adapted from Encyclopaedia Britannica, Inc

Figure 1.10 Schematic of a combination ion-selective electrode

The use of potentiometry in this research work has a number of purposes. It aims to define the effect of selective pH adjustment during manufacture on overall metal proteinate stability, determine the suitability of copper ion selective electrodes (ISE) in monitoring the presence of Cu^{2+} ions and thus indirectly determine the relative

proportion of bound copper over a wide pH range. It will also be used for the determination of stability constants for a selection of copper and ligand complexes which will aid in analysing the suitability of such complexes for use in nutritional feed supplements.

The concentrations of unbound or free mineral, free ligand, and bound mineral can be used to calculate the stability of the organic mineral. As the stability constant increases, the affinity of the ligand for the metal increases. However, chelates with very high stability constants are not advantageous and examples of such include chelates formed from EDTA and its derivatives which have stability constants in excess of 10^{16}. The mineral-ligand association may be indicative of the bioavailability of the trace mineral in the digestive system of livestock and poultry. High stability constants indicate that the bonds formed are so strong that the metal is unlikely to be biologically available and may pass intact through most biological systems which use (stomach) acids to dissociate the metal from the ligand (Ashmead, 1980b). Conversely, yet just as important, low stability constant values indicate that the metal-ligand is not only soluble in water but readily dissociates into the ionic form of the metal and the ligand. Consequently, these metallic ions are available for absorption but may also react with dietary antagonists rendering the metal insoluble or reducing biological availability. Examples of such include citrates and ascorbates which form much weaker chelate bonds on the order of $10^2 – 10^4$. The citrates and ascorbates tend to decompose before they can be assimilated into a biological system and it is much more difficult to absorb a positive metal ion than a chelate (Ashmead, 1980b). Ideally mineral dietary supplements will have stability constants between these two extremes enabling them to be sufficiently stable during the digestive process yet remain biologically available with the metal not so tightly bound to its respective ligand as to prevent its release at the appropriate point.

There are several standard methods for obtaining equilibrium constants from titrimetric data, one of the most sophisticated and current being the Hyperquad 2008 computer program which allows one to calculate stability constants for suggested multispecies equilibrium situations. Through its use, a satisfactory fit of the

potentiometric data to a proposed multiequilibrium process involving several sequential metal-ligand associations may be obtained.

1.6.6 WinCOMICS and Hyperquad

Speciation calculations are commonly used to describe chemical systems and the associated diagrams are a convenient way to display such calculations. Developments in software programs have enabled construction of speciation diagrams for any given concentration of metal ions. Programs such as WinCOMICS (Hynes, 2005) illustrate the concentration of different species as a function of pH and allow identification of the predominant species occurring at a given pH. Such speciation diagrams provide an insight into the pH ranges where ionisation is effectively complete and where it is not. The theoretical results produced refer to end-point data and are based solely on the input parameters selected.

Progress in the field of computation of equilibrium constants from experimental data has been reviewed on numerous occasions (Leggett, 1977; Garcia *et al.*, 1984). More recently an improved software suite (Hyperquad) was described, which has the advantage over older programs of determining equilibrium constants from both potentiometric and spectrophotometric (absorbance) data simultaneously on the same set of reaction solutions (Sabatini *et al.*, 1992). The use of the Hyperquad software permits the determination of formation constants from potentiometric data especially when different equilibrium reactions can take place in the aqueous solution (Gans *et al.*, 1996). This software provides a means of obtaining "live data" as the titration progresses which is a distinct advantage over the theoretical WinCOMICS program. Although the quality of the complexation model that can be obtained from the calculations is limited by the experimental data (potentiometric accuracy, kinetic effects, precipitation, etc.) species may be detected that are absent in WinCOMICS. It is important that all experimental work is carried out in a systematic way avoiding analytical errors in the concentrations and verifying the equilibrium state of the chemical system (Escoda *et al.*, 1999). The information obtained from WinCOMICS can be used

as a complimentary method to Hyperquad to determine if species identified based on experimental data correlate with those theoretically expected under defined conditions.

Hyperquad 2008, which was used in this work, has some notable differences in comparison to previous versions, including the way the mass-balance equations are solved. The parameters to refine are the logarithms of the free concentrations of the metal ion and not the free concentrations themselves. The convergence criteria are also different and another difference is that the table of concentrations is available at any time, not just after refinement. The species included in the speciation diagrams in Hyperquad refer only to the major species calculated but it is important to note that numerous minor species may also be present that may not be detected. As a result, the log β values are overall stability constant values but these values are only valid at the pH the titrations were carried out at, and as such, may be referred to as "conditional" stability constants. Due to the fact that amino acids contain dissociable protons, the free ligand concentration will depend on the pH of the ambient solution. Given the total concentration of amino acid and metal present in solution together with the stability constants of the complexes formed (readily available for most amino acid complexes of Cu^{2+} and Zn^{2+} in compilations of stability constants), it is possible to calculate the percentage of the metal complexed at any given pH value. The combined use of potentiometry and Hyperquad provided a novel, accurate and cost effective method for further characterisation of metal ligand interactions in nutritional mineral supplements.

Covalent linking of minerals to amino acids or peptides may provide essential trace minerals with multiple routes for absorption in the intestine. Some absorption could occur through normal mineral transport mechanisms. Alternatively, uptake may occur via transport proteins for amino acids and short-chain polypeptides in the intestinal mucosa. Furthermore, the different fractions of metal ions that are present in free and bound forms perform different functions. The ability to obtain information on the variety of species present using techniques such as mass spectrometry and potentiometry is extremely valuable from a nutritional perspective. Furthermore, the development of a method to obtain stability constants of ligands contained in metal proteinates provides a means of comparing and contrasting products based on stability and chelation properties.

1.7 Aims and objectives of the study

The focus of this work was on metal proteinates for use as nutritional supplements in feed and measures were taken to add to the previously published body of work regarding metal proteinate production. One of the initial aims of the project was to identify the most suitable protein source for the production of metal proteinates. From an industry standpoint, escalating production costs are of considerable concern and a further aim of this work was to produce effective metal proteinates from a cost-benefit perspective by examining the enzymatic hydrolysis procedure in terms of pH, temperature and enzyme concentration. Additionally, a wide selection of enzymes were also examined to determine which enzyme produced the highest free α-amino nitrogen (FAN) release.

Reliable methods that provide a means of qualitatively and quantitatively analysing metal proteinates are also required to ensure products meet manufacturer and regulatory specifications. There are a wide variety of products available on the market and not all are equal in terms of bioavailability, stability or nutritional value. Assessment of a variety of analytical techniques such as Flame Atomic Absorption Spectroscopy (FAAS), Fourier transform Infrared Spectroscopy (FTIR), Surface-Enhanced Laser Desorption/Ionisation Time-of-Flight Mass Spectrometry (SELDI-ToF-MS), carbon, hydrogen and nitrogen (CHN) analysis, amino acid profiling and potentiometry, to determine their effectiveness at comparing and contrasting proteinates, was a further goal of this work. Additionally, many of the aforementioned techniques can also be used as quality control measures to ensure product consistency between batches and satisfies another objective which was to assess the suitability of a range of techniques as methods of quality control. Another objective was to apply the knowledge gained to identification of metal proteinates in premixes and in feed.

Potentiometry and computer simulation were used to model speciation of copper with the aim of understanding the stability of copper proteinates over a wide pH range. Furthermore, identification of many of the metal-ligand species present using computer models such as WinCOMICS and Hyperquad was another objective and if met, may provide an explanation regarding the increased bioavailability of some proteinates over others. Another important aim of this work relates to the area of chelation. There are few

definitive published methods which conclusively determine whether a metal is truly chelated or merely complexed. Using a number of the aforementioned techniques, the aim of this work was to determine a method, or combination of methods, to conclusively determination chelation.

2. Materials and Methods

2.1 Reagents and equipment

All materials used were of ACS grade or higher where appropriate.

2-2'-azino-bis 3-ethylbenzthiazoline-6-sulfonic acid (ABTS), acetonitrile, anhydrous sodium phosphate, alpha-cyano-4-hydroxycinnamic acid (CHCA), cupric(II) nitrate hydrate, copper(II) sulphate pentahydrate, ethanolamine, ethylenediaminetetraacteic acid (EDTA), fructose, glycine, hydrochloric acid, iron(II) sulphate heptahydrate, manganese sulphate monohydrate , ninhydrin, nitric acid, oxalic acid, potassium chloride, potassium iodate, potassium phosphate , sodium bicarbonate, sodium chloride, sodium hydroxide (carbonate free), sodium nitrate, sodium phosphate, sulphuric acid, trifluoroacetic acid (TFA), Triton X-100, zinc(II) sulphate heptahydrate and all amino acids used were supplied by Sigma-Aldrich, Tallaght, Ireland.

Ethanol (Lennox, Dublin, Ireland), liquid nitrogen (BOC Gases, Dublin, Ireland), synthetic peptides (GenScript USA Inc., New Jersey, U.S.A.), protein sources including soy flour, whey and casein (Alltech Bioscience Centre, Dunboyne, Co. Meath, Ireland) and alkaline and acidic protease enzymes (Dr. Richard Murphy, Alltech Bioscience Centre, Dunboyne, Co. Meath, Ireland) were used as supplied.

Maxisorp 96-well micro-titre plates were obtained from Bio-Sciences Ltd. Dublin, Ireland.

The All-in-One Peptide Standard and all SELDI-ToF-MS arrays were supplied by Ciphergen Biosystems, Fremont, CA, U.S.A.

Monoclonal antibodies based on peptide sequences provided by our laboratory were prepared by Fusion Antibodies Ltd., Belfast, N. Ireland.

2.2 Laboratory preparation and analysis of metal proteinates

2.2.1 Hydrolysis of a protein source

Enzymatic hydrolyses were carried out in the laboratory under acidic and alkaline conditions by preparing a 16.67 % (w/v) aqueous suspension of soy flour and distilled water. A portion of soy flour (50 g) was added to distilled water (500 mL) in a glass beaker. An aliquot of the enzyme (1 mL) was added to the soy flour suspension. The remainder of the soy flour (50 g) was immediately added followed by a second aliquot of the enzyme (1.5 mL). The total enzyme concentration was 0.42 % (v/v). Over the course of the hydrolysis, a visual inspection determined the viscosity of the sample had decreased dramatically.

The pH dropped rapidly during the first 40 minutes of the hydrolysis and required constant monitoring. Adjustments to temperature, pH and enzyme volume were carried out according to a previously established protocol (Murphy, 2005) before the effect of changing these parameters was investigated. For acidic hydrolyses, the pH was maintained at pH 3 and temperature at 55 °C. Alkaline hydrolyses were carried out at pH 8.5 and 55 °C. After two hours of maintaining the pH at the predetermined optimum value, the hydrolysis was allowed to continue for a further four hours without pH adjustment. The pH of the final soy hydrolysate was noted in addition to the properties of the suspension.

2.2.2 Formation of metal proteinates from soy flour hydrolysate

The sulphate form of each element (Cu, Fe, Mn and Zn) was used to prepare batches of metal proteinates with a metal content of 10 % (w/w) dry weight. The metal content was confirmed by Flame Atomic Absorption Spectrometry (Section 2.2.6). The calculated amount of metal salt for each element to obtain a 10 % (w/w) metal content was added to a soy hydrolysate (90 mL) and the contents were mixed for 1 hour at room temperature prior to being cooled and frozen at -70 °C before lyophilisation. The dried

powders were homogenised using a pestle and mortar and stored in sterile, high density polyethylene (HDPE) airtight containers.

2.2.3 Determination of total nitrogen

A selection of protein sources was tested to determine the most suitable for this work. Whey, casein, skim milk, corn steep liquor and soy flour were assessed. Total nitrogen for all protein sources examined was determined using the Kjeldahl method (Cohen, 1924) and consequently, crude protein could be determined by multiplying this value by 6.25 for soy proteins or 6.38 for milk proteins. The total nitrogen analysis was carried out by Independent Analytical Supplies Ltd., Carlow, Ireland.

2.2.4 Free α-Amino Nitrogen (FAN) determination

Using a modified version of the official procedure of the Association of Official Analytical Chemists (Association of Official Analytical Chemists, 1990), α-amino nitrogen was monitored to determine the hydrolysis time required for maximum conversion of soy flour protein into lower molecular mass peptides. The effects of pH, time and temperature on the production of FAN were investigated. The optical density of the blank, standards and coloured complexes formed when free amino nitrogen reacted with ninhydrin under the prescribed conditions was measured at 570nm on a UV-Vis Shimadzu 160-A spectrophotometer. A simple calculation was employed to convert optical density to FAN:

$$Alpha\ Amino\ Nitrogen = \frac{(Net\ absorbance\ of\ test\ solution\ x\ 2\ x\ Dilution\ factor)}{Net\ absorbance\ of\ Glycine\ standard} \qquad (\mathbf{2.1})$$

2.2.5 CHN analysis

Carbon, hydrogen and nitrogen analyses on the metal proteinates were carried out in the Microanalytical Laboratory of the Department of Chemistry, NUI Galway, using a PerkinElmer Model 2400 Series II CHNS/O Analyzer.

2.2.6 Flame Atomic Absorption Spectroscopy

To verify that the laboratory batch proteinates contained 10 % (w/w) metal, a quality control procedure to determine the exact percent by unit mass of metal in the proteinate was carried out using Flame Atomic Absorption Spectrometry (FAAS). The atomic absorption spectrometer used in this case was a PerkinElmer AAnalyst 100 equipped with a deuterium background corrector and air: acetylene (3:1) flame.

Calibration standards (1–5 mg/L for Cu and 0.5–2.5 mg/L for Fe, Mn and Zn) were prepared by dilution of a 1,000 mg/L stock solution with HCl (0.1 M). A calibration curve was obtained by plotting the standard absorbances against their concentration.

In brief, the procedure involved digestion of the sample in 10 mL nitric acid at 180 °C for 30 minutes. The digest was diluted with 0.1 M hydrochloric acid so that the metal concentration fell within the concentration range used to calibrate the instrument. The percentage metal in the sample is calculated from the following equations:

$$PPM\ (sample) = \frac{(PPM\ (dilutant) x\ dilution\ factor)}{sample\ mass} \quad \textbf{(2.2)}$$

$$\%\ metal = \frac{(PPM\ (sample) x\ 100)}{1{,}000{,}000} \quad \textbf{(2.3)}$$

2.2.7 Fourier Transform Infrared (FTIR) Spectroscopy

Infrared spectroscopy was carried out on a selection of metal proteinates, soy hydrolysates and metal control samples. Analysis was carried out using a PerkinElmer Spectrum 100 FT-IR spectrometer with a universal Attenuated Total Reflectance (ATR) sampling accessory. All samples were ground using an agate mortar and pestle prior to loading to ensure homogeneity.

2.2.8 Amino acid profiling

Amino acid profiling was carried out by Alta Bioscience, University of Birmingham, Edgbaston, Birmingham, U.K. Profiling was performed using modular HPLC components and the technique has been designed to give maximum versatility in methods of separation and detection. Separation is based on the very well tried and tested Steine and Moore method of ion exchange chromatography, followed by post column colourimetric or fluorimetric detection (Spackman *et al.*, 2002).

2.2.9 Preparation of a metal proteinate mimic

A metal proteinate mimic was prepared by dissolving 5 mg of Ranatensin (Sigma R9002) in water (1 mL) in 1.5 mL push-cap microcentrifuge tubes. Ranatensin was chosen based on the fact that its molecular mass is similar to that of some of the peptides of interest in the metal proteinate samples. Aliquots (10 μL) of this solution were transferred to new tubes and deionised water (20 μL) and 0.1 M copper(II) sulphate pentahydrate (10 μL) were added. The mixture was left to stand at room temperature for 10 minutes before being frozen at -70 °C and lyophilised. The dried material was resuspended in deionised water (40 μL) prior to analysis.

2.3 Mass spectrometry

A PBS IIc ProteinChip® reader system (Ciphergen Biosystems, Fremont, CA, USA) was used to acquire the mass spectra using Surface Enhanced Laser Desorption / Ionisation Time-of-Flight Mass Spectrometry (SELDI-ToF-MS). The energy absorbing molecule (EAM) matrix was prepared by adding 200 µL of EAM buffer (1.0 % TFA in 50 % acetonitrile) to 0.05 g of CHCA (alpha-cyano-4-hydroxycinnamic acid) in a 1.5 mL push-cap microcentrifuge tube. This saturated solution was mixed and allowed to stand for 10 minutes before centrifugation at 14,000 rpm (20,400 g) for 2 minutes using an Eppendorf® 5417C microfuge. An aliquot of the supernatant (50 µL) was added to 200 µL of EAM buffer to prepare a 20 % (v/v) CHCA solution of EAM matrix. This solution was stored under refrigeration (4 °C) and prepared fresh daily.

2.3.1 Calibration of Surface Enhanced Laser Desorption / Ionisation Time-of-Flight Mass Spectrometer (SELDI-ToF-MS) Instrument

The instrument was calibrated using a mixture of standard peptides. The peptides contained in the calibration mixture and their molecular masses are listed in Table 2.1. The calibration mixture was applied to an NP20 chip (normal phase) as described in Section 2.3.2 and inserted into the ProteinChip® reader. Analysis was performed using optimised instrument and data acquisition settings (Table 2.2). The calibration spectrum is displayed in Section 3.3.6.1. The molecular mass of the appropriate peptide standard was assigned to each peak in the spectrum, resulting in the generation of a calibration equation. Application of the calibration equation to the set equation which converts the ToF-axis to a m/z-axis rectifies any deviations that may have occurred between runs by inserting the extraction delay (t_0) and calibration parameters (Dijkstra *et al.*, 2007).

Table 2.1 SELDI-ToF-MS calibration peptides

Peptide	Molecular mass (Da)
Vasopressin	1,084.25
Somatostatin	1,637.90
Dynorphin A (porcine)	2,147.50
ACTH (human)	2,933.50
Insulin β-chain (bovine)	3,495.94
Insulin (human recombinant)	5,807.65
Hirudin (recombinant)	7,034.00

All-in-one peptide mixture (Ciphergen Biosystems Inc.)

Table 2.2 Optimised SELDI-ToF-MS instrument settings

Parameter	Setting
High mass	10,000 Da
Digitizer rate	250.0 MHz
Ion mode	Positive
Chamber vacuum	4.350e-007 Torr
Source voltage	20,000 V
Detector voltage	1,950 V
Time lag focusing	On
Pulse voltage	3,000 V
Pulse lag time	600 ns
Focus mass	600.00 nS
Laser intensity	180
Detector sensitivity	8

Manufacturer (Ciphergen) recommended instrument settings

2.3.2 Analysis of suitable array surfaces and buffers for SELDI-ToF-MS

The arrays listed in Table 2.3 were assessed and three arrays were chosen for initial analysis based on their surface chemistry (NP20, CM10 and IMAC30). Furthermore, a gold array was selected for MALDI-ToF-MS analysis to determine if reproducible spectra could be obtained. A selection of buffers were tested to determine if higher intensity peptide peaks could be obtained but it was determined that distilled water produced equivalent results at a fraction of the cost and preparation time and was selected for use in this work.

Table 2.3 Array surfaces used for SELDI-ToF-MS analysis

Array ID	Function	Use
SAX2, Q10	Mimic strong anion exchange chromatography with a quaternary amine functionality	Protein profiling and protein purification
WCX2, CM10	Mimic weak cation exchange chromatography with carboxylate functionality	Protein profiling and protein purification
IMAC3, IMAC30	Coated with an NTA functional group to entrap transition metals for subsequent metal affinity binding to proteins	6X His-tagged protein capture, protein profiling and protein purification
H50	Binds proteins through reversed phase or hydrophobic interaction chromatography and have binding characteristics similar to that of a C6 to C12 alkyl chromatographic resin	Protein profiling and protein purification
H4	Mimic reversed phase chromatography with C16 functionality	Protein profiling and on-chip desalting
SEND ID	Incorporates an energy absorbing molecule (EAM) into the chemistry of the array reducing chemical noise and allowing analysis of lower molecular mass species with less interference	Protein identification by either peptide mass fingerprinting or MS/MS sequencing
RS100, PS10	Preactivated with carbonyldiimidazole chemistry that covalently binds to free primary amine groups	Immunoassays, receptor-ligand binding studies and transcription factor analysis
PS20	Preactivated with epoxide chemistry that covalently binds to free primary amine groups	Immunoassays, receptor-ligand binding studies and transcription factor analysis
NP20	Mimic normal phase chromatography with silicate functionality	Protein molecular mass validation and QC assays
Gold chip	Relatively non-binding, reusable	MALDI-ToF-MS experiments

2.3.3 SELDI-ToF-MS analysis of metal proteinates

Samples of metal proteinates were prepared by adding 50 mg of the lyophilised proteinate in deionised water (1 mL) to 1.5 mL push-cap microcentrifuge tubes. The contents were vortexed for 1 minute before centrifugation at 14,000 rpm (20,400 g) for 2 minutes. Aliquots (5 μL) of the supernatant were applied to each spot on the chip surface. The chip was then incubated in a humidity chamber for 20 minutes to allow for interaction of the sample with the chip surface. The chip was removed from the humidity chamber and each spot was washed twice with 0.5 mL of deionised water. A vacuum pump with suitable tubing was used to assist in the washing steps by aspirating the liquid from the spot surface. The chip and spot surfaces were allowed to air-dry for 10 minutes before the application of EAM matrix (1 μL) to each spot. The surfaces were again allowed to air-dry for 10 minutes before the chip was inserted into the mass spectrometer. A ProteinChip® reader system (Ciphergen Biosystems, Fremont, CA, USA) was used to acquire the mass spectra. Data management and spectral analysis were performed using Ciphergen ProteinChip® software version 3.2.1.

2.3.4 Tandem MS Collision-Activated Dissociation

Fractionation using cut-off membranes was carried out and Microcon® filtration units (Millipore) with a molecular mass cut off of 10 kDa (YM-10) were used. Optimisation and detection was carried out on the ProteinChip® Array used for discovery (i.e. IMAC30 for metal proteinates). Protein complexity analysis was then carried out on a NP20 array. The metal proteinate sample containing the marker peptides was then spotted onto a CM10 array in preparation for MS/MS analysis. The instrument used was an Applied Biosystems Q-STAR XL with a PCI-1000 interface. For each sample, results were obtained in MS mode 800-2500 Da or 500-1000 Da depending on the size of peptide. The non-enhanced mode feature in the ABI software was used for all peptides.

2.3.5 Premix analysis

A range of animal feed premix samples was analysed using SELDI-ToF-MS to monitor the specific pattern of peaks outlined in Section 3.3.6. As the premix samples contained laboratory manufactured metal proteinates at various concentrations ranging from 1 % to 15 % (w/w) metal inclusion, the presence of the 5 peptides of interest was investigated. Premix samples were diluted in distilled water at an initial concentration of 50 mg/mL. The samples were extracted for 30 minutes and then centrifuged. Aliquots (5 μL) of the supernatant were applied to an IMAC30 array and the protocol used for metal proteinate analysis using SELDI-ToF-MS in Section 2.3.3 was followed.

2.3.6 Feed analysis

The inclusion rate of all premix samples containing metal proteinates "in-feed" was 2.5 mg/g. This value was chosen as it was close to the maximum permitted metal level typically found in finished feed samples (E.U., 2003b). Due to difficulties encountered in detection of the peptide peaks of interest, it was necessary to concentrate the spiked feed samples. This was achieved by lyophilising the sample and resuspending it in a minimum amount of solute prior to spotting on an IMAC30 array.

2.3.7 Synthetic peptide production

Synthetic peptides were created using the selected peptide sequences obtained from tandem mass spectrometry sequencing (Section 2.3.4) by GenScript USA Inc., New Jersey, U.S.A. using FlexPeptide^{TM} . This is an advanced integrated approach based on automated synthesizers for liquid and solid phase peptide synthesis, microwave technologies and proprietary ligation technology.

2.4 Enzyme Linked Immunosorbent Assay (ELISA)

A modification of the method described by Medina was used (Medina, 1988). The methodology for obtaining the standard curve and the sample analysis was identical. Each sample containing antigen (50 µL/well) was added to a 96-well micro-titre plate and the solution was incubated overnight at 4 °C. The micro-titre plate was then emptied and washed three times with 200 µL wash buffer (10 mM sodium phosphate buffer, pH 7.5). Subsequently, 100 µL of blocking solution (2 % skim milk in 10 mM sodium phosphate buffer) was added to each well. The 96-well plate was incubated at room temperature for 1 hour. After blocking the surface to prevent non-specific binding, the plate was washed three times with 200 µL washing buffer as above. Each well was then treated with 100 µL of the primary antibody and the plate was incubated at 37 °C for 1 hour. The plate was washed as before and 50 µL of a secondary antibody (anti-mouse HRP conjugated antibody) in blocking solution (1:500 v/v) was added to the plate prior to incubation at 37 °C for 1 hour. After three additional post-incubation washes, as previously described, 50 µL of substrate (2, 2'-Azino-bis 3-ethylbenzthiazoline-6-sulfonic acid) was added to each well. The reaction was stopped, following incubation at room temperature for 20 minutes, by the addition of stopping reagent (0.5 M oxalic acid, 100 µL) to each well. Optical density was read at 410 nm, using a BioTek Synergy HT micro-titre plate reader (BioTek Instruments Inc., Winooski, Vermont, USA).

2.5 Stability constant determination using potentiometry and ion-selective electrodes (ISE)

Potentiometric titrations were carried out with two Orion pH-meters (precision of 0.1 mV or 0.001 units of pH). One monitored pH using a combination glass electrode and an automatic temperature controller. The second meter was connected to a Jenway copper combination ion selective electrode with a solid-state crystalline membrane and an integral driTEK built-in reference electrode (Barloworld Scientific Ltd., U.K.) and was used for measuring EMF.

Calibration for the Orion glass electrode was accomplished by immersing the electrode in standardised aqueous buffers at pH 4.01 and 7.00 followed by rinsing the electrode with deionised water before and after each series of measurements based on the standard scale of the U.S National Bureau of Standards.

Calibration of the ISE electrode was carried out by immersing the electrode in a series of standard copper(II) solutions with concentrations of 10^{-1} to 10^{-5} M with constant ionic strength of 0.1 M and measuring the observed EMF (mV). The slope of the calibration graph represented the mV response per decade of concentration change. This is typically *ca.* 59.2 mV/decade for monovalent ions and 29.6 for divalent ions (Nagele *et al.*, 1999; Trojanowicz, 2000).

The relationship between the ionic concentration (activity) and the electrode potential is given by the Nernst equation:

$$E = E^o + \left(\frac{2.303\,RT}{nF}\right)\log(a) \qquad (\mathbf{2.4})$$

where E is the total potential (in mV) developed between the sensing and reference electrodes. E^0 is a constant which is characteristic of the particular ISE/reference pair. (It is the sum of all the liquid junction potentials in the electrochemical cell).

2.303 = the conversion factor from natural to base10 logarithm.

R = the Gas Constant (8.314 joules/degree/mole).

T = the Absolute Temperature.

n = the charge on the ion (with sign).

F = the Faraday Constant (96,500 coulombs).
log (a) = the logarithm of the activity of the measured ion.

2.303RT/nF is the slope of the line (from the straight line plot of E versus log (a) which is the basis of ISE calibration plots), an important diagnostic characteristic of the electrode. In general, the slope gradually decreases as the electrode ages or becomes contaminated, and the lower the slope the higher the errors on the sample measurements (Rundle, 2005). Due to reductions of the slope as the electrode degrades, conditioning of the ISE was necessary from time to time. The crystalline surface of the copper(II) ion-selective electrode was gently polished with fine (600 grit) abrasive paper, rinsed with deionised water and soaked in a solution of copper(II) (10 ppm) for 15 minutes until a constant potential value was obtained.

Titrations were performed in a 50 mL commercial double-walled glass vessel. Temperature was maintained inside the cell at 25 ± 0.1 °C by water circulation through the vessel. By addition of the requisite amount of $NaNO_3$ as a supporting electrolyte; the ionic strength of the solutions was maintained at constant level (0.1 M). pH was kept constant at pH 5.5 using carbonate free NaOH (0.01 M). Aliquots (0.5 mL) of a ligand solution were added to a solution of Cu^{2+} ions in the form of copper(II) nitrate hydrate in the titration vessel. Concentrations were such that after 20 additions the M:L ratio in solution was 1:1 and consequently 1:2 after 40 additions. The pH was monitored throughout and aliquots of carbonate free NaOH were added as required to maintain a constant pH. EMF values (mV) were recorded after each metal and base addition. The results were input into Microsoft Office Excel© and, using a batch import function, imported to Hyperquad for subsequent data analysis.

The Hyperquad suite of computational programs (Gans *et al.*, 1996) was used in this work for potentiometric data analysis. The 2008 version of the software has some significant improvements over earlier versions including the manner in which the mass-balance equations are solved. The parameters to refine are the logarithms of the free concentrations and not the actual free concentrations. The convergence criteria are also different and another difference is that the table of concentrations is available at any time, not just after refinement. Further adaptations to the Hyperquad software were

required to suit experimental procedures used in this work with the inclusion of a batch data import file for EMF data and the option to calculate the apparent stability constants at a constant pH. Data relevant to the chemical model including the names of the reagents, the equilibrium constants defined by initial value and stoichiometric coefficients, keys to indicate refineable quantities and whether or not a species absorbs light are input in the Model file. The titration conditions and all titration data such as the total amounts (mmol), burette concentrations, volumes added and EMF values are added to the Potentiometric data file. Tables of calculated values and concentrations can also be viewed in the Hyperquad program.

3. Results and Discussion

3.1 Assessment of potential protein sources for metal proteinate production

The initial focus of this work was the determination of a suitable protein source from which metal proteinates could be produced and subsequently analysed. According to the AAFCO definitions for organic mineral complexes (Table 1.4, Section 1.5), a metal proteinate is the product resulting from the chelation of a soluble salt with amino acids and/or partially hydrolysed protein. Wide variability exists between products in the marketplace so the ability to produce an effective proteinate which is characterised in detail is highly desirable. Furthermore, the ability to compare and contrast products enables informed decisions to be made regarding the most suitable proteinate for use as a nutritional supplement.

Requirements for an effective proteinate include the ability to chelate a metal enabling effective absorption in the animal and increased metal status. Successful chelation of a metal is highly dependent on the ligand and it is generally accepted that amino acids and peptides are most suitable (Ashmead *et al.*, 1989). The advantages of using organic ligands in place of inorganic ligands have been described previously (Sections 1.3 and 1.4). In the present work, protein sources were partially hydrolysed to produce a mixture of polypeptides, peptides and amino acids prior to reacting with a metal salt to form a proteinate. The protein sources assessed were soy flour, whey, skim milk, corn steep liquor and casein. From an industrial perspective, there were a number of points to consider such as ligand suitability, cost and ease of use. Hydrolysis of a protein source is necessary as large proteins can hinder metal binding due to steric hindrances and shielding, thereby reducing chelation potential. Additionally, large unhydrolysed proteins can be poorly absorbed or utilised in the body and have poor solubility. There are distinct advantages to having a mix of ligands such as those produced by hydrolysis instead of just one. For example, the potential for a wide range of metal-ligand interactions is increased which is beneficial from a nutritional perspective. Costs can vary considerably between protein sources and it is necessary to

select one that is economically viable in addition to one which produces a suitable mix of ligands for metal binding. In a 1:2, M:L chelate, the metal ion is bonded to both the amino and carboxyl moieties of the amino acid in such a way as to form two 5 membered rings as shown in Figure 3.1.

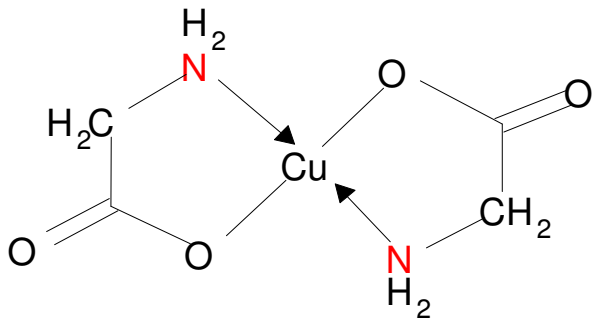

Figure 3.1 Schematic diagram of a 1:2, copper:glycine chelate

As previously outlined in Sections 1.4 and 1.5, binding can occur via oxygen, nitrogen or sulphur atoms acting as electron donors either by replacement of hydrogen ions or by coordination (Wolf, 1986). The formation of metal-ligand complexes is often highly dependent on the pH of the solution. This is because there is a competition for the ligand between the metal ion and a proton as they both bind to the same atoms of the ligand. Anions of carboxylic acids are completely protonated below a pH of approximately 4 and a metal can combine only by displacing a proton (Metzler *et al.*, 2001). At higher pH there is less competition from protons although this is highly ligand dependent (e.g. in the case of ethylenediamine, whose pK_a values are 10.2 and 7.5, protons are very strong competitors at pH 7, even with a strongly complexing metal such as Cu^{2+}). At high pH there may be competition between the ligand and the hydroxyl ion (Metzler *et al.*, 2001).

To determine the most suitable protein source, analysis of the nitrogen content of the five aforementioned protein sources was carried out (Section 3.1.1). A nitrogen:metal ratio of 2:1 was selected as a guideline for choosing the protein source based on chelation potential. The nitrogen:metal ratio can only serve as a guideline due to the fact that other groups such as those containing sulphur or oxygen may also be involved. From an industrial perspective it was also necessary to take into account financial considerations.

3.1.1 Total nitrogen analysis of protein sources

Nitrogen is an indicator of the presence of protein or amino acids, and the Kjeldahl method was employed to determine the total nitrogen content in the five protein sources selected for examination. Total nitrogen is the sum of that derived from amino acids (the vast majority), and that from non-protein nitrogen (NPN) sources (generally minor in quantity), existing in the foodstuff (EDA, 2005). The total nitrogen derived from the analysis is converted into total protein by multiplying by a factor that takes into account the nitrogen content of a known or average amino acid composition (approximately 16 %). An E.U. directive recommended two conversion factors depending on the type of protein. For milk proteins, nitrogen content x 6.38 was suggested (E.U., 1991). For soy protein isolates, nitrogen content x 6.25 was used. It can be seen from Table 3.1 that whey and skim milk can be eliminated as potential ligand sources due to their low protein (11.9 & 33.2) and nitrogen (1.9 & 5.2) contents. Sources with low protein content would provide less polypeptides, peptides and amino acids for potential chelation post hydrolysis.

Table 3.1 Total nitrogen and crude protein content determined using the Kjeldahl method

Sample ID	Total Nitrogen (%)	Crude Protein (%)
Soy flour	8.3	51.9
Whey	1.9	11.9
Skim milk	5.2	33.2
Casein	13.6	86.8
Corn steep liquor	7.8	48.8

Financial considerations are important from an industrial perspective and casein was eliminated due to high cost and supply issues. Viscosity issues were encountered with corn steep liquor which made it difficult to work with. Consequently, corn steep liquor was not selected for further analysis. The ready availability and low cost of soy flour contributed to the decision to focus on soy flour as the protein source for the remainder of this work. In addition to being the most suitable based on total nitrogen

analysis and cost considerations, soy flour is also the ligand source most commonly used by manufacturers of feed additives in the European Union (Hard, 2002). Furthermore, a high nitrogen:crude protein ratio is important to generate chelates having mineral levels that are economically feasible. There is little reason to produce a chelate with low percentage metal as the physical quantity needed for inclusion in a premix or feed sample would be too high.

3.1.2 Hydrolysis of protein sources

Catabolism of peptide bonds that link amino acids together in a polypeptide chain is achieved by use of a protease enzyme (Figure 3.2). The peptide fragments are then available to chelate to the desired metal forming a metal complex.

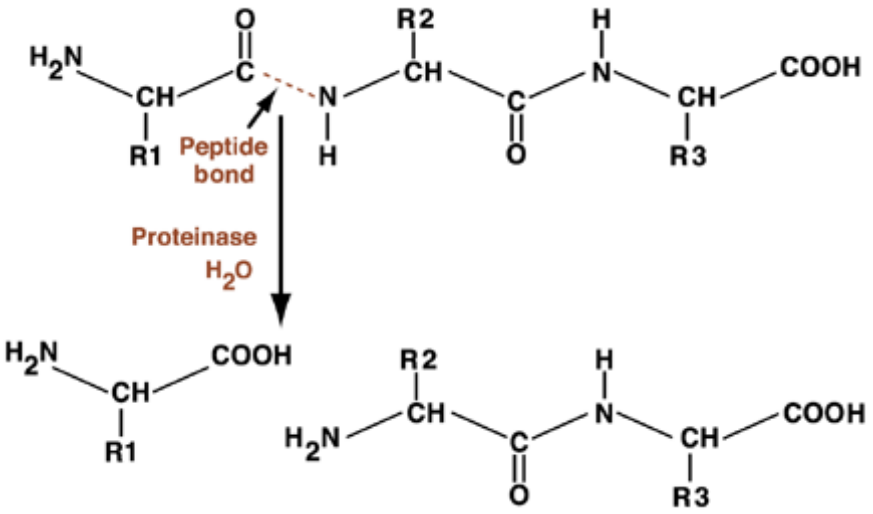

Figure 3.2 Proteolysis of peptide linkage

An effective hydrolysis procedure which provides amino acids and small polypeptides suitable for metal binding is of paramount importance to manufacturing an effective metal proteinate. From an industrial perspective, alkaline proteases are most commonly used for hydrolysis (Murphy, 2005) and a serine protease from a strain of *Bacillus licheniformis*, was selected for initial hydrolysis investigations in this work.

Proteases belong to the class of enzymes known as hydrolases, which catalyse the hydrolysis of various bonds with the participation of a water molecule. They can be subdivided into two major groups; exopeptidases and endopeptidases, depending on their sites of action. Exopeptidases cleave the peptide bond proximal to the amino or carboxy termini of the substrate, whereas endopeptidases cleave peptide bonds distant form the termini of the substrate (Rao *et al.*, 1998). Within these groups there are various subclasses of proteases including serine proteases, cysteine proteases, aspartate proteases and metalloproteases. Serine proteases utilise an active site serine residue in a covalent catalytic cleavage of peptide bonds. Trypsin, which cleaves lysine and arginine residues, and chymotrypsin, which cleaves aromatic amino acids such as tryptophan, tyrosine and phenylalanine, are members of this subclass (Kies, 1981). Cysteine proteases include bromelain and papain. Aspartate proteases include pepsin, which is optimally active at acidic pH. Metalloproteases are characterised by the requirement for a divalent metal ion for their activity and they include enzymes from a wide variety of origins such as collagenases from higher organisms, hemorrhagic toxins from snake venoms, and thermolysin from bacteria (Rao *et al.*, 1998).

The performance of all enzymes is dependent on pH and temperature, and optimum conditions are normally within quite a narrow range. Generally, an enzyme will be examined under a range of pH, temperature and concentration conditions to determine the values at which the enzyme is most effective. Based on manufacturer recommendations for the serine protease selected for this work, hydrolysis was initially carried out at 55 °C and pH 8.5. However, additional research involving pH, temperature and enzyme concentration changes was carried out to determine if the hydrolysis procedure could be optimised further. Free amino nitrogen (FAN) measurement was employed as an indicator of reaction efficiency (Section 3.1.3). To determine FAN, a ninhydrin assay was employed. This is a colorimetric assay and the method is dependent on the reaction between free α-amino groups ($-NH_2$) and ninhydrin (2,2-dihydroly-1,3-indanedione) solution which forms a purple-coloured product. Although ninhydrin reacts with the α-amino group, which is contained in all amino acids, peptides and proteins, the decarboxylation reaction - an essential part of the reaction, only occurs for free amino acids and not for peptides and proteins (Sun Wang,

2007). Limitations of this method include the inability of the assay to differentiate between other forms of FAN such as ammonium ions and short chain peptides (dipeptides and tripeptides) (Abernathy *et al.*, 2009). Essentially, the ninhydrin method does not give an entirely accurate estimation of true FAN but gives a good indication of the presence of amino acids and thus hydrolysis potential in the samples. Another limitation of the method is that it does not react with tertiary or aromatic amines which results in the underestimation of the total amino acid composition of a sample that contains high levels of amino acids that possess aromatic groups (Sun Wang, 2007; Abernathy *et al.*, 2009). Notwithstanding the limitations of the ninhydrin assay, it is the official method of the European Brewery Convention and is acknowledged as being a rapid, inexpensive method which is applicable to a large number of samples (Abernathy *et al.*, 2009).

Upon enzyme addition to the protein source, the protease enzyme cleaves peptide bonds resulting in the formation of free amino groups and therefore an increase in the levels of free amino nitrogen. The cleavage of these peptides into amino acids lowers the pH of the solution due to the ionisation of carboxylic groups which result from each cleaved peptide bond liberating a proton. The decrease in pH was expected due to the low pK_a values of the –COOH groups. Due to the bond cleavage, it was essential to monitor the pH and maintain it between 8.5 and 9.0 in order for the alkaline enzyme to continue proteolysis at optimum capacity according to manufacturer specifications.

3.1.3 Optimisation of hydrolysis parameters

As a complimentary technique to the total nitrogen analysis (Section 3.1.1), free α-amino nitrogen (FAN) analysis (Figure 3.3) was carried out on the five protein sources selected for assessment prior to, and after the hydrolysis procedure outlined in Section 2.2.1, to determine the amount of α-amino nitrogen present after enzymatic hydrolysis using the serine protease. This method was also employed to determine the effect of adjusting pH, temperature and enzyme concentration on the hydrolysis.

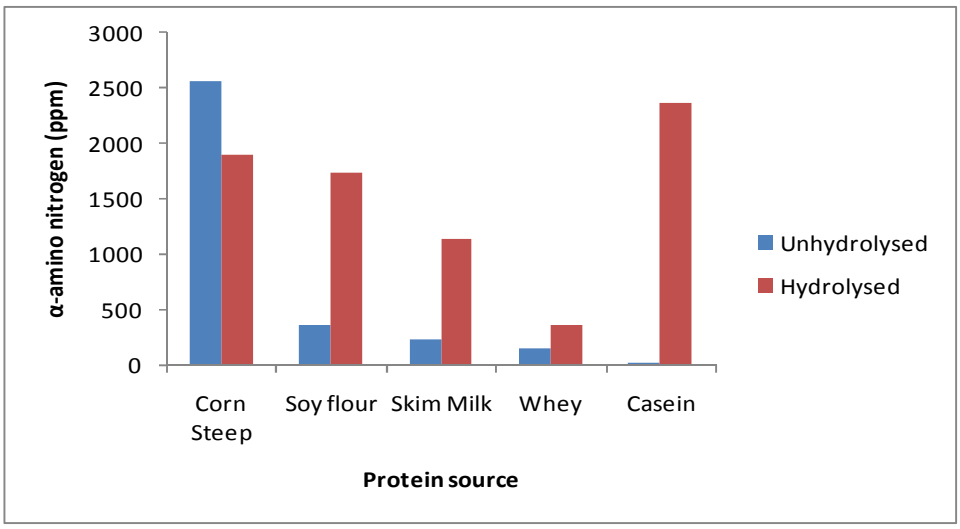

Figure 3.3 Free α-amino nitrogen (ppm) before and after hydrolysis

Based on costing considerations and ease of use, soy flour was chosen as the protein source for this work. The results in Figure 3.3 show an increase in free α-amino nitrogen for four of the five protein sources after enzymatic hydrolysis. From the total protein results outlined in Table 3.1, the low FAN values for skim milk and whey were expected based on their low total protein content. Over four times as much FAN was detected in soy flour after enzymatic hydrolysis indicating multiple cleavage recognition sites in this protein source. Casein and corn steep also produced high FAN values but were not selected due to previously highlighted issues such as cost and viscosity. Hydrolysis parameters based on manufacturer recommendations for the serine protease were initially utilised to produce the hydrolysate from which the metal proteinate was formed (pH 8.5 and 55 °C). Research was carried out to determine if adjustments to the manufacturer recommended pH, temperature and experiment duration could increase FAN release or be used on a cost beneficial basis in an industrial setting. Shorter experimental time, lower pH and temperature conditions, with minimal effect on FAN release, could reduce production costs considerably. Protein sources with high protein and consequently high nitrogen content have the potential to release significant quantities of FAN under optimised conditions. Consequently, such sources can minimise the enzyme concentration requirement while still producing high FAN values, thereby reducing production costs further with no detrimental effect on the quality of the hydrolysate.

3.1.3.1 Optimisation of hydrolysis temperature

The effect of temperature on FAN release for the serine protease was monitored over a range of 40 °C to 60 °C and the results described in Figure 3.4 confirm the highest FAN release was observed at a temperature of 55 °C. Enzyme concentration and pH values were maintained at levels recommended by the manufacturer (pH 8.5 and 0.42 % v/v). It was observed that decreasing the temperature to 40 °C resulted in a 17 % reduction in the final FAN level (Table 3.2). In deference to this and with respect to the speed of the hydrolysis, there is a distinct benefit with regard to using an increased temperature in that a higher level of FAN release occurs in a shorter time. After 150 minutes at 55 °C, similar amounts of FAN were released as those observed at 40 °C after 360 minutes. It should also be noted that at 55 °C for instance, extending the hydrolysis beyond 180 minutes to 360 minutes only yields an additional 14 % increase in FAN.

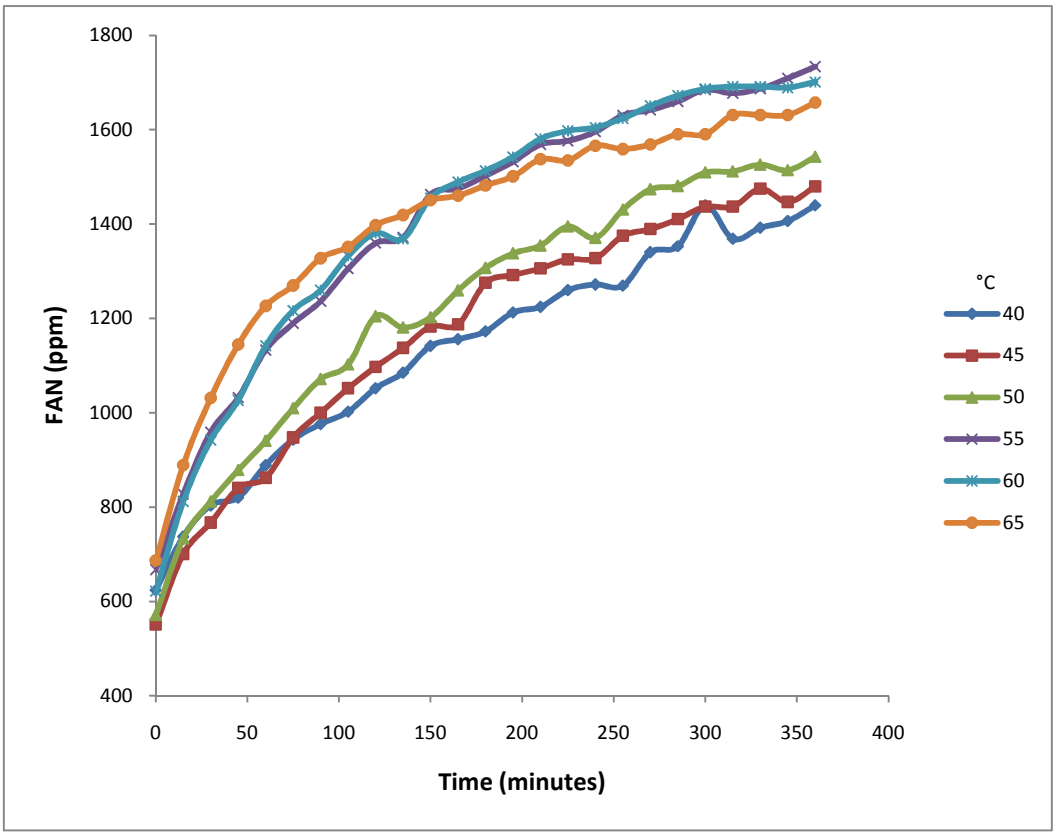

Figure 3.4 Effect of temperature adjustment on FAN release from soy flour. Hydrolysis conditions included used of a serine protease (0.42 % v/v) and pH 8.5.

Table 3.2 End-point FAN level with varying hydrolysis temperatures

Temperature (°C)	FAN (ppm)*
40	1440 ± 13[a]
45	1479 ± 8[a]
50	1543 ± 3[a]
55	1734 ± 17[c]
60	1702 ± 12[b]
65	1658 ± 3[b]

*n = 3, mean ± standard deviation
a = $p \leq 0.05$, b = $p > 0.05$, c = control conditions

Statistical analysis using Minitab version 15 (Minitab, Coventry, U.K.) with control conditions of 55 °C, pH 7 and 100 % enzyme concentration (0.42 % v/v), indicated significant differences were observed at temperature values of 40 °C, 45 °C and 50 °C with p values ≤ 0.05. At temperatures of 60 °C and 65 °C the differences were not statistically significant.

Surface-Enhanced-Laser-Desorption/Ionisation-Time-of-Flight-Mass-Spectrometry (SELDI-ToF-MS) was employed to assess the peptide patterns produced during the temperature profiling experiments (Figure 3.5). This mass spectrometry technique is described in detail in Section 3.3.6 and was applied to a range of proteinate samples to aid with characterisation. As can be appreciated from the mass spectral analysis, consistent peptide patterns were obtained for all hydrolysates. The consistency in the peptide profiles was expected as the same enzyme was used in all cases resulting in cleavage of the same bonds. Minor peak and intensity deviations are observed at differing temperatures but as the SELDI-ToF-MS technique is not fully quantitative no definitive conclusion can be drawn from these differences.

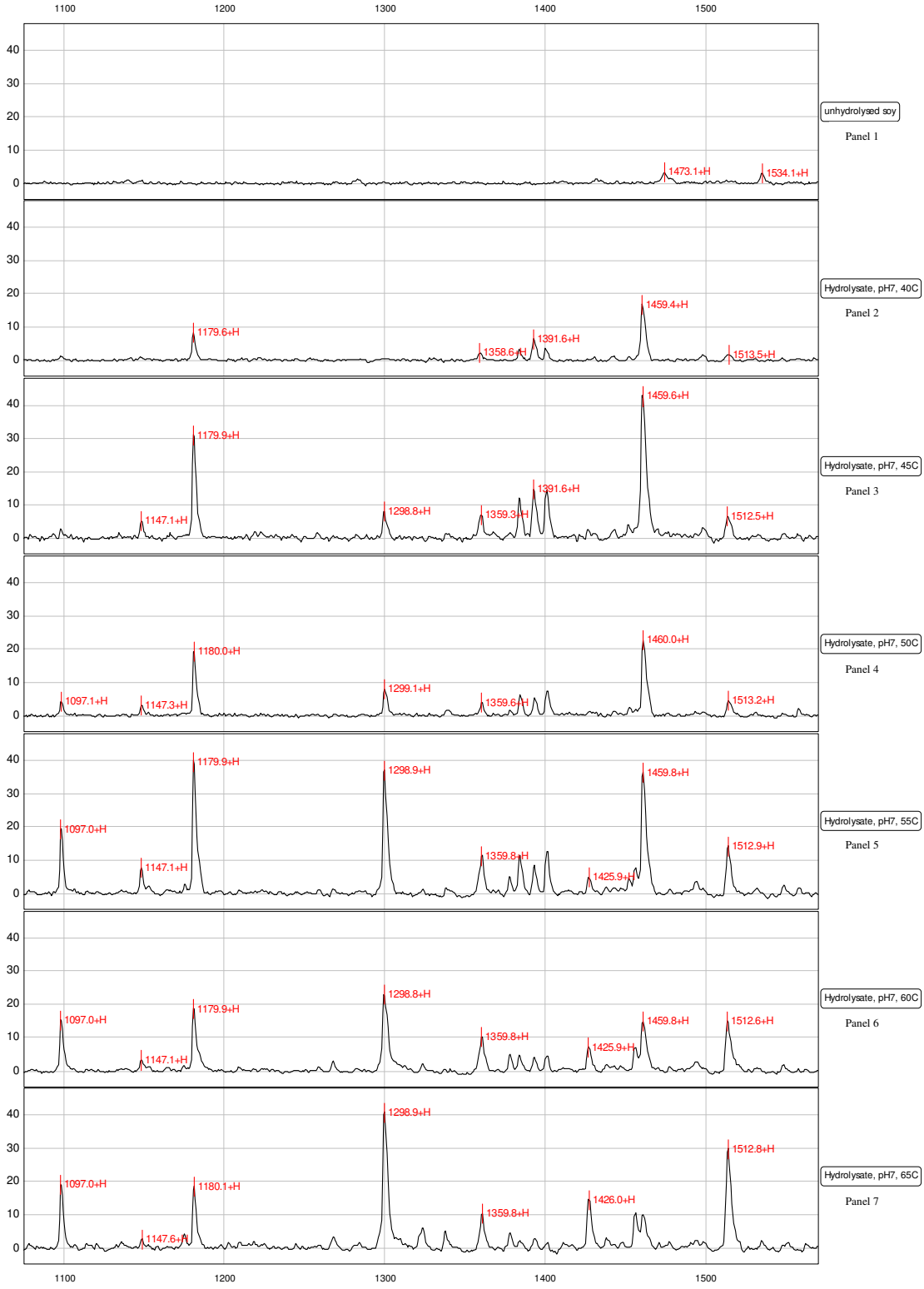

Figure 3.5 Assessment of thermal effects on enzymatic hydrolysates using SELDI-ToF-MS. The molecular mass (Da) of the peptides is displayed on the x-axis and the mass-to-charge ratio (m\z) is shown on the y-axis.

3.1.3.2 Optimisation of hydrolysis pH

Following on from the results obtained from temperature optimisation, which found the optimum temperature for FAN release to be 55 °C, a pH optimisation step was carried out. According to manufacturer recommendations, the expected optimal pH range for the alkaline protease is between pH 7 and 9 and the results described in Figure 3.6 confirm this is indeed the case. Examination of the enzymatic profile of the serine protease suggested complete inactivation of the enzyme occurred at pH 11.

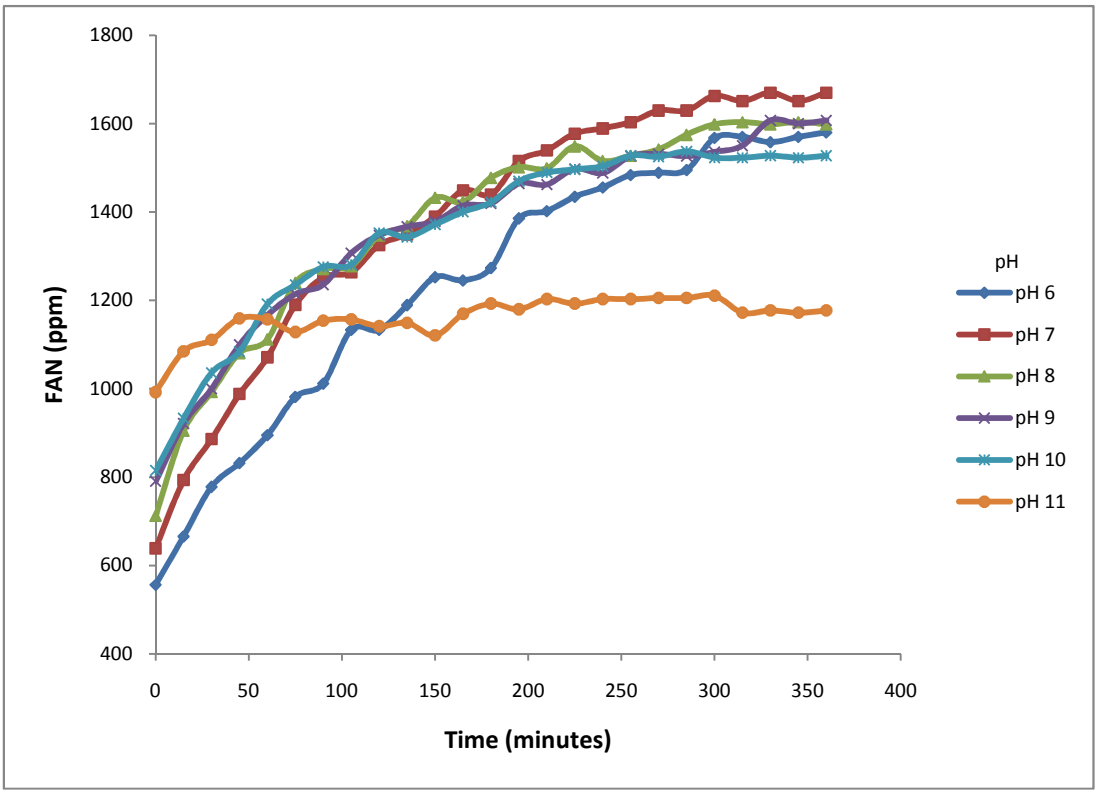

Figure 3.6 Effect of pH adjustment on FAN release from soy flour. Hydrolysis conditions included used of a serine protease (0.42 % v/v) and a temperature of 55 °C.

Maintaining the hydrolysis at pH 7 appeared optimal for FAN release at 55 °C. However on closer examination it can be seen that decreasing the pH to 6 would only reduce final FAN levels by 13 % (Table 3.3). Similar to the results observed in the thermal profiling experiment, the speed of the hydrolysis is a factor and there appears to be a distinct benefit with regard to using a higher pH. After 225 minutes at pH 7, FAN

release observed is similar to that seen after 360 minutes at pH 6. Extending the hydrolysis at pH 7 from 180 minutes to 360 minutes only yields an additional 14 % increase in FAN. A pH of 7 was selected for the remaining hydrolysis experiments as it produced the highest FAN release.

Table 3.3 End-point FAN level with varying hydrolysis pH values

pH	FAN (ppm)*
6	1458 ± 21^{a}
7	1669 ± 25^{c}
8	1599 ± 10^{b}
9	1607 ± 12^{b}
10	1524 ± 12^{a}
11	1093 ± 7^{a}

*n = 3, mean ± standard deviation
a = $p \leq 0.05$, b = $p > 0.05$, c = control conditions

Statistical analysis (Minitab, Coventry, U.K.) with control conditions of 55 °C, pH 7 and 100 % enzyme concentration (0.42 % v/v) indicated significant differences were observed at pH values of 6, 10 and 11 with p values ≤ 0.05 but not at pH 8 or 9.

3.1.3.3 Optimisation of enzyme concentration

Research was also carried out to determine the effect of reducing the enzyme concentration in the hydrolysate from an initial concentration of 0.42 % (v/v), using pH 7 and 55 °C as standard reaction conditions (Figure 3.7). The initial concentration of 0.42 % (v/v) was chosen based on manufacturer recommendations for the serine enzyme. It was discovered that a 20 % reduction in enzyme concentration would have a negligible effect on the hydrolysis in terms of FAN liberation (Table 3.4). Furthermore, reducing the enzyme concentration by 60 % would merely result in an 11 % decrease in final FAN levels. Consistent with results obtained for the thermal and pH profiling experiments, a distinct benefit with respect to the speed of the hydrolysis was observed.

Extending the reaction time from 180 minutes to 360 minutes at maximum enzyme concentration inclusion only resulted in a 14 % increase in FAN.

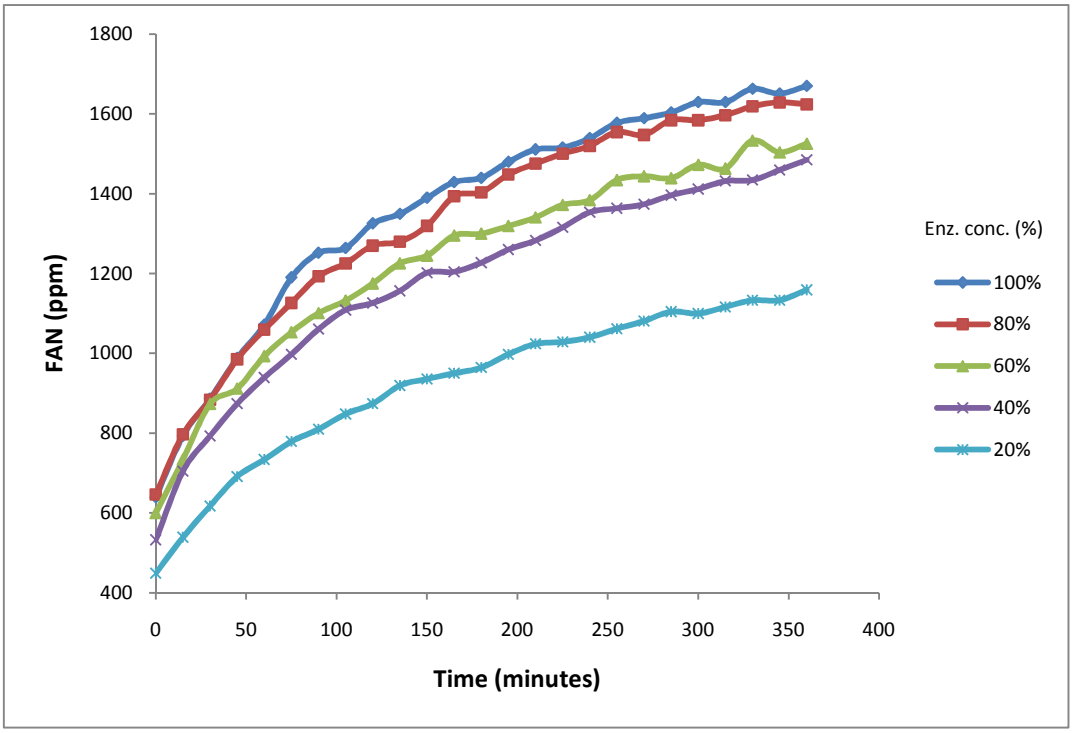

Figure 3.7 Effect of adjusting enzyme concentration on FAN release from soy flour. Hydrolysis conditions included used of a serine protease, pH 7 and a temperature of 55 °C.

Table 3.4 End-point FAN level with varying enzyme concentrations

Enzyme concentration (%)	FAN (ppm)*
100	1669 ± 25^{c}
80	1625 ± 5^{b}
60	1526 ± 8^{a}
40	1485 ± 14^{a}
20	1159 ± 1^{a}

*n = 3, mean ± standard deviation
a = $p \leq 0.05$, b = $p > 0.05$, c = control conditions

Statistical analysis (Minitab, Coventry, U.K.) with control conditions of 55 °C, pH 7 and 100 % enzyme concentration (0.42 % v/v) indicated significant differences

were observed at when the enzyme concentration was less than 80 %, i.e. at 60 %, 40 % and 20 % enzyme concentration had p values ≤ 0.05.

Surface-Enhanced-Laser-Desorption/Ionisation-Time-of-Flight-Mass-Spectrometry (SELDI-ToF-MS) was again employed to analyse the peptide profiles obtained with reduced enzyme concentrations. As can be seen from the panels in Figure 3.8, no significant effects were noted with respect to the peptide profiles observed. A decrease in peptide intensities was observed as the enzyme concentration was reduced but the peptide patterns remained consistent. The fact that the peptide profiles remain consistent even when hydrolysis parameters are adjusted allows potential cost saving changes to be made to the hydrolysis procedure without affecting the peptide profiles. Further work on the peptide profiles obtained using mass spectrometry is outlined in Section 3.3.6.

Similar trends were observed for all three profiling experiments (temperature, pH and enzyme concentration). The concentration of α-amino nitrogen in the hydrolysate reached close to a maximum value after 5 hours and appeared to plateau off by this time. Additional increases were negligible in comparison to the dramatic increase in FAN at the beginning of the hydrolysis procedure. The plots in Figures 3.4, 3.6 and 3.7 indicate that protein hydrolysis proceeded very rapidly during the first hour of the process in comparison to later in the hydrolysis. If an average value of 1700 mg/kg is taken as the total amount of α-amino nitrogen produced overall during hydrolysis, it can be seen that over 50 % (850 mg/kg) was present after the first hour. This correlated with the observation of a high requirement of base (4 M NaOH) during this initial stage of the process to maintain a constant pH value in the reaction mixture. Cleavage of peptide bonds would have lowered the pH of the hydrolysate and most of the bond cleavage would have occurred quite rapidly at the start of the hydrolysis procedure. Furthermore, a significant increase in α-amino nitrogen was expected due to the release of peptides and free amino acids during the protein hydrolysis caused by cleavage of peptide bonds resulting in an increase in free amino groups. It was also observed that the relationship between the increase in FAN and levels of enzyme addition were not directly proportional. When economic considerations are borne in mind, it is clear that significant cost savings on an industrial basis are feasible in terms

of optimising the various hydrolysis parameters. Specifically, changes could be made in terms of the duration of the hydrolysis, the volume of enzyme required, the pH and also the temperature at which the reaction is carried out.

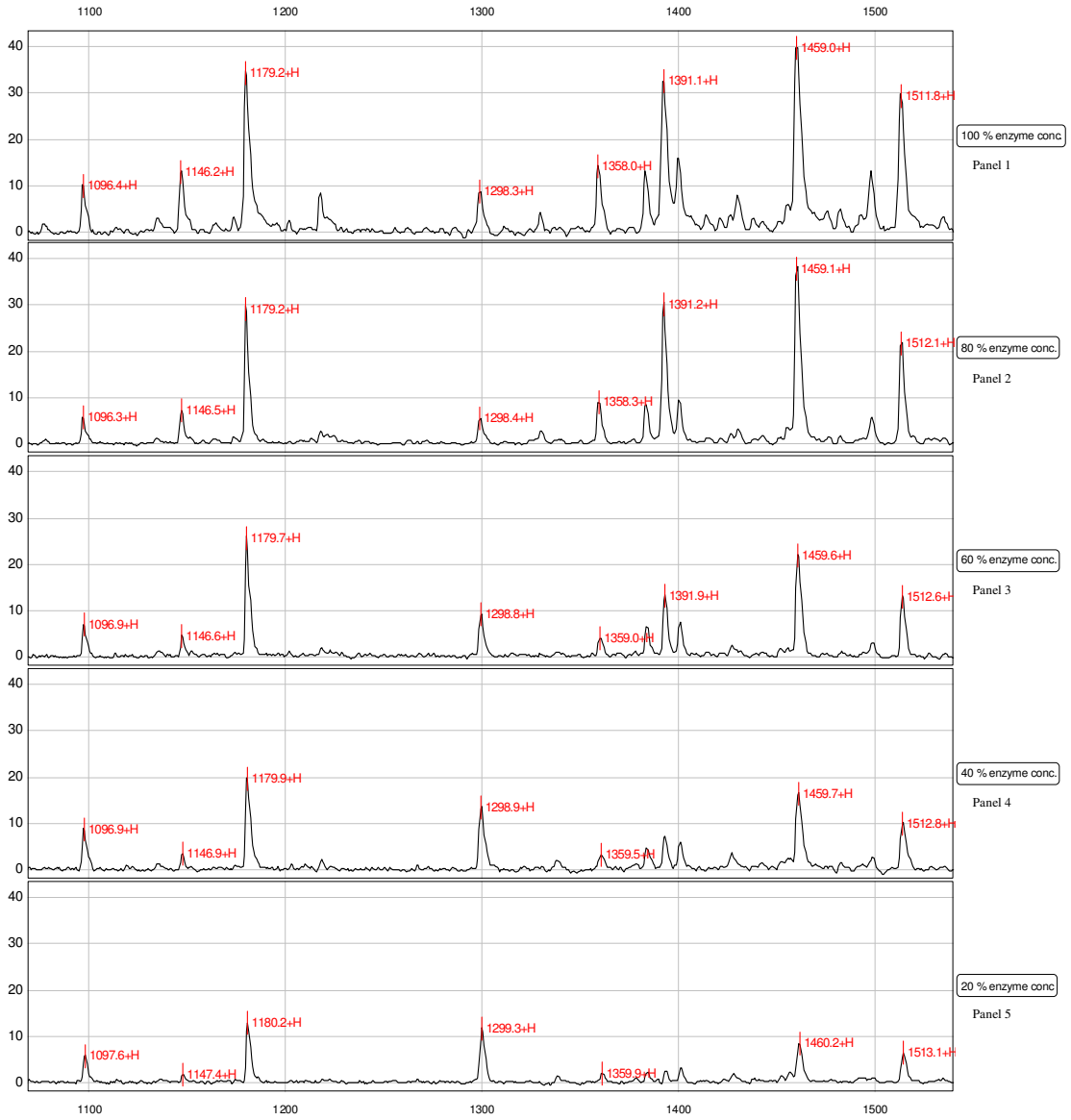

Figure 3.8 Assessment of the effect of varying enzyme concentration on soy hydrolysates using SELDI-ToF-MS (100 % enzyme conc. refers to an enzyme inclusion level of 0.42 % (v/v), 80 % to 0.33 % (v/v), 60 % to 0.25 % (v/v), 40 % to 0.17 % (v/v) and 20 % enzyme conc. refers to an enzyme inclusion level of 0.08 % (v/v) or 0.5 mL of enzyme in 600 mL hydrolysate). The molecular mass (Da) of the peptides is displayed on the x-axis and the mass-to-charge ratio (m\z) is shown on the y-axis.

3.2 Metal proteinate production

Production of metal proteinates is achieved by adding a metal salt to a hydrolysed protein source and neutralising the protons released under appropriate conditions as described in Section 3.2.1. The transition metals Cu, Fe, Mn and Zn were selected as the metal sources due to their nutritional importance as previously detailed (Section 1.2). In order to ensure optimum chelation conditions are present for metal proteinate formation, protons liberated on coordination of the metal ion must be neutralised by addition of base. The pH must be adjusted to a point that is sufficiently basic to remove interfering protons from solution which allows the heterocyclic rings to form from covalent bonds between the positive metal ions and the lone pairs of electrons on the carboxyl and amine groups. Although not a prerequisite, removing such protons can increase chelation potential. Simple mixing of hydrolysates with water in the presence of a metal salt will not result in a chelate or proteinate because the protons on the carboxyl and amine groups can interfere with chelate formation (Ashmead, 1980a).

3.2.1 Formation of metal proteinates

The transition metals selected for analysis were copper (Cu), iron (Fe), manganese (Mn) and zinc (Zn). Hydrolysis of soy flour was carried out as previously described (Section 2.2.1). At this stage, the resultant proteinate formed was separated into two identical aliquots (A and B). The relevant quantity of metal salt was added to each of the aliquots to achieve a 10 % (w/w) metal content (Section 2.2.2). The viscosity of the hydrolysate was visually monitored throughout the experiment but little change was noted over the course of the hydrolysis. However, on addition of the metal to the hydrolysate, the change in viscosity was significant and constant stirring over a 30 minute time period was required to reduce the viscosity and obtain a homogeneous solution. The pH of proteinate A was noted (Table 3.5) and the sample was subsequently lyophilised. The pH of proteinate B was adjusted to 7.0 prior to lyophilisation to determine the effect of adjusting the pH on proteinate formation. As previously mentioned, neutralising the

protons liberated on coordination of the metal may increase chelation potential. Precipitation of the metal was not visually observed when the pH was increased to 7.0.

Table 3.5 Observed pH of proteinates prior to lyophilisation

Aliquot	Cu(II) proteinate	Fe(II) proteinate	Mn(II) proteinate	Zn(II) proteinate
A (unadjusted)	3.34	5.84	6.87	5.24
B (adjusted)	7.00	7.00	7.00	7.00

The magnitude of the pH drop upon addition of metals of the first transition series follows the order Mn < Fe < Co < Ni << Cu > Zn (< pH 7.5) (Khanna *et al.*, 1962) and similar results were observed in this work. Although first established by Mellor and Maley, the series has become known as the Irving-Williams stability series (Khanna *et al*., 1962*).*

The colour of the hydrolysate was observed to be pale yellow. Addition of manganese or zinc salts did not affect the colour significantly, but significant colour changes were observed with copper and iron. The addition of iron produced a proteinate that was brown in colour, and copper inclusion turned the solution green. For the proteinate B samples, the effect of increasing the pH to 7.0 did not change the colour significantly in iron, zinc or manganese proteinates but the copper proteinate B turned from green to blue (Figure 3.9). At various pH values unique bonding mechanisms occur and different complexes are formed. Most transition metal ions form complex ions with water molecules when in aqueous solution. However, water is not a particularly strong ligand and such complexes are prone to substitution reactions in which the water molecules are successively replaced with other ligands. Such reactions are often accompanied by a change in the colour of the solution. For example, the blue-green $[Cu(H_2O)_6]^{2+}$ ion is formed when many copper(II) salts are dissolved in water. Upon the addition of concentrated NH_3 however, the colour changes to dark blue as the tetraaminediaquacopper(II) complex (known as Schweizers reagent) is formed at high pH.

$$[Cu(H_2O)_6]^{2+} + 4NH_3 \rightleftharpoons [Cu(NH_3)_4(H_2O)_2]^{2+} + 4H_2O \qquad (\mathbf{3.1})$$

The lyophilised samples were ground into a fine homogeneous powder using a pestle and mortar prior to analysis. Further batches of each of the metal proteinates were produced and analysed to determine consistency between batches.

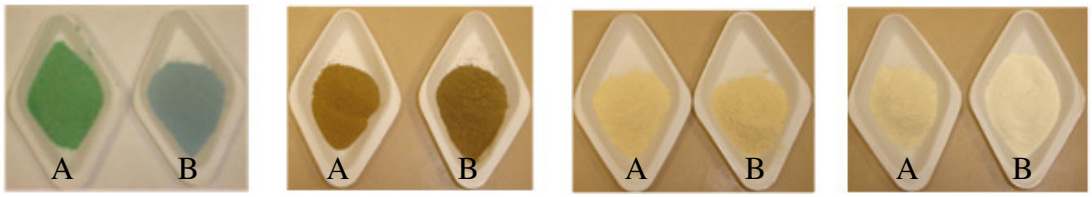

Cu proteinates Fe proteinates Mn proteinates Zn proteinates

Figure 3.9 Colour comparisons of copper, iron, manganese and zinc proteinates. A refers to proteinates without pH adjustment and B refers to proteinates with pH adjusted to 7.0

3.3 Metal proteinate characterisation

The lyophilised metal proteinates were subsequently analysed using a range of techniques including free α-amino nitrogen analysis (FAN), Flame Atomic Absorption Spectrometry (FAAS), carbon, hydrogen and nitrogen (CHN) analysis, Fourier Transform Infrared (FTIR) spectroscopy, Surface-Enhanced Laser Desorption/Ionisation Time-of-Flight Mass Spectrometry (SELDI-ToF-MS), amino acid profiling and potentiometric titrations using an ion-selective electrode (ISE).

Analysis of FAN values can determine the amount of α-amino nitrogen present before and after hydrolysis and can serve as a guideline for chelation potential. Flame AAS allows for the determination of the metal content in the proteinates and CHN analysis gives an accurate indication of the percentage of carbon, hydrogen and nitrogen in the samples which can also be a useful indication of chelation potential. One potential drawback of this technique is the very small sample size (< 10 mg) used for analysis. For samples with non-uniform particle size this can be an issue.

Band shifts in FTIR spectra in relation to groups such as N-H and C=O (< 3000 cm^{-1} and 1700 cm^{-1} – 1500 cm^{-1} region) can be indicative of complex formation as these groups are known to be involved. Further band shifts in the fingerprint region (~ 1600 –

500 cm^{-1}) allude to complex formation when compared to control samples. SELDI-ToF-MS can be used to analyse peptide profiles for consistency between metal proteinate batches and identify new peptide peaks on complex formation which may be peptide-metal adducts indicative of chelation which is important from an industrial standpoint. Amino acid profiling outlines the amino acids present in the sample and their percentage abundance. Potentiometry can provide information on the stability of the proteinates over a wide pH range and can be used to determine stability constants in some cases.

The importance of metal proteinates as nutritional supplements in the feed industry has previously been outlined (Section 1.1), and effective characterisation methods such as those described in this section are of significant importance to aid product development and assessment in addition to providing means of comparing and contrasting products. Furthermore, from a regulatory standpoint, the methods used in this section provide an acceptable level of detail to satisfy legal requirements.

3.3.1 FAN analysis of metal proteinates

Copper, iron, manganese and zinc proteinates were analysed for free amino nitrogen using the protocol outlined in Section 2.2.4. Unhydrolysed soy flour was analysed as a control and a hydrolysed soy flour sample was also analysed. Based on the results obtained in Figure 3.10, a 2.5 fold increase in free amino nitrogen was observed in the hydrolysed soy sample when compared to the unhydrolysed sample. This was expected due to the cleavage of peptide bonds which increased the number of amino acids and short polypeptides present in the hydrolysate.

Increased FAN was also observed in the proteinates in comparison to the unhydrolysed soy control, although FAN values were not as high as those obtained from analysis of hydrolysed soy flour. As free amino acids are involved in metal-ligand complex formation, this reduction of approximately 491 ppm (32 % of total) in FAN between the hydrolysate and the highest mineral proteinate value is of significance as it may be explained by peptide-metal bond formation. The reduction was also due in part to dilution following the addition of the metal salt to the hydrolysate but the expected reduction based solely on dilution effects was only approximately 152 ppm (10 %).

Previous research found the metal itself did not interfere with the FAN assay (Connolly, 2009).

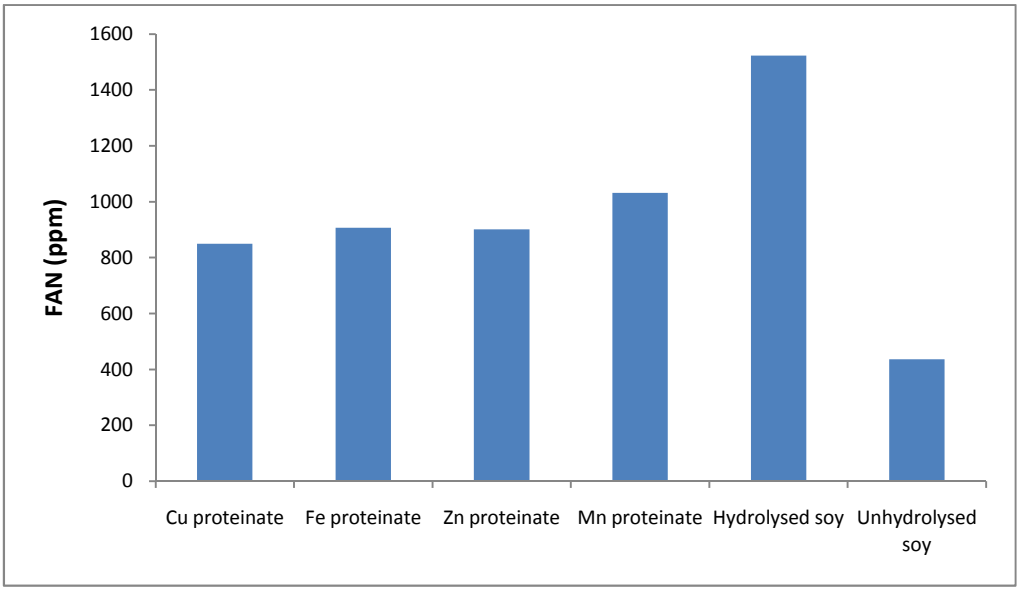

Figure 3.10 Free α-amino nitrogen analyses of metal proteinates

3.3.2 Determination of total metal content using flame Atomic Absorption Spectrometry

Flame Atomic Absorption Spectrometry (FAAS) was employed to assess the percentage metal content in the proteinate samples. Based on the percentage metal salt added to the hydrolysates, the calculated metal content of the proteinates was 10.18 % (w/w). Flame Atomic Absorption Spectrometry confirmed the metal content in all cases was within an acceptable range (± 3 %) of the theoretically calculated value (Table 3.6).

The consistency of the metal content between batches can also be investigated using this technique and based on the results obtained in Table 3.6 it can be concluded that variation between batches is quite low.

Table 3.6 Assessment of proteinate total metal content

Sample ID	Metal content (% w/w)
Cu proteinate 1	10.19 ± 0.01
Cu proteinate 2	10.23 ± 0.04
Cu proteinate 3	10.20 ± 0.01
Fe proteinate 1	10.14 ± 0.03
Fe proteinate 2	10.06 ± 0.08
Fe proteinate 3	10.15 ± 0.02
Mn proteinate 1	10.16 ± 0.01
Mn proteinate 2	10.19 ± 0.01
Mn proteinate 3	10.23 ± 0.04
Zn proteinate 1	10.33 ± 0.11
Zn proteinate 2	10.22 ± 0.03
Zn proteinate 3	10.20 ± 0.01

*n = 3, mean ± standard deviation

3.3.3 CHN analysis

Carbon, hydrogen and nitrogen analyses were performed as described in Section 2.2.5 and the results are presented in Table 3.7. It is generally accepted that a nitrogen:metal ratio of 2:1 is required for complete chelation of a divalent metal by amino acid or peptide ligands. However, not all nitrogen present in the proteinates is available for chelation. Some is present in free amino acid groups and some may be contained in ring structures which may not be freely available for metal binding so this ratio was used only as a guide for interpreting Table 3.7. Additionally, it should be noted that in addition to nitrogen, other electron-donating groups or atoms such as oxygen and sulphur may be involved in metal coordination. Schematic representations of the coordination modes of some amino acid side chains containing sulphur and oxygen have been previously outlined (Figure 1.5, Section 1.5). Based on the fact that the nitrogen:metal ratio was greater than 2:1 in all of the proteinates assessed, the analytical data in Table 3.7 indicated that the metal proteinate preparations selected for analysis

were capable of supporting complete chelation of the transition metal in all cases. The phenacetin standard was included to monitor the accuracy of the analytical procedure.

Table 3.7 CHN analysis for a selection of metal proteinates

Sample ID	C (%)	H (%)	N (%)	Metal (%)	N:Metal
Cu proteinate 1	29.72	4.82	5.70	10.19	2.54
Cu proteinate 2	28.48	4.80	5.51	10.23	2.44
Cu proteinate 3	28.35	4.21	5.44	10.20	2.42
Fe proteinate 1	26.94	4.67	5.18	10.14	2.04
Fe proteinate 2	26.85	4.75	5.22	10.06	2.07
Fe proteinate 3	27.35	4.48	5.24	10.15	2.06
Zn proteinate 1	28.15	4.39	6.10	10.33	2.76
Zn proteinate 2	26.63	3.89	5.93	10.22	2.71
Zn proteinate 3	25.83	3.83	5.97	10.20	2.73
Mn proteinate 1	28.61	4.87	5.49	10.16	2.12
Mn proteinate 2	27.40	4.35	5.56	10.19	2.14
Mn proteinate 3	27.36	4.77	5.81	10.23	2.23
Phenacetin standard (theoretical)	67.01	7.32	7.82	-	-
Phenacetin standard (experimental)	67.24	7.47	7.77	-	-

Compiling a selection of the results obtained in Sections 3.3.1, 3.3.2 and 3.3.3 to compare the FAN, total N and metal values illustrates how much of the total N detected is present as FAN (Table 3.8). Based on the results observed, it can be seen that most of the nitrogen detected in the proteinates is not free α-amino nitrogen. The percentage FAN recovered is similar in all proteinates (approximately 0.10 %).

Table 3.8 FAN, N and M content for a selection of metal proteinates

Sample	FAN (%)	N (%)	M (%)	N : M (Molar ratio)
Cu proteinate 1	0.09	5.70	10.19	**2.54 : 1.00**
Fe proteinate 1	0.09	5.18	10.14	**2.04 : 1.00**
Mn proteinate 1	0.10	5.49	10.16	**2.12 : 1.00**
Zn proteinate 1	0.09	6.10	10.33	**2.76 : 1.00**

3.3.4 Fourier Transform InfraRed (FTIR) spectroscopy

The purpose of employing Fourier Transform Infrared (FTIR) spectroscopy was to determine the possibility of monitoring the modification in the vibrational absorption bands of a ligand due to metal-ligand complex formation. When a metal ion forms a bond with a ligand, the vibrational frequencies of the functional groups involved in the bond formation will be altered. The simple stretching vibrations in the 1600 cm^{-1} to 3500 cm^{-1} region are the most characteristic and predictable, and absorptions in this region are used to identify functional groups in molecules. The region of an IR spectrum from approximately 1600 cm^{-1} to 500 cm^{-1} is called the fingerprint region and contains a unique set of absorptions for a given molecule. Specifically, by comparing the spectra of both free and complexed ligands in this region, the occurrence of complexation may be verified.

The utility of FTIR for analysis of metal complexes is well illustrated by an examination of IR spectra for a selection of the proteinates. Figure 3.11 is comprised of spectral views of the 4000 cm^{-1} to 650 cm^{-1} region for an unhydrolysed soy control sample, a soy hydrolysate, the metal used in complex formation ($CuSO_4.5H_2O$) and copper proteinates with and without pH adjustment. Adjusting the pH was investigated to determine if chelation potential could be increased as previously discussed in Section 3.2.

Involvement of the carboxylic oxygen and the nitrogen atom of the amino group in coordination is expected and shifts in the υ(C=O) and δ(N-H) vibrations are expected in the FTIR spectra. The υ(N-H) stretching vibrations appear in the region above 3000 cm^{-1} and shifts in this region provide evidence for the involvement of the $–NH_2$ group in complex formation (Çakir *et al.*, 2001; Stanila *et al.*, 2007; Marcu *et al.*, 2008). Band shifts in the region above 3000 cm^{-1} are visible in the metal proteinate spectra when compared to control soy samples in Figure 3.11 and may be indicative of $–NH_2$ group involvement in complex formation. Additionally, band shifts in the region of 1600 cm^{-1} to 1700 cm^{-1} are indicative of changes in the υ(C=O) stretching vibration and shifts in the 1500 cm^{-1} – 1600 cm^{-1} can be assigned to symmetric and asymmetric bending vibrations of the N-H bond providing further evidence of complexation (Çakir *et al.*,

2001; Stanila *et al.*, 2007; Marcu *et al.*, 2008). These band shifts are also present in the spectra of the metal proteinates (Figure 3.11).

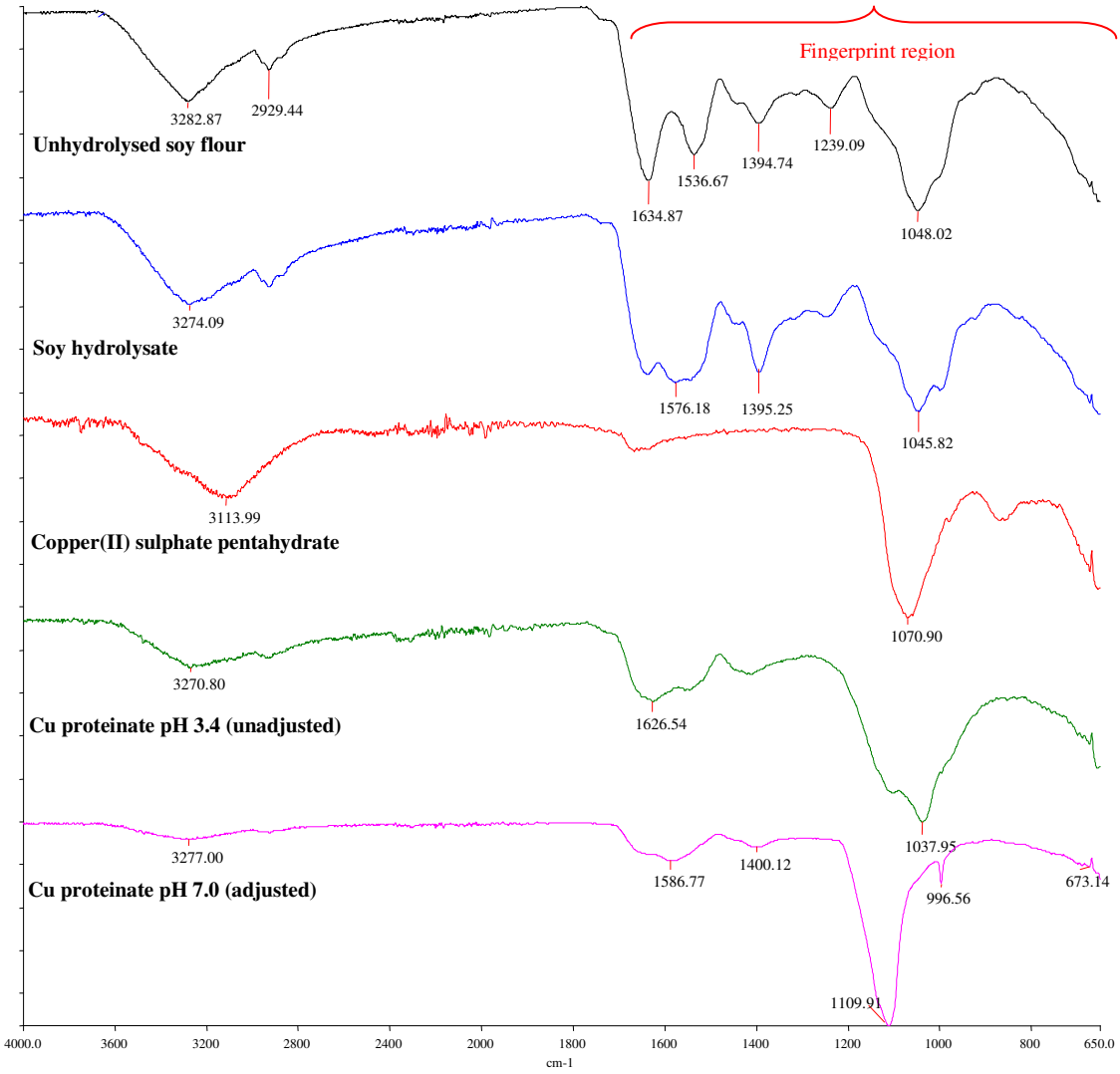

Figure 3.11 FTIR spectra of copper(II) proteinates and soy ligand controls

The chemical structure of the samples cannot be deduced from the infrared spectrum due to overlapping bonds, however, changes in chemical structure can be detected (Barth, 2007). Differences in the spectral results between the unhydrolysed soy and the soy hydrolysate controls indicated that the hydrolysis procedure had an effect on functional groups although the addition of the mineral resulted in the most significant

spectral differences. The most noticeable shifts are observed in the 1200 cm^{-1} – 1700 cm^{-1} region (Figure 3.11). This was to be expected based on peptide bond cleavage.

The copper(II) sulphate pentahydrate sample was assessed as an additional control sample to determine if spectral differences were observed in the proteinates containing copper. Based on the spectra obtained for the two copper proteinate samples analysed, clear differences are observed between the spectra of the proteinates and the copper and soy controls. This could indicate metal-ligand bond formation. Furthermore, the IR spectra in Figure 3.11 clearly showed that pH adjustment significantly affected the spectral results in the fingerprint region of the metal proteinates. This can be observed from the IR band shifts in the 1000 cm^{-1} to 1200 cm^{-1} region (Figure 3.11) which indicated perturbations of the functional groups. In the pH unadjusted proteinate, which is acidic, a band is observed at 1045.82 cm^{-1} whereas a higher frequency band at 1109.91 cm^{-1} is observed in the proteinate adjusted to pH 7.00.

Protonation changes cause shifts in mid-infrared vibrational spectra (Rich *et al.*, 2008) and numerous publications have observed such shifts in IR spectra (Dunn *et al.*, 1969; Cabaniss *et al.*, 1998; Hay *et al.*, 2007; Lanigan *et al.*, 2007). One study has described the complexation of EDTA and EDDS with Pb(II), Zn(II), Ni(II), and Cu(II) ions which was indicated primarily by the shift of the asymmetric carboxyl group band frequencies at low pH values (Lanigan *et al.*, 2007). The large polarities of the C-O bonds result in high infrared activity, giving rise to strong, characteristic vibrational bands, which vary significantly with pH (Hay *et al.*, 2007). Figure 3.12 illustrates the independent vibrational modes for C=O and C-OH highlighting the differences in C-O bonds in a protonated carboxyl group (Hay *et al.*, 2007) and previous research by this group on the effect of pH on fulvic acid is displayed. The protonated carboxylic acid yields absorption bands corresponding to a carbonyl stretch ($\nu_{C=O}$) between 1690 and 1750 cm^{-1}, and C-OH vibrations ($\nu_{C\text{-}OH}$) between 1200 and 1300 cm^{-1} (comprised of a mixture of C-O stretch and C-O-H bend that often yields a single, broad absorption band). On deprotonation, $\nu_{C=O}$ shifts to lower energy as its vibrational mode becomes coupled to that of the other oxygen, giving rise to an asymmetric feature (ν_{as}) between 1540 and 1650 cm^{-1}. Similarly, the C-OH band shifts to higher energy on deprotonation, yielding a symmetric COO- mode (ν_{s}) between 1300 and 1420 cm^{-1} (Hay *et al.*, 2007).

Examination of the metal proteinate spectra in Figure 3.11 found a similar shift for the C-OH vibrations ($\nu_{C\text{-}OH}$) between 1200 and 1300 cm^{-1} (1239.09 cm^{-1} in the soy controls) which shifts to higher energy on deprotonation (1400.12 cm^{-1} for the Cu proteinate at pH 7).

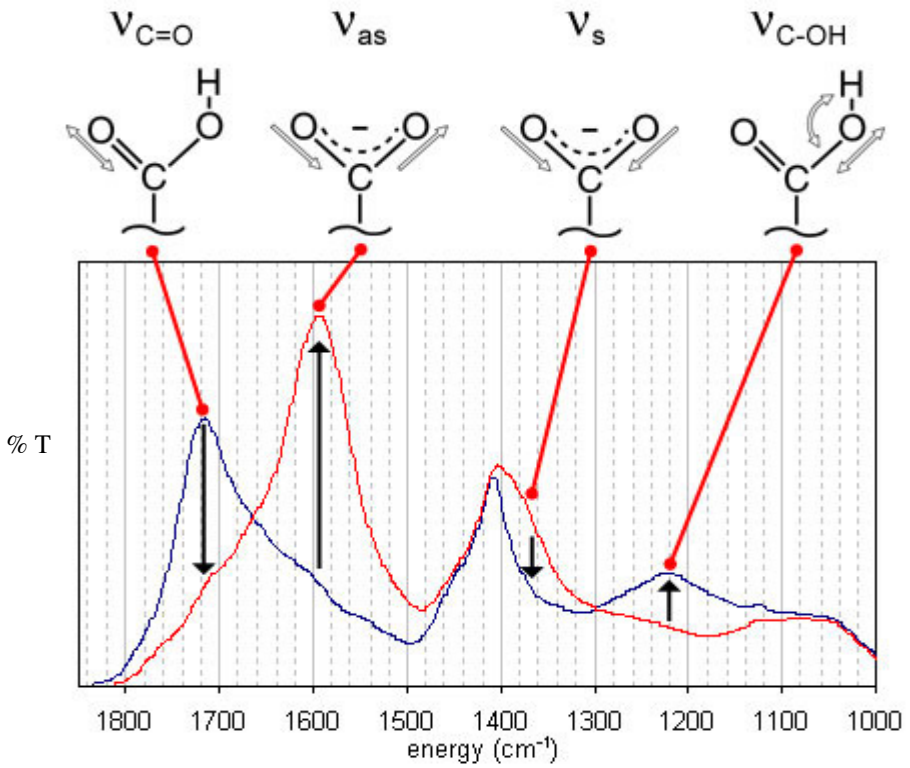

Figure 3.12 IR spectra of soil fulvic acid at pH 2 (blue) and pH 6 (red). The black arrows indicate the spectral changes that occurred on deprotonation (adapted from Hay *et al*., 2007)

The arrows in Figure 3.12 highlight the disappearance of the carbonyl and C-OH bands and the appearance of bands corresponding to the asymmetric and symmetric modes of the carboxylate anion. The structures above the graph in Figure 3.12 illustrate the vibrational modes of the carboxylic acid and the carboxylate anion. The symbols $\nu_{C=O}$, $\nu_{C\text{-}OH}$, ν_{as} and ν_{s} represent the different vibrations. The precise energies of the bands are dependent on a number of factors including the electron density on the carboxyl, as affected by the presence of electron donating / withdrawing functional groups on the molecule, and inter- or intramolecular H-bonding involving a carboxylic oxygen and/or

the proton in the carboxylic acid. Interactions with metal cations and coupling with other vibrational modes in the molecule may also affect the energy of the carboxylate absorption bands. The degree of shift is dependent on the ionic or covalent character of the complex formed. The more covalent the $–CO_2–M$ bond, the higher the frequency of the asymmetric stretching band and the lower the symmetric stretching band (Sawyer *et al.*, 1959; Chapman *et al.*, 1963).

Band width is also informative. Flexible structures will give broader bands than rigid structures and the band width is indicative of conformational freedom (Barth, 2007). A restriction in conformational freedom is indicative of binding (Barth, 2007). FTIR spectra, obtained from metal ions binding to amino acids and polypeptides in the hydrolysate to form metal proteinates, should show narrower band width than a control hydrolysate sample if binding had occurred. The 1109.91 cm^{-1} band in the pH 7.00 copper proteinate sample is narrower than the band observed in the pH unadjusted copper proteinate at 1037.95 cm^{-1} and the 1045.82 cm^{-1} band seen in the soy hydrolysate sample (Figure 3.11). This could be indicative of stronger binding in the pH 7.00 proteinate sample. Potentiometric titrations provided further insight into this postulation (Section 3.6).

FTIR can be used to identify conformational change in the proteinate samples and was applied to all metal proteinate samples produced for this work. In addition to the Cu spectra outlined in Figure 3.11, full spectral information for Fe, Mn and Zn proteinates are outlined in Appendix 1.1.

3.3.5 Amino acid profiling

Amino acid profiling provided accurate measurement of the individual amino acids present in the soy ligand sample. Only amino acids that are stable to acid hydrolysis (6 M HCl, 110 °C) were quantified. Tryptophan is usually completely destroyed during normal acid hydrolysis of proteins and cysteine is partially lost. In addition, asparagine and glutamine are fully converted to aspartic and glutamic acid respectively so it is necessary to take into account the fact that the value for aspartic acid in Table 3.9 consists of Asp and Asn. Similarly, the value for glutamic acid is an overall value of all

Glu and Gln in the sample combined. Figure 3.13 displays the percentage of each amino acid present in the samples and provides a clearer picture of the most abundant amino acids present. A practical application of the technique could be to employ amino acid profiling profiling as a fingerprinting method to differentiate products in the marketplace.

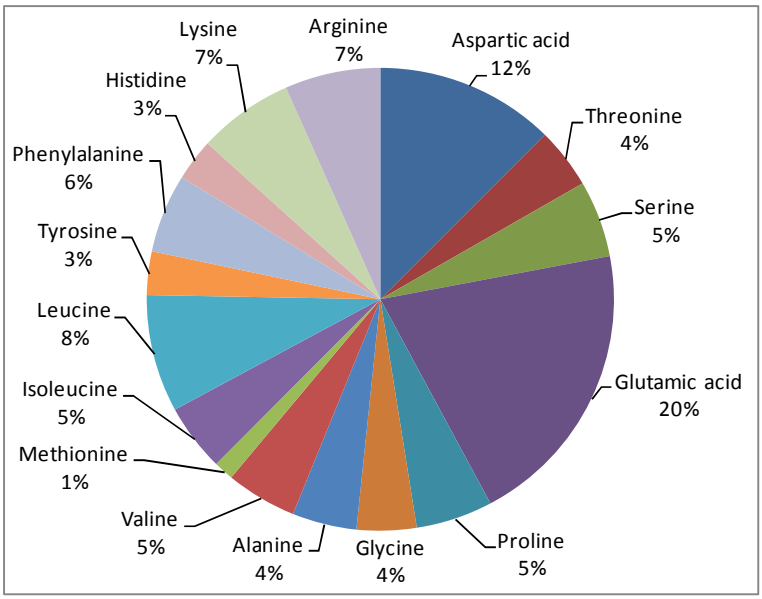

Figure 3.13 Amino acid profile of a soy ligand

Table 3.9 illustrates the concentration of the individual amino acids (% of total) present in the soy ligand. Cysteine, which was absent in the copper proteinates, was observed at low levels in the hydrolysed and unhydrolysed soy control sample. Cysteine is partially lost during the acid hydrolysis step so any residual cysteine would be present at very low levels. It is possible that any cysteine present was below the level of detection in the case of the proteinates and was only marginally above the level of detection in the case of the soy controls. The primary purpose of measuring the total amino acid content of the samples was from a quality control perspective; to determine the consistency of the amino acid content between proteinate batches. Based on the results shown in Table 3.9, it can be concluded that the variation between batches is very low.

Table 3.9 Amino acid profiles of soy based metal proteinates

AA (% of total)	Cu proteinate 1	Cu proteinate 2	Cu proteinate 3	Cu proteinate 4	Cu proteinate 5	Cu proteinate 6	Cu proteinate 7	Hyd. Soy	Soy Flour	Average	Std. Dev
Cysteic acid	-	-	-	-	-	-	-	-	-	-	-
Aspartic acid	12.72	12.60	12.55	12.50	12.14	12.28	12.35	12.12	12.05	12.45	0.24
Threonine	4.24	4.25	4.15	4.18	4.21	4.27	4.30	4.37	4.28	4.23	0.07
Serine	4.96	5.19	5.02	4.87	5.52	5.77	6.00	5.53	5.50	5.33	0.39
Glutamic acid	20.09	20.09	20.09	20.22	19.92	20.12	20.43	19.63	19.97	20.14	0.22
Proline	5.43	5.36	5.32	5.39	5.20	5.27	5.35	5.26	5.23	5.33	0.08
Glycine	4.35	4.30	4.16	4.18	3.96	4.05	4.01	3.78	3.85	4.15	0.19
Alanine	4.57	4.60	4.47	4.47	4.37	4.44	4.43	4.15	4.25	4.48	0.14
Cysteine	-	-	-	-	-	-	-	1.14	1.19	-	0.03
Valine	5.04	5.06	5.02	5.13	4.88	4.73	4.65	4.57	4.59	4.93	0.22
Methionine	1.09	1.09	1.18	1.12	2.38	1.40	1.41	1.42	1.38	1.38	0.40
Isoleucine	4.78	4.77	4.81	4.82	4.64	4.56	4.43	4.27	4.28	4.69	0.22
Leucine	8.28	8.13	8.30	8.25	8.02	8.13	8.04	7.98	8.04	8.16	0.12
Tyrosine	2.77	2.94	3.08	2.93	3.16	3.04	3.25	3.09	2.81	3.02	0.16
Phenylalanine	5.60	5.53	5.53	5.61	5.36	5.52	5.35	5.65	5.63	5.50	0.11
Histidine	3.03	2.94	2.97	2.95	2.68	3.00	2.81	3.04	2.98	2.91	0.12
Tryptophan	-	-	-	-	-	-	-	-	-	-	-
Lysine	6.77	6.72	6.72	6.80	6.59	6.43	6.35	6.59	6.67	6.63	0.15
Arginine	6.16	6.26	6.85	6.71	6.87	6.76	6.87	7.48	7.28	6.64	0.42

3.3.6 Surface-Enhanced-Laser-Desorption/Ionisation-Time-of-Flight-Mass-Spectrometry (SELDI-ToF-MS) analysis of metal proteinates

Mass spectrometric techniques have been successfully applied to the analysis of proteins and peptides (Schmelzer *et al.*, 2004; Xiao *et al.*, 2005) and are ideally suited to characterising metal proteinates by providing additional information to complement other techniques such as electrophoresis or chromatography. Mass spectrometry can be used for peptide profiling to establish the molecular mass of peptides available for chelation with trace elements in addition to providing a method to compare proteinates based on their respective peptide profiles. The emphasis during the course of the present work was on the evaluation of a particular type of mass spectrometry for characterisation of proteinates called Surface-Enhanced-Laser-Desorption/Ionisation-Time-of-Flight-Mass-Spectrometry (SELDI-ToF-MS).

As previously mentioned (Section 1.6.1), SELDI-ToF-MS has limitations with respect to quantitative analysis. Due to competition during binding steps and variation in ionisation efficiency, peak heights in mass spectra do not always reflect absolute concentrations in samples (Piperno *et al.*, 2009). Robotic systems, automated protocols, and strictly controlled SELDI-ToF-MS settings may allow semi-quantitative assessment of the peptide profiles to be obtained but, due to the fact that a manual protocol was used for the assessment of the proteinates in this work, quantitative assertions regarding concentrations could not be made. However, based on the fact that the aim of employing SELDI-ToF-MS in this work was to aid the characterisation of proteinates and not for quantitative purposes, this was not a major disadvantage. Matrix effects which can shield low molecular mass peptides and amino acids below 500 Da, and variations in array surfaces which may occur during the manufacturing process can also present difficulties. However, stringent adherence to sample handling protocols and data analysis methods can identify differences in peptide profiles obtained due to issues such as these, thereby alleviating such difficulties (Albrethsen *et al.*, 2006; Dijkstra *et al.*, 2007; Poon, 2007). Advantages of SELDI-ToF-MS include high sensitivity and selectivity and these outweigh such limitations as outlined earlier. As such, SELDI-ToF-MS was selected to establish the molecular masses of peptides in the metal proteinates.

Peptide profiles were obtained for the metal proteinates using this technique and as a result, consistency between metal proteinate batches could be determined by comparing their respective peptide profiles. Based on the profiles obtained in this work, marker peptides were identified that appeared to be specific to the protein hydrolysis procedure used (Section 3.3.6.6). As a further application of this mass spectrometric technique, the selected marker peptides were used to identify the presence of the metal proteinates in premixes (Section 3.3.6.7) and in feed (Section 3.3.6.8).

3.3.6.1 Calibration of SELDI-ToF-MS Instrument

The instrument was calibrated using an All-in-One peptide mixture (Ciphergen Biosystems Inc.) which contained a mixture of standard peptides (Figure 3.14). Slight variations in molecular mass were observed between the stated molecular masses for the calibrants (Table 2.1) and the peptide peaks observed. However, the values observed for the calibrants were well within an acceptable margin of error. According to the manufacturer (Ciphergen Biosystems), instrument resolution may contribute to differences of ± 1 Da and the values obtained are within this range. The presence of low intensity minor peaks in the spectra may be indicative of proteolytic degradation of the All-In-One peptide standard over time or minor contaminants in the sample. Irrespective of the presence of the minor peaks, high intensity peptide standards are visible with accurate molecular masses and are readily identifiable to enable calibration of the spectrometer.

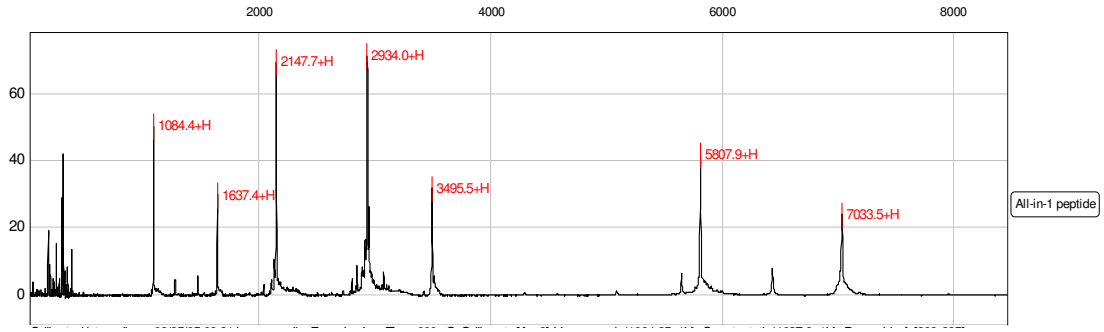

Figure 3.14 Internal calibration spectra obtained using All-in-One peptide mixture containing: Vasopressin (1,084.4 Da), Somatostatin (1,637.4 Da), Dynorphin A (porcine) (2,147.7 Da), ACTH (human) (2,934.0 Da), Insulin β-chain (bovine) (3,495.5 Da), Insulin (human recombinant) (5,807.9 Da) and Hirudin (recombinant) (7,033.5 Da) (Ciphergen Biosystems Inc.). The x-axis indicates the molecular mass (Da) of the peptides and the y-axis displays the mass-to-charge ratio (m/z).

3.3.6.2 Selection of suitable array surfaces

A wide range of array surfaces (Figure 1.7, Section 1.6.1) are available for various analyses such as biomarker discovery, protein profiling, protein interaction analysis, peptide mapping applications, immunoassay, receptor-ligand binding and DNA-binding protein applications (Seibert *et al.*, 2004). However, only a select number of these arrays are suitable for use in the current work. Although the main focus was on profiles obtained from a range of chromatographic surfaces using SELDI-ToF-MS, an inert gold array was also examined using MALDI-ToF-MS as it has the advantage of reducing costs since the gold arrays are reusable.

Based on the surface properties which were deemed to be most suitable for metal proteinate assessment, four arrays from those listed in Table 2.3 were selected for analysis. The arrays chosen were: gold (Au), normal phase (NP20), cation (CM10) and immobilised metal affinity capture (IMAC30). Figures 3.15-3.18 illustrate the differences in peptide profiles observed between the four array surfaces for Cu(II), Fe(II), Mn(II) and Zn(II) proteinates without pH adjustment.

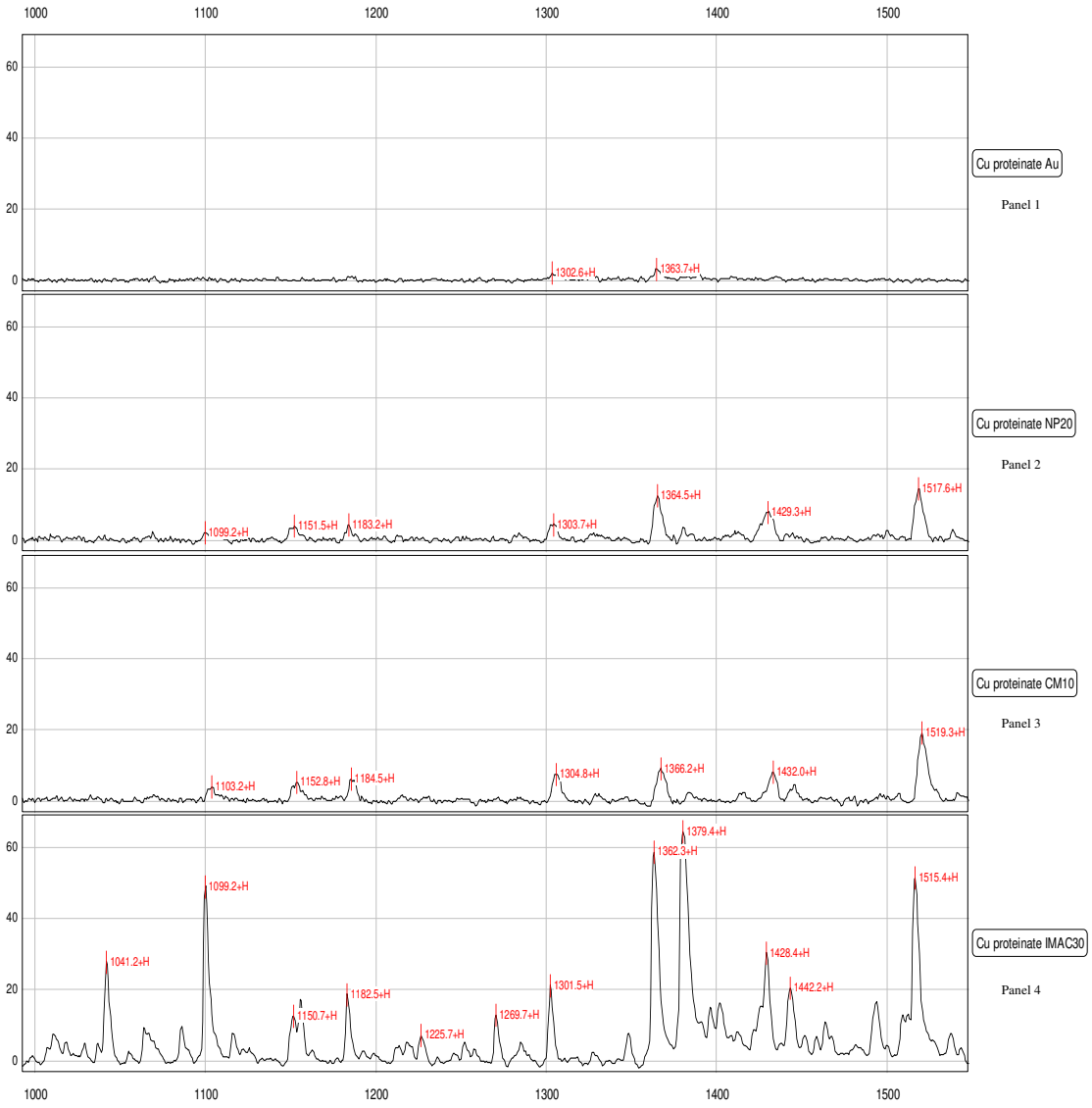

Figure 3.15 Cu proteinate analyses on a selection of array surfaces (Cu proteinate Au = Panel 1, Cu proteinate NP20 = Panel 2, Cu proteinate CM10 = Panel 3 and Cu proteinate IMAC30 = Panel 4). The x-axis indicates the molecular mass (Da) of the peptides and the y-axis displays the mass-to-charge ratio (m/z).

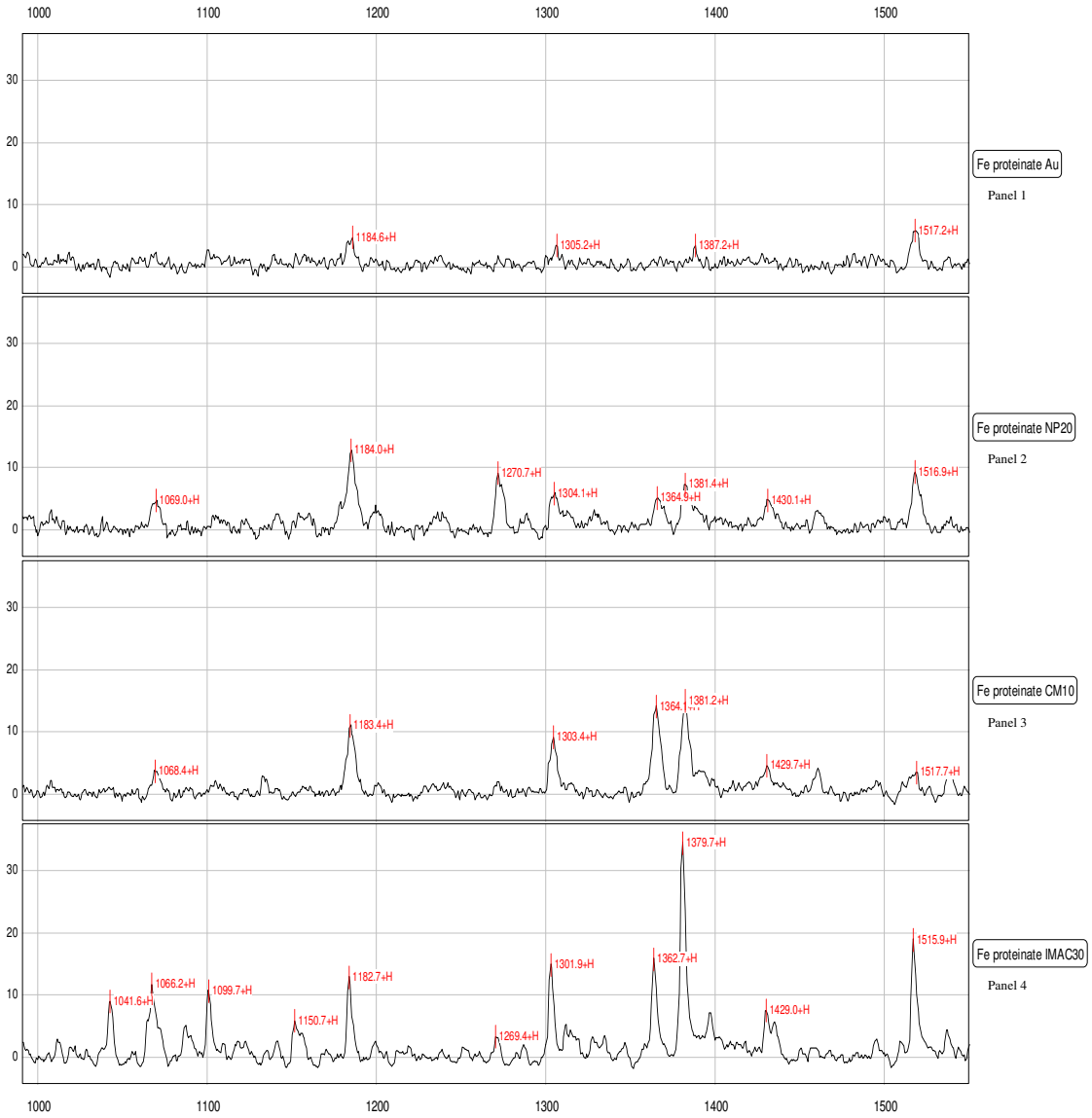

Figure 3.16 Fe proteinate analyses on a selection of array surfaces (Fe proteinate Au = Panel 1, Fe proteinate NP20 = Panel 2, Fe proteinate CM10 = Panel 3 and Fe proteinate IMAC30 = Panel 4). The x-axis indicates the molecular mass (Da) of the peptides and the y-axis displays the mass-to-charge ratio (m/z).

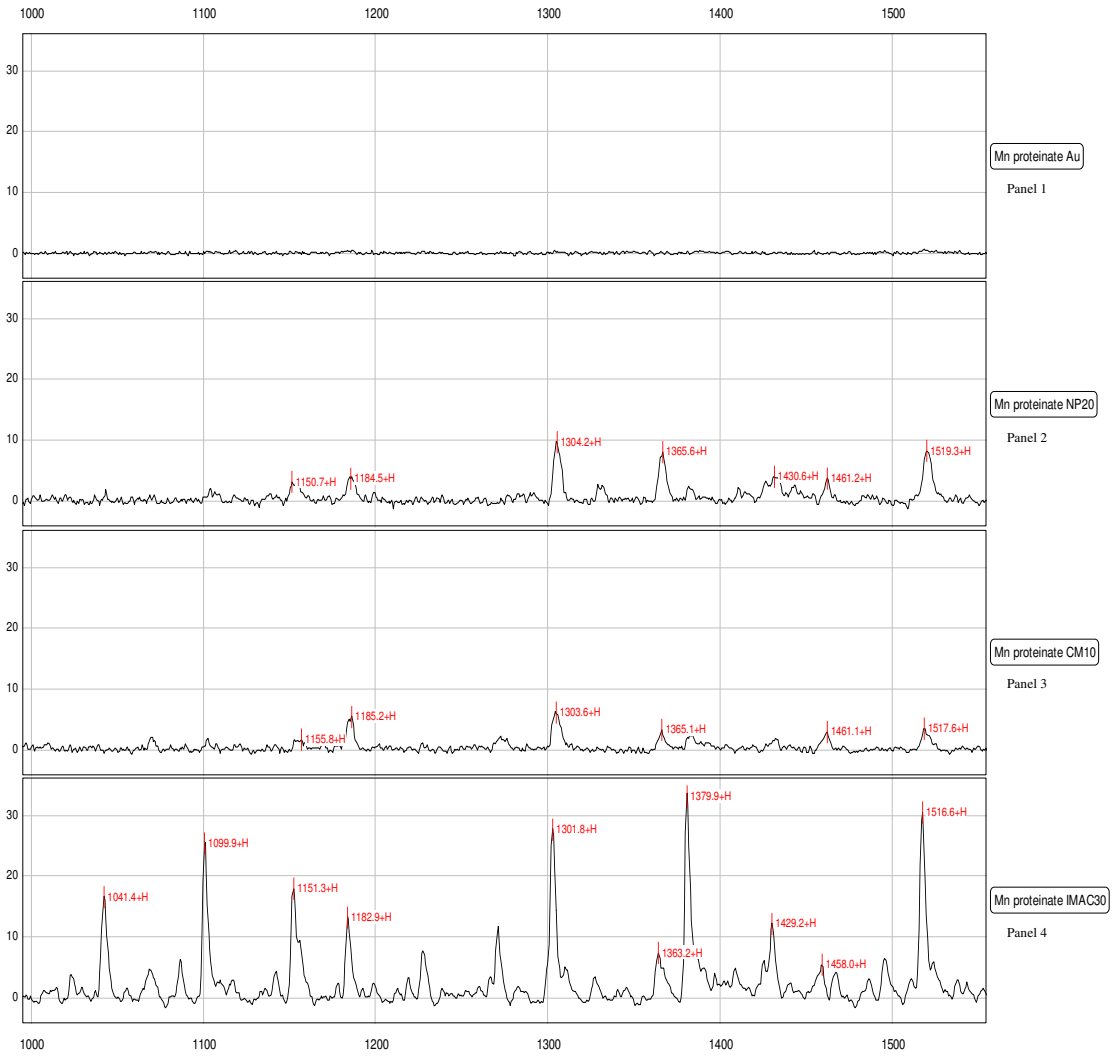

Figure 3.17 Mn proteinate analyses on a selection of array surfaces (Mn proteinate Au = Panel 1, Mn proteinate NP20 = Panel 2, Mn proteinate CM10 = Panel 3 and Mn proteinate IMAC30 = Panel 4). The x-axis indicates the molecular mass (Da) of the peptides and the y-axis displays the mass-to-charge ratio (m/z).

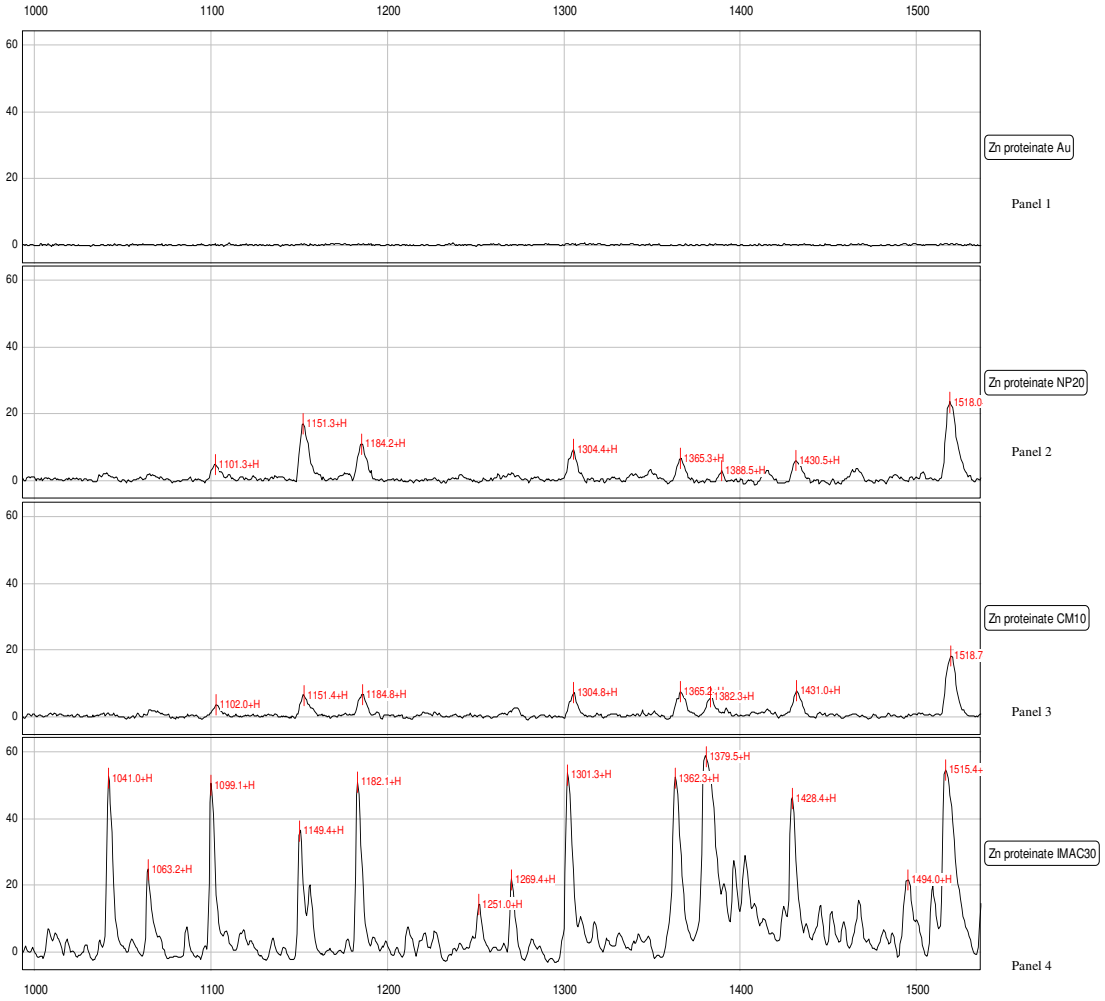

Figure 3.18 Zn proteinate analyses on a selection of array surfaces (Zn proteinate Au = Panel 1, Zn proteinate NP20 = Panel 2, Zn proteinate CM10 = Panel 3 and Zn proteinate IMAC30 = Panel 4). The x-axis indicates the molecular mass (Da) of the peptides and the y-axis displays the mass-to-charge ratio (m/z).

Gold arrays were chosen for initial analysis on a cost basis as the arrays are reusable; a factor which would significantly reduce experimental costs. MALDI-ToF-MS was used for analysis of this particular array surface in place of SELDI-ToF-MS. Although both methods are quite similar, notable differences between SELDI-ToF-MS and MALDI-ToF-MS include the construction of the sample targets, the design of the analyser and the software tools used to interpret the acquired data (Vorderwulbecke *et al.*, 2005). Binding was very weak however, and the difficulty in finding "hot spots" on the array surface produced significant background noise and poor peptide intensity

(Figures 3.15-3.18, Panel 1). “Hot spots” is a term used to describe positions on the MALDI-ToF-MS array surface where clear spectra are obtained with low background noise and high intensity peaks. The absence of clear peptide peaks of reasonable intensity and low background noise makes this inert gold surface unsuitable.

Normal phase (NP20) arrays, which have silicon dioxide (SiO_2) surface chemistry, were also investigated. Binding to these arrays can be through hydrophilic and charged residues on the protein surface, electrostatic and dipole-dipole interactions or hydrogen bonds. These arrays can be used to give an overview of all the peptides present in a sample as a wide range of proteins can bind to this surface. A disadvantage of this array however, is its ability to potentially bind large proteins present in samples such that lower molecular mass peptide peaks of interest may be shielded or of lower intensity (Figure 3.15-3.18, Panel 2). To illustrate this point, a wider spectral range is shown in Figure 3.19. High molecular mass proteins up to 9,000 Da are noted although their intensities are very weak. As the peptides of interest in this work were of low molecular mass (below 2,000 Da) based on the fact that the hydrolysis procedure of the soy ligand should produce a selection of amino acids and low molecular mass polypeptides, the matrix choice and spectral range were limited to detecting proteins and peptides below 10 kDa. The matrix chosen for all analyses carried out during the course of this work was 20 % alpha-cyano-4-hydroxycinnamic acid (CHCA). According to manufacturer recommendations, this matrix is used for peptides and proteins below 15 kDa. Sinapinic acid (SPA) is the recommended matrix for detection of higher molecular weight proteins.

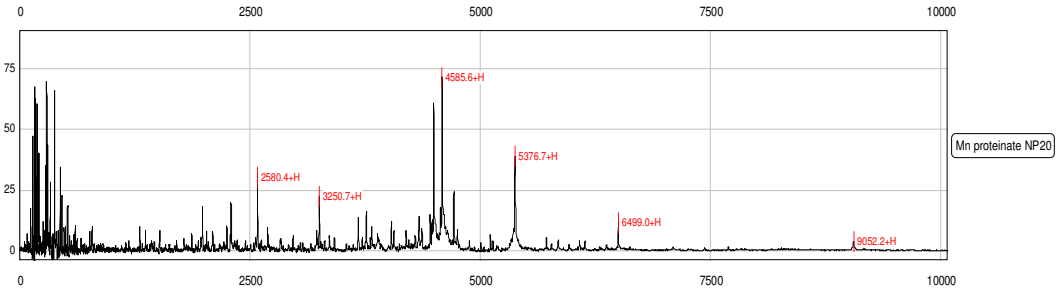

Figure 3.19 Wide spectral range analysis of a Mn(II) proteinate using an NP20 array. The x-axis indicates the molecular mass (Da) of the peptides and the y-axis displays the mass-to-charge ratio (m/z).

Sample preparation prior to analysis may be able to remove high molecular mass proteins but, due to the fact that the surface is reactive to such a significant number of proteins, the intensities of smaller peptides can still occasionally appear of low intensity due to shielding by larger proteins. However, NP20 arrays are often selected instead of more specific chromatographic array surfaces to obtain a more complete view of the proteins in a sample. NP20 arrays are also used to obtain calibration equations for SELDI-ToF-MS (Sections 2.3.1 and 3.3.6.1). Based on the results obtained in Figures 3.15-3.18, it can be concluded that NP20 arrays can be used for metal proteinate analysis but the peak intensities are rather low and a more specific chromatographic surface is required to obtain higher quality spectra.

CM10 arrays have a cationic surface derivatised with carboxylate groups. The peptide profile obtained using the CM10 arrays in Figures 3.15-3.18 (Panel 3) was very similar to that obtained from NP20 arrays and, although peptide peaks could clearly be identified, the intensities were again rather low. CM10 arrays are commonly used for tandem mass spectrometry (MS/MS) so it was encouraging to obtain peptide profiles for the metal proteinates using these arrays as MS/MS may be employed as a further characterisation technique and to obtain sequence data for particular peptides at a later stage.

The surface chemistry of IMAC30 arrays consists of nitrilotriacetic acid (NTA) functional groups which are capable of capturing metals (and attached peptides) and immobilising them on the chip. These arrays can chelate transition metal ions such as Zn^{2+}, Co^{2+}, Ni^{2+}, Cu^{2+}, Fe^{2+}, Mn^{2+}, and Mg^{2+} in addition to Al^{3+}, Fe^{3+} and Ga^{3+}.

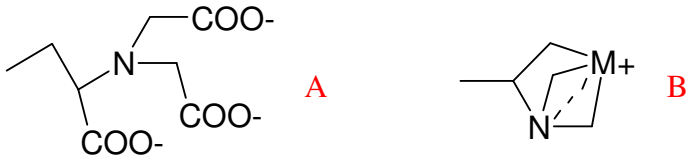

Figure 3.20 Diagrams illustrating the NTA surface structure (A) and the binding of a metal ion M^+ to the NTA group (B)

Based on the presence of an increased number of peptides and the significantly improved peak intensities obtained using these arrays (Figures 3.15-3.18, Panel 4), IMAC30 arrays were the obvious choice of array for this work.

3.3.6.3 Analysis of hydrolysed soy using Immobilised Metal Affinity Capture (IMAC) arrays

Immobilised Metal Affinity Capture (IMAC) arrays were used for this procedure and the samples were prepared for analysis as described in Section 2.3.3. The spectra for soy flour before and after hydrolysis are shown in Figure 3.21. Advantages of IMAC arrays include their selectivity and the ability to wash unbound peptides from the surface of the array before reading, thereby reducing potential interferences. As previously mentioned, the presence of intense matrix signals up to approximately 500 Da is a feature of this technique, making peak identification in this region of the spectrum quite difficult.

The hydrolysed and unhydrolysed soy flour used for the preparation of the metal proteinates was analysed by SELDI-ToF-MS so that the molecular mass distribution of peptides could be observed. Data for compounds greater than 10 kDa was not acquired because only low molecular mass peptides were of interest in this study. There are clear differences between the two spectra with an increase in the presence of low molecular mass peptides in the hydrolysed soy preparation (Figure 3.21, Panels 1 and 2).

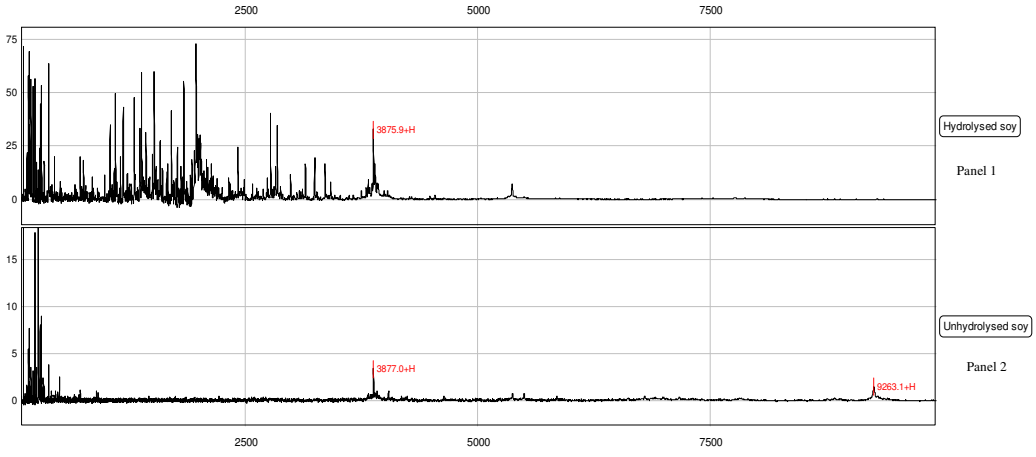

Figure 3.21 SELDI-ToF-MS spectra of a hydrolysed and unhydrolysed soy sample. The x-axis indicates the molecular mass (Da) of the peptides and the y-axis displays the mass-to-charge ratio (m/z).

The spectra for the soy samples provided additional information regarding the hydrolysis of proteins in the soy flour and their conversion into lower molecular mass peptides. For example, the appearance of peaks below 2,500 Da in the hydrolysate spectrum which were absent in the unhydrolysed soy sample was clearly illustrated. It was concluded therefore, that SELDI-ToF-MS could be used to distinguish peptide profiles in soy hydrolysate ligands used for metal proteinate manufacture. Based on the fact that the majority of the peptides were found below 2,000 Da, this area of the spectrum was focused on for the remainder of this work.

3.3.6.4 SELDI-ToF-MS analysis of a metal-peptide mimic

SELDI-ToF-MS, in addition to identifying peptide profiles as seen in Sections 3.1.3 and 3.3.6.2, can also be used to establish the molecular mass of peptides available for chelation with trace elements such as Cu(II), Fe(II), Mn(II) and Zn(II). Furthermore, potential metal chelation may be demonstrated by firstly detecting shifts in the molecular mass of peptides corresponding to metal binding (metal-peptide adducts) and then monitoring their response to conditions such as the addition of stronger chelating ligands which would strip the metal adduct from the original parent peptide. The absence or reduction in intensity of the adduct peak in the SELDI-ToF-MS spectra on treatment with ligands such as ethylenediaminetetraacetic acid (EDTA) can confirm this. EDTA is a useful chelating agent due to its ability to sequester metal ions such as Cu^{2+} (log K = 18.8, [ML] / [M][L] (Martell *et al.*, 2004)). It is a hexadentate ligand when fully deprotonated and can coordinate to metals through its two amine and four carboxyl groups (Figure 3.22). Based on the affinity of EDTA for divalent metals, it was employed to determine if it could strip the metal from the peptide chelate. If successful, the metal adduct peak in the mass spectrum should be removed or significantly reduced, leaving behind only the parent peptide.

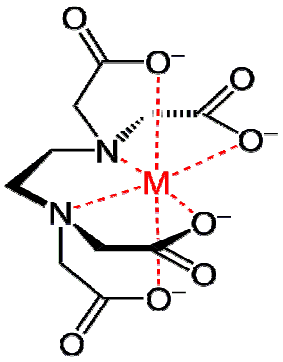

Figure 3.22 Fully deprotonated EDTA molecule illustrating metal (M) coordination

To confirm the usefulness of SELDI-ToF-MS to provide reliable information regarding metal proteinate characterisation, ranatensin, a peptide with known amino acid sequence and molecular mass 1281.5 Da was selected to create a metal proteinate mimic. The amino acid sequence of ranatensin is Glu-Val-Pro-Gln-Trp-Ala-Val-Gly-His-Phe-Met and its molecular mass is similar to the peptide peaks in the region of interest (below 2000 Da). Furthermore, ranatensin contained amino acid residues such as histidine which were expected to react and form complexes with transition metal ions such as copper(II) (Farkas *et al.*, 1984; Bruni *et al.*, 2000; Sanna *et al.*, 2001; Kozlowski *et al.*, 2005; Matera *et al.*, 2008).

An experiment was set up whereby ranatensin was applied to a spot on an IMAC30 array. A sample of a ranatensin-copper complex was applied to two additional spots on the array surface. The first two spots were washed twice with distilled water, removing any unbound sample. The third spot was washed once with distilled water and then treated with 0.1 M EDTA. Examination of the resultant SELDI-ToF-MS spectra (Figure 3.23) indicated the presence of a putative peptide-metal adduct in Panel 2 at 1343.7 Da with a molecular mass difference from the parent peptide of 62.1 Da. The molecular mass of this adduct is close to that of Cu (63.5 Da) (allowing for calibration deviations). This adduct was not detected in the original ranatensin spectra and treatment with EDTA demonstrated the removal of the Cu peptide-metal peak (1343.7 Da) from the SELDI-ToF-MS spectrum of ranatensin (1281.6 Da) (Figure 3.23, Panel 3). This experiment confirmed the presence of a metal-peptide adduct when a parent peptide was reacted with copper sulphate under appropriate conditions. It also confirmed

EDTA could effectively be used as a sequestering agent for copper. Successfully applying this procedure to metal proteinate samples would show the ability to remove the bound metal from the parent peptide.

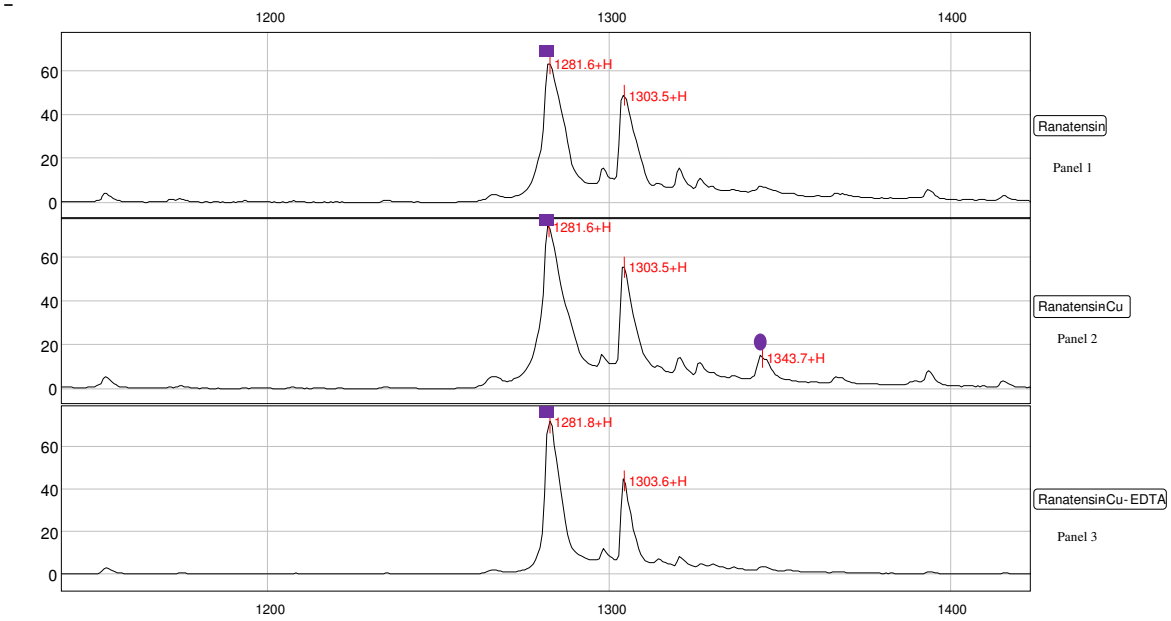

Figure 3.23 SELDI-ToF-MS spectra of ranatensin before and after treatment with EDTA (■ represent parent peptide peaks and ● refers to potential peptide-metal adducts). Ranatensin = Panel 1, Ranatensin-Cu = Panel 2 and Ranatensin-Cu- EDTA = Panel 3. The x-axis indicates the molecular mass (Da) of the peptides and the y-axis displays the mass-to-charge ratio (m/z).

The presence of a peak at 1304 Da was unexpected in the SELDI-ToF-MS spectra of ranatensin (1281.6 Da) prior to any treatment. Impurities in the commercially manufactured ranatensin sample may be the cause. The difference of 22 Da in the impurity from the 1281.6 Da parent peak may be indicative of the presence of sodium (Na) which has an atomic mass of 23. Regardless of the impurity present, the presence of a copper adduct at 1343.7 Da is clearly visible in the second panel of Figure 3.23 as is its removal on treatment with EDTA in the third panel.

Based on the results obtained using ranatensin, EDTA treatment was applied to the metal proteinate samples to determine the presence of peptide-metal adducts by attempting to strip the peptide-metal adduct from the parent peak using EDTA as a sequestering agent.

3.3.6.5 Immobilised Metal Affinity Capture (IMAC) analysis of metal proteinates

Arrays containing samples of metal proteinates were prepared for SELDI-ToF-MS analysis in accordance with the procedure outlined previously (Section 2.3.3) using IMAC 30 arrays. The spectra in Figure 3.24 show peptides in the molecular mass range from 0 Da to 5,000 Da for Cu, Fe, Mn and Zn metal proteinates. Although, peptides are visible up to 5000 Da, the majority of the peptide peaks are in the region below 2000 Da and were the focus of this work. The spectrum of the batch of soy hydrolysate used to prepare each of these samples was also included so that the peptide peaks before metal addition could be clearly observed. An unhydrolysed soy sample was also included as a control. The molecular mass labels were omitted from this plot to allow for similarities and differences between the spectra to be more readily apparent.

In order to interpret the plots more effectively, it was necessary to separate them into different molecular mass ranges. Difficulties in identifying amino acids and low molecular mass peptides were encountered due to the presence of intense matrix peaks in the 0 – 500 Da molecular mass region of the spectra (Figure 3.25). The full spectral view of the proteinates obtained in Figure 3.24 was separated into 500 Da molecular mass intervals to aid interpretation (Figures 3.25, 3.26, 3.28 and 3.30).

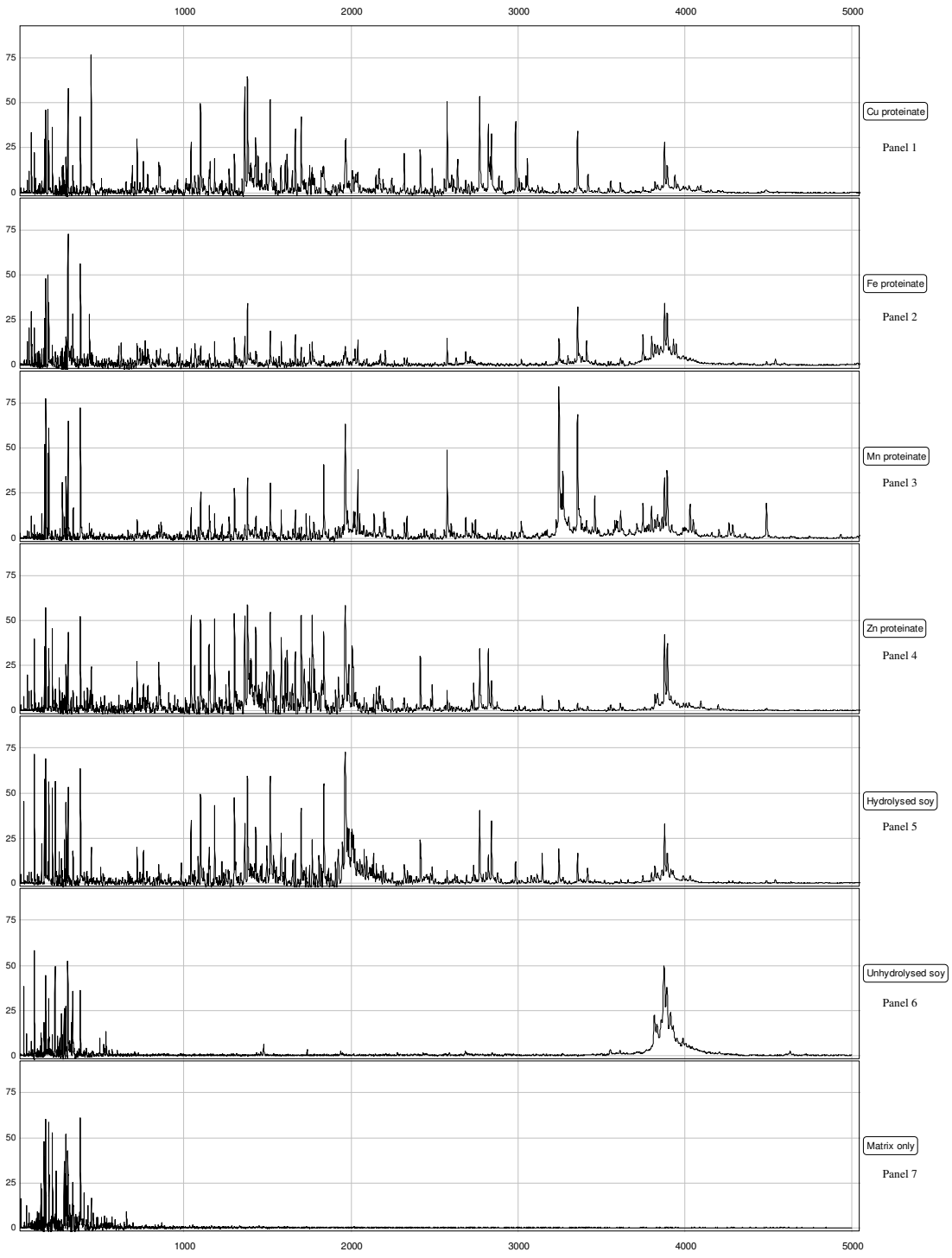

Figure 3.24 SELDI-ToF-MS spectra (0 Da – 5000 Da) of a selection of metal proteinates and controls. The x-axis indicates the molecular mass (Da) of the peptides and the y-axis displays the mass-to-charge ratio (m/z).

Appropriate molecular mass labels are shown in Figures 3.25, 3.26, 3.28 and 3.30 where specific molecular mass regions have been enlarged to show the presence of potential peptide-metal adducts in some of the metal proteinate preparations.

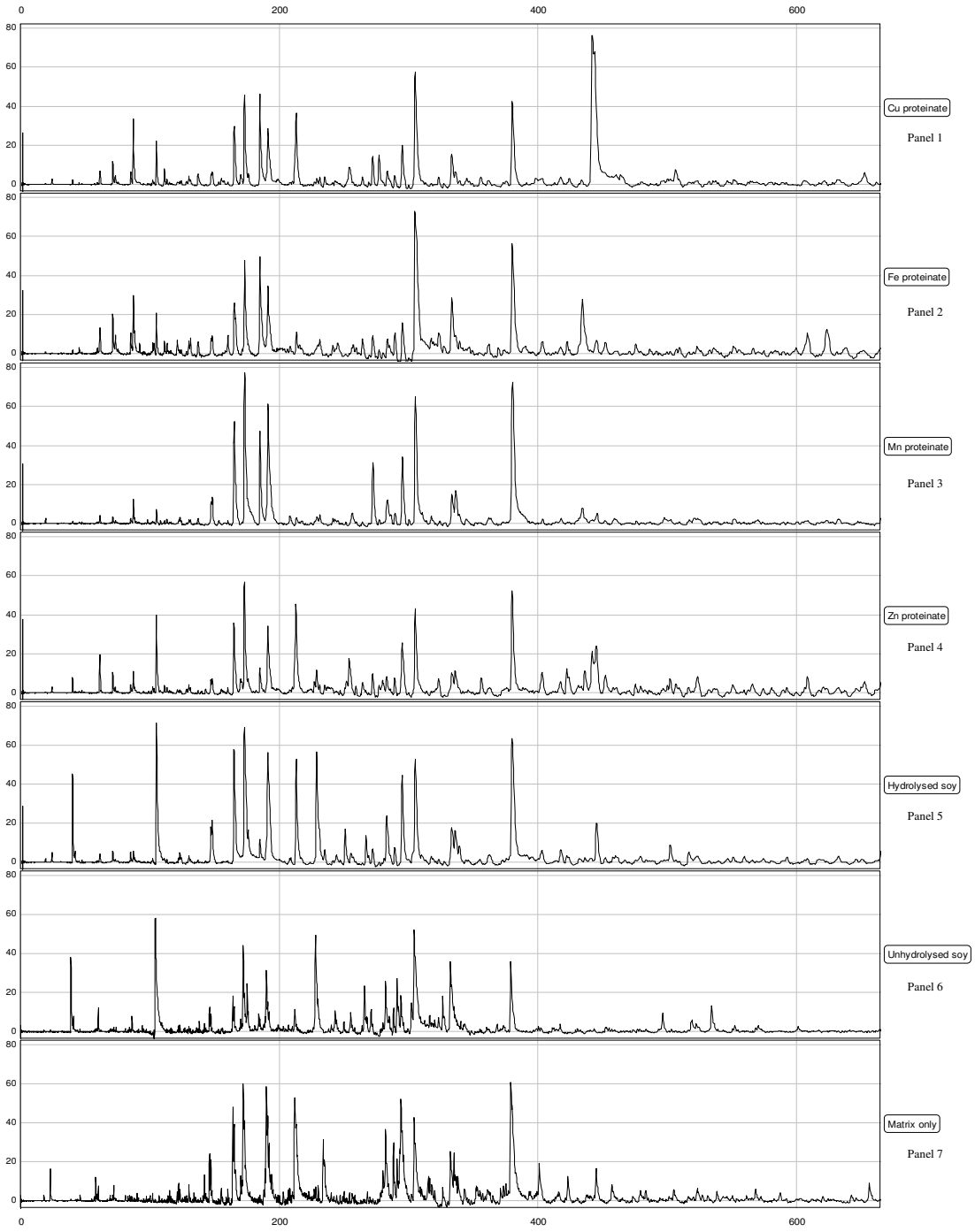

Figure 3.25 SELDI-ToF-MS spectra (0 Da – 500 Da) of a selection of metal proteinates and controls. The x-axis indicates the molecular mass (Da) of the peptides and the y-axis displays the mass-to-charge ratio (m/z).

Matrix peaks are clearly visible in the low molecular mass region of the spectra in Figure 3.25 and can interfere with detection of low molecular mass peptides. Panel 7 (Figure 3.25), which contains only the CHCA matrix, illustrates the extent of the matrix peaks in this region and conclusive identification of low molecular mass peptides was not possible in this region.

Few high intensity peptides are visible in the 500 Da – 1000 Da region of the SELDI-ToF-MS spectra of the proteinates. However, peptide peaks at approximately 718.8 Da and 849.6 Da which are present in the proteinates and in the soy hydrolysate may be parent peptides (Figure 3.26, Panels 1-5). Putative peptide-metal adducts are visible at 782.8 Da and 913.1 Da in the copper proteinate (Figure 3.26, Panel 1). Similarly, potential peptide-metal adducts are visible in the zinc proteinate (Figure 3.26, Panel 4) at 782.9 Da and 916.1 Da. As before, based on the affinity of EDTA for sequestering metal ions, the two proteinate samples (copper and zinc) containing detectable peptide-metal adducts were analysed further (Figure 3.27).

For all spectral data obtained, the intensities for Fe and Mn are lower than those of Cu and Zn. The metal is of great importance with regard to binding to an IMAC30 array. If the metal is weakly bound to the peptide when reacted with the IMAC30 array, the array surface will bind the metal but may contain very little of the peptides after the wash step. This would explain the low intensities of the peptide peaks in the Fe and Mn spectra. However, if the metal is strongly bound to the peptide, it will markedly improve peptide identification potential. Based on the spectral results for the proteinates in this section, the peak intensities for the metal proteinates appear to follow the Irving-Williams series in the majority of cases:

$$Mn(II) < Fe(II) < Co(II) < Ni(II) < Cu(II) > Zn(II)$$

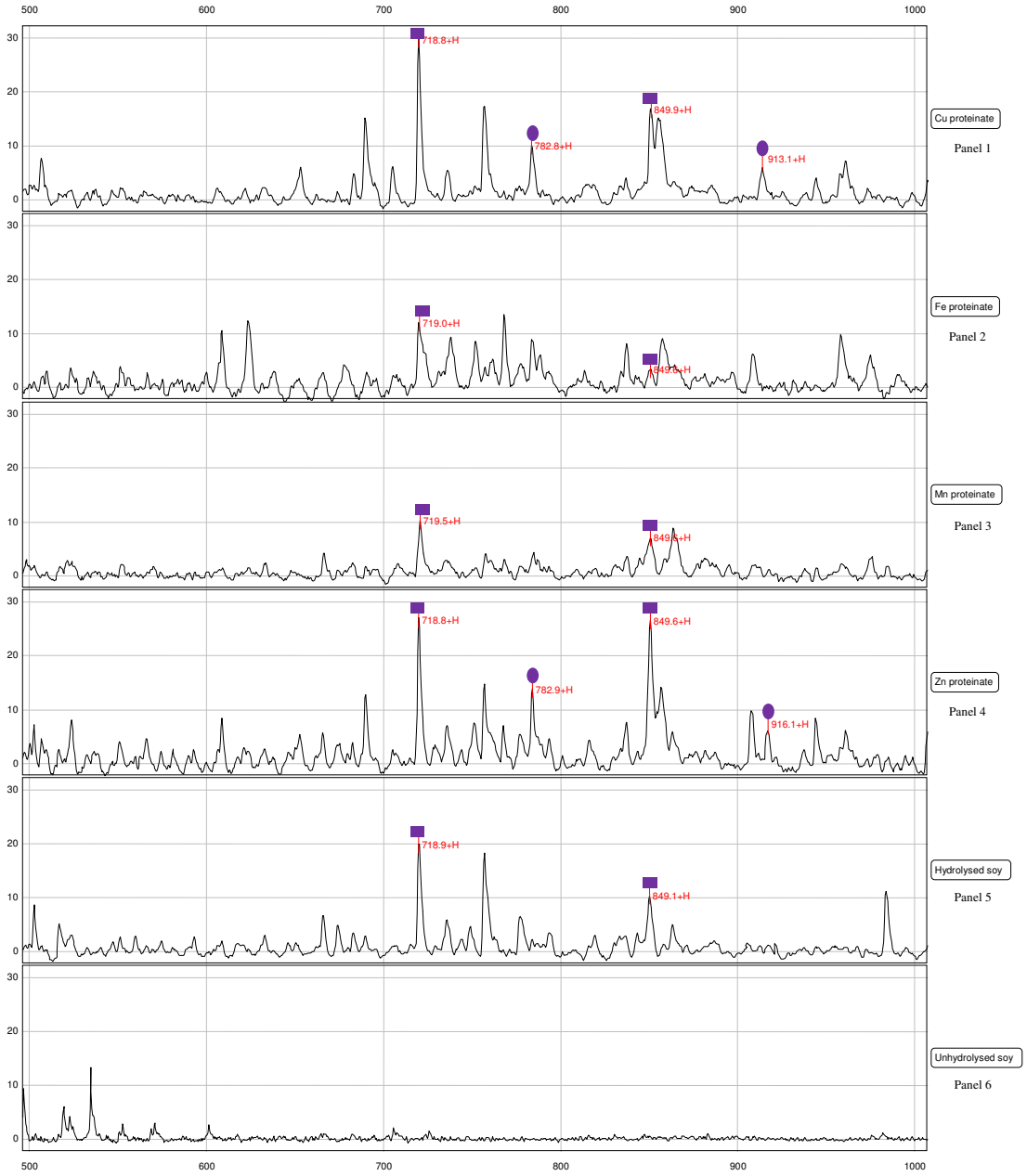

Figure 3.26 SELDI-ToF-MS spectra (500 Da – 1000 Da) of a selection of metal proteinates and controls (■ represent parent peptide peaks and ● refers to potential peptide-metal adducts) Cu proteinate = Panel 1, Fe proteinate = Panel 2, Mn proteinate = Panel 3, Zn proteinate = Panel 4, Hydrolysed soy = Panel 5, Unhydrolysed soy = Panel 6. The x-axis indicates the molecular mass (Da) of the peptides and the y-axis displays the mass-to-charge ratio (m/z).

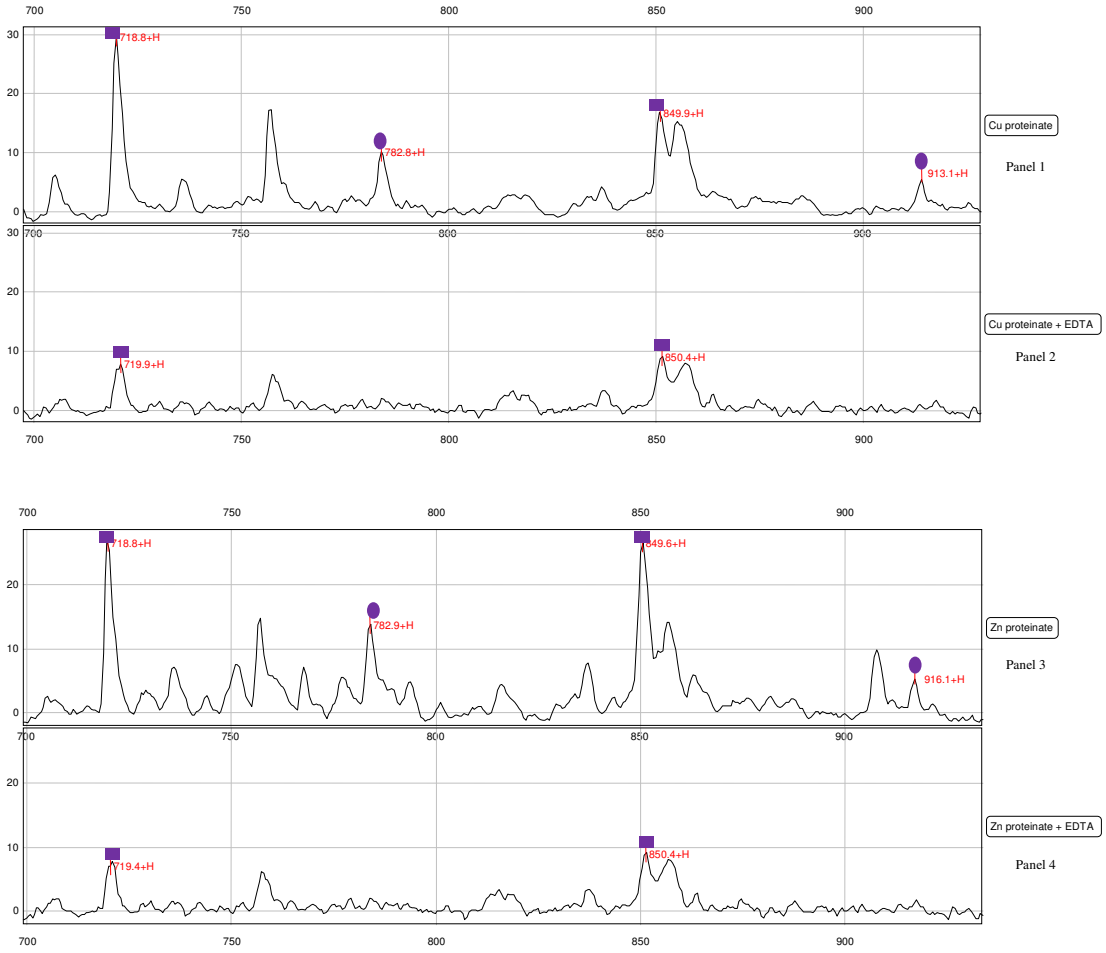

Figure 3.27 SELDI-ToF-MS spectra (700 Da – 950 Da) of copper and zinc proteinates treated with EDTA (■ represent parent peptide peaks and ● refers to potential peptide-metal adducts). Cu proteinate = Panel 1, Cu proteinate + EDTA = Panel 2, Zn proteinate = Panel 3, Zn proteinate + EDTA = Panel 4. The x-axis indicates the molecular mass (Da) of the peptides and the y-axis displays the mass-to-charge ratio (m/z).

In Figure 3.27, which is a slightly narrower molecular mass view of the copper and zinc proteinates analysed in Figure 3.26, the 718.8 Da and 849.6 Da parent peptides previously identified in the metal proteinates are present. Potential copper adducts at 782.8 Da and 913.1 Da are observed (Panel 1). The putative copper adducts were removed on treatment with EDTA leaving only the parent peptides present in the spectra (Panel 2). The spectra of the zinc proteinate in Panel 3 also contained two potential peptide-metal adducts at 782.9 Da and 916.1 Da and the spectral results in Panel 4 illustrate the disappearance of the adduct peaks on treatment with the sequestering

agent. This confirmed that the effect of EDTA treatment was the same as that previously observed in the case of ranatensin.

A significant number of peptide peaks are visible in the 1000 Da – 1500 Da region of the proteinate spectra (Figure 3.28). Nine intense peaks for each of the metal proteinates and the hydrolysed soy sample were observed. The approximate molecular masses of these peaks are: 1041 Da, 1099 Da, 1150 Da, 1182, Da, 1301 Da, 1362 Da, 1379 Da, 1428 Da and 1514 Da. These peptide peaks are noticeably absent in the unhydrolysed soy control and may be considered to be parent peptides. Identification of some peptide-metal adducts in this region may be somewhat hindered due to the high intensities of the parent peptides, but putative adducts for copper at 1442.2 Da (Figure 3.28, Panel 1) and zinc at 1251.0 Da and 1450.8 Da (Figure 3.28, Panel 4) were detected in the proteinates that were absent in the soy hydrolysate (Figure 3.28, Panel 5). Potentiometric analysis in conjunction with SELDI-ToF-MS may provide further insight into the peptide-metal adducts (Section 3.6). Difficulties in determining peptide-metal adducts of reasonable intensity were encountered for Fe(II) and Mn(II) but in the case of Cu and Zn, potential adducts based on the atomic mass of Cu (63.5 Da) and Zn (65.4 Da) were visible and the aforementioned peptide-metal adducts were examined in further detail using EDTA treatment (Figure 3.29).

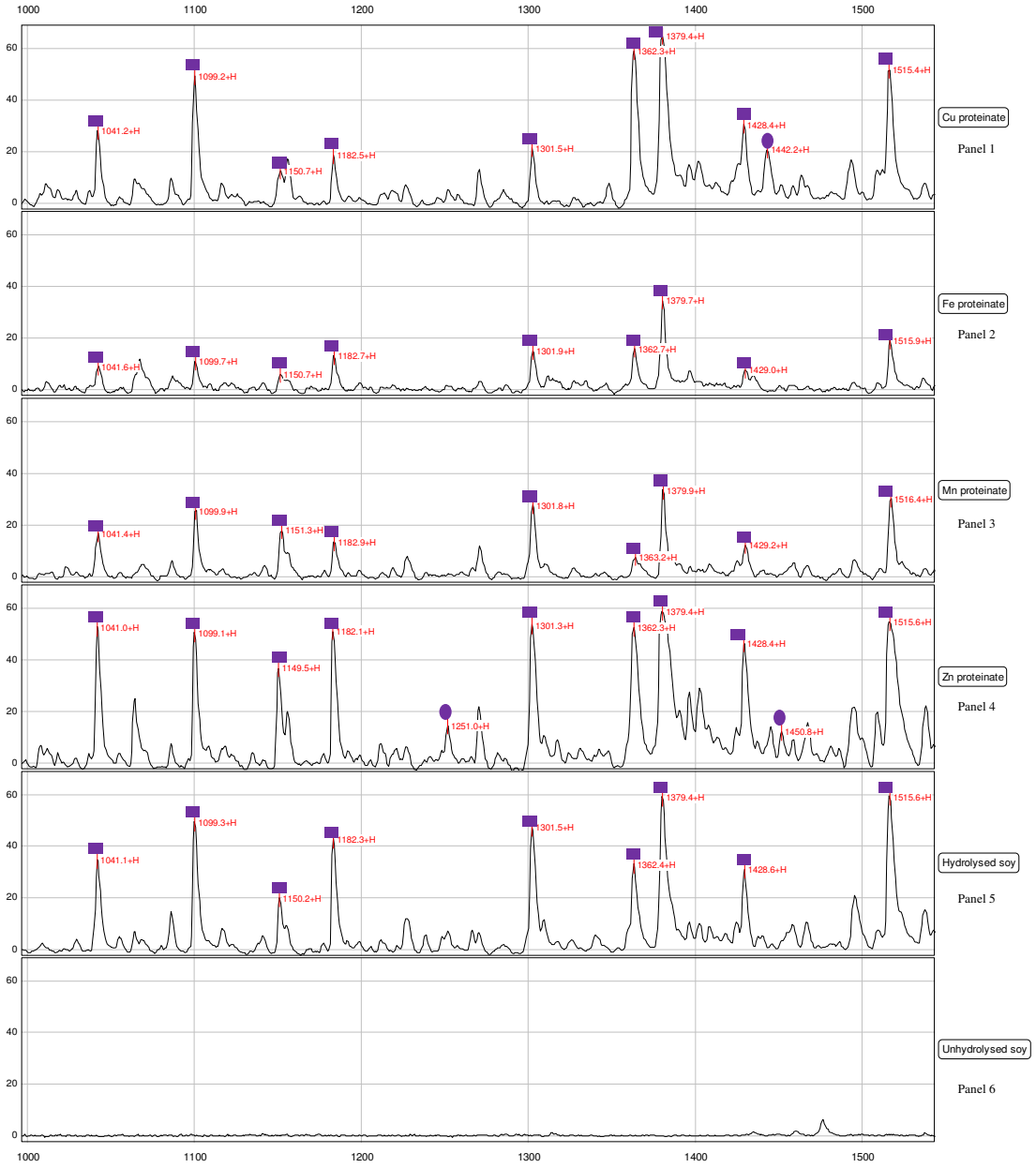

Figure 3.28 SELDI-ToF-MS spectra (1000 Da – 1500 Da) of a selection of metal proteinates and controls (■ represent parent peptide peaks and ● refers to potential peptide-metal adducts). The x-axis indicates the molecular mass (Da) of the peptides and the y-axis displays the mass-to-charge ratio (m/z).

Figure 3.29 illustrates the effect of EDTA treatment on a zinc and copper proteinate sample in the 1150 Da – 1500 Da region of the spectrum. The previously postulated peptide-metal adducts based on examination of the spectra in Figure 3.28 for copper at 1442.2 Da (Figure 3.28, Panel 1) and zinc at 1251.0 Da and 1450.8 Da (Figure 3.28, Panel 4) were examined and their removal on treatment with EDTA (Figure 3.29, Panels 2 and 4) was observed. The 1182.1 Da parent peak has a putative zinc adduct at 1251.0 Da which is a difference in molecular mass of 68.9 Da (Figure 3.29, Panel 3). With the loss of two protons and minor calibration deviations in the spectra, this adduct could imply zinc(II) binding. The adduct peak is not visible on treatment with EDTA (Figure 3.29, Panel 4) or in the hydrolysate (Figure 3.29, Panel 5). Similarly, in relation to the 1379.4 Da parent peptide present in both the copper and zinc proteinates, the corresponding potential peptide-metal adduct for copper was observed at 1442.2 Da (Figure 3.29, Panel 1) and at 1450.8 Da for zinc (Figure 3.29, Panel 3). Both putative adducts were absent on treatment with the sequestering agent (Figure 3.29, Panels 2 and 4). Furthermore, these peptide-metal adducts were absent in the corresponding soy hydrolysate (Figure 3.29, Panel 5) which provided further evidence that these particular peptide peaks were in fact peptide-metal adducts.

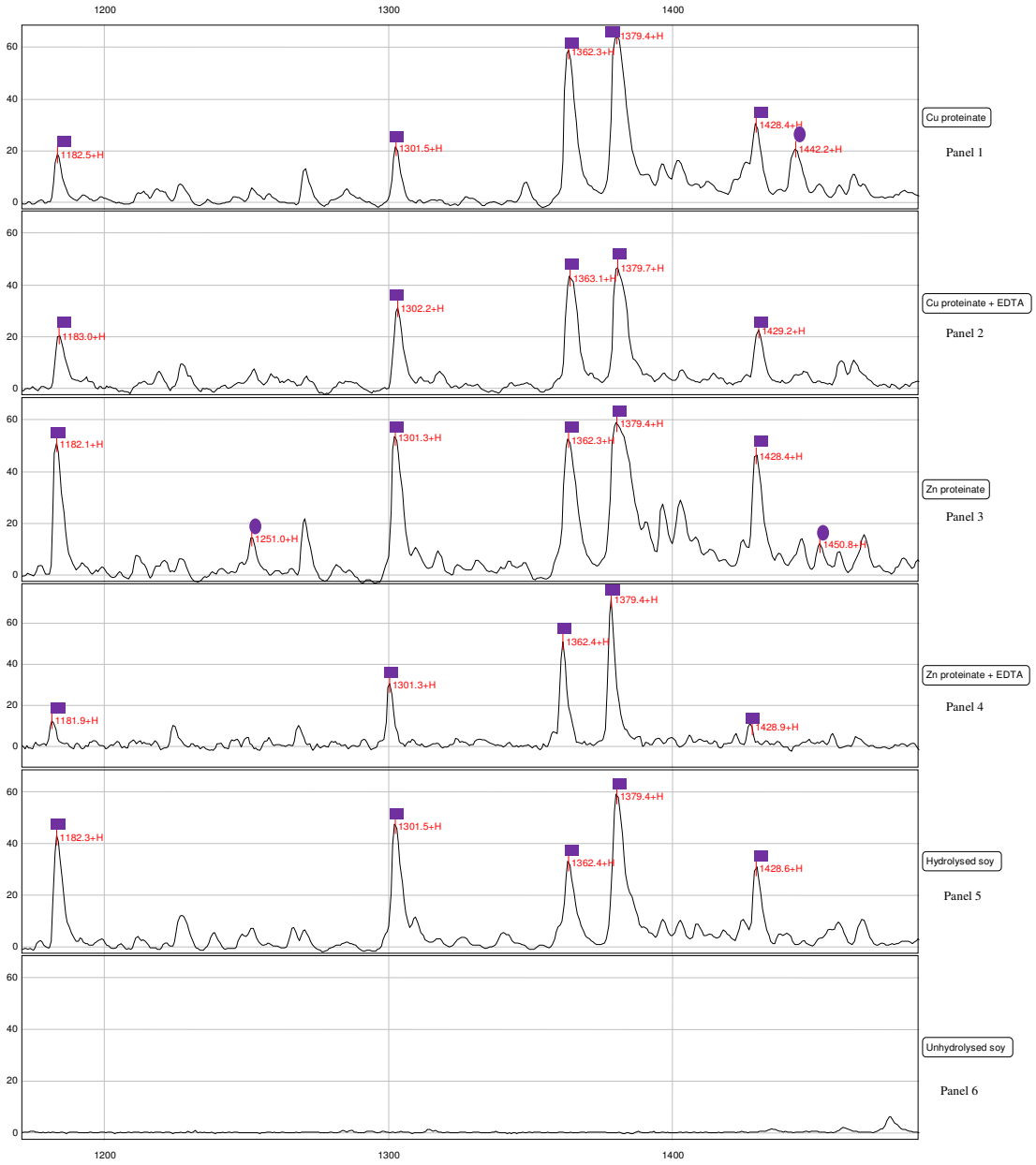

Figure 3.29 SELDI-ToF-MS spectra (1150 Da – 1370 Da) of a zinc(II) proteinate treated with EDTA (■ represent parent peptide peaks and ● refers to potential peptide-metal adducts). Zn proteinate = Panel 1, Zn proteinate + EDTA = Panel 2, Hydrolysed soy = Panel 3 and unhydrolysed soy = Panel 4. The x-axis indicates the molecular mass (Da) of the peptides and the y-axis displays the mass-to-charge ratio (m/z).

Figure 3.30 displays the molecular mass region from 1500 Da to 2000 Da. Potential peptide-metal adduct peaks are still identifiable in this region, such as the 1647.0 Da and the 1727.7 Da adducts in the spectra of the copper proteinate (Figure

3.30, Panel 1). A similar adduct was observed in the spectra of the zinc proteinate at 1651.3 Da based on the parent peptide being that of the 1581.4 Da peptide peak (Figure 3.30, Panel 3). As before, treatment with EDTA removed the metal adducts from the parent peptides and were absent from the EDTA treated proteinate spectra (Figure 3.30, Panels 2 and 4).

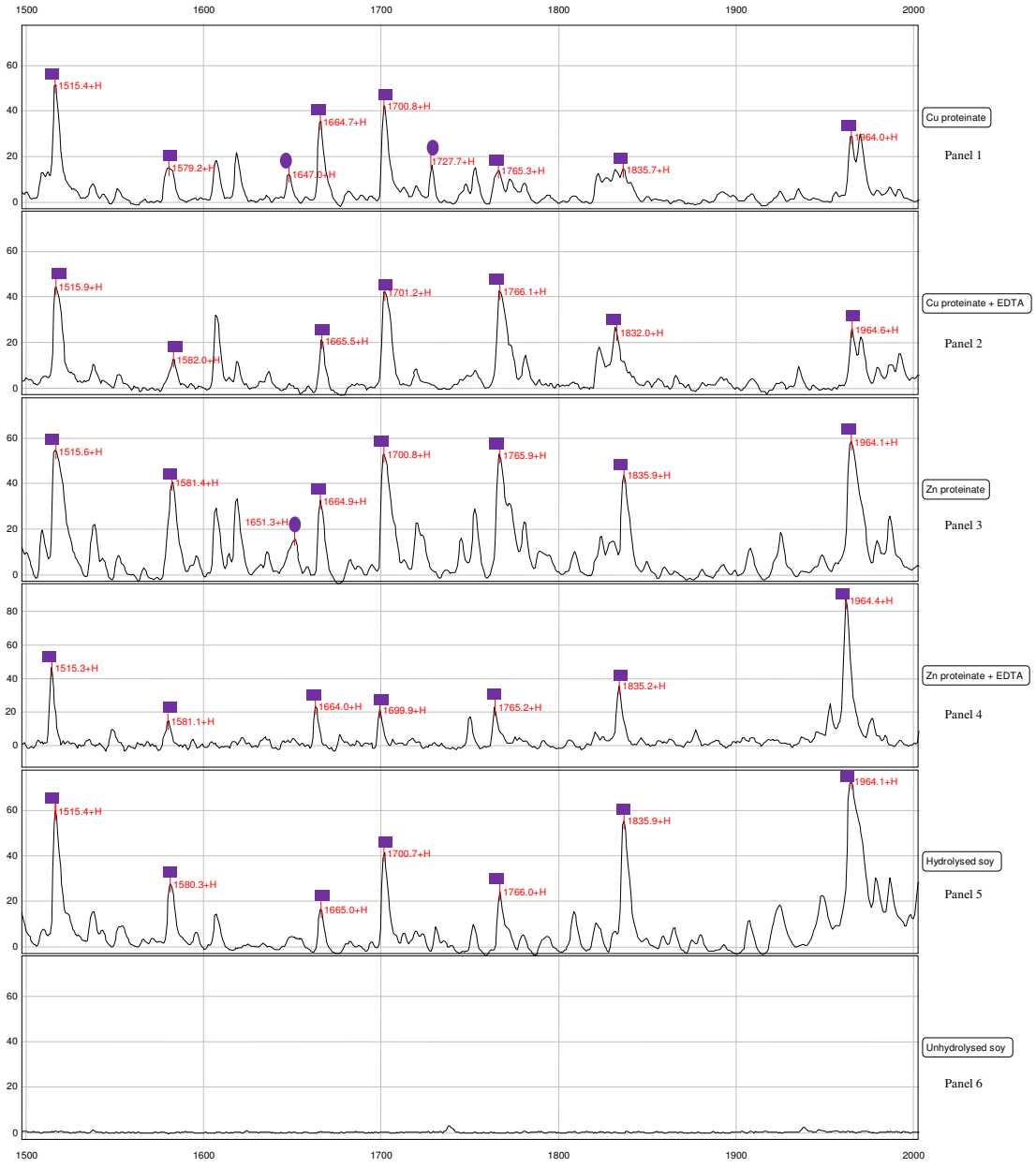

Figure 3.30 SELDI-ToF-MS spectra (1500 Da – 2000 Da) of a selection of metal proteinates and controls (■ represent parent peptide peaks and ● refers to potential peptide-metal adducts). The x-axis indicates the molecular mass (Da) of the peptides and the y-axis displays the mass-to-charge ratio (m/z).

The presence of multi-metal species is possible although this is dependent on the properties of the ligand and the number of potential binding sites for metal ions. Previously published reviews have acknowledged the formation of M_2L species (two metal ions bound to one ligand) for ligands with a range of cations at 1:1, metal:ligand concentrations (Anderegg *et al.*, 2005). A putative copper adduct was visible at 1647.0 Da which could be indicative of a M_2L species if the 1515.4 Da peptide peak is the parent peptide (Figure 3.31). Additionally, assuming the 1150 Da peak is the parent peptide, a putative adduct peak at 1347 Da could imply the presence of an M_3L species. Another example of an M_3L species may be the 1428 Da parent peptide and the 1617 Da metal adduct although further analysis is required to conclusively determine if this is the case. Potentiometric analysis has the potential to determine metal-ligand species and may provide further evidence of multi-metal species (Section 3.6).

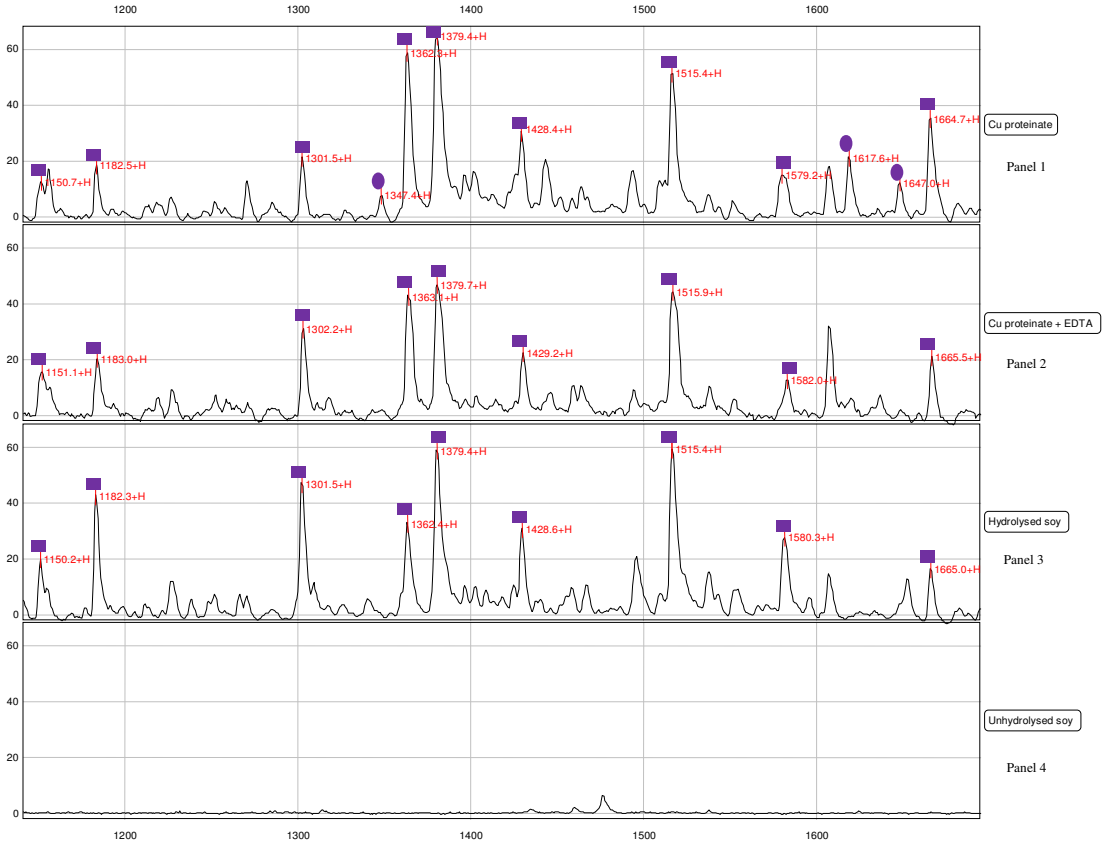

Figure 3.31 SELDI-ToF-MS spectra (1140 Da – 1700 Da) of a copper proteinate and controls (■ represent parent peptide peaks and ● refers to potential peptide-metal adducts). The x-axis indicates the molecular mass (Da) of the peptides and the y-axis displays the mass-to-charge ratio (m/z).

Due to the inconsistent response of SELDI-ToF-MS to show metal-peptide binding from a quantitative perspective, it is apparent that this method is best applied to marker peptide identification. Factors such as peak broadening or masking and the relative binding affinity of the array surface may have contributed to the difficulties in identifying clear metal-peptide adducts. From the peptide profiles acquired, peptide markers specific to the hydrolysis procedure used are readily identified using this technique. Section 3.3.6.6 describes this particular application in greater detail.

Based on the spectral results obtained (Figure 3.28), copper and zinc proteinates provided clearest spectra with respect to the visibility of peptide-metal adducts. Of these, copper proteinates were selected for further analysis. Copper proteinates, manufactured using four separate batches of soy flour, were analysed to determine consistency between the batches. A broad range of peptides less than 2000 Da in size provided signature profiles unique to the metal proteinates which indicated this mass spectrometric technique could also be applied as a quality control measure (Figure 3.32). One cannot underestimate the importance of having a reliable method to ensure a product's consistency and reliability from an industrial perspective and, based on the results obtained, SELDI-ToF-MS provides the means to obtain such results. Furthermore, SELDI-ToF-MS can provide semi-quantitative analysis with respect to metal proteinate chelation which has been difficult to ascertain using other methods. Based on the importance of metal proteinates in the feed industry, techniques that allow identification and characterisation of such products are of great importance. Further analysis of peptide-metal adducts, based on the results obtained using SELDI-ToF-MS, could provide additional information regarding the stability of the proteinates, of which little is known at the present time.

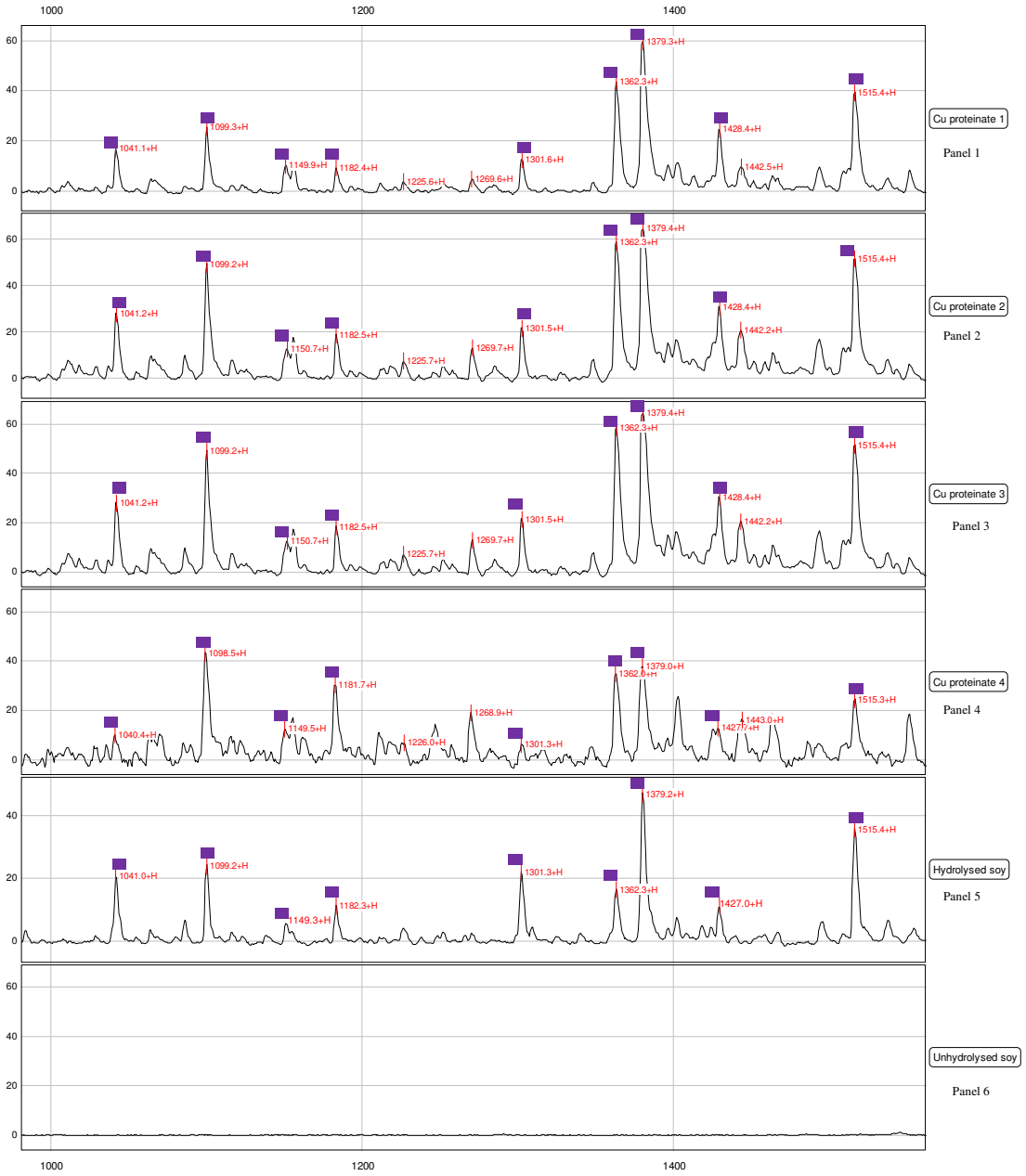

Figure 3.32 SELDI-ToF-MS sample analysis of Cu proteinate batches manufactured using four different batches of soy flour (■ indicate consistent peaks at approximately 1041 Da, 1099 Da, 1150 Da, 1182, Da, 1301 Da, 1362 Da, 1379 Da, 1428 Da and 1514 Da). The x-axis indicates the molecular mass (Da) of the peptides and the y-axis displays the mass-to-charge ratio (m/z).

Little variation was noted in the unique peptide patterns characteristic of the copper proteinates and metal specific fingerprints were clearly identified (Figure 3.32). The peptide peaks observed are identical to those seen in Figure 3.28 for the copper proteinate sample with the same potential peptide-metal adducts previously discussed. Slight differences between the observed and theoretical mass shifts for the parent peptide and adduct peaks can be justified by a number of reasons, some of which have been previously mentioned:

- Regarding the SELDI-ToF-MS calibration (Section 3.3.6.1), instrument resolution may play a part (± 1 Da)
- The molecular mass label on each peak corresponds to the average value for that peptide which can account for a few Daltons deviation
- The broadness of some of the peptide peaks would also encompass a few Daltons in range
- Metal-peptide complex formation may also play a part by displacing protons
- The mass shift is reduced by 1 Da for every proton displaced

Based on the profiles obtained in this section it was determined that only copper and zinc proteinates show clearly visible adducts. As mentioned previously, the proteinates appear to follow the trend in the Irving-Williams series which would explain the poor spectra obtained for Fe(II) and Mn(II). Later investigations into the stability of a selection of the ligands identified in Figure 3.32 may further clarify why adducts are formed with some of these particular peptides (Section 3.6).

3.3.6.6 Marker peptide identification

Analysis of the spectra obtained for each of the metal proteinates led to the identification of a pattern of peaks unique to the hydrolysis procedure employed (Figure 3.33). The highest intensity peptide peaks in all the proteinates, with the potential to form metal adducts, were identified and selected for detailed study. Matrix, pH and selectivity effects did not influence the peptide pattern and consistent peak patterns were identified in all proteinate samples using SELDI-ToF-MS. From the SELDI-ToF-MS spectra obtained using the protocol outlined in Section 2.3.3, five peptides in particular were chosen (■, Figure 3.33). The molecular masses of the five peptides were as follows: 1148 Da, 1181 Da, 1300 Da, 1428 Da and 1514 Da. Reasons for the slight variations in molecular mass between calculated and observed values were proposed earlier. The primary focus was on peptides with a molecular mass less than 2,000 Da based on the fact that the focus of this work was on short chain polypeptides in the proteinate samples which have molecular masses of less than 2,000 Da. Preliminary comparisons with other metal proteinates indicated that these 5 peptides were specific to the hydrolysis procedure described in Section 2.2.1.

Other peptide peaks could also have been chosen based on their presence in the spectra but on analysing a number of pilot scale batches kindly provided by Dr. Ronan Power (Alltech, Lexington, Ky, U.S.A.) some of the peaks are of lower intensity, possibly due to slight differences in the industrial scale-up production method (■, Figure 3.34). An example of such peptide peaks are the 1363 Da and the 1379 Da peptides which are very prominent in the laboratory manufactured samples but are of a lower intensity in the pilot scale batches although their presence was still detected using SELDI-ToF-MS.

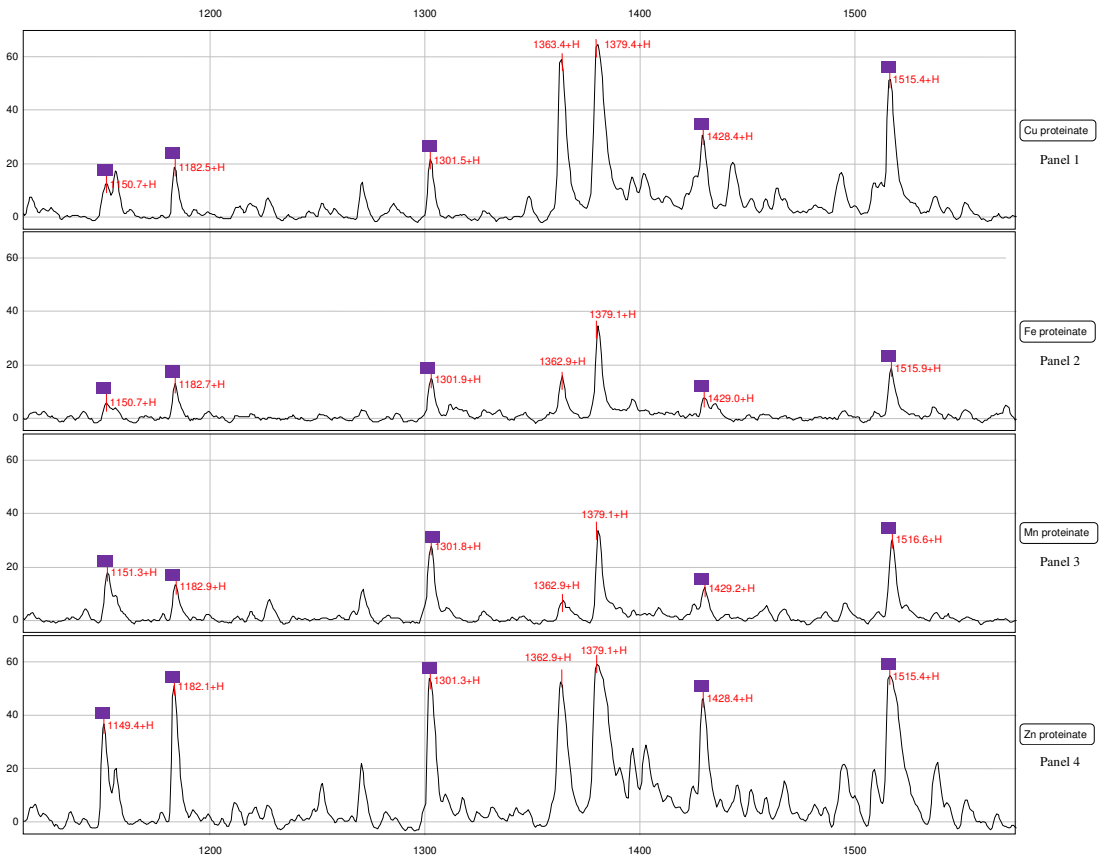

Figure 3.33 SELDI-ToF-MS spectra of the peptides of interest in laboratory manufactured metal proteinate samples (■ indicate consistent peaks at approximately 1150 Da, 1182, Da, 1301 Da, 1428 Da and 1514 Da). The x-axis indicates the molecular mass (Da) of the peptides and the y-axis displays the mass-to-charge ratio (m/z).

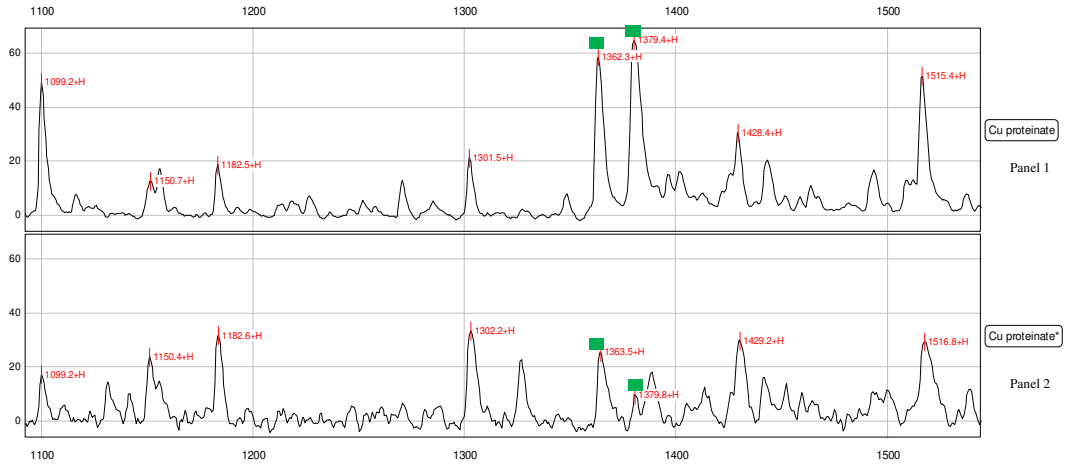

Figure 3.34 SELDI-ToF-MS spectra of copper proteinates manufactured on a pilot scale (■ refers to peaks not selected for further analysis - 1362 Da and 1379 Da). Laboratory Cu proteinate = Panel 1 and Pilot scale Cu proteinate* = Panel 2

Having clearly identifiable marker peptides in a proteinate allows for the detection of same when the product is included in a premix or in feed and can provide confirmation of inclusion which is advantageous from an industrial perspective. Based on the sensitivity of the technology with the ability to detect concentrations as low as femtomolar, SELDI-ToF-MS analysis of premixes and feedstuffs should be able to identify the markers of the metal proteinates if said proteinates are contained in the finished products.

3.3.6.7 Premix analysis

Premixes contain a multitude of constituents including vitamins, trace minerals and carrier proteins. Their purpose is to supplement feed with required levels of these ingredients to improve its nutritional quality. The ability to identify particular metal proteinates in a premix is of significant value from an industrial perspective for a number of reasons. Advantages of including trace minerals in the diet have been outlined previously (Section 1.2) and a high quality premix containing the appropriate vitamin and mineral levels can contribute significantly to improved animal health and performance. Vitamins and minerals are available in different forms and their bioavailability can vary between sources. A poor quality premix may result in poor consumer confidence, potential regulatory issues or even product recall situations.

Premix manufacturers often go to great lengths to try to differentiate their particular products from those of their competitors. The advantage of employing the method outlined in this section is that it provides the means to do this. The peptide patterns specific to a particular hydrolysis procedure as illustrated in Section 3.3.6.6 may be identified in premix samples thereby confirming the presence of a particular proteinate. This is also advantageous from a consumer perspective as it provides evidence that a certain proteinate is present in the sample. Not all metal proteinates are of the same quality and the ability to identify a particular proteinate in the premix ensures confidence in a particular brand. The method can also be used as a quality control measure to ensure consistency between batches of premixes.

Mineral free commercial premixes (Alltech Bioscience Centre, Dunboyne, Co. Meath, Ireland) were spiked with the proteinates of interest (10 % (w/w) metal content) and analysed using SELDI-ToF-MS. The inclusion levels of the proteinates in the premix samples ranged from 5 % to 10 % (w/w) (Table 3.10). Prior to applying the SELDI-ToF-MS method outlined in Section 2.3.3, the premixes were extracted for 30 minutes in distilled water before centrifugation. Analysis was carried out on the resultant supernatant.

The SELDI-ToF-MS panels shown in Figure 3.35 illustrate the consistent appearance of a number of main peaks in the premix material containing metal proteinates. Five of these marker peptides (1148 Da, 1181 Da, 1300 Da, 1428 Da and 1514 Da) are quite distinct and have the same molecular masses as those observed in earlier metal proteinate analysis (Figure 3.33). From the spectra obtained, development of a qualitative assay for the detection of metal proteinates in premix material was possible. Further optimisation was necessary to obtain spectra as sharp as those obtained for initial proteinate analysis, although the peptides of interest can be easily detected in premix samples using this method.

Table 3.10 Metal proteinate content in a selection of premix batches

Sample ID	Proteinate content (% w/w)
Premix 1	Fe proteinate (10 %)
Premix 2	Mn proteinate (10 %)
Premix 3	Zn proteinate (10 %)
Premix 4	Cu proteinate (10 %)
Premix 5	Cu proteinate (5 %)

Based on the results of previously recorded spectra (Figure 3.33), it is unsurprising that the Cu(II) and Zn(II) proteinates are most prominent due to their respective metals apparent specificity for the array surface, which in turn enables more effective peptide binding. The high intensity peaks produced allow these particular metals to be detected at lower levels in the premixes than either iron or manganese. A lower Cu proteinate inclusion level (5 % w/w) was examined in Premix 5 to determine if

proteinates with lower metal content could be detected in premix samples. The SELDI-ToF-MS results for the 5 % (w/w) copper proteinate in Panel 5 show that detection is possible at lower inclusion rates (Figure 3.35, Panel 5) but as SELDI-ToF-MS is not fully quantitative; the peak intensity cannot be taken to be a representative measure of amount.

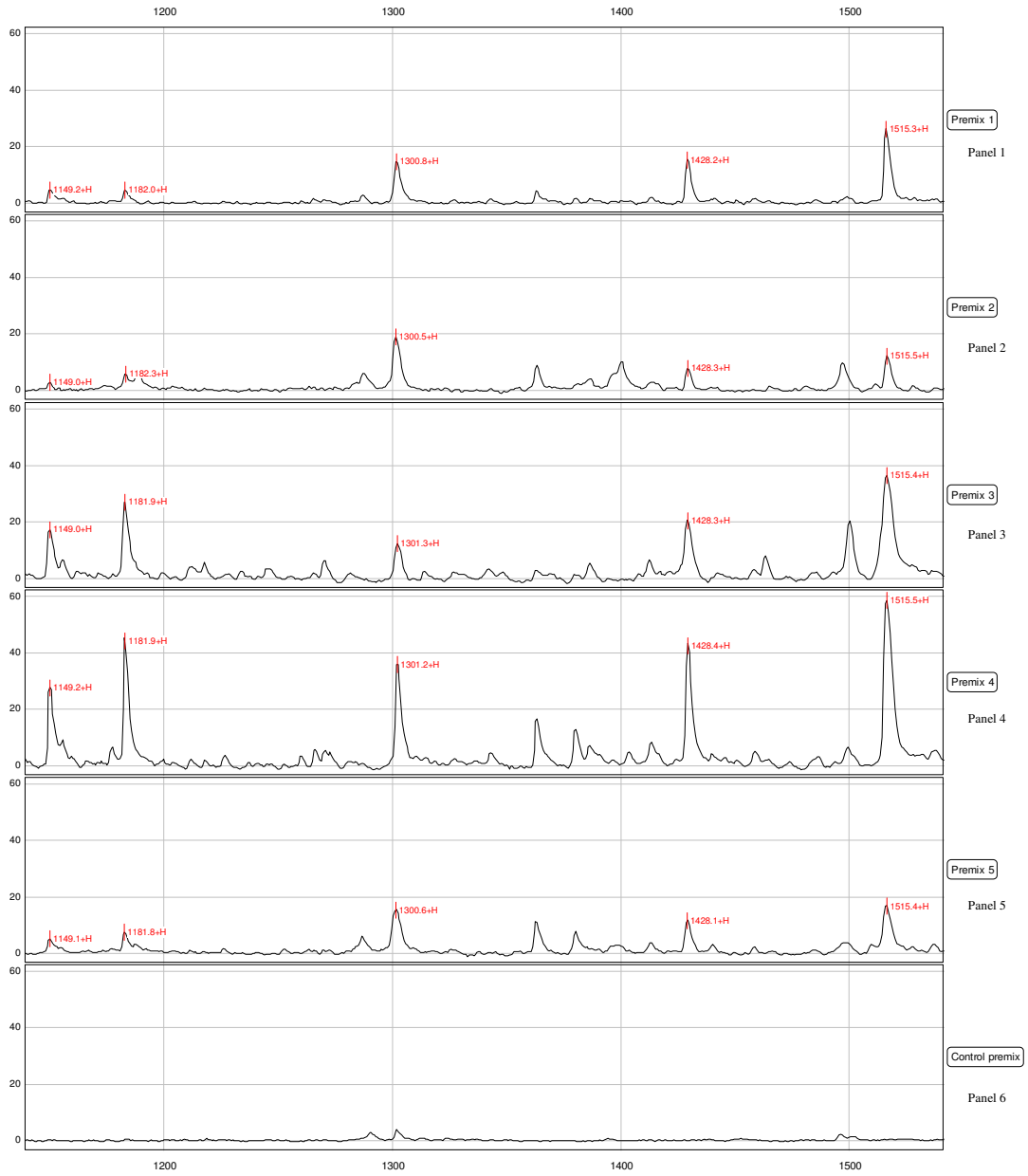

Figure 3.35 Assessment of SELDI-ToF-MS for qualitative detection of metal proteinates in premix material. The x-axis indicates the molecular mass (Da) of the peptides and the y-axis displays the mass-to-charge ratio (m/z).

An additional analysis was carried out to determine the detection limit of the copper proteinate in the premix samples (Figure 3.36). Figure 3.36 contains a representative sample of the results. From the results obtained, it can be seen that a copper proteinate can be detected in a premix sample at high intensities using this method at inclusion levels as low as 1 % (w/w). Below 1 % (w/w), detection becomes increasingly difficult although low intensity marker peptides are visible (Figure 3.36, Panel 5). The results are promising and allow progression to the next stage of analysis – detection in feed.

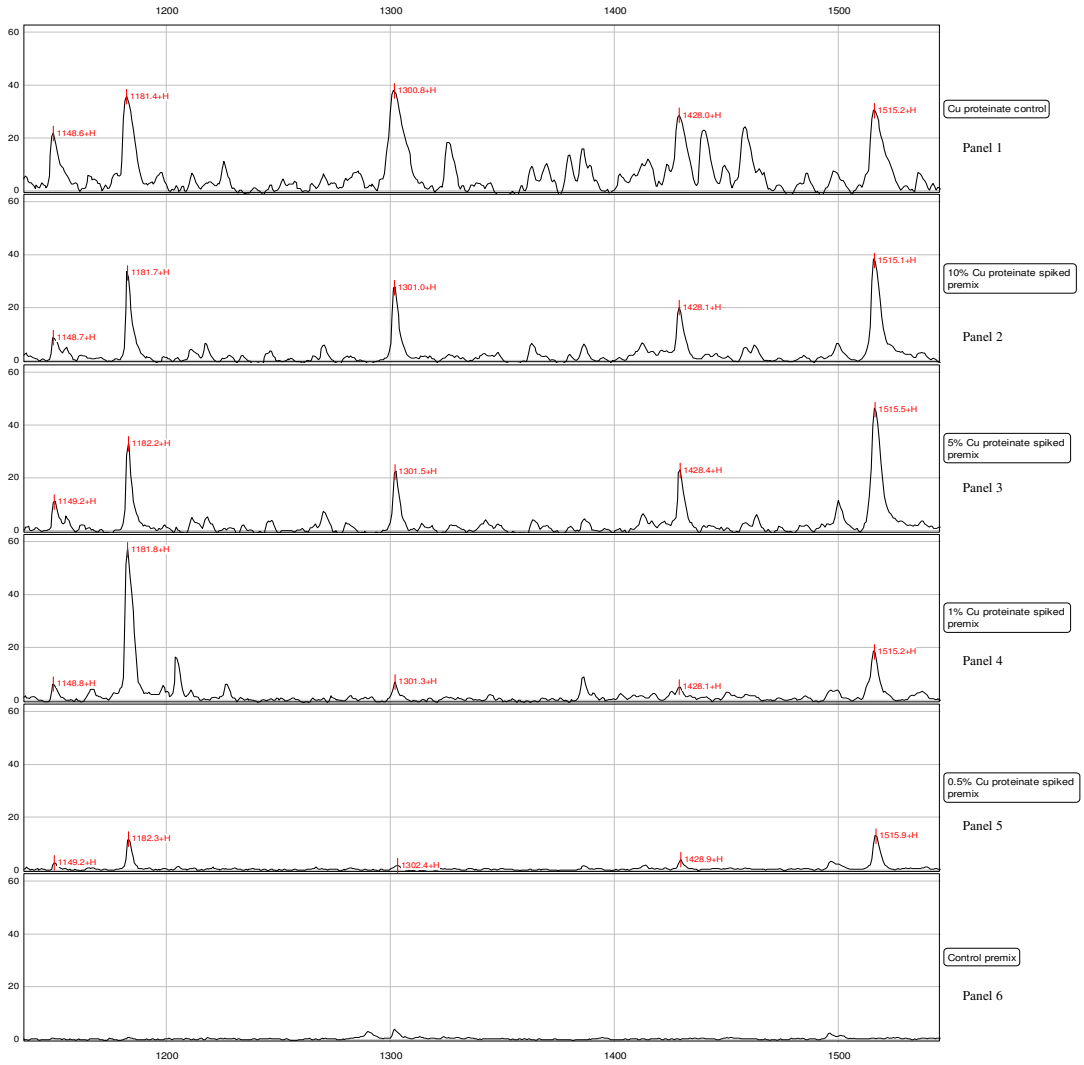

Figure 3.36 Assessment of SELDI-ToF-MS for qualitative detection of metal proteinates in premix material at a range of inclusion levels. The x-axis indicates the molecular mass (Da) of the peptides and the y-axis displays the mass-to-charge ratio (m/z).

3.3.6.8 Feed analysis

Detection of the metal proteinate products based on their respective peptide markers is much more challenging on an in-feed basis. There are numerous reasons which may explain the increased difficulty in detecting the marker peptides and their low intensities. Based on the typical inclusion levels of the mineral in feed (Table 3.11), the low concentration of the metal proteinate may be a factor. Every species requires a different inclusion rate of minerals in feed. Other parameters for determining suitable levels include the specific reason for supplementation; improved performance or supplementing a deficiency. Additionally, E.U. directives place a restriction on inclusion levels (Table 3.11).

Table 3.11 Maximum permitted metal inclusion levels in feedstuffs for producing animals

Species	Cu (mg/kg)	Fe (mg/kg)	Mn (mg/kg)	Zn (mg/kg)
Poultry	15	500	150	150
Pig	25	750	150	150
Beef	35	750	150	150
Dairy	35	750	150	200

(Data taken from: The Minerals Directory, (Ewing *et al.*, 2007))

Mineral-free commercial feed was spiked with premixes containing metal proteinates at a copper(II) inclusion level of 25 mg/kg. This particular level was chosen as it lies in the middle of the range of permitted mineral inclusion levels for a range of species. In comparison to the metal proteinate and premix spectra obtained in previous sections (Section 3.3.6.5 and Section 3.3.6.7), the peptide peaks in the feed spectra are of much lower intensity and not all of the 5 peptide peaks of interest can be easily detected (Figure 3.37). The potential peptide markers are identified (■), but due to their low intensities this method could not be confidently used for detection. The most prominent peaks present in each spectra are identified and it can be seen from Figure 3.37 that most of these peaks do not match the molecular masses of the previously identified five peptide markers (1148 Da, 1181 Da, 1300 Da, 1428 Da and 1514 Da).

Furthermore, the increased presence of low intensity peptide peaks not previously seen in the proteinate or premix samples may infer components in the feed may have prevented binding of the peptides or contributed to non-specific binding.

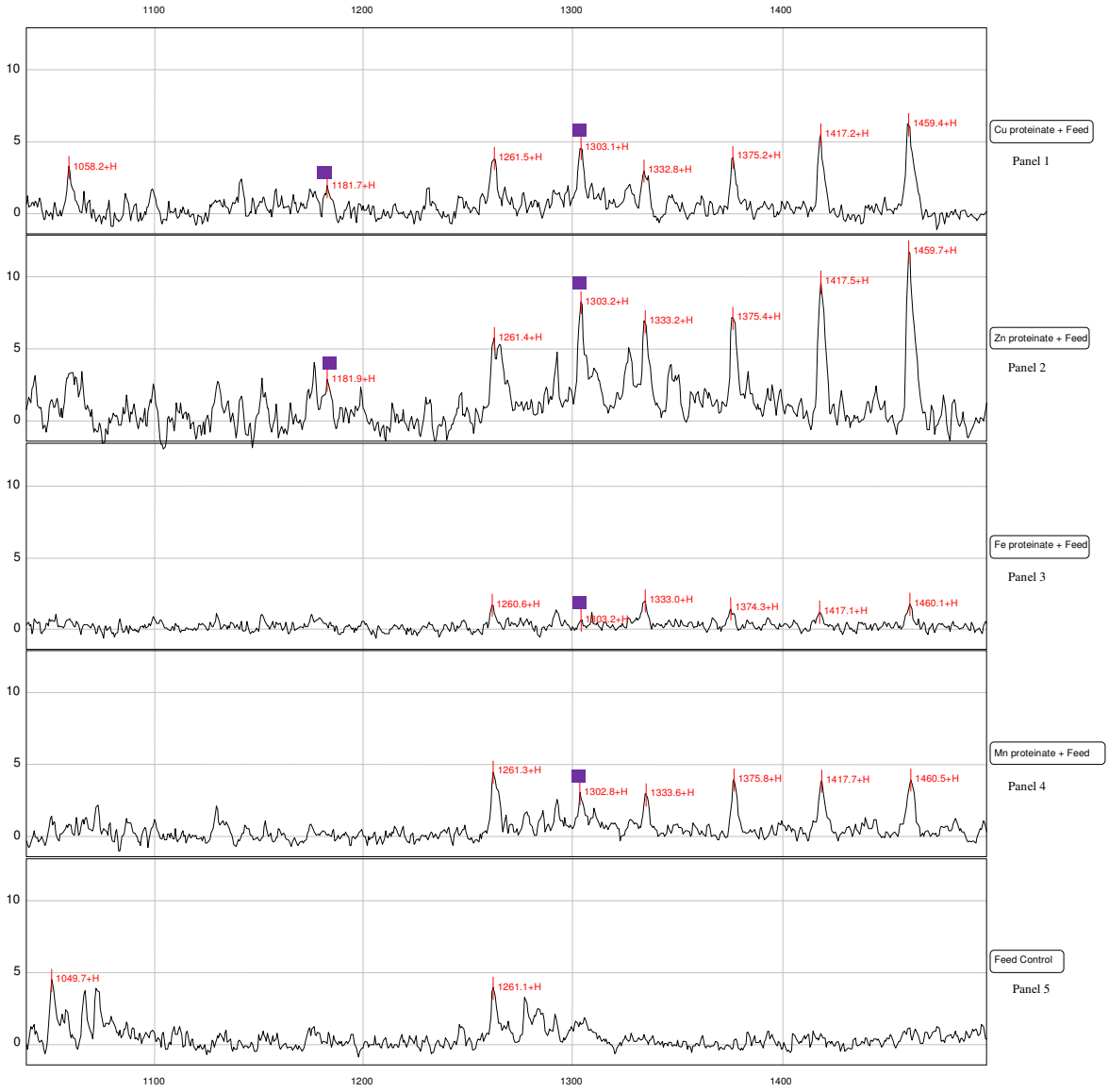

Figure 3.37 Assessment of SELDI-ToF-MS for qualitative detection of metal proteinates in feed (■ represent potential peptide markers). The x-axis indicates the molecular mass (Da) of the peptides and the y-axis displays the mass-to-charge ratio (m/z).

The qualitative procedure determined in Section 3.3.6.7 for metal proteinate detection in premix material is not suitable for in-feed detection of proteinates due to the difficulty in identifying the marker peptides. From the results obtained for the premix samples at low inclusion levels (Figure 3.36), it appears that factors such as dilution effects or inclusion levels are the primary cause of the difficulty in identifying the peptide peaks in Figure 3.37. To confirm this theory, the premix samples containing the copper(II) proteinates were analysed using SELDI-ToF-MS at levels close to those expected in feed.

The metal proteinates in this work contained 10 % copper (w/w) which is equivalent to 100 g/kg. Peptide profiles were successfully obtained for these proteinate samples using SELDI-ToF-MS (Section 3.3.6.5). Furthermore, the 10 % (w/w) metal proteinates were spiked into mineral free premixes at inclusion rates of 10 % to 0.5 % (w/w), equivalent to a copper content of 10 g/kg to 500 mg/kg in the premixes with successful detection (Figure 3.36). However, at a metal proteinate inclusion rate of 0.5 % (w/w), equivalent to 500 mg/kg Cu(II) in the premix samples, the intensities of the peptide peaks are low (Figure 3.36, Panel 5). To obtain a copper(II) inclusion level of 25 mg/kg (w/w) in feed, a further 20 fold dilution is required. The results obtained for the premix samples indicated that it was highly unlikely the marker peptides would be detected at such a low level in feed. Figure 3.38 illustrates the spectral results for the copper proteinate samples spiked into premixes at copper(II) inclusion levels of 1 g/kg, 100 mg/kg and 25 mg/kg (w/w), the latter resembling the copper(II) inclusion level of the copper proteinates in feed (Figure 3.38, Panel 3). Based on the spectra obtained, it can be clearly seen that difficulties were encountered in marker peptide detection at low inclusion levels and consequently explains why the marker peptides cannot be detected in feed.

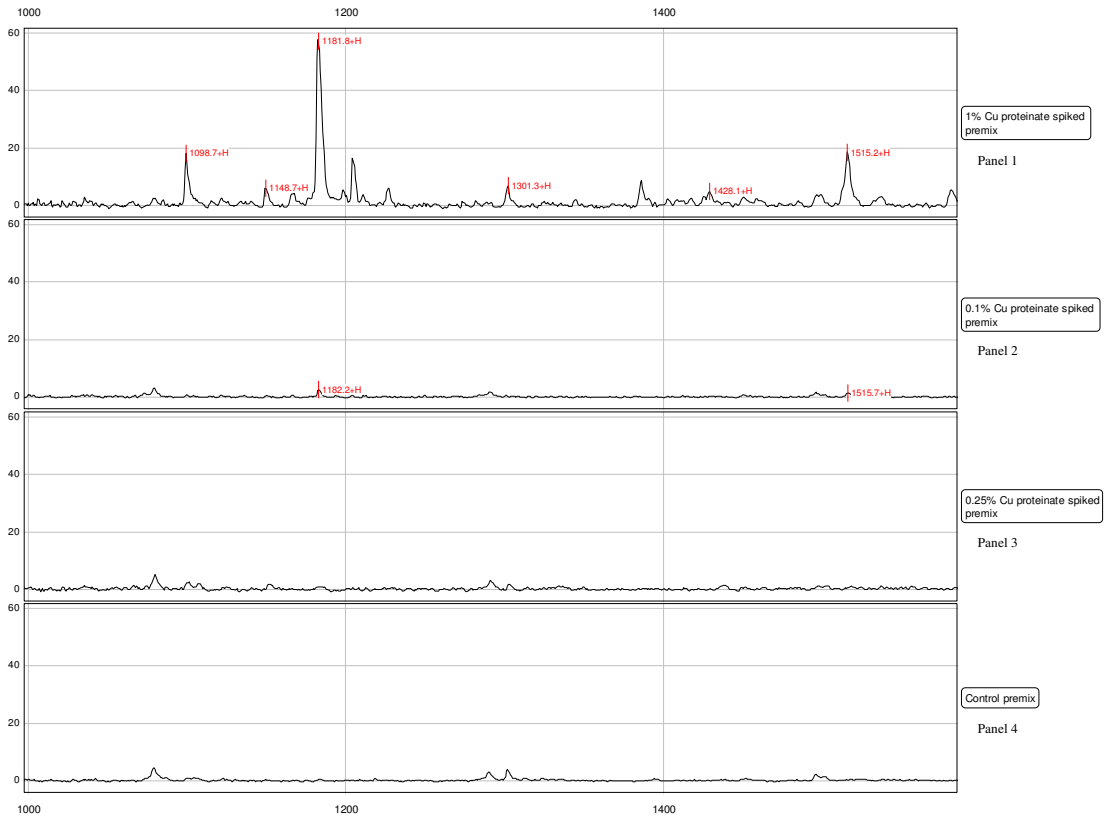

Figure 3.38 Assessment of SELDI-ToF-MS for qualitative detection of metal proteinates in premix material at low inclusion levels. The x-axis indicates the molecular mass (Da) of the peptides and the y-axis displays the mass-to-charge ratio (m/z).

Antibodies to small peptides have become an essential tool in life science research, with applications including gene product detection and identification, protein processing studies, diagnostic tests, protein localisation, active site determination, protein homology studies and protein purification (Sigma, 2000). Previously published studies have illustrated the success of employing antibodies for soy protein quantification (Medina, 1988; Macedo-Silva *et al.*, 2001; Bittencourt *et al.*, 2005).

As such, generation of antibodies towards the marker peptides was investigated to enable development of a quantitative assay sensitive enough for in-feed detection of proteinates (Section 3.5). The first step in the process was the determination of the peptide sequence for the marker peptides. Tandem mass spectrometry was selected to obtain the sequences of interest.

3.3.6.9 Tandem Mass Spectrometry (MS/MS)

To sequence the marker peptides of interest, a triple-quadrupole mass spectrometer with a time-of-flight mass spectrometer replacing the third quadrupole (QqTOF) was employed. Based on the equipment and facilities required, the majority of the tandem mass spectrometry (MS/MS) work was sub-contracted to Ciphergen Biosystems Inc. When combined with tandem mass spectrometry, ionisation methods such as SELDI-ToF-MS allow protein identification by comparing partial amino acid sequences obtained with the protein database for that organism. The sequences obtained could then be used for further characterisation of the metal proteinates using techniques such as Enzyme Linked Immunosorbent Assays (ELISAs) (Section 3.5) and potentiometry (Section 3.6)

A useful secondary application of MS/MS was to verify that the peptide sequence was consistent and that changes in the metal proteinate production process over a range of batches did not result in significant differences in the peptide sequence.

Using the protocol outlined in Section 2.3.3 for the preparation of metal proteinates for SELDI-ToF-MS analysis, CM10 arrays were spotted with the prepared proteinate solution and a 20 % alpha-cyano-4-hydroxycinnamic acid (CHCA) matrix. The tandem mass spectrometer had a SELDI-ToF-MS user interface and the sequencing process was carried out from the peptides on the surface of the array. As mentioned in Section 3.3.6.2, CM10 arrays are commonly used for MS/MS as a broad range of peptides can be detected using these arrays. Although IMAC30 arrays provided the clearest intensity SELDI-ToF-MS peaks for the metal proteinates, the selectivity of the array can be too high to obtain information on the large amount of peptides present in the samples. Successful sequencing was carried out on the metal proteinates using the CM10 arrays.

Prior to carrying out MS/MS analysis, the metal proteinates were subjected to filtration using a 10 kDa membrane to remove high molecular mass proteins allowing lower molecular mass peptides to be detected with greater ease. The result of the initial MS/MS analysis using a CM10 array on the resultant filtrate is shown in Figure 3.39. The 1148 Da, 1181 Da, 1300 Da and 1514 Da marker peptides can be seen in the filtrate

spectrum and tandem MS was successfully carried out on these particular marker peptides (Figures 3.40 – 3.43). The fifth peptide selected for sequencing was the 1428 Da marker peptide however issues were encountered with regards to obtaining a sequence for this peptide.

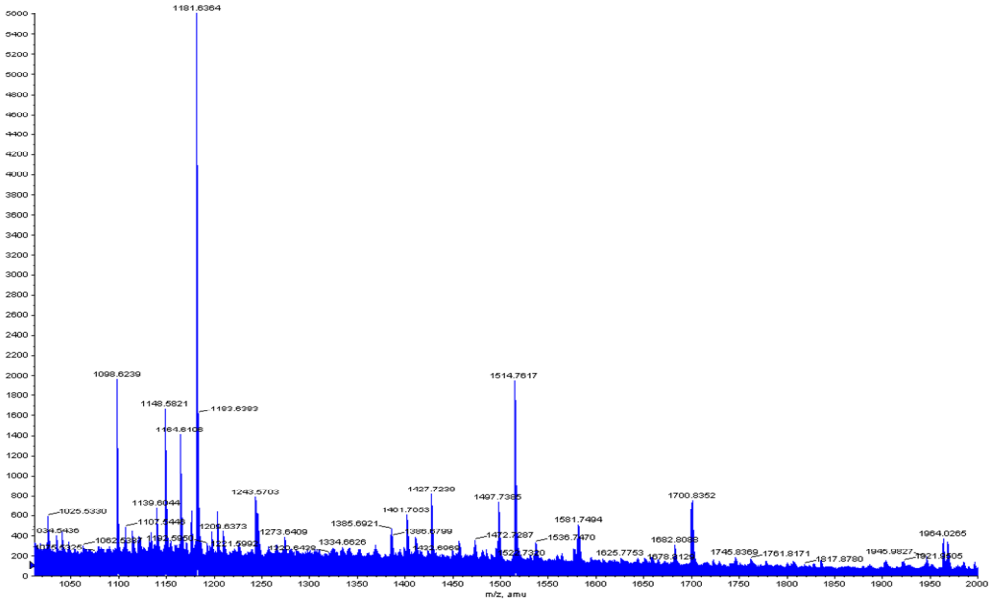

Figure 3.39 Tandem MS spectra of a copper proteinate sample

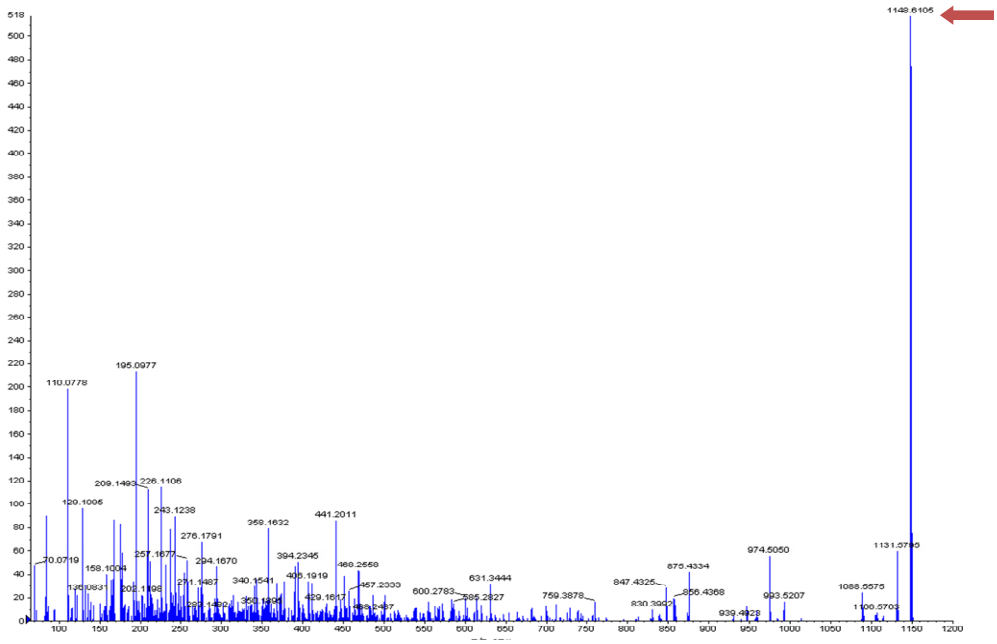

Figure 3.40 Tandem MS spectra of the 1148 Da marker peptide

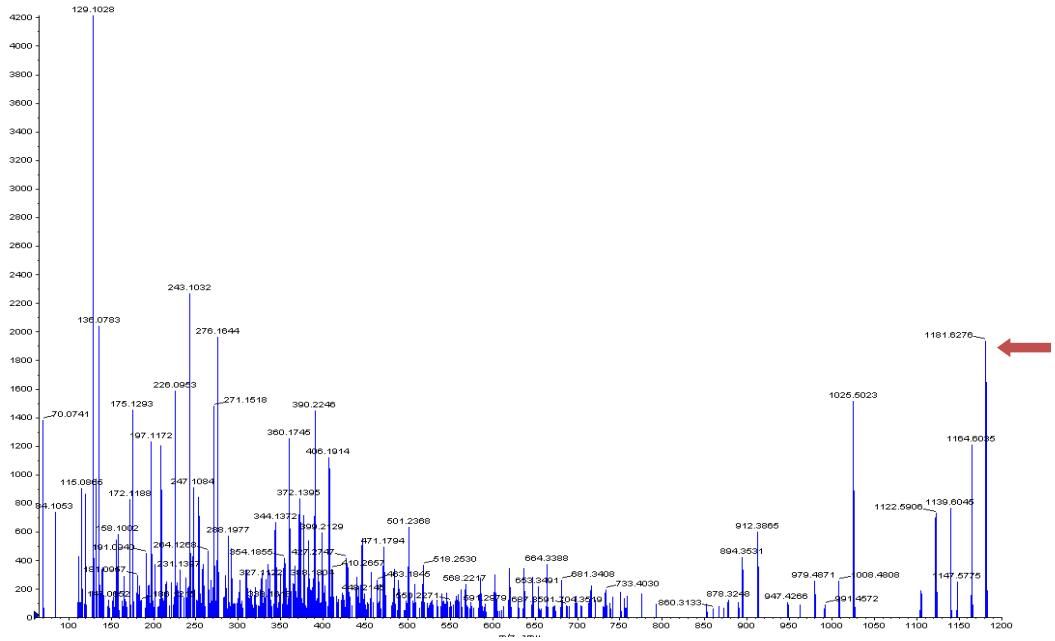

Figure 3.41 Tandem MS spectra of the 1181 Da marker peptide

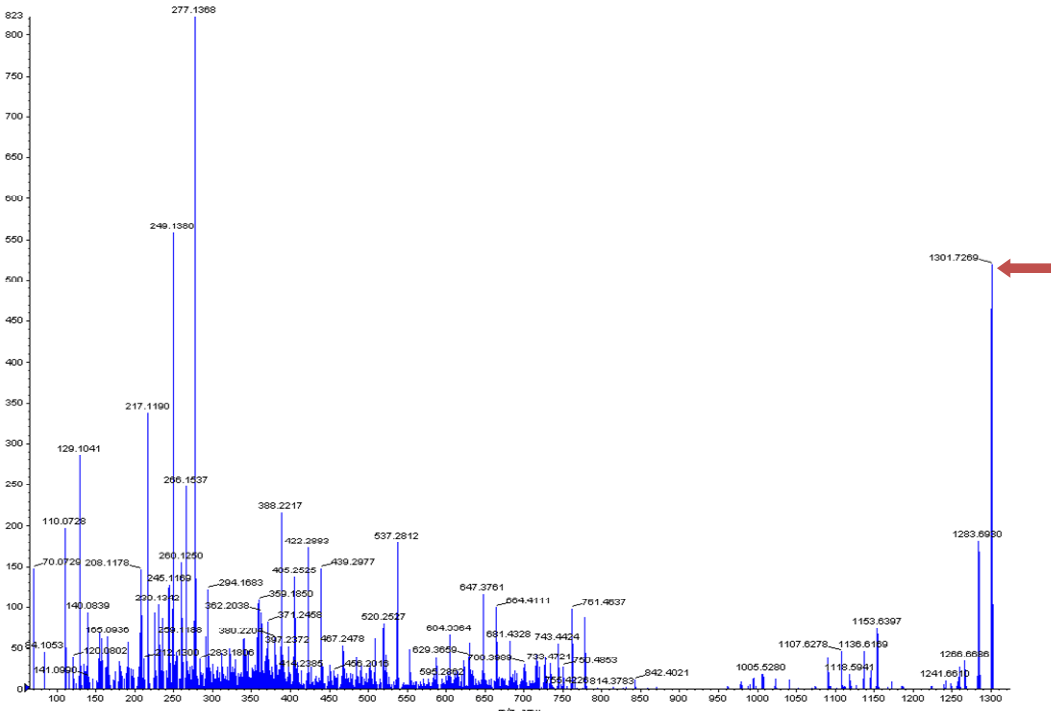

Figure 3.42 Tandem MS spectra of the 1300 Da marker peptide

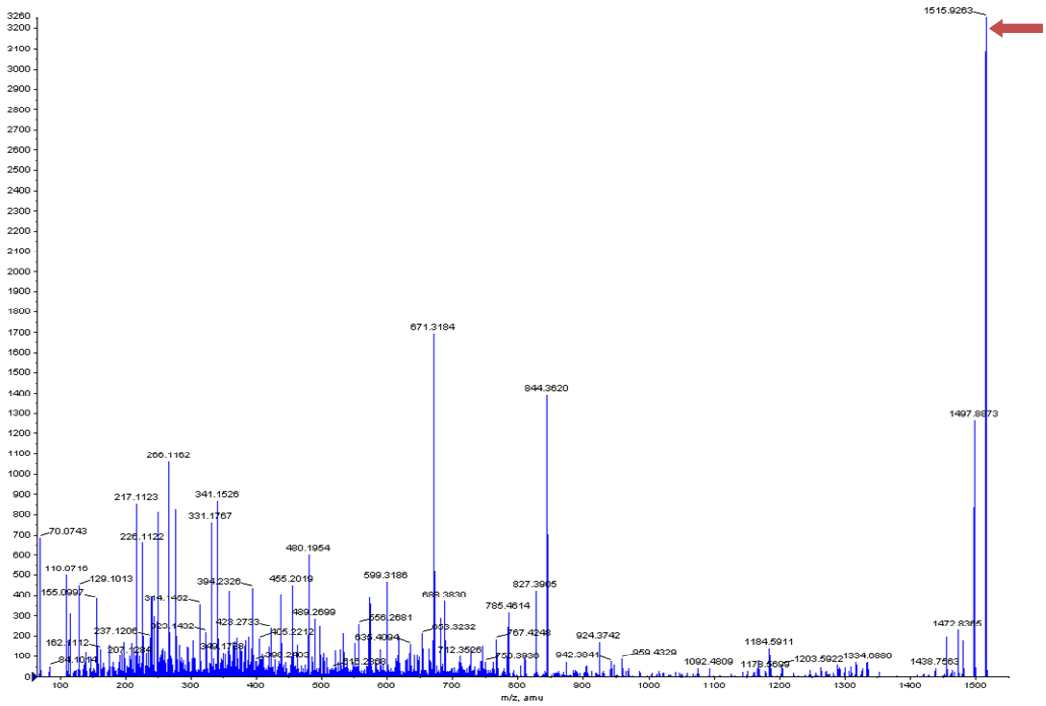

Figure 3.43 Tandem MS spectra of the 1514 Da marker peptide

Sequences were obtained for four of the five marker peptides (Table 3.12a) but multiple batches were not analysed using MS/MS. Due to the high costs involved in sequencing the metal proteinates, only the 1300 Da peptide was chosen to determine the presence of a marker peptide in a selection of the proteinates (Table 3.12b) although the other marker peptides are clearly present in the SELDI-ToF-MS spectra. Once the sequences were obtained for the four marker peptides of interest (Table 3.12a), synthetic peptides were produced for further research; employing techniques such as SELDI-ToF-MS (Section 3.4), ELISA (Section 3.5) and potentiometry (Section 3.6).

Table 3.12a Tandem MS sequencing results for the marker peptides in the metal proteinate samples

Peptide mass (Da)	Sequence
1148	FKNQYGHVR
1181	FKNQYGRIR
1300	RHKNKNPFLF
1514	SSRPQDRHQKIY

Table 3.12b Tandem MS sequencing results of the 1300 Da marker peptide in a selection of metal proteinates

No.	Sample. ID	M.W	Sequence	Description
1	Cu proteinate	1300.7	R.RHKNKNPFLF.G	GLCA SOYBN
2	Cu proteinate	1300.7	R.RHKNKNPFLF.G	GLCA SOYBN
3	Cu proteinate	1300.7	R.RHKNKNPFLF.G	GLCA SOYBN
4	Cu proteinate	1300.7	R.RHKNKNPFLF.G	GLCA SOYBN
5	Fe proteinate	1300.7	R.RHKNKNPFLF.G	GLCA SOYBN
6	Fe proteinate	1300.7	R.RHKNKNPFLF.G	GLCA SOYBN
7	Fe proteinate	1300.7	R.RHKNKNPFLF.G	GLCA SOYBN
8	Fe proteinate	1300.7	R.RHKNKNPFLF.G	GLCA SOYBN
9	Zn proteinate	1300.7	R.RHKNKNPFLF.G	GLCA SOYBN
10	Zn proteinate	1300.7	R.RHKNKNPFLF.G	GLCA SOYBN
11	Zn proteinate	1300.7	R.RHKNKNPFLF.G	GLCA SOYBN
12	Zn proteinate	1300.7	R.RHKNKNPFLF.G	GLCA SOYBN
13	Mn proteinate	1300.7	R.RHKNKNPFLF.G	GLCA SOYBN
14	Mn proteinate	1300.7	R.RHKNKNPFLF.G	GLCA SOYBN
15	Mn proteinate	1300.7	R.RHKNKNPFLF.G	GLCA SOYBN
16	Mn proteinate	1300.7	R.RHKNKNPFLF.G	GLCA SOYBN

The results shown in Table 3.12b verify the identity of the peptide as that of conglycinin-A from soy and also confirm that the 1300 Da peptide is consistent between individual proteinate batches. Tandem MS spectra, from which confirmatory peptide sequencing results of the 1300 Da marker peptide were obtained using two databases ProFound (Zhang *et al.*, 2000) and Mascot (David *et al.*, 1999), were previously illustrated in Figures 3.39 and 3.42.

3.4 Synthetic peptide analysis

Using the sequences obtained from tandem mass spectrometry for the marker peptides, synthetic peptides were generated (GenScript USA Inc., New Jersey, U.S.A.). SELDI-ToF-MS was used to obtain spectra of the synthetic peptides to confirm the molecular masses agreed with those of the original marker peptides. Additionally, the purity of the synthetic peptide was determined using SELDI-ToF-MS. If the synthetic peptide was 100 % pure, only a single peptide peak would be visible in the SELDI-ToF-MS spectra.

To determine if the synthetic peptides could display properties similar to those of the marker peptides on which they were based, the metal proteinate mimic experiment (Section 3.3.6.4) was repeated. Replacing ranatensin, a polypeptide with similar physical characteristics to the 1300 Da peptide such as sequence length and molecular mass, by the 1300 Da synthetic peptide and repeating the procedure outlined in Section 3.3.6.4 for ranatensin and EDTA (Figure 3.23) successfully showed copper binding to the synthetic peptide and removal of the copper by the EDTA treatment (Figure 3.44) thereby confirming the similarities of the synthetic and native peptides. The 1363.5 Da peak is only present on addition of Cu and it disappears on addition of EDTA indicating the metal is stripped from the peptide.

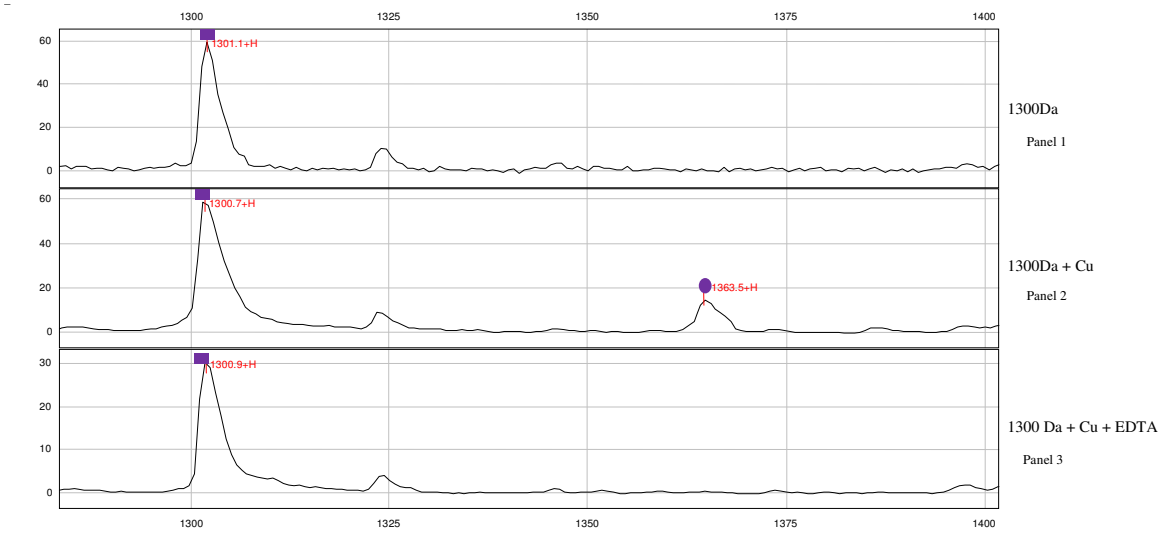

Figure 3.44 Analysis of the 1300 Da synthetic peptide using SELDI-ToF-MS (■ represent parent peptide peaks and ● refers to potential peptide-metal adducts). 1300 Da peptide = Panel 1, 1300 Da-Cu = Panel 2 and 1300 Da-Cu- EDTA = Panel 3

A similar impurity to that previously seen in the ranatensin spectra (Figure 3.23) was observed in the spectra of the 1300 Da synthetic peptide (Figure 3.44). The presence of a peak at approximately 1323 Da, a difference of approximately 23 Da from the parent 1300 Da peptide peak may be indicative of the presence of sodium (Na) which has an atomic mass of 23. Regardless of the impurity present, the presence of a copper adduct at 1363.5 Da is clearly visible in the second panel of Figure 3.44 as is its removal on treatment with EDTA in the third panel.

3.5 Antibody assay

Due to increasing stringency of legislative and regulatory requirements in the animal feed industry, the ability to detect and quantify products such as metal proteinates in feedstuffs is advantageous. In addition, development of such an assay system would further build and maintain confidence in a product.

The initial development of an assay for the detection and quantification of marker peptides in feed was based on the use of antibodies. Due to the high costs associated with antibody generation only the 1300 Da peptide, which appeared to be the most prominent marker peptide, was selected for examination. A synthetic peptide, based on the sequence results obtained from tandem mass spectrometry, was used to generate protein-reactive antibodies. This approach involved synthesising the 1300 Da peptide sequence, coupling the synthetic peptide to a large carrier molecule, and immunising the animal of choice with the peptide-carrier molecule. Conjugation to a carrier protein is important because peptides are small molecules that alone do not tend to be immunogenic, thus possibly eliciting a weak immune response (Sigma, 2000). The most commonly selected carriers are keyhole limpet hemocyanin (KLH) and bovine serum albumin (BSA). The 1300 Da peptide was successfully synthesised but conjugation to KLH for immunisation resulted in an insoluble peptide. However, when BSA was used as a conjugation partner, a soluble peptide conjugate was obtained. Due to facility and license requirements, the monoclonal antibody generation was sub-contracted to Fusion Antibodies Ltd., Belfast, N. Ireland.

Figure 3.45 outlines the procedure employed in this work based on a modified Enzyme Linked Immunosorbent Assay (ELISA) method (Medina, 1988) and illustrates the theory behind the assay. In brief, the marker protein is bound to the microtitre plate and unoccupied sites are blocked. The primary antibody which is specific for the marker protein in question is added and should bind to the protein. A secondary antibody is then added followed by a substrate and a colourimetric reaction is observed.

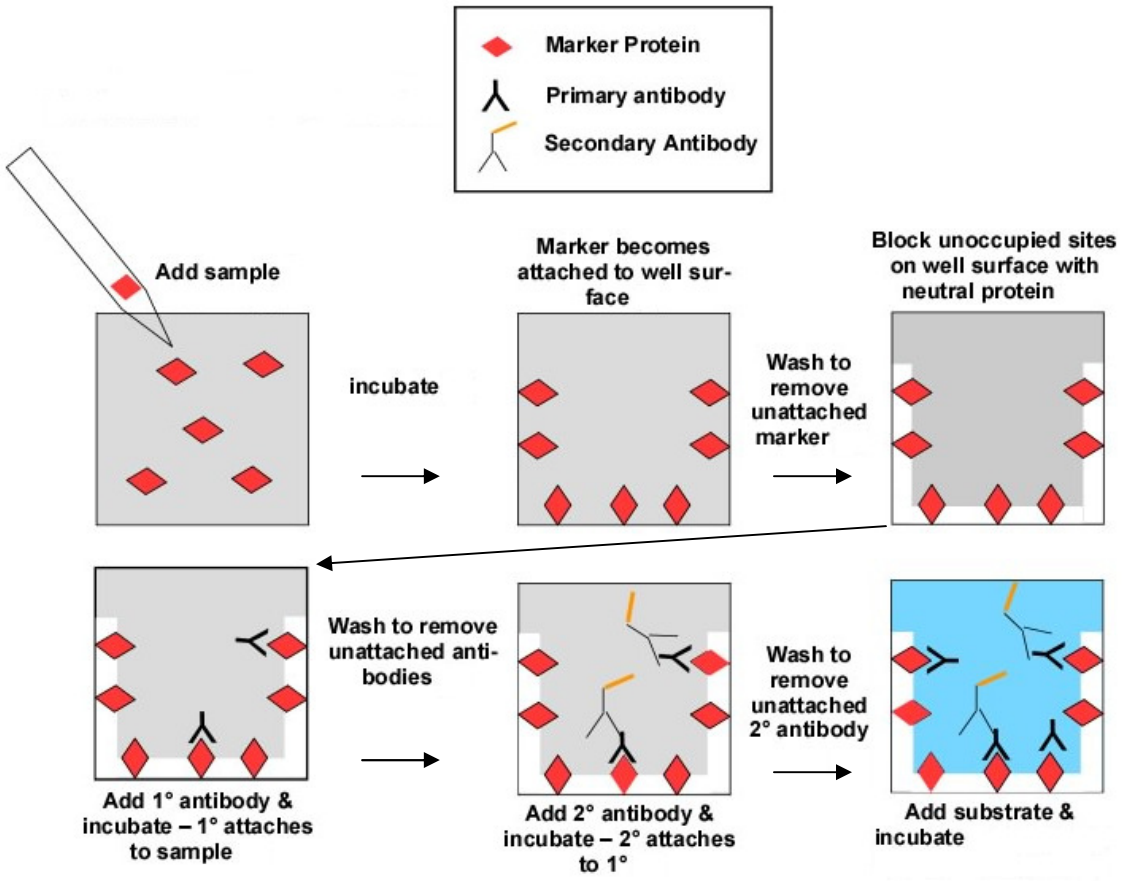

Figure 3.45 Schematic diagrams outlining an ELISA method
Adapted from http://entomology.tfrec.wsu.edu/VPJ_Lab/images/indirect_elisa.jpg

Enzyme-Linked Immunosorbent Assays (ELISAs) which tested the specificity of the antibodies (1H5 and 1E2) to the 1300 Da synthetic peptide were successful and a standard curve (0.07 to 5 mg/mL) was obtained (Figure 3.46).

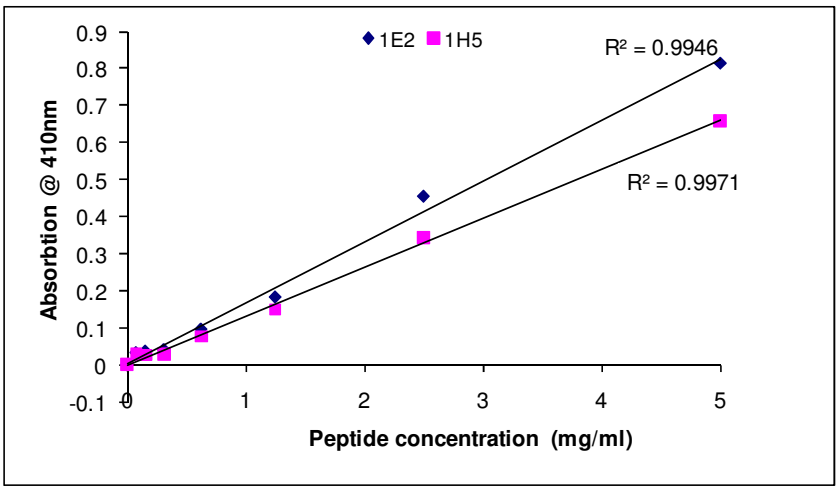

Figure 3.46 Standard curve of antibodies 1E2(♦) and 1H5(■) raised against the 1300Da synthetic peptide

Two antibodies (1E2 and 1H5) were selected to determine their specificity to the 1300 Da synthetic peptide and standard curves were successfully obtained for each (Figure 3.46). Once the specificity of the antibodies to the 1300 Da synthetic peptide had been successfully demonstrated, the method was applied to hydrolysed soy and metal proteinate samples to investigate whether the antibodies were specific to the 1300 Da native peptide.

Little or no absorbance was observed in ELISAs for hydrolysed soy samples and metal proteinates containing the 1300 Da native peptide (Figure 3.47). Several reasons can be postulated for the low absorbance observed. Anti-peptide antibodies will always recognise the peptide. However, the same antibody may not recognise the sequence within the folded intact protein (Sigma, 2000). The ability of anti-peptide antibodies to recognise the native protein depends on whether the peptide sequence displayed on the surface of the native protein is in a conformation similar to that found in the peptide-carrier protein conjugate. A denaturation step which would alter the secondary and tertiary structures but leave the peptide bonds between the amino acids intact was carried out prior to ELISA analysis in an attempt to aid detection. Heat and dithiothreitol (DTT) were used in an attempt to denature the antigen containing metal proteinates. DTT was chosen as it is a strong reducing agent which is frequently used to cleave the disulfide bonds of proteins (Cleland, 2002). In Figure 3.47 it can be seen that the 1HS antibody clearly shows specificity to the 1300 Da synthetic peptide but not to

hydrolysed soy or metal proteinates containing the native 1300 Da peptide. Furthermore, denaturing the samples appears to reduce the absorbance values of the 1300 Da synthetic peptide and detection of the antigen containing metal proteinates was still unsuccessful.

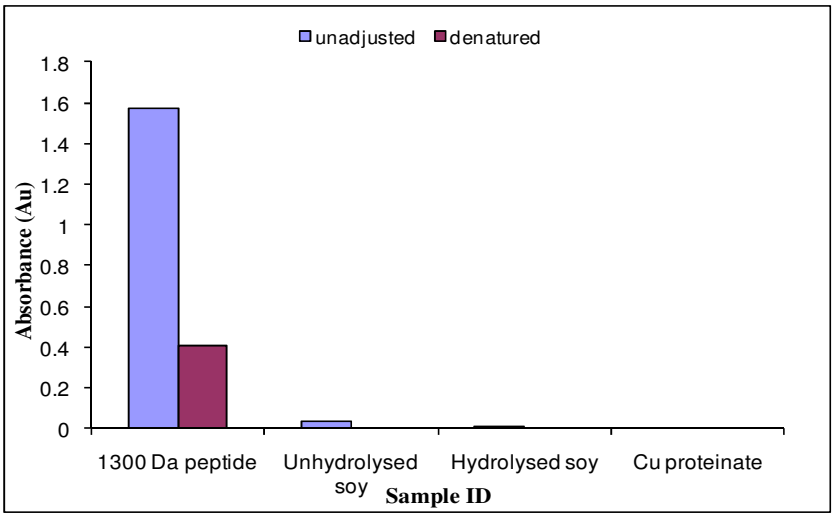

Figure 3.47 ELISA of synthetic (1H5) and native antigen containing samples and an unhydrolysed soy control

Another possible reason for the low absorbance observed may be due to interferences from the secondary antibody or other peptides in the hydrolysed soy and metal proteinate samples which may hinder antigen detection. To eliminate the possibility of any interference from the secondary antibody, an ELISA was run in the absence of the primary antibody. No absorbance was detected thus confirming the secondary antibody was not interfering with the assay and that it could be used without problems.

A third possible reason may involve the concentration of the antigen in the proteinate samples. The 1300 Da peptide may only represent a tiny fraction of the entire protein. Chessboard titrations are often employed to determine the optimum concentration of antigen to coat plate wells in addition to determining the optimum dilution of enzyme-linked antibody. The basis of this assay is to dilute the antigen across the plate one way and then dilute the conjugate across the plate the opposite way to the antigen obtaining a chessboard titration of antigen against conjugate. Thus, the colour

developing in each well depends on (a) the amount of antigen and (b) the amount of conjugate that has bound to the antigen (Crowther, 1995). Chessboard titrations were carried out to try to detect the 1300 Da peptide in the metal proteinates over a wide concentration range but no absorbance was detected at any concentration of antigen and antibody.

The limit of detection (LOD) of an individual analytical procedure is the lowest amount of analyte in a sample which can be detected but not necessarily quantitated as an exact value (ICH, 1995). Several approaches for determining the LOD are possible, depending on whether the procedure is instrumental or non-instrumental. These include determination based on visual evaluation, signal-to-noise ratio and the standard deviation of the response and the slope of the standard curve (ICH, 1996). Based on the method employed in this work, visual evaluation was relied upon. The undiluted concentration of synthetic peptide analysed was 2.4 mg/well. The peptide could be diluted 128-fold to a concentration of 18.75 μg/well and a colorimetric reaction could still be visually observed. From the ELISA results obtained, the 1:128 synthetic peptide dilution factor was chosen for a theoretical calculation as it was the lowest concentration to give a visible colorimetric reaction. This dilution factor would give a detection limit of 18.75 μg/well. This suggest that the level of the native 1300 Da peptide in the metal proteinate samples must be lower than this value and is therefore not being detected.

The particular batch of soy flour used in this work is known to contain 51.9 % crude protein (Table 3.1). A ratio of 1:5, soy:water is used during the hydrolysis procedure resulting in a protein content of 8.65 % protein. Formation of the proteinates uses approximately 60 % of the hydrolysate with the remainder consisting of the metal of choice. This gives a final protein content of approximately 5.19 %. However, the 1300 Da peptide will only represent a minor fraction of this 5.19 %.

On examination of the results for the synthetic peptide, it was concluded that a peptide concentration of 18.75 μg/well can be visually detected. Since 100 mg of the copper proteinate is present per well, which is equivalent to a total protein concentration of 5.19 mg/well, the 1300 Da peptide would need to consist of at least 0.36 % of the total protein in order to be detected. The fact that the 1300 Da peptide is not detected would indicate that a significantly lower percentage of the total protein consists of the

1300 Da native peptide, possibly less than 0.1 % and is therefore below the current level of detection.

Although ELISAs have been widely used for detection of a wide selection of antigens under various conditions, this particular method was unsuitable for use in this work. Alternative methods were investigated to characterise the metal proteinates further and to determine their suitability in feedstuffs.

Potentiometry provided the means to do this. A significant section of work involved ion-selective electrode (ISE) titrations to determine the presence of metal ions in the proteinates, the stability of the complexes formed, the effect of pH on stability and the proportion of free metal over a wide pH range for a selection of metal proteinates.

3.6 The use of potentiometry and ISE titrations to determine stability constants.

A considerable amount of information was obtained using the techniques outlined in previous sections which aided metal proteinate characterisation. Potentiometry was selected as an additional technique to complement some of the methods already employed in addition to providing further information on the stability of the metal proteinates and postulating some of the metal-ligand species present.

In Section 3.3.2, the total metal content of the proteinates was determined using Flame Atomic Absorption Spectrometry (FAAS) and found to be approximately 10 % (w/w). An ion selective electrode measures only free metal ions, the ones not bound but free in solution. If a solution contains for example, 10 % metal, determined by atomic absorption, and very little of this 10 % is free, (say 2 %), as determined by the ion selective electrode, then one can be reasonably confident that the metal is still bound to its ligand. On the other hand, if the ion electrode reveals a considerable portion of the metal as free, there is an indication of inadequate binding of metal and protein, and there is justification in being sceptical of the degree of chelation of the metal and the stability of the complex (Leach *et al.*, 1997).

Band shifts in FTIR spectra and identification of potential peptide-metal adducts by SELDI-ToF-MS provided evidence of complexation. Potentiometric analysis in conjunction with Hyperquad, a computer program used to determine stability constants from titration data (Gans *et al.*, 1996), may provide further insight into the metal peptide adducts mentioned in section 3.3.6.5 by identifying species also observed in the SELDI-ToF-MS spectra.

Potentiometric titrations with an ion-selective electrode (ISE) were also used to evaluate apparent stability constants for metal-ligand interactions. The stability constant of a complex, which is the equilibrium constant for its formation from the component parts, gives an indication of how strongly the ligands coordinate to the metal. A relatively high stability constant indicates a stable complex in which the ligands are not displaced to any significant extent in solution. However, in many cases the stability constants of complexes are quite low, which means they can be difficult to isolate and, in solution, there may be a mixture of complex species present.

Experimental work in this section of the project included:

- Investigation of the suitability of a Cu(II) ion selective electrode for monitoring the concentration of Cu(II) ions for a selection of Cu(II)–ligand titrations.

- Determination of stability constants for Cu(II)-amino acid complexes and assessment of the accuracy of the experimental procedure through comparison with published values.

- Application of the technique to study interactions between Cu(II) ions and peptides and to determine their apparent stability constants.

- Determination of the relative proportion of free copper over a wide pH range in a selection of test samples and analysis of the effect of selective pH adjustment during manufacture on overall metal chelate stability.

Since quantitative investigations of metal proteinates as well as of the pure ligands themselves have not been previously described in the literature, the applications, success and limitations of this study represent a new area in stability constant determinations.

Ion-selective electrodes are robust and durable and are relatively inexpensive to use. Other advantages include their applicability to a wide range of analyses and their ease of use (Rundle, 2005).

The main disadvantage of ISEs in relation to this work is that iron, manganese and zinc electrodes are not readily available. As a result, the work in this section is based solely on the formation of copper complexes although the protocols and techniques developed and outlined will apply to other metals, especially when using the same or similar ligands. Additionally, ISEs are not entirely ion-specific and can permit the passage of other ions through the membrane. This problem can be minimised by ensuring the solutions analysed are free of any of the potential interfering ions. The electrodes are also sensitive to changes in temperature and ionic strength and experiments were carried out at constant ionic strength and temperature to minimise deviations. Ion selective electrodes tend to be unsuitable for detection of concentrations lower than 10^{-7} moles/L (Ohzeki *et al.*, 1980; Wang, 2000). However, this was not an issue in this work and all analyses were carried out at concentrations in excess of 10^{-5} moles/L.

The use of Hyperquad software (Gans *et al.*, 1996) permits the determination of formation constants from potentiometric data especially when different equilibrium reactions occur in the aqueous solution. For this purpose, a data-fitting criterion based on the minimisation of the least-squares sum defined by the difference between the calculated and the experimental potential of the titration curves was used (Gans *et al.*, 1996; Escoda *et al.*, 1999). In the program, a proposed model with initial constant values was entered and as a result the program generated refined values of the formation constants and statistical parameters which indicate the goodness of the fit. These parameters are the minimising function, the global standard deviation of the model, the estimated values of the formation constants of the mixed species proposed and the standard deviation of each value (Escoda *et al.*, 1999). The standard deviation is a commonly used measure of variability within a dataset indicating how dispersed the data

points are from the mean (Tucker, 2003). To obtain a low sigma value (σ) and good experimental fit on the curve, it is necessary to test a range of combinations of species present in the model.

3.6.1 Calibration of the Cu(II) ion selective electrode

Copper(II) nitrate hydrate ($Cu(NO_3)_2.2.5H_2O$) and copper(II) sulphate pentahydrate ($CuSO_4.5H_2O$) were initially examined to determine whether copper salts other than the one recommended by the manufacturer ($Cu(NO_3)_2.2.5H_2O$) may be used to calibrate the ISE. Both solutions produced acceptable standard curves with similar slope and intercept values and r^2 values above 0.99 in each case. However, copper(II) nitrate hydrate was chosen for the stock solutions based on manufacturer recommendations for the copper ion selective electrode. Copper concentrations ranging from 10^{-1} to 10^{-5} M were chosen for the calibration curve (Figure 3.48).

Nernstian response occurs when an ion-selective electrode responds according to "local" thermodynamic equilibrium, over a given range of activity (or concentration) (Inczédy *et al.*, 1997). For Nernstian response, a plot of the potential difference of the ISE cell (ISE with an outer reference electrode) *vs*. the logarithm of the ionic activity of a given species (a_A) is linear with a slope of $2.303\left(\frac{RT}{z_AF}\right)$. A slope value of $\frac{59.16}{z_A}$ mV per unit change of pa_A at 298.15 K is obtained (Inczédy *et al.*, 1997).

R is the gas constant equal to 8.314510 J $K^{-1}mol^{-1}$;
T is the absolute temperature, K;
F is the Faraday constant, 9.6485309 x 10^4 C mol^{-1};
z_A is the charge number: an integer with sign and magnitude corresponding to the charge of the principal ion, A;
a_A is the activity of ion A;
pa_A (-log activity of the measured species A)

Nernstian response implies ideal sensitivity, but not necessarily ideal selectivity since interfering ions may also give Nernstian response when present as the sole potential determining species (Inczédy *et al.*, 1997).

Although it has been reported that the accuracy of the ion selective electrode is still within acceptable limits at concentrations as low as 10^{-7} M (Nakagawa *et al.*, 1980), it has been noted that deviations from a Nernstian response can occur at low concentrations due to the presence of coexisting ions (Ohzeki *et al.*, 1980; Wang, 2000). A minor deviation in the calibration curve was observed at low concentrations (10^{-5}) using $CuSO_4.5H_2O$ indicating the SO_4^{2-} ions present a problem at low Cu^{2+} concentrations. Based on literature information regarding the accuracy of the ISE at low concentrations (Nakagawa *et al*., 1980; Ohzeki *et al*., 1980; Wang, 2000) and the minor deviation observed during initial calibration experiments, the minimum Cu^{2+} concentration selected was 10^{-5} M. Cupric nitrate hydrate $(CuNO_3)_2.2.5H_2O$ produced a linear standard curve from 10^{-1} to 10^{-5} with a Nernstian slope of 29.6 and was chosen for all calibrations in this work (Figure 3.48). The slope is what one would expect for a 2+ ion (i.e. half of 59.16 – the value for a monovalent ion). These results from the calibration curve indicate the suitability of the Cu(II) ISE to detect Cu^{2+} ions in solution.

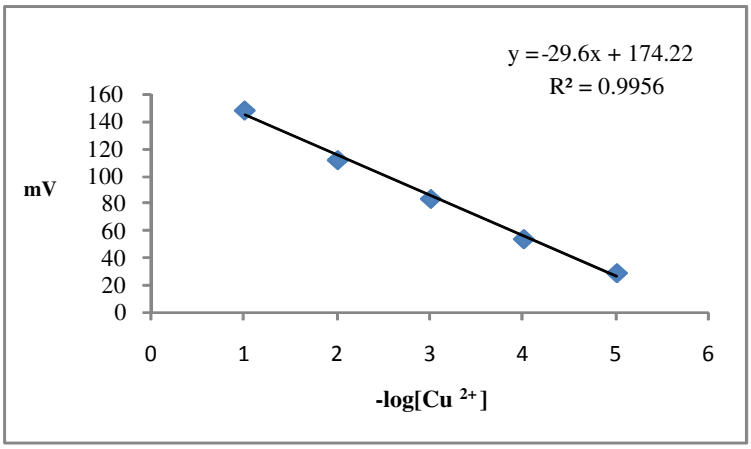

Figure 3.48 Calibration curve for a Cu^{2+} ISE with $(CuNO_3)_2.2.5H_2O$ at 25 °C and 0.1 M ionic strength

3.6.2 Potentiometric titrations of amino acids and Cu^{2+} using an ISE.

A selection of amino acids were titrated with Cu^{2+} ions in the form of copper(II) nitrate hydrate to determine their stability constants at 25 °C and 0.1 M ionic strength. Stepwise stability constants: log K_1, $K_2 \ldots K_n$, were obtained experimentally and calculated using Hyperquad for a selection of amino acids (Table 3.13). The experimentally obtained values were compared to the corresponding published values obtained from the National Institute of Standards and Technology (NIST) database (Martell *et al.*, 2004) to examine the accuracy of the experimental procedure. An introduction to the theory and stability constant relationships is described in Section 1.6.4.

Table 3.13 displays the stability constants obtained experimentally for the amino acid titrations with Cu(II). Some of the amino acids were unsuitable for titration under the conditions employed and were omitted. For example, solubility issues were encountered with tyrosine and tryptophan required heat to aid solubility prior to the titration. In the case of the basic amino acids lysine and arginine, copper uptake was immediate which affected the data analysis as there were no measurable Cu^{2+} ions in solution. Limited data for arginine and lysine was available using the NIST and SC-Databases. A logarithmic value of 15.205, referring to the cumulative stability constant (β_2), was obtained for the complex $[ML_2] / [M][L]^2$ for lysine, and a value for log K_1 of 7.65 for the complex [ML] / [M][L] was obtained for arginine. The percentage agreement of the theoretical versus the experimental values for arginine was outside acceptable margins of error as determined by the NIST database (Table 3.13). Arginine and lysine are basic amino acids due to the presence of a strongly basic group in addition to the α-amino group and are positively charged over a wide pH range (pH 1-9). Basic amino acids can in principle bind to metal ions through the α-amino carboxylate and ω-amino or guanidinium groups. However the side chains of Arg and Lys are not involved in metal binding under physiological conditions (Yamauchi *et al.*, 1996). Illustrations for each amino acid are contained in Appendix 2.

Table 3.13 Comparison of published and experimental stepwise stability constant (log K) values for amino acid ligands with Cu^{2+}

Ligand	log K	Theoretical logβ*	Experimental logβ	% agreement
Glycine	K_1	8.19	8.04	101.87
	K_2	15.10	14.78	102.17
Alanine	K_1	8.11	7.91	102.53
	K_2	14.90	14.74	101.09
Leucine	K_1	8.14	7.95	102.39
	K_2	14.90	14.87	100.20
Methionine	K_1	7.85	8.22	95.50
	K_2	14.50	14.98	96.80
Tryptophan	K_1	8.21	7.68	106.90
	K_2	15.50	14.98	103.47
Glutamine	K_1	7.70	8.74	88.10
	K_2	14.1	10.54	133.78
Glutamic acid	K_1	8.32	9.59	86.76
	K_2	14.92	16.63	89.72
Serine	K_1	7.90	7.96	99.25
	K_2	14.50	14.51	99.93
Proline	K_1	8.83	8.77	100.68
	K_2	16.37	16.32	100.31
Valine	K_1	8.10	8.50	95.29
	K_2	14.90	15.53	95.94
Isoleucine	K_1	8.14	8.21	99.15
	K_2	15.00	15.00	100.00
Histidine	K_1	10.16	10.10	100.59
	K_2	18.07	18.01	100.33
Arginine	K_1	7.65	6.42	116.82
Asparagine	K_1	7.84	7.55	103.84
	K_2	14.40	14.42	99.86
Aspartic Acid	K_1	8.89	8.50	104.59
	K_2	15.89	15.73	101.02
Threonine	K_1	7.99	8.15	98.04
	K_2	14.69	15.59	94.23

* Data obtained from NIST and SC databases

Comparing the experimentally obtained results with the published values (Table 3.13) it can be seen that the K_1 and K_2 values obtained from titrations of histidine and proline with Cu(II) had the closest agreement with the literature values obtained from the NIST and SC databases. Numerous publications have shown the affinity of these particular amino acids to bind copper (Broomhead *et al.*, 1961; Wapnir, 1990; Irtelli *et al.*, 2009) complimenting the stability results obtained experimentally. The correlation plot shown in Figure 3.49 illustrates the excellent agreement between the majority of experimental results and the published data from the NIST and SC databases.

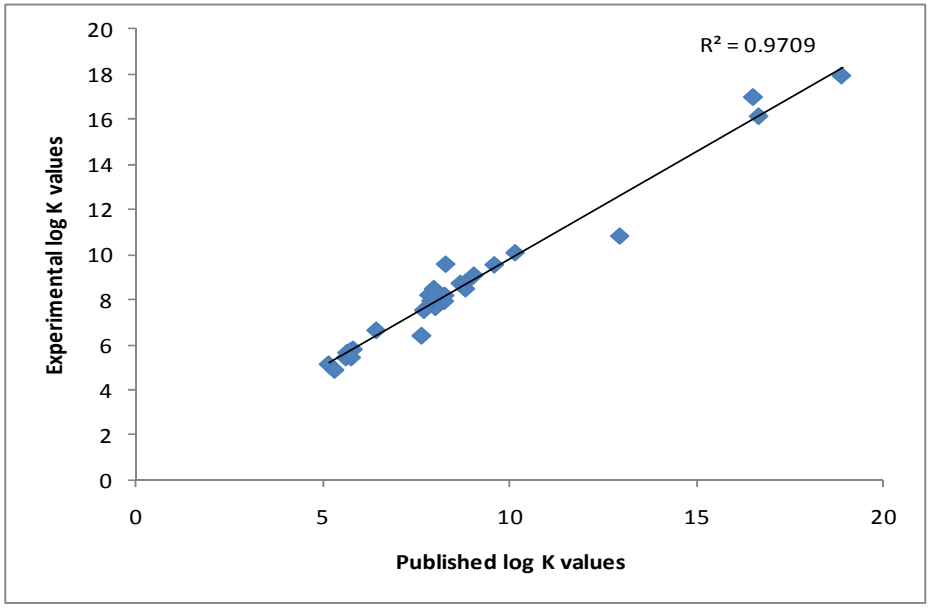

Figure 3.49 Comparative analysis of published and experimental log K values for amino acid ligands with Cu^{2+}

Glycine, which has the simplest structure of the amino acids with a single hydrogen as its R group (side chain), was used to standardise the titration prior to investigating the remaining amino acids. Glycine can act as a bidentate ligand in its interactions with many divalent metal ions, forming mono, bis and tris complexes having stable 5-membered chelate rings via the amino N and the carboxylate O donors (Kiss *et al.*, 1991). With some metal ions e.g. Fe(III) and Zn(II), protonated complexes can also be formed via the monodentate coordination of the carboxylate or the amino group. Figure 3.50 shows the formation of a Cu-glycinate. A covalent bond is formed between the carboxylate oxygen and the copper and a coordinate covalent (also known

as dative) bond forms via the amino nitrogen and the copper. This complex still has a single positive charge.

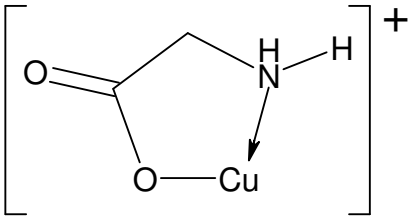

Figure 3.50 Schematic of the complex formed between Cu and glycine

At higher pH, especially when there is only a slight excess of ligand, formation of soluble mixed hydroxo complexes must also be taken into account (Kiss *et al.*, 1991). In this work, the ligand is in excess at the end of the titration which reduces the possibility of the formation of such species.

A modelling computer program called WinCOMICS (Hynes, 2005), which calculates and plots species concentrations relative to pH, was employed to create speciation diagrams for the copper complexes formed with a selection of ligands. Input parameters include the pK_w (the negative log of the water ion product, K_w), the number of reactants and complex species (including protonated and hydrolysed species) and the total starting concentrations of all species. Information on each complex species such as the log of the overall stability constant of the species, the number of molecules of reactant, the number of hydroxyl ions, the number of protons and the minimum and maximum pH values in addition to the pH increment are additional input parameters (Hynes, 2005). The relative contribution of each component as well as the pH value determines which species of complex exists and whether one species is dominant. Speciation diagrams created using WinCOMICS illustrate the complex formation clearly over a wide pH range and were used in this work to provide theoretical models based on set input parameters from which experimental data could be compared. The Hyperquad suite of programs provide a means of calculating equilibrium constants and identifying the chemical species present in appreciable concentrations in the reaction mixture (Gans *et al.*, 1996). The speciation data obtained experimentally and analysed

using Hyperquad can be compared to the theoretically obtained data created using WinCOMICS to determine if many of the same species are present.

A graphical illustration of the experimental data for the Cu(II)-glycine titration is provided in Figure 3.51 and the reduction in free copper is clearly seen with increasing pH. The corresponding theoretical speciation diagram created using WinCOMICS outlines the depletion of free copper and the formation of the resultant 1:1 and 1:2 metal:ligand complexes (Figure 3.52). Hyperquad calculations based on the experimental data from the Cu-Gly titration using a 1:2, metal:ligand ratio confirmed the presence of the same species observed using WinCOMICS (Figure 3.53) and provided values for log β_1 (8.04) and log β_2 (14.78) which were in excellent agreement with published data (Table 3.13).

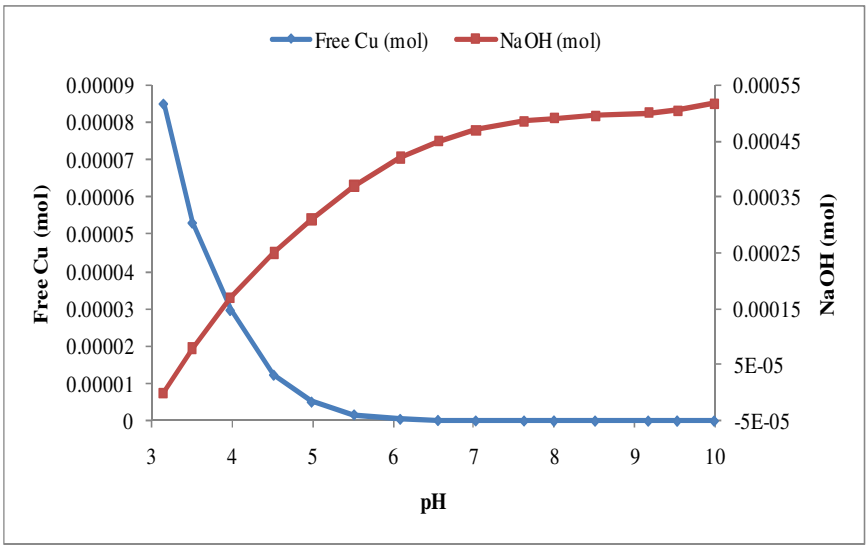

Figure 3.51 Experimental titration curves for 10mM Cu + 20mM Glycine at 25 °C and 0.1 M ionic strength illustrating the decrease in free Cu with increasing pH

The speciation diagram (Figure 3.52) clearly illustrates the decrease in free Cu^{2+} concentration with the formation of a 1:1, M:L complex over a pH range of approximately 3 – 5.2. At pH 4, the formation of a 1:2, M:L complex is observed and above pH 6 this becomes the dominant species.

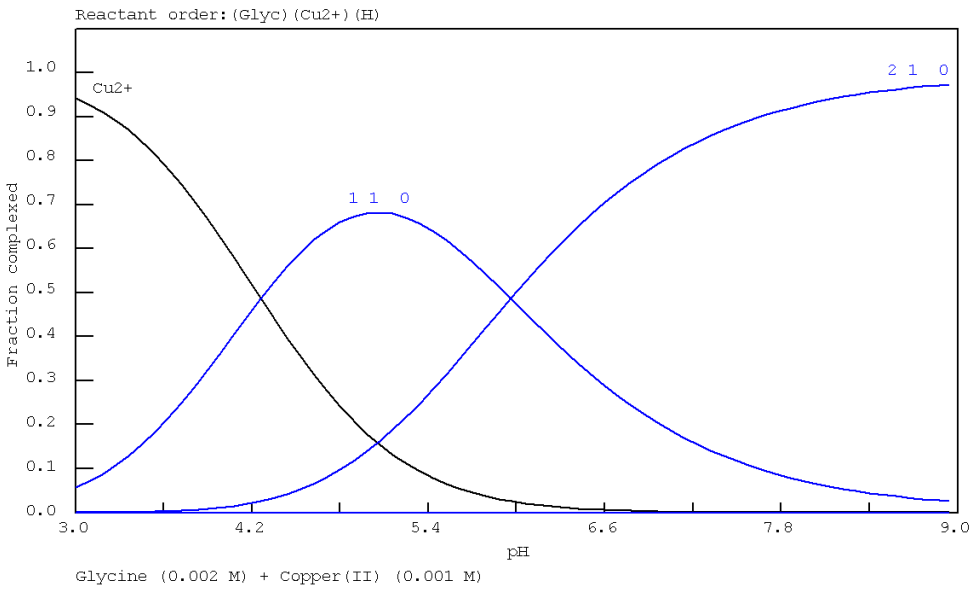

Figure 3.52 Speciation diagram created using WinCOMICS for Cu (0.001 M) and Glycine (0.002 M) at 25 °C and 0.1 M ionic strength, [M]:[L] = 1:2, (1,1,0 refers to a 1:1, L:M species and 2,1,0 refers to the formation of a 2:1, L:M species. 0 refers to a proton, negative values in this position indicate deprotonation)

Speciation diagrams provide an insight into the pH ranges where ionisation is effectively complete, and where it is not (Maurin *et al.*, 2008). The area of the diagram may be divided into three regions: two of them are those where only one of the species is present. They are separated by a region of transition where one species is decreasing while the other is increasing. Over the intermediate region, the unionised form begins to decrease, while the anion increases. In this particular range, a shift in pH immediately causes a shift of the proportions of the ionised and unionised species. The point where the distribution lines for the two species intersect and each species is present in equal fractions, i.e. 0.5 or 50 %, marks the pK_a. Examination of Figure 3.52 identifies two pK_a values, one at pH 4.3 and a second at pH 6.0 indicative of deprotonation.

The 1:1, M:L species identified using WinCOMICS refers to the complex previously described in Figure 3.50 and has a single positive charge as previously mentioned. The 1:2, M:L species in which the metal ion is bonded to both the amino and carboxyl moieties of the amino acid in such a way as to form two 5 membered rings is a chelate and has previously been discussed (Section 3.1). This 1:2. M:L species is uncharged and unreactive.

Figure 3.53 shows the change in free copper concentration determined by Hyperquad calculations over the course of the titration in addition to illustrating the complex species formed. To obtain the best curve fit, a manual trial and error data fitting method is required with regard to the species formed (Gans *et al.*, 1996). Criteria to determine whether or not the computed equilibrium model is satisfactory in a chemical sense and if the calculated data points agree with those observed enables reasonably accurate model selection. Sigma values which indicate the goodness of fit in relation to the curves are provided by the program.

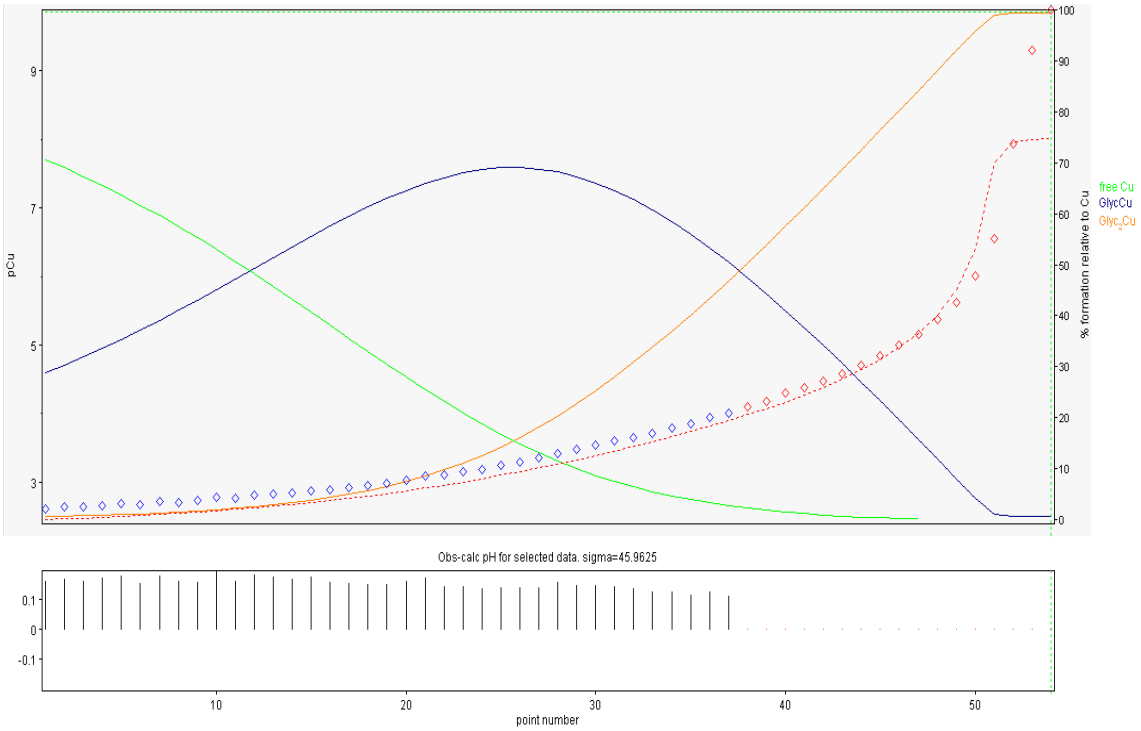

Figure 3.53 Screenshot capture of the Hyperquad file for a Cu-Gly titration. - = free Cu^{2+}, - = 1:1, M:L species (GlycCu, log β = 8.04) and - = 1:2, M:L species ($Glyc_2Cu$, log β = 14.78). The experimental data (◊) closely follows the theoretically calculated Hyperquad values (---)

The 1:1 and 1:2, M:L species postulated by Hyperquad for the Cu-Gly titration over a pH range of 3 to 9 at 25 °C and 0.1 M ionic strength agree with those obtained using WinCOMICS (Figure 3.52). Furthermore, these species are frequently referred to in numerous publications (Borsook *et al.*, 1932; Li *et al.*, 1956; Kiss *et al.*, 1991; Fan, 1995; D'Angelo *et al.*, 1998). Based on the results of the ISE titrations of the amino

acids with Cu(II), it can be concluded that the results obtained for the majority of the complexes formed are reasonably close to the corresponding published values. This enabled progression to examine the interactions between larger ligands such as polypeptides and Cu(II). If successful, this technique could be applied to the determination of stability constants for ligands with no published information. In the context of this work, the method could also be applied to investigating the stability of metal proteinates under a range of conditions such as various pH and temperature values.

Further analysis was carried out on the resultant complexes formed from the potentiometric titration. A sample of copper(II) sulphate pentahydrate was selected as a control analyte, the amino acid prior to titration was analysed and finally an aliquot of the resultant complex formed from the titration was investigated to determine if differences could be detected which may indicate complexation. Fourier Transform Infrared (FTIR) spectroscopy was employed to monitor the band shifts that occurred during complex formation for all samples. Based on previous work in relation to assessment of parent peptide and corresponding peptide-metal adduct peaks for larger polypeptide complexes, SELDI-ToF-MS was also employed as an additional characterisation technique. However, this method could not be used for single amino acids due to difficulties in accurately identifying low molecular mass peptides in the matrix region. As discussed in Section 3.3.6.5, high intensity matrix peaks can shield low molecular mass peptides in the 0 – 500 Da spectral region. Figure 3.25 illustrates the matrix effect quite clearly.

The FTIR spectra in Figure 3.54 illustrate the shifts observed when histidine is reacted with Cu^{2+}. The spectral results for a selection of other amino acids with Cu^{2+} are outlined in Appendix 1.2. Noticeable band shifts were observed for the His-Cu complex when compared to the spectra for the amino acid or the copper(II) sulphate pentahydrate controls on their own. This was considered to be indicative of complex formation. Assignments based on literature data allude to frequency shifts in groups expected to be involved in the chelation of Cu(II) (Çakir *et al.*, 2001; Wagner *et al.*, 2004; Stanila *et al.*, 2007; Marcu *et al.*, 2008). The majority of spectral differences were observed in the fingerprint region although changes to the υ(N-H) stretching vibration were observed

above 3100 cm^{-1} which suggested involvement of the $–NH_2$- group in complex formation. Shifts in the υ(C=O) stretching vibration were observed in the region of 1560 cm^{-1} to 1660 cm^{-1} depending on the ligand and were indicative of involvement of the carboxylic group in covalent bonding to the metal ion.

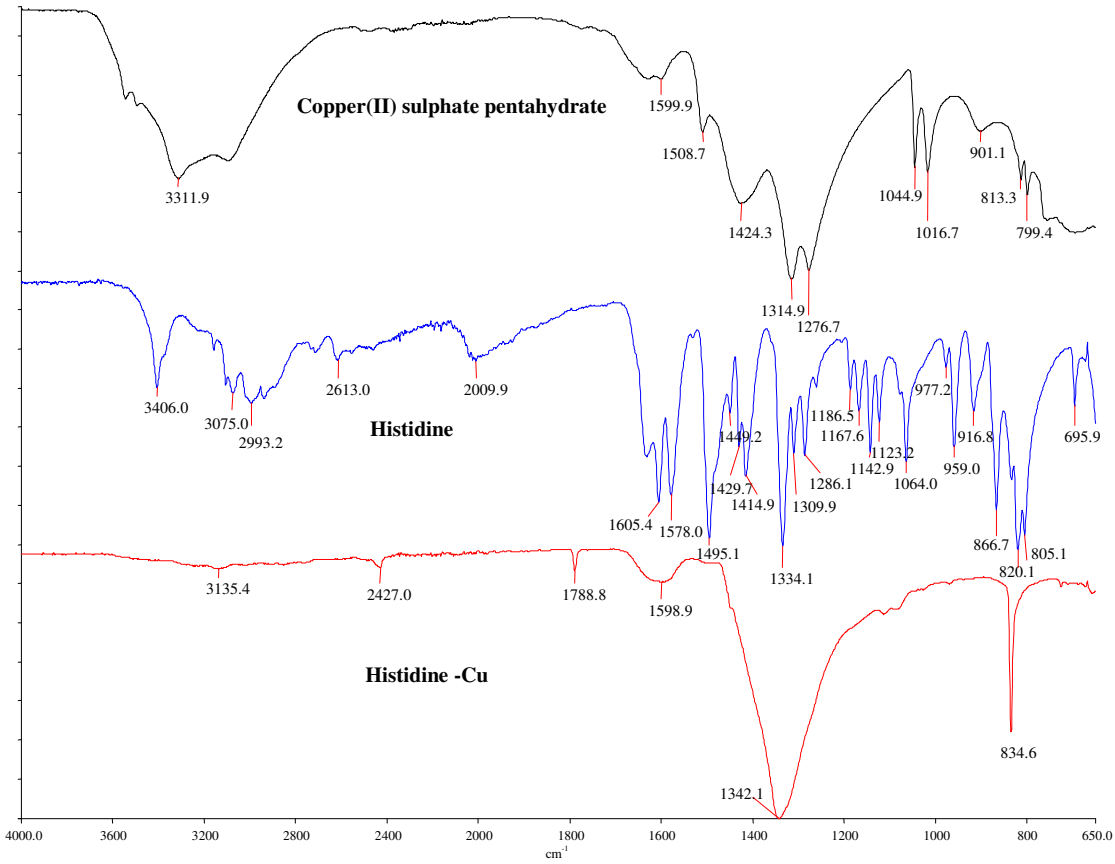

Figure 3.54 FTIR spectra of a copper(II) sulphate pentahydrate control, histidine and a His-Cu complex

3.6.3 Potentiometric titrations of peptide ligands and Cu^{2+} using an ISE

The results obtained in Section 3.6.2 confirmed that the potentiometric method selected was suitable for analysing complexes formed with amino acids and could now be applied to longer chain peptides. Following on from the analysis of amino acids in section 3.6.2, short chain peptides with published stability constants for complexes with copper were analysed. Of particular interest were metal-ligand complexes containing glycine due to their use as nutritional supplements in the form of metal glycinates. Peptides of di-, tri-, tetra- and pentaglycine were investigated in addition to short chain mixed peptides containing glycine.

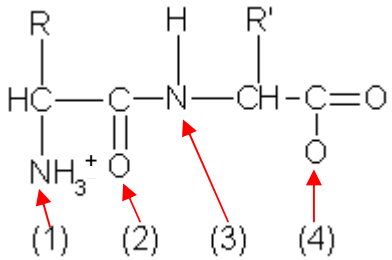

Figure 3.55 The general formula for a dipeptides comprised of two amino acids. R and R' refer to unspecified amino acid side chains. The potential metal-binding sites are the terminal NH_2 group (1), the carbonyl group (2), the amide nitrogen (3), and the carbonyl oxygen (4) (Pettit *et al.*, 1977)

The Cu^{2+} ion forms rather stable complexes, even with simple dipeptides (Sóvágó *et al.*, 1996). In these, the nitrogen of the deprotonated amide acts as the strongest donor, but the terminal carboxylic and amino groups as well as the carbonyl oxygen are also implicated in the metal binding (Sigel *et al.*, 1982; Sóvágó *et al.*, 1996). However, it should be noted that chelation reactions can occur without the release of two protons per atom of added Cu(II) (Khanna *et al.*, 1962). A study into metallo-organic complexes in soil demonstrated that the number of protons released per atom of added Cu(II) did not approach the theoretical value of two for the reaction of Cu(II) with strong chelation groups (such as α-amino and α-hydroxy acids). These findings indicated that the groupings in soil organic matter which bind metals are types which normally ionise in aqueous media (such as carboxyl groups) and that the metals may be

held largely by electrostatic forces (Khanna *et al.*, 1962). Additionally, it was postulated that some of the chelation sites may have been already occupied by metals resulting in fewer protons released.

For simple dipeptides, the amide nitrogen is usually not involved in the bonding because resonance with the carbonyl group reduces its basicity, however when one or more of the constituent amino acids of the dipeptide has a coordinating centre in the side chain, the equilibria become more complicated (Pettit *et al.*, 1977). For example, with glycyl-histidine there is another potential binding centre in the molecule, the imidazole nitrogen. With metal ions such as Co^{2+} and Zn^{2+}, it appears that the bonding involves the terminal $–NH_2$ and the carbonyl group resulting in a five membered chelate ring. The presence of an additional ionisable proton on the metal-peptide complexes containing Cu^{2+} or Ni^{2+} however, has a significant effect. This proton resides on the amide nitrogen and, in the absence of a metal, extremely high pH values are required to effect ionisation/deprotonation. However, with Cu^{2+} present, the proton ionises at pH values as low as 4 and it must be concluded that the amide nitrogen now plays an important part in the bonding (Pettit *et al.*, 1977).

The complex formation involving Cu^{2+} with di-, tri- and tetraglycine has been thoroughly investigated (Sóvágó *et al.*, 1996) and complexes such as the 1:1 and 1:2, M:L complexes suggested in that work have been observed over the course of this work in speciation diagrams and Hyperquad data. Additionally the stability constant values are very similar. Table 3.14 shows the stability constants obtained from the NIST database (theoretical log β), the values from the literature (Sóvágó *et al.*, 1996) and the experimentally-obtained values for 1:1, ligand:metal complexes. The species postulated by Hyperquad (Figure 3.56) for the titration of diglycine with copper(II) are the same as those described in the literature.

Table 3.14 Comparison of sample stability constant values for a selection of Cu-Glycine complexes at 25 °C

Ligand	Theoretical log β*	Experimental log β	Published log β (Sóvágó, Sanna *et al.*, 1996)
Diglycine	5.55	5.61	5.56
Triglycine	5.05	5.13	5.25
Tetraglycine	5.10	5.16	5.06

* Data obtained from NIST database

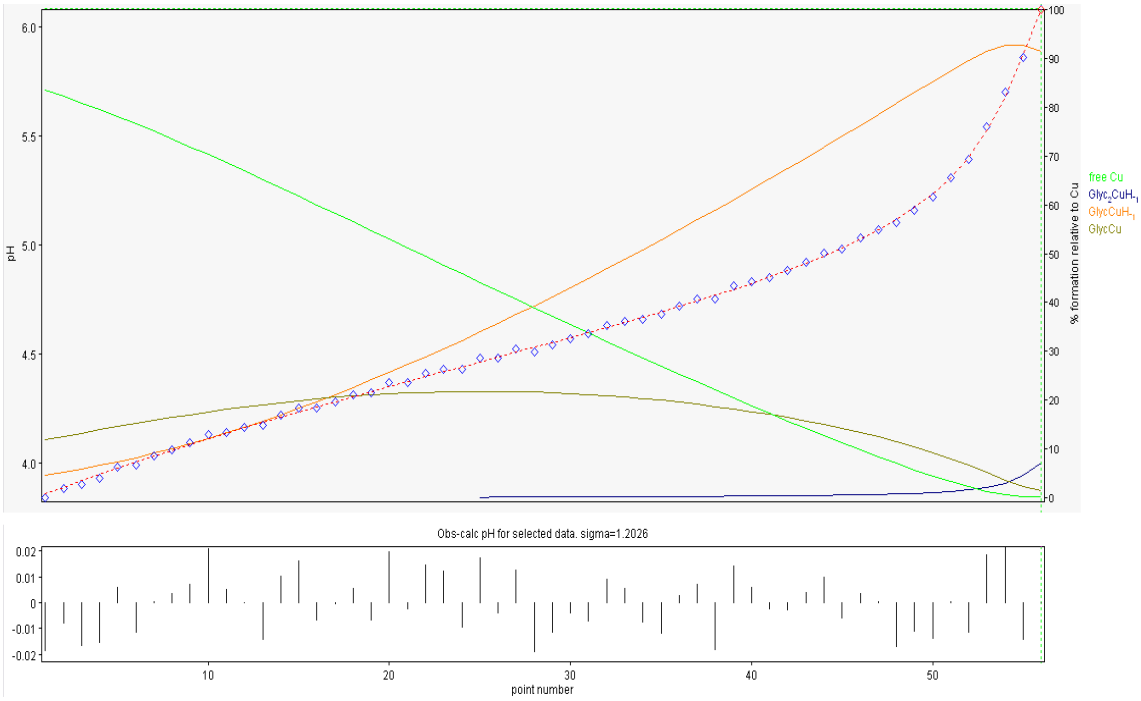

Figure 3.56 Screenshot capture of the Hyperquad file for a copper(II)-glygly titration. - = free Cu^{2+}, - = 1:1, M:L species (GlycCu, log β = 5.61), - = 1:1, M:L species minus 1 proton ($GlycCuH_{-1}$, log β = 1.34) and - = 1:2, M:L species minus 1 proton ($Glyc_2CuH_{-1}$, log β = 4.72). The experimental data (◊) closely follows the theoretically calculated Hyperquad values (---)

As mentioned previously, when one or more of the constituent amino-acids of the dipeptides had a coordinating centre in the side chain such as in the case of glycyl-histidine, there is another potential binding centre in the molecule, the imidazole nitrogen (Figure 3.57).

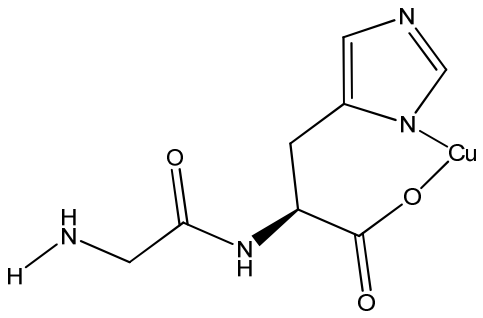

Cu(Gly-His)

Figure 3.57 Chelate formed from copper and the dipeptide Gly-His

With tripeptides, two amide protons can be displaced by Cu^{2+} as the pH is increased and the resultant 1:1 complex is extremely stable. Table 3.15 contains theoretical and experimental stability data for a selection of such polypeptides and there are significant differences in the stability constant values of copper with different ligands at 25 °C and 0.1 M ionic strength.

Table 3.15 Comparison of published logβ values of polypeptides with Cu^{2+} vs. experimentally obtained values monitoring pH.

Ligand	L:M	Theoretical log β	Experimental log β	Agreement (%)
Diglycine	1:1	5.55	5.61	98.93 %
Triglycine	1:1	5.05	5.13	98.44 %
	2:1	9.60	9.56	100.42 %
Tetraglycine	1:1	5.10	5.16	98.84 %
EDTA	1:1	18.90	17.95	105.29 %
Pentaglycine	1:1	5.30	4.90	108.16 %
NTA	1:1	12.96	10.84	119.56 %
	2:1	17.43	18.97	91.88 %
Gly-Phe	1:1	5.70	5.81	98.11 %
Gly-Ser	1:1	5.66	5.67	99.82 %
Gly-Leu	1:1	5.81	5.75	101.04 %
Gly-Pro	1:1	6.44	6.65	96.84 %
	2:1	11.50	11.57	99.40 %
Gly-Val	1:1	5.71	5.45	104.77 %
	2:1	11.26	11.31	99.56 %
Gly-His	1:1	8.98	6.54	137.31 %
	2:1	16.1	16.99	94.76 %
Gly-Gly-His	1:1	7.59	8.37	90.68 %
	2:1	16.68	17.54	95.10 %
Gly-His-Gly	1:1	9.39	9.10	103.19 %
	2:1	15.96	17.76	89.87 %

Data obtained from NIST database

Examination of the data in Table 3.15 indicated significant differences in stability constant values for a range of ligands complexed with copper under the same physiological conditions. The results indicate that it is not only the type of amino acid that influences the stability of a given chelate but the configuration of amino acids in a peptide can also significantly influence how the ligand and metal interact. Increased amino acid chain length does not necessarily increase the stability of the metal complex as can be observed by comparing the tetrapeptide (tetraglycine, $\log\beta_{11} = 5.10$) and dipeptide data (Gly-Pro, $\log\beta_{11} = 6.44$). Analysis of three tripeptides; Gly-Gly-Gly ($\log\beta_{11} = 5.05$), Gly-Gly-His ($\log\beta_{11} = 7.59$) and Gly-His-Gly ($\log\beta_{11} = 9.39$) provides evidence that the sequence and position of amino acids in the peptide will greatly affect the stability of a chelate. Clearly the substitution of a histidine into the tripeptide Gly-Gly-Gly enhances the stability value. Furthermore, altering the position of the histidine within the tripeptide sequence can result in a further increase in the stability constant value. The ability to analyse larger peptides with differences in configuration of amino acids in the peptide sequence can provide details regarding the proportion of bound metal relative to free metal and ligand. This can enable further information to be obtained regarding the stability of metal proteinates and provide an effective means for product comparison.

Due to the increasing complexity of the ligands investigated, it was necessary to make some adjustments to the experimental procedure. For simple amino acids and the majority of the short chain peptides, the titrations were carried out by monitoring pH, but for larger polypeptides it was necessary to keep the pH constant and monitor EMF instead. In order to use Hyperquad to calculate stability constants, the pK_a values of the ligands are required. The input data for stability constant calculation is the base volume and the pH value. These values were unavailable for larger peptides and it was not particularly straightforward to measure them. Furthermore, there were no known literature values available. Instead, the “apparent stability constant” (or conditional stability constant) was measured at a constant pH. By measuring free Cu^{2+} with the ISE, the bound Cu could be calculated and an apparent stability constant (or equilibrium constant) obtained which is valid only at that particular pH.

Further adaptions to the Hyperquad software were required to suit experimental procedures outlined in this work. It was necessary to consult with the program developer to further expand the capabilities of the software with the inclusion of a batch data import function for EMF data and the option to calculate the apparent stability constants at a constant pH. Hyperquad 2008 had not been tested on experimental data using a divalent ISE prior to this work. The sensitivity of the fitting program allowed models that included several complex species of different stoichiometries and formation constants to be considered. Several ratios and initial formation constants were tested, introducing the model or the species that yield more reasonable fittings. The model which provided the best fit to the experimental data was selected. Species included in the Hyperquad speciation diagrams refer only to the major species calculated but it is important to note that numerous minor species may also be present at concentrations too low to be detected. The titrations of di-, tri-, tetra- and pentaglycine were repeated using EMF data analysis instead of pH to validate the procedure (Figures 3.59, 3.62, 3.65 and 3.68). The experimental results obtained were very close to theoretical values calculated by Hyperquad. Optimisation was necessary to obtain the best curve fit by adjusting the major species formed. WinCOMICS was employed to create speciation diagrams for the copper complexes formed with di-, tri-, tetra- and pentaglycine enabling comparison with experimentally determined species obtained using Hyperquad (Figures 3.58, 3.61, 3.64 and 3.67).

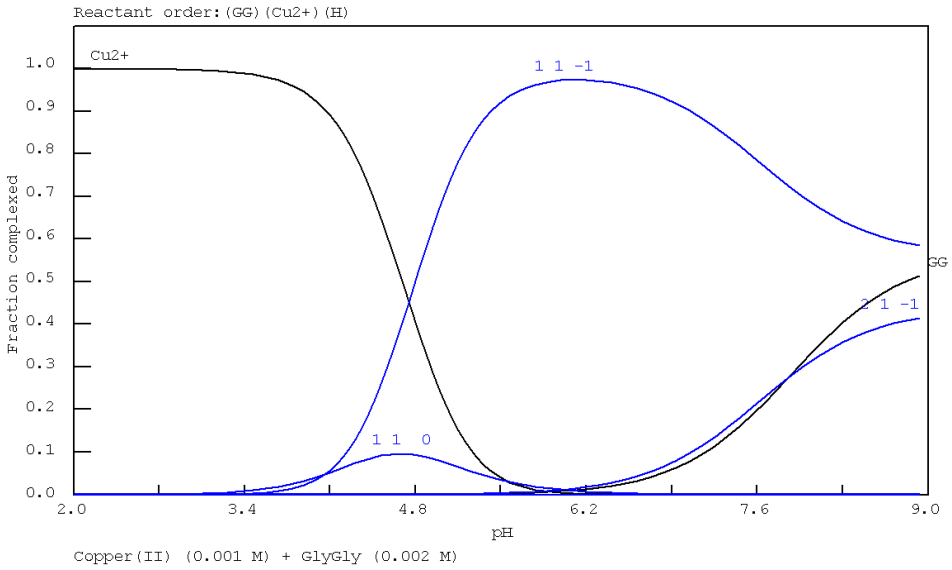

Figure 3.58 Speciation diagram created using WinCOMICS for Cu (0.001 M) and diglycine (0.002 M) at 25 °C and 0.1 M ionic strength, [M]:[L] = 1:2, (1,1,0 refers to a 1:1, L:M species; 1,1,-1 refers to 1 ligand, 1 metal and the loss of 1 proton and 2,1,-1 refers to a species comprised of 2 ligands, 1 metal and the loss of 1 proton)

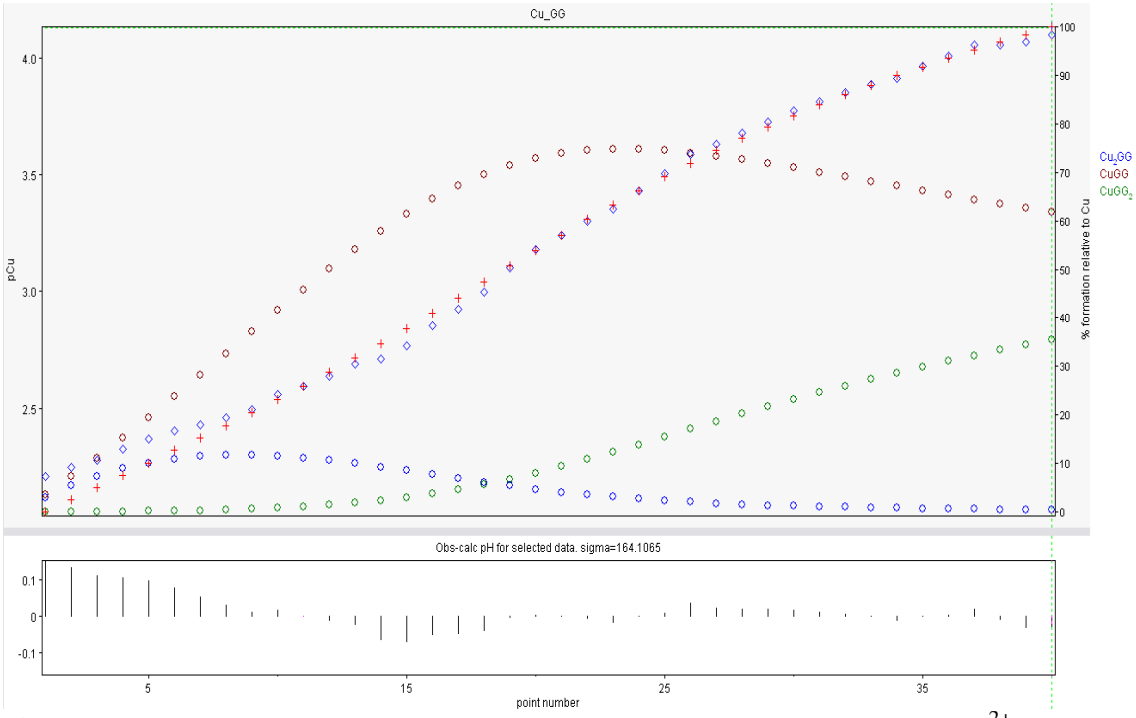

Figure 3.59 Screenshot capture of the Hyperquad file of diglycine with Cu^{2+}. ○ = 1:1, M:L species (CuGG, ML), ○ = 2:1, M:L species (Cu_2GG, M_2L) and ○ = 1:2, M:L species ($CuGG_2$, ML_2). The experimental data (◊) closely follows the theoretically calculated Hyperquad values (+)

The formation of multiple species (ML, M_2L and ML_2) was observed in the Hyperquad file (Figure 3.59) with the 1:1, ML species dominating. Comparing the Hyperquad results with those obtained from WinCOMICS (Figure 3.58), it was observed that at pH 5.5 the 1:1, M:L species suggested as the dominant species at this particular pH in WinCOMICS was also detected as the dominant species in Hyperquad. Furthermore, a minor 1:2, M:L species was also suggested in WinCOMICS which was present in Hyperquad. The final species suggested in Hyperquad (2:1, M:L), was not observed in the speciation diagram. This can be explained by the input parameters chosen for WinCOMICS speciation - an excess of ligand was used (0.001 M Cu and 0.002 M diglycine) rather than an excess of metal which would prevent the formation of a 2:1, M:L species on a theoretical basis. As the majority of literature data contains values based on an excess of ligand, the log K input parameters were selected from those available and WinCOMICS plots were created using an excess of ligand. Reversing the input parameters to include an excess of metal would also eliminate theoretical postulation of a 1:2, M:L species. Hyperquad has the ability to detect this species, even with an initial excess of metal based on experimental data and has advantages over the theoretical WinCOMICS modelling program in this case.

The experimental fit closely follows the theoretically calculated values (Figure 3.59) and the calculated Hyperquad values for the species obtained were: ML = 4.095, M_2L = 5.775 and ML_2 = 6.53, although it must noted that these values refer to 'conditional' stability constants at pH 5.5, 25 °C and an ionic strength of 0.1 M. To confirm the accuracy of the results, a brief calculation was carried out to determine if the Hyperquad stability constant results for ML (log K = 4.095) could be replicated. Based on the theory outlined in Section 1.6.4, Equation 3.2 was selected to represent the metal-ligand interaction. In the Hyperquad program, a table of observed and calculated concentration values is provided and from this the following values were obtained:

Free ligand (diglycine) = HL = 2.9941×10^{-6} M
ML = CuL = 3.2923×10^{-4} M
Free metal (copper) = Cu^{2+} = 8.8308×10^{-3} M

$$Cu^{2+} + HL = CuL + H^{+} \quad \textbf{(3.2)}$$

Provided the equation selected is the correct one used by Hyperquad for the calculations, substituting the values from the table of concentrations should produce the same log K value as that obtained from Hyperquad.

$$K = \frac{3.2923\ x\ 10^{-4}}{(8.8308\ x\ 10^{-3})(2.9941\ x\ 10^{-6})} = 12452 \quad \textbf{(3.3)}$$

log (12452) = 4.095 (validated from Hyperquad)

From Figure 3.59 it is clear that the 1:1, M:L species is the major species present. The reason for including the M_2L and the ML_2 minor species was to improve the curve fit. However, these species are viable as the titration was carried out with excess metal. The majority of literature values are based on titrations with excess ligand which would explain the absence of such species. If copper is not limiting, which is the case in this work, binding of multiple Cu^{2+} ions is possible. For this to occur, the involvement of the backbone amide groups is important. When two backbone amide groups are involved in binding to Cu^{2+}, two protons are released for each copper bound with the result that the charge is balanced and no increase in positive charge on the peptide occurs (Hynes, 2009). This can facilitate binding of additional Cu^{2+} ions and a previously published example has shown binding of up to six Cu(II) ions in the unstructured N-terminal region of the prion protein (Wells *et al.*, 2006). The formation of a selection of metal-ligand species, even with such simple ligands as diglycine, extends the potential for interactions of metal-ligand complexes and chelates. The availability of such a selection of complexes with differing stability constants may increase the nutritional potential of feed supplements.

Samples were also analysed by FTIR to obtain further information on the complexes and similar to the band shifts observed for the single amino acids, significant differences can been seen in the FTIR spectra of the Gly-Gly-Cu complex in comparison to the Gly-Gly and copper(II) control spectra. These band shifts, indicative of complex formation, are visible in all the copper(II) glycine complexes analysed (Figures 3.60,

3.63, 3.66 and 3.69). As mentioned previously, band shifts in the υ(C=O) stretching vibration were observed in the region of 1560 cm^{-1} to 1660 cm^{-1-} and are indicative of involvement of the carboxylic group in covalent bonding to the metal ion. Additionally, changes to the υ(N-H) stretching vibration were observed above 3100 cm^{-1} suggesting the involvement of the $–NH_2-$ group in complex formation.

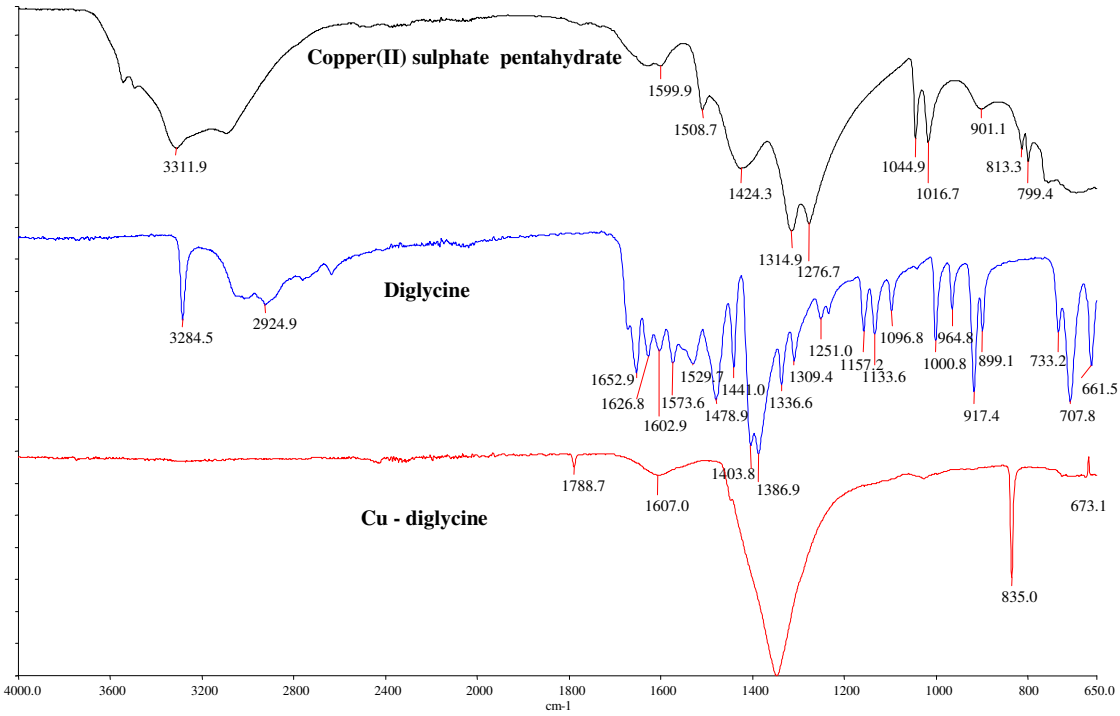

Figure 3.60 FTIR spectra of a copper(II) sulphate pentahydrate control, diglycine and a GlyGly-Cu complex

Speciation diagrams, metal-ligand titrations with Hyperquad data analysis and FTIR provided a considerable amount of information on the copper complexes formed with diglycine. The resultant data confirmed the formation of a range of metal-ligand complexes in addition to their respective stability constants and FTIR spectral data identified band shifts indicative of chelation as previously discussed. Consequently, the methods were applied to copper complexes formed with larger glycine ligands such as tri-, tetra and pentaglycine (Figures 3.61 – 3.69). Additional FTIR spectra for a selection of di- and tri- peptides are contained in Appendix 1.3.

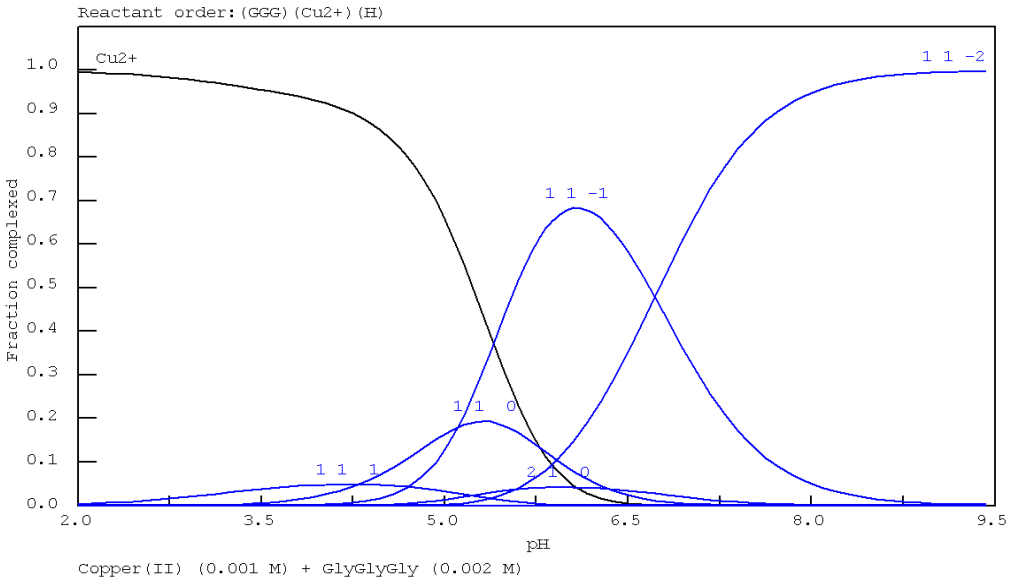

Figure 3.61 Speciation diagram created using WinCOMICS for Cu (0.001 M) and triglycine (0.002 M) at 25 °C and 0.1 M ionic strength, [M]:[L] = 1:2, (1,1,1 refers to a species containing 1 ligand, 1 metal and 1 proton, 1,1,0 refers to a 1:1, L:M species; 1,1,-1 refers to 1 ligand, 1 metal and the loss of 1 proton, 1,1,-2 refers to 1 ligand, 1 metal and the loss of 2 protons and 2,1,0 refers to a species comprised of 2 ligands and 1 metal)

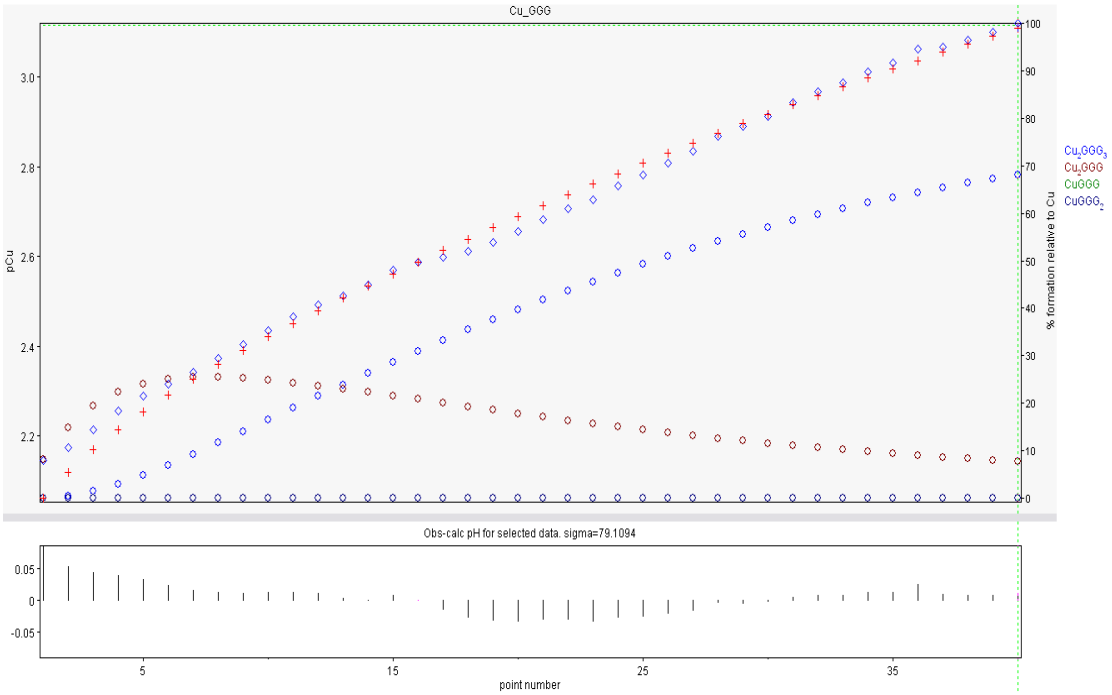

Figure 3.62 Screenshot capture of the Hyperquad file of triglycine with Cu^{2+}. ○ = 2:1, M:L species (Cu_2GGG, M_2L), ○ = 2:3, M:L species (Cu_2GGG_3, M_2L_3) and ○ =1:2, M:L species ($CuGGG_2$, ML_2). The experimental data (◊) closely follows the theoretically calculated Hyperquad values (+)

The two major species observed from the Hyperquad file for triglycine are M_2L_3 and M_2L. Neither of these species was observed in the WinCOMICS speciation diagram. As previously observed in the speciation diagram of diglycine, the speciation diagram for triglycine also contains no multi metal species. As before, this is partly due to the fact that the ligand concentration exceeds that of the metal, in addition to the limited data available for use as input parameters, and the resultant diagrams reflect this. However, reversing the data to examine species formed with excess metal would not necessarily identify multi ligand species without firstly obtaining stability constants for such species to use as input parameters. As the Hyperquad results are based on experimental data, the identification of such species in addition to obtaining their corresponding stability constants is advantageous. WinCOMICS is useful as a reference to determine if certain species are present but has limitations based on theoretical input parameters. The final species suggested by Hyperquad, the ML_2 species was observed in the WinCOMICS speciation diagram for Cu-GGG. However, this particular species was not present at high concentrations at pH 5.5 according to the speciation diagram and the Hyperquad data confirms this as the ML_2 species resides on the baseline (Figure 3.62). The additional microspecies observed in the WinCOMICS plot were not detected in Hyperquad which only displays the major species present in solution. However, it is possible that these species exist in solution but were not detected. The experimental fit closely follows the theoretically calculated values (Figure 3.62) and the Hyperquad values for the species obtained were: $M_2L_3 = 10.81$ and $M_2L = 4.83$. Although an ML_2 species was initially postulated, it was ignored during refinement to obtain the best curve fit. This acceptable method of trial and error fitting has been carried out by other authors based on the original method suggested by the developer (Gans *et al.*, 1996). As mentioned previously, the values for the observed species refer to ‘conditional’ stability constants at pH 5.5, 25 °C and an ionic strength of 0.1 M.

Based on extensive literature investigations it was found that the M_2L_3 species had not been previously suggested or discussed. Very little information has been published in relation to the formation of such species and even less (if any) has examined such species in the context of nutritional feed supplements. When compared to available products such as glycinates (metal complexes with glycine ligands)

containing a single metal ion bound, the advantage of multi species complexes is apparent. As discussed earlier, during the formation of the Cu-glycinate, a covalent bond forms between the O and Cu and a coordinate covalent bond forms between the N and copper. This complex still has a single positive charge and has the propensity to react with negatively charged molecules (Figure 3.50). As such, its stability and ability to effectively deliver mineral may be impaired. For multi-ligand species, a covalent bond can form between the O and Cu and a second covalent bond forms between the N and copper. These complexes are chelates and form a heterocyclic ring structure with the metal ion. With regard to such species, increased potential for a wider range of metal-ligand interactions exists and increased metal concentration is present in multi-metal species. A wider range of complexes and chelates with different stability constants may be formed which may have different modes of action and some of the species formed may be absorbed more effectively during digestion.

Additional FTIR analysis was carried out on the Cu-triglycine complex and similar band shifts to those previously observed in the case of the copper complexes with amino acids and diglycine were observed in the FTIR spectra of the Cu-GGG complex in comparison to the control spectra and were indicative of complexation as previously discussed.

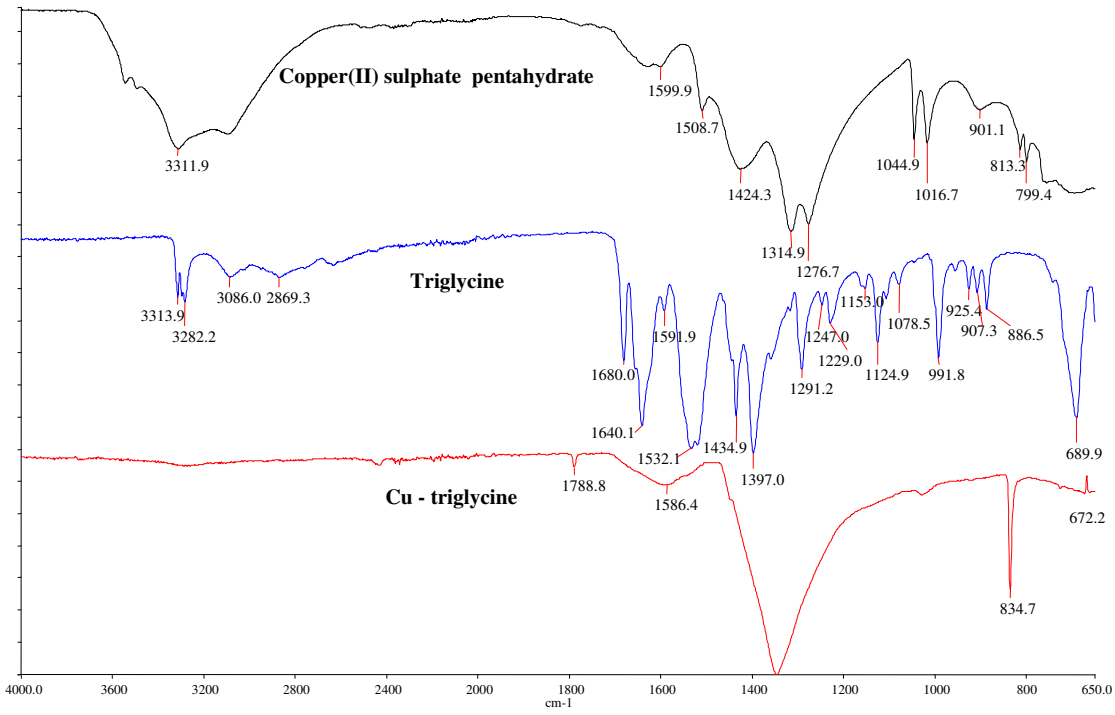

Figure 3.63 FTIR spectra of a copper(II) sulphate pentahydrate control, triglycine and a $(Gly)_3$-Cu complex

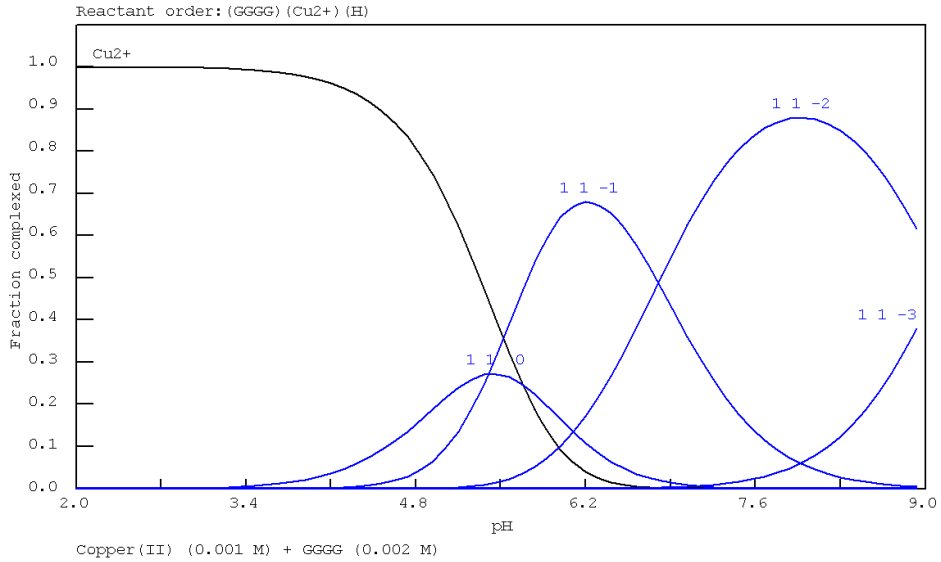

Figure 3.64 Speciation diagram created using WinCOMICS for Cu (0.001 M) and tetraglycine (0.002 M) at 25 °C and 0.1 M ionic strength, [M]:[L] = 1:2, (1,1,0 refers to a 1:1, L:M species; 1,1,-1 refers to 1 ligand, 1 metal and the loss of 1 proton, 1,1,-2 refers to 1 ligand, 1 metal and the loss of 2 protons and 1,1,-3 refers to a species comprised of 1 ligand, 1 metal and the loss of 3 protons)

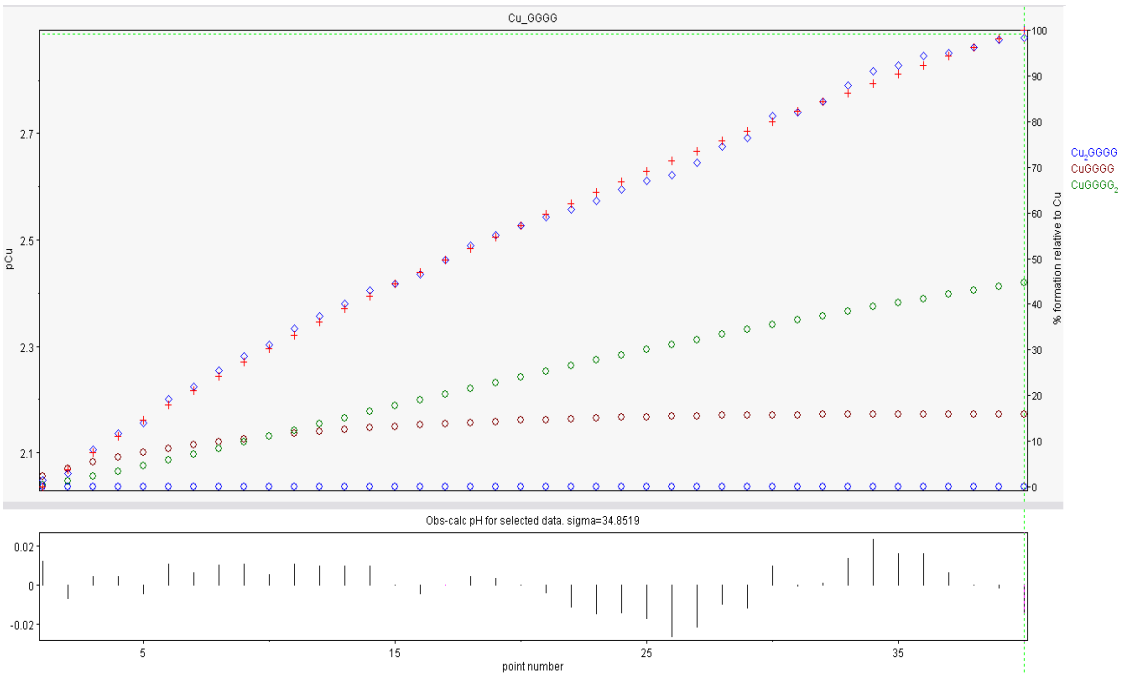

Figure3.65 Screenshot capture of the Hyperquad file of tetraglycine with Cu^{2+}. ○ = 1:1, M:L species (CuGGGG, ML), ○ = 2:1, M:L species (Cu_2GGGG, M_2L) and ○ = 1:2, M:L species ($CuGGGG_2$, ML_2). The experimental data (◊) closely follows the theoretically calculated Hyperquad values (+)

The experimental fit is excellent in relation to the theoretically calculated conditional stability constant values at 25 °C and 0.1 M ionic strength for tetraglycine (Figure 3.65). The Hyperquad values for the species obtained were: ML = 2.12 and ML_2 = 5.08. Although a M_2L species was initially postulated, it was ignored during refinement to obtain the best curve fit. The species observed for the Cu(II)-tetraglycine complex are similar to those formed with diglycine as the ligand. The complexes formed with copper(II) and triglycine (M_2L_3 and M_2L) are not observed but may be present as minor species. Comparing the Hyperquad results for Cu-tetraglycine to those obtained from WinCOMICS, it can be seen that the ML species was observed using both methods. The ML_2 species suggested by Hyperquad was not seen in the speciation diagram. With increasing ligand size and an excess of ligand taken into account in the WinCOMICS calculations, this result was not unexpected.

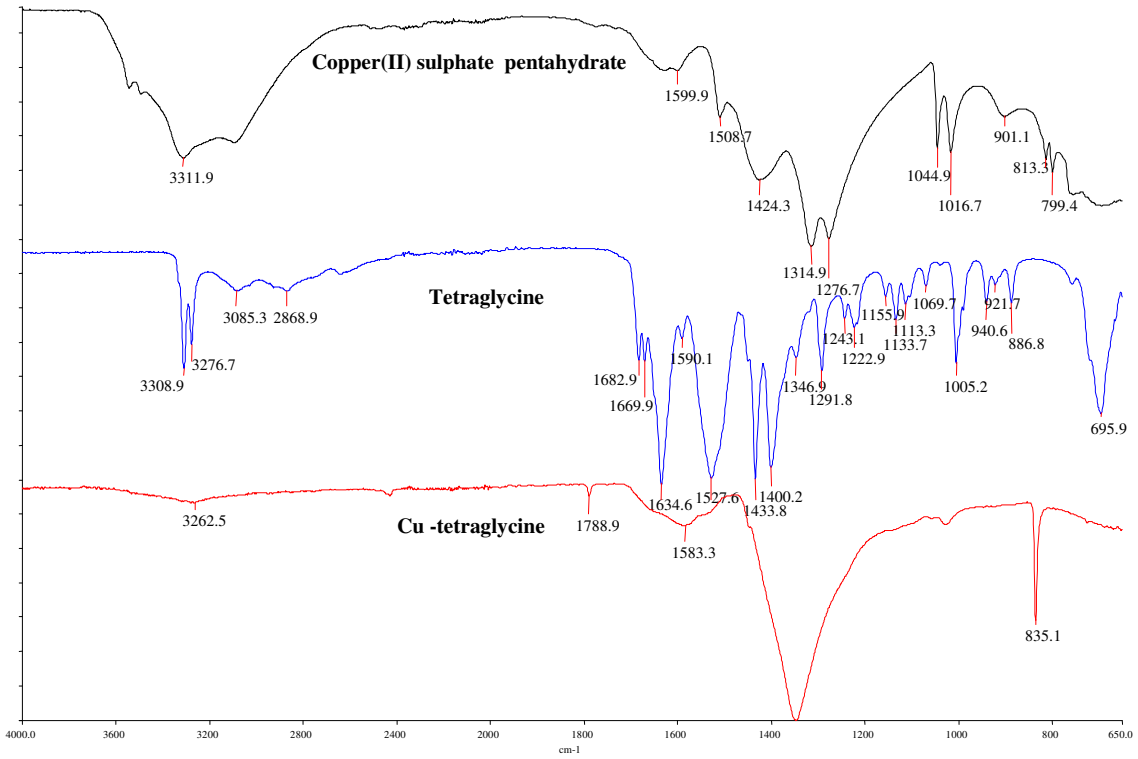

Figure 3.66 FTIR spectra of a copper(II) sulphate pentahydrate control, tetraglycine and a $(Gly)_4$-Cu complex

Spectral results from FTIR analysis for tetraglycine were similar to those obtained for the smaller complexes previously discussed. Band shifts in the υ(C=O) stretching vibration indicative of involvement of the carboxylic group in the covalent bonding to the metal ion and changes to the υ(N-H) stretching vibration suggesting the involvement of the $–NH_2$- group in complex formation were observed.

The largest of the glycine ligands analysed in this work was pentaglycine. Pentaglycine species obtained from the NIST database were as follows: ML, $M(H_{-1})L$, $M(H_{-2})L$ and $M(H_{-3})L$. This suggests loss of four protons which would give a -2 complex (three peptide protons and one carboxylate proton compensated by the +2 charge on Cu^{2+}). The aforementioned species were used to create a speciation diagram using WinCOMICS (Figure 3.67) and the pH values where deprotonation occurs are clearly visible.

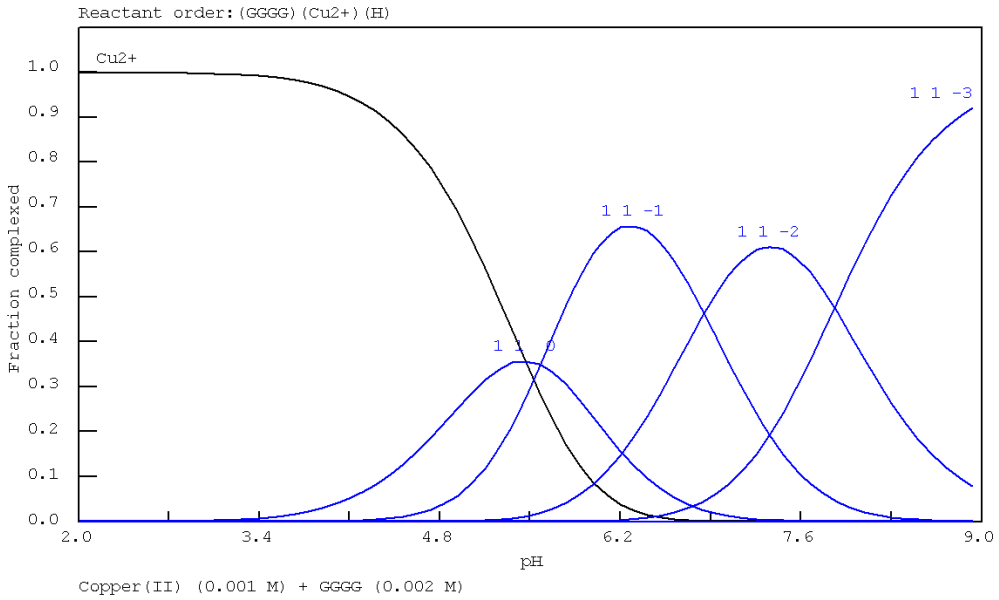

Figure 3.67 Speciation diagram created using WinCOMICS for Cu (0.001 M) and pentaglycine (0.002 M) at 25 °C and 0.1 M ionic strength, [M]:[L] = 1:2, (1,1,0 refers to a 1:1, L:M species; 1,1,-1 refers to 1 ligand, 1 metal and the loss of 1 proton, 1,1,-2 refers to 1 ligand, 1 metal and the loss of 2 protons and 1,1,-3 refers to a species comprised of 1 ligand, 1 metal and the loss of 3 protons)

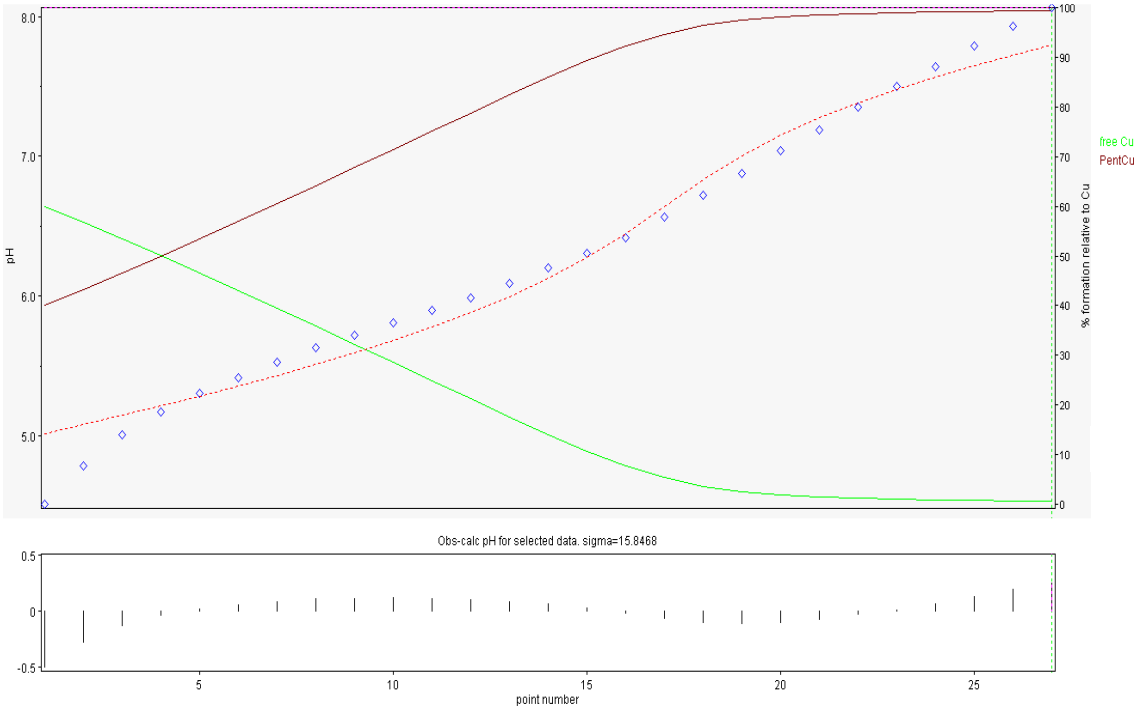

Figure 3.68 Screenshot capture of the Hyperquad file of pentaglycine with Cu^{2+}. - = free Cu^{2+}, - = 1:1, M:L species (CuGGGGG, ML). The experimental data (◊) closely follows the theoretically calculated Hyperquad values (---)

Hyperquad proposed only one major species – that of the 1:1, M:L (Figure 3.68). From the speciation diagram (Figure 3.67) it can be seen that at pH 5.5, the 1:1 species is indeed the major species and the two programs correlate well. As the pH is increased in the speciation diagram, further deprotonations occur and the pH values at which each proton is removed is quite clear (Figure 3.67).

As observed in the FTIR spectra for di-, tri- and tetraglycine with copper, band shifts indicative of complexation are observed in the case of pentaglycine with copper (Figure 3.69).

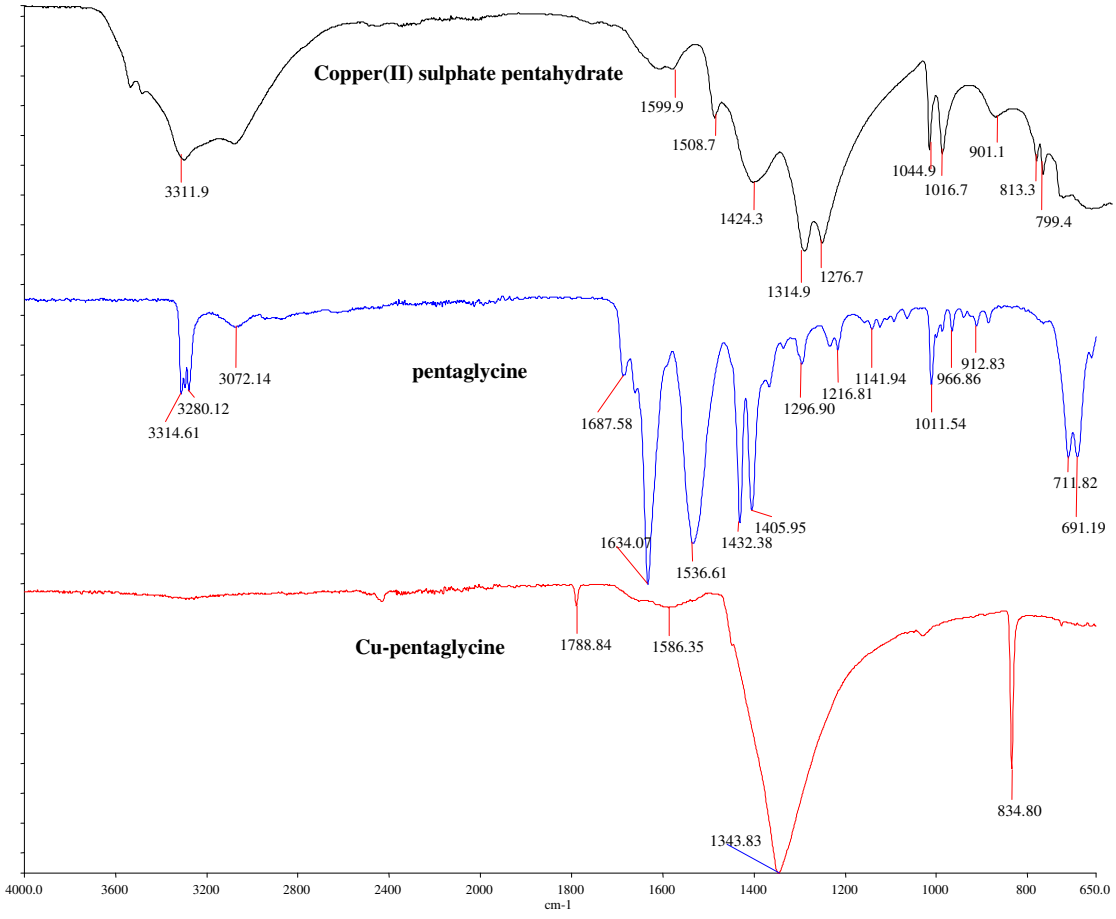

Figure 3.69 FTIR spectra of pentaglycine and a $(Gly)_5$-Cu complex

The speciation diagrams obtained using WinCOMICS are a useful indication of the effect of pH on the copper-glycine complexes. The stability constant values, obtained from pH titrations for di-, tri-, tetra- and pentaglycine ligands with Cu(II) using

Hyperquad, closely resemble those obtained from the literature (Table 3.15). Hyperquad can be used as a complementary analytical method to WinCOMICS confirming the presence of some of the theoretically postulated species in solution but has the advantage of identifying additional species based on experimental data that may not be present in the WinCOMICS speciation diagrams. With increasing ligand complexity however, modifications were made to the analytical procedure and prior to progressing to longer polypeptides it was necessary to confirm if the values obtained from Hyperquad under the conditions used were accurate. As previously mentioned, apparent stability constants were obtained from Hyperquad based on potentiometric titrations carried out at 25 °C, 0.1 M ionic strength and pH 5.5. Literature values are not available for the copper-glycine complexes under these conditions but algebraic manipulation of readily-available data should provide conclusive evidence that the modified procedure is accurate. Diglycine is selected to illustrate the theory. Based on values obtained in the literature for diglycine (Martell *et al.*, 1974), the following data were obtained:

$\log K_1 = 3.13$, $\log K_2 = 8.07$,
$\log \beta_{11\text{-}1} = 8.07$, $\log \beta_{21\text{-}1} = 11.20$,
$\log \beta_{110} = 5.50$ ([ML]/[M][L])

The successive stability constants, K_n, are related to the overall stability constants, β, as follows: $\beta = K_1K_2...K_n$. β terms in subscript refer to the species. M refers to the metal ion, L to the ligand and ML to the complex formed between M and L. Terms in square brackets refer to molar concentrations.

$$\log K = \frac{[ML]}{[MLH_{-1}][H^+]} = 4.07 \quad \text{(Martell } \textit{et al.}\text{, 1974)} \qquad \textbf{(3.4)}$$

Using The Chemical Society notation which is widely used for stability constants, the following equation is obtained:

$$M + L = MLH_{-1} + H^+ \qquad \textbf{(3.5a)}$$

$$\beta_{11-1} = \frac{[MLH_{-1}][H^+]}{[M][L]} \quad \textbf{(3.5b)}$$

$$= \frac{[ML]}{K.[H^+]} \cdot \frac{[H^+]}{[M][L]} \quad \textbf{(3.5c)}$$

$$= \frac{[ML]}{[M][L].K} \quad \textbf{(3.5d)}$$

$$= \frac{\beta_{110}}{K} \quad \textbf{(3.5e)}$$

$$= \frac{10^{5.50}}{10^{4.07}} \quad \textbf{(3.5f)}$$

$$= 10^{1.43}$$

$$\therefore \boldsymbol{\beta_{11-1}\, for\, [MLH_{-1}] = 10^{1.43}}$$

$$M + HL = MLH_{-1} + H^+ \quad \textbf{(3.6)}$$

and

$$HL = H^+ + L^-, \qquad K_a = \frac{[H^+][L^-]}{[HL]} \quad \textbf{(3.7, 3.8)}$$

from Hyperquad:

$$K_{meas} = \frac{[MLH_{-1}]}{[M][HL]} \quad \textbf{(3.9a)}$$

$$= \frac{\beta_{11-1}\,[M][L^-]}{[H^+]} \cdot \frac{1}{[M][HL]} \quad \textbf{(3.9b)}$$

$$= \frac{\beta_{11-1}}{[H^+]} \frac{.[L^-].K_a}{[H^+][L^-]} \quad \textbf{(3.9c)}$$

$$K_{meas} = \frac{\beta_{11-1}.K_a}{[H^+]^2} \quad \textbf{(3.9d)}$$

at pH 5.5:

$$= \frac{10^{1.43}.10^{-8.62}}{(10^{-5.5})^2} \quad (\mathbf{3.9e})$$

$$\mathbf{\log K_{meas} = 3.81}$$

Based on the above calculation it can be seen that at pH 5.5 a value of 3.81 was obtained for ML; the value returned by Hyperquad was 4.095. Variations in temperature and ionic strength would also affect the values obtained so it can be concluded that the values are sufficiently close to progress to more complex ligands using the modified method.

Comparing the results of the speciation diagrams created by WinCOMICS, an increase in complexity and richness of species was observed as the glycine ligands increased in size from diglycine to pentaglycine. With increasing pH, the larger ligands provided more sites for deprotonation. Furthermore, larger ligands with multidentate characteristics have the potential to bind more than one metal ion. The M_2L_3 species formed from the reaction of triglycine with copper is an example of such. The ability to identify the major species in a complex in addition to their respective stability constants is of great value. Due to the wide variety of products commercially available, the ability to identify chemical species which may play a significant role in nutritional supplementation is highly advantageous. Not all of the products available are equally effective, some use inorganic ligands, others are not chelates and the ability to identify the species present in the trace metal supplements allows superior products to be identified. Stability constants can play an important role in identifying the suitability of ligands for metal complexation and large variation in stability can exist. Effectively determining stability constants for a range of metal-ligand species is of immense value and can provide an additional means to compare and contrast products.

3.6.4 Potentiometric titrations of polypeptides and Cu^{2+} using an ISE.

The success of the previous two sections (Sections 3.6.2 and 3.6.3) provided enough confidence in the experimental technique to extend investigations in this area to ligands with little or no published stability constant information. Prior to assessing the marker peptides identified in Section 3.3.6.6, ranatensin ($C_{61}H_{84}N_{16}O_{13}S$), a peptide of similar molecular mass was analysed (Figure 3.70). There are no published protonation constants available for ligands such as ranatensin, a factor that hinders stability constant determination using the present methods. Therefore, it was necessary to develop a method for the determination of protonation constants and subsequently, stability constants for such ligands to expand current knowledge. Ranatensin contains some of the amino acid residues found in the peptide markers of interest in the present study including a histidine side chain which is known to aid metal complexation (Casolaro *et al.*, 1999; Kozlowski *et al.*, 1999; Kozlowski *et al.*, 2005; Remelli *et al.*, 2005; Kruppa *et al.*, 2006; Matera *et al.*, 2008). The reason for choosing ranatensin for initial investigations, prior to analysing the marker peptides of interest, was mainly due to the excessive cost of manufacturing the required synthetic peptides. From a cost perspective, ranatensin is less expensive to obtain than peptides produced from custom synthesis as it is available off the shelf and was therefore chosen for optimisation of the experimental parameters.

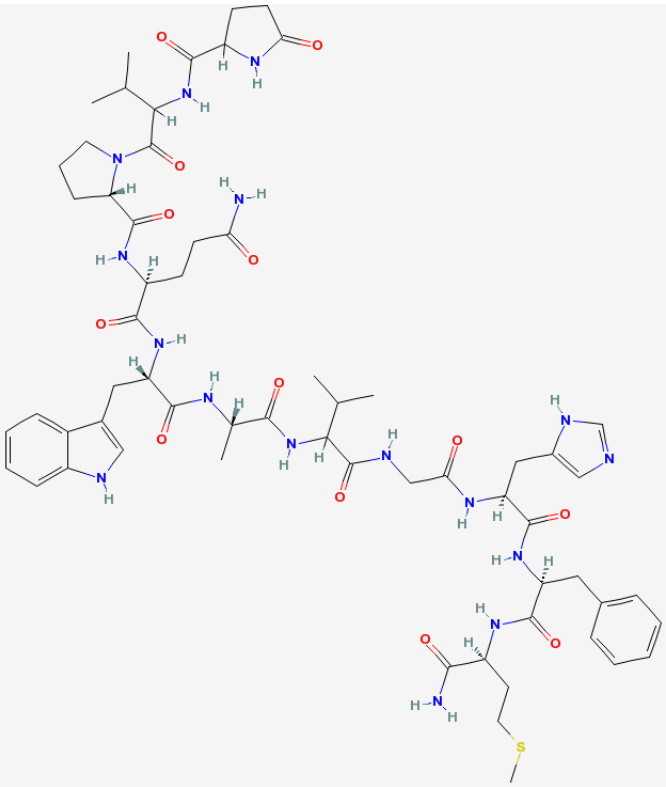

Figure 3.70 Structure of ranatensin, a polypeptide used as a metal peptide mimic (From PubChem)

Aliquots of ranatensin (0.5 mL) were titrated with copper(II) nitrate (1.95×10^{-4} M) at pH 5.5, 0.01 M ionic strength and 25 °C. Due to the lower concentrations of metal and ligand used than in previous experiments with amino acids and short chain peptides, the ionic strength of the solution was also reduced. Measurements of EMF over the course of the titration suggested that complex formation had occurred but that binding was weak (Figure 3.72). Considering the pH at which the titration was conducted, there was the possibility that a precipitate of copper hydroxide may have formed. Some straightforward calculations relating to the solubility product (K_{sp}) for $Cu(OH)_2$ provide further clarity on this situation. The solubility product for $Cu(OH)_2$ is 2.2×10^{-20} M (Patnaik, 2002) and based on this solubility product, any $Cu(OH)_2$ formed will be insoluble.

$$Cu(OH)_2 \rightleftharpoons Cu^{2+} + 2OH^- \qquad (\mathbf{3.10})$$

$$K_{sp} = [Cu^{2+}] [OH^-]^2 \quad (\mathbf{3.11})$$

$$K_w = [H^+] [OH^-] = 1 \times 10^{-14} \quad (\mathbf{3.12})$$

At pH 5.5 which was the pH at which the titration was carried out; pOH = 8.5. Substituting into Equation **3.11** provided the following data:

$$2.2 \times 10^{-20} = [Cu^{2+}] (1.0 \times 10^{-8.5}) \text{ and } [Cu^{2+}] = 2.2 \times 10^{-3}$$

Based on the results of the calculations it can be concluded that the maximum permissible copper concentration at pH 5.5 is 2.2×10^{-3}. Provided the concentration is below this value (which is the case for the Cu-ranatensin titration), a precipitate will not occur. The copper concentration for the Cu-ranatensin titration was 1.95×10^{-4}. To determine the maximum pH of the solution with the aforementioned copper concentration to prevent precipitation it was necessary to again employ Equation **3.11** and the following data was obtained:

$$2.2 \times 10^{-20} = [1.95 \times 10^{-4}] [OH^-]^2 \text{ and } [OH^-] = 1.06 \times 10^{-8}$$

$$-\log[OH^-] = pOH = 7.98 \therefore pH = 6.02$$

From the results obtained it is clear that the pH must be below 6.02 to prevent precipitation at a copper(II) concentration of 1.95×10^{-4}. Constant stirring was carried out over the course of all titrations to prevent localised conditions that fall outside these ranges which may contribute to a precipitate. As the pH was maintained at a value of 5.5 throughout, the possibility of precipitate formation was eliminated. It can be concluded that the reduction in free copper in the experiment was due to complexation rather than precipitation. Furthermore, according to Martell (1957), transition metals will not precipitate as hydroxides in the presence of an excess of chelating agent even at pH values as high as 11.0. This however, is highly dependent on the stability constants of the complexes.

In addition to Hyperquad analysis to determine stability constants for the Cu-ranatensin titration (Figure 3.72), SELDI-ToF-MS was employed to confirm the presence of copper-peptide adducts (Figure 3.71). The visible appearance of an adduct peak 62.1 Da greater in mass than the parent peak of 1281.6 Da in the SELDI-ToF-MS spectra confirms the presence of a putative metal adduct and suggested binding had taken place (Figure 3.71, Panel 2). To verify that this is indeed a complex, EDTA, which has a very high affinity for divalent metal ions was added and the resultant spectrum was monitored for the disappearance of the adduct peak (Figure 3.71, Panel 3). The resultant spectrometric data confirmed the disappearance of the adduct peak indicating EDTA had successfully stripped the metal adduct from the parent peptide.

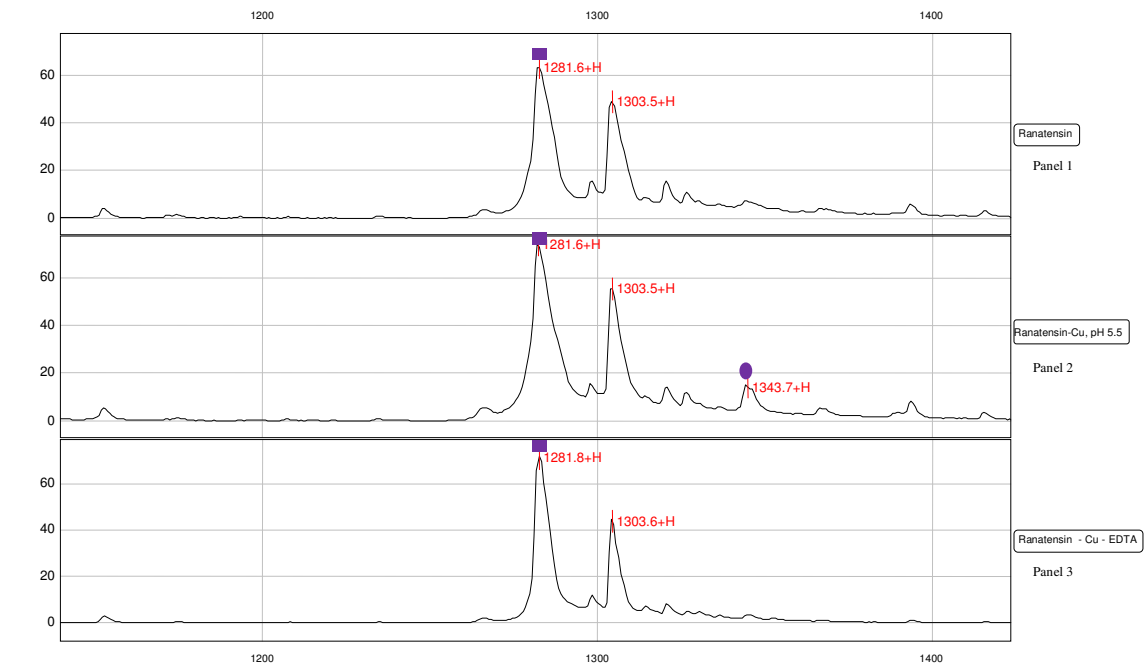

Figure 3.71 SELDI-ToF-MS spectra of ranatensin (Panel 1), the formation of a ranatensin-Cu complex (Panel 2) and the complex after treatment with EDTA (Panel 3) (■ indicates the parent peptide in each panel and ● indicates the metal-peptide adduct)

A protocol developed by R.J Angelici (Angelici *et al.*, 1999) was used to determine the pK_a of ranatensin using a standard acid-base titration in an attempt to examine additional means of obtaining stability constants. The protocol was first applied to glycine, an amino acid with a known protonation constant, to ensure experimental

accuracy. In brief, a solution of glycine in 1.0 M KNO_3 was titrated with aliquots of 1.0 M NaOH and the pH of the solution was measured after each addition of NaOH. Substituting the values obtained into the expression derived for pK_a determination (**3.13**), the pK_a for glycine was calculated.

$$pK_a = -\log[H^+] + \log\left(\frac{L_{tot} - ([Na^+] + [H^+] - [OH^-])}{[Na^+] + [H^+] - [OH^-]}\right) \quad \textbf{(3.13)}$$

L_{tot} refers to the total concentration of glycine, $[OH^-]$ can be calculated by making use of the autoionisation constant of water, K_w (**3.12**) and $[Na^+]$ will vary based on the aliquot volume. Since all quantities on the right-hand side of the expression are either known or may be calculated, the pK_a for glycine can be obtained. The value obtained experimentally for glycine at 25 °C was 9.56 ([HL] / [H][L]). The theoretical value obtained using the NIST database was 9.57. Based on the success of the protocol for glycine, the method was subsequently applied to ranatensin.

As the titration of copper(II) and ranatensin was carried out at pH 5.5, the pK_a value for ranatensin was investigated at this pH value. A pK_a value of 4.56 was obtained for the ranatensin ligand. However, with adjustments to the Hyperquad program including modifications by the developer allowing the importation of EMF data, it was found that conditional stability constants could be determined for metal:ligand complexes in the absence of the ligand pK_a values solely by concentrating on the metal ligand species formed in the titration and maintaining a constant pH (Figure 3.72). This was of significance as it provided a means to assess a large selection of ligands with no published protonation constants, and obtain stability constants for a number of metal-ligand species. Results obtained for ranatensin indicate very weak binding took place with a conditional stability constant of 2.77 for the 1:1, L:M complex.

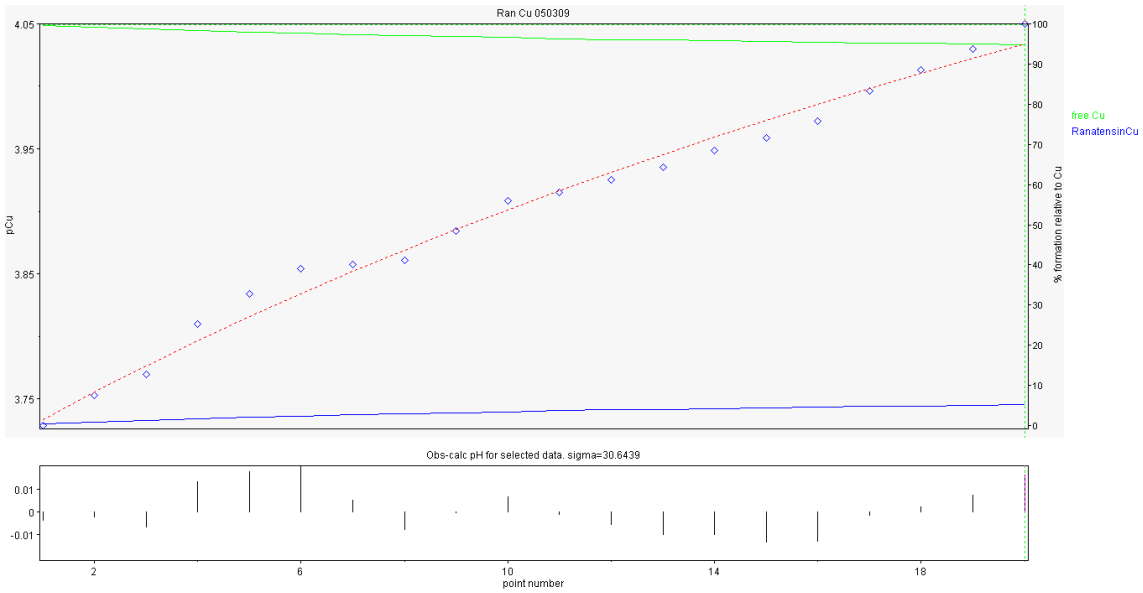

Figure 3.72 Screenshot capture of the Hyperquad file of the reaction between Cu^{2+} and ranatensin at pH 5.5. - = free Cu^{2+} and - = 1:1, M:L species (Cu-Ranatensin, ML). The experimental data (◊) closely follows the theoretically calculated Hyperquad values (---)

Consultations with the developer to improve the Hyperquad software and development of suitable titration conditions (pH, temperature and ionic strength) using ranatensin as a ligand, provided a means to obtain stability constants for larger ligands with unknown protonation constants and little or no literature data available. Use of SELDI-ToF-MS provided a complimentary method of analysis, identifying the molecular mass of the unknown ligand in addition to confirming the presence and removal of a copper adduct. Based on the results obtained for ranatensin with Cu, the methods and techniques could now be applied to the marker peptides previously identified in the metal proteinates to obtain information on the species formed with copper in addition to their respective stability constants.

3.6.5 Potentiometric titrations of novel peptide ligands and Cu^{2+} using an ISE

Four of the five marker peptides of interest (1148 Da, 1181 Da, 1300 Da and 1514 Da) identified in Section 3.3.6.6 were analysed once the titration procedure had been optimised. Due to the high manufacturing cost involved in the peptide synthesis, very small quantities were used for the titrations and as a result, the ligand concentrations were very low. In some aspects this was advantageous as the metal concentration was also low (based on final titrant ratios of 1:2, M:L), discouraging potential precipitate formation. In addition to potentiometric titrations and the use of Hyperquad to interpret the results for the 1148 Da, 1181 Da, 1300 Da and 1514 Da synthetic peptides, SELDI-ToF-MS analysis was carried out on the ligands before and after the titrations to determine if complexation had taken place and if the species identified by Hyperquad were present in the mass spectrometric data.

Section 3.6 outlined the fitting criteria used to create proposed models in the Hyperquad program. Based on these proposed models, the species combinations resulting in the best curve fit are reported for each peptide in this section and the reasoning behind the Hyperquad model selection is also outlined. Care needed to be taken not to "invent" additional complex species solely for the purpose of improving the fit of the calculated results to the experimental curves. The species considered to be present in the experimental solutions are those that one would expect to form according to established principles of coordination chemistry while taking into account types of donor groups, the nature of the metal ion, and analogous known metal complex systems including protonated metal chelates and hydroxo-metal chelate species. As mentioned previously, only the major species are included in the Hyperquad data although a number of minor species may also be present. The fit of the experimental curve is good however, so the omission of minor species that may be present has little or no effect on the overall results.

3.6.5.1 Determination of stability constants for the 1148 Da marker peptide with Cu^{2+}

A Cu^{2+} ISE was used to obtain EMF values for the titration of 2.1771 x 10^{-4} M copper(II) (10 mL) with aliquots (0.5 mL) of the 1148 Da synthetic peptide (2.1771 x 10^{-4} M) at pH 5.5, 0.01 M ionic strength and 25 °C. The metal was initially in excess which could allow formation of multi-metal species. After 20 ligand additions the M:L ratio was 1:1 and subsequent ligand additions ensured an excess of ligand. The resultant data was input to Hyperquad and stability constants were obtained. The titration data provided quite a good fit with deviations distributed evenly throughout the titration. There was no indication of systematic deviations but there did appear to be a slight irregularity in the experimental data between points 18 – 22 which lie below the theoretical values on the curve (Figure 3.73). Possible explanations for the irregularity may be a surge in electrical current or a minor temperature deviation during the course of the titration. Steps were taken to minimise effects of temperature fluctuations by carrying out all experiments in a jacketed beaker.

To obtain the best curve fit it was necessary to investigate a number of potential models with a range of species combinations. Bearing in mind the necessity of the species to make chemical sense, a trial and error method was used to identify the species formed that provided the closest curve fit between the theoretical values postulated by Hyperquad and the experimental values obtained. Comparison of the titration curve and the pCu (pCu = -log [Cu^{2+}]) values can provide an indication of the stability of the complexes formed and will be monitored for all potentiometric titrations.

The first Hyperquad model identified three major species:

ML	Cu (1148 Da)	$\log\beta_{11} = 4.62 \pm 0.03$
M_2L	Cu_2 (1148 Da)	$\log\beta_{21} = 8.20 \pm 0.12$
ML_2	Cu (1148 Da)$_2$	$\log\beta_{12} = 8.54 \pm 0.26$ (Excessive)
	Sigma value for this model = 74.3	

$\log\beta$ refers to the log of the stability constant and the corresponding subscript referring to the metal:ligand ratio.

In Hyperquad, the stability constants, β, (not log β) are the parameters that are refined and a standard deviation was labelled as excessive if it was more than 33 % of the parameter value (Gans *et al.*, 2008). Although this value was user-definable, the default value of 33 % was used. The sigma value is an indication of the goodness of fit. The lower the value, the closer the curve fit of experimental and calculated data.

A second Hyperquad model suggested the presence of only two major species, a 1:1, M:L complex and a 2:1, M:L complex:

ML	Cu (1148 Da)	$\log\beta_{11} = 4.66 \pm 0.02$
M_2L	Cu_2 (1148 Da)	$\log\beta_{21} = 7.94 \pm 0.10$
	Sigma value for this model = 79.6	

Removal of the ML_2 complex which was identified in the first model did not result in a significant difference to the fit which remained quite good. The sigma value is marginally better in the first model.

A third model postulated the presence of three species. Overall, this model had the lowest sigma value and produced the best curve fit of the three models:

ML	Cu (1148 Da)	$\log\beta_{11} = 4.50 \pm 0.08$
M_2L	Cu_2 (1148 Da)	$\log\beta_{21} = 8.18 \pm 0.09$
M_2L_3	Cu_2 (1148 Da)$_3$	$\log\beta_{23} = 17.26 \pm 0.23$ (Excessive)
	Sigma value for this model = 72.7	

This was the model selected for inclusion in this work (Figure 3.73).

Based on the Hyperquad data which corresponds to the graph in Figure 3.73, much more of the Cu_2L_3 and CuL complexes were present at the end of the titration and a reduction in the concentration of the Cu_2L complex was observed as the concentration of the M_2L_3 species increased. With increasing ligand concentration over the course of the titration, the propensity towards multi metal-ligand species formation is increased due to the availability of additional metal binding sites. Thorough examination of

published data provided limited information on such complexes and the ability of Hyperquad to determine these species is highly advantageous.

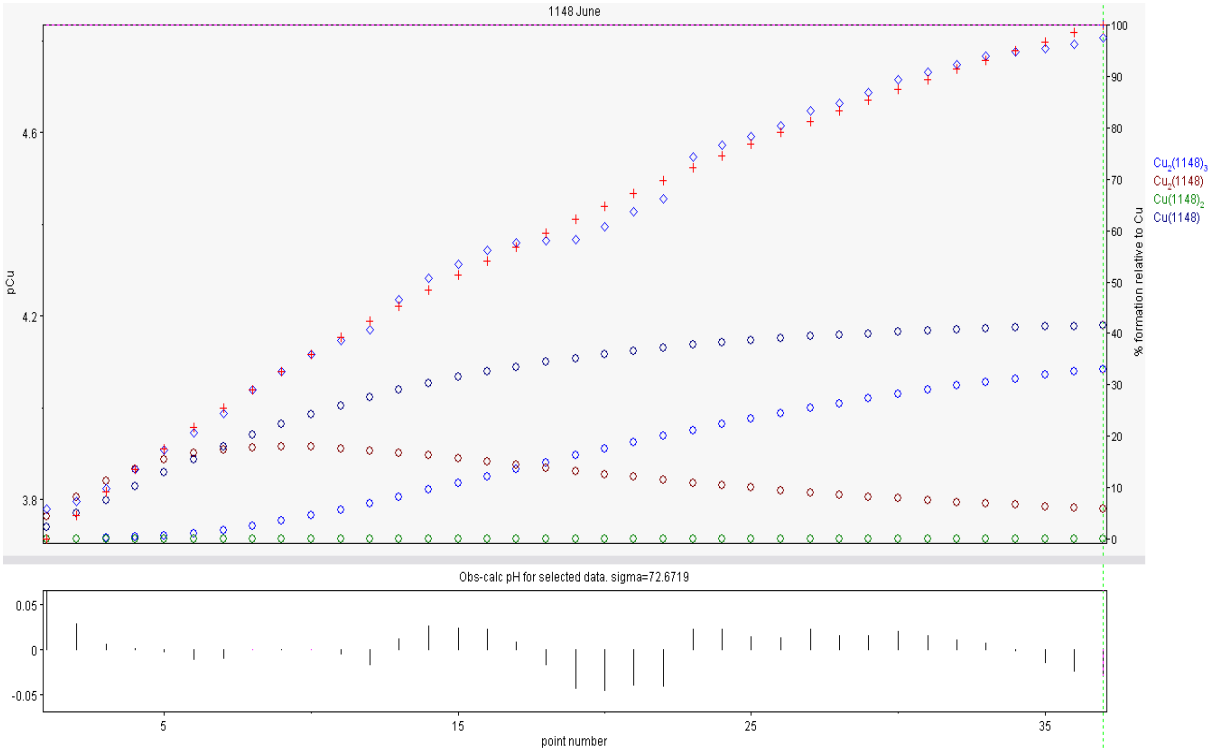

Figure 3.73 Screenshot capture of the Hyperquad file of the 1148 Da synthetic peptide with Cu^{2+} at pH 5.5 and 0.1 M ionic strength at 25 ^{o}C. ○ = 2:1, M:L species (Cu_2(1148), M_2L), ○ = 2:3, M:L species ($Cu_2(1148)_3$, M_2L_3), ○ =1:1, M:L species (Cu(1148), ML) and ○ = 1:2, M:L species ($Cu(1148)_2$, ML_2). The experimental data (◊) closely follows the theoretically calculated Hyperquad values (+)

To determine the purity of the 1148 Da peptide, SELDI-ToF-MS was employed and based on the results in Figure 3.74 a slight impurity was detected at 1205.4 Da. The second panel in Figure 3.74 illustrates the spectra for the 1148 Da peptide titrated with copper. A potential Cu adduct can be seen at 1210.7 Da in the spectra. This compliments the proposed 1:1, L:M species from Hyperquad which would have a similar molecular mass (minor deviations in molecular mass may be due to reasons previously discussed in Section 3.3.6.5). Finally, based on previous success with EDTA as a sequestering agent, this ligand was selected to determine if the metal could be stripped from the peptide. The third panel in Figure 3.74 clearly illustrates the removal of the 1210.7 Da metal adduct using EDTA. Two additional peaks present in the

SELDI-ToF-MS spectra containing the copper salt at 1170.8 Da and 1192.7 Da may be indicative of the presence of Na with an atomic mass of 23.

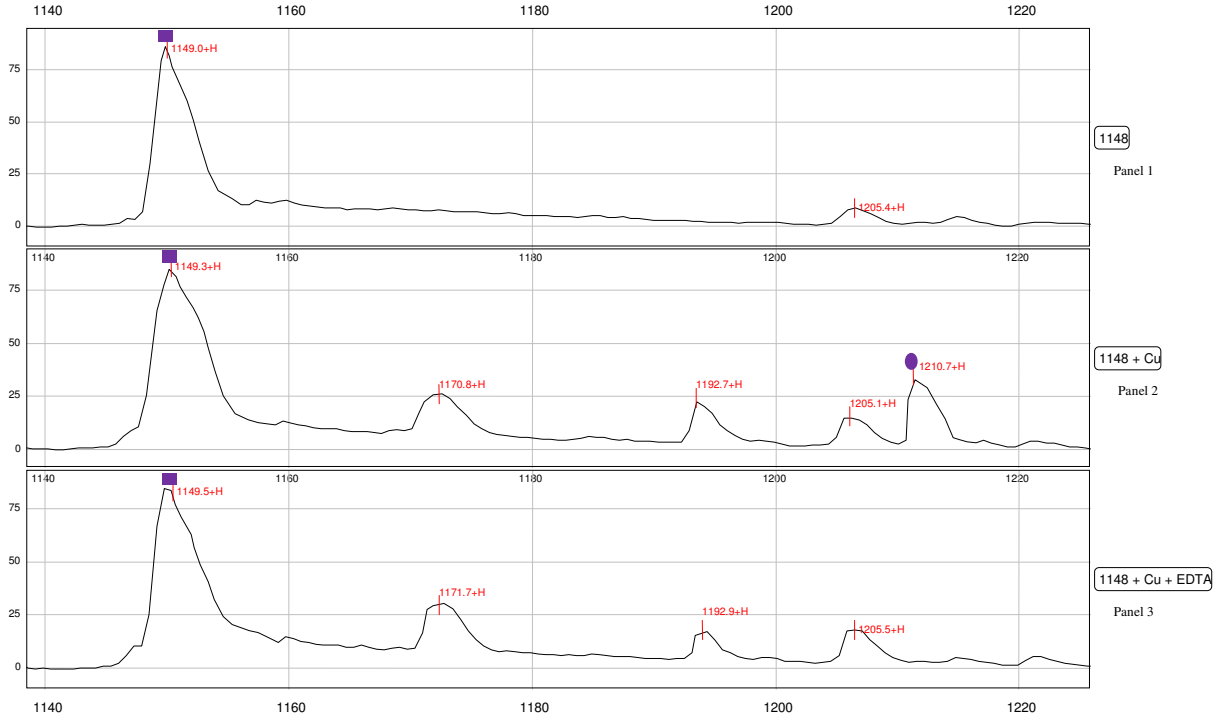

Figure 3.74 SELDI-ToF-MS spectra of the 1148 Da synthetic peptide before and after titration with Cu and on treatment with EDTA (■ indicates the parent peptide in each panel and ● indicates the metal-peptide adduct)

Infrared spectroscopy was also employed to determine if spectral shifts indicative of complexation were observed after the synthetic peptide was titrated with Cu(II). Copper(II) sulphate pentahydrate which was the metal salt used to prepare the chelate, was analysed as a control sample alongside the 1148 Da synthetic peptide on its own and the titrated L:M sample. Band shifts were observed in the FTIR spectrum (Figure 3.75) and based on previous spectral analyses (Sections 3.3.4 and 3.6.2) were indicative of complexation with the involvement of $-NH_2$ and C=O groups.

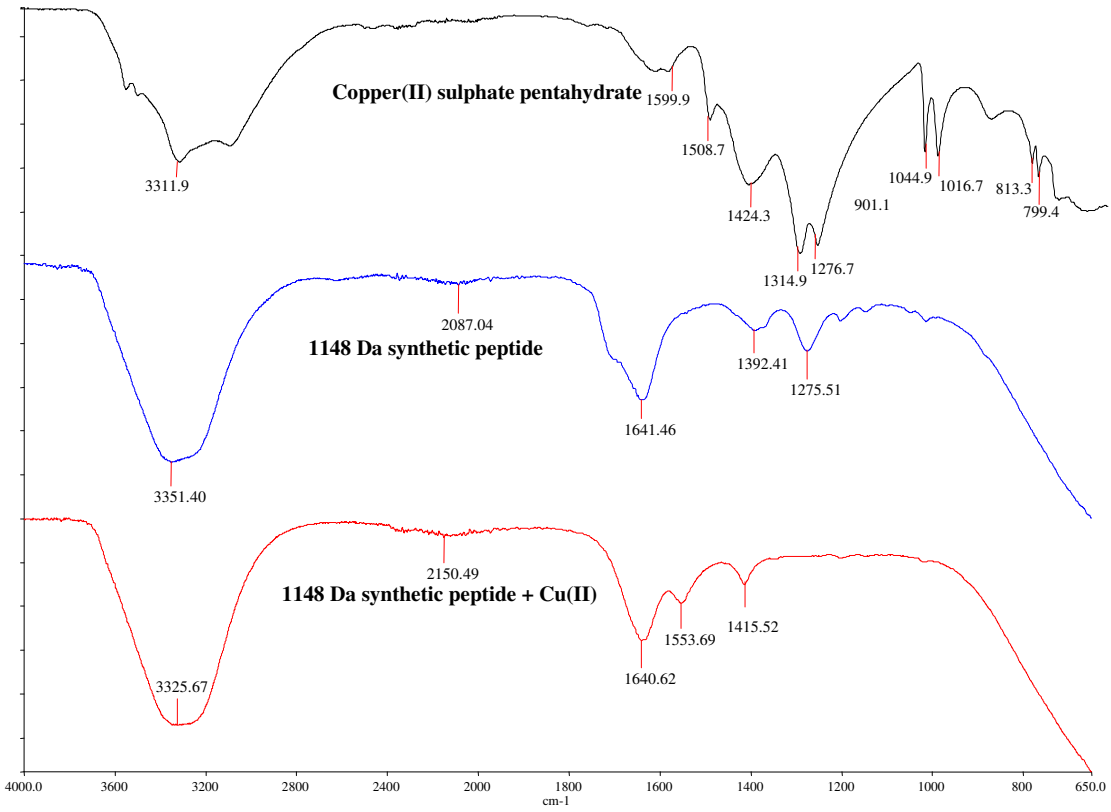

Figure 3.75 FTIR spectra of the 1148 Da synthetic peptide titrated with Cu(II) and a copper and a peptide control

The amino acid sequence for the 1148 Da synthetic peptide was determined from tandem mass spectrometry analysis as: Phe-Lys-Asn-Gln-Tyr-Gly-His-Val-Arg (Section 3.3.6.9). Factors contributing to the stability of the complex may include residues containing aromatic rings such as Tyr, Phe or Trp, hydrophobic interactions or ring stacking (Kozlowski *et al.*, 1999). In relation to the presence of histidine in the peptide sequence which is known to have a stabilising effect in some positions, separation of the N-terminal amine and the imidazole donors by two or more intervening amino acid residues removes the possibility of concerted formation of the fused chelate system, because there are five or more potential nitrogen donors for four equatorial sites around the metal ion (Kozlowski *et al.*, 1999). This is the case in relation to the 1148 Da peptide and the stabilising effect of histidine is minimal in this position. Previous studies (Pettit *et al.*, 1990; Kozlowski *et al.*, 1999) have examined the effect of histidine at various positions in a peptide sequence (Figure 3.76).

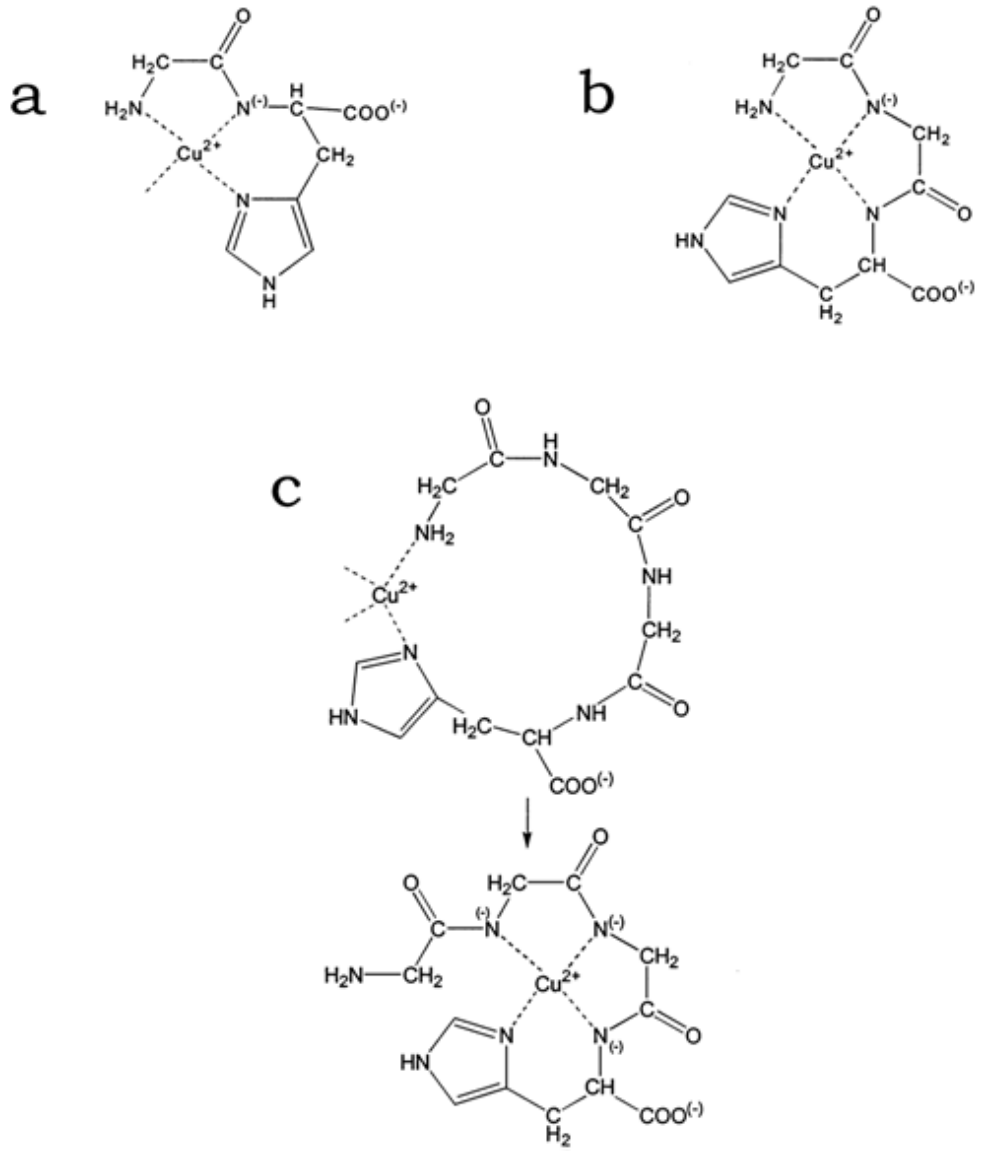

Figure 3.76 Structures of 1:1, metal:ligand complex species for (a) Gly-His ($CuH_{-1}L$), (b) Gly-Gly-His ($CuH_{-2}L$) and (c) Gly-Gly-Gly-His. Diagram adapted from Kozlowski *et al*., 1999

The presence of histidine in position two results in the formation of a pair of fused chelate rings, the 5 membered (NH_2) and the six membered (N^-, N_{im}) (a). Histidine in position 3 allows for the simultaneous formations of 3 fused chelate rings and thus saturation of the coordination plane (b). When histidine is found in position four as seen in the tetrapeptide Gly-Gly-Gly-His (c), the formation of a 15-membered macrochelate loop with NH_2, N_{im} coordination at neutral pH for the 2N complex species was postulated (Kozlowski *et al.*, 1999). With increasing pH, amide deprotonations occur

and imidazole anchoring is preferred, forming a system of two (3N) and subsequently three (4N) chelate rings. The amine donor remains uncoordinated (Kozlowski *et al.*, 1999).

The 1148 Da peptide has a relatively low stability constant for the 1:1 metal:ligand complex ($\log\beta_{11} = 4.50 \pm 0.08$). The aforementioned analysis of the amino acid sequence, and the weak effect of histidine on stability due to its position in the sequence, provides an indication as to why this may be the case.

3.6.5.2 Determination of stability constants for the 1181 Da marker peptide with Cu^{2+}

Aliquots (0.5 mL) of the 1181 Da synthetic peptide (2.1162×10^{-4} M) at pH 5.5, 0.01 M ionic strength and 25 °C were titrated against a 2.1162×10^{-4} M copper(II) solution. The resultant data were input to Hyperquad and stability constants were obtained. A range of models were again tested using Hyperquad to obtain the best curve fit for the 1181 Da synthetic peptide but this particular peptide appeared to refine best with a 1:1, metal:ligand complex only (Figure 3.77). As previously mentioned, logβ refers to the log of the stability constant and the corresponding subscript referring to the metal:ligand ratio.

Cu (1181 Da) $\log\beta_{11} = 4.18. \pm 0.01$

Sigma value for this model = 37.1

The fit was excellent over the entire titration apart from points 22 – 25 where there appeared to be a minor discrepancy in the experimental data with these points lying above the theoretical values on the curve (Figure 3.77). The low sigma value confirms the goodness of fit for this titration. A similar irregularity was observed in the titration results of the 1148 Da synthetic peptide and similar explanations for the irregularity such as a surge in current or a temporary change in temperature may be proposed. The logβ value for the 1:1 complex was similar to that obtained for the 1148 Da synthetic peptide.

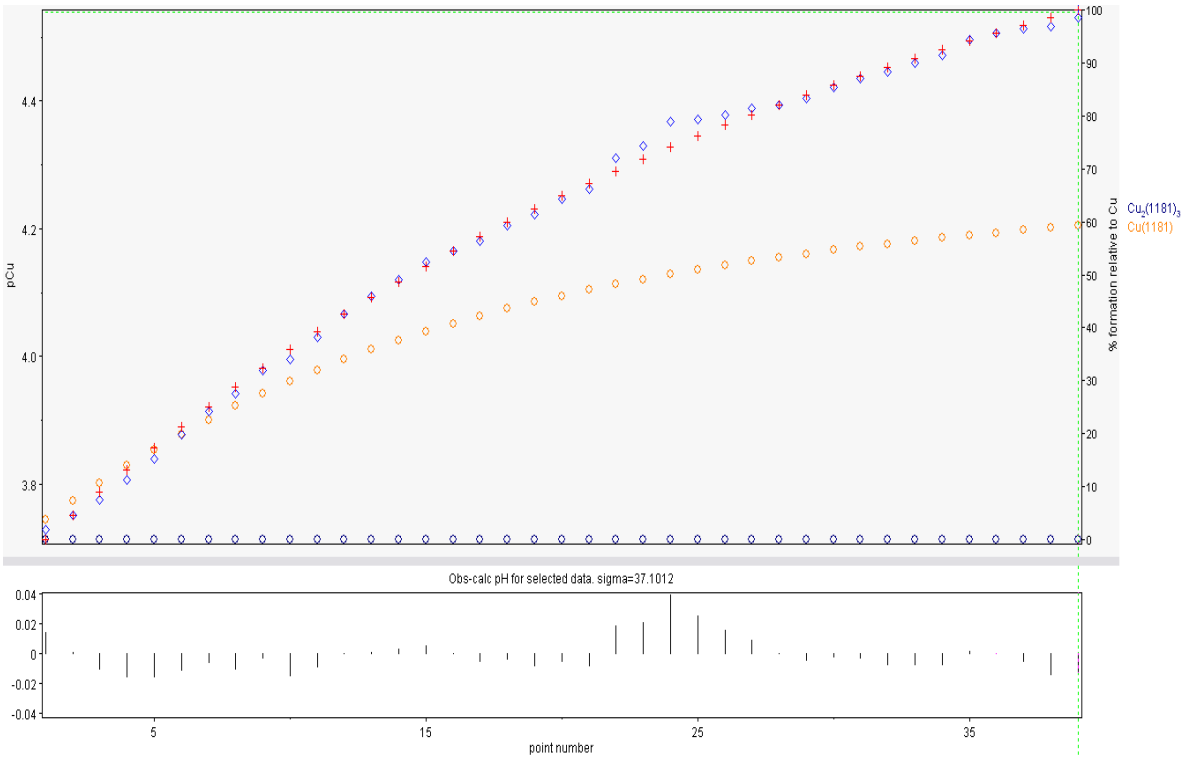

Figure 3.77 Screenshot capture of the Hyperquad file of the 1181 Da synthetic peptide with Cu^{2+} at pH 5.5 and 0.1 M ionic strength at 25 ^{o}C. ○ = 1:1, M:L species (Cu(1181), ML) and ○ = 2:3, M:L species ($Cu_2(1181)_3$, M_2L_3). The experimental data (◊) closely follows the theoretically calculated Hyperquad values (+)

The purity of the 1181 Da synthetic peptide was investigated using SELDI-ToF-MS and only minor impurities were observed in the spectra (Figure 3.78, Panel 1). The solution formed at the end of the metal:ligand titration was also analysed and the presence of a metal adduct at 1244.2 Da is clearly visible in the second panel which is within acceptable limits based on mass spectrometric deviations for a copper adduct. This correlates with the Hyperquad model which indicated that the major species present was a 1:1, M:L complex. EDTA was used as a sequestering agent and the resultant absence of the 1244.2 Da adduct can be seen in the third SELDI-ToF-MS panel in Figure 3.78.

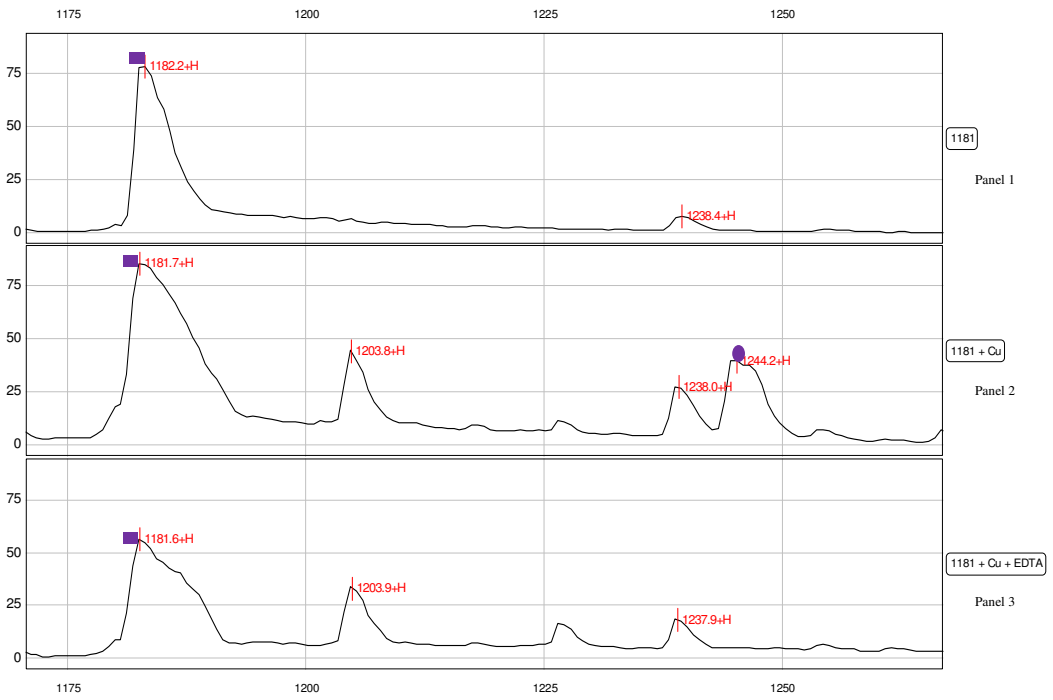

Figure 3.78 SELDI-ToF-MS spectra of the 1181 Da synthetic peptide before and after titration with Cu. EDTA was added to an aliquot to determine if the Cu adduct could be removed (■ indicates the parent peptide in each panel and ● indicates the metal-peptide adduct)

Infra-red spectroscopy showed shifts in the fingerprint region of the 1181 Da peptide titrated sample similar to those seen for the 1148 Da synthetic peptide titration indicating similar complexation had occurred with copper(II) in this case (Figure 3.79).

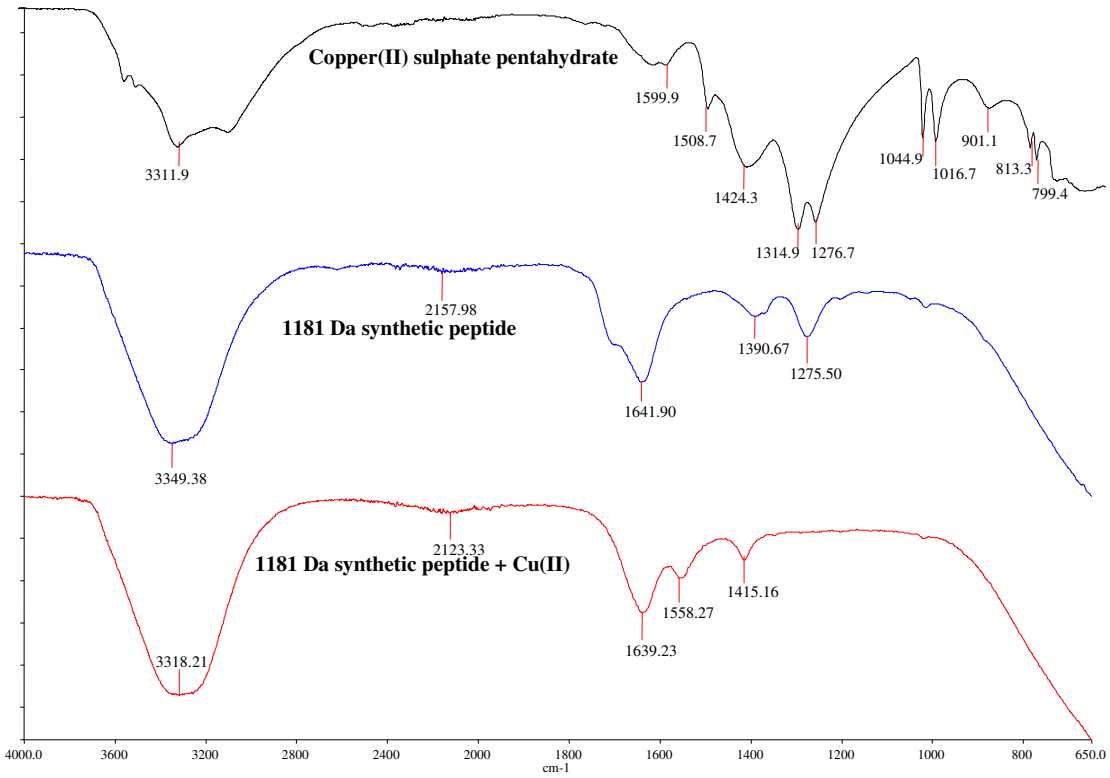

Figure 3.79 FTIR spectra of the 1181 Da synthetic peptide titrated with Cu(II) and a copper and a peptide control

The 9 amino acids contained in the sequence for the 1181 Da synthetic peptide are: Phe-Lys-Asn-Gln-Tyr-Gly-Arg-Ile-Arg (Section 3.3.6.9). Similarities between the 1181 Da peptide sequence and the 1148 Da synthetic peptide are clear with only two amino acids differing in the entire sequence, however, positional changes with respect to amino acids in a peptide sequence can significantly impact on stability as previously observed in Section 3.6.3. Due to the similarities observed, it is unsurprising that the $\log\beta_{11}$ values obtained using Hyperquad are close for both peptides. Tyr and Phe are present in the 1181 Da peptide which may contribute to the stability of the complex as previously mentioned in the case of the 1148 Da synthetic peptide. The absence of His in this sequence may contribute to the lower stability constant compared to the 1148 Da peptide. However, due to the position of the histidine residue in the 1148 Da chain as discussed previously, it was unlikely to have played a major role in the stability of the complex and may explain why its stability constant is only moderately higher ($\log \beta_{11}$ of 4.50 for the 1148 Da peptide vs. a $\log \beta_{11}$ of 4.18 for the 1181 Da peptide for a 1:1, L:M ratio).

3.6.5.3 Determination of stability constants for the 1300 Da marker peptide with Cu^{2+}

Potentiometric data for the titration of 1.9215 x 10^{-4} M copper(II) with aliquots (0.5 mL) of the 1300 Da synthetic peptide (1.9215 x 10^{-4} M) at pH 5.5, 0.01 M ionic strength and 25 °C was obtained and the resultant EMF values were analysed using Hyperquad. Comparison of the titration curve and the pCu (pCu = -log [Cu^{2+}]) values showed that this ligand formed by far the most stable complexes with Cu^{2+} (Figure 3.80). At a titrant volume of 10 ml (point 20) one mole of peptide had been added per mole of Cu^{2+} present. Consequently, at point 30, 1.5 moles of peptide had been added per mole of Cu^{2+} present. If this represented an endpoint, we could assume $Cu_2(1300\ Da)_3$ as a species present where the average number of metals bound per ligand is 0.66.

Of the models tested, the following appeared to give the best curve fit:

Cu (1300 Da)	$\log\beta_{11} = 6.63 \pm 0.03$
Cu_2 (1300 Da)	$\log\beta_{21} = 10.64 \pm 0.08$
Cu_2 (1300 Da)$_3$	$\log\beta_{23} = 25.08 \pm 0.15$

Sigma value for this model = 94.8

where logβ refers to the log of the stability constant and the corresponding subscript referring to the metal:ligand ratio.

The results make chemical sense as $\log\beta_{11}$ for the 1:1 complex was the largest of all the peptides investigated here. Similarly, $\log\beta_{21}$ for the Cu_2L complex was the largest when compared to all of the other Cu-ligand complexes containing a 2:1, metal:ligand species. Both of these observations were consistent with the large pCu (i.e. low [Cu^{2+}]) values observed during the titration. The fact that this ligand formed the most stable complexes with Cu^{2+} compared to the other marker peptides presented difficulties at the latter part of the titration which was carried out at the lower linear region of the standard curve as it was previously established that the linear response of the Cu^{2+} ISE at pCu values larger than 5, (i.e. at Cu^{2+} concentrations lower than ca. 10^{-5} M) was reduced. This may have been the reason for the sharp endpoint relative to the titrations with the other marker peptides. Furthermore, the sigma value in this example is higher than in

previous titrations indicating the fit is not as good. It appeared that virtually all of the Cu was complexed and very little free Cu remained which caused the sharp endpoint when the M:L ratio was 1:1.

Analysis of the Hyperquad data and the potentiometric graph in Figure 3.80 indicated that the largest increase in formation was in relation to the Cu_2L_3 species. A reduction was noted in the Cu_2L species and the 1:1, M:L species increased over the mid section of the titration but was only marginally higher at the titration endpoint than at the start of the titration. As observed in previous titrations, the increased ligand concentration over the course of the titration increased the potential for larger multi metal-ligand species formation.

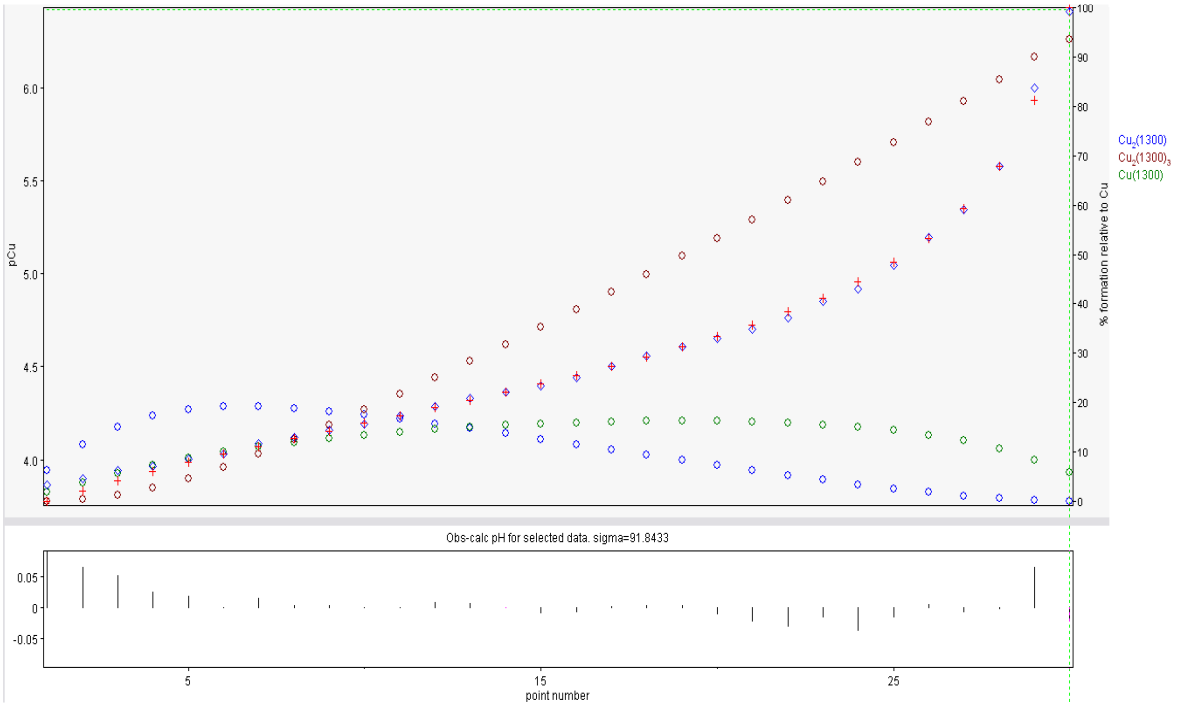

Figure 3.80 Screenshot capture of the Hyperquad file of the 1300 Da synthetic peptide with Cu^{2+} at pH 5.5 and 0.1 M ionic strength at 25 ^{o}C. ○ = 2:1, M:L species ($Cu_2(1300)$, M_2L), ○ = 2:3, M:L species ($Cu_2(1300)_3$, M_2L_3) and ○ = 1:1, M:L species (Cu(1300), ML). The experimental data (◊) closely follows the theoretically calculated Hyperquad values (+)

The purity of the 1300 Da peptide was examined by SELDI-ToF-MS and found to be reasonably high with only the parent 1300 Da peptide peak present at high

intensities (Figure 3.81, Panel 1). The complex formed at the end of the titration was also investigated and Panel 2 shows the presence of the copper metal adduct at 1363.5 Da. The metal adduct was removed with EDTA treatment (Panel 3). The M:L complex shown in the second SELDI-ToF-MS panel confirms the presence of the 1:1 species, again correlating with the Hyperquad model which proposed a Cu(1300 Da) species.

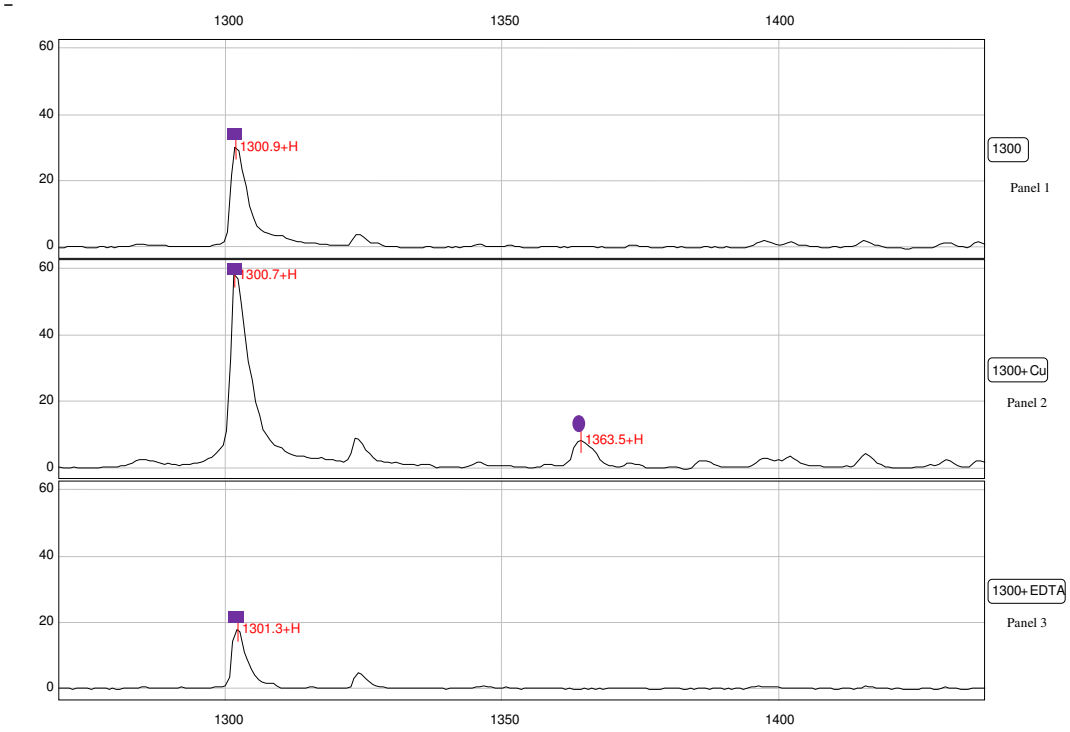

Figure 3.81 SELDI-ToF-MS spectra of the 1300 Da synthetic peptide before and after titrating with Cu. EDTA was added to an aliquot to determine if the Cu adduct could be removed (■ indicates the parent peptide in each panel and ● indicates the metal-peptide adduct)

Results produced by FTIR were similar to those previously seen in the other titrations of the synthetic peptides and the band shifts are indicative of complex formation (Figure 3.82). As in all experiments, copper(II) sulphate pentahydrate and the synthetic peptide prior to titration were analysed in addition to the end-point titration complex for comparative analysis. The majority of the band shifts are in the fingerprint region of the spectrum between 1800 cm^{-1} and 1000 cm^{-1} and were indicative of complexation as discussed for previous metal-ligand complexes.

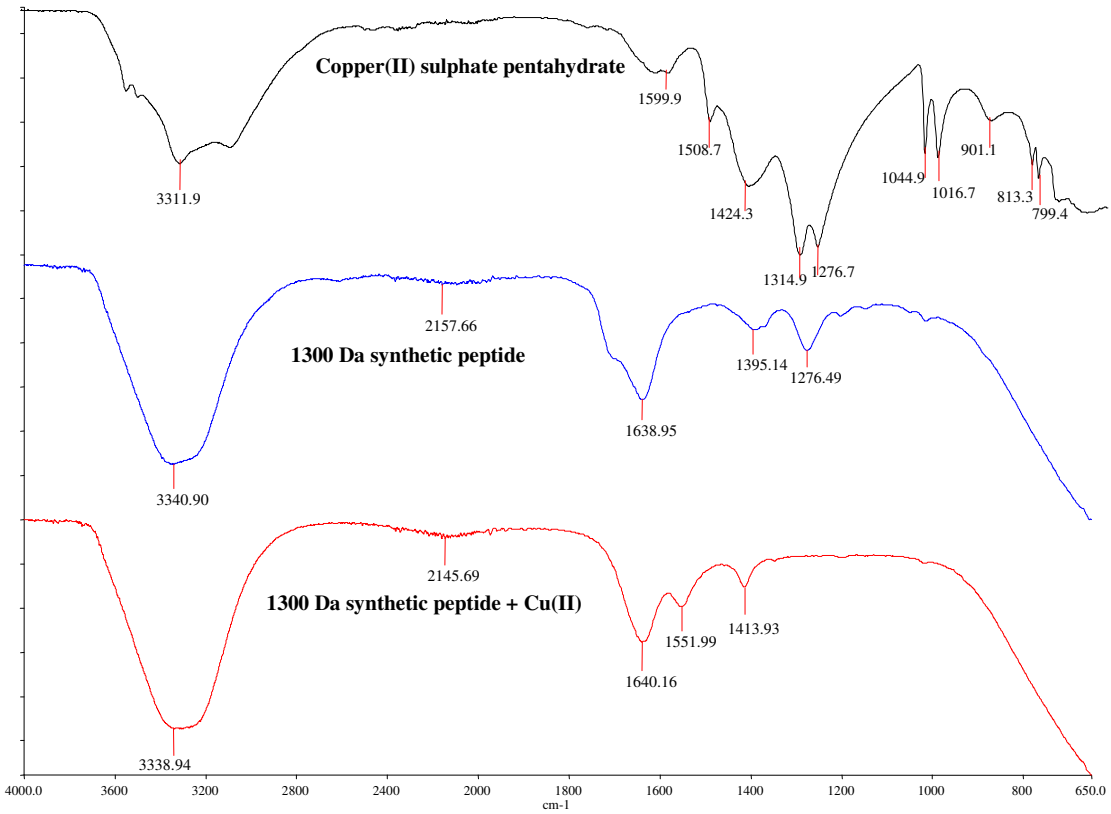

Figure 3.82 FTIR spectra of the 1300 Da synthetic peptide titrated with Cu(II) and a copper and a peptide control

The 1300 Da peptide contains 10 amino acids: Arg-His-Lys-Asn-Lys-Asn-Pro-Phe-Leu-Phe (Section 3.3.6.9). Several studies showed that various strongly coordinating side chain residues in appropriate locations can behave as anchors for the coordination of the amide donors of peptides (Casolaro *et al.*, 1999; Kozlowski *et al.*, 1999; Kozlowski *et al.*, 2005; Matera *et al.*, 2008). Histidyl residues are among the most common metal binding sites of proteins and their presence has a significant impact on the coordination chemistry of peptide molecules. The histidine residue possesses a very efficient nitrogen donor in its side chain imidazole ring. The His residue provides two nitrogen donors and a six-membered chelate ring for coordination (Figure 3.83).

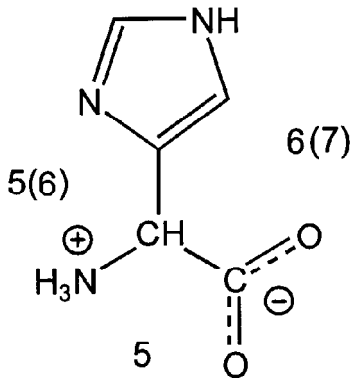

Figure 3.83 Chelating abilities of histidine. The numbers denote sizes of potential chelate rings. Diagram adapted from Kozlowski *et al*., 1999

The presence of histidine in position two of the peptide chain, which is the case for the 1300 Da synthetic peptide, allows for the simultaneous participation of the amine, the imidazole and the intervening histidyl amide nitrogens in the binding. The very high stability of this complex results from the formation of the fused rings previously mentioned in Section 3.6.5.1 (Kozlowski *et al.*, 1999). This would explain why the logβ values calculated by Hyperquad for the 1300 Da peptide were so high. An additional residue that may also contribute to the high stability of this peptide is proline which may increase the propensity of a peptide chain to bend (Kozlowski *et al.*, 1999). Steric hindrances would affect the stability of the complex so the presence of proline in the chain may reduce this problem. As in the previous two peptides, aromatic rings are present in the 1300 Da peptide. Two Phe residues are present and, as previously mentioned, aromatic residues may also contribute to the stability. As previously discussed, positioning in a sequence can greatly affect the stability of a complex. It is possible that the increased stability constant value obtained for the 1300 Da peptide when compared to the 1148 Da and the 1181 Da peptides may be partly due to the histidine in position two of the 1300 Da sequence having a positive effect on stability. Additionally, the sequences of the 1148 Da and the 1181 Da peptides are very similar with only two amino acids differing in the entire chain. The sequence for the 1300 Da peptide is quite different and it can be concluded that in addition to the amino acids contained in the sequence, their configuration also contributes to the stability of the peptide.

3.6.5.4 Determination of stability constants for the 1514 Da marker peptide with Cu^{2+}

The final synthetic peptide analysed was the largest of the four with a molecular mass of 1514 Da. Aliquots (0.5 mL) of the 1514 Da synthetic peptide (1.6505×10^{-4} M) at pH 5.5, 0.01 M ionic strength and 25 °C were titrated against a 1.6505×10^{-4} M copper(II) solution and the EMF values obtained were analysed using Hyperquad. An excellent fit was observed throughout the titration for the 1514 Da marker peptide with even distribution of deviations and the lowest sigma value of all of the titrations. Inclusion of two species provided the best curve fit in the Hyperquad model, with metal:ligand ratios of 1:1 and 1:2 respectively (Figure 3.84).

Cu (1514 Da) $\log\beta_{11} = 4.81. \pm 0.01$

$Cu(1514\ Da)_2$ $\log\beta_{12} = 8.73 \pm 0.07$

Sigma value for this model = 33.2

$\log\beta$ refers to the log of the stability constant and the corresponding subscript referring to the metal:ligand ratio. The results appear to make sense from analysis of the Hyperquad data-file which indicated more of the $Cu(1514\ Da)_2$ species was present at the end of the titration.

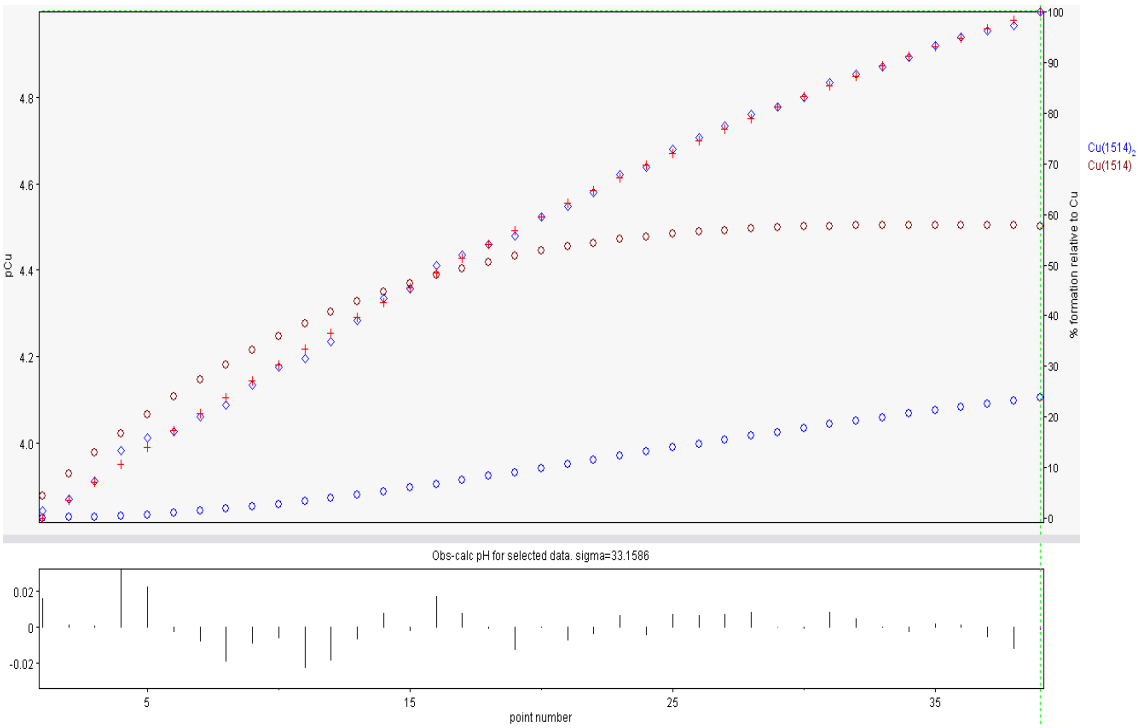

Figure 3.84 Screenshot capture of the Hyperquad file of 1514 Da synthetic peptide with Cu^{2+} at pH 5.5 and 0.1 M ionic strength at 25 ^{o}C. ○ = 1:2, M:L species ($Cu(1514)_2$, ML_2) and ○ = 1:1, M:L species (Cu(1514), ML). The experimental data (◊) closely follows the theoretically calculated Hyperquad values (+)

SELDI-ToF-MS was again employed to investigate the purity of the sample and determine if complex formation had occurred. Based on the spectral panels shown in Figure 3.85 it can be seen that an impurity is observed in the synthetic peptide (Panel 1) but does not interfere with complex formation (Panel 2). The second panel clearly shows the presence of a copper adduct at 1578.3 Da and its removal when the species is treated with EDTA (Panel 3). The results obtained in panel two are consistent with the 1:1, M:L species proposed in Hyperquad. The larger molecular mass species (ML_2) was expected at 3091.5 Da in the SELDI-ToF-MS spectra. A putative possible species at 3084.0 Da is seen in the wider spectral view of the full copper(II) proteinate sample in Figure 3.88 but the intensity is very weak and it is not possible to imply this is the ML_2 species with confidence.

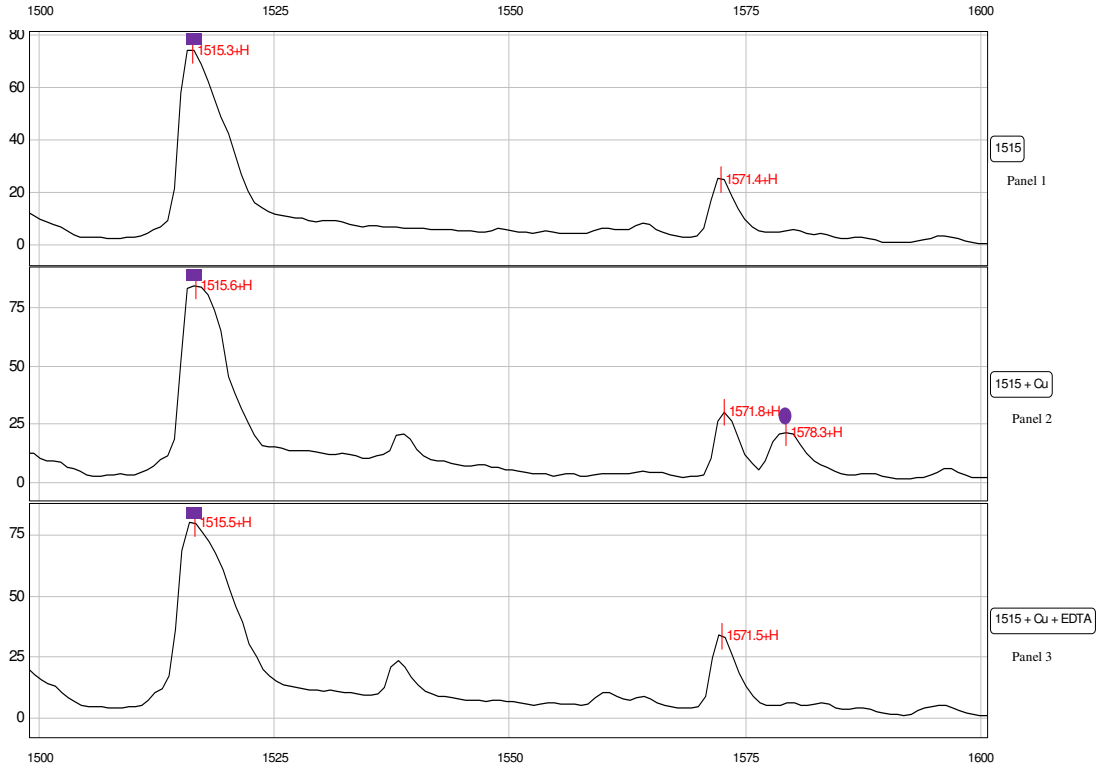

Figure 3.85 SELDI-ToF-MS spectra of 1514 Da synthetic peptide before and after titration with Cu (■ indicates the parent peptide in each panel and ● indicates the metal-peptide adduct)

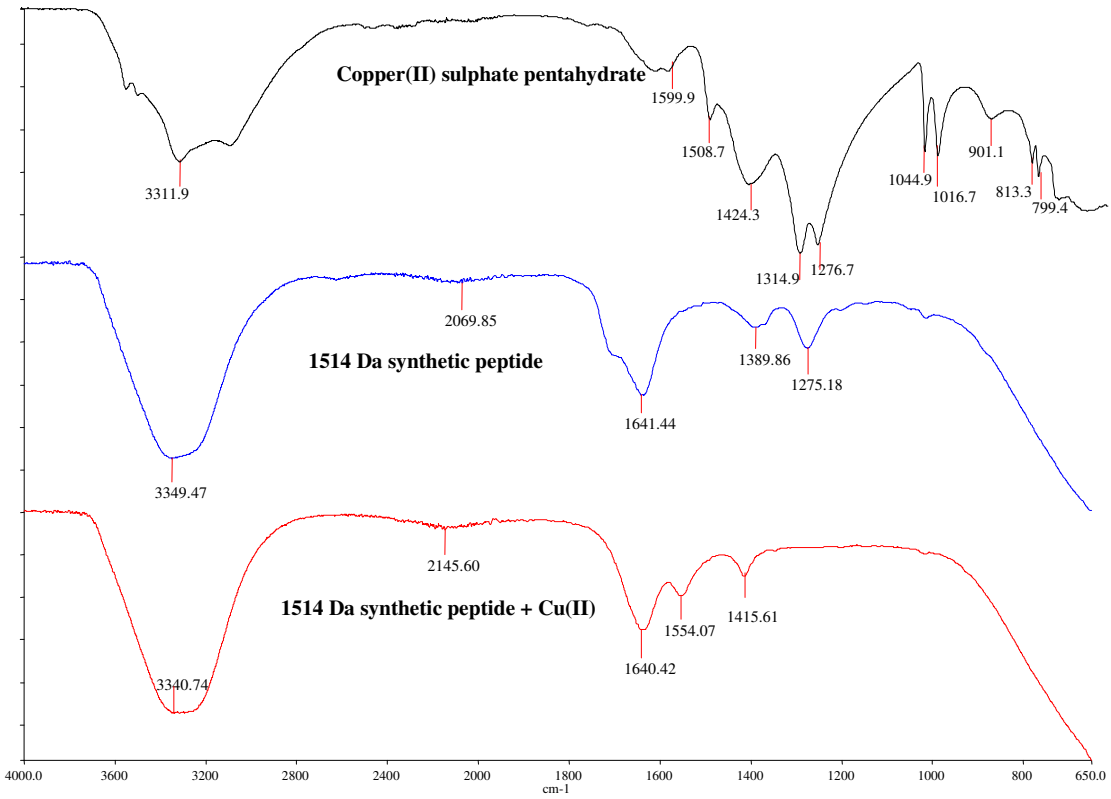

Figure 3.86 FTIR spectra of the 1514 Da synthetic peptide titrated with Cu(II) and a copper and a peptide control

The 12 amino acid sequence of the 1514 Da peptide was the largest of the synthetic peptides investigated and has a sequence of Ser-Ser-Arg-Pro-Gln-Asp-Arg-His-Gln-Lys-Ile-Tyr (Section 3.3.6.9). While a proline residue inserted as the N-terminal residue in the peptide sequence can be an effective anchoring site for metal ions (Kozlowski *et al.*, 1999), its introduction into the peptide chain in position two, three or further (position 4 in the 1514 Da synthetic peptide), results in a peptide bond that does not have an amide proton that may be displaced by metal ions. As a consequence, the simple stepwise coordination of consecutive amide nitrogens is no longer possible (Kozlowski *et al.*, 1999). As mentioned previously however, the presence of a Pro residue in the peptide sequence increases the propensity of a peptide chain to bend which may aid stability and may contribute to the higher $\log\beta_{11}$ value for this peptide compared to the 1148 Da and the 1181 Da peptides as determined by Hyperquad. The effects of His and Tyr in the chain have already been outlined for previous peptides and may contribute in a similar way to the stability in the case of this particular peptide. The

interactions between peptide residues may favour a particular peptide conformation, which in turn may have an essential impact on metal-peptide coordination equilibria, both in a thermodynamic and a structural sense.

In essence, mineral chelate stability can be significantly influenced by not only the type of amino acid but also the configuration of amino acids in a peptide sequence. The presence of certain amino acids at particular points in the amino acid sequence plays an important role provided they have the ability to react in a particular structural conformation. Sections 3.6.5.1 to 3.6.5.4 examined four synthetic peptides in terms of their respective stability constants, FTIR band shifts and SELDI-ToF-MS profiles. From sequencing information obtained it was observed that three of the four synthetic peptide ligands investigated contained a histidine residue in their sequence (1148 Da, 1300 Da and 1514 Da). This residue was absent in the 1181 Da peptide and may have contributed to the lack of species richness with regard to this ligand and differences in sequence conformation may also have had a negative impact. No multi-metal species were detected with the 1181 Da peptide, in fact the only species suggested was the 1:1, M:L species. Furthermore, the stability constant for the 1:1, M:L species was lower for this peptide than 1:1, M:L stability constants for the remaining three peptides examined.

It is reasonable to expect that peptides which have a greater number of donor atoms and hence the potential to form a number of chelate rings when binding to a metal ion would have higher stabilities than simple amino acids such as glycine. This is however, dependent on the peptide being able to actually form more than one chelate ring. The multidentate character of the ligands containing residues such as histidine, can enable multi-metal binding in some cases and provide complexes with high stability constants as seen in the case of the 1148 Da and the 1300 Da synthetic peptides which form M_2L complexes with copper(II). Tridentate coordination via the terminal amino, deprotonated amide and the imidazole nitrogen donor can facilitate dinuclear complex formation in which the imidazole nitrogen may be a bridging residue. Alternatively, simultaneous coordination of the N- and C- termini to two different metal ions may also permit formation of dinuclear complexes. The existence of such complexes was supported by SELDI-ToF-MS (Section 3.6.5.5).

3.6.5.5 Identification of species proposed by Hyperquad in metal proteinates using SELDI-ToF-MS

From the results obtained by ISE titrations and Hyperquad analysis in the previous sections (Sections 3.6.5.1 – 3.6.5.4), the complexes outlined in Table 3.16 were suggested as being present following the reaction of the synthetic peptides with Cu^{2+}.

Table 3.16 $\log\beta_{ML}$ and molecular masses of species suggested from Hyperquad based on the results of the ISE titrations for marker peptides and Cu^{2+}

Synthetic peptide	$\log\beta_{11}$, (*Da)	$\log\beta_{21}$, (*Da)	$\log\beta_{12}$, (*Da)	$\log\beta_{23}$, (*Da)
1148Da	4.50, (1211.5 Da)	8.18, (1275.0 Da)	-	17.26, (3571.0 Da)
1181Da	4.18, (1244.5 Da)	-	-	-
1300Da	6.63, (1363.5 Da)	10.64, (1427.0 Da)	-	25.08, (4027.0 Da)
1514Da	4.81, (1577.5 Da)	-	8.73, (3091.5 Da)	-

*Molecular mass may differ by 1 or 2 protons (Da) due to complex formation

Using the information obtained in the previous sections (Sections 3.6.5.1 – 3.6.5.4), a copper proteinate was assessed using SELDI-ToF-MS to determine if the multi metal-ligand species proposed by Hyperquad for the synthetic marker peptides were present in the copper proteinate sample (Figures 3.87 and 3.88). The synthetic peptide markers were derived from sequences obtained from the proteinate and as such, many of the same reactions were anticipated. As expected, no marker peptides were detected in the unhydrolysed soy control sample but the marker peptides were seen in the soy hydrolysate. The copper proteinate spectra contained peptide-metal adduct peaks that may be indicative of metal:ligand complexation so the molecular masses of these peptides were compared to the proposed Hyperquad species to determine if agreement was satisfactory. Furthermore, the copper proteinate was treated with EDTA in an attempt to strip the metal adducts from the parent peptide (Figures 3.87 and 3.88, Panel 2). The majority of previously detected adducts were successfully removed while others were markedly reduced in intensity.

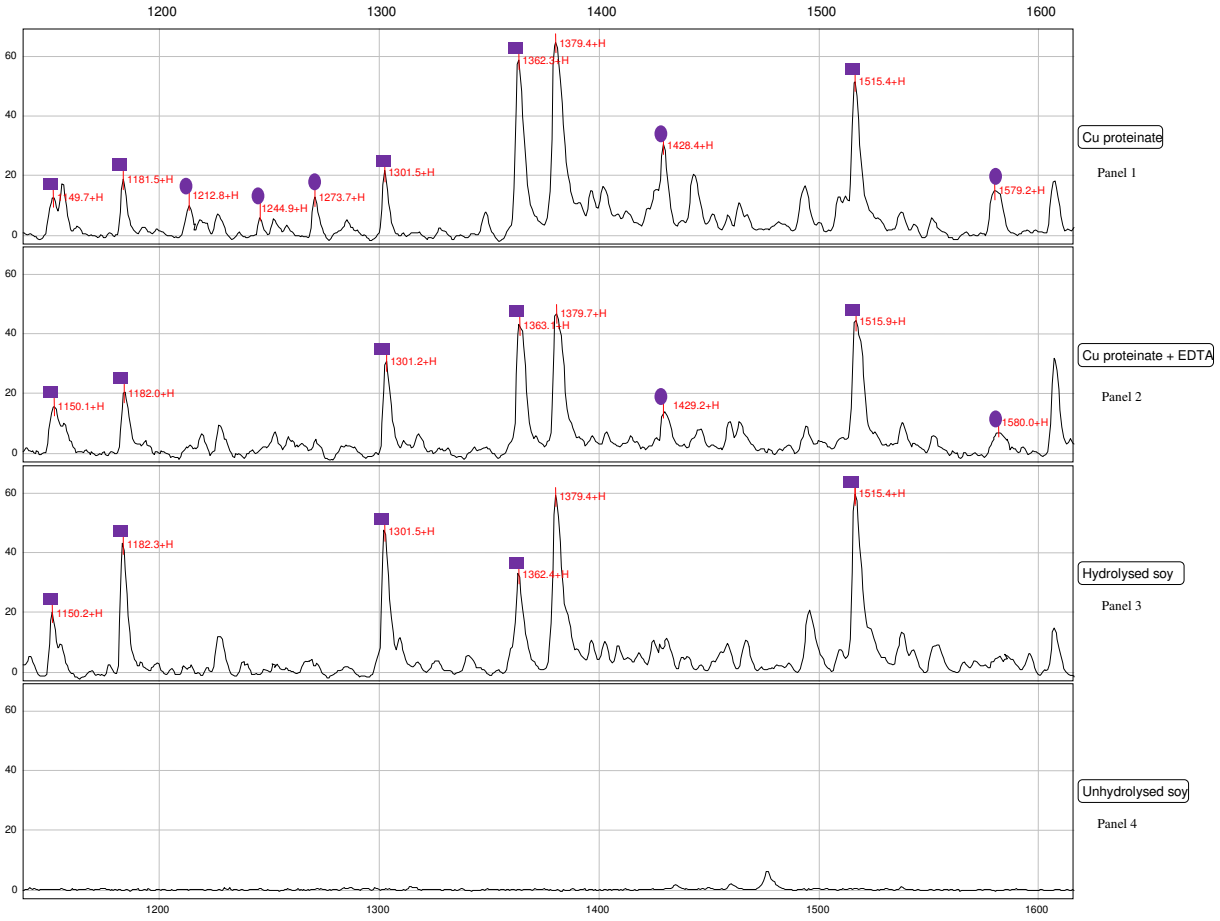

Figure 3.87 Low molecular weight SELDI-ToF-MS spectra of a metal proteinate (Panel 1), the metal proteinate after treatment with EDTA (Panel 2), the hydrolysed ligand prior to the addition of the metal (Panel 3), and the unhydrolysed soy flour (Panel 4) (■ indicates the parent peptide in each panel and ● indicates the metal-peptide adduct / complex species)

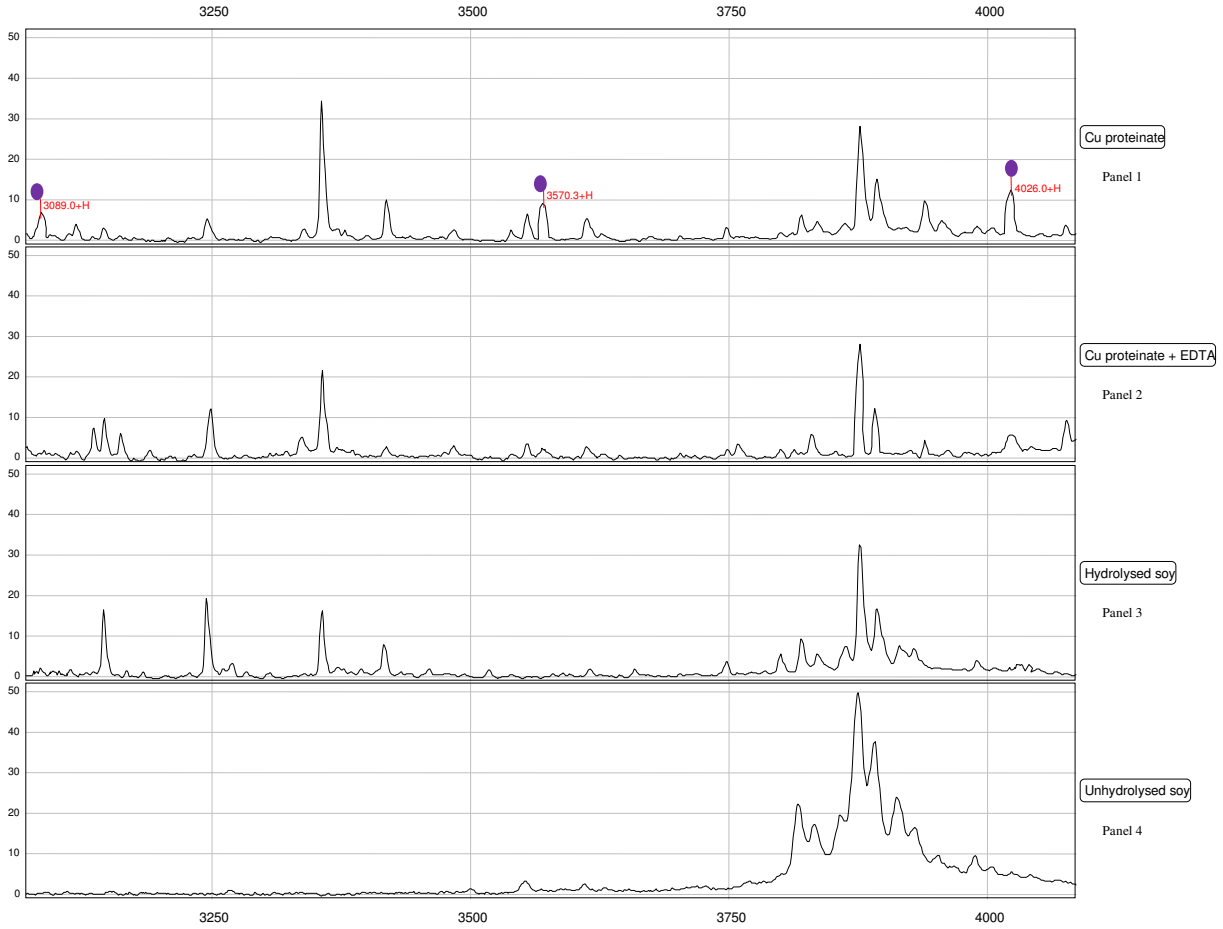

Figure 3.88 High molecular weight SELDI-ToF-MS spectra of a metal proteinate (Panel 1), the metal proteinate after treatment with EDTA (Panel 2), the hydrolysed ligand prior to the addition of the metal (Panel 3), and the unhydrolysed soy flour (Panel 4) (● indicates the metal-peptide adduct / complex species, parent peptides are of lower molecular mass below 2000 Da)

Based on the SELDI-ToF-MS results in Figures 3.87 and 3.88, it can be clearly seen that the majority of the species proposed in Hyperquad are present in the copper proteinate sample and are removed or reduced on treatment with EDTA. For clarity, the low and high molecular mass peptides were separated into two figures (3.87 and 3.88) but only Figure 3.87 contains the molecular mass region for the parent peptides. Table 3.17 contains a summary showing the agreement between the Hyperquad species and the SELDI-ToF-MS proteinate sample.

Table 3.17 Comparison of the molecular masses of species suggested from Hyperquad and SELDI-ToF-MS peptides

Hyperquad species	*Molecular mass (Da)	SELDI-ToF-MS peptide (Da)
1149 Da	1148.6 Da	1150.7 Da
Cu:1148 Da	1211.5 Da	1212.9 Da
Cu_2:1148 Da	1275.0 Da	1269.7 Da
Cu_2:(1148 Da)$_3$	3571.0 Da	3570.0 Da
1181 Da	1181.6 Da	1182.5 Da
Cu:1181 Da	1244.5 Da	1244.9 Da
1300 Da	1301.7 Da	1301.5 Da
Cu:1300 Da	1363.5 Da	**
Cu_2:1300 Da	1427.0 Da	1428.4 Da
Cu_2:(1300 Da)$_3$	4027.0 Da	4022.0 Da
1514 Da	1515.9 Da	1515.4 Da
Cu:1514 Da	1577.5 Da	1579.2 Da
Cu:(1514 Da)$_2$	3091.5 Da	3085.1 Da

*Molecular mass may differ by 1 or 2 protons due to complex formation
** A parent peptide was detected in the spectra at this molecular mass and no adduct could be conclusively identified.

Other minor species that were not identified in Hyperquad but were formed during the course of the titration were also identified using SELDI-ToF-MS. The greater the number of complex species, the more difficult it is to find an unambiguous set of equilibrium constants. The different methods are not equally sensitive to the concentrations of different species, and it is possible therefore, that different properties of the same system can be quantitatively explained by postulating different numbers of species (Beck, 1977).

Use of techniques such as those outlined in this work, provide a range of useful information regarding metal-ligand complex formation. Band shifts observed in FTIR spectra provided information regarding the groups involved in complex formation. The

SELDI-ToF-MS spectra identified peptide profiles, from which conclusions could be drawn in relation to the formation of peptide-metal adducts. The existence of multi-metal species such as dinuclear complex formation was supported by SELDI-ToF-MS data and complimentary data analysis was provided by potentiometric means in addition to speciation diagrams. The ability to obtain stability constants for complex species is advantageous as it can provide a relative measure of the strength of the interaction between a metal and the ligand in a chelate or complex including multi-metal or multi-ligand species. In general, the stability constant, β, can be defined as a measure of the ratio of the chelate concentration to the concentrations of the free metal and ligand under a given set of conditions. For simplicity it can be represented by the following equation:

$$\beta = \frac{[ML]}{[L][M]} \quad \textbf{(3.14)}$$

From the equation, it can be concluded that the greater the value of the stability constant β, the greater the proportion of the chelate or complex which is present relative to free ligand ([L]) or free metal ([M]) at a given pH. This information can serve as a useful guide when comparing different ligands such as amino acids and polypeptides. In general, the higher the stability constant value, the greater the relative proportion of bound mineral to free mineral and free ligand under a given set of conditions although exceptions can exist. Likewise, the very nature of the complex chemistry governing chelation dictates that additional factors will ultimately contribute to stability of ligand-mineral complexes. Furthermore, not all metal complexes or chelates with high stability constants are suitable as feed supplements; copper complexes formed with EDTA as a ligand are an example of such. As mentioned earlier (Section 3.3.6.4), EDTA is often employed as a chelating agent due to its ability to sequester metal ions such as Cu^{2+}, and a log K value of 18.8 is returned for the 1:1, M:L complex. Due to the very high stability constant, it is highly unlikely the metal is released at any stage during digestion and is therefore unavailable for absorption.

3.6.6 Further applications of ISE electrodes in this work

Over the last thirty years, interest in the formation of metal complexes in aqueous solutions has changed from the more basic purposes of interpreting the mechanism of formation and correlating stability constant data, to numerous applied fields ranging from the formation of complexes in biological fluids to the treatment of sewage (Nancollas *et al.*, 1982). An example of such is the use of copper ion-selective electrodes for investigations of copper(II) complexes with humic and fulvic acids in soil (Saha *et al.*, 1985; Stevenson *et al.*, 1991; Stevenson *et al.*, 1993; Se Young Choi *et al.*, 1994; Buffle *et al.*, 2002). In the present work, a Cu^{2+} ISE was used to determine the suitability of the electrode in monitoring the presence of Cu^{2+} ions in aqueous solutions of copper proteinate samples over a wide pH range. The results also provided an indication of the effects of varying production conditions on the stability of the copper proteinate samples.

3.6.6.1 Potentiometric titrations of hydrolysed soy and Cu^{2+} using an ISE

Initial experiments in this section focused on the titration of a soy hydrolysate with Cu^{2+}. The soy protein used in this work contains approximately 50 % protein, giving a percentage nitrogen content of approximately 8 %. Previous titrations, which were carried out at a 1:2, metal:ligand molar ratio cannot be performed in this case due to the molecular weight of the soy protein not being accurately known. As a result, a 1:2 metal:nitrogen ratio was used instead. Section 1.5 outlined that other atoms such as oxygen or sulphur can also be involved in metal binding but nitrogen was selected for this analysis based on conventional theory regarding metal proteinate formation. Section 3.2.1 described the formation of metal proteinates with (B), and without (A) pH adjustment prior to lyophilisation. There is a water-insoluble fraction in the hydrolysates and resultant proteinates due to insoluble particulates in soy flour so all of the lyophilised hydrolysates and proteinates were reconstituted in distilled water and vortexed prior to centrifugation (Figure 3.89). The resultant soluble fraction was used for all potentiometric titrations. The reason behind adjusting the pH to 7 in some

samples was to examine if an increase in chelation potential was observed by neutralising any protons liberated on coordination of the metal.

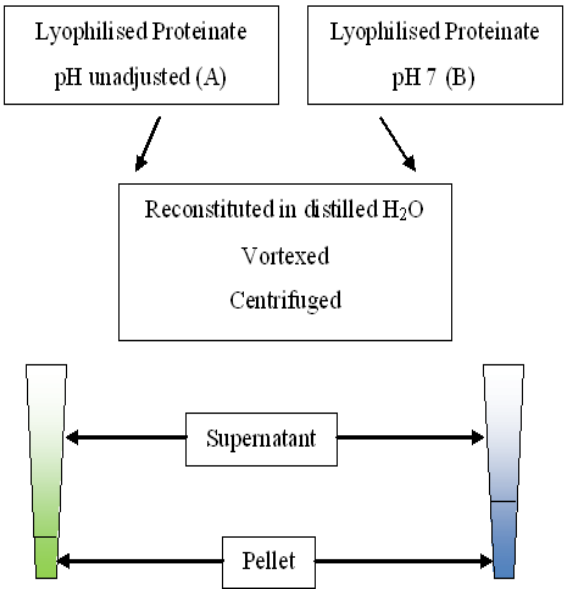

Figure 3.89 Schematic outlining the steps involved prior to potentiometric titrations of proteinate supernatants

Distinct differences in colour were observed between the pH unadjusted and pH 7 adjusted copper proteinate samples and a larger pellet was observed in the pH 7 samples. The increase in pellet size/weight may be due to the formation of an insoluble chelate which formed when the pH of the proteinate B was increased to 7. In aqueous solution, H^+ ions compete for the basic coordinating groups that form a metal binding site, and thus the pK_a of the coordinating groups and the pH of the solutions are determinants of the stability of a metal complex. At a pH of 7 or higher the backbone amide groups are deprotonated and there is less competition for binding sites.

A solution of copper(II) was titrated with aliquots of the resultant supernatant obtained after centrifugation of a hydrolysed soy sample and Figure 3.90 illustrates the decrease in free Cu^{2+} on addition of the ligand with increasing pH. However, the presence of a precipitate above pH 6 was observed. One possible explanation was that the reduction in free Cu^{2+} was due to M:L binding as carboxyl groups were deprotonated with increasing pH and that the resultant chelated species formed was insoluble.

Another reason may be that although increasing pH aided complexation, any remaining free Cu^{2+} precipitated as the metal hydroxide above pH 6. Further examination of this rationale was carried out using FTIR on a selection of additional hydrolysates (Section 3.6.6.2), to determine conclusively whether the precipitate observed was an insoluble complex or a metal precipitate.

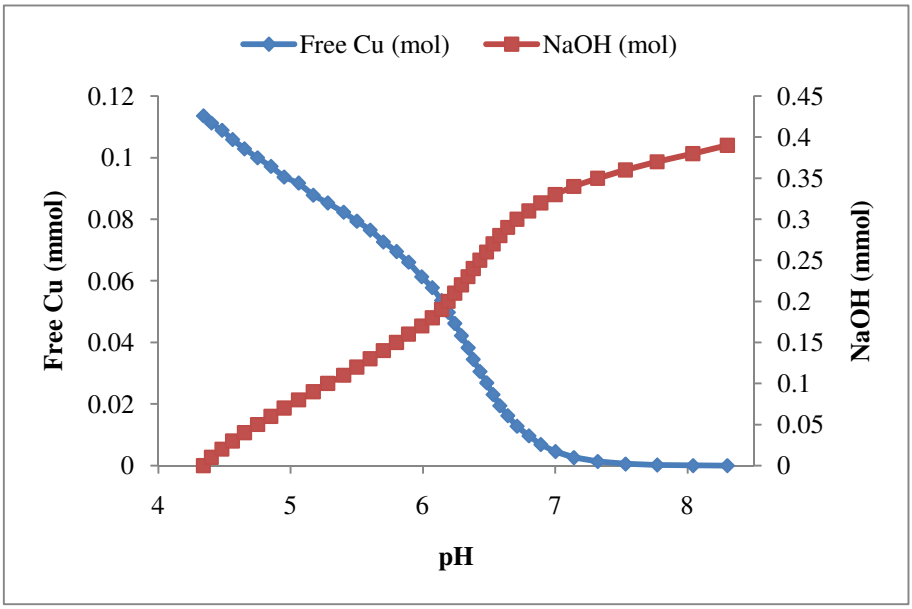

Figure 3.90 Titration of hydrolysed soy and copper(II) at a 2:1 N: M concentration over a pH range of 4-9

A detailed analysis on the proteinates was carried out and the effects of changing the original enzyme were investigated. In addition, analysis of the chelates formed and differences observed between proteinates formed from different enzymes over a pH range of 3 to 8 were also examined (Section 3.6.6.2).

3.6.6.2 Effect of ligand hydrolysis on proteinate stability

Section 3.1.2 outlined the effect of enzymes on the catabolism of peptide bonds that link amino acids together in a polypeptide chain. Enzymes will cleave peptides differently depending on their mode of action and on the recognition sequence. Some enzymes are more efficient than others in relation to generating suitable peptide fragments for

chelation with a metal ion. The aim of this section was to use the experimental techniques previously outlined (Sections 3.3.1 – 3.3.6), in addition to potentiometry, to determine the effect of different enzymes on the hydrolysis procedure and their effect on stability of the resultant proteinates formed from each enzymatic hydrolysis. The hydrolysis procedure outlined in Section 2.2.1 was repeated using a variety of enzymes and enzyme combinations. The enzymes and combinations thereof, chosen for examination, are listed in Table 3.18.

Table 3.18 Enzymes used for ligand hydrolysis

Hydrolysate number	Enzyme used*	Abbreviation
1	Cysteine Protease 1	CP1
2	Serine Protease	SP
3	Fungal Protease	FP
4	Cysteine Protease 2	CP2
5	Acidic Fungal Protease	AFP
6	Serine Protease + Fungal Protease	SP + FP
7	Serine Protease + Cysteine Protease 1	SP + CP1
8	Serine Protease + Cysteine Protease 2	SP + CP2
9	Serine Protease + Acidic Fungal Protease	SP + AFP
10	Cysteine Protease 1 + Serine Protease + Fungal Protease + Cysteine Protease 2 + Acidic Fungal Protease	Enzyme cocktail
11	Serine Protease + Acidic Fungal Protease pH 7 then after 2.5 hours pH 3	Dual hydrolysis 1
12	Serine Protease + Acidic Fungal Protease pH 3 then after 2.5 hours pH 7	Dual hydrolysis 2

* All enzymes supplied by Dr. R. Murphy, Alltech Bioscience Centre, Dunboyne, Co. Meath, Ireland.

Both alkaline and acidic hydrolyses were investigated individually and in combination. Two dual hydrolyses (Samples 11 and 12, Table 3.18) were also tested, with the start of the hydrolysis carried out under either alkaline (Sample 11) or acidic (Sample 12) conditions for the first 2.5 hours and the pH reversed for the remaining 2.5 hours. This was to give each type of enzyme an opportunity to work separately.

Enzymatic hydrolysis can enhance the biological value of the protein source and the hydrolysate can be characterised by physiochemical properties superior to the original protein (Darewicz *et al.*, 2000; Surówka *et al.*, 2004) . Varying the enzyme can result in the generation of hydrolysates with different properties and thus differing in their ability to bind metals. Free α-amino nitrogen (FAN) was measured in each of the hydrolysates (Figure 3.91) to monitor the effect of different enzymatic treatments. In general terms, increasing FAN is an indication of hydrolysis progression. Significant differences in the FAN levels were noted with different enzyme preparations. The highest FAN level was achieved with the use of a multi-enzyme cocktail and resulted in an increase in FAN of over 30 % relative to the lowest enzymatic FAN release observed with the cysteine protease enzyme (CP1). The hydrolysates with the four highest FAN levels were generated with the enzyme cocktail, the serine and fungal protease combination (SP + FP), the serine and cysteine protease 1 combination (SP + CP1) and the serine and cysteine protease 2 combination (SP + CP2) (hydrolysate numbers 10, 6, 7 and 8 from Table 3.18 respectively). Subsequent potentiometric work in this section illustrated that the hydrolysis procedure had a significant role in defining the pH dependant stability of metal proteinates produced from such hydrolysates.

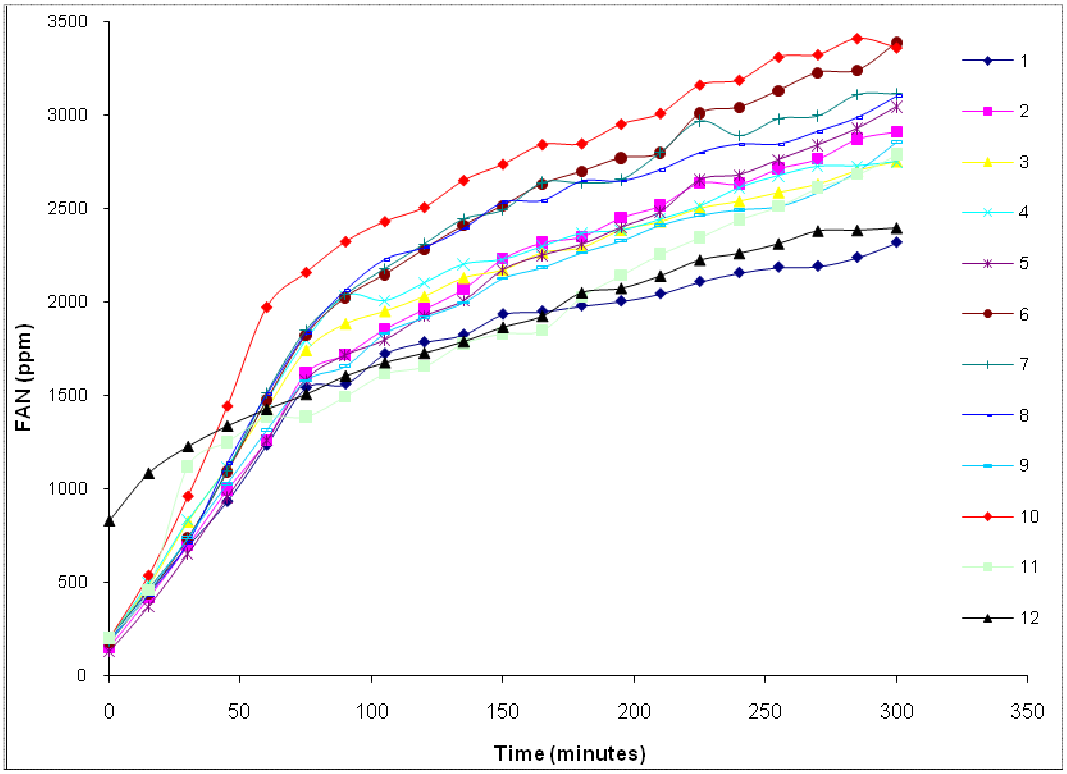

Figure 3.91 Enzymatic release of FAN from soy flour using different enzymes: (1 = CP1, 2 = SP, 3 = FP, 4 = CP2, 5 = AFP, 6 = SP + FP, 7 = SP + CP1, 8 = SP + CP2, 9 = SP + AFP 10 = Enzyme cocktail, 11 = Dual hydrolysis 1, 12 = Dual hydrolysis 2)

Free amino acid profiling (as distinct from total amino acid profiling, Section 3.3.5) was carried out on the 12 enzyme hydrolysates to determine the free amino acid content of each (Table 3.19). Given that proteolytic enzymes will have different cleavage patterns and recognition sites, one can appreciate the wide variation in levels of individual free amino acids such as arginine, glycine, glutamic acid and valine for instance. The acid hydrolysis step used to determine the amino acid content of a protein/peptide hydrolysate destroys tryptophan and cysteine. Serine and threonine may also be partially destroyed. Additionally, isoleucine and valine residues may be only partially cleaved and methionine can undergo oxidation during acid hydrolysis. Therefore a separate analysis is required to quantitatively determine the presence of such amino acids. A range of analyses are available including variations on pre and postcolumn derivatisation techniques enabling exploitation of the advantages of each method (NIHS, 2002).

Table 3.19 Free amino acid profile of soy based enzymatic hydrolyses

	1	2	3	4	5	6	7	8	9	10	11	12
% total	% total	% total	% total	% total	% total	% total	% total	% total	% total	% total	% total	% total
Aspartic acid	6.14	7.24	3.25	6.76	5.51	4.17	7.22	7.26	5.74	5.56	5.26	5.35
Threonine	3.42	5.50	5.78	3.08	1.74	5.46	4.26	4.28	4.67	4.31	3.92	2.09
Serine	4.26	3.64	5.19	3.68	1.24	4.62	4.72	4.15	3.80	4.48	2.88	1.48
Glutamic acid	18.75	17.36	8.43	15.52	21.11	9.22	13.64	12.37	12.01	11.61	20.22	18.64
Asparagine	1.72	3.64	3.85	2.08	3.01	3.76	2.58	2.63	2.78	3.04	2.59	3.23
Glutamine	3.82	3.70	3.94	1.46	2.05	3.24	3.22	1.73	2.28	2.03	1.44	0.72
Proline	0.57	0.58	0.79	0.43	0.56	0.58	0.45	0.50	0.55	0.54	0.42	1.40
Glycine	2.54	1.80	1.85	5.08	0.49	1.39	1.58	2.63	1.13	2.11	0.72	0.79
Alanine	7.99	9.61	7.39	7.44	3.04	7.16	8.18	8.43	8.37	7.21	6.77	2.96
Cystine	-	-	0.10	-	0.68	0.12	0.16	0.22	0.17	0.09	0.64	1.43
Valine	4.67	6.07	7.20	5.26	1.57	6.99	5.38	6.00	5.91	5.96	3.73	1.32
Methionine	2.71	2.97	2.44	3.06	2.95	2.64	3.22	3.48	3.13	2.92	3.29	3.17
Isoleucine	2.48	4.64	5.96	3.19	0.93	5.77	4.03	4.46	4.76	4.71	2.63	1.09
Leucine	12.04	12.64	11.29	10.98	13.78	11.99	12.27	12.13	13.25	13.15	12.66	12.12
Tyrosine	5.30	1.27	5.92	5.49	5.45	5.87	6.23	6.22	6.34	5.84	5.67	5.10
Phenylalanine	5.42	7.03	6.29	6.63	9.43	6.97	7.10	7.22	8.11	7.61	7.92	7.88
Tryptophan	1.98	2.21	1.75	1.57	0.74	2.11	2.02	1.99	2.11	1.99	1.44	1.58
Lysine	6.46	7.18	6.83	5.75	11.93	6.56	5.55	4.61	5.07	6.83	7.56	13.74
Histidine	1.61	2.56	2.66	1.74	0.40	2.56	1.71	2.03	2.02	2.16	1.36	0.48
Arginine	8.03	0.41	9.07	10.75	13.32	8.82	6.42	7.72	7.82	7.87	8.93	15.51

In addition to analysing the soy hydrolysates, copper proteinates were created from each enzymatic hydrolysis and assessed using CHN microanalysis, atomic absorption spectroscopy for metal content, FTIR spectroscopy, amino acid profiling and potentiometry. From each of the 12 hydrolysates, six copper proteinates were formed:

I 7.5 % (w/w) copper content, pH unadjusted

II 7.5 % (w/w) copper content, pH 7 adjusted

III 10 % (w/w) copper content, pH unadjusted

IV 10 % (w/w) copper content, pH 7 adjusted

V 15 % (w/w) copper content, pH unadjusted

VI 15 % (w/w) copper content, pH 7 adjusted

Once the lyophilised proteinates had been resuspended and separated into their respective supernatants and pellets (Figure 3.89), Flame Atomic Absorption Spectrometry was employed to determine the copper partitioning in the samples (Tables 3.20 – 3.22).

Table 3.20 Metal partitioning in copper proteinates (7.5 % w/w). A refers to pH unadjusted proteinates and B refers to pH 7 adjusted proteinates

Sample*	Supernatant (% of total Cu)	Pellet (% of total Cu)	Total Recovery (%)
1A	71.72	30.88	102.60
1B	32.93	66.40	99.33
2A	69.84	31.42	101.27
2B	36.47	54.83	91.30
3A	82.32	26.66	108.99
3B	25.80	67.62	93.41
4A	82.16	39.85	122.00
4B	40.17	83.19	123.36
5A	93.07	9.10	102.17
5B	50.05	56.33	106.38
6A	70.77	28.53	99.30
6B	38.26	68.24	106.50
7A	55.61	38.45	94.06
7B	52.58	62.66	115.24
8A	65.32	51.63	116.95
8B	44.59	66.39	110.98
9A	70.28	38.18	108.46
9B	37.94	73.84	111.78
10A	72.50	25.50	97.99
10B	37.76	59.48	97.24
11A	95.67	11.57	107.24
11B	44.57	48.71	93.28
12A	65.42	21.49	86.91
12B	50.76	42.69	93.45

* Samples were generated using enzymes outlined in Table 3.18

The total copper recovery based on the values obtained from analysis of the supernatant and the pellet was excellent. From Table 3.21 it was observed that in the case of the 7.5 % (w/w) Cu proteinates, the majority of the copper was present in the supernatant of the pH unadjusted samples (A) and in the pellet of the pH 7 adjusted

samples (B). Similar patterns were observed in the case of the 10 % (w/w) and 15 % (w/w) proteinate samples although the percentage copper in the supernatant and pellet samples increased with increasing copper content (Tables 3.21 and 3.22).

Table 3.21 Metal partitioning in copper proteinates (10 % w/w). A refers to pH unadjusted proteinates and B refers to pH 7 adjusted proteinates

Sample*	Supernatant (% of total Cu)	Pellet (% of total Cu)	Total Recovery (%)
1A	74.30	18.52	92.81
1B	8.37	97.32	105.69
2A	87.47	14.67	102.15
2B	17.75	83.72	101.47
3A	86.00	15.90	101.91
3B	11.98	90.33	102.31
4A	83.22	10.80	94.03
4B	12.25	91.53	103.78
5A	100.20	6.85	107.05
5B	15.87	84.28	100.15
6A	86.67	15.97	102.64
6B	15.14	88.91	104.06
7A	70.97	18.20	89.16
7B	12.94	83.25	96.19
8A	79.48	18.40	97.88
8B	13.34	85.05	98.39
9A	79.58	18.12	97.71
9B	11.48	87.90	99.38
10A	85.57	17.24	102.82
10B	11.64	86.24	97.88
11A	97.55	6.72	104.27
11B	13.81	83.97	97.79
12A	84.56	19.45	104.01
12B	15.56	83.14	98.71

* Samples were generated using enzymes outlined in Table 3.18

Table 3.21 illustrates the percentage of total copper in the supernatant of the 10 % (w/w) copper proteinates. The most significant differences in supernatant and pellet copper partitioning between the 7.5 % (w/w) and the 10 % (w/w) copper proteinates were observed in the proteinates adjusted to pH 7.

In the case of the 15 % (w/w) copper proteinates, the copper content in the supernatant of the pH unadjusted samples was as high as 95.63 % of the total in one case with the majority of pH unadjusted samples containing above 90 % of the total copper in the supernatant (Table 3.22). Similarly, the pellet contained over 90 % of the total copper when the pH was adjusted to 7. The average partitioning of the copper was far greater in the 15 % (w/w) metal proteinates (90:10) than in the 10 % (w/w) copper content (80:20) or the 7.5 % (w/w) copper proteinates (70:30).

Table 3.22 Metal partitioning in copper proteinates (15 % w/w). A refers to pH unadjusted proteinates and B refers to pH 7 adjusted proteinates

Sample*	Supernatant (% of total Cu)	Pellet (% of total Cu)	Total Recovery (%)
1A	89.60	10.95	100.54
1B	4.39	98.42	102.81
2A	87.44	6.82	94.25
2B	6.30	99.05	105.34
3A	86.83	8.95	95.77
3B	4.96	100.62	105.58
4A	90.91	9.78	100.69
4B	5.01	100.58	105.59
5A	96.28	5.30	101.58
5B	6.60	98.43	105.04
6A	90.06	9.55	99.61
6B	6.43	104.04	110.47
7A	85.05	8.59	93.64
7B	6.51	95.12	101.63
8A	86.36	8.89	95.25
8B	6.15	97.31	103.46
9A	93.34	8.80	102.15
9B	5.92	96.53	102.45
10A	86.31	8.49	94.80
10B	4.12	93.92	98.04
11A	95.82	4.37	100.20
11B	4.96	93.98	98.94
12A	89.93	8.31	98.25
12B	6.42	95.39	101.81

* Samples were generated using enzymes outlined in Table 3.18

Examination of the Flame AAS results (Tables 3.20 – 3.22) indicated an increase in copper in the supernatants of the pH unadjusted samples with increasing overall metal content. This may have been due to the ability of water-soluble ligands to successfully bind up to 15 % (w/w) copper or it could indicate the presence of unbound inorganic copper that did not precipitate. Similarly, an increase in the copper content of the pellet of the pH 7 adjusted samples was observed as the total metal content increased. It is possible that in the case of the 15 % (w/w) copper proteinates that the nitrogens are saturated. However, copper can still bind under such conditions, albeit very weakly. This was examined further by determining the CHN content of the metal proteinates and subsequently assessing the nitrogen:metal ratios.

A representative set of samples from the copper proteinates formed using the twelve separate enzymatic hydrolysis procedures were selected for initial CHN analysis. The copper proteinate sample sets chosen were those containing 7.5 % (w/w), 10 % (w/w) and 15 % (w/w) metal content and formed using a serine protease (SP), an acidic fungal protease (AFP) and a 5 enzyme cocktail (enzymes 1-5, Table 3.18). Nitrogen to metal ratios were determined for the unpartitioned proteinates at each of the three copper contents (Table 3.23). Furthermore, the N:M ratio was measured in the supernatant and pellet fractions in addition to the unpartitioned proteinate N:M ratio for a representative sample set; in this instance the 10 % (w/w) copper proteinates were assessed (Tables 3.24). Inspection of the results for the unpartitioned proteinate samples indicated that for the 7.5 % (w/w) copper proteinates (Table 3.23), the majority of the samples have a N:M ratio of greater than 3:1. The sole exception to this is the pH unadjusted sample of the acidic fungal protease (5A). It can be postulated that one histidine N, two amide backbone nitrogens and one oxygen may be involved in the copper binding in the case of the 7.5 % (w/w) copper proteinates which would give a N:M ratio of 3:1 (Hynes, 2009). The N:M ratios for the 10 % (w/w) copper proteinates indicate the majority of samples in this case have ratios of greater than 2:1 with the exception of the acidic fungal protease without pH adjustment which has a N:M ratio of 1.8:1. For proteinates containing 15 % (w/w) copper, the N:M ratio is slightly greater than 1:1 in most cases (Table 3.23). Two exceptions are the pH unadjusted proteinate formed using a serine protease and the pH 7 proteinate formed using an acidic fungal

protease which have N:M ratios of less than 1:1. The results indicate there is enough nitrogen to support complexation (charged) and/or chelation (usually electrostatically neutral) depending on the metal content.

Table 3.23 CHN results for a representative sample set of unpartitioned proteinates, with and without pH adjustment

Sample	Total (% w/w Cu)	C (%)	H (%)	N (%)	N:M
Cu (7.5 % w/w)					
2A (unadjusted)	7.55	27.97	5.01	4.99	3.00
2B (pH 7)	7.34	19.55	3.63	4.85	3.00
5A (unadjusted)	7.59	15.60	4.56	3.91	2.34
5B (pH 7)	7.40	27.40	4.35	5.56	3.41
10A (unadjusted)	7.48	28.15	4.39	6.10	3.70
10B (pH 7)	7.36	20.23	3.98	5.86	3.61
Cu (10 % w/w)					
2A (unadjusted)	10.75	29.35	4.79	5.32	2.24
2B (pH 7)	9.99	27.00	3.88	4.88	2.22
5A (unadjusted)	10.50	27.37	4.84	4.20	1.81
5B (pH 7)	9.79	26.55	3.90	4.61	2.14
10A (unadjusted)	10.21	33.15	4.92	5.83	2.59
10B (pH 7)	9.45	27.27	3.95	4.94	2.37
Cu (15 % w/w)					
2A (unadjusted)	15.30	18.81	4.69	3.10	0.92
2B (pH 7)	14.45	18.07	3.09	3.27	1.03
5A (unadjusted)	15.06	19.35	4.76	3.58	1.08
5B (pH 7)	14.06	17.23	2.80	2.15	0.69
10A (unadjusted)	14.86	19.98	4.74	3.61	1.10
10B (pH 7)	15.08	19.36	3.02	3.54	1.07

In addition to assessing CHN and the resultant N:M ratios for unpartitioned proteinate samples (Table 3.23), the supernatant and pellet fractions of the proteinates were also individually analysed. Noticeable differences were observed in the percentage carbon, nitrogen and hydrogen values between fractions. Table 3.24 displays the CHN values for a representative sample set of proteinates containing 10 % (w/w) copper. A number of soy hydrolysates were analysed as control samples and gave consistently similar values, an example of which is outlined in Table 3.25.

Table 3.24 CHN results for a representative sample set of unpartitioned proteinates (10 % w/w Cu) with and without pH adjustment and their respective supernatant and pellet fractions

Sample	S'nat Cu (% w/w)	C (%)	H (%)	N (%)	N:M	Pellet Cu (% w/w)	C (%)	H (%)	N (%)	N:M	Total Cu (% w/w)	C (%)	H (%)	N (%)	N:M
2A	9.41	24.47	4.62	5.52	2.66	1.58	37.34	5.64	4.78	13.75	10.75	29.35	4.79	5.32	2.24
2B	1.77	21.52	3.40	3.15	8.06	8.36	30.42	4.89	5.70	3.09	9.99	27.00	3.88	4.88	2.22
5A	10.52	22.38	4.67	5.01	2.16	0.72	37.73	5.95	5.30	33.43	10.50	27.37	4.84	4.20	1.81
5B	1.55	20.55	3.33	3.76	10.98	8.25	30.23	4.45	5.67	3.12	9.79	26.55	3.90	4.61	2.14
10A	8.74	24.39	4.53	5.15	2.67	1.76	37.62	5.62	5.63	14.50	10.21	33.15	4.92	6.38	2.83
10B	1.10	21.99	3.65	3.87	15.97	8.15	29.25	5.28	5.43	3.02	9.45	27.27	3.95	4.94	2.37

Table 3.25 CHN results for a sample soy hydrolysate control

Sample	C (%)	H (%)	N (%)
Soy hydrolysate	41.81	6.57	7.09

Examination of Table 3.24 indicated marked differences in the N:M ratio between the supernatant and the pellet samples for each of the enzyme treatments. For example, in the case of the proteinate formed from the hydrolysis of soy flour with an enzyme cocktail (Table 3.24, Samples 10 A and B) the N:M ratio in the unpartitioned sample without pH adjustment (Sample 10 A) was 2.81:1. Analysis of the corresponding supernatant after centrifugation indicated a N:M ratio of 2.67:1 and the resultant pellet N:M ratio was found to be 14.50:1. In this example, the majority of metal was present in the supernatant as detected using FAAS (Table 3.21) which explains the significant different in N:M ratios in the partitioned samples. Increasing the pH to 7 (Sample 10 B) significantly altered the N:M value for each fraction. With the majority of metal now contained in the pellet (Table 3.21), the N:M ratio was 3.02 in this fraction and the supernatant had a N:M ratio of 15.97.

The 12 enzymatic hydrolysates were assessed using FTIR spectroscopy in addition to their respective copper(II) complexes with and without pH adjustment. Visible differences are present in the fingerprint region for the copper(II) proteinates adjusted to pH 7. Band shifts previously observed in metal:ligand complexes such as those in the υ(C=O) stretching vibration region (1560 cm^{-1} to 1660 cm^{-1}) which are indicative of involvement of the carboxylic group in covalent bonding to the metal ion were observed. In addition, changes to the υ(N-H) stretching vibration (> 3100 cm^{-1}) suggesting the involvement of the $-NH_2$ group in complex formation were also detected in the FTIR spectra of the proteinates formed from the 12 hydrolysates. Spectra for a hydrolysate and proteinates formed from an enzymatic soy hydrolysis procedure using the enzyme cocktail are shown in Figure 3.92. The remaining FTIR enzymatic hydrolyses results are outlined in Appendix 1.4.

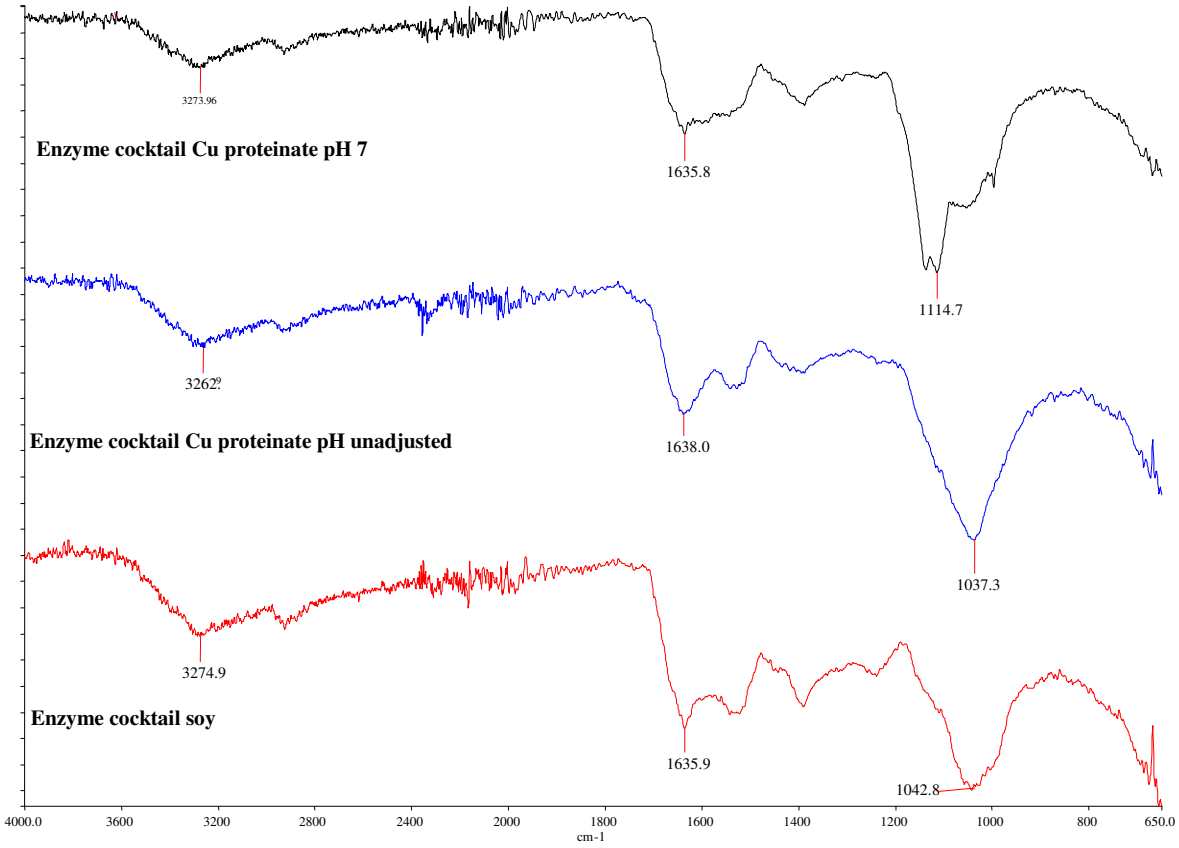

Figure 3.92 FTIR spectra for Cu complexes formed using an enzyme cocktail hydrolysis procedure with and without pH adjustment and an enzyme cocktail soy hydrolysate control

Potentiometric analysis was employed to assess the copper binding of proteinates produced by the different enzymes over a pH range of 3 to 8. The benefits of incorporating proteinates in feed has previously been outlined (Section 1.5) but the effectiveness of such products relies on preserving the bioavailability of the active ingredients. A large proportion of bioactive compounds can remain poorly available after inclusion due to factors such as low permeability and/or solubility within the gut, lack of stability during food processing (temperature, oxygen, light) and challenges in the gastrointestinal tract such as pH conditions, the presence of enzymes or other nutrients (Tedeschi *et al.*, 2009). Examining a selection of proteinates over a wide pH range can provide valuable information regarding the stability and potential bioavailability of the samples and enable further product comparison.

The lyophilised pH unadjusted and pH 7 adjusted copper proteinates formed from the 12 different enzyme combinations containing copper contents of either 7.5 % (w/w), 10 % (w/w) or 15 % (w/w), were resuspended in distilled water prior to centrifugation (Figure 3.89). The resultant supernatant and pellet fractions were separated and the soluble fraction (25 mL) was used for the potentiometric titration at 25 °C and 0.1 M ionic strength. The insoluble fraction was assessed at a later stage using FTIR spectroscopy. The initial pH of each of the soluble fractions varied between proteinates so each supernatant was adjusted to pH 3 prior to titration to obtain a consistent start point and no precipitate was observed in any of the supernatants at this pH. Aliquots of base (0.1 M NaOH) were added incrementally over the course of the titration up to pH 8 to determine the extent of copper binding over a wide pH range. Precipitates were observed in the supernatants of the pH unadjusted samples analysed as the pH was increased and were examined separately using FTIR.

As the titration data for each of the three copper contents (7.5 % (w/w), 10 % (w/w) and 15 % (w/w)) is difficult to decipher in a single graph (Figures 3.93, 3.99 and 3.105), the data was separated into a pH unadjusted set (Figures 3.94, 3.100 and 3.106) and a pH 7 adjusted set (Figures 3.95, 3.101 and 3.107) for each percentage Cu content. Additionally, three separate titrations from the pH unadjusted and pH 7 adjusted enzymatic hydrolysates were selected to illustrate the main trends. The serine protease (SP) was selected as the alkaline enzyme example (Figures 3.96, 3.102 a&b and 3.108) and the acidic fungal protease (AFP) as the acidic example (Figures 3.97, 3.103 and 3.109). Finally, an enzyme cocktail containing 5 enzymes was selected to illustrate the results obtained from using a combination of enzymes (Figures 3.98, 3.104 and 3.110).

An important point to note is that graphical representations of pH unadjusted and pH 7 adjusted values are only relative. Based on the flame atomic absorption results in Tables 3.20 – 3.22, it is clear that a far greater percentage of copper is present in the supernatant of the pH unadjusted supernatant than in the pH 7 adjusted supernatant. If the graphs were to scale, the pH 7 adjusted sample data would be difficult to decipher as it would lie close to the baseline (Figure 3.102 b).

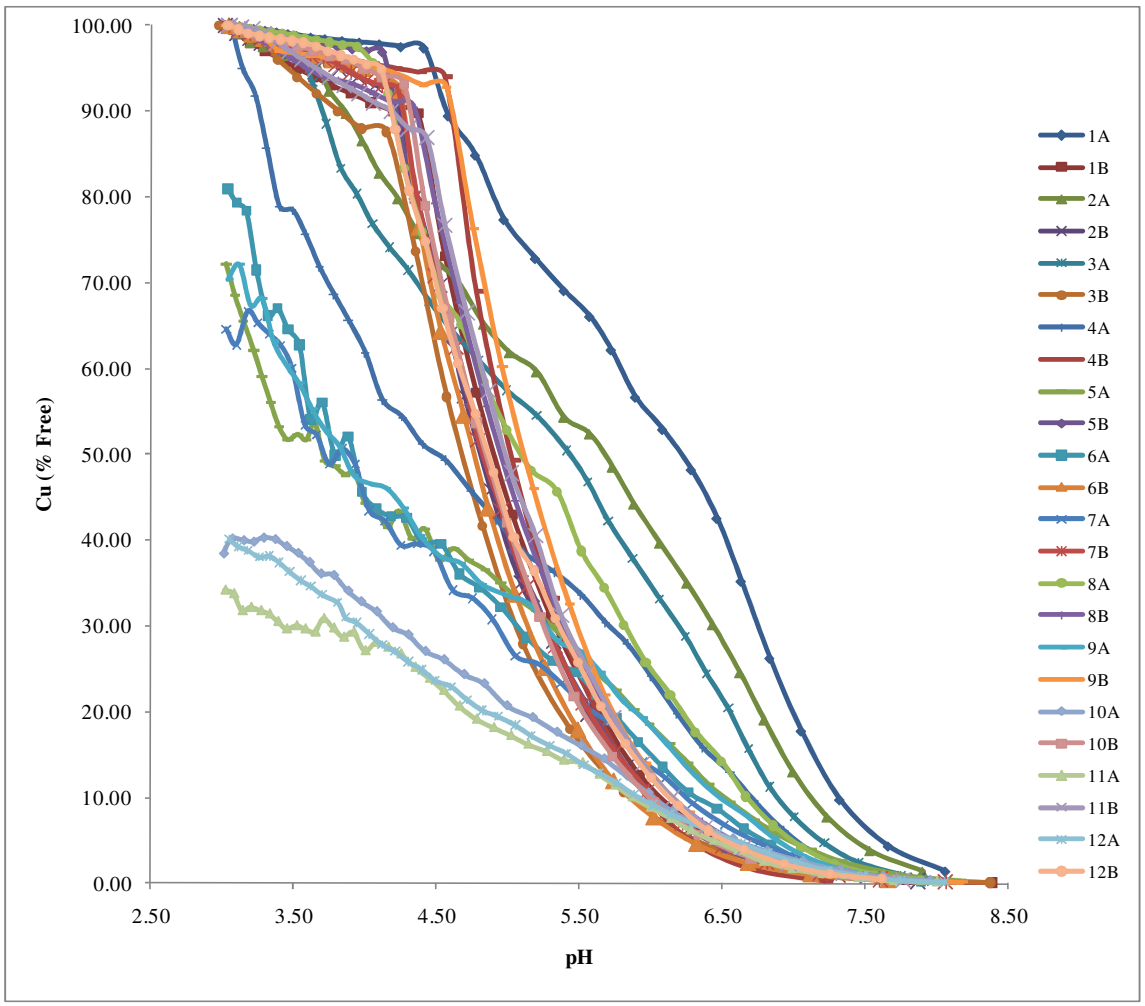

Figure 3.93 ISE titrations of free Cu in proteinates containing 7.5 % (w/w) Cu. A refers to pH unadjusted samples, B refers to pH 7 adjusted samples. (1 = CP1, 2 = SP, 3 = FP, 4 = CP2, 5 = AFP, 6 = SP + FP, 7 = SP + CP1, 8 = SP + CP2, 9 = SP + AFP 10 = Enzyme cocktail, 11 = Dual hydrolysis 1, 12 = Dual hydrolysis 2)

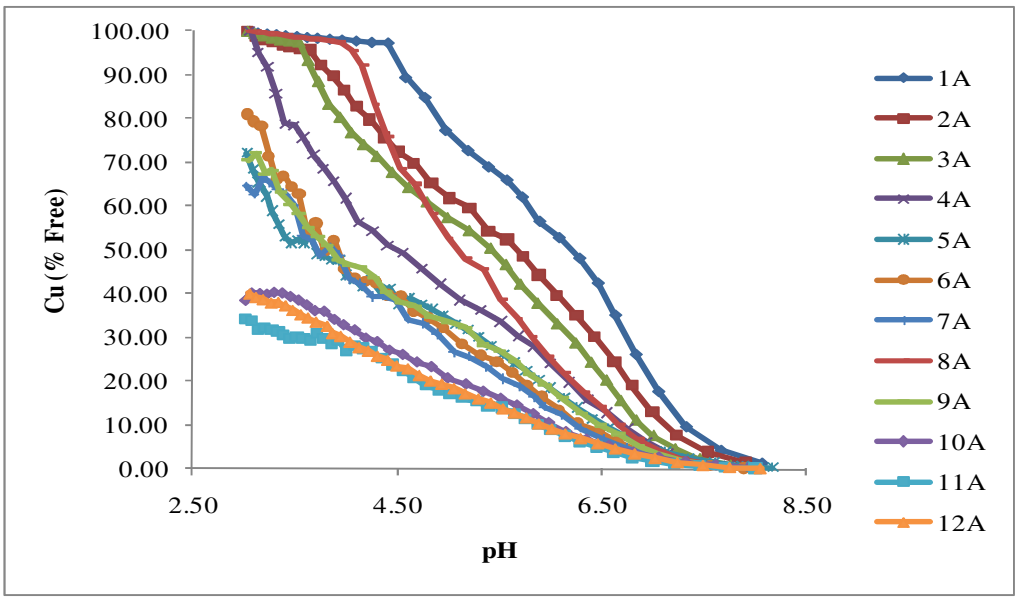

Figure 3.94 ISE titrations of free Cu in proteinates containing 7.5 % (w/w) Cu. A refers to pH unadjusted samples. (1 = CP1, 2 = SP, 3 = FP, 4 = CP2, 5 = AFP, 6 = SP + FP, 7 = SP + CP1, 8 = SP + CP2, 9 = SP + AFP 10 = Enzyme cocktail, 11 = Dual hydrolysis 1, 12 = Dual hydrolysis 2)

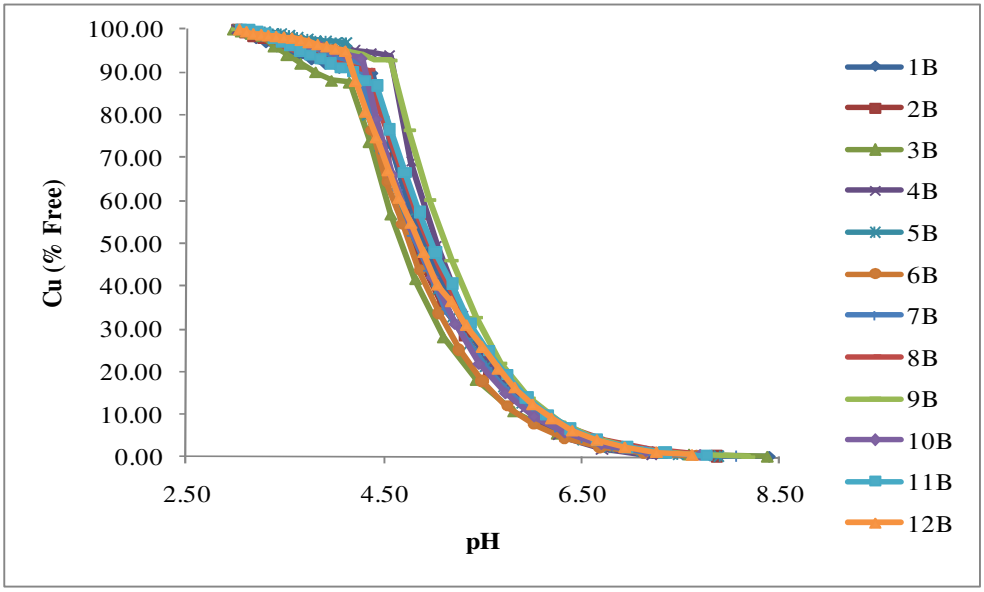

Figure 3.95 ISE titrations of free Cu in proteinates containing 7.5 % (w/w) Cu. B refers to pH 7 adjusted samples. (1 = CP1, 2 = SP, 3 = FP, 4 = CP2, 5 = AFP, 6 = SP + FP, 7 = SP + CP1, 8 = SP + CP2, 9 = SP + AFP 10 = Enzyme cocktail, 11 = Dual hydrolysis 1, 12 = Dual hydrolysis 2)

Figure 3.94 illustrates the percentage of free Cu(II) over a pH range of approximately pH 3 to pH 8 for the soluble fraction of a selection of copper proteinates containing approximately 7.5 % (w/w) Cu without pH adjustment. It is apparent from the data that the extent of hydrolysis and as such, the choice of enzyme, plays an important role in the ability of soy based proteinates to bind metal. Samples 10A, 11A and 12A, which were pH unadjusted proteinates formed from the enzymatic hydrolyses of an enzyme cocktail and two dual hydrolyses respectively, appear to have the highest binding ability based on the fact that there is less free Cu^{2+} detected by the ISE (Figure 3.94). Previously obtained FAN data (Figure 3.91) indicated the extent of hydrolysis was greatest in the enzyme cocktail sample (Sample 10), and thus free amino acids and smaller peptides would be more prevalent. Over the course of the titrations of the pH unadjusted soluble proteinate fractions (Figure 3.94), a precipitate was observed to form above pH 5 in all cases. To investigate whether this precipitate was unbound precipitated metal or an insoluble bound metal complex, FTIR spectroscopy was employed to assess the resultant precipitates (*vide infra,* Figures 3.111-3.113). Figure 3.95 illustrates the titration curves obtained from the pH 7 adjusted soluble fractions and although very little copper is present in the supernatant (Table 3.20), no visible precipitate of the low level copper present was detected over the course of the titrations. Comparing the general trend between the pH unadjusted (A) and the pH 7 adjusted (B) samples in Figures 3.94 and 3.95, a distinct difference in terms of relative free copper is observed. For the pH 7 adjusted samples (Figure 3.95), the titration curves are very similar whereas greater variation is observed in the pH unadjusted samples (Figure 3.94).

Three sample titration sets were chosen to illustrate the differences in the proteinates formed from the various enzymes. Although the pH unadjusted and the pH 7 adjusted soluble fractions cannot be directly compared due to differing initial copper concentrations, the data were plotted relative to each other (Figures 3.96 – 3.98). Similar trends were observed in the titrations of all the pH 7 adjusted soluble fractions which contained low levels of copper. Analysis of the pH unadjusted soluble fractions showed that the proteinate formed using a serine protease had the highest percentage free copper at pH 3, the corresponding acidic fungal protease preparation had less free copper at pH

3 and finally the enzyme cocktail in Figure 3.98 had only 40 % free copper at the start of the titration indicating a significant portion of the metal was bound at pH 3.

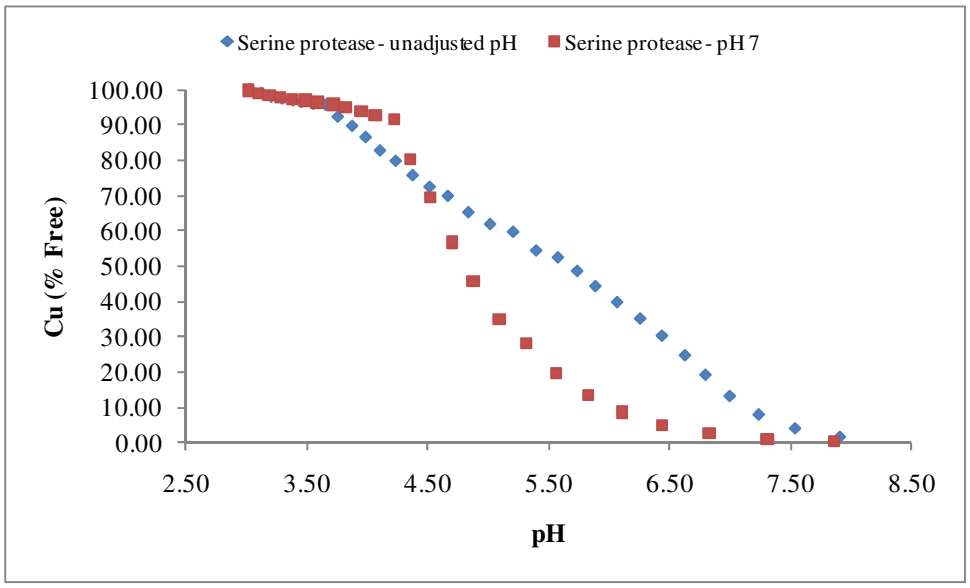

Figure 3.96 ISE titrations of proteinates formed using a serine protease, containing 7.5 % (w/w) Cu, with and without pH adjustment

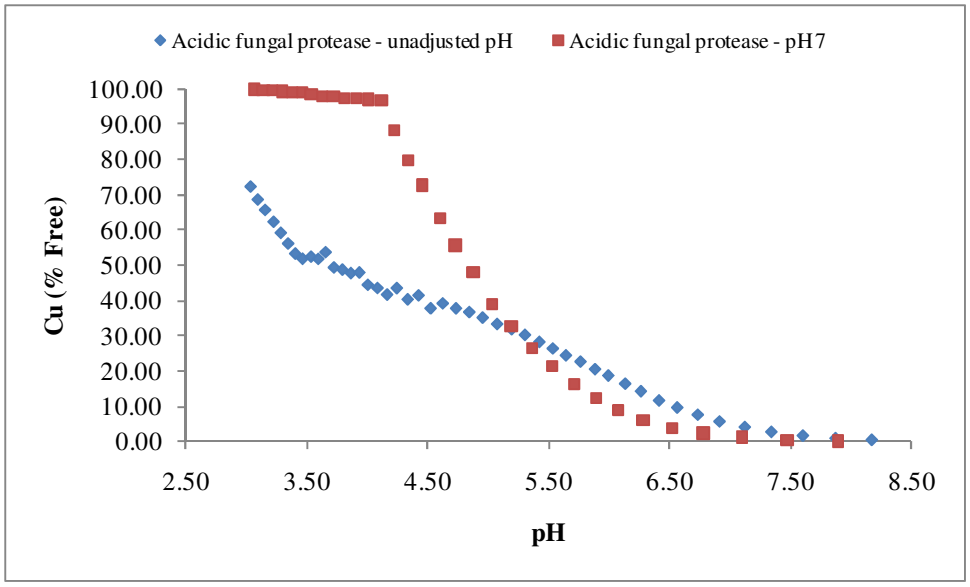

Figure 3.97 ISE titrations of proteinates formed using an acidic fungal protease, containing 7.5 % (w/w) Cu, with and without pH adjustment

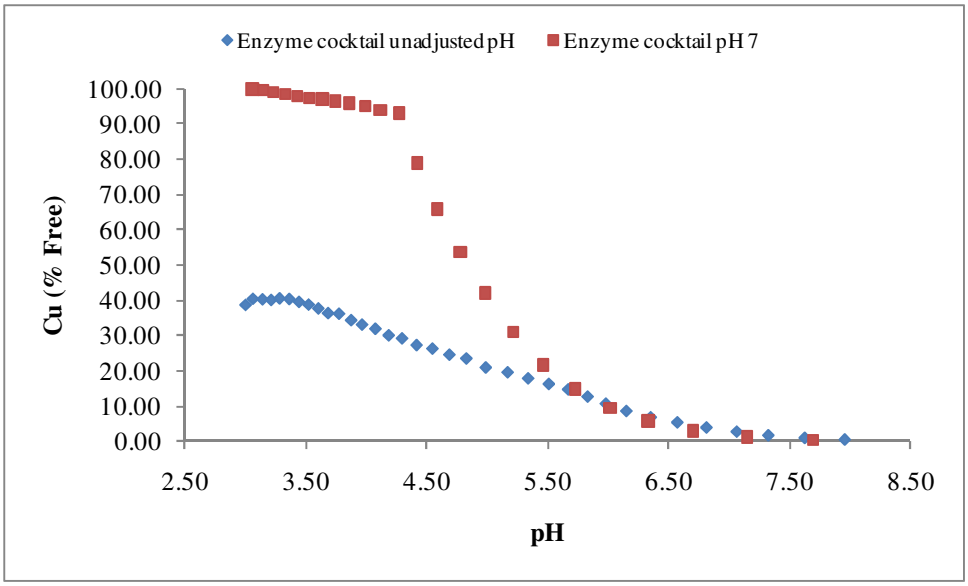

Figure 3.98 ISE titrations of proteinates formed using an enzyme cocktail, containing 7.5 % (w/w) Cu, with and without pH adjustment

Noticeable differences were observed between the percentage of free copper in the pH 7 adjusted and pH unadjusted soluble fractions of the 7.5 % (w/w) copper proteinates (Figures 3.96 – 3.98). For the pH 7 adjusted fractions, which contained a lower total copper concentration in the soluble fraction, close to 100 % of the copper was found to be free at pH 3 and by pH 6 very little free copper was detected in solution. The pH unadjusted samples contained a significantly higher proportion of copper in the soluble fraction (Table 3.20) and increased binding at lower pH was detected in most cases when compared to the pH 7 adjusted samples. Relating the extent of copper binding to the degree of hydrolysis and referring to previous FAN analysis (Figure 3.91), it was observed that copper binding was highest in the proteinate formed from the enzyme cocktail hydrolysis which provided the highest FAN release. The proteinate formed from the serine protease hydrolysis provided the lowest FAN release and from Figure 3.96 it was observed copper binding was lowest at pH 3 for this pH unadjusted sample.

Figures 3.99 – 3.104 relate to the 10 % (w/w) Cu proteinates and as before, the graphs of the pH unadjusted and pH 7 adjusted samples are plotted relative to each other, although it should be kept in mind that the copper content in the supernatant of

the pH 7 adjusted samples was much less than in the supernatant of the pH unadjusted samples as determined by FAAS (Table 3.21).

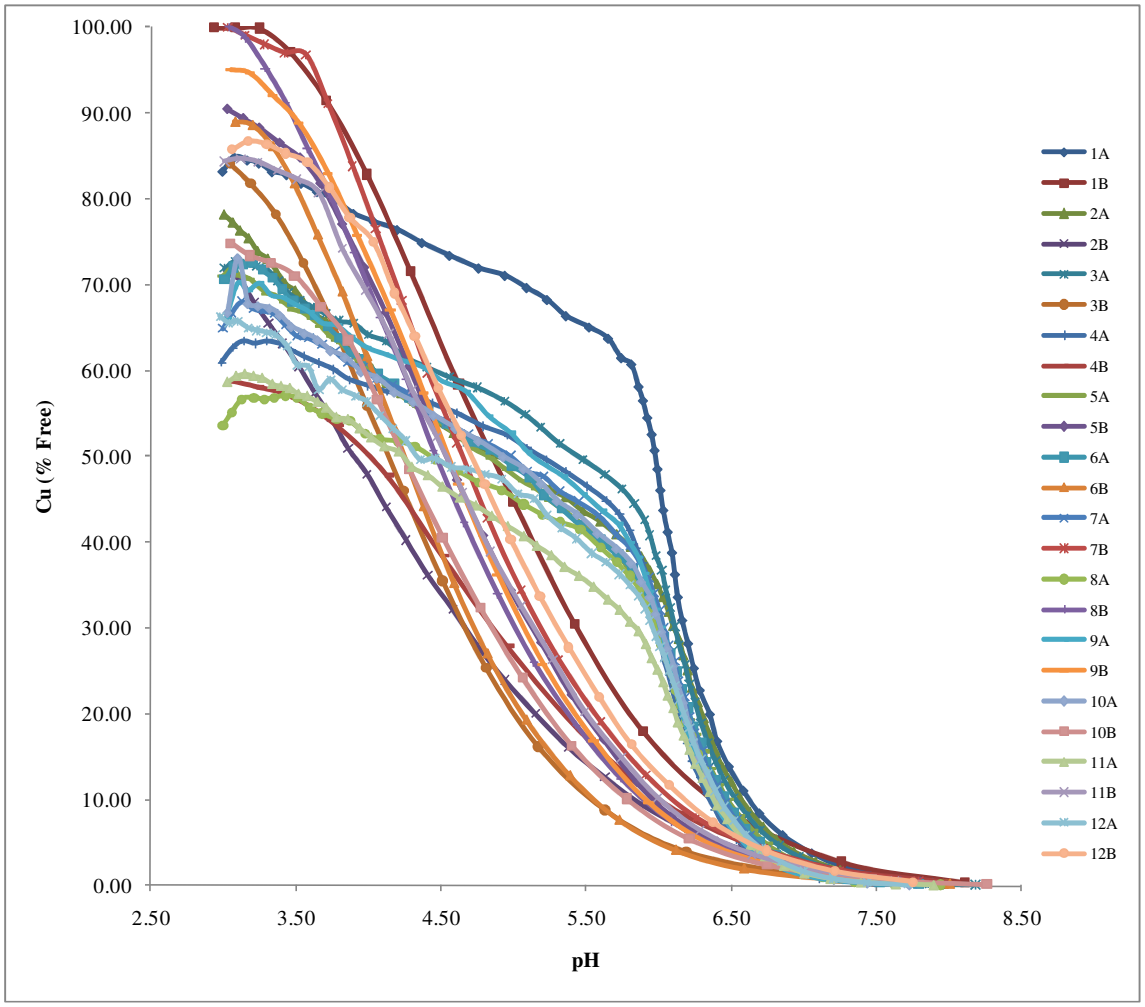

Figure 3.99 ISE titrations of free Cu in proteinates containing 10 % (w/w) Cu. A refers to pH unadjusted samples, B refers to pH 7 adjusted samples. (1 = CP1, 2 = SP, 3 = FP, 4 = CP2, 5 = AFP, 6 = SP + FP, 7 = SP + CP1, 8 = SP + CP2, 9 = SP + AFP 10 = Enzyme cocktail, 11 = Dual hydrolysis 1, 12 = Dual hydrolysis 2)

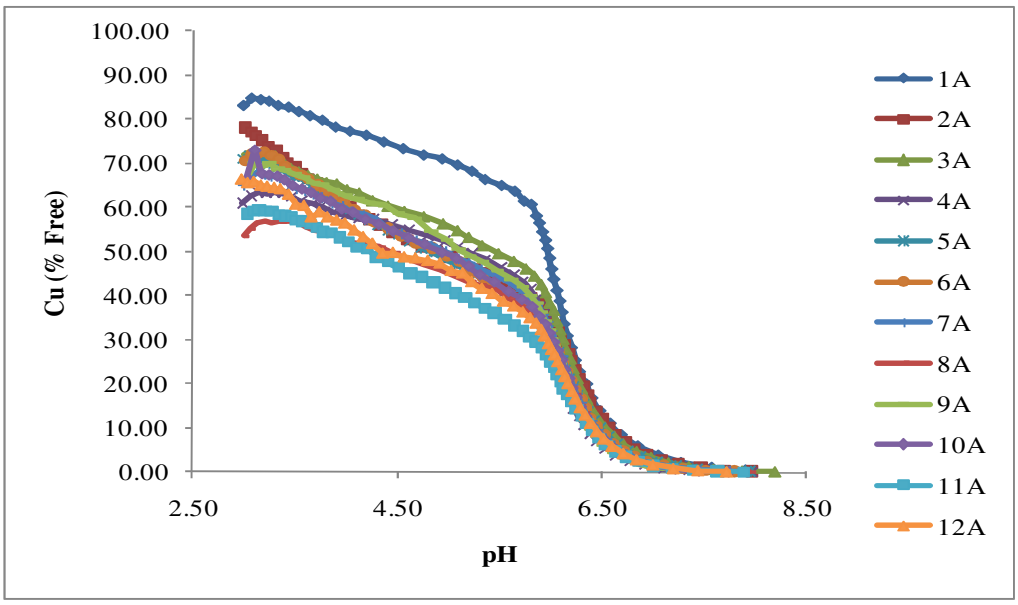

Figure 3.100 ISE titrations of free Cu in proteinates containing 10 % (w/w) Cu. A refers to pH unadjusted samples. (1 = CP1, 2 = SP, 3 = FP, 4 = CP2, 5 = AFP, 6 = SP + FP, 7 = SP + CP1, 8 = SP + CP2, 9 = SP + AFP 10 = Enzyme cocktail, 11 = Dual hydrolysis 1, 12 = Dual hydrolysis 2)

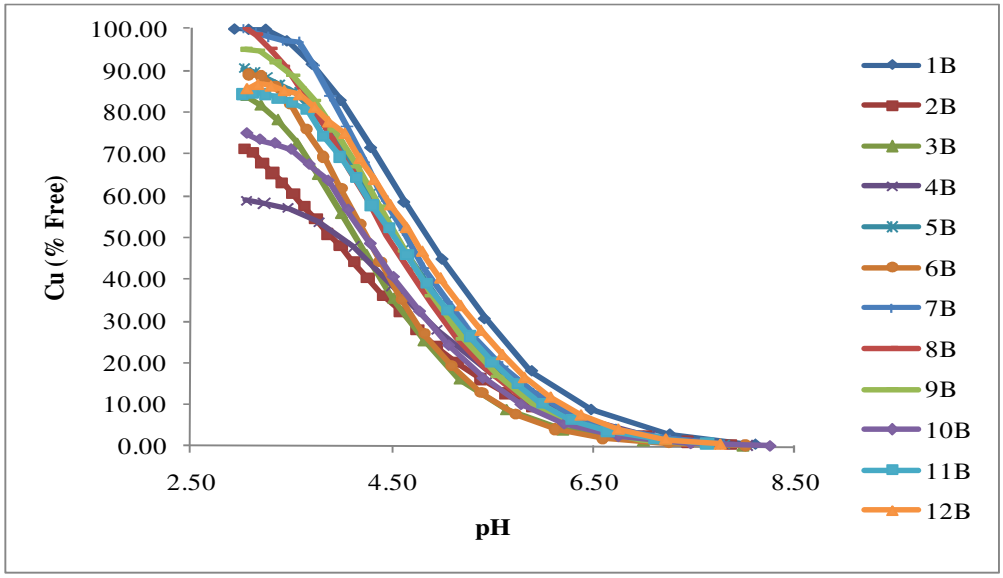

Figure 3.101 ISE titrations of free Cu in proteinates containing 10 % (w/w) Cu. B refers to pH 7 adjusted samples. (1 = CP1, 2 = SP, 3 = FP, 4 = CP2, 5 = AFP, 6 = SP + FP, 7 = SP + CP1, 8 = SP + CP2, 9 = SP + AFP 10 = Enzyme cocktail, 11 = Dual hydrolysis 1, 12 = Dual hydrolysis 2)

The titration data of the pH unadjusted samples in Figure 3.100 had a characteristic profile of a titration end-point at approximately pH 6. The pK_a of a peptide nitrogen is approximately 6 and examination of the WinCOMICS plot obtained from pentaglycine (Figure 3.67) illustrated the pH values at which deprotonation occurs for this polypeptide (approximately pH 5.6, 6.85 and 7.86). It is possible that a similar deprotonation occurred at approximately pH 6 in the case of the pH unadjusted samples in Figure 3.100 corresponding to the sharp change in curve at this point and increased metal binding (Hynes, 2009).

To emphasise the previously mentioned point regarding the scaling of the graphs, a sample plot of the titration results from the proteinate formed using a serine protease hydrolysis is shown in Figure 3.102a. This graph illustrates the actual copper concentration in the supernatant of the pH 7 adjusted proteinate compared to the concentration in the supernatant of the pH unadjusted sample. Marked differences were observed and it is clear, based on previous FAAS results, that the majority of copper in the pH 7 adjusted samples is contained in the pellet. Once titration data had been obtained for all the soluble proteinate fractions, an examination of the pellets was carried out to determine if the metal had merely precipitated or if it had formed an insoluble complex.

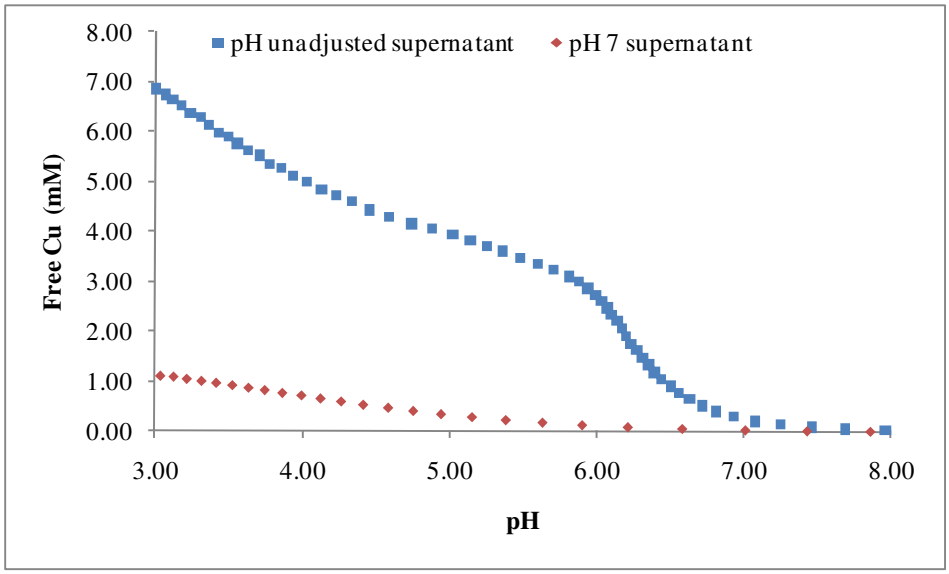

Figure 3.102a ISE titrations of proteinates formed using a serine protease, containing 10 % (w/w) Cu, with and without pH adjustment

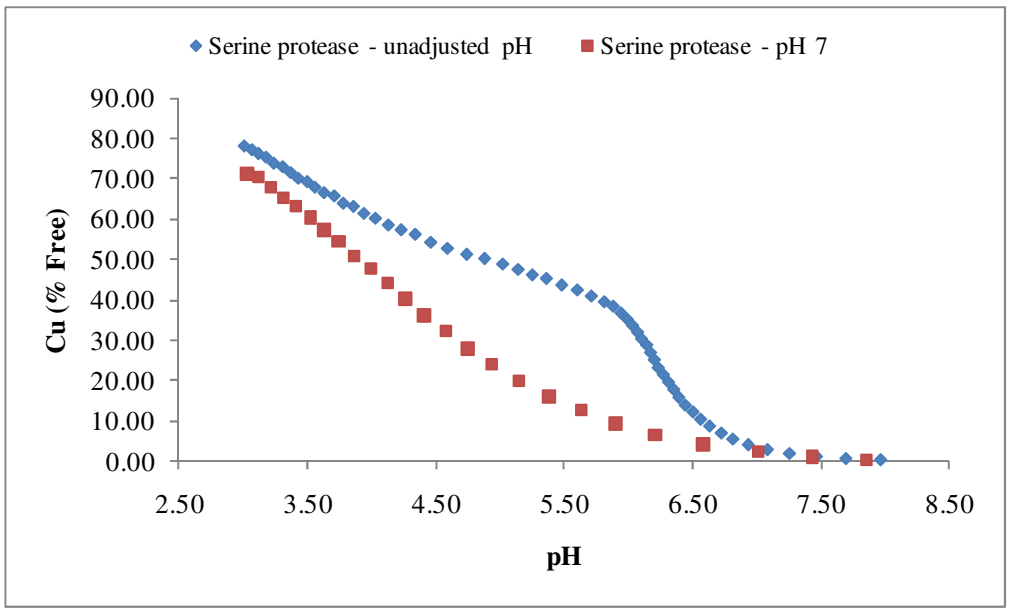

Figure 3.102b ISE titrations of proteinates formed using a serine protease, containing 10 % (w/w) Cu, with and without pH adjustment

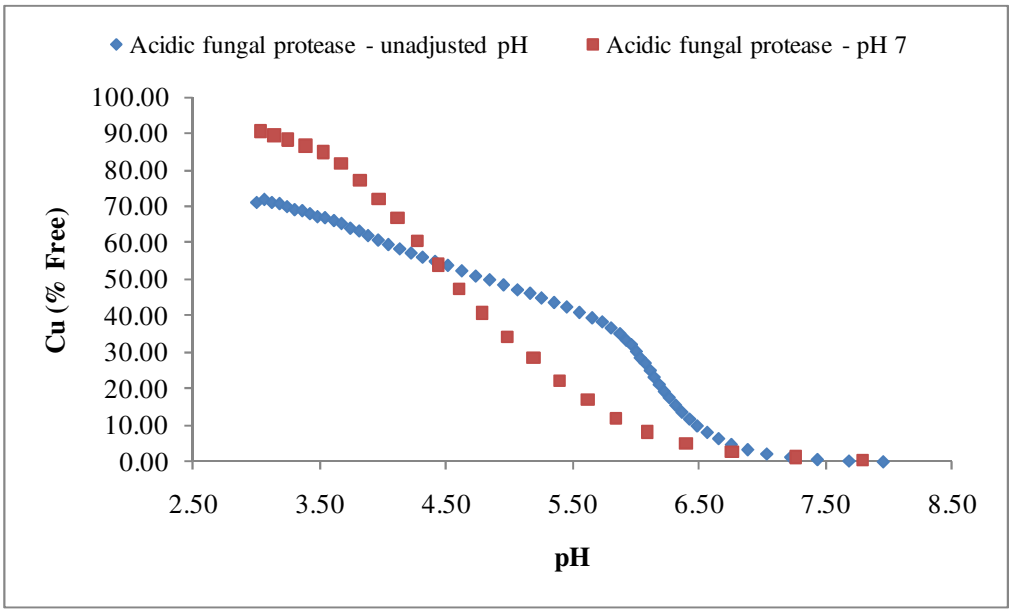

Figure 3.103 ISE titrations of proteinates formed using an acidic fungal protease, containing 10 % (w/w) Cu, with and without pH adjustment

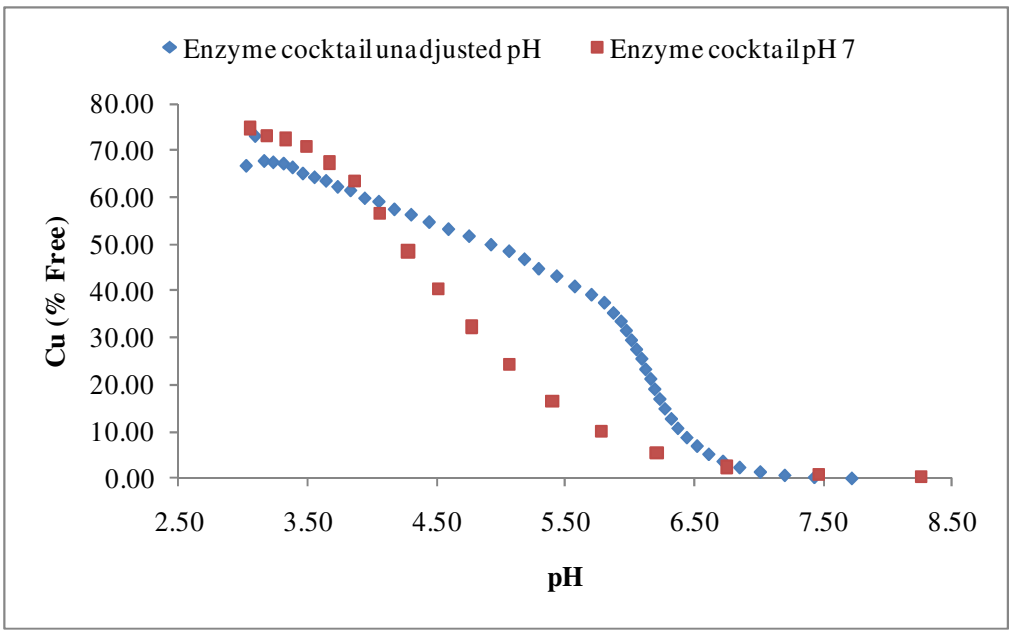

Figure 3.104 ISE titrations of proteinates formed using an enzyme cocktail, containing 10 % (w/w) Cu, with and without pH adjustment

Comparison of the curves obtained from titration of the 10 % (w/w) copper proteinate soluble fractions with those of the 7.5 % (w/w) samples indicated differences in the percentage of free copper detected at the start of the titration for the pH unadjusted and pH 7 adjusted samples between the two proteinate sets. Less free copper was detected using the ISE electrode for the 10 % (w/w) Cu proteinate pH 7 adjusted soluble fractions. Figures 3.96 – 3.98 indicated almost 100 % of the total copper present in the 7.5 % (w/w) Cu proteinate pH 7 adjusted soluble fractions was free. For the 10 % (w/w) proteinates, 70 – 90 % of the total copper was found to be free (Figures 3.102b – 3.104). Examination of the FAAS analysis of the copper content in the pH 7 adjusted soluble fractions of the 10 % (w/w) samples (Table 3.21) found less copper was present than in the pH 7 adjusted 7.5 % (w/w) samples (Table 3.20). It may be postulated that only a certain proportion of the copper present in the soluble fraction would bind and that the excess copper contained in the 7.5 % (w/w) soluble fraction would be detected as free copper.

One notable difference between the 7.5 % (w/w) and 10 % (w/w) soluble fractions was in the case of the pH unadjusted proteinate formed using the enzyme cocktail. A far greater proportion of free copper was detected in the 10 % (w/w) copper

proteinate sample (Figure 3.104) than in the 7.5 % (w/w) sample (Figure 3.98). FAAS of the soluble fractions of the pH unadjusted copper proteinates found the 10 % (w/w) sample formed using the enzyme cocktail contained over 13 % more copper than that of the corresponding 7.5 % (w/w) sample. The additional copper in the 10 % (w/w) sample appears to be free at low pH thereby contributing to the higher percentage free copper detected in this case using an ISE.

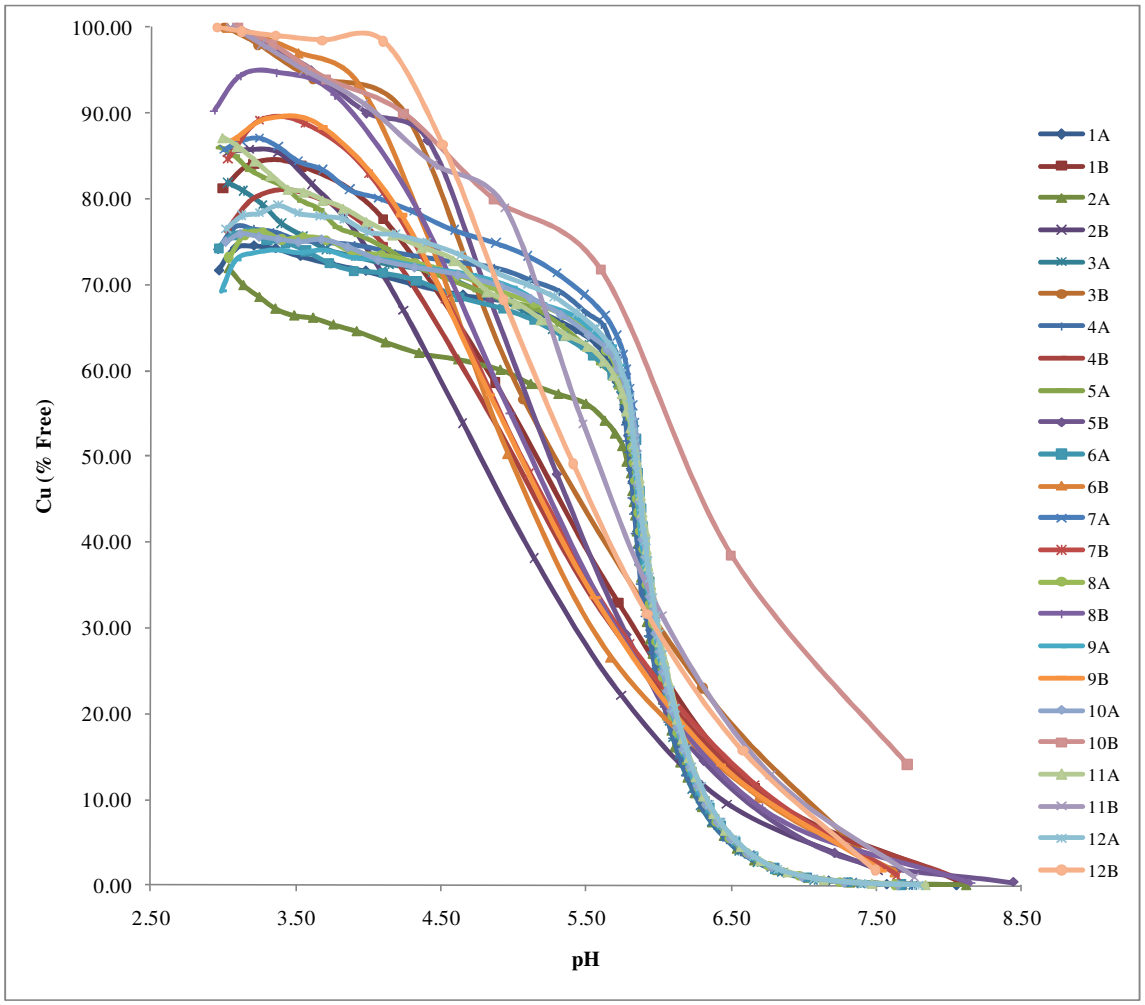

Figure 3.105 ISE titrations of free Cu in proteinates containing 15 % (w/w) Cu. A refers to pH unadjusted samples, B refers to pH 7 adjusted samples. (1 = CP1, 2 = SP, 3 = FP, 4 = CP2, 5 = AFP, 6 = SP + FP, 7 = SP + CP1, 8 = SP + CP2, 9 = SP + AFP 10 = Enzyme cocktail, 11 = Dual hydrolysis 1, 12 = Dual hydrolysis 2)

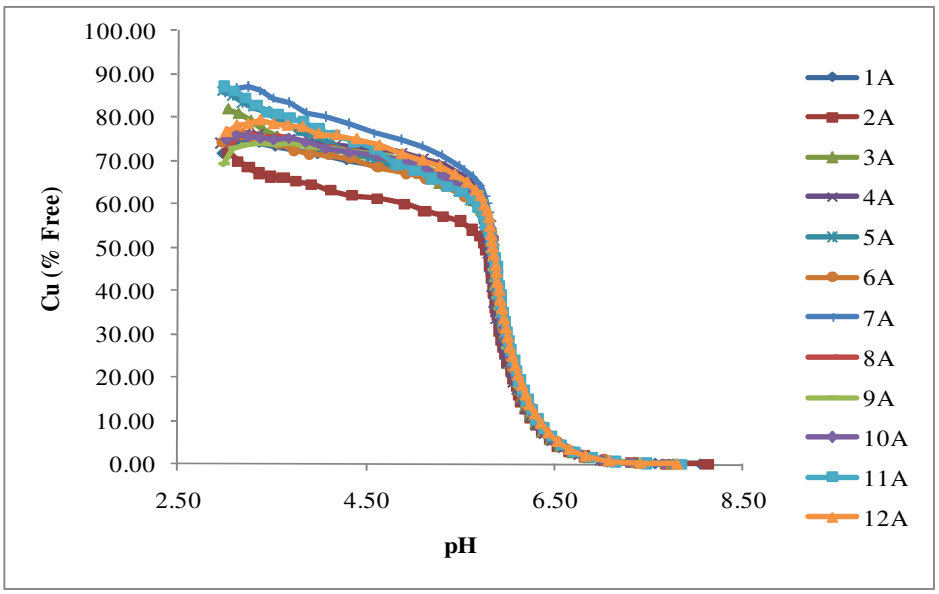

Figure 3.106 ISE titrations of free Cu in proteinates containing 15 % (w/w) Cu. A refers to pH unadjusted samples. (1 = CP1, 2 = SP, 3 = FP, 4 = CP2, 5 = AFP, 6 = SP + FP, 7 = SP + CP1, 8 = SP + CP2, 9 = SP + AFP 10 = Enzyme cocktail, 11 = Dual hydrolysis 1, 12 = Dual hydrolysis 2)

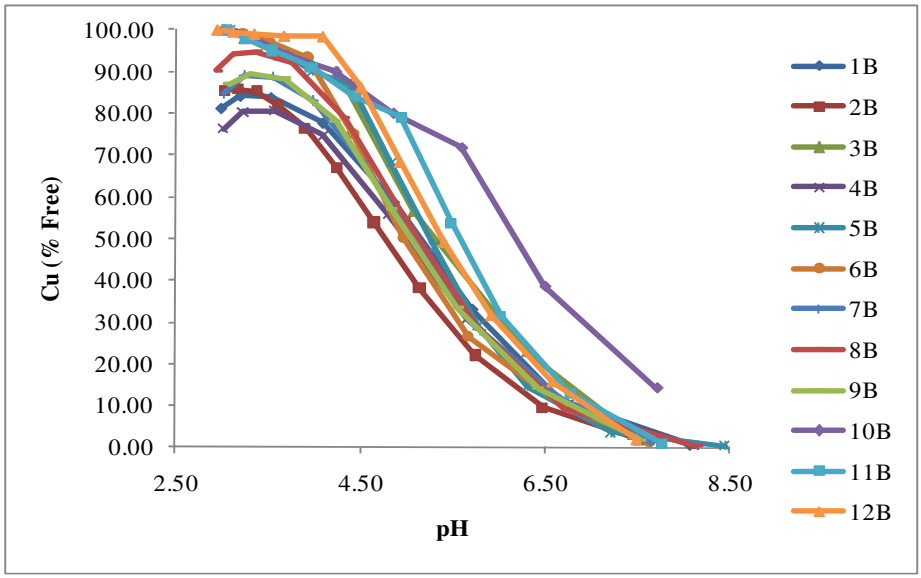

Figure 3.107 ISE titrations of free Cu in proteinates containing 15 % (w/w) Cu. B refers to pH 7 adjusted samples. (1 = CP1, 2 = SP, 3 = FP, 4 = CP2, 5 = AFP, 6 = SP + FP, 7 = SP + CP1, 8 = SP + CP2, 9 = SP + AFP 10 = Enzyme cocktail, 11 = Dual hydrolysis 1, 12 = Dual hydrolysis 2)

The trend observed for the 15 % (w/w) copper proteinates closely resembled that of the 10 % (w/w) proteinate samples albeit more pronounced with regard to the

characteristic end-point previously observed in the soluble fraction of the 10 % (w/w) proteinates at approximately pH 6 (Figures 3.105 – 3.110). Comparing the titration results for the 7.5 % (w/w), 10 % (w/w) and 15 % (w/w) soluble fractions it was observed that groupings/similar trends were more apparent for the 10 % (w/w) and 15 % (w/w) proteinates than for the 7.5 % (w/w) proteinates. The increased metal content may have contributed to more specific binding. As the metal concentration was increased there was a proportional decrease in ligand concentration and binding may have been less random at 15 % (w/w) copper content. However, the binding would have been weaker at 15 % (w/w) copper content as the amide nitrogens would have to be deprotonated to bind metal at this concentration. Taking into consideration the basic mass balance effect: $M^+ + L^- \rightleftharpoons ML$, if there is physically more copper and ligand in the same volume of sample, binding may be somewhat forced. To determine if complexation had occurred at 15 % (w/w) copper content, FTIR spectroscopy (Figures 3.111-3.113) was employed to examine the insoluble fraction produced on centrifugation of the unpartitioned proteinate samples prior to titration.

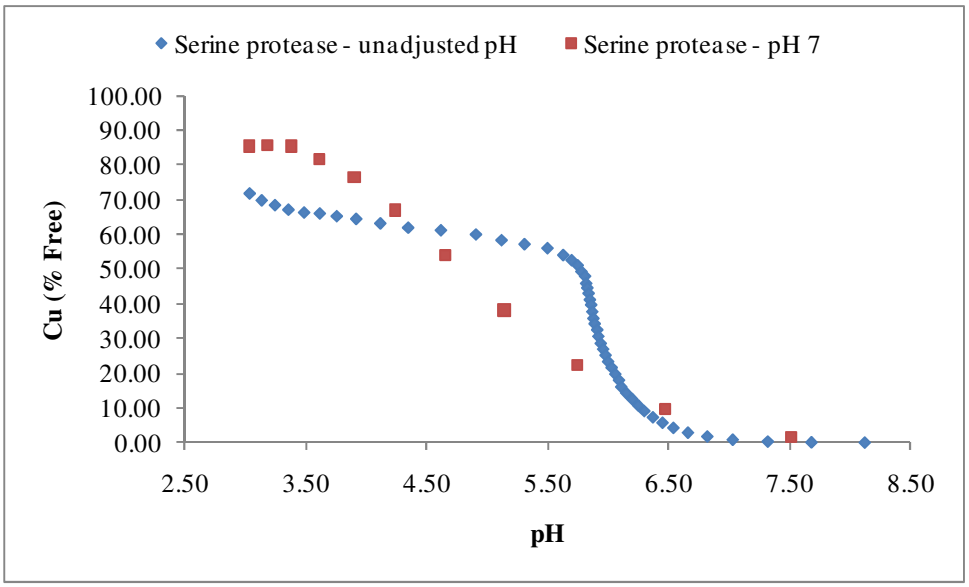

Figure 3.108 ISE titrations of proteinates formed using a serine protease, containing 15 % (w/w) Cu, with and without pH adjustment

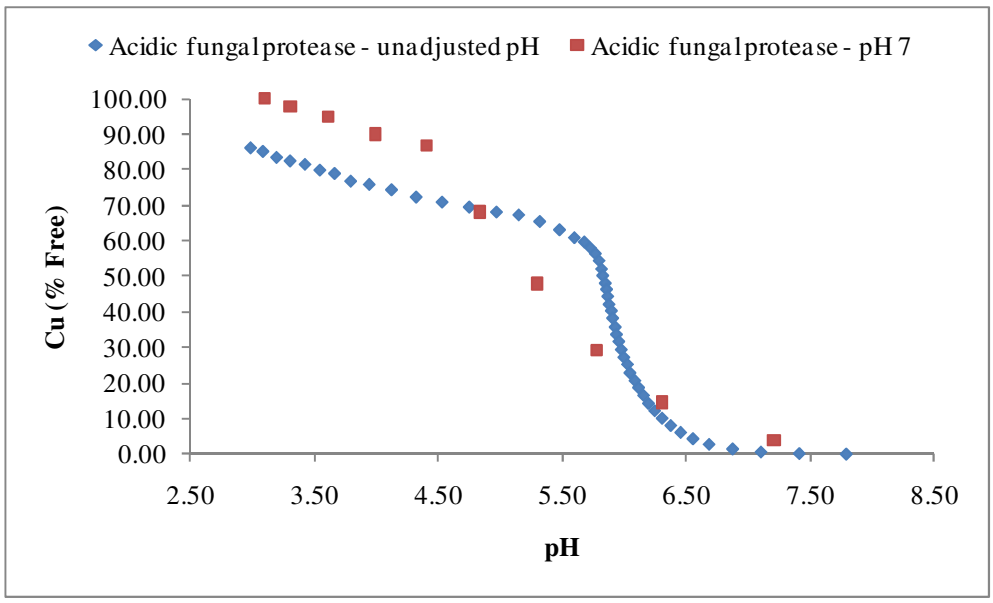

Figure 3.109 ISE titrations of proteinates formed using an acidic fungal protease, containing 15 % (w/w) Cu, with and without pH adjustment

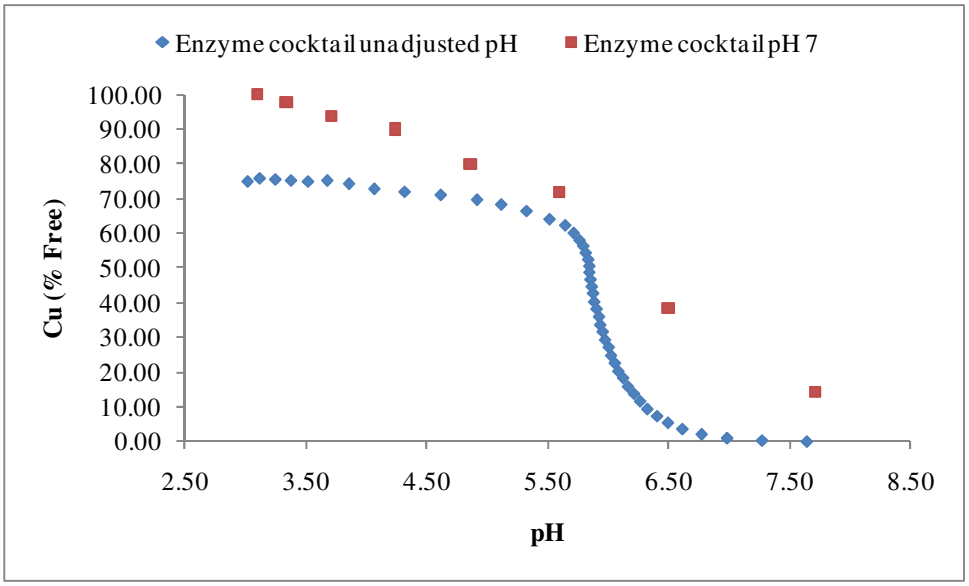

Figure 3.110 ISE titrations of proteinates containing 15 % (w/w) Cu(II) formed using an enzyme cocktail, with and without pH adjustment

During the course of the titrations of the soluble fraction from the pH unadjusted 15 % (w/w) copper proteinates, a precipitate was observed to form above pH 6 corresponding to the end-point seen in the graphical representation of the titration. This precipitate was also observed to form during the titrations of the 7.5 % (w/w) and 10 %

(w/w) pH unadjusted soluble fractions but was absent over the course of the titrations of the pH 7 adjusted soluble fractions. As the majority of copper was present in the soluble fractions of the pH unadjusted samples for all copper proteinates, it was necessary to examine whether complexation or precipitation had occurred at higher pH values. The importance of this from a nutritional perspective cannot be underestimated. Due to the variety of pH values encountered during the digestion process, it is imperative that the metal proteinate retains its bioavailability on ingestion and releases the metal at the appropriate point. Provided the precipitate observed is a complex or chelate, the integrity of the metal proteinate for use as an effective nutritional supplement would be preserved.

Prior to potentiometric titration, an examination of all copper proteinates (7.5 % (w/w), 10 % (w/w) and 15 % (w/w)) formed with and without pH adjustment indicated the presence of a substantially larger pellet in the pH 7 adjusted samples on centrifugation (Figure 3.89). Flame AAS confirmed the majority of the copper present in the pH 7 adjusted samples was contained in the pellet for all proteinates (Tables 3.20 – 3.23). No precipitate was observed over the course of the titrations of the soluble fraction of the pH 7 adjusted proteinates which can be explained by the fact that an insoluble chelate may have formed on initial pH adjustment and formed the original pellets observed on centrifugation. In the case of the pH unadjusted samples for all proteinates, a small pellet was observed on centrifugation and FAAS confirmed very little copper present (Tables 3.20 – 3.23). As the soy hydrolysate contained insoluble particulates, the presence of a minor pellet on centrifugation of the proteinate was not unexpected. The majority of the copper was present in the supernatant of the pH unadjusted samples for all proteinates and on titration of this soluble fraction a precipitate was observed to form at higher pH. In theory, the precipitate formed over the course of the titrations of the pH unadjusted soluble fractions should be the same product as the large pellet observed on initial centrifugation of the pH 7 adjusted proteinates (although the pH 7 adjusted proteinate pellet will also contain some insoluble soy particulates from the original sample). To confirm this, FTIR spectroscopy was employed to compare the precipitate formed from the titration of the pH unadjusted 10 % (w/w) Cu proteinates with the original pellet of the 10 % (w/w) Cu pH 7 adjusted

proteinates. Furthermore, with no additional precipitate formed over the course of the titration in the pH 7 adjusted soluble fractions, it can be concluded that the remainder of the proteinate is truly water-soluble and that the metal in the pellet is at least complexed.

FTIR analysis of 10 % (w/w) Cu proteinates formed using a serine protease hydrolysis (Sample 2), an acidic fungal protease hydrolysis (Sample 5) and a hydrolysate formed using an enzyme cocktail (Sample 10) was carried out (Figures 3.111-3.113). All three examples clearly illustrated that the precipitate formed during the course of the titration of the pH unadjusted samples with increasing pH was a similar product to that formed in the original pellet of the pH 7 adjusted proteinates.

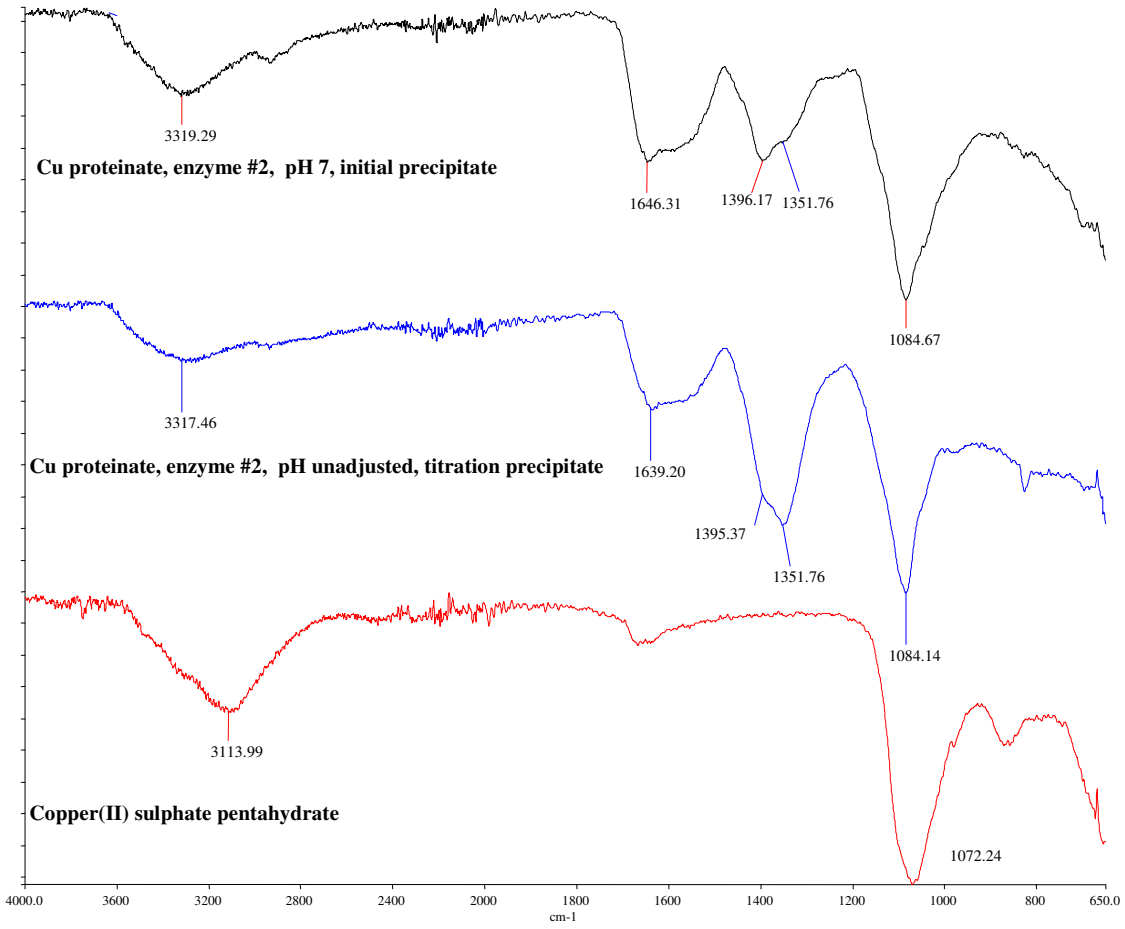

Figure 3.111 FTIR spectra of a 10 % (w/w) Cu proteinate formed using a serine protease hydrolysis (Sample 2), comparing a pH unadjusted titration precipitate against a pH 7 original pellet and a copper(II) sulphate pentahydrate control

On examination of the FTIR spectra of Figures 3.111-3.113, it can be seen that the majority of comparable peaks lie in the fingerprint region. Three bands in particular can be compared with ease (1650 cm^{-1} – 1080 cm^{-1} region), and based on the spectral results obtained, it is clear that the patterns are very similar between those of the pH unadjusted titration precipitate and the pH 7 original pellet. Due to the fact that some of the bands are quite broad, slight variations are observed but the general trend for each chelate is identical.

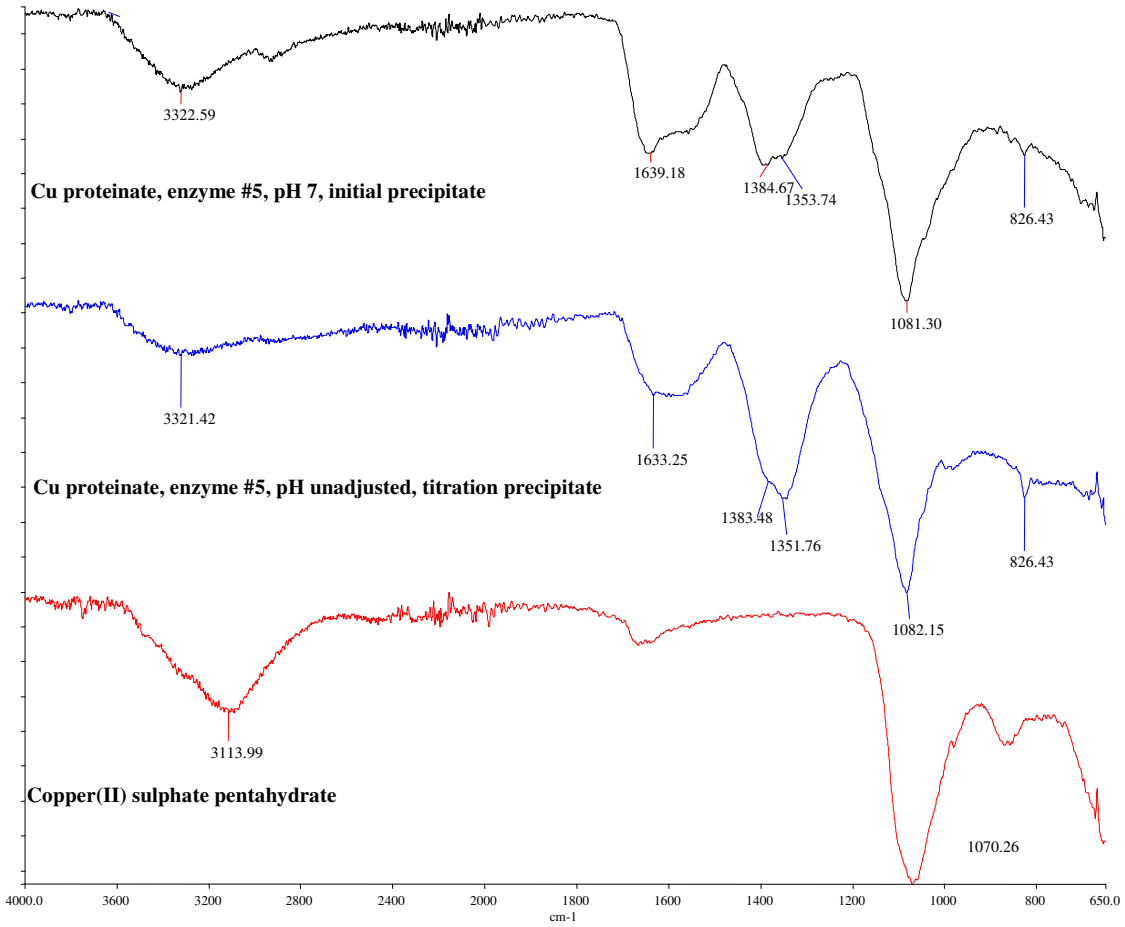

Figure 3.112 FTIR spectra of a 10 % (w/w) Cu proteinate formed using an acidic fungal protease hydrolysis (Sample 5), comparing a pH unadjusted titration precipitate against a pH 7 original pellet and a copper(II) sulphate pentahydrate control

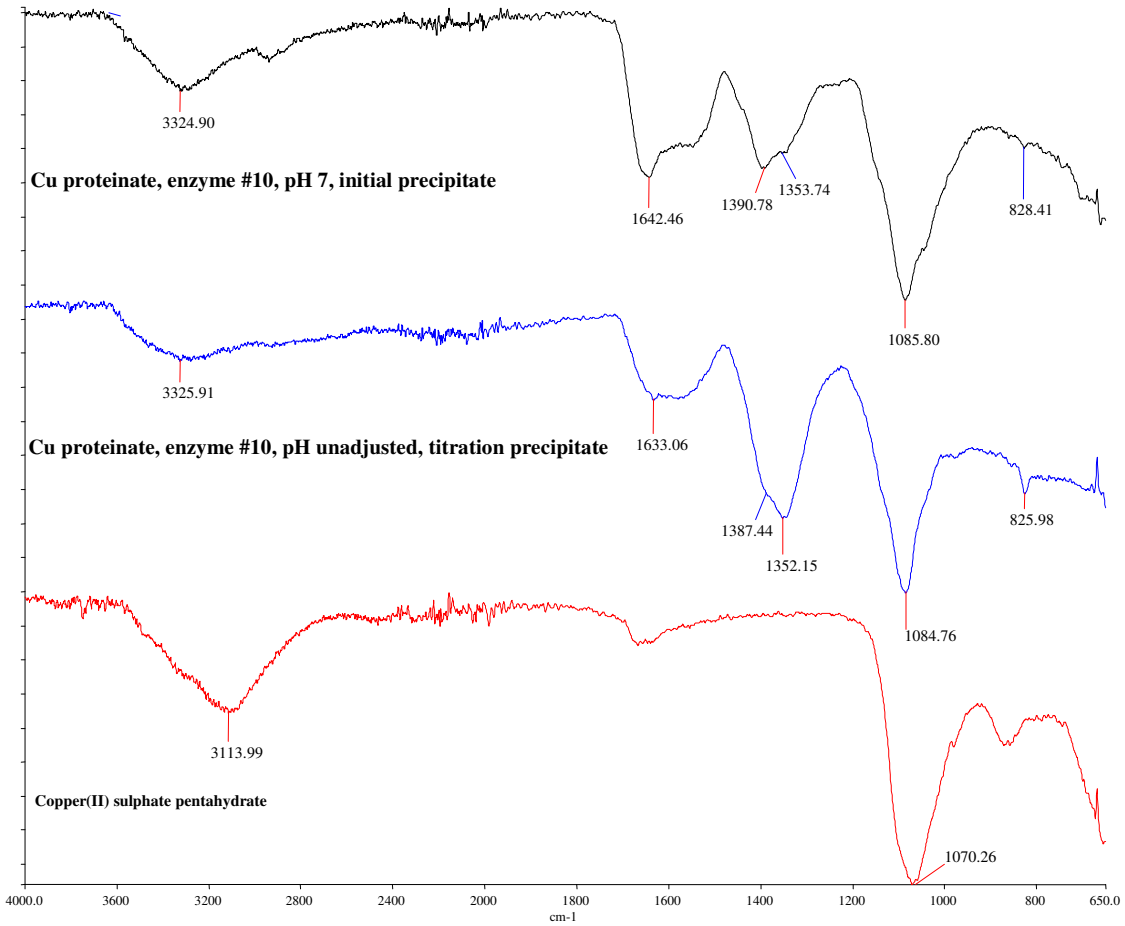

Figure 3.113 FTIR spectra of a 10 % (w/w) Cu proteinate formed using an enzyme cocktail hydrolysis (Sample 10), comparing a pH unadjusted titration precipitate against a pH 7 original pellet and a copper(II) sulphate pentahydrate control

Band shifts previously highlighted as indicative of groups involved in complex formation (Section 3.3.4) were also observed in the precipitate of the pH unadjusted soluble fraction and the original pH 7 adjusted proteinate pellet. To reiterate, shifts in the region above 3000 cm^{-1} can be indicative of the involvement of the $–NH_2$ group in complex formation. Deprotonation of the carboxylic acid group yields absorption bands corresponding to a carbonyl stretch ($\upsilon_{C=O}$) and C-OH vibrations (υ_{C-OH}) in the regions 1540 – 1650 cm^{-1} and 1300 and 1420 cm^{-1} respectively.

It can be concluded that the precipitate detected during the pH unadjusted soluble fraction titrations for the 7.5 % (w/w), 10 % (w/w) and 15 % (w/w) proteinates is indeed an insoluble complex and not precipitated metal. Furthermore, the pellet observed on centrifugation of the pH 7 adjusted samples is similarly complexed for all

metal proteinates. From a chemical perspective, greater solubility can decrease the protection of the metal ion in some cases (Leach, 2007). Insolubility can provide the chelate with kinetic stability as well as thermodynamic stability which can aid rumen or stomach bypass resulting in improved delivery of the metal to the area of absorption in the small intestine (Leach, 2007). Previous work has indicated solubility alone is not an accurate indicator of bioavailability (Sandberg, 1997) and as such, the formation of insoluble complexes in this work is not a major concern. Furthermore, the results obtained in this study related to solubility in water. However, gastric juices (pH < 3) could significantly affect the insoluble chelate and render it soluble at a particular point.

Based on the results of the potentiometric titrations, the free amino acid profiling results obtained for each enzymatic hydrolysis (Table 3.19) were extensively assessed to determine if any correlation existed between the individual free amino acids and the percentage free Cu in the pH unadjusted and pH 7 samples. This may indicate whether the metal was associated with free amino acids or with peptides produced from the various enzymatic hydrolyses. Individual amino acids (Table 3.19), classes of amino acids (Table 3.26) and combinations of classes of amino acids were investigated for the pH unadjusted and pH 7 samples (Tables 3.27 – 3.29).

Table 3.26: Summary of amino acid properties

Amino acid	Abbreviation	pK_a1	pK_a2	pK_a side chain	Polar properties	Acidic/Basic
Alanine	A – Ala	2.34	9.69		Non-polar	Neutral
Arginine	R – Arg	2.17	9.04	12.48	Polar	Basic
Asparagine	N – Asn	2.02	8.80		Polar	Neutral
Aspartic acid	D – Asp	1.88	9.60	3.65	Polar	Acidic
Cysteine	C – Cys	1.96	10.28	8.18	Slightly polar	Neutral
Glutamic acid	E – Glu	2.19	9.67	4.25	Polar	Acidic
Glutamine	Q – Gln	2.17	9.13		Polar	Neutral
Glycine	G – Gly	2.34	9.60		Non-polar	Neutral
Histidine	H – His	1.82	9.17	6.00	Polar	Basic
Isoleucine	I – Ile	2.36	9.60		Non-polar	Neutral
Leucine	L – Leu	2.36	9.60		Non-polar	Neutral
Lysine	K – Lys	2.18	8.95	10.53	Polar	Basic
Methionine	M – Met	2.28	9.21		Non-polar	Neutral
Phenylalanine	F – Phe	1.83	9.13		Non-polar	Neutral
Proline	P – Pro	1.99	10.60		Non-polar	Neutral
Serine	S – Ser	2.21	9.15		Polar	Neutral
Threonine	T – Thr	2.09	9.10		Polar	Neutral
Tryptophan	W – Trp	2.83	9.39		Slightly polar	Neutral
Tyrosine	Y – Tyr	2.20	9.11	10.07	Polar	Neutral
Valine	V - Val	2.32	9.62		Non-polar	Neutral

pK_a1: carboxyl group pK_a2: amino group

(adapted from: Lide, D.R., 1991)

Table 3.27 Individual amino acid analysis of 12 enzymatic preparations (Table 3.18) containing 7.5 % (w/w), 10 % (w/w) or 15 % (w/w) Cu without pH adjustment

		Ranked by highest level of Individual aa											
		8	**2**	**7**	**4**	**1**	**9**	**10**	**5**	**12**	**11**	**6**	**3**
	% Individual aa (Asp)	**7.26**	**7.24**	**7.22**	**6.76**	**6.14**	**5.74**	**5.56**	**5.51**	**5.35**	**5.26**	**4.17**	**3.25**
7.5 % Cu	pH 3 (% Free Cu)	100.00	100.00	64.61	100.00	100.00	70.44	38.51	72.16	40.10	34.24	80.99	100.00
pH unadj	pH 5 (% Free Cu)	52.80	61.85	28.56	40.06	77.37	33.60	20.78	33.66	18.66	17.27	30.05	57.46
10 % Cu	pH 3 (% Free Cu)	53.62	78.10	64.94	60.97	83.21	66.15	66.76	70.96	66.30	58.61	70.66	71.93
pH unadj	pH 5 (% Free Cu)	45.07	48.80	50.11	51.43	70.06	52.75	49.06	48.00	45.66	41.13	48.99	55.47
15 % Cu	pH 3 (% Free Cu)	73.21	71.85	85.81	74.07	71.64	69.29	75.06	86.02	76.57	87.18	74.30	81.91
pH unadj	pH 5 (% Free Cu)	68.17	59.37	74.21	70.83	67.97	74.75	69.08	67.99	71.06	67.83	66.19	67.70
		3	**2**	**6**	**9**	**10**	**8**	**7**	**11**	**1**	**4**	**12**	**5**
	% Individual aa (Thr)	**5.78**	**5.50**	**5.46**	**4.67**	**4.31**	**4.28**	**4.26**	**3.92**	**3.42**	**3.08**	**2.09**	**1.74**
7.5 % Cu	pH 3 (% Free Cu)	100.00	100.00	80.99	70.44	38.51	100.00	64.61	34.24	100.00	100.00	40.10	72.16
pH unadj	pH 5 (% Free Cu)	57.46	61.85	30.05	33.60	20.78	52.80	28.56	17.27	77.37	40.06	18.66	33.66
10 % Cu	pH 3 (% Free Cu)	71.93	78.10	70.66	66.15	66.76	53.62	64.94	58.61	83.21	60.97	66.30	70.96
pH unadj	pH 5 (% Free Cu)	55.47	48.80	48.99	52.75	49.06	45.07	50.11	41.13	70.06	51.43	45.66	48.00
15 % Cu	pH 3 (% Free Cu)	81.91	71.85	74.30	69.29	75.06	73.21	85.81	87.18	71.64	74.07	76.57	86.02
pH unadj	pH 5 (% Free Cu)	67.70	59.37	66.19	74.75	69.08	68.17	74.21	67.83	67.97	70.83	71.06	67.99
		3	**7**	**6**	**10**	**1**	**8**	**9**	**4**	**2**	**11**	**12**	**5**
	% Individual aa (Ser)	**5.19**	**4.72**	**4.62**	**4.48**	**4.26**	**4.15**	**3.80**	**3.68**	**3.64**	**2.88**	**1.48**	**1.24**
7.5 % Cu	pH 3 (% Free Cu)	100.00	64.61	80.99	38.51	100.00	100.00	70.44	100.00	100.00	34.24	40.10	72.16
pH unadj	pH 5 (% Free Cu)	57.46	28.56	30.05	20.78	77.37	52.80	33.60	40.06	61.85	17.27	18.66	33.66
10 % Cu	pH 3 (% Free Cu)	71.93	64.94	70.66	66.76	83.21	53.62	66.15	60.97	78.10	58.61	66.30	70.96
pH unadj	pH 5 (% Free Cu)	55.47	50.11	48.99	49.06	70.06	45.07	52.75	51.43	48.80	41.13	45.66	48.00
15 % Cu	pH 3 (% Free Cu)	81.91	85.81	74.30	75.06	71.64	73.21	69.29	74.07	71.85	87.18	76.57	86.02
pH unadj	pH 5 (% Free Cu)	67.70	74.21	66.19	69.08	67.97	68.17	74.75	70.83	59.37	67.83	71.06	67.99
		5	**11**	**1**	**12**	**2**	**4**	**7**	**8**	**9**	**10**	**6**	**3**
	% Individual aa (Glu)	**21.11**	**20.22**	**18.75**	**18.64**	**17.36**	**15.52**	**13.64**	**12.37**	**12.01**	**11.61**	**9.22**	**8.43**
7.5 % Cu	pH 3 (% Free Cu)	72.16	34.24	100.00	40.10	100.00	100.00	64.61	100.00	70.44	38.51	80.99	100.00
pH unadj	pH 5 (% Free Cu)	33.66	17.27	77.37	18.66	61.85	40.06	28.56	52.80	33.60	20.78	30.05	57.46
10 % Cu	pH 3 (% Free Cu)	70.96	58.61	83.21	66.30	78.10	60.97	64.94	53.62	66.15	66.76	70.66	71.93
pH unadj	pH 5 (% Free Cu)	48.00	41.13	70.06	45.66	48.80	51.43	50.11	45.07	52.75	49.06	48.99	55.47
15 % Cu	pH 3 (% Free Cu)	86.02	87.18	71.64	76.57	71.85	74.07	85.81	73.21	69.29	75.06	74.30	81.91
pH unadj	pH 5 (% Free Cu)	67.99	67.83	67.97	71.06	59.37	70.83	74.21	68.17	74.75	69.08	66.19	67.70

Table 3.27 continued:

		3	6	2	12	10	5	9	8	11	7	4	1
	% Individual aa (Asn)	**3.85**	**3.76**	**3.64**	**3.23**	**3.04**	**3.01**	**2.78**	**2.63**	**2.59**	**2.58**	**2.08**	**1.72**
7.5 % Cu	pH 3 (% Free Cu)	100.00	80.99	100.00	40.10	38.51	72.16	70.44	100.00	34.24	64.61	100.00	100.00
pH unadj	pH 5 (% Free Cu)	57.46	30.05	61.85	18.66	20.78	33.66	33.60	52.80	17.27	28.56	40.06	77.37
10 % Cu	pH 3 (% Free Cu)	71.93	70.66	78.10	66.30	66.76	70.96	66.15	53.62	58.61	64.94	60.97	83.21
pH unadj	pH 5 (% Free Cu)	55.47	48.99	48.80	45.66	49.06	48.00	52.75	45.07	41.13	50.11	51.43	70.06
15 % Cu	pH 3 (% Free Cu)	81.91	74.30	71.85	76.57	75.06	86.02	69.29	73.21	87.18	85.81	74.07	71.64
pH unadj	pH 5 (% Free Cu)	67.70	66.19	59.37	71.06	69.08	67.99	74.75	68.17	67.83	74.21	70.83	67.97
		3	**1**	**2**	**6**	**7**	**9**	**5**	**10**	**8**	**4**	**11**	**12**
	% Individual aa (Gln)	**3.94**	**3.82**	**3.70**	**3.24**	**3.22**	**2.28**	**2.05**	**2.03**	**1.73**	**1.46**	**1.44**	**0.72**
7.5 % Cu	pH 3 (% Free Cu)	100.00	100.00	100.00	80.99	64.61	70.44	72.16	38.51	100.00	100.00	34.24	40.10
pH unadj	pH 5 (% Free Cu)	57.46	77.37	61.85	30.05	28.56	33.60	33.66	20.78	52.80	40.06	17.27	18.66
10 % Cu	pH 3 (% Free Cu)	71.93	83.21	78.10	70.66	64.94	66.15	70.96	66.76	53.62	60.97	58.61	66.30
pH unadj	pH 5 (% Free Cu)	55.47	70.06	48.80	48.99	50.11	52.75	48.00	49.06	45.07	51.43	41.13	45.66
15 % Cu	pH 3 (% Free Cu)	81.91	71.64	71.85	74.30	85.81	69.29	86.02	75.06	73.21	74.07	87.18	76.57
pH unadj	pH 5 (% Free Cu)	67.70	67.97	59.37	66.19	74.21	74.75	67.99	69.08	68.17	70.83	67.83	71.06
		12	**3**	**2**	**6**	**1**	**5**	**9**	**10**	**8**	**7**	**4**	**11**
	% Individual aa (Pro)	**1.40**	**0.79**	**0.58**	**0.58**	**0.57**	**0.56**	**0.55**	**0.54**	**0.50**	**0.45**	**0.43**	**0.42**
7.5 % Cu	pH 3 (% Free Cu)	40.10	100.00	100.00	80.99	100.00	72.16	70.44	38.51	100.00	64.61	100.00	34.24
pH unadj	pH 5 (% Free Cu)	18.66	57.46	61.85	30.05	77.37	33.66	33.60	20.78	52.80	28.56	40.06	17.27
10 % Cu	pH 3 (% Free Cu)	66.30	71.93	78.10	70.66	83.21	70.96	66.15	66.76	53.62	64.94	60.97	58.61
pH unadj	pH 5 (% Free Cu)	45.66	55.47	48.80	48.99	70.06	48.00	52.75	49.06	45.07	50.11	51.43	41.13
15 % Cu	pH 3 (% Free Cu)	76.57	81.91	71.85	74.30	71.64	86.02	69.29	75.06	73.21	85.81	74.07	87.18
pH unadj	pH 5 (% Free Cu)	71.06	67.70	59.37	66.19	67.97	67.99	74.75	69.08	68.17	74.21	70.83	67.83
		4	**8**	**1**	**10**	**3**	**2**	**7**	**6**	**9**	**12**	**11**	**5**
	% Individual aa (Gly)	**5.08**	**2.63**	**2.54**	**2.11**	**1.85**	**1.80**	**1.58**	**1.39**	**1.13**	**0.79**	**0.72**	**0.49**
7.5 % Cu	pH 3 (% Free Cu)	100.00	100.00	100.00	38.51	100.00	100.00	64.61	80.99	70.44	40.10	34.24	72.16
pH unadj	pH 5 (% Free Cu)	40.06	52.80	77.37	20.78	57.46	61.85	28.56	30.05	33.60	18.66	17.27	33.66
10 % Cu	pH 3 (% Free Cu)	60.97	53.62	83.21	66.76	71.93	78.10	64.94	70.66	66.15	66.30	58.61	70.96
pH unadj	pH 5 (% Free Cu)	51.43	45.07	70.06	49.06	55.47	48.80	50.11	48.99	52.75	45.66	41.13	48.00
15 % Cu	pH 3 (% Free Cu)	74.07	73.21	71.64	75.06	81.91	71.85	85.81	74.30	69.29	76.57	87.18	86.02
pH unadj	pH 5 (% Free Cu)	70.83	68.17	67.97	69.08	67.70	59.37	74.21	66.19	74.75	71.06	67.83	67.99

Table 3.27 continued:

		2	**8**	**9**	**7**	**1**	**4**	**3**	**10**	**6**	**11**	**5**	**12**
	% Individual aa (Ala)	**9.61**	**8.43**	**8.37**	**8.18**	**7.99**	**7.44**	**7.39**	**7.21**	**7.16**	**6.77**	**3.04**	**2.96**
7.5 % Cu	pH 3 (% Free Cu)	100.00	100.00	70.44	64.61	100.00	100.00	100.00	38.51	80.99	34.24	72.16	40.10
pH unadj	pH 5 (% Free Cu)	61.85	52.80	33.60	28.56	77.37	40.06	57.46	20.78	30.05	17.27	33.66	18.66
10 % Cu	pH 3 (% Free Cu)	78.10	53.62	66.15	64.94	83.21	60.97	71.93	66.76	70.66	58.61	70.96	66.30
pH unadj	pH 5 (% Free Cu)	48.80	45.07	52.75	50.11	70.06	51.43	55.47	49.06	48.99	41.13	48.00	45.66
15 % Cu	pH 3 (% Free Cu)	71.85	73.21	69.29	85.81	71.64	74.07	81.91	75.06	74.30	87.18	86.02	76.57
pH unadj	pH 5 (% Free Cu)	59.37	68.17	74.75	74.21	67.97	70.83	67.70	69.08	66.19	67.83	67.99	71.06
		12	**5**	**11**	**8**	**9**	**7**	**6**	**3**	**10**	**-**	**-**	**-**
	% Individual aa (Cys)	**1.43**	**0.68**	**0.64**	**0.22**	**0.17**	**0.16**	**0.12**	**0.10**	**0.09**	**-**	**-**	**-**
7.5 % Cu	pH 3 (% Free Cu)	40.10	72.16	34.24	100.00	70.44	64.61	80.99	100.00	38.51			
pH unadj	pH 5 (% Free Cu)	18.66	33.66	17.27	52.80	33.60	28.56	30.05	57.46	20.78			
10 % Cu	pH 3 (% Free Cu)	66.30	70.96	58.61	53.62	66.15	64.94	70.66	71.93	66.76			
pH unadj	pH 5 (% Free Cu)	45.66	48.00	41.13	45.07	52.75	50.11	48.99	55.47	49.06			
15 % Cu	pH 3 (% Free Cu)	76.57	86.02	87.18	73.21	69.29	85.81	74.30	81.91	75.06			
pH unadj	pH 5 (% Free Cu)	71.06	67.99	67.83	68.17	74.75	74.21	66.19	67.70	69.08			
		3	**6**	**2**	**8**	**10**	**9**	**7**	**4**	**1**	**11**	**5**	**12**
	% Individual aa (Val)	**7.20**	**6.99**	**6.07**	**6.00**	**5.96**	**5.91**	**5.38**	**5.26**	**4.67**	**3.73**	**1.57**	**1.32**
7.5 % Cu	pH 3 (% Free Cu)	100.00	80.99	100.00	100.00	38.51	70.44	64.61	100.00	100.00	34.24	72.16	40.10
pH unadj	pH 5 (% Free Cu)	57.46	30.05	61.85	52.80	20.78	33.60	28.56	40.06	77.37	17.27	33.66	18.66
10 % Cu	pH 3 (% Free Cu)	71.93	70.66	78.10	53.62	66.76	66.15	64.94	60.97	83.21	58.61	70.96	66.30
pH unadj	pH 5 (% Free Cu)	55.47	48.99	48.80	45.07	49.06	52.75	50.11	51.43	70.06	41.13	48.00	45.66
15 % Cu	pH 3 (% Free Cu)	81.91	74.30	71.85	73.21	75.06	69.29	85.81	74.07	71.64	87.18	86.02	76.57
pH unadj	pH 5 (% Free Cu)	67.70	66.19	59.37	68.17	69.08	74.75	74.21	70.83	67.97	67.83	67.99	71.06
		8	**11**	**7**	**12**	**9**	**4**	**2**	**5**	**10**	**1**	**6**	**3**
	% Individual aa (Met)	**3.48**	**3.29**	**3.22**	**3.17**	**3.13**	**3.06**	**2.97**	**2.95**	**2.92**	**2.71**	**2.64**	**2.44**
7.5 % Cu	pH 3 (% Free Cu)	100.00	34.24	64.61	40.10	70.44	100.00	100.00	72.16	38.51	100.00	80.99	100.00
pH unadj	pH 5 (% Free Cu)	52.80	17.27	28.56	18.66	33.60	40.06	61.85	33.66	20.78	77.37	30.05	57.46
10 % Cu	pH 3 (% Free Cu)	53.62	58.61	64.94	66.30	66.15	60.97	78.10	70.96	66.76	83.21	70.66	71.93
pH unadj	pH 5 (% Free Cu)	45.07	41.13	50.11	45.66	52.75	51.43	48.80	48.00	49.06	70.06	48.99	55.47
15 % Cu	pH 3 (% Free Cu)	73.21	87.18	85.81	76.57	69.29	74.07	71.85	86.02	75.06	71.64	74.30	81.91
pH unadj	pH 5 (% Free Cu)	68.17	67.83	74.21	71.06	74.75	70.83	59.37	67.99	69.08	67.97	66.19	67.70

Table 3.27 continued:

		3	**6**	**9**	**10**	**2**	**8**	**7**	**4**	**11**	**1**	**12**	**5**
	% Individual aa (Ile)	**5.96**	**5.77**	**4.76**	**4.71**	**4.64**	**4.46**	**4.03**	**3.19**	**2.63**	**2.48**	**1.09**	**0.93**
7.5 % Cu	pH 3 (% Free Cu)	100.00	80.99	70.44	38.51	100.00	100.00	64.61	100.00	34.24	100.00	40.10	72.16
pH unadj	pH 5 (% Free Cu)	57.46	30.05	33.60	20.78	61.85	52.80	28.56	40.06	17.27	77.37	18.66	33.66
10 % Cu	pH 3 (% Free Cu)	71.93	70.66	66.15	66.76	78.10	53.62	64.94	60.97	58.61	83.21	66.30	70.96
pH unadj	pH 5 (% Free Cu)	55.47	48.99	52.75	49.06	48.80	45.07	50.11	51.43	41.13	70.06	45.66	48.00
15 % Cu	pH 3 (% Free Cu)	81.91	74.30	69.29	75.06	71.85	73.21	85.81	74.07	87.18	71.64	76.57	86.02
pH unadj	pH 5 (% Free Cu)	67.70	66.19	74.75	69.08	59.37	68.17	74.21	70.83	67.83	67.97	71.06	67.99
		5	**9**	**10**	**11**	**2**	**7**	**8**	**12**	**1**	**6**	**3**	**4**
	% Individual aa (Leu)	**13.78**	**13.25**	**13.15**	**12.66**	**12.64**	**12.27**	**12.13**	**12.12**	**12.04**	**11.99**	**11.29**	**10.98**
7.5 % Cu	pH 3 (% Free Cu)	72.16	70.44	38.51	34.24	100.00	64.61	100.00	40.10	100.00	80.99	100.00	100.00
pH unadj	pH 5 (% Free Cu)	33.66	33.60	20.78	17.27	61.85	28.56	52.80	18.66	77.37	30.05	57.46	40.06
10 % Cu	pH 3 (% Free Cu)	70.96	66.15	66.76	58.61	78.10	64.94	53.62	66.30	83.21	70.66	71.93	60.97
pH unadj	pH 5 (% Free Cu)	48.00	52.75	49.06	41.13	48.80	50.11	45.07	45.66	70.06	48.99	55.47	51.43
15 % Cu	pH 3 (% Free Cu)	86.02	69.29	75.06	87.18	71.85	85.81	73.21	76.57	71.64	74.30	81.91	74.07
pH unadj	pH 5 (% Free Cu)	67.99	74.75	69.08	67.83	59.37	74.21	68.17	71.06	67.97	66.19	67.70	70.83
		9	**7**	**8**	**3**	**6**	**10**	**11**	**4**	**5**	**1**	**12**	**2**
	% Individual aa (Tyr)	**6.34**	**6.23**	**6.22**	**5.92**	**5.87**	**5.84**	**5.67**	**5.49**	**5.45**	**5.30**	**5.10**	**1.27**
7.5 % Cu	pH 3 (% Free Cu)	70.44	64.61	100.00	100.00	80.99	38.51	34.24	100.00	72.16	100.00	40.10	100.00
pH unadj	pH 5 (% Free Cu)	33.60	28.56	52.80	57.46	30.05	20.78	17.27	40.06	33.66	77.37	18.66	61.85
10 % Cu	pH 3 (% Free Cu)	66.15	64.94	53.62	71.93	70.66	66.76	58.61	60.97	70.96	83.21	66.30	78.10
pH unadj	pH 5 (% Free Cu)	52.75	50.11	45.07	55.47	48.99	49.06	41.13	51.43	48.00	70.06	45.66	48.80
15 % Cu	pH 3 (% Free Cu)	69.29	85.81	73.21	81.91	74.30	75.06	87.18	74.07	86.02	71.64	76.57	71.85
pH unadj	pH 5 (% Free Cu)	74.75	74.21	68.17	67.70	66.19	69.08	67.83	70.83	67.99	67.97	71.06	59.37
		5	**9**	**11**	**12**	**10**	**8**	**7**	**2**	**6**	**4**	**3**	**1**
	% Individual aa (Phe)	**9.43**	**8.11**	**7.92**	**7.88**	**7.61**	**7.22**	**7.10**	**7.03**	**6.97**	**6.63**	**6.29**	**5.42**
7.5 % Cu	pH 3 (% Free Cu)	72.16	70.44	34.24	40.10	38.51	100.00	64.61	100.00	80.99	100.00	100.00	100.00
pH unadj	pH 5 (% Free Cu)	33.66	33.60	17.27	18.66	20.78	52.80	28.56	61.85	30.05	40.06	57.46	77.37
10 % Cu	pH 3 (% Free Cu)	70.96	66.15	58.61	66.30	66.76	53.62	64.94	78.10	70.66	60.97	71.93	83.21
pH unadj	pH 5 (% Free Cu)	48.00	52.75	41.13	45.66	49.06	45.07	50.11	48.80	48.99	51.43	55.47	70.06
15 % Cu	pH 3 (% Free Cu)	86.02	69.29	87.18	76.57	75.06	73.21	85.81	71.85	74.30	74.07	81.91	71.64
pH unadj	pH 5 (% Free Cu)	67.99	74.75	67.83	71.06	69.08	68.17	74.21	59.37	66.19	70.83	67.70	67.97

Table 3.27 continued:

		2	**6**	**9**	**7**	**8**	**10**	**1**	**3**	**12**	**4**	**11**	**5**
	% Individual aa (Trp)	**2.21**	**2.11**	**2.11**	**2.02**	**1.99**	**1.99**	**1.98**	**1.75**	**1.58**	**1.57**	**1.44**	**0.74**
7.5 % Cu	pH 3 (% Free Cu)	100.00	80.99	70.44	64.61	100.00	38.51	100.00	100.00	40.10	100.00	34.24	72.16
pH unadj	pH 5 (% Free Cu)	61.85	30.05	33.60	28.56	52.80	20.78	77.37	57.46	18.66	40.06	17.27	33.66
10 % Cu	pH 3 (% Free Cu)	78.10	70.66	66.15	64.94	53.62	66.76	83.21	71.93	66.30	60.97	58.61	70.96
pH unadj	pH 5 (% Free Cu)	48.80	48.99	52.75	50.11	45.07	49.06	70.06	55.47	45.66	51.43	41.13	48.00
15 % Cu	pH 3 (% Free Cu)	71.85	74.30	69.29	85.81	73.21	75.06	71.64	81.91	76.57	74.07	87.18	86.02
pH unadj	pH 5 (% Free Cu)	59.37	66.19	74.75	74.21	68.17	69.08	67.97	67.70	71.06	70.83	67.83	67.99
		12	**5**	**11**	**2**	**3**	**10**	**6**	**1**	**4**	**7**	**9**	**8**
	% Individual aa (Lys)	**13.74**	**11.93**	**7.56**	**7.18**	**6.83**	**6.83**	**6.56**	**6.46**	**5.75**	**5.55**	**5.07**	**4.61**
7.5 % Cu	pH 3 (% Free Cu)	40.10	72.16	34.24	100.00	100.00	38.51	80.99	100.00	100.00	64.61	70.44	100.00
pH unadj	pH 5 (% Free Cu)	18.66	33.66	17.27	61.85	57.46	20.78	30.05	77.37	40.06	28.56	33.60	52.80
10 % Cu	pH 3 (% Free Cu)	66.30	70.96	58.61	78.10	71.93	66.76	70.66	83.21	60.97	64.94	66.15	53.62
pH unadj	pH 5 (% Free Cu)	45.66	48.00	41.13	48.80	55.47	49.06	48.99	70.06	51.43	50.11	52.75	45.07
15 % Cu	pH 3 (% Free Cu)	76.57	86.02	87.18	71.85	81.91	75.06	74.30	71.64	74.07	85.81	69.29	73.21
pH unadj	pH 5 (% Free Cu)	71.06	67.99	67.83	59.37	67.70	69.08	66.19	67.97	70.83	74.21	74.75	68.17
		3	**6**	**2**	**10**	**8**	**9**	**4**	**7**	**1**	**11**	**12**	**5**
	% Individual aa (His)	**2.66**	**2.56**	**2.56**	**2.16**	**2.03**	**2.02**	**1.74**	**1.71**	**1.61**	**1.36**	**0.48**	**0.40**
7.5 % Cu	pH 3 (% Free Cu)	100.00	80.99	100.00	38.51	100.00	70.44	100.00	64.61	100.00	34.24	40.10	72.16
pH unadj	pH 5 (% Free Cu)	57.46	30.05	61.85	20.78	52.80	33.60	40.06	28.56	77.37	17.27	18.66	33.66
10 % Cu	pH 3 (% Free Cu)	71.93	70.66	78.10	66.76	53.62	66.15	60.97	64.94	83.21	58.61	66.30	70.96
pH unadj	pH 5 (% Free Cu)	55.47	48.99	48.80	49.06	45.07	52.75	51.43	50.11	70.06	41.13	45.66	48.00
15 % Cu	pH 3 (% Free Cu)	81.91	74.30	71.85	75.06	73.21	69.29	74.07	85.81	71.64	87.18	76.57	86.02
pH unadj	pH 5 (% Free Cu)	67.70	66.19	59.37	69.08	68.17	74.75	70.83	74.21	67.97	67.83	71.06	67.99
		12	**5**	**4**	**3**	**11**	**6**	**1**	**10**	**9**	**8**	**7**	**2**
	% Individual aa (Arg)	**15.51**	**13.32**	**10.75**	**9.07**	**8.93**	**8.82**	**8.03**	**7.87**	**7.82**	**7.72**	**6.42**	**0.41**
7.5 % Cu	pH 3 (% Free Cu)	40.10	72.16	100.00	100.00	34.24	80.99	100.00	38.51	70.44	100.00	64.61	100.00
pH unadj	pH 5 (% Free Cu)	18.66	33.66	40.06	57.46	17.27	30.05	77.37	20.78	33.60	52.80	28.56	61.85
10 % Cu	pH 3 (% Free Cu)	66.30	70.96	60.97	71.93	58.61	70.66	83.21	66.76	66.15	53.62	64.94	78.10
pH unadj	pH 5 (% Free Cu)	45.66	48.00	51.43	55.47	41.13	48.99	70.06	49.06	52.75	45.07	50.11	48.80
15 % Cu	pH 3 (% Free Cu)	76.57	86.02	74.07	81.91	87.18	74.30	71.64	75.06	69.29	73.21	85.81	71.85
pH unadj	pH 5 (% Free Cu)	71.06	67.99	70.83	67.70	67.83	66.19	67.97	69.08	74.75	68.17	74.21	59.37

Table 3.28 Individual amino acid analysis of 12 enzymatic preparations (Table 3.18) containing 7.5 % (w/w), 10 % (w/w) or 15 % (w/w) Cu with pH adjustment

		Ranked by highest level of Individual aa											
		8	**2**	**7**	**4**	**1**	**9**	**10**	**5**	**12**	**11**	**6**	**3**
	% Individual aa (Asp)	**7.26**	**7.24**	**7.22**	**6.76**	**6.14**	**5.74**	**5.56**	**5.51**	**5.35**	**5.26**	**4.17**	**3.25**
7.5 % Cu	pH 3 (% Free Cu)	100.00	100.00	100.00	100.00	100.00	100.00	100.00	100.00	100.00	100.00	100.00	100.00
pH 7	pH 5 (% Free Cu)	45.64	38.03	41.44	49.40	43.01	57.36	42.01	38.79	41.32	47.84	33.64	31.01
10 % Cu	pH 3 (% Free Cu)	100.00	71.24	100.00	58.82	100.00	95.05	78.45	90.52	85.76	84.39	89.03	84.09
pH 7	pH 5 (% Free Cu)	30.00	22.99	36.41	26.88	44.79	32.19	25.21	34.37	40.34	33.56	23.02	20.35
15 % Cu	pH 3 (% Free Cu)	90.33	85.42	84.69	76.28	81.19	86.98	100.00	100.00	100.00	100.00	100.00	100.00
pH 7	pH 5 (% Free Cu)	55.00	42.15	50.01	50.97	51.63	51.11	78.36	58.18	65.29	76.98	50.29	58.57
		3	**2**	**6**	**9**	**10**	**8**	**7**	**11**	**1**	**4**	**12**	**5**
	% Individual aa (Thr)	**5.78**	**5.50**	**5.46**	**4.67**	**4.31**	**4.28**	**4.26**	**3.92**	**3.42**	**3.08**	**2.09**	**1.74**
7.5 % Cu	pH 3 (% Free Cu)	100.00	100.00	100.00	100.00	100.00	100.00	100.00	100.00	100.00	100.00	100.00	100.00
pH 7	pH 5 (% Free Cu)	31.01	38.03	33.64	57.36	42.01	45.64	41.44	47.84	43.01	49.40	41.32	38.79
10 % Cu	pH 3 (% Free Cu)	84.09	71.24	89.03	95.05	78.45	100.00	100.00	84.39	100.00	58.82	85.76	90.52
pH 7	pH 5 (% Free Cu)	20.35	22.99	23.02	32.19	25.21	30.00	36.41	33.56	44.79	26.88	40.34	34.37
15 % Cu	pH 3 (% Free Cu)	100.00	85.42	100.00	86.98	100.00	90.33	84.69	100.00	81.19	76.28	100.00	100.00
pH 7	pH 5 (% Free Cu)	58.57	42.15	50.29	51.11	78.36	55.00	50.01	76.98	51.63	50.97	65.29	58.18
		3	**7**	**6**	**10**	**1**	**8**	**9**	**4**	**2**	**11**	**12**	**5**
	% Individual aa (Ser)	**5.19**	**4.72**	**4.62**	**4.48**	**4.26**	**4.15**	**3.80**	**3.68**	**3.64**	**2.88**	**1.48**	**1.24**
7.5 % Cu	pH 3 (% Free Cu)	100.00	100.00	100.00	100.00	100.00	100.00	100.00	100.00	100.00	100.00	100.00	100.00
pH 7	pH 5 (% Free Cu)	31.01	41.44	33.64	42.01	43.01	45.64	57.36	49.40	38.03	47.84	41.32	38.79
10 % Cu	pH 3 (% Free Cu)	84.09	100.00	89.03	78.45	100.00	100.00	95.05	58.82	71.24	84.39	85.76	90.52
pH 7	pH 5 (% Free Cu)	20.35	36.41	23.02	25.21	44.79	30.00	32.19	26.88	22.99	33.56	40.34	34.37
15 % Cu	pH 3 (% Free Cu)	100.00	84.69	100.00	100.00	81.19	90.33	86.98	76.28	85.42	100.00	100.00	100.00
pH 7	pH 5 (% Free Cu)	58.57	50.01	50.29	78.36	51.63	55.00	51.11	50.97	42.15	76.98	65.29	58.18
		5	**11**	**1**	**12**	**2**	**4**	**7**	**8**	**9**	**10**	**6**	**3**
	% Individual aa (Glu)	**21.11**	**20.22**	**18.75**	**18.64**	**17.36**	**15.52**	**13.64**	**12.37**	**12.01**	**11.61**	**9.22**	**8.43**
7.5 % Cu	pH 3 (% Free Cu)	100.00	100.00	100.00	100.00	100.00	100.00	100.00	100.00	100.00	100.00	100.00	100.00
pH 7	pH 5 (% Free Cu)	38.79	47.84	43.01	41.32	38.03	49.40	41.44	45.64	57.36	42.01	33.64	31.01
10 % Cu	pH 3 (% Free Cu)	90.52	84.39	100.00	85.76	71.24	58.82	100.00	100.00	95.05	78.45	89.03	84.09
pH 7	pH 5 (% Free Cu)	34.37	33.56	44.79	40.34	22.99	26.88	36.41	30.00	32.19	25.21	23.02	20.35
15 % Cu	pH 3 (% Free Cu)	100.00	100.00	81.19	100.00	85.42	76.28	84.69	90.33	86.98	100.00	100.00	100.00
pH 7	pH 5 (% Free Cu)	58.18	76.98	51.63	65.29	42.15	50.97	50.01	55.00	51.11	78.36	50.29	58.57

Table 3.28 continued:

		3	6	2	12	10	5	9	8	11	7	4	1
	% Individual aa (Asn)	**3.85**	**3.76**	**3.64**	**3.23**	**3.04**	**3.01**	**2.78**	**2.63**	**2.59**	**2.58**	**2.08**	**1.72**
7.5 % Cu	pH 3 (% Free Cu)	100.00	100.00	100.00	100.00	100.00	100.00	100.00	100.00	100.00	100.00	100.00	100.00
pH 7	pH 5 (% Free Cu)	31.01	33.64	38.03	41.32	42.01	38.79	57.36	45.64	47.84	41.44	49.40	43.01
10 % Cu	pH 3 (% Free Cu)	84.09	89.03	71.24	85.76	78.45	90.52	95.05	100.00	84.39	100.00	58.82	100.00
pH 7	pH 5 (% Free Cu)	20.35	23.02	22.99	40.34	25.21	34.37	32.19	30.00	33.56	36.41	26.88	44.79
15 % Cu	pH 3 (% Free Cu)	100.00	100.00	85.42	100.00	100.00	100.00	86.98	90.33	100.00	84.69	76.28	81.19
pH 7	pH 5 (% Free Cu)	58.57	50.29	42.15	65.29	78.36	58.18	51.11	55.00	76.98	50.01	50.97	51.63
		3	**1**	**2**	**6**	**7**	**9**	**5**	**10**	**8**	**4**	**11**	**12**
	% Individual aa (Gln)	**3.94**	**3.82**	**3.70**	**3.24**	**3.22**	**2.28**	**2.05**	**2.03**	**1.73**	**1.46**	**1.44**	**0.72**
7.5 % Cu	pH 3 (% Free Cu)	100.00	100.00	100.00	100.00	100.00	100.00	100.00	100.00	100.00	100.00	100.00	100.00
pH 7	pH 5 (% Free Cu)	31.01	43.01	38.03	33.64	41.44	57.36	38.79	42.01	45.64	49.40	47.84	41.32
10 % Cu	pH 3 (% Free Cu)	84.09	100.00	71.24	89.03	100.00	95.05	90.52	78.45	100.00	58.82	84.39	85.76
pH 7	pH 5 (% Free Cu)	20.35	44.79	22.99	23.02	36.41	32.19	34.37	25.21	30.00	26.88	33.56	40.34
15 % Cu	pH 3 (% Free Cu)	100.00	81.19	85.42	100.00	84.69	86.98	100.00	100.00	90.33	76.28	100.00	100.00
pH 7	pH 5 (% Free Cu)	58.57	51.63	42.15	50.29	50.01	51.11	58.18	78.36	55.00	50.97	76.98	65.29
		12	**3**	**2**	**6**	**1**	**5**	**9**	**10**	**8**	**7**	**4**	**11**
	% Individual aa (Pro)	**1.40**	**0.79**	**0.58**	**0.58**	**0.57**	**0.56**	**0.55**	**0.54**	**0.50**	**0.45**	**0.43**	**0.42**
7.5 % Cu	pH 3 (% Free Cu)	100.00	100.00	100.00	100.00	100.00	100.00	100.00	100.00	100.00	100.00	100.00	100.00
pH 7	pH 5 (% Free Cu)	41.32	31.01	38.03	33.64	43.01	38.79	57.36	42.01	45.64	41.44	49.40	47.84
10 % Cu	pH 3 (% Free Cu)	85.76	84.09	71.24	89.03	100.00	90.52	95.05	78.45	100.00	100.00	58.82	84.39
pH 7	pH 5 (% Free Cu)	40.34	20.35	22.99	23.02	44.79	34.37	32.19	25.21	30.00	36.41	26.88	33.56
15 % Cu	pH 3 (% Free Cu)	100.00	100.00	85.42	100.00	81.19	100.00	86.98	100.00	90.33	84.69	76.28	100.00
pH 7	pH 5 (% Free Cu)	65.29	58.57	42.15	50.29	51.63	58.18	51.11	78.36	55.00	50.01	50.97	76.98
		4	**8**	**1**	**10**	**3**	**2**	**7**	**6**	**9**	**12**	**11**	**5**
	% Individual aa (Gly)	**5.08**	**2.63**	**2.54**	**2.11**	**1.85**	**1.80**	**1.58**	**1.39**	**1.13**	**0.79**	**0.72**	**0.49**
7.5 % Cu	pH 3 (% Free Cu)	100.00	100.00	100.00	100.00	100.00	100.00	100.00	100.00	100.00	100.00	100.00	100.00
pH 7	pH 5 (% Free Cu)	49.40	45.64	43.01	42.01	31.01	38.03	41.44	33.64	57.36	41.32	47.84	38.79
10 % Cu	pH 3 (% Free Cu)	58.82	100.00	100.00	78.45	84.09	71.24	100.00	89.03	95.05	85.76	84.39	90.52
pH 7	pH 5 (% Free Cu)	26.88	30.00	44.79	25.21	20.35	22.99	36.41	23.02	32.19	40.34	33.56	34.37
15 % Cu	pH 3 (% Free Cu)	76.28	90.33	81.19	100.00	100.00	85.42	84.69	100.00	86.98	100.00	100.00	100.00
pH 7	pH 5 (% Free Cu)	50.97	55.00	51.63	78.36	58.57	42.15	50.01	50.29	51.11	65.29	76.98	58.18

Table 3.28 continued:

		2	**8**	**9**	**7**	**1**	**4**	**3**	**10**	**6**	**11**	**5**	**12**
	% Individual aa (Ala)	**9.61**	**8.43**	**8.37**	**8.18**	**7.99**	**7.44**	**7.39**	**7.21**	**7.16**	**6.77**	**3.04**	**2.96**
7.5 % Cu	pH 3 (% Free Cu)	100.00	100.00	100.00	100.00	100.00	100.00	100.00	100.00	100.00	100.00	100.00	100.00
pH 7	pH 5 (% Free Cu)	38.03	45.64	57.36	41.44	43.01	49.40	31.01	42.01	33.64	47.84	38.79	41.32
10 % Cu	pH 3 (% Free Cu)	71.24	100.00	95.05	100.00	100.00	58.82	84.09	78.45	89.03	84.39	90.52	85.76
pH 7	pH 5 (% Free Cu)	22.99	30.00	32.19	36.41	44.79	26.88	20.35	25.21	23.02	33.56	34.37	40.34
15 % Cu	pH 3 (% Free Cu)	85.42	90.33	86.98	84.69	81.19	76.28	100.00	100.00	100.00	100.00	100.00	100.00
pH 7	pH 5 (% Free Cu)	42.15	55.00	51.11	50.01	51.63	50.97	58.57	78.36	50.29	76.98	58.18	65.29
		12	**5**	**11**	**8**	**9**	**7**	**6**	**3**	**10**	**-**	**-**	**-**
	% Individual aa (Cys)	**1.43**	**0.68**	**0.64**	**0.22**	**0.17**	**0.16**	**0.12**	**0.10**	**0.09**	**-**	**-**	**-**
7.5 % Cu	pH 3 (% Free Cu)	100.00	100.00	100.00	100.00	100.00	100.00	100.00	100.00	100.00			
pH 7	pH 5 (% Free Cu)	41.32	38.79	47.84	45.64	57.36	41.44	33.64	31.01	42.01			
10 % Cu	pH 3 (% Free Cu)	85.76	90.52	84.39	100.00	95.05	100.00	89.03	84.09	78.45			
pH 7	pH 5 (% Free Cu)	40.34	34.37	33.56	30.00	32.19	36.41	23.02	20.35	25.21			
15 % Cu	pH 3 (% Free Cu)	100.00	100.00	100.00	90.33	86.98	84.69	100.00	100.00	100.00			
pH 7	pH 5 (% Free Cu)	65.29	58.18	76.98	55.00	51.11	50.01	50.29	58.57	78.36			
		3	**6**	**2**	**8**	**10**	**9**	**7**	**4**	**1**	**11**	**5**	**12**
	% Individual aa (Val)	**7.20**	**6.99**	**6.07**	**6.00**	**5.96**	**5.91**	**5.38**	**5.26**	**4.67**	**3.73**	**1.57**	**1.32**
7.5 % Cu	pH 3 (% Free Cu)	100.00	100.00	100.00	100.00	100.00	100.00	100.00	100.00	100.00	100.00	100.00	100.00
pH 7	pH 5 (% Free Cu)	31.01	33.64	38.03	45.64	42.01	57.36	41.44	49.40	43.01	47.84	38.79	41.32
10 % Cu	pH 3 (% Free Cu)	84.09	89.03	71.24	100.00	78.45	95.05	100.00	58.82	100.00	84.39	90.52	85.76
pH 7	pH 5 (% Free Cu)	20.35	23.02	22.99	30.00	25.21	32.19	36.41	26.88	44.79	33.56	34.37	40.34
15 % Cu	pH 3 (% Free Cu)	100.00	100.00	85.42	90.33	100.00	86.98	84.69	76.28	81.19	100.00	100.00	100.00
pH 7	pH 5 (% Free Cu)	58.57	50.29	42.15	55.00	78.36	51.11	50.01	50.97	51.63	76.98	58.18	65.29
		8	**11**	**7**	**12**	**9**	**4**	**2**	**5**	**10**	**1**	**6**	**3**
	% Individual aa (Met)	**3.48**	**3.29**	**3.22**	**3.17**	**3.13**	**3.06**	**2.97**	**2.95**	**2.92**	**2.71**	**2.64**	**2.44**
7.5 % Cu	pH 3 (% Free Cu)	100.00	100.00	100.00	100.00	100.00	100.00	100.00	100.00	100.00	100.00	100.00	100.00
pH 7	pH 5 (% Free Cu)	45.64	47.84	41.44	41.32	57.36	49.40	38.03	38.79	42.01	43.01	33.64	31.01
10 % Cu	pH 3 (% Free Cu)	100.00	84.39	100.00	85.76	95.05	58.82	71.24	90.52	78.45	100.00	89.03	84.09
pH 7	pH 5 (% Free Cu)	30.00	33.56	36.41	40.34	32.19	26.88	22.99	34.37	25.21	44.79	23.02	20.35
15 % Cu	pH 3 (% Free Cu)	90.33	100.00	84.69	100.00	86.98	76.28	85.42	100.00	100.00	81.19	100.00	100.00
pH 7	pH 5 (% Free Cu)	55.00	76.98	50.01	65.29	51.11	50.97	42.15	58.18	78.36	51.63	50.29	58.57

Table 3.28 continued:

		3	6	9	10	2	8	7	4	11	1	12	5
	% Individual aa (Ile)	**5.96**	**5.77**	**4.76**	**4.71**	**4.64**	**4.46**	**4.03**	**3.19**	**2.63**	**2.48**	**1.09**	**0.93**
7.5 % Cu	pH 3 (% Free Cu)	100.00	100.00	100.00	100.00	100.00	100.00	100.00	100.00	100.00	100.00	100.00	100.00
pH 7	pH 5 (% Free Cu)	31.01	33.64	57.36	42.01	38.03	45.64	41.44	49.40	47.84	43.01	41.32	38.79
10 % Cu	pH 3 (% Free Cu)	84.09	89.03	95.05	78.45	71.24	100.00	100.00	58.82	84.39	100.00	85.76	90.52
pH 7	pH 5 (% Free Cu)	20.35	23.02	32.19	25.21	22.99	30.00	36.41	26.88	33.56	44.79	40.34	34.37
15 % Cu	pH 3 (% Free Cu)	100.00	100.00	86.98	100.00	85.42	90.33	84.69	76.28	100.00	81.19	100.00	100.00
pH 7	pH 5 (% Free Cu)	58.57	50.29	51.11	78.36	42.15	55.00	50.01	50.97	76.98	51.63	65.29	58.18
		5	9	10	11	2	7	8	12	1	6	3	4
	% Individual aa (Leu)	**13.78**	**13.25**	**13.15**	**12.66**	**12.64**	**12.27**	**12.13**	**12.12**	**12.04**	**11.99**	**11.29**	**10.98**
7.5 % Cu	pH 3 (% Free Cu)	100.00	100.00	100.00	100.00	100.00	100.00	100.00	100.00	100.00	100.00	100.00	100.00
pH 7	pH 5 (% Free Cu)	38.79	57.36	42.01	47.84	38.03	41.44	45.64	41.32	43.01	33.64	31.01	49.40
10 % Cu	pH 3 (% Free Cu)	90.52	95.05	78.45	84.39	71.24	100.00	100.00	85.76	100.00	89.03	84.09	58.82
pH 7	pH 5 (% Free Cu)	34.37	32.19	25.21	33.56	22.99	36.41	30.00	40.34	44.79	23.02	20.35	26.88
15 % Cu	pH 3 (% Free Cu)	100.00	86.98	100.00	100.00	85.42	84.69	90.33	100.00	81.19	100.00	100.00	76.28
pH 7	pH 5 (% Free Cu)	58.18	51.11	78.36	76.98	42.15	50.01	55.00	65.29	51.63	50.29	58.57	50.97
		9	7	8	3	6	10	11	4	5	1	12	2
	% Individual aa (Tyr)	**6.34**	**6.23**	**6.22**	**5.92**	**5.87**	**5.84**	**5.67**	**5.49**	**5.45**	**5.30**	**5.10**	**1.27**
7.5 % Cu	pH 3 (% Free Cu)	100.00	100.00	100.00	100.00	100.00	100.00	100.00	100.00	100.00	100.00	100.00	100.00
pH 7	pH 5 (% Free Cu)	57.36	41.44	45.64	31.01	33.64	42.01	47.84	49.40	38.79	43.01	41.32	38.03
10 % Cu	pH 3 (% Free Cu)	95.05	100.00	100.00	84.09	89.03	78.45	84.39	58.82	90.52	100.00	85.76	71.24
pH 7	pH 5 (% Free Cu)	32.19	36.41	30.00	20.35	23.02	25.21	33.56	26.88	34.37	44.79	40.34	22.99
15 % Cu	pH 3 (% Free Cu)	86.98	84.69	90.33	100.00	100.00	100.00	100.00	76.28	100.00	81.19	100.00	85.42
pH 7	pH 5 (% Free Cu)	51.11	50.01	55.00	58.57	50.29	78.36	76.98	50.97	58.18	51.63	65.29	42.15
		5	9	11	12	10	8	7	2	6	4	3	1
	% Individual aa (Phe)	**9.43**	**8.11**	**7.92**	**7.88**	**7.61**	**7.22**	**7.10**	**7.03**	**6.97**	**6.63**	**6.29**	**5.42**
7.5 % Cu	pH 3 (% Free Cu)	100.00	100.00	100.00	100.00	100.00	100.00	100.00	100.00	100.00	100.00	100.00	100.00
pH 7	pH 5 (% Free Cu)	38.79	57.36	47.84	41.32	42.01	45.64	41.44	38.03	33.64	49.40	31.01	43.01
10 % Cu	pH 3 (% Free Cu)	90.52	95.05	84.39	85.76	78.45	100.00	100.00	71.24	89.03	58.82	84.09	100.00
pH 7	pH 5 (% Free Cu)	34.37	32.19	33.56	40.34	25.21	30.00	36.41	22.99	23.02	26.88	20.35	44.79
15 % Cu	pH 3 (% Free Cu)	100.00	86.98	100.00	100.00	100.00	90.33	84.69	85.42	100.00	76.28	100.00	81.19
pH 7	pH 5 (% Free Cu)	58.18	51.11	76.98	65.29	78.36	55.00	50.01	42.15	50.29	50.97	58.57	51.63

Table 3.28 continued:

		2	**6**	**9**	**7**	**8**	**10**	**1**	**3**	**12**	**4**	**11**	**5**
	% Individual aa (Trp)	**2.21**	**2.11**	**2.11**	**2.02**	**1.99**	**1.99**	**1.98**	**1.75**	**1.58**	**1.57**	**1.44**	**0.74**
7.5 % Cu	pH 3 (% Free Cu)	100.00	100.00	100.00	100.00	100.00	100.00	100.00	100.00	100.00	100.00	100.00	100.00
pH 7	pH 5 (% Free Cu)	38.03	33.64	57.36	41.44	45.64	42.01	43.01	31.01	41.32	49.40	47.84	38.79
10 % Cu	pH 3 (% Free Cu)	71.24	89.03	95.05	100.00	100.00	78.45	100.00	84.09	85.76	58.82	84.39	90.52
pH 7	pH 5 (% Free Cu)	22.99	23.02	32.19	36.41	30.00	25.21	44.79	20.35	40.34	26.88	33.56	34.37
15 % Cu	pH 3 (% Free Cu)	85.42	100.00	86.98	84.69	90.33	100.00	81.19	100.00	100.00	76.28	100.00	100.00
pH 7	pH 5 (% Free Cu)	42.15	50.29	51.11	50.01	55.00	78.36	51.63	58.57	65.29	50.97	76.98	58.18
		12	**5**	**11**	**2**	**3**	**10**	**6**	**1**	**4**	**7**	**9**	**8**
	% Individual aa (Lys)	**13.74**	**11.93**	**7.56**	**7.18**	**6.83**	**6.83**	**6.56**	**6.46**	**5.75**	**5.55**	**5.07**	**4.61**
7.5 % Cu	pH 3 (% Free Cu)	100.00	100.00	100.00	100.00	100.00	100.00	100.00	100.00	100.00	100.00	100.00	100.00
pH 7	pH 5 (% Free Cu)	41.32	38.79	47.84	38.03	31.01	42.01	33.64	43.01	49.40	41.44	57.36	45.64
10 % Cu	pH 3 (% Free Cu)	85.76	90.52	84.39	71.24	84.09	78.45	89.03	100.00	58.82	100.00	95.05	100.00
pH 7	pH 5 (% Free Cu)	40.34	34.37	33.56	22.99	20.35	25.21	23.02	44.79	26.88	36.41	32.19	30.00
15 % Cu	pH 3 (% Free Cu)	100.00	100.00	100.00	85.42	100.00	100.00	100.00	81.19	76.28	84.69	86.98	90.33
pH 7	pH 5 (% Free Cu)	65.29	58.18	76.98	42.15	58.57	78.36	50.29	51.63	50.97	50.01	51.11	55.00
		3	**6**	**2**	**10**	**8**	**9**	**4**	**7**	**1**	**11**	**12**	**5**
	% Individual aa (His)	**2.66**	**2.56**	**2.56**	**2.16**	**2.03**	**2.02**	**1.74**	**1.71**	**1.61**	**1.36**	**0.48**	**0.40**
7.5 % Cu	pH 3 (% Free Cu)	100.00	100.00	100.00	100.00	100.00	100.00	100.00	100.00	100.00	100.00	100.00	100.00
pH 7	pH 5 (% Free Cu)	31.01	33.64	38.03	42.01	45.64	57.36	49.40	41.44	43.01	47.84	41.32	38.79
10 % Cu	pH 3 (% Free Cu)	84.09	89.03	71.24	78.45	100.00	95.05	58.82	100.00	100.00	84.39	85.76	90.52
pH 7	pH 5 (% Free Cu)	20.35	23.02	22.99	25.21	30.00	32.19	26.88	36.41	44.79	33.56	40.34	34.37
15 % Cu	pH 3 (% Free Cu)	100.00	100.00	85.42	100.00	90.33	86.98	76.28	84.69	81.19	100.00	100.00	100.00
pH 7	pH 5 (% Free Cu)	58.57	50.29	42.15	78.36	55.00	51.11	50.97	50.01	51.63	76.98	65.29	58.18
		12	**5**	**4**	**3**	**11**	**6**	**1**	**10**	**9**	**8**	**7**	**2**
	% Individual aa (Arg)	**15.51**	**13.32**	**10.75**	**9.07**	**8.93**	**8.82**	**8.03**	**7.87**	**7.82**	**7.72**	**6.42**	**0.41**
7.5 % Cu	pH 3 (% Free Cu)	100.00	100.00	100.00	100.00	100.00	100.00	100.00	100.00	100.00	100.00	100.00	100.00
pH 7	pH 5 (% Free Cu)	41.32	38.79	49.40	31.01	47.84	33.64	43.01	42.01	57.36	45.64	41.44	38.03
10 % Cu	pH 3 (% Free Cu)	85.76	90.52	58.82	84.09	84.39	89.03	100.00	78.45	95.05	100.00	100.00	71.24
pH 7	pH 5 (% Free Cu)	40.34	34.37	26.88	20.35	33.56	23.02	44.79	25.21	32.19	30.00	36.41	22.99
15 % Cu	pH 3 (% Free Cu)	100.00	100.00	76.28	100.00	100.00	100.00	81.19	100.00	86.98	90.33	84.69	85.42
pH 7	pH 5 (% Free Cu)	65.29	58.18	50.97	58.57	76.98	50.29	51.63	78.36	51.11	55.00	50.01	42.15

Data analysis of both the pH unadjusted and the pH 7 adjusted samples at pH 3 and pH 5 (Tables 3.27 and 3.28) showed no clear correlation between free copper and individual amino acids. Histidine was selected to illustrate this point for the 10 % (w/w) Cu pH unadjusted samples outlined in Table 3.27 (Figure 3.114). It can be proposed that metal binding is not significantly dependent on individual amino acids to any extent but that it is more dependent on short chain peptides present in the hydrolysate. Ultimately, when one considers the extent of hydrolysis generated through use of the multi-enzyme cocktail, as evidenced by the increase in FAN in this hydrolysate, it is clear that the presence of peptides and the amino acid sequence within peptides plays a more important role in metal chelation.

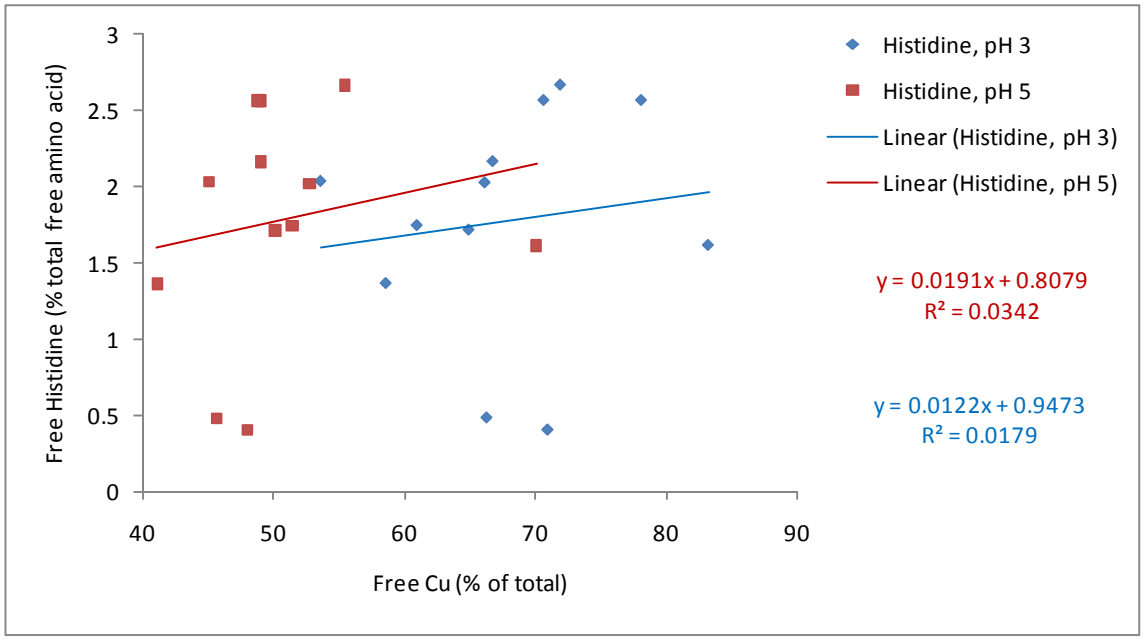

Figure 3.114 Correlation between free copper (at pH 3 and pH 5) and free histidine

Table 3.29 Amino acid analysis of 12 enzymatic preparations (Table 3.18) containing 7.5 % (w/w), 10 % (w/w) or 15 % (w/w) Cu without pH adjustment

		Ranked by highest level of Neutral AA											
		1	**2**	**9**	**8**	**10**	**6**	**3**	**7**	**4**	**11**	**5**	**12**
	% Neutral aa	**53.39**	**47.55**	**47.33**	**46.83**	**46.19**	**45.60**	**44.97**	**44.22**	**43.63**	**39.57**	**33.50**	**32.29**
7.5 % Cu	pH 3 (% Free Cu)	100.00	100.00	70.44	100.00	38.51	80.99	100.00	64.61	100.00	34.24	72.16	40.10
pH unadj	pH 5 (% Free Cu)	77.37	61.85	33.60	52.80	20.78	30.05	57.46	28.56	40.06	17.27	33.66	18.66
10 % Cu	pH 3 (% Free Cu)	83.21	78.10	66.15	53.62	66.76	70.66	71.93	64.94	60.97	58.61	70.96	66.30
pH unadj	pH 5 (% Free Cu)	70.06	48.80	52.75	45.07	49.06	48.99	55.47	50.11	51.43	41.13	48.00	45.66
15 % Cu	pH 3 (% Free Cu)	71.64	71.85	69.29	73.21	75.06	74.30	81.91	85.81	74.07	87.18	86.02	76.57
pH unadj	pH 5 (% Free Cu)	67.97	59.37	74.75	68.17	69.08	66.19	67.70	74.21	70.83	67.83	67.99	71.06
		Ranked by highest level of Basic AA											
		12	**5**	**3**	**4**	**6**	**11**	**10**	**1**	**9**	**8**	**7**	**2**
	% Basic aa	**29.72**	**25.66**	**18.56**	**18.24**	**17.94**	**17.85**	**16.87**	**16.10**	**14.92**	**14.36**	**13.68**	**10.15**
7.5 % Cu	pH 3 (% Free Cu)	40.10	72.16	100.00	100.00	80.99	34.24	38.51	100.00	70.44	100.00	64.61	100.00
pH unadj	pH 5 (% Free Cu)	18.66	33.66	57.46	40.06	30.05	17.27	20.78	77.37	33.60	52.80	28.56	61.85
10 % Cu	pH 3 (% Free Cu)	66.30	70.96	71.93	60.97	70.66	58.61	66.76	83.21	66.15	53.62	64.94	78.10
pH unadj	pH 5 (% Free Cu)	45.66	48.00	55.47	51.43	48.99	41.13	49.06	70.06	52.75	45.07	50.11	48.80
15 % Cu	pH 3 (% Free Cu)	76.57	86.02	81.91	74.07	74.30	87.18	75.06	71.64	69.29	73.21	85.81	71.85
pH unadj	pH 5 (% Free Cu)	71.06	67.99	67.70	70.83	66.19	67.83	69.08	67.97	74.75	68.17	74.21	59.37
		Ranked by highest level of Acidic AA											
		5	**11**	**1**	**2**	**12**	**4**	**7**	**8**	**9**	**10**	**6**	**3**
	% Acidic aa	**26.62**	**25.48**	**24.89**	**24.60**	**23.99**	**22.28**	**20.87**	**19.63**	**17.75**	**17.17**	**13.39**	**11.68**
7.5 % Cu	pH 3 (% Free Cu)	72.16	34.24	100.00	100.00	40.10	100.00	64.61	100.00	70.44	38.51	80.99	100.00
pH unadj	pH 5 (% Free Cu)	33.66	17.27	77.37	61.85	18.66	40.06	28.56	52.80	33.60	20.78	30.05	57.46
10 % Cu	pH 3 (% Free Cu)	70.96	58.61	83.21	78.10	66.30	60.97	64.94	53.62	66.15	66.76	70.66	71.93
pH unadj	pH 5 (% Free Cu)	48.00	41.13	70.06	48.80	45.66	51.43	50.11	45.07	52.75	49.06	48.99	55.47
15 % Cu	pH 3 (% Free Cu)	86.02	87.18	71.64	71.85	76.57	74.07	85.81	73.21	69.29	75.06	74.30	81.91
pH unadj	pH 5 (% Free Cu)	67.99	67.83	67.97	59.37	71.06	70.83	74.21	68.17	74.75	69.08	66.19	67.70
		Ranked by highest level of Polar AA											
		3	**6**	**7**	**9**	**10**	**8**	**1**	**2**	**11**	**4**	**5**	**12**
	% Polar aa	**24.77**	**23.07**	**21.18**	**20.03**	**19.78**	**19.23**	**18.52**	**17.75**	**17.14**	**15.80**	**14.17**	**14.05**
7.5 % Cu	pH 3 (% Free Cu)	100.00	80.99	64.61	70.44	38.51	100.00	100.00	100.00	34.24	100.00	72.16	40.10
pH unadj	pH 5 (% Free Cu)	57.46	30.05	28.56	33.60	20.78	52.80	77.37	61.85	17.27	40.06	33.66	18.66
10 % Cu	pH 3 (% Free Cu)	71.93	70.66	64.94	66.15	66.76	53.62	83.21	78.10	58.61	60.97	70.96	66.30
pH unadj	pH 5 (% Free Cu)	55.47	48.99	50.11	52.75	49.06	45.07	70.06	48.80	41.13	51.43	48.00	45.66
15 % Cu	pH 3 (% Free Cu)	81.91	74.30	85.81	69.29	75.06	73.21	71.64	71.85	87.18	74.07	86.02	76.57
pH unadj	pH 5 (% Free Cu)	67.70	66.19	74.21	74.75	69.08	68.17	67.97	59.37	67.83	70.83	67.99	71.06

Table 3.29 continued:

		Ranked by highest level of combined basic and acidic AA											
		12	**5**	**11**	**1**	**4**	**2**	**7**	**10**	**8**	**9**	**6**	**3**
	% B+A aa	**53.71**	**52.28**	**43.33**	**40.99**	**40.52**	**34.75**	**34.55**	**34.04**	**33.99**	**32.67**	**31.33**	**30.23**
7.5 % Cu	pH 3 (% Free Cu)	40.10	72.16	34.24	100.00	100.00	100.00	64.61	38.51	100.00	70.44	80.99	100.00
pH unadj	pH 5 (% Free Cu)	18.66	33.66	17.27	77.37	40.06	61.85	28.56	20.78	52.80	33.60	30.05	57.46
10 % Cu	pH 3 (% Free Cu)	66.30	70.96	58.61	83.21	60.97	78.10	64.94	66.76	53.62	66.15	70.66	71.93
pH unadj	pH 5 (% Free Cu)	45.66	48.00	41.13	70.06	51.43	48.80	50.11	49.06	45.07	52.75	48.99	55.47
15 % Cu	pH 3 (% Free Cu)	76.57	86.02	87.18	71.64	74.07	71.85	85.81	75.06	73.21	69.29	74.30	81.91
pH unadj	pH 5 (% Free Cu)	71.06	67.99	67.83	67.97	70.83	59.37	74.21	69.08	68.17	74.75	66.19	67.70
		Ranked by highest level of combined polar and neutral AA											
		1	**3**	**6**	**9**	**8**	**10**	**7**	**2**	**4**	**11**	**5**	**12**
	% P+N aa	**71.91**	**69.74**	**68.67**	**67.36**	**66.07**	**65.98**	**65.39**	**65.30**	**59.43**	**56.71**	**47.67**	**46.34**
7.5 % Cu	pH 3 (% Free Cu)	100.00	100.00	80.99	70.44	100.00	38.51	64.61	100.00	100.00	34.24	72.16	40.10
pH unadj	pH 5 (% Free Cu)	77.37	57.46	30.05	33.60	52.80	20.78	28.56	61.85	40.06	17.27	33.66	18.66
10 % Cu	pH 3 (% Free Cu)	83.21	71.93	70.66	66.15	53.62	66.76	64.94	78.10	60.97	58.61	70.96	66.30
pH unadj	pH 5 (% Free Cu)	70.06	55.47	48.99	52.75	45.07	49.06	50.11	48.80	51.43	41.13	48.00	45.66
15 % Cu	pH 3 (% Free Cu)	71.64	81.91	74.30	69.29	73.21	75.06	85.81	71.85	74.07	87.18	86.02	76.57
pH unadj	pH 5 (% Free Cu)	67.97	67.70	66.19	74.75	68.17	69.08	74.21	59.37	70.83	67.83	67.99	71.06
		Ranked by highest level of combined Basic and Polar											
		12	**3**	**6**	**5**	**10**	**11**	**9**	**7**	**1**	**4**	**8**	**2**
	%B+P aa	**43.77**	**43.33**	**41.02**	**39.82**	**36.65**	**34.99**	**34.95**	**34.86**	**34.62**	**34.04**	**33.59**	**27.90**
7.5 % Cu	pH 3 (% Free Cu)	40.10	100.00	80.99	72.16	38.51	34.24	70.44	64.61	100.00	100.00	100.00	100.00
pH unadj	pH 5 (% Free Cu)	18.66	57.46	30.05	33.66	20.78	17.27	33.60	28.56	77.37	40.06	52.80	61.85
10 % Cu	pH 3 (% Free Cu)	66.30	71.93	70.66	70.96	66.76	58.61	66.15	64.94	83.21	60.97	53.62	78.10
pH unadj	pH 5 (% Free Cu)	45.66	55.47	48.99	48.00	49.06	41.13	52.75	50.11	70.06	51.43	45.07	48.80
15 % Cu	pH 3 (% Free Cu)	76.57	81.91	74.30	86.02	75.06	87.18	69.29	85.81	71.64	74.07	73.21	71.85
pH unadj	pH 5 (% Free Cu)	71.06	67.70	66.19	67.99	69.08	67.83	74.75	74.21	67.97	70.83	68.17	59.37

* B+A aa= Basic and Acidic amino acids, P+N aa= Polar and Neutral amino acids, B+P aa = Basic and Polar amino acids

Table 3.29 continued:

		Ranked by highest level of combined basic and neutral											
		1	**6**	**3**	**10**	**9**	**12**	**4**	**8**	**5**	**7**	**2**	**11**
	%B+N aa	**69.49**	**63.54**	**63.52**	**63.06**	**62.25**	**62.02**	**61.88**	**61.19**	**59.16**	**57.90**	**57.70**	**57.42**
7.5 % Cu	pH 3 (% Free Cu)	100.00	80.99	100.00	38.51	70.44	40.10	100.00	100.00	72.16	64.61	100.00	34.24
pH unadj	pH 5 (% Free Cu)	77.37	30.05	57.46	20.78	33.60	18.66	40.06	52.80	33.66	28.56	61.85	17.27
10 % Cu	pH 3 (% Free Cu)	83.21	70.66	71.93	66.76	66.15	66.30	60.97	53.62	70.96	64.94	78.10	58.61
pH unadj	pH 5 (% Free Cu)	70.06	48.99	55.47	49.06	52.75	45.66	51.43	45.07	48.00	50.11	48.80	41.13
15 % Cu	pH 3 (% Free Cu)	71.64	74.30	81.91	75.06	69.29	76.57	74.07	73.21	86.02	85.81	71.85	87.18
pH unadj	pH 5 (% Free Cu)	67.97	66.19	67.70	69.08	74.75	71.06	70.83	68.17	67.99	74.21	59.37	67.83
		Ranked by highest level of combined acidic and neutral											
		1	**2**	**8**	**4**	**7**	**9**	**11**	**10**	**5**	**6**	**3**	**12**
	%A+N aa	**78.28**	**72.15**	**66.47**	**65.91**	**65.09**	**65.08**	**65.05**	**63.36**	**60.12**	**58.98**	**56.64**	**56.28**
7.5 % Cu	pH 3 (% Free Cu)	100.00	100.00	100.00	100.00	64.61	70.44	34.24	38.51	72.16	80.99	100.00	40.10
pH unadj	pH 5 (% Free Cu)	77.37	61.85	52.80	40.06	28.56	33.60	17.27	20.78	33.66	30.05	57.46	18.66
10 % Cu	pH 3 (% Free Cu)	83.21	78.10	53.62	60.97	64.94	66.15	58.61	66.76	70.96	70.66	71.93	66.30
pH unadj	pH 5 (% Free Cu)	70.06	48.80	45.07	51.43	50.11	52.75	41.13	49.06	48.00	48.99	55.47	45.66
15 % Cu	pH 3 (% Free Cu)	71.64	71.85	73.21	74.07	85.81	69.29	87.18	75.06	86.02	74.30	81.91	76.57
pH unadj	pH 5 (% Free Cu)	67.97	59.37	68.17	70.83	74.21	74.75	67.83	69.08	67.99	66.19	67.70	71.06
		Ranked by highest level of combined acidic and polar											
		1	**11**	**2**	**7**	**5**	**8**	**4**	**12**	**9**	**10**	**6**	**3**
	%A+P aa	**43.41**	**42.62**	**42.36**	**42.04**	**40.79**	**38.86**	**38.08**	**38.04**	**37.78**	**36.96**	**36.46**	**36.45**
7.5 % Cu	pH 3 (% Free Cu)	100.00	34.24	100.00	64.61	72.16	100.00	100.00	40.10	70.44	38.51	80.99	100.00
pH unadj	pH 5 (% Free Cu)	77.37	17.27	61.85	28.56	33.66	52.80	40.06	18.66	33.60	20.78	30.05	57.46
10 % Cu	pH 3 (% Free Cu)	83.21	58.61	78.10	64.94	70.96	53.62	60.97	66.30	66.15	66.76	70.66	71.93
pH unadj	pH 5 (% Free Cu)	70.06	41.13	48.80	50.11	48.00	45.07	51.43	45.66	52.75	49.06	48.99	55.47
15 % Cu	pH 3 (% Free Cu)	71.64	87.18	71.85	85.81	86.02	73.21	74.07	76.57	69.29	75.06	74.30	81.91
pH unadj	pH 5 (% Free Cu)	67.97	67.83	59.37	74.21	67.99	68.17	70.83	71.06	74.75	69.08	66.19	67.70

* B+N aa= Basic and Neutral amino acids, A+N aa= Acidic and Neutral amino acids, A+P aa = Acidic and Polar amino acids

Table 3.30 Amino acid analysis of 12 enzymatic preparations (Table 3.18) containing 7.5 % (w/w), 10 % (w/w) or 15 % (w/w) Cu at pH 7

		Ranked by highest level of Neutral AA											
		1	**2**	**9**	**8**	**10**	**6**	**3**	**7**	**4**	**11**	**5**	**12**
	% Neutral aa	**53.39**	**47.55**	**47.33**	**46.83**	**46.19**	**45.60**	**44.97**	**44.22**	**43.63**	**39.57**	**33.50**	**32.29**
7.5 % Cu	pH 3 (% Free Cu)	100.00	100.00	100.00	100.00	100.00	100.00	100.00	100.00	100.00	100.00	100.00	100.00
pH 7	pH 5 (% Free Cu)	43.01	38.03	57.36	45.64	42.01	33.64	31.01	41.44	49.40	47.84	38.79	41.32
10 % Cu	pH 3 (% Free Cu)	100.00	71.24	95.05	100.00	78.45	89.03	84.09	100.00	58.82	84.39	90.52	85.76
pH 7	pH 5 (% Free Cu)	44.79	22.99	32.19	30.00	25.21	23.02	20.35	36.41	26.88	33.56	34.37	40.34
15 % Cu	pH 3 (% Free Cu)	81.19	85.42	86.98	90.33	100.00	100.00	100.00	84.69	76.28	100.00	100.00	100.00
pH 7	pH 5 (% Free Cu)	51.63	42.15	51.11	55.00	78.36	50.29	58.57	50.01	50.97	76.98	58.18	65.29
		Ranked by highest level of Basic AA											
		12	**5**	**3**	**4**	**6**	**11**	**10**	**1**	**9**	**8**	**7**	**2**
	% Basic aa	**29.72**	**25.66**	**18.56**	**18.24**	**17.94**	**17.85**	**16.87**	**16.10**	**14.92**	**14.36**	**13.68**	**10.15**
7.5 % Cu	pH 3 (% Free Cu)	100.00	100.00	100.00	100.00	100.00	100.00	100.00	100.00	100.00	100.00	100.00	100.00
pH 7	pH 5 (% Free Cu)	41.32	38.79	31.01	49.40	33.64	47.84	42.01	43.01	57.36	45.64	41.44	38.03
10 % Cu	pH 3 (% Free Cu)	85.76	90.52	84.09	58.82	89.03	84.39	78.45	100.00	95.05	100.00	100.00	71.24
pH 7	pH 5 (% Free Cu)	40.34	34.37	20.35	26.88	23.02	33.56	25.21	44.79	32.19	30.00	36.41	22.99
15 % Cu	pH 3 (% Free Cu)	100.00	100.00	100.00	76.28	100.00	100.00	100.00	81.19	86.98	90.33	84.69	85.42
pH 7	pH 5 (% Free Cu)	65.29	58.18	58.57	50.97	50.29	76.98	78.36	51.63	51.11	55.00	50.01	42.15
		Ranked by highest level of Acidic AA											
		5	**11**	**1**	**2**	**12**	**4**	**7**	**8**	**9**	**10**	**6**	**3**
	% Acidic aa	**26.62**	**25.48**	**24.89**	**24.60**	**23.99**	**22.28**	**20.87**	**19.63**	**17.75**	**17.17**	**13.39**	**11.68**
7.5 % Cu	pH 3 (% Free Cu)	100.00	100.00	100.00	100.00	100.00	100.00	100.00	100.00	100.00	100.00	100.00	100.00
pH 7	pH 5 (% Free Cu)	38.79	47.84	43.01	38.03	41.32	49.40	41.44	45.64	57.36	42.01	33.64	31.01
10 % Cu	pH 3 (% Free Cu)	90.52	84.39	100.00	71.24	85.76	58.82	100.00	100.00	95.05	78.45	89.03	84.09
pH 7	pH 5 (% Free Cu)	34.37	33.56	44.79	22.99	40.34	26.88	36.41	30.00	32.19	25.21	23.02	20.35
15 % Cu	pH 3 (% Free Cu)	100.00	100.00	81.19	85.42	100.00	76.28	84.69	90.33	86.98	100.00	100.00	100.00
pH 7	pH 5 (% Free Cu)	58.18	76.98	51.63	42.15	65.29	50.97	50.01	55.00	51.11	78.36	50.29	58.57
		Ranked by highest level of Polar AA											
		3	**6**	**7**	**9**	**10**	**8**	**1**	**2**	**11**	**4**	**5**	**12**
	% Polar aa	**24.77**	**23.07**	**21.18**	**20.03**	**19.78**	**19.23**	**18.52**	**17.75**	**17.14**	**15.80**	**14.17**	**14.05**
7.5 % Cu	pH 3 (% Free Cu)	100.00	100.00	100.00	100.00	100.00	100.00	100.00	100.00	100.00	100.00	100.00	100.00
pH 7	pH 5 (% Free Cu)	31.01	33.64	41.44	57.36	42.01	45.64	43.01	38.03	47.84	49.40	38.79	41.32
10 % Cu	pH 3 (% Free Cu)	84.09	89.03	100.00	95.05	78.45	100.00	100.00	71.24	84.39	58.82	90.52	85.76
pH7	pH 5 (% Free Cu)	20.35	23.02	36.41	32.19	25.21	30.00	44.79	22.99	33.56	26.88	34.37	40.34
15 % Cu	pH 3 (% Free Cu)	100.00	100.00	84.69	86.98	100.00	90.33	81.19	85.42	100.00	76.28	100.00	100.00
pH 7	pH 5 (% Free Cu)	58.57	50.29	50.01	51.11	78.36	55.00	51.63	42.15	76.98	50.97	58.18	65.29

Table 3.30 continued:

		Ranked by highest level of combined basic and acidic AA											
		12	**5**	**11**	**1**	**4**	**2**	**7**	**10**	**8**	**9**	**6**	**3**
	% B+A aa	**53.71**	**52.28**	**43.33**	**40.99**	**40.52**	**34.75**	**34.55**	**34.04**	**33.99**	**32.67**	**31.33**	**30.23**
7.5 % Cu	pH 3 (% Free Cu)	100.00	100.00	100.00	100.00	100.00	100.00	100.00	100.00	100.00	100.00	100.00	100.00
pH 7	pH 5 (% Free Cu)	41.32	38.79	47.84	43.01	49.40	38.03	41.44	42.01	45.64	57.36	33.64	31.01
10 % Cu	pH 3 (% Free Cu)	85.76	90.52	84.39	100.00	58.82	71.24	100.00	78.45	100.00	95.05	89.03	84.09
pH 7	pH 5 (% Free Cu)	40.34	34.37	33.56	44.79	26.88	22.99	36.41	25.21	30.00	32.19	23.02	20.35
15 % Cu	pH 3 (% Free Cu)	100.00	100.00	100.00	81.19	76.28	85.42	84.69	100.00	90.33	86.98	100.00	100.00
pH 7	pH 5 (% Free Cu)	65.29	58.18	76.98	51.63	50.97	42.15	50.01	78.36	55.00	51.11	50.29	58.57
		Ranked by highest level of combined polar and neutral AA											
		1	**3**	**6**	**9**	**8**	**10**	**7**	**2**	**4**	**11**	**5**	**12**
	% P+N aa	**71.91**	**69.74**	**68.67**	**67.36**	**66.07**	**65.98**	**65.39**	**65.30**	**59.43**	**56.71**	**47.67**	**46.34**
7.5 % Cu	pH 3 (% Free Cu)	100.00	100.00	100.00	100.00	100.00	100.00	100.00	100.00	100.00	100.00	100.00	100.00
pH 7	pH 5 (% Free Cu)	43.01	31.01	33.64	57.36	45.64	42.01	41.44	38.03	49.40	47.84	38.79	41.32
10 % Cu	pH 3 (% Free Cu)	100.00	84.09	89.03	95.05	100.00	78.45	100.00	71.24	58.82	84.39	90.52	85.76
pH 7	pH 3.5 (% Free Cu)	44.79	20.35	23.02	32.19	30.00	25.21	36.41	22.99	26.88	33.56	34.37	40.34
15 % Cu	pH 3 (% Free Cu)	81.19	100.00	100.00	86.98	90.33	100.00	84.69	85.42	76.28	100.00	100.00	100.00
pH 7	pH 3.5 (% Free Cu)	51.63	58.57	50.29	51.11	55.00	78.36	50.01	42.15	50.97	76.98	58.18	65.29
		Ranked by highest level of combined Basic and Polar											
		12	**3**	**6**	**5**	**10**	**11**	**9**	**7**	**1**	**4**	**8**	**2**
	%B+P aa	**43.77**	**43.33**	**41.02**	**39.82**	**36.65**	**34.99**	**34.95**	**34.86**	**34.62**	**34.04**	**33.59**	**27.90**
7.5 % Cu	pH 3 (% Free Cu)	100.00	100.00	100.00	100.00	100.00	100.00	100.00	100.00	100.00	100.00	100.00	100.00
pH 7	pH 5 (% Free Cu)	41.32	31.01	33.64	38.79	42.01	47.84	57.36	41.44	43.01	49.40	45.64	38.03
10 % Cu	pH 3 (% Free Cu)	85.76	84.09	89.03	90.52	78.45	84.39	95.05	100.00	100.00	58.82	100.00	71.24
pH 7	pH 5 (% Free Cu)	40.34	20.35	23.02	34.37	25.21	33.56	32.19	36.41	44.79	26.88	30.00	22.99
15 % Cu	pH 3 (% Free Cu)	100.00	100.00	100.00	100.00	100.00	100.00	86.98	84.69	81.19	76.28	90.33	85.42
pH 7	pH 5 (% Free Cu)	65.29	58.57	50.29	58.18	78.36	76.98	51.11	50.01	51.63	50.97	55.00	42.15

* B+A aa= Basic and Acidic amino acids, P+N aa= Polar and Neutral amino acids, B+P aa = Basic and Polar amino acids

Table 3.30 continued:

		Ranked by highest level of combined basic and neutral											
		1	**6**	**3**	**10**	**9**	**12**	**4**	**8**	**5**	**7**	**2**	**11**
	%B+N aa	**69.49**	**63.54**	**63.52**	**63.06**	**62.25**	**62.02**	**61.88**	**61.19**	**59.16**	**57.90**	**57.70**	**57.42**
7.5 % Cu	pH 3 (% Free Cu)	100.00	100.00	100.00	100.00	100.00	100.00	100.00	100.00	100.00	100.00	100.00	100.00
pH 7	pH 5 (% Free Cu)	43.01	33.64	31.01	42.01	57.36	41.32	49.40	45.64	38.79	41.44	38.03	47.84
10 % Cu	pH 3 (% Free Cu)	100.00	89.03	84.09	78.45	95.05	85.76	58.82	100.00	90.52	100.00	71.24	84.39
pH unadj	pH 5 (% Free Cu)	44.79	23.02	20.35	25.21	32.19	40.34	26.88	30.00	34.37	36.41	22.99	33.56
15 % Cu	pH 3 (% Free Cu)	81.19	100.00	100.00	100.00	86.98	100.00	76.28	90.33	100.00	84.69	85.42	100.00
pH unadj	pH 5 (% Free Cu)	51.63	50.29	58.57	78.36	51.11	65.29	50.97	55.00	58.18	50.01	42.15	76.98
		Ranked by highest level of combined acidic and neutral											
		1	**2**	**8**	**4**	**7**	**9**	**11**	**10**	**5**	**6**	**3**	**12**
	%A+N aa	**78.28**	**72.15**	**66.47**	**65.91**	**65.09**	**65.08**	**65.05**	**63.36**	**60.12**	**58.98**	**56.64**	**56.28**
7.5 % Cu	pH 3 (% Free Cu)	100.00	100.00	100.00	100.00	100.00	100.00	100.00	100.00	100.00	100.00	100.00	100.00
pH unadj	pH 5 (% Free Cu)	43.01	38.03	45.64	49.40	41.44	57.36	47.84	42.01	38.79	33.64	31.01	41.32
10 % Cu	pH 3 (% Free Cu)	100.00	71.24	100.00	58.82	100.00	95.05	84.39	78.45	90.52	89.03	84.09	85.76
pH unadj	pH 5 (% Free Cu)	44.79	22.99	30.00	26.88	36.41	32.19	33.56	25.21	34.37	23.02	20.35	40.34
15 % Cu	pH 3 (% Free Cu)	81.19	85.42	90.33	76.28	84.69	86.98	100.00	100.00	100.00	100.00	100.00	100.00
pH unadj	pH 5 (% Free Cu)	51.63	42.15	55.00	50.97	50.01	51.11	76.98	78.36	58.18	50.29	58.57	65.29
		Ranked by highest level of combined acidic and polar											
		1	**11**	**2**	**7**	**5**	**8**	**4**	**12**	**9**	**10**	**6**	**3**
	%A+P aa	**43.41**	**42.62**	**42.36**	**42.04**	**40.79**	**38.86**	**38.08**	**38.04**	**37.78**	**36.96**	**36.46**	**36.45**
7.5 % Cu	pH 3 (% Free Cu)	100.00	100.00	100.00	100.00	100.00	100.00	100.00	100.00	100.00	100.00	100.00	100.00
pH unadj	pH 5 (% Free Cu)	43.01	47.84	38.03	41.44	38.79	45.64	49.40	41.32	57.36	42.01	33.64	31.01
10 % Cu	pH 3 (% Free Cu)	100.00	84.39	71.24	100.00	90.52	100.00	58.82	85.76	95.05	78.45	89.03	84.09
pH unadj	pH 5 (% Free Cu)	44.79	33.56	22.99	36.41	34.37	30.00	26.88	40.34	32.19	25.21	23.02	20.35
15 % Cu	pH 3 (% Free Cu)	81.19	100.00	85.42	84.69	100.00	90.33	76.28	100.00	86.98	100.00	100.00	100.00
pH unadj	pH 5 (% Free Cu)	51.63	76.98	42.15	50.01	58.18	55.00	50.97	65.29	51.11	78.36	50.29	58.57

* B+N aa= Basic and Neutral amino acids, A+N aa= Acidic and Neutral amino acids, A+P aa = Acidic and Polar amino acids

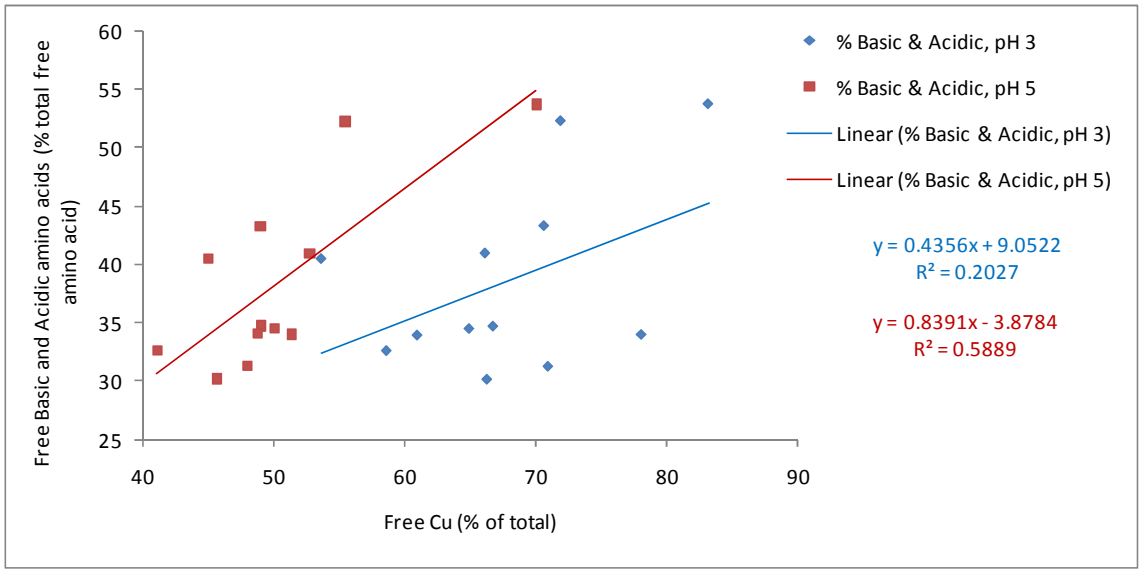

Figure 3.115 Correlation between free copper (at pH 3 and pH 5) and total free basic and acidic amino acids

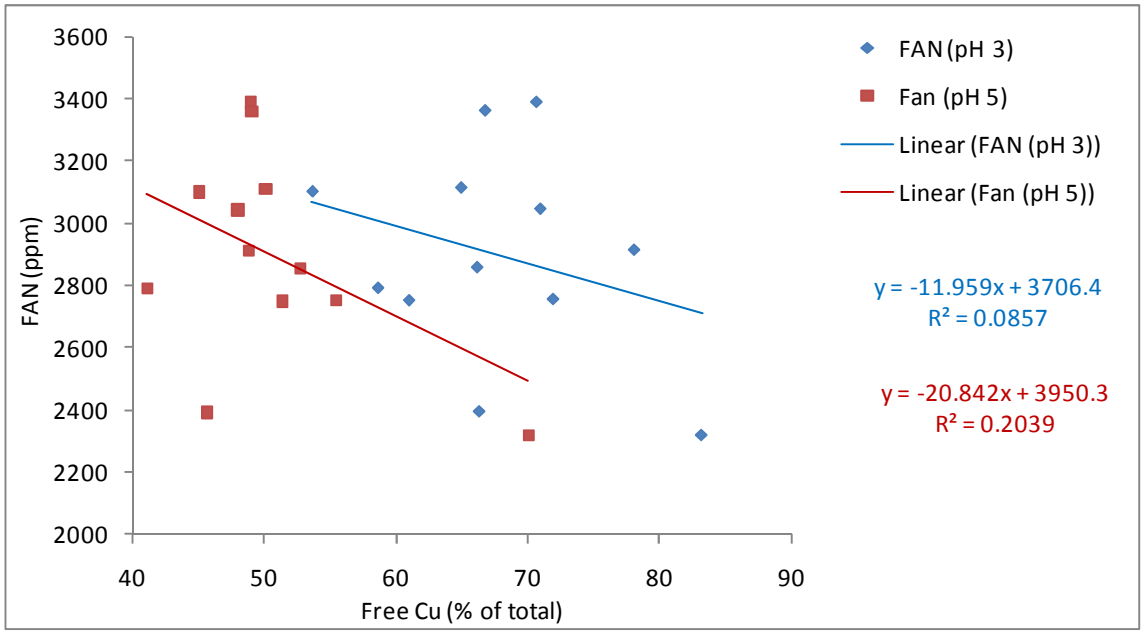

Figure 3.116 Correlation between FAN and free copper at pH 3 and pH 5

From the results obtained, it appeared that there was no clear correlation between the percentage free Cu, FAN release and free amino acid profiles (Figures 3.115, 3.116 and Tables 3.27 – 3.30). This was indicative of stability and binding being due to

peptide interaction and more significantly, amino acid configuration within the peptides as opposed to the individual amino acids.

As discussed earlier (Section 3.6.5) certain individual amino acids such as histidine have a greater affinity for Cu(II) ions than others and can contribute to metal binding. In this study however, successful chelate formation appeared not to be dependent on the presence of individual amino acids (Tables 3.27, 3.28 and Figure 3.114) but more on the sequence of amino acids in peptides present in the hydrolysate. Amino acid configuration in a peptide can significantly influence how the ligand and metal interact and consequently affect the overall stability of the chelate. Table 3.31 contains the stability constant values for a selection of tripeptides complexed with Cu(II) under the same physiological conditions.

Table 3.31 ML stability constant values for a selection of tripeptides

Tripeptides	$\log\beta_{ML}$*
Gly-Gly-Gly	5.13
Gly-Gly-His	7.55
Gly-His-Gly	9.25
Gly-His-Lys	16.44
Gly-Gly-Tyr	10.01

* Values sourced from NIST database

On examination of Table 3.31, it is clear that the sequence and position of amino acids in the peptide greatly affects the stability of a chelate. The inclusion of histidine unsurprisingly enhances the stability of the tripeptide. Additionally, the position of histidine in the sequence also affects the stability constant of the chelate. Comparing the values obtained for Gly-Gly-Gly and Gly-Gly-His, it is clear that the addition of histidine into the sequence at position 3 markedly enhances the stability constant ($\log\beta_{ML}$ =5.13 for GGG and $\log\beta_{ML}$ = 7.55 for GGH). Inclusion of histidine in position 2

of the amino acid sequence increases the stability constant even further ($\log\beta_{ML} = 9.25$). Sections 3.6.5.1 and 3.6.5.3 assessed the effect of positional substitution of histidine in the tri-peptide sequence and factors such as folding and structural rearrangements (*e.g.* the formation of fused rings) can contribute to enhanced stability. Applying this knowledge to the marker peptides identified during the course of this work further strengthens the theory of the importance of the configuration of amino acids in a peptide sequence. As previously discussed in detail (Section 3.6.5), the highest [ML] stability value obtained was for the 1300 Da peptide ($\log\beta_{11} = 6.63$) comprised of the sequence: RHKNKNPFLF. The lowest [ML] stability value was found in the 1181 Da peptide ($\log\beta_{11} = 4.18$) consisting of the sequence: FKNQYGRIR. The absence of histidine and proline residues in the 1181 Da peptide which were identified in the 1300 Da peptide appeared to have a considerable affect in addition to the peptide configuration itself. Histidine in position two of the peptide sequence of the 1300 Da peptide may have contributed to increased stability as previously discussed and it can be concluded that the configuration of the amino acids in the peptide sequence is of extreme importance.

Another factor which can influence the binding of Cu(II) to unstructured peptides is pH. In aqueous solution, H^+ ions compete for the basic coordinating groups that form a metal binding site and thus the pK_a of the coordinating groups and the pH of the solution are both determinants of the stability of a metal complex. Furthermore, the choice of enzyme is important with respect to obtaining a hydrolysate consisting of small molecular mass peptides. All enzymatic hydrolysates chosen for this work appeared to produce ligands capable of binding metal ions and little correlation was observed between free Cu, FAN release and free amino acid profiles. Interestingly, although no clear correlation was observed, analysis of FAN values indicated the enzyme cocktail produced the highest FAN release (Figure 3.91) which may merit further analysis into the use of enzyme cocktails. Based on the fact that a multi-enzyme cocktail will have multiple cleavage recognition sites due to the combinations of enzymes contained in the cocktail (e.g. serine proteases, cysteine proteases, aspartate proteases and metalloproteases etc.), the potential for a more effective hydrolysis is increased, resulting in enhanced production of short chain peptides suitable for metal binding. Table 3.19 examined the free amino acid profiles of 12 soy based enzymatic

hydrolyses and, due to the variation in cleavage patterns and recognition sites, a wide variation in the level of individual free amino acids was observed. Other factors such as properties of the ligand itself, metal:ligand concentrations and ionic strength also play a role in the stability of a chelate. Applying the knowledge gained to products in the marketplace allowed information to be obtained regarding the quality of the proteinates available.

3.6.6.3 Potentiometric titrations of metal proteinate test samples.

All of the techniques previously described in this work were applied to a selection of proteinate test samples commercially available in the marketplace. Analysis of a range of these metal proteinate test samples, manufactured under different conditions, was carried out to determine their stability over a wide pH range (Figures 3.117 and 3.118). As before, the lyophilised samples were reconstituted and separated into their respective supernatants and pellets prior to titration of the supernatants. Figure 3.117 illustrates the percentage free copper detected for all test proteinate samples over a pH range of 3 to 8. Figure 3.118 displays the actual free copper detected (mM), enabling clearer comparative analysis based on the actual copper content of each of the proteinate supernatants. Observations during the course of the titrations of the soluble fractions found the majority of the samples precipitated above pH 5.5. This can be seen from the kink in the curves for these proteinates which appears to represent an end-point (Figure 3.117). In the case of samples 2, 4 and 6 however, no precipitate was observed at any point over the course of the titrations from pH 3 - pH 8.

Flame AAS was employed to confirm the metal content of the unpartitioned proteinates and found all to contain approximately 10 % (w/w) Cu (data not shown). Further analysis of the proteinates confirmed the pH of three of these proteinates had been increased (samples 2, 4 and 6) and results similar to those previously obtained using Flame AAS for the pH 7 adjusted proteinates indicated the majority of copper was contained in the pellet of these three samples (data not shown). This explained the absence of the precipitate in these samples over the course of the potentiometric

titrations and the increased pH during production would have increased chelation potential and contribute to their increased stability.

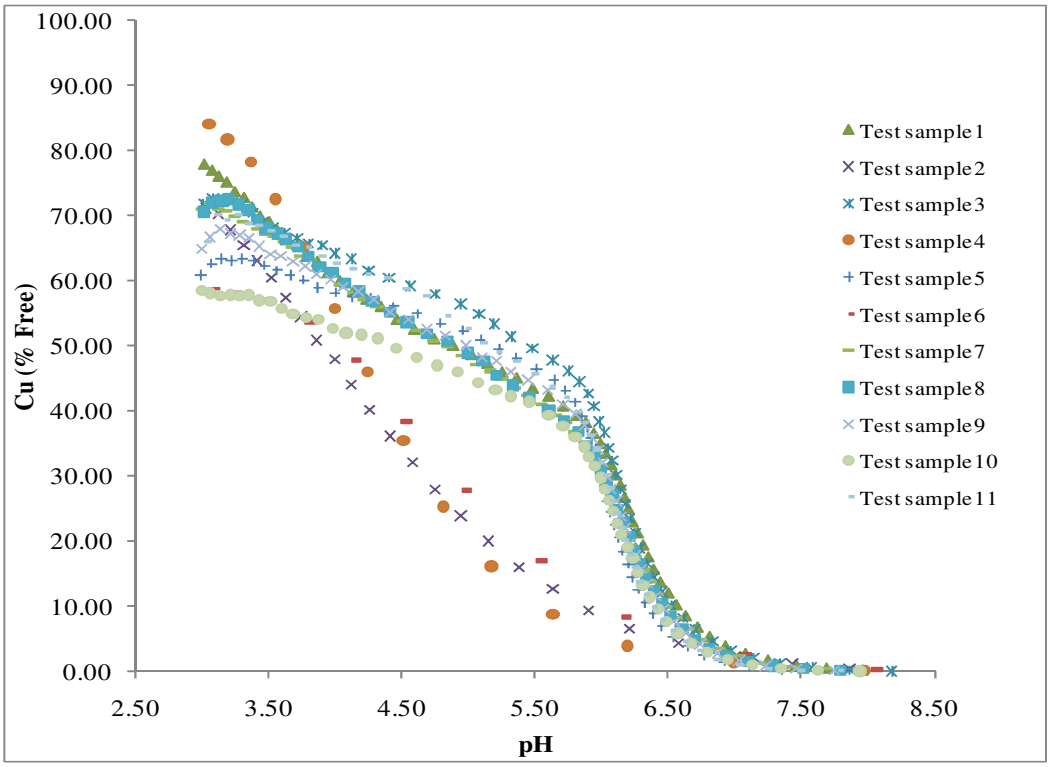

Figure 3.117 ISE titrations of a selection of commercial copper proteinate test samples titrated over a pH range of 3-8. Samples provided by Dr. R. Murphy, Alltech Bioscience Centre, Dunboyne, Co. Meath, Ireland

All commercial samples tested were manufactured using differing hydrolysis procedures and enzymes which contributed to the difference in initial free copper detected at the start of the potentiometric titrations. Figure 3.118 displays the actual free copper detected in mM which clearly shows the differences between the three samples which were pH adjusted. Very little free copper was detected in the soluble fraction of these samples.

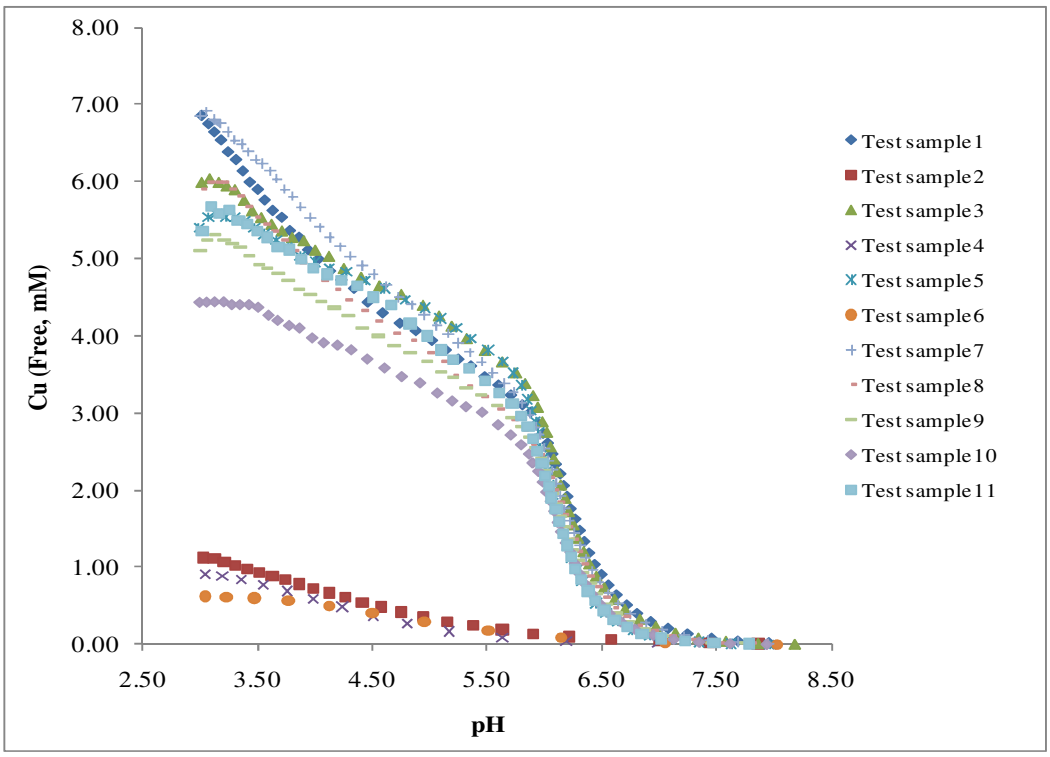

Figure 3.118 ISE titrations of a selection of commercial copper proteinate test samples titrated over a pH range of 3-8. Samples provided by Dr. R. Murphy, Alltech Bioscience Centre, Dunboyne, Co. Meath, Ireland

In addition to the results obtained from potentiometry, SELDI-ToF-MS was used to assess the samples further. Clear differences were observed in the peptide profiles of the various commercial test samples providing further evidence that the hydrolysis procedures and enzymes used varied greatly between manufacturers (Figure 3.119). Additionally, many of the test proteinates analysed did not appear to contain metal-peptide adducts. Of further concern was the fact that a number of the test proteinates assessed appeared to have significant high molecular mass proteins and few low molecular mass peptides. This raises questions regarding the effectiveness of the hydrolysis procedure selected for the production of these commercial proteinates in addition to their chelation ability. FTIR spectra provided further evidence of significant differences between products (data not shown) and band shifts indicative of groups involved in chelation were noticeably absent in some cases.

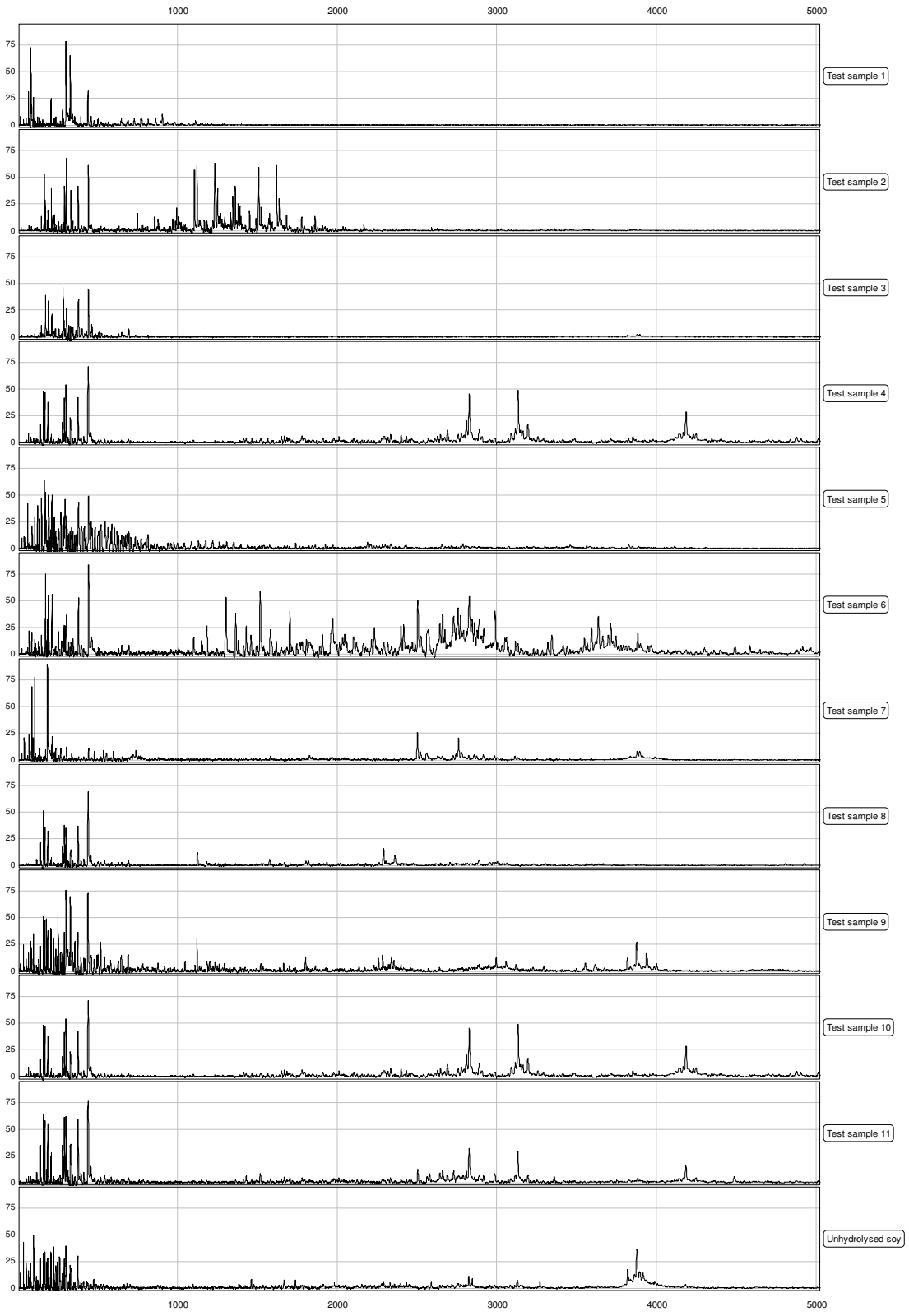

Figure 3.119 SELDI-ToF-MS analysis of a selection of Cu proteinate test samples

The effect of pH adjustment during the course of proteinate production appears to have an effect on the overall stability of the complexes. Previous work on the overall stability constants for humic acids with divalent metals concluded successive and overall stability constants increased as pH increased (Takamatsu *et al.*, 1978). The authors suggested three possible explanations for this. Firstly, it was proposed that the charge densities of the functional groups bound to metal cations would increase with increased acid dissociation constants of functional groups adjacent to the metal-ion-bound sites. A second reason related to the fact that in the higher pH region, metal cations would be bound selectively to the functional groups, forming the strongest complexes among those whose binding capacities are heterogeneous. It was noted that in the lower pH region such functional groups may have been partly occupied with hydrogen ions. Thirdly, the authors suggested steric stabilisations would occur due to the formation of chelate rings. The necessity to neutralise protons liberated on coordination of the metal ion during metal proteinate formation has been discussed previously (Sections 3.1 and 3.2) and, based on the potentiometric and mass spectrometric results over the course of this work, it is clear that pH adjustments during metal proteinate formation can contribute to improving the chelation potential of the products.

Examination of the data obtained from potentiometric and spectrometric analysis (Figures 3.117 – 3.119) confirms that large variation exists between metal proteinates currently on the market. The efficiency of the hydrolysis procedure and the choice of enzyme are only two of the many factors that can affect the quality of the final product. Additional differences in manufacturing methods relating to pH, temperature and the duration of the hydrolysis can also contribute to the variation in the quality of the products. The metal content of the proteinates also varies considerably between manufacturers. Previous FAAS analysis on such proteinates over a number of years identified deviations of up to 30 % above or below the stated metal content in some cases (data not shown). Many *in vivo* trials have been carried out examining whether the organic forms of metal supplements are in fact superior to inorganic forms. In the majority of cases, the organic forms have shown increased metal status in the animal, thereby confirming the benefits of this form of supplementation. However, some

published data has shown little or no advantage to using organic forms. The effectiveness of the proteinate used in such trials may certainly play a role as not all proteinates are of equal quality. This was clearly demonstrated from the analysis of metal proteinates carried out in this work and it is clear that variation exists between the organic forms of the metal proteinates and not all may be equally bioavailable. The needs of the individual animal would also influence absorption and differences in bioavailability of metal sources may not be evident until a deficiency exists. It is imperative that methods of effective metal proteinate characterisation exist which can differentiate products on the market in addition to identifying which of these products may be effective nutritional supplements. There is no single technique to comprehensively characterise metal proteinates and provide the required information regarding chelation and stability. Instead, it is necessary to combine a range of analytical methods to obtain a complete evaluation of the samples. Clearly the techniques employed in this work can provide substantial information relating to the metal proteinates, their stability and whether they are actual chelates or simply metal-peptide complexes. Furthermore, individual peptide profiles can be obtained allowing identification of particular proteinates enhancing traceability, quality control is achievable using a variety of methods and consequently, confidence in a particular product can be achieved.

4. Conclusion

It used to be a common assumption that the nutritional value of a trace element depended largely on the total concentration of the nutrients as measured by analytical methods. However, recent research in chemical speciation of trace elements in biological systems has shown that it is the form in which the trace element occurs that influences its bioavailability and not the total concentration (Cao *et al*., 2002; Spears, 2003; Veum *et al*., 2004; Li *et al*., 2005; Ao *et al*., 2006; Nollet *et al*., 2007; Lamb *et al*., 2008; Leeson *et al*., 2008).

One of the initial aims of the work was to identify a suitable protein source from which metal proteinates could be produced. Using a range of analytical techniques such as carbon, hydrogen and nitrogen analysis and free α-amino nitrogen analysis, a comprehensive assessment of potential protein sources was achieved. Based on the results obtained, and an examination of the costs associated with the respective protein sources, soy flour was chosen for the production of metal proteinates.

Once the protein source had been selected, steps were taken to ensure optimum hydrolysis conditions were in place. Assessment of the enzymatic hydrolysis procedure in terms of pH, temperature and enzyme concentration using FAN release as an indication of hydrolysis potential provided a means to select hydrolysis conditions providing highest FAN release on a cost-benefit basis and increase chelation potential. Optimum conditions for a serine protease initially selected for the hydrolysis procedure were found to be pH 7, 55 °C and an enzyme concentration of 0.33 % (v/v).

The effectiveness of the hydrolysis procedure was also examined using Surface-Enhanced Laser Desorption/Ionisation Time-of-Flight Mass Spectrometry (SELDI-ToF-MS) as a complimentary method to FAN as the size and distribution of peptides present in the metal chelates could be identified. The advantage of having two very different methods of analysis added strength to the resultant data.

Both essential and non-essential elements can be toxic at high levels and there is a fine line between essentiality and toxicity in some cases. Therefore, it is imperative that a reliable technique is in place that can conclusively determine the metal content in the proteinates formed. Additionally, concentrations of metal proteinates in feedstuffs

are strictly regulated and it is necessary to have a method in place which can accurately determine the total metal content to satisfy regulatory requirements. Flame Atomic Absorption Spectrometry met these requirements and was used to confirm the metal content of the proteinates throughout this work.

One of the primary aims of this work was to develop methods which enabled qualitative and quantitative analysis of metal proteinates in the marketplace. Assessment of a variety of analytical techniques, in addition to development of protocols suitable for metal proteinate analysis, provided a wide range of data that, when combined, provided a means to characterise the metal proteinates. Flame Atomic Absorption Spectrometry (FAAS) accurately determined the metal content in the proteinates and also satisfied quality control requirements to determine metal content consistency between batches. Peptide profiling based on molecular mass was achieved using Surface-Enhanced Laser Desorption/Ionisation Time-of-Flight Mass Spectrometry (SELDI-ToF-MS). Prior to SELDI-ToF-MS analysis it was necessary to select the most suitable array surface for metal proteinate analysis. Immobilised Metal Affinity Capture (IMAC 30) arrays were chosen after analysing a wide range of surface arrays as they provided the highest intensity peptide peaks. Array binding and washing protocols were optimised and SELDI-ToF-MS parameters such as laser intensity and sensitivity were examined to determine the settings which provided the clearest spectral results. This enabled characterisation of the metal proteinates and provided an additional means of comparing and contrasting proteinates based on their respective peptide profiles. This technique also provided an additional means of quality control by demonstrating consistency (or lack of) in peptide profiles between proteinate batches. From the results obtained, the consistency in peptide profiles was excellent. Furthermore, the presence of peptide-metal adducts which may have been indicative of chelation were detected in most of the proteinates analysed. Treatment with a sequestering agent such as EDTA removed or significantly reduced the metal adduct. This indicated the metal had bound to the peptide, complexation had occurred, and that a stronger chelating agent with a greater metal affinity could remove the metal adduct. Extensive analysis of a wide range of proteinates indicated significant differences in the peptide profiles of the products between manufacturers. It could be concluded that not all proteinates available in the

marketplace are equally effective as nutritional supplements based on the spectral data which indicated poor hydrolysis or the absence of metal adducts in some products. A further and extremely important extension of this technique was the ability to detect metal proteinates in premixes based on the mass spectrometric profiles characteristic of each of the metal proteinates generated. The ability to identify a particular product whether by simply comparing proteinate products or in more complex environments such as in premixes or in feed is of immense value. It can confirm a particular product is in a certain batch, whether the product has been replaced by a cheaper version in a premix or even if the product is present at all. Difficulties were encountered in relation to identification of the proteinates in feed due to the low proteinate inclusion levels but SELDI-ToF-MS analysis of premix samples was a success and clearly identified the proteinates in the premix batches. This approach was shown to significantly improve traceability which is a distinct advantage from an industrial perspective.

Fourier Transform Infrared Spectroscopy (FTIR) aided in demonstrating chelation in metal proteinates and was employed as a complimentary technique to the other methods of assessment. Band shifts relating to functional groups potentially involved in metal chelation were observed and comparing the proteinates with control soy and copper samples demonstrated significant spectral differences. Furthermore, batch-to-batch consistency could also be demonstrated and provided an additional technique for quality control with SELDI-ToF-MS.

The techniques outlined in this work were found to successfully compare and contrast proteinate samples and demonstrated their suitability for used as quality control methods in addition to meeting manufacturer and regulatory specifications.

Speciation modelling and measurement can help in formulating supplements of higher bioavailabilities by assessing the strength of metal-ligand interactions. These models can be used as a convenient and cost effective tool in evaluating metal supplement bioavailabilities and results obtained in this work identified stability constants for a range of metal-ligand complexes in addition to confirming the presence of multi metal-ligand species. In this study, computer simulation using WinCOMICS was used effectively to model the speciation of Cu(II) with a variety of ligands from a selection of protein sources. As with most modelling techniques, it was also important to

validate such models by experimental means. Potentiometry with the use of an ion-selective electrode (ISE) was employed for metal-ligand titrations and the Hyperquad program proved effective for analysing the resultant data. Techniques previously used for proteinate characterisation such as SELDI-ToF-MS and FTIR provided additional complimentary data regarding complexation.

WinCOMICS demonstrated the distribution of metal species present at given concentrations of metal and ligand was found to depend on the pH of the solution and resultant data from potentiometric titrations confirmed this was indeed the case. Furthermore, Cu^{2+} ions had different stability constants with a range of ligands and thus the percentage of copper present as a particular species depended not only on the pH of the solution, but also on the stability constant of the complex. Initial experiments using ligands such as amino acids and short chain peptides with known stability constants allowed for comparison of the experimental data with published values. The methods and techniques employed (WinCOMICS speciation, pK_a determination, ISE titrations and Hyperquad calculations) were used to generate stability constants that were similar to published values for these ligands and aided in validating the method for use with ligands of interest in metal proteinates.

The ligands of interest in the metal proteinates assessed were identified using SELDI-ToF-MS and included the 1148 Da, 1181 Da, 1300 Da and 1514 Da peptides. Tandem mass spectrometry (MS/MS) provided sequences for the peptides of interest and synthetic peptides based on the sequences provided were subsequently produced. The marker peptides were consistently present in the metal proteinates and were recovered from premix samples using SELDI-ToF-MS. Consistent identification was advantageous from a quality control perspective and their mass spectrometry profiles confirmed the presence of metal adducts in most cases. Stability constant data for these marker peptides was obtained and a range of metal-ligand species was identified. Employment of techniques such as FTIR and SELDI-ToF-MS provided complimentary data regarding the species identified from the potentiometric titrations and resultant Hyperquad analysis. FTIR band shifts were indicative of chelation and SELDI-ToF-MS data confirmed the presence of peptide peaks with molecular masses that corresponded to the masses of the species identified in Hyperquad including dimer/trimer formation.

The effect of enzymatic hydrolysis on peptide profiles was also investigated. From initial SELDI-ToF-MS profiling it was confirmed that a consistent hydrolysate could be produced with the same enzyme under the same conditions. However, due to the fact that not all proteinate manufacturers use the same conditions, it was necessary to examine the effect of hydrolysates produced from many different enzymes on FAN release, peptide profiles, complexation and stability. The nature of this approach, along with the use of these powerful techniques, demonstrated it was possible to discriminate between enzymatic hydrolyses. FAN release illustrated significant differences between the resultant hydrolysates. Potentiometry confirmed notable differences in relation to metal binding between the proteinates formed from the various hydrolysates and stability over a wide pH range varied considerably between samples.

The techniques developed as part of this project were applied to products from different suppliers and enabled comparative analysis. SELDI-ToF-MS profiles illustrated marked differences between the proteinates and the absence of low molecular mass peptides in the case of some samples was indicative of a poor hydrolysis procedure. This would have implications regarding chelation as low molecular mass peptides and amino acids are required for optimum chelation potential. Potentiometry confirmed substantial differences in metal complexation over a pH range of 3 to 8 and it can be concluded that a number of commercially available proteinates appear to be inferior products.

The original aims of this thesis were largely achieved and commercially available instruments have provided a means to characterise metal proteinates. Methods outlined in this work can aid product development and nutritionally superior supplements can be produced. Furthermore, quality control methods have been outlined which are important from an industrial perspective and regulatory requirements can be satisfied. Another important achievement has been the ability to compare and contrast commercially available proteinates. The work on sequencing and stability has provided a wealth of information including the importance of amino acid configuration in the peptide chain and identification of multi metal-ligand species previously unseen.

Bibliography

AAFCO. (2000) Official Publication. Oxford, IN.

AAFCO. (2005). Official publication. Association of American Feed Control Officials: 307-308.

Abernathy, D. G., Spedding, G. and Starcher, B. (2009). Analysis of Protein and Total Usable Nitrogen in Beer and Wine Using a Microwell Ninhydrin Assay. *Journal of the Institute of Brewing*. **115**: (2) 122-127.

Aiba, H., Yokoyama, A. and Tanaka, H. (1974). Copper(II) Complexes of Glycyl-L-histidine, Glycyl-L-histidylglycine, and Glycylglycyl-L-histidine in Aqueous Solution. *Bulletin of the Chemical Society of Japan*. **47**: (6) 1437-1441.

Albrethsen, J., Bogebo, R., Olsen, J., Raskov, H. and Gammeltoft, S. (2006). Preanalytical and analytical variation of surface-enhanced laser desorption-ionization time-of-flight mass spectrometry of human serum. *Clinical Chemistry and Laboratory Medicine*. **44**: (10) 1243-1252.

Ammerman, C. B., Baker, D. H., Lewis, A. J., Clarence, B. A., David, H. B. and Austin, J. L. (1995). Bioavailability of Nutrients for Animals: *Amino acids, Minerals and Vitamins.* In Bioavailability of Nutrients for Animals, Academic Press, San Diego.

Anderegg, G., Arnaud-Neu, F., Rita Delgado, Judith Felcman and Popov, K. (2005). Critical Evaluation of Stability Constants Of Metal Complexes of Complexones for Biomedical and Environmental Applications. *Pure Appl. Chem.* **77**: (8) 1445-1495.

Angelici, R. J., Girolami, G. S. and Rauchfuss, T. B. (1999). Synthesis and technique in inorganic chemistry : a laboratory manual. University Science Books, Sausalito, Calif.

Ao, T., Pierce, J. L., Power, R., K.A. Dawson, A.J. Pescatore, and, A. H. C. and Ford, M. J. (2006). Evaluation of Bioplex Zn® as an Organic Zinc Source for Chicks *International Journal of Poultry Science*. **5**: (9) 808-811.

Ashmead, H. H. (1980a). Oil cooked foods containing metal proteinates. **4201793**: (05/743456) United States

Ashmead, H. H. (1980b). Soluble non-ferrous metal proteinates. **4216143**: United States

Ashmead, H. H., Ashmead, D. H. and Graff, D. J. (1989). Amino acid chelated compositions for delivery to specific biological tissue sites. **826786**: United States

Association of Official Analytical Chemists. (1990). p. 735

Bailey, P. D. (1990). An introduction to peptide chemistry. Wiley . SalleSauerländer, Chichester (England) and New York : Aarau (Switzerland)

Baker. D.H., Odle, J., Funk, M. A. and Wieland, T. M. (1991). Research note: bioavailability of copper in cupric oxide, cuprous oxide, and in a copper-lysine complex. *Poult Sci.* **70**: (1) 177-179.

Barth, A. (2007). Infrared spectroscopy of proteins. *Biochimica et Biophysica Acta (BBA) - Bioenergetics*. **1767**: (9) 1073-1101.

Beck, M. T. (1977). Critical evaluation of equilibrium constants in solution. Stability constants of metal complexes. *Pure Appl. Chem.* **49**: (1) 127-136.

Bittencourt, A. L., Fernandes, I., Pereira, I. R. O., Honmoto, C. S., Tanaka, M. K., Lima, F. S. P. and Abdalla, D. S. P. (2005). Detection of 7S and 11S soy protein fractions by monoclonal antibody-based immunoassays in food. *Food and Agricultural Immunology*. **16**: (2) 91 - 100.

Bjerrum, N. (1908). Ph.D Dissertation, Copenhagen

Blackstock, W.P. and Weir M.P. (1999). Proteomics: Quantitative and physical mapping of cellular proteins, *Trends in Biotechnology*. **17:** (3) 121-127

Boot, R. G., Verhoek, M., de Fost, M., Hollak, C. E. M., Maas, M., Bleijlevens, B., van Breemen, M. J., van Meurs, M., Boven, L. A., Laman, J. D., Moran, M. T., Cox, T. M. and Aerts, J. M. F. G. (2004). Marked elevation of the chemokine CCL18/PARC in Gaucher disease: a novel surrogate marker for assessing therapeutic intervention. *Blood*. **103**: (1) 33-39.

Borsook, H. and Thimann, K. V. (1932). The Cupric Complexes of Glycine and of Alanine. *The Journal of Biological Chemistry*. **98**: (2) 671-705.

Brønsted, J.N. (1922). Z. Phys. Chem. **102:** 169-207

Broomhead, J. A., McKenzie, H. A. and Mellor, D. P. (1961). Complexes of copper(II) with pyrrolidine. *Australian Journal of Chemistry*. **14**: (4) 649-655.

Bruni, S., Cariati, F., Daniele, P. G. and Prenesti, E. (2000). Speciation and structure of copper(II) complexes with histidine-containing peptides in aqueous medium: a combined potentiometric and spectroscopic study. *Spectrochimica Acta Part A: Molecular and Biomolecular Spectroscopy*. **56**: (4) 815-827.

Buffle, J., Greter, F. L. and Haerdi, W. (2002). Measurement of complexation properties of humic and fulvic acids in natural waters with lead and copper ion-selective electrodes. *Analytical Chemistry*. **49**: (2) 216-222.

Bull, R., C. (1999). Trace Minerals and Immunology. In Beef Cattle Handbook. pp. 1-5

Burlingame, A. L., Boyd, R. K. and Gaskell, S. J. (1996). Mass Spectrometry. *Analytical Chemistry*. **68**: (12) 599-652.

Cabaniss, S. E., Leenheer, J. A. and McVey, I. F. (1998). Aqueous infrared carboxylate absorbances: aliphatic di-acids. *Spectrochimica Acta Part A: Molecular and Biomolecular Spectroscopy*. **54**: (3) 449-458.

Çakir, S., Biçer, E. and Eleman, A. (2001). Synthesis, spectroscopic and voltammetric studies of mixed-ligand copper(II) complexes of amino acids. *Transition Metal Chemistry*. **26**: (1) 89-95.

Cao, J., Henry, P. R., Davis, S. R., Cousins, R. J., Miles, R. D., Littell, R. C. and Ammerman, C. B. (2002). Relative bioavailability of organic zinc sources based on tissue zinc and metallothionein in chicks fed conventional dietary zinc concentrations. *Animal Feed Science and Technology*. **101**: (1-4) 161-170.

Cao, J., Henry, P. R., Guo, R., Holwerda, R. A., Toth, J. P., Littell, R. C., Miles, R. D. and Ammerman, C. B. (2000). Chemical characteristics and relative bioavailability of supplemental organic zinc sources for poultry and ruminants. *J. Anim. Sci.* **78**: (8) 2039-2054.

Casolaro, M., Chelli, M., Ginanneschi, M., Laschi, F., Muniz-Miranda, M., Papini, A. M. and Sbrana, G. (1999). Spectroscopic and potentiometric study of copper(II) complexes with -histidyl-glycyl--histidyl-glycine in aqueous solution. *Spectrochimica Acta Part A: Molecular and Biomolecular Spectroscopy*. **55**: (7-8) 1675-1689.

Chapman, D., Lloyd, D. R. and Prince, R. H. (1963). An infrared and nuclear magnetic resonance study of the nature of ethylenediaminetetra-acetic acid and some related substances in solution: hydrogen bonding in -amino-polycarboxylic acid systems. *J. Chem. Soc.*: 3645-3658.

Clarke, C. H., Buckley, J. A. and Fung, E. T. (2005). SELDI-ToF-MS proteomics of breast cancer. *Clinical Chemistry & Laboratory Medicine*. **43**: (12) 1314-1320.

Cleland, W. W. (2002). Dithiothreitol, a New Protective Reagent for SH Groups*. *Biochemistry*. **3**: (4) 480-482.

Cohen, J. B. (1924). Practical organic chemistry. Macmillan, London

Connolly, C. D. (2009) Personal communication.

Cottingham, K. (2003). Clinical Proteomics: Are We There Yet? *Analytical Chemistry*. **75**: (21) 472 A - 476 A.

Crichton, R. R. (2008). Biological Inorganic Chemistry - An Introduction. Elsevier

Crowther, J. R. (1995). ELISA: theory and practice. *Methods Mol. Biol.* **42**: 1-218.

D'Angelo, P., Bottari, E., Festa, M. R., Nolting, H. F. and Pavel, N. V. (1998). X-ray Absorption Study of Copper(II) Glycinate Complexes in Aqueous Solution. *The Journal of Physical Chemistry B*. **102**: (17) 3114-3122.

Darewicz, M., Dziuba, J., Petra, W. J. and Caessens, R. (2000). Effect of enzymatic hydrolysis on the emulsifying and foaming properties of milk proteins - a review. *Polish Journal of Food and Nutrition Sciences*. **9/50**: (1) 3-8.

David, N. P., Darryl, J. C. P., David, M. C. and John, S. C. (1999). Probability-based protein identification by searching sequence databases using mass spectrometry data. **20**: (18) 3551-3567.

Davies, C.W. (1962). *Ion association.* London. Butterworths, pp. 37-53.

Debye, P. and Huckel, E. (1923). The theory of electrolytes. 1. Lowering of freezing point and related phenomena. *Physikalische Zeitschrift. **24:** 185-206.*

Dembowski, J. S., Kurtz, D. C. and Nakon, R. (1988). Aminoacidate dechelation upon hydroxo complex formation in mixed ligand metal chelates. *Inorganica Chimica Acta*. **152**: (4) 209-210.

Dijkstra, M., Vonk, R. J. and Jansen, R. C. (2007). SELDI-ToF mass spectra: A view on sources of variation. *Journal of Chromatography B*. **847**: (1) 12-23.

Du, Z., Hemken, R. W., Jackson, J. A. and Trammell, D. S. (1996). Utilisation of copper in copper proteinate, copper lysine and cupric sulfate using the rat as an experimental model. *J. Anim. Sci.* **74**: 1657-1663.

Dunn, G. E. and McDonald, R. S. (1969). Infrared spectra of aqueous sodium benzoates and salicylates in the carboxyl-stretching region: chelation in aqueous sodium salicylates. *Canadian Journal of Chemistry*. **47**: (24) 4577-4588.

E.U. (1970). Council Directive 70/524/EEC concerning additives in feedstuffs.

E.U. (1991). Commission Directive 91/321/EEC of 14 May 1991 on infant formulae and follow-on formulae European Union: 35-49.

E.U. (2003a). Commission Regulation (EC) No 1334/2003 of 25 July 2003 amending the conditions for authorisation of a number of additives in feedingstuffs belonging to the group of trace elements. European Union: 1-5.

E.U. (2003b). Opinion of the Scientific Committee for Animal Nutrition on the use of copper in feedingstuffs. European Union:

EDA. (2005) DG SANCO Consultation on a proposal to recast commission directive 91/321 on infant formulae and follow-on formulae.

Ekblad, L., Baldetorp, B., Ferno, M., Olsson, H. and Bratt, C. (2007). In-Source Decay Causes Artifacts in SELDI-TOF MS Spectra. *Journal of Proteome Research*. **6**: (4) 1609-1614.

Eriks, J. C., Gaisser, H. D., Van Der Goot, H. and Timmerman, H. (1983). Determination of formation constants of copper(II) complexes of Adler medium components with a solid-state copper(II) ionselective electrode. *Pharmacy World & Science*. **5**: (6) 319-324.

Escoda, M. L., de la Torre, F. and Salvadó, V. (1999). The formation of mixed ligand complexes of Fe(III) with phosphoric and citric acids in 0.5 M NaNO3 aqueous solutions. *Polyhedron*. **18**: (25) 3269-3274.

Ewing, W. N. and Charlton, S. J. (2007). The Minerals Directory. Context

Fakhari, A. R., Alaghemand, M. and Shamsipur, M. (2000). Zinc-Selective Membrane Electrode Based On 5, 6, 14, 15-Dibenzo-l, 4-Dioxa-8, 12-Diazacyclopentadecane-5, 14-Diene. *Analytical Letters*. **33**: (11) 2169 - 2181.

Fan, J. (1995). Determination of stability constants of copper(II) complex of glycine in water + alcohol mixed solvents with ion selective electrode technique. *Talanta*. **42**: (3) 317-321.

FAO. (2002) Protein Sources for the Animal Feed Industry. Bangkok.

Farkas, E., Sóvágó, I., Kiss, T. and Gergely, A. (1984). Studies on transition-metal–peptide complexes. Part 9. Copper(II) complexes of tripeptides containing histidine. *J. Chem. Soc., Dalton Trans.*: 611-614.

Fenn, J. B., Mann, M., Meng, C. K., Wong, S. F. and Whitehouse, C. M. (1989). Electrospray Ionization for Mass Spectrometry of Large Biomolecules. *Science*. **246**: (4926) 64-71.

Fiedler-Linnersund, U. and Bhatti, K. M. (1979). Development of polymeric membranes for zinc ion-selective electrodes. *Analytica Chimica Acta*. **111**: 57-70.

Florence, T. M. (1989). Trace Element Speciation in Biological Systems. In Trace Element Speciation: Analytical Methods and Problems, CRC Press, Inc.

Fraker, P.J. (1983). Zinc deficiency: A common immunodeficiency state. *Sur. Immunol. Res*. **2**. 155-175.

Fricker, G., Bruns, C., Munzer, J., Briner, U., Albert, R., Kissel, T. and Vonderscher, J. (1991). Intestinal absorption of the octapeptide sms-201995 visualized by Fluorescence derivatisation. *Gastroenterology*. **100**: 1544-1552.

Fricker, G., Drewe, J., Vonderscher, J., Kissel, T. and Beglinger, C. (1992). Enteral absorption of ocreotide. *British Journal of Pharmacology*. **105**: 783-786.

Gans, P., Sabatini, A. and Vacca, A. (1996). Investigation of equilibria in solution. Determination of equilibrium constants with the HYPERQUAD suite of programs. *Talanta*. **43**: (10) 1739-1753.

Gans, P., Sabatini, A. and Vacca, A., (2008), Hyperquad 2008,

Garcia, A. and Madariaga, J. M. (1984). Applications of computers in the study of solutions equilibria-III Evaluation of some programs for known ionic equilibria. *Computers & Chemistry*. **8**: (3) 193-199.

Gorton, L. and Fiedler, U. (1977). A zinc-sensitive polymeric membrane electrode. *Analytica Chimica Acta*. **90**: 233-236.

Green, M., Husband, J. and Green, L. (2008). Variability in feed components of animal diets: Implications for animal performance and decision-making. In Recent Advances in Animal Nutrition, Nottingham University Press

Guo, R., Henry, P. R., Holwerda, R. A., Cao, J., Littell, R. C., Miles, R. D. and Ammerman, C. B. (2001). Chemical characteristics and relative bioavailability of supplemental organic copper sources for poultry. *J. Anim. Sci.* **79**: (5) 1132-1141.

Gupta, V. K., Al Khayat, M., Minocha, A. K. and Kumar, P. (2005). Zinc(II)-selective sensors based on dibenzo-24-crown-8 in PVC matrix. *Analytica Chimica Acta*. **532**: (2) 153-158.

Gupta, V. K., Jain, A. K., Singh, L. P. and Khurana, U. (1998). Zn^{2+} sensor based on Zn-bis(2,4,4-trimethylpentyl)dithiophosphinicacid complex in PVC matrix. *Electrochimica Acta*. **43**: (14-15) 2047-2052.

Hard, D. L. (2002). Innovative developments in the production and delivery of alternative protein sources. FAO, Protein sources for the animal feed industry, Bangkok.

Hardy, B. (2003). Trace minerals for sows - a new approach. *Pig International*:

Hay, M. B. and Myneni, S. C. B. (2007). Structural environments of carboxyl groups in natural organic molecules from terrestrial systems. Part 1: Infrared spectroscopy. *Geochimica et Cosmochimica Acta*. **71**: (14) 3518-3532.

Hopgood, D. and Angelici, R. J. (2002). Equilibrium and stereochemical studies of the interactions of amino acids and their esters with divalent metal nitrilotriacetate complexes. *Journal of the American Chemical Society*. **90**: (10) 2508-2513.

Hunt, D. F., Yates, J. R., Shabanowitz, J., Winston, S. and Hauer, C. R. (1986). Protein sequencing by tandem mass spectrometry. *Proc. Natl. Acad. Sci.* **83**: (17) 6233-6237.

Hutchens, T. W. and Yip, T.-T. (1993). New desorption strategies for the mass spectrometric analysis of macromolecules. *Rapid Communications in Mass Spectrometry*. **7**: (7) 576-580.

Hynes, M., J., (2005), WinCOMICS, Version 1.20

Hynes, M., J. (2009) Personal communication.

ICH. (1995) Validation of analytical procedures, ICH Topic Q2A. International Conference on Harmonisation (ICH) of Technical Requirements for the Registration of Pharmaceuticals for Human Use,

ICH. (1996) Validation of Analytical Procedures: Methodology; ICH Topic Q2B. International Conference on Harmonisation (ICH) of Technical Requirements for the Registration of Pharmaceuticals for Human Use

Inczédy, J., Lengyel, T. and Ure, A. M. (1997). Compendium of Analytical Nomenclature, Definitive Rules 1997. (Science, B., ed.), International Union of Pure and Applied Chemistry

Irtelli, B., Petrucci, W. A. and Navari-Izzo, F. (2009). Nicotianamine and histidine/proline are, respectively, the most important copper chelators in xylem sap of *Brassica carinata* under conditions of copper deficiency and excess. *Journal of Experimental Botany*. **60**: (1) 269-277.

Irving, H. and Rossotti, H. S. (1953). Methods for computing successive stability constants from experimental formation curves. *J. Chem. Soc.*: 3397-3405.

Jacques, K. and McKenzie, C. (1991). Organic Trace Minerals on the Farm. *Feeds & Feeding*: (40.7)

Jain, A. K., Sondhi, S. M. and Rajvanshi, S. (2002). A PVC Based Hematoporphyrin IX Membrane Potentiometric Sensor for Zinc(II). *Electroanalysis*. **14**: (4) 293-296.

Jain, K. K. (2010). The Handbook of Biomarkers. Humana Press

Jondreville, C. and Revy, P. S. (2003) An update on use of organic minerals in swine nutrition. 1-16, Qubec, Canada.

Jourdain, S. (2004) Clinical Proteomic using SELDI-MS. Ciphergen Biosystems Inc

Karas, M. and Hillenkamp, F. (1988). Laser desorption ionization of proteins with molecular masses exceeding 10,000 daltons. *Analytical Chemistry*. **60**: (20) 2299-2301.

Kessler, J., Morel, I., Dufey, P. A., Gutzwiller, A., Stern, A. and Geyer, H. (2003). Effect of organic zinc sources on peformance, zinc status and carcass, meat and claw quality in fattening bulls. *Livestock Prod. Sci.* **81**: 161-171.

Khanna, S. S. and Stevenson, F. J. (1962). Metallo-organic complexes in soil: 1. Potentiometric titration of some soil organic matter isolates in the presence of transition metals. *Soil Science*. **93**: (5) 298-305.

Kies, C. (1981). Bioavailability: a factor in protein quality. *Journal of Agricultural and Food Chemistry*. **29**: (3) 435-440.

Kincaid, R. L., Blauwiekel, R. M. and Cronrath, J. D. (1986). Supplementation of Copper as Copper Sulfate or Copper Proteinate for Growing Calves Fed Forages Containing Molybdenum. *Journal of Dairy Science*. **69**: (1) 160-163.

Kiss, T., Sovago, I. and Gergely, A. (1991). Critical survey of stability constants of complexes of glycine. *Pure Appl. Chem.* **63**: (4) 597-638.

Koeln, L. L. and Webb, K. E., Jr. (1982). Peptide, erythrocyte and plasma amino acid transport across the gastrointestinal tract and liver of calves. *Fed Proc.* **41**: 948.

Kojima, R. and Kamata, S. (1994). Zinc-Selective Membrane Electrode Using Tetrabutyl Thiuram Disulfide Neutral Carrier. *Analytical Sciences*. **Vol.10**: (No.3) 409-412.

Kozak, K. R., Amneus, M. W., Pusey, S. M., Su, F., Luong, M. N., Luong, S. A., Reddy, S. T. and Farias-Eisner, R. (2003). Identification of biomarkers for ovarian cancer using strong anion-exchange ProteinChips: Potential use in diagnosis and prognosis. *Proc. Natl. Acad. Sci.* **100**: (21) 12343-12348.

Kozlowski, H., Bal, W., Dyba, M. and Kowalik-Jankowska, T. (1999). Specific structure-stability relations in metallopeptides. *Coordination Chemistry Reviews*. **184**: (1) 319-346.

Kozlowski, H., Kowalik-Jankowska, T. and Jezowska-Bojczuk, M. (2005). Chemical and biological aspects of Cu2+ interactions with peptides and aminoglycosides. *Coordination Chemistry Reviews*. **249**: (21-22) 2323-2334.

Kruppa, M., Frank, D., Leffler-Schuster, H. and König, B. (2006). Screening of metal complex-amino acid side chain interactions by potentiometric titration. *Inorganica Chimica Acta*. **359**: (4) 1159-1168.

Lamb, G. C., Brown, D. R., Larson, J. E., Dahlen, C. R., DiLorenzo, N., Arthington, J. D. and DiCostanzo, A. (2008). Effect of organic or inorganic trace mineral supplementation on follicular response, ovulation, and embryo production in superovulated Angus heifers. *Animal Reproduction Science*. **106**: (3-4) 221-231.

Lanigan, K. C. and Pidsosny, K. (2007). Reflectance FTIR spectroscopic analysis of metal complexation to EDTA and EDDS. *Vibrational Spectroscopy*. **45**: (1) 2-9.

Leach, G. A. (2007). Micro ingredients with macro benefits. *Feed Mix*. **13**: (3) 2-3.

Leach, G. A. and Patton, R. S. (1997). Analysis techniques for chelated minerals evaluated. *Feedstuffs*. **69**: (13) 13-15.

Leeson, S. and Caston, L. (2008). Using minimal supplements of trace minerals as a method of reducing trace mineral content of poultry manure. *Animal Feed Science and Technology*. **142**: (3-4) 339-347.

Leggett, D. J. (1977). Machine computation of equilibrium concentrations-some practical considerations. *Talanta*. **24**: (9) 535-542.

Lennon, J. J. and Walsh, K. A. (1997). Direct sequence analysis of proteins by in-source fragmentation during delayed ion extraction. *Protein Sci.* **6**: (11) 2446-2453.

Li, N. C., White, J. M. and Yoest, R. L. (1956). Some Metal Complexes of Glycine and Valine. *Journal of the American Chemical Society*. **78**: (20) 5218-5222.

Li, S. F., Luo, X. G., Lu, L., Crenshaw, T. D., Bu, Y. Q., Liu, B., Kuang, X., Shao, G. Z. and Yu, S. X. (2005). Bioavailability of organic manganese sources in broilers fed high dietary calcium. *Animal Feed Science and Technology*. **123-124**: (Part 2) 703-715.

Lill, J. (2003). Proteomic tools for quantitation by mass spectrometry. *Mass Spectrometry Reviews*. **22**: 182-194.

Macedo-Silva, A., Shimokomaki, M., Vaz, A. J., Yamamoto, Y. Y. and Tenuta-Filho, A. (2001). Textured Soy Protein Quantification in Commercial Hamburger. *Journal of Food Composition and Analysis*. **14**: (5) 469-478.

Marcu, A., Stanila, A., Cozar, O. and David, L. (2008). Structural investigations of some metallic complexes with threonine as ligand. *Journal of Optoelectronics and Advanced Materials*. **10**: (4) 830-833.

Martell, A. E. and Hancock, R. D. (1996). Metal complexes in aqueous solutions. Plenum Press, New York

Martell, A. E. and Motekaitis, R. J. (1988). Determination and use of stability constants. VCH Publishers, New York

Martell, A. E. and Smith, R. M. (1974). Critical Stability Constants. Plenum Press, New York

Martell, A. E., Smith, R. M. and Motekaitis, R. J., (2004), NIST standard reference database 46, Version 8.0

Martin, R. B. and Edsall, J. T. (1960). The Association of Divalent Cations with Acylated Histidine Derivatives1. *Journal of the American Chemical Society*. **82**: (5) 1107-1111.

Matera, A., Brasun, J., Cebrat, M. and Swiatek-Kozlowska, J. (2008). The role of the histidine residue in the coordination abilities of peptides with a multi-histidine sequence towards copper(II) ions. *Polyhedron*. **27**: (6) 1539-1555.

Maurin, M. B., Grant, D. J. W. and Stahl, P. H. (2008). The Physicochemical background: Fundamentals of Ionic Equilibria. In Handbook of pharmaceutical salts: properties, selection and use (Stahl, P. H. and Wermuth, C. G., eds.), Wiley-VCH, Germany.

McDowell, L. R. (2003). Minerals in animal and human nutrition, 2nd. ed. Elsevier Science B.V., Amsterdam

Medina, M. B. (1988). Extraction and quantitation of soy protein in sausages by ELISA. *J. Agric. Food Chem.* **36**: (4) 766-771.

Mertz, W. (1977). Criteria for Adequacy and Safety of Trace Elements in Animal Nutrition. *J. Anim. Sci.* **44**: (3) 469-474.

Metzler, D. E. and Metzler, C. M. (2001). Biochemistry: the chemical reactions of living cells. Harcourt / Academic Press, Burlington, MA.

Murphy, R. M. (2005) Personal communication.

Nagele, M., Bakker, E. and Pretsch, E. (1999). General Description of the Simultaneous Response of Potentiometric Ionophore-Based Sensors to Ions of Different Charge. *Analytical Chemistry*. **71**: (5) 1041-1048.

Nakagawa, G., Wada, H. and Sako, T. (1980). Performances of lead and copper(II) ion-selective electrodes in metal buffer solutions and the determination of the stability constants of lead and copper(II) complexes. *Bulletin of the Chemical Society of Japan*. **53**: (5) 1303-1307.

Nancollas, G. H. and Tomson, M. B. (1982). Guidelines for the determination of stability constants. *Pure Appl. Chem.* **54**: (12) 2675-2692.

Nielsen, F. H., Girand, S. H. and Myron, D. R. (1975). Evidence of a possible requirement for arsenic by the rat. *Fed. Proc.* **34**: 923.

NIHS. (2002) Amino acid analysis. National Institute of Health Sciences (NIHS)

Nollet, L., van der Klis, J. D., Lensing, M. and Spring, P. (2007). The Effect of Replacing Inorganic With Organic Trace Minerals in Broiler Diets on Productive Performance and Mineral Excretion. *J. Appl. Poult. Res.* **16**: (4) 592-597.

O'Dell, B. L. (1983). Bioavailability of essential and toxic trace elements. *Fed Proc.* **42**: (6) 1714-1715.

Oda, Y., Huang, K., Cross, F. R., Cowburn, D. and Chait, B. T. (1999). Accurate quantitation of protein expression and site-specific phosphorylation. *Proc. Natl. Acad. Sci. USA*. **96**: (12) 6591-6596.

Ohzeki, K., Saruhashi, M. and Kambara, T. (1980). Use of the Copper(II) Ion-selective Electrode for the Determination of the Stability Constant of Binuclear Copper(II) Complex with 3,6-Dioxaoctane-1,8-diamine-N,N,N′,N′-tetraacetric Acid. *Bulletin of the Chemical Society of Japan*. **53**: (9) 2548-2551.

Osterberg, R., Sjoberg, B. and Soderquist, R. (1972). Models of Copper-Protein Interaction: The Crystal Structure of (Glycyl-L-histidylglycinato)-copper(II) Sodium Perchlorate Hydrate. *Acta Chemica Scandinavica*. **26**: 4184-4185.

Parks, F. P. and Harmston, K. J. (1994). An assay method from proteinates: Judging organic trace minerals. *Feed Management*. **45**: (10) 35-38.

Patnaik, P. (2002). Handbook of Inorganic Chemicals. McGraw-Hill

Patton, R. S. (1990). *Feedstuffs*. **62**: 14.

Peng, J., Stanley, A. J., Cairns, D., Selby, P. J. and Banks, R. E. (2009). Using the protein chip interface with quadrupole time-of-flight mass spectrometry to directly identify peaks in SELDI profiles - initial evaluation using low molecular weight serum peaks. *Proteomics*. **9**: (2) 492-498.

Pettit, L. D. and Brookes, G. (1977). Why stability constants? J.N. Bradley, R.D. Gillard and R.F. Hudson

Pettit, L. D., Pyburn, S., Wojciech, B., Kozlowski, H. and Bataille, M. (1990). A study of the comparative donor properties to CuII of the terminal amino and imidazole nitrogens in peptides. *J. Chem. Soc., Dalton Trans.*: 3565-3570.

Piperno, A., Mariani, R., Trombini, P. and Girelli, D. (2009). Hepcidin modulation in human diseases: From research to clinic. *World Journal of Gastroenterology*. **15**: (5) 538-551.

Poon, T. C. W. (2007). Opportunities and limitations of SELDI-TOF-MS in biomedical research: practical advices. *Expert Review of Proteomics*. **4**: (1) 51-65.

Predieri, G., Elviri, L., Tegoni, M., Zagnoni, I., Cinti, E., Biagi, G., Ferruzza, S. and Leonardi, G. (2005). Metal chelates of 2-hydroxy-4-methylthiobutanoic acid in animal feeding: Part 2: further characterizations, in vitro and in vivo investigations. *Journal of Inorganic Biochemistry*. **99**: (2) 627-636.

ProFound. The Rockefeller University, http://prowl.rockefeller.edu/

Radcliffe, J. S., Aldridge, B. E. and Saddoris, K. L. (2007) Understanding organic mineral uptake mechanisms: experiments with Bioplex Cu. www.engormix.com

Rao, M. B., Tanksale, A. M., Ghatge, M. S. and Deshpande, V. V. (1998). Molecular and Biotechnological Aspects of Microbial Proteases. *Microbiology and Molecular Biology Reviews*. **62**: (3) 597-635.

Remelli, M., Donatoni, M., Guerrini, R., Janicka, A., Pretegiani, P. and Kozlowski, H. (2005). Copper-ion interaction with the 106-113 domain of the prion protein: a solution-equilibria study on model peptides. *Dalton transactions*: (17) 2876-2885.

Rich, P. R. and Maréchal, A. (2008). Carboxyl group functions in the heme-copper oxidases: Information from mid-IR vibrational spectroscopy. *Biochimica et Biophysica Acta*. **1777**: (7-8) 912-918.

Roat-Malone, R. M. (2007). Bioinorganic Chemistry: A Short Course, 2nd ed. John Wiley & Sons, Inc., New Jersey

Rompala, R. E. and Halley, J. T. (1995). Explaining the absorption of chelated trace minerals: The Trojan horse of nutrition. *Feed Management*. **46**: (4) 52-58.

Rossi, L., Moharram, R., Martin, B. M., White, R. L. and Panelli, M. C. (2006). Detection of human MCP-4/CCL13 isoforms by SELDI immunoaffinity capture. *J Transl Med.* **4**:

Rundle, C. C. (2005) A Beginners Guide to Ion-Selective Electrode Measurements. London.

Ryan, J. P., Kearns, P. and Quinn, T. (2002). Bioavailability of dietary copper and zinc in adult Texel sheep: A comparative study of the effects of sulfate and Bioplex supplementation. *Irish Veterinary Journal*. **55**: (5) 221-224.

Sabatini, A., Vacca, A. and Gans, P. (1992). Mathematical algorithms and computer programs for the determination of equilibrium constants from potentiometric and spectrophotometric measurements. *Coordination Chemistry Reviews*. **120**: 389-405.

Saha, S. K., Choudhury, R. N. and Chakravarti, S. K. (1985). Multiple equilibrium in humic acid-metal system: Determination of successive stability constants of Cu(II) and Ca-complexes with the aid of ion selective electrodes. *j. Surf. Sci. Tech.* **1**: 63-68.

Samavat, S., Gholami, N. and Nazari, K. (2007). Complexation of Iron (III) With Citrate and Tartarate Anions in Perturbed Aqueous Solutions Using Potentiometry and Difference UV/Vis. and IR Spectrophotometric Methods. *Acta Chim. Slov.* **54**: 565-573.

Sandberg, A. S. (1997). Food processing influencing iron and zinc bioavailability. In In: 9th International symposium on Trace Elements in Man and Animals (Fischer, P. W. F., L'Abbé, M. R., Cockell, K. A. and Gibson, R. S., eds.), National Research Council of Canada, Banff, Alberta.

Sanna, D., Gábor Ágoston, C., Sóvágó, I. and Micera, G. (2001). Potentiometric and spectroscopic studies on the copper(II) complexes formed by oligopeptides containing histidine with a protection at the terminal amino group. *Polyhedron*. **20**: (9-10) 937-947.

Sawyer, D. T. and Paulsen, P. J. (1959). Properties and Infrared Spectra of Ethylenediaminetetraacetic Acid Complexes. II. Chelates of Divalent Ions1. *Journal of the American Chemical Society*. **81**: (4) 816-820.

Schlegel, P. (2006). Experimental designs to study organic trace mineral sources in animal nutrition. In Windisch, W. und Plitzner, Chr. (Eds): Experimentelle Modelle der Spurenelementforschung

Schmelzer, C. E. H., Schöps, R., Ulbrich-Hofmann, R., Neubert, R. H. H. and Raith, K. (2004). Mass spectrometric characterization of peptides derived by peptic cleavage of bovine [beta]-casein. *Journal of Chromatography A*. **1055**: (1-2) 87-92.

Schwarz, K. (1974). New essential trace elements (Sn, V, F, Si). Progress report and outlook. In Trace Element Metabolism in Animals -2 (Hoekstra, W. G., Suttie, I. W., Ganther, H. E. and Mertz, W., eds.). p. 366, University Park Press, Baltimore, MD.

Scrimgeour, W. A., Ward, T. L. and Fakler, T. M. (2004) Building an effective organic trace mineral. AFMA Forum 2004.

Se Young Choi, Hichung Moon, Songhui Jun and Chung, K. H. (1994). Comparison of the Stability Constants of Cd(II)-, Cu(II)-, and Pb(II)-Humate Complexes. *Bulletin of the Korean Chemical Society*. **15**: (7) 581-584.

Seibert, V., Wiesner, A., Buschmann, T. and Meuer, J. J. (2004). Surface-enhanced laser desorption ionization time-of-flight mass spectrometry (SELDI TOF-MS) and ProteinChip® technology in proteomics research. *Pathology - Research and Practice*. **200**: (2) 83-94.

Shamsipur, M., Rouhani, S., Ganjali, M. R., Sharghi, H. and Eshghi, H. (1999). Zinc-selective membrane potentiometric sensor based on a recently synthesized benzo-substituted macrocyclic diamide. *Sensors and Actuators B: Chemical*. **59**: (1) 30-34.

Sharma, G. and Tandon, J. P. (1971). Potentiometric studies of ternary complex formation : Cu(II), Ni, Zn or Cd iminodiacetic acid/amino-acid complexes. *Talanta*. **18**: (11) 1163-1167.

Sigel, H. and Martin, R. B. (1982). Coordinating properties of the amide bond. Stability and structure of metal ion complexes of peptides and related ligands. *Chemical Reviews*. **82**: (4) 385-426.

Sigma. (2000) Antigen Design and Sera Purification Tech Sheet. Sigma Genosys

Singh, A. K., Bhattacharjee, G., Singh, M. and Chandra, S. (1997). A new macrocyclic polystyrene based membrane sensor for zinc. *Electroanalysis*. **9**: (13) 1005-1008.

Smith, B. C. (1996). Fundamentals of Fourier transform infrared spectroscopy. CRC Press LLC, Florida

Solassol, J., Marin, P., Demettre, E., Rouanet, P., Bockaert, J., Maudelonde, T. and Mangé, A. (2005). Proteomic detection of prostate-specific antigen using a serum fractionation procedure: potential implication for new low-abundance cancer biomarkers detection. *Analytical Biochemistry*. **338**: (1) 26-31.

Sóvágó, I., Sanna, D., Dessí, A., Várnagy, K. and Micera, G. (1996). EPR and potentiometric reinvestigation of copper(II) complexation with simple oligopeptides and related compounds. *Journal of Inorganic Biochemistry*. **63**: (2) 99-117.

Spackman, D. H., Stein, W. H. and Moore, S. (2002). Automatic Recording Apparatus for Use in Chromatography of Amino Acids. *Analytical Chemistry*. **30**: (7) 1190-1206.

Spears, J. W. (2003). Trace Mineral Bioavailability in Ruminants. *Journal of Nutrition*. **133**: (5) 1506S-1509.

Srivastava, S. K., Vardhan, H., Singh, M., Rao, G. N. and Srivastava, S. (1995). A new chelating ion exchange resin based sensor for zinc ions. *Anal. Proc.* **32**: 173-174.

Stanila, A., Marcu, A., Rusu, D., Rusu, M. and David, L. (2007). Spectroscopic studies of some copper(II) complexes with amino acids. *Journal of Molecular Structure*. **834-836**: 364-368.

Stevenson, F. J. and Chen, Y. (1991). Stability Constants of Copper(II)-Humate Complexes Determined by Modified Potentiometric Titration. *Soil Science Society of America Journal*. **55**: (6) 1586-1591.

Stevenson, F. J., Fitch, A. and Brar, M. S. (1993). Stability constants of Cu(II)-humate complexes: comparison of select models. *Soil Science*. **155**: (2) 77-91.

Subramanian, A. and Rodriguez-Saona, L. (2009). Infrared spectroscopy for food quality analysis and control. Elsevier

Sun Wang, N. (2007) Amino acid assay by ninhydrin colorimetric assay. http://www.eng.umd.edu/~nsw/ench485/lab3a.htm

Surówka, K., Zmudzinski, D. and Surówka, J. (2004). Enzymic modification of extruded soy protein concentrates as a method of obtaining new functional food components. *Trends in Food Science & Technology*. **15**: (3-4) 153-160.

Takamatsu, T. and Yoshida, Y. (1978). Determination of stability constants of metal-humic acid complexes by potentiometric titration and ion-selective electrodes. *Soil Science*. **125**: (6) 377-386.

Tastet, L., Schaumloffel, D., Yiannikouris, A., Power, R. and Lobinski, R. (2009). Insight in the transport behaviour of copper glycinate complexes through the porcine gastrointestinal membrane using an Ussing chamber assisted by mass spectrometry analysis. *J. Trace Elements Med. Biol.*:

Tedeschi, C., Clement, V., Rouvet, M. and Valles-Pamies, B. (2009). Dissolution tests as a tool for predicting bioaccessibility of nutrients during digestion. *Food Hydrocolloids*. **23**: (4) 1228-1235.

Teixeira, M. F. S., Aniceto, C. and Fatibello-Filho, O. (1998). Ion-Selective Electrode for the Determination of Iron(III) in Vitamin Formulations in Citric Medium. *J. Braz. Chem. Soc.* **9**: (5) 506-510.

Trojanowicz, M. (2000). Flow injection analysis : instrumentation and applications. World Scientific, Singapore; River Edge, NJ

Tucker, L. A. (2003). Simplistic Statistics - A Basic Guide to the Statistical Analysis of Biological Data. Chalcombe Publications

Underwood, E. J. (1971). Trace elements in human and animal nutrition. Acad. Press, New York.

Underwood, E. J. and Suttle, N. F. (1999). The mineral nutrition of livestock. CABI Publishing, New York

Uselová-Vceláková, K., Zusková, I. and Gascaron, B. (2007). Stability constants of amino acids, peptides, proteins, and other biomolecules determined by CE and related methods: Recapitulation of published data. *Electrophoresis*. **28**: (13) 2145-2152.

Vandergrift, B. (1992). Mineral Proteinates. *Feed Compounder*: 42-44.

Veum, T. L., Carlson, M. S., Wu, C. W., Bollinger, D. W. and Ellersieck, M. R. (2004). Copper proteinate in weanling pig diets for enhancing growth performance and reducing fecal copper excretion compared with copper sulfate. *Journal of Animal Science*. **82**: (4) 1062-1070.

Vorderwulbecke, S., Cleverley, S., Weinberger, S. R. and Wiesner, A. (2005). Protein quantification by the SELDI-TOF-MS-based ProteinChip[reg] System. *Nature Methods*. **2**: (5) 393-395.

Wagner, C. C. and Baran, E. J. (2004). Spectroscopic and Magnetic Behaviour of the Copper(II) Complex of L-Tryptophan. *Acta Farm. Bonaerense*. **23**: (3) 339-342.

Walker, M. and Shah, H. H. (1997). Everything you should know about chelation therapy. Keats Pub., New Canaan, Conn.

Wang, J. (2000). Analytical electrochemistry. Wiley-VCH, New York

Wapnir, R. A. (1990). Protein nutrition and mineral absorption. CRC Press, Boca Raton

Ward, J. D., Spears, J. W. and Kegley, E. B. (1996). Bioavailability of Copper Proteinate and Copper Carbonate Relative to Copper Sulfate in Cattle. *Journal of Dairy Science*. **79**: (1) 127-132.

Webb, K. E., Dirienzo, D. B. and Matthews, J. C. (1993). Recent Developments in Gastrointestinal Absorption and Tissue Utilization of Peptides: A Review. *J. Dairy Sci.* **76**: (1) 351-361.

Webb, K. E., Matthews, J. C. and DiRienzo, D. B. (1992). Peptide absorption: a review of current concepts and future perspectives. *J. Anim. Sci.* **70**: (10) 3248-3257.

Wedekind, K. J., Hortin, A. E. and Baker, D. H. (1992). Methodology for assessing zinc bioavailability: efficacy estimates for zinc-methionine, zinc sulfate, and zinc oxide. *Journal of Animal Science*. **70**: (1) 178-187.

Wells, M. A., Jelinska, C., Hosszu, L. L. P., Craven, C. J., Clarke, A. R., Collinge, J., Waltho, J. P. and Jackson, G. S. (2006). Multiple forms of copper (II) co-ordination occur throughout the disordered N-terminal region of the prion protein at pH 7.4. *Biochem. J.* **400**: (3) 501-510.

Wilde, D. (2006). Influence of macro and micro minerals in the peri-parturient period on fertility in dairy cattle. *Anim. Reprod. Sci.* **96**: 240-249.

Wilson, J. and Seymour, W. (2003). Animal production agriculture: Is this a new frontier for nutraceuticals? *Nutraceuticals World*:

Wolf, H. U. (1986). Metal-chelating properties of organic compounds with biological significance: An overview. In Intracellular calcium regulation (Bader, H., Gietzen, K., Rosenthal, J., Rudel, R. and Wolf, H. U., eds.). pp. 95-104, Manchester University Press

Wright Jr, G. L., Cazares, L. H., Leung, S. M., Nasim, S., Adam, B. L., Yip, T. T., Schellhammer, P. F., Gong, L. and Vlahou, A. (1999). Proteinchip® surface enhanced laser desorption/ionization (SELDI) mass spectrometry: a novel protein biochip technology for detection of prostate cancer biomarkers in complex protein mixtures. *Prostate Cancer & Prostatic Diseases*. **2**: (5/6) 264.

Xiao, Z., Luke, B. T., Izmirlian, G., Umar, A., Lynch, P. M., Phillips, R. K. S., Patterson, S., Conrads, T. P., Veenstra, T. D., Greenwald, P., Hawk, E. T. and Ali, I. U. (2004). Serum Proteomic Profiles Suggest Celecoxib-Modulated Targets and Response Predictors. *Cancer Research*. **64**: (8) 2904-2909.

Xiao, Z., Prieto, D., Conrads, T. P., Veenstra, T. D. and Issaq, H. J. (2005). Proteomic patterns: their potential for disease diagnosis. *Molecular and Cellular Endocrinology*. **230**: (1-2) 95-106.

Yamauchi, O. and Odani, A. (1996). Stability constants of metal complexes of amino acids with charged side chains - Part I: Positively charged side chains (Technical Report). *Pure Appl. Chem.* **68**: (2) 469-496.

Zhang, W. and Chait, B. T. (2000). ProFound: An Expert System for Protein Identification Using Mass Spectrometric Peptide Mapping Information. *Analytical Chemistry*. **72**: (11) 2482-2489.

Zhang, Z., Bast, R. C., Yu, Y., Li, J., Sokoll, L. J., Rai, A. J., Rosenzweig, J. M., Cameron, B., Wang, Y. Y., Meng, X.-Y., Berchuck, A., van Haaften-Day, C., Hacker, N. F., de Bruijn, H. W. A., van der Zee, A. G. J., Jacobs, I. J., Fung, E. T. and Chan, D. W. (2004). Three Biomarkers Identified from Serum Proteomic Analysis for the Detection of Early Stage Ovarian Cancer. *Cancer Research*. **64**: (16) 5882-5890.

Appendix 1.1 FTIR spectra of a selection of Fe, Mn and Zn proteinates and soy ligand controls

Appendix 1.1a

FTIR spectra of a iron(II) proteinates and soy ligand controls

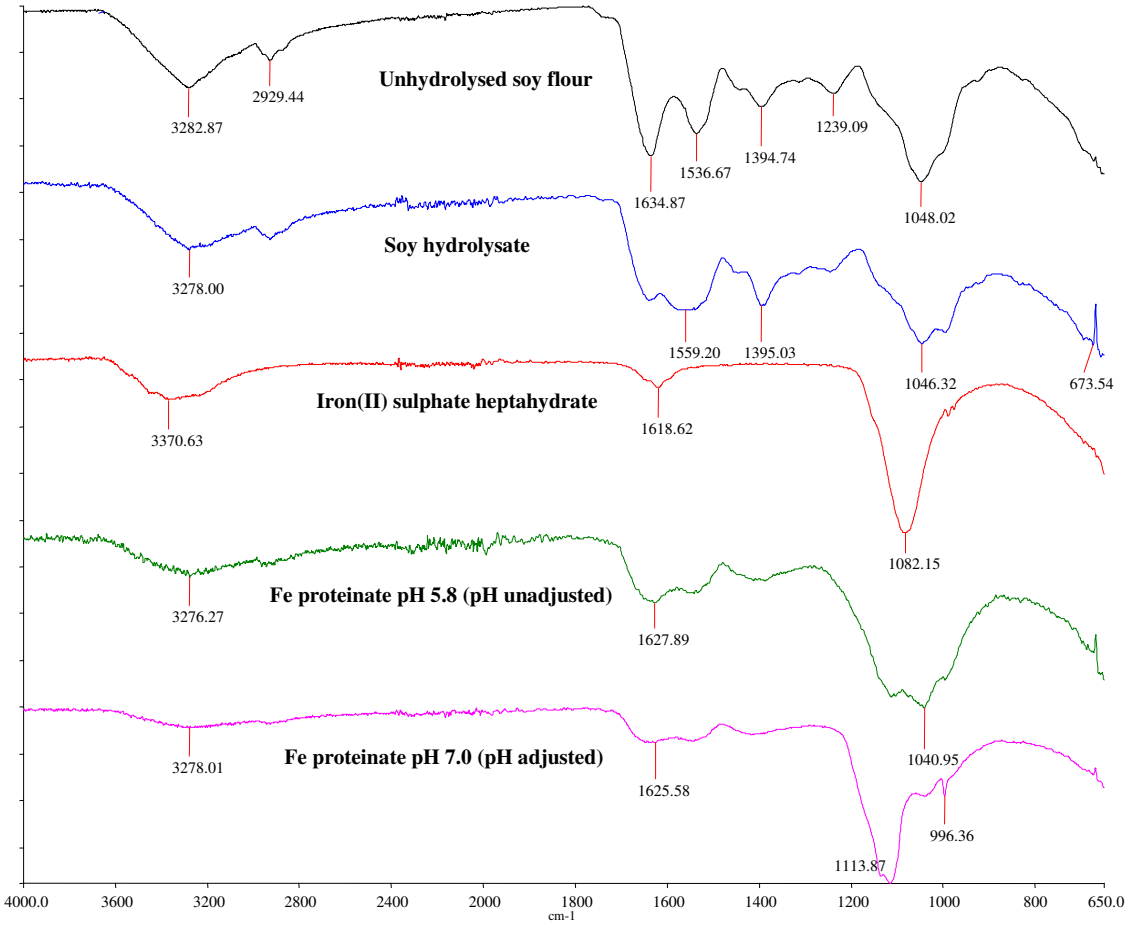

Appendix 1.1b

FTIR spectra of a manganese(II) proteinates and soy ligand controls

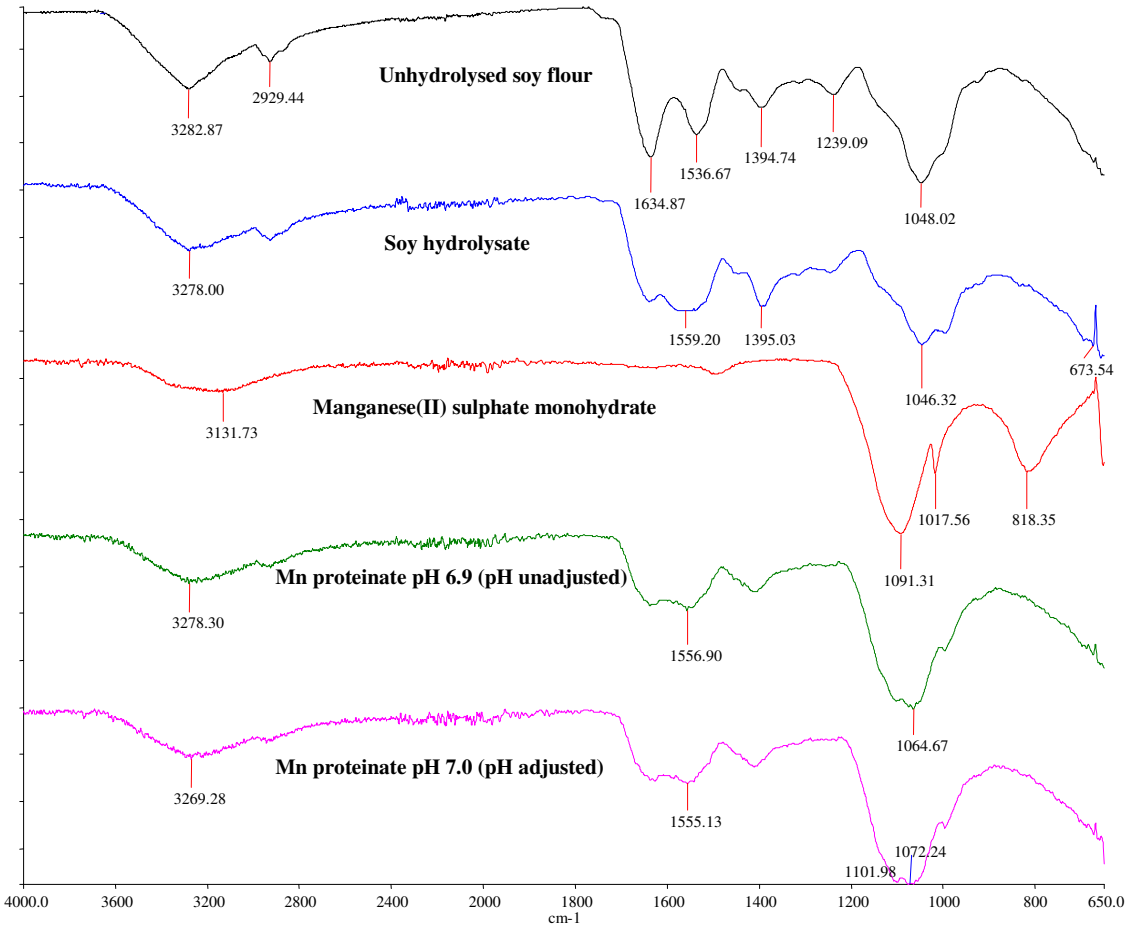

Appendix 1.1c

FTIR spectra of a zinc(II) proteinates and soy ligand controls

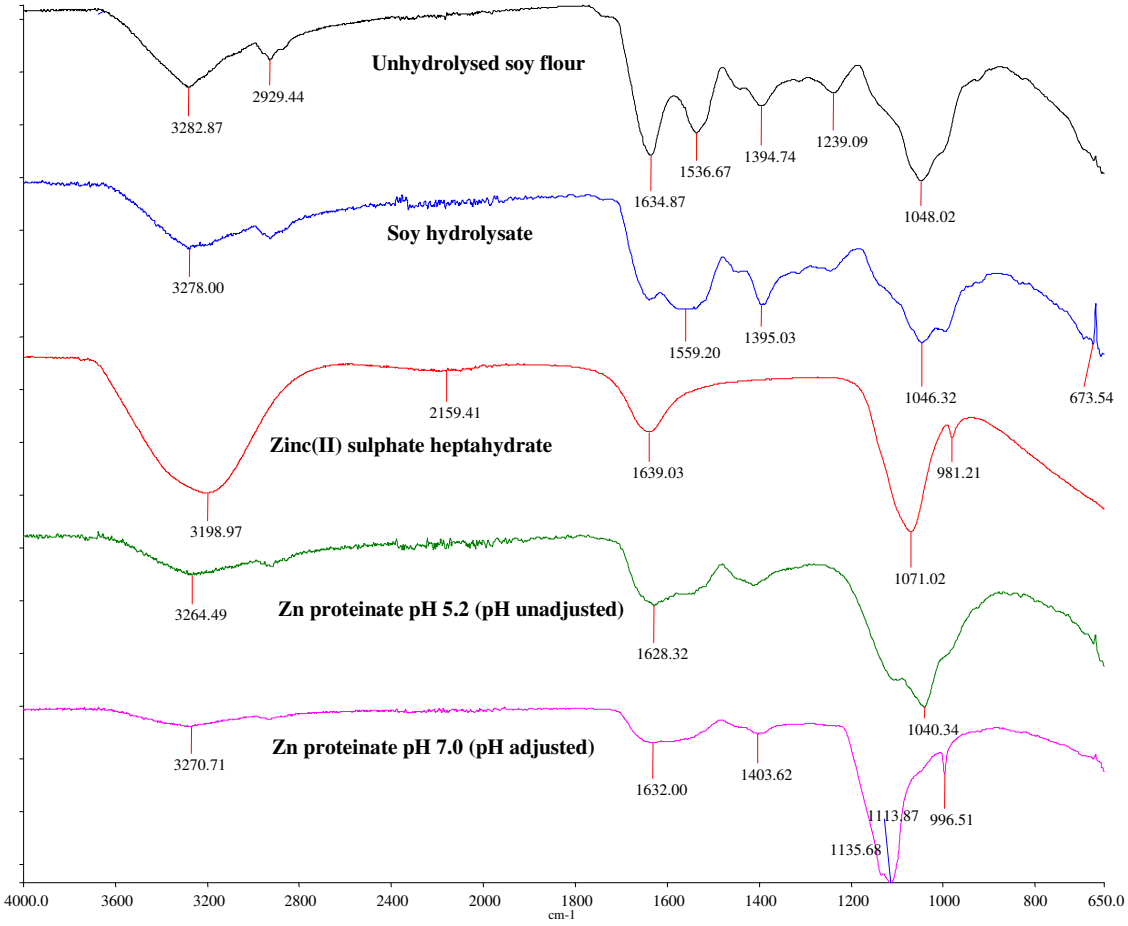

Appendix 1.2 FTIR spectra of a selection of amino acid-Cu complexes and controls

Appendix 1.2a

FTIR spectra of a copper(II) sulphate pentahydrate control, alanine and an alanine-Cu complex

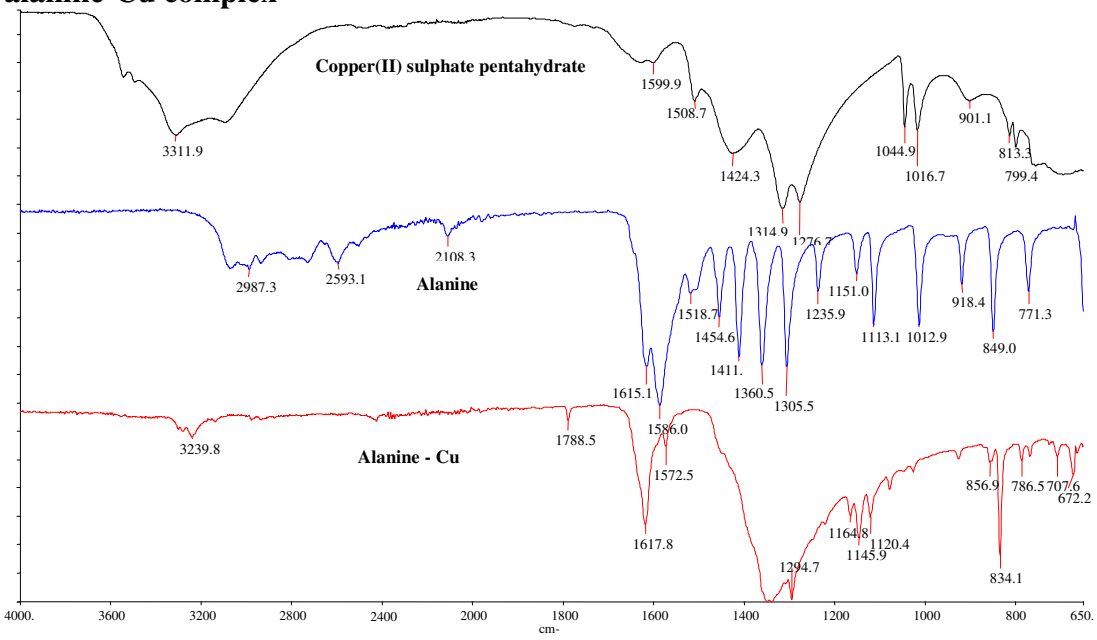

Appendix 1.2b

FTIR spectra of a copper(II) sulphate pentahydrate control, arginine and an arginine-Cu complex

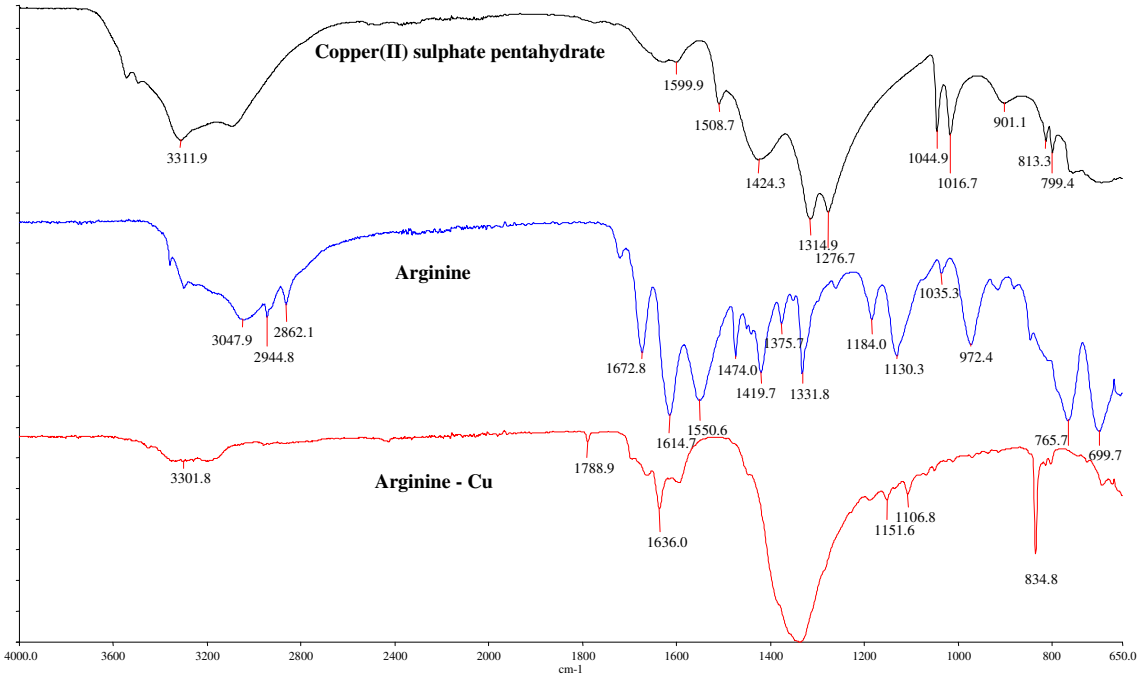

Appendix 1.2c

FTIR spectra of a copper(II) sulphate pentahydrate control, asparagine and an aspargine-Cu complex

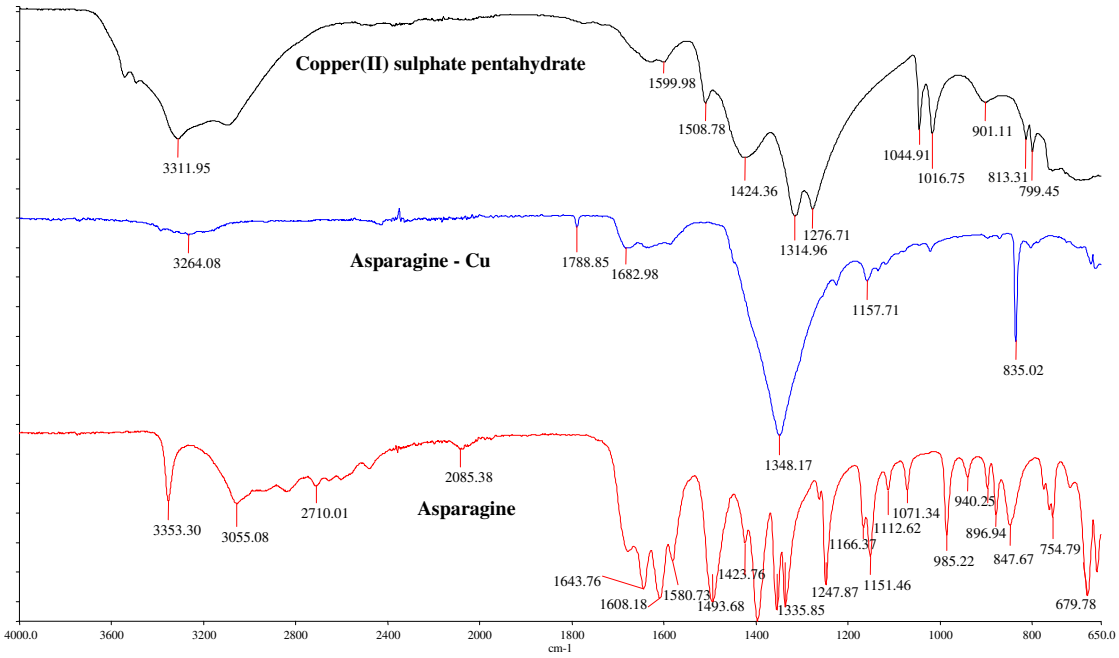

Appendix 1.2d

FTIR spectra of a copper(II) sulphate pentahydrate control, aspartic acid and an aspartic acid-Cu complex

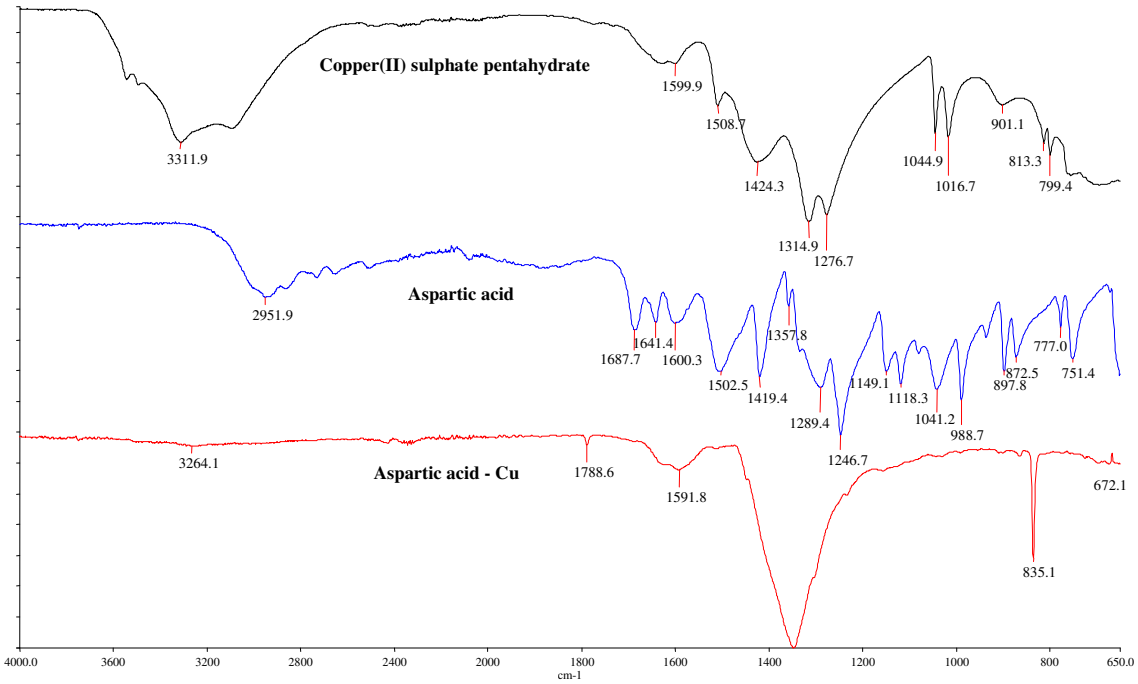

Appendix 1.2e

FTIR spectra of a copper(II) sulphate pentahydrate control, cysteine and a cysteine-Cu complex

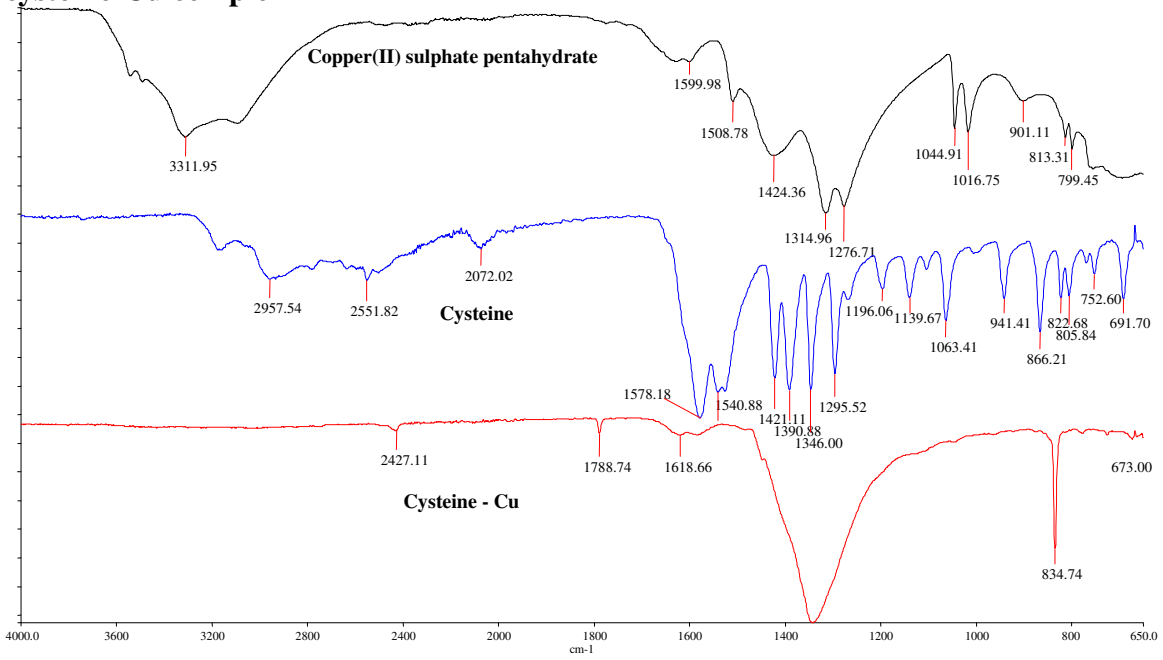

Appendix 1.2f

FTIR spectra of a copper(II) sulphate pentahydrate control, glutamic acid and a glutamic acid-Cu complex

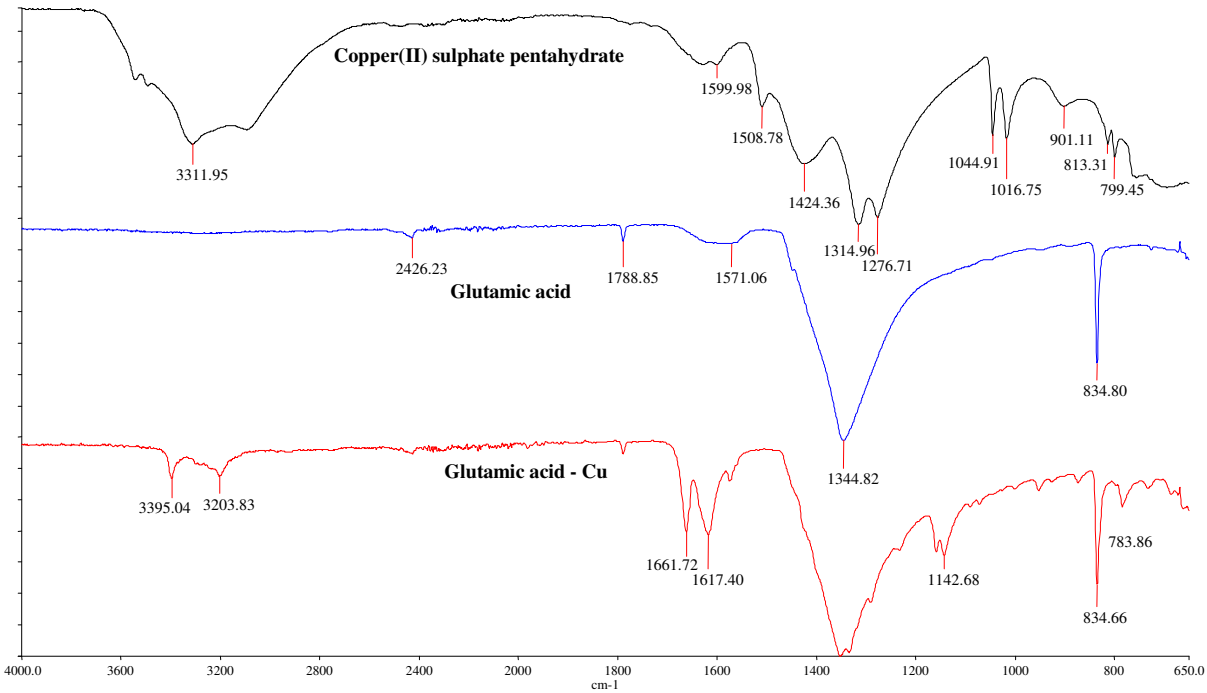

Appendix 1.2g

FTIR spectra of a copper(II) sulphate pentahydrate control, glutamine and a glutamine-Cu complex

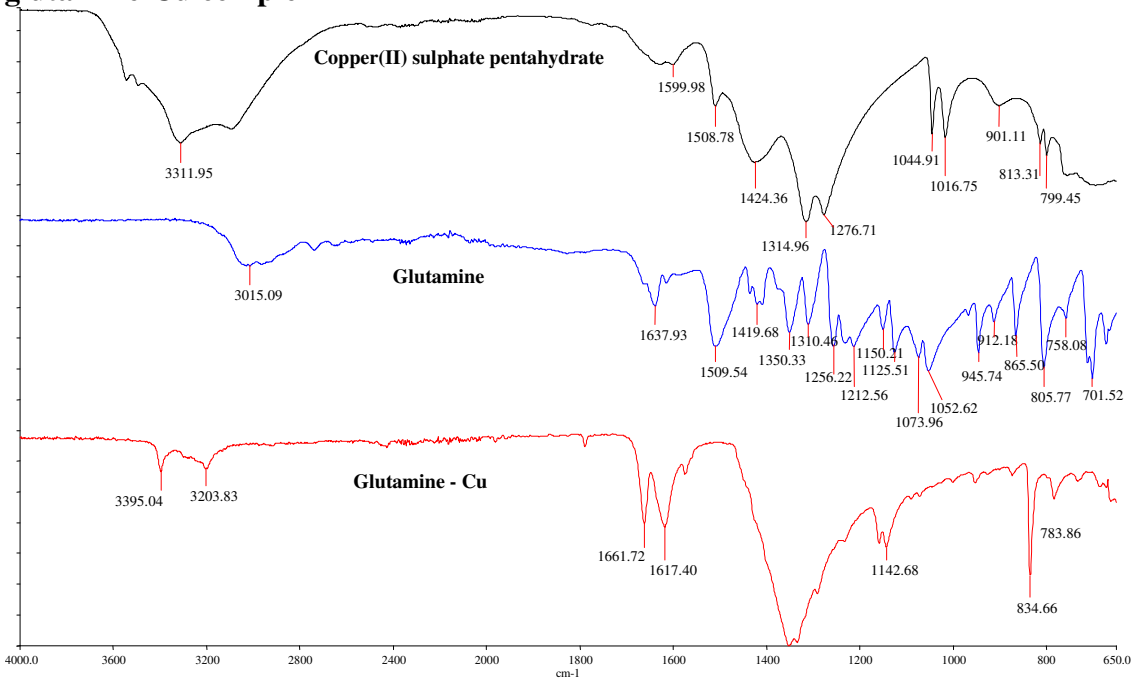

Appendix 1.2h

FTIR spectra of a copper(II) sulphate pentahydrate control, histidine and a histidine-Cu complex

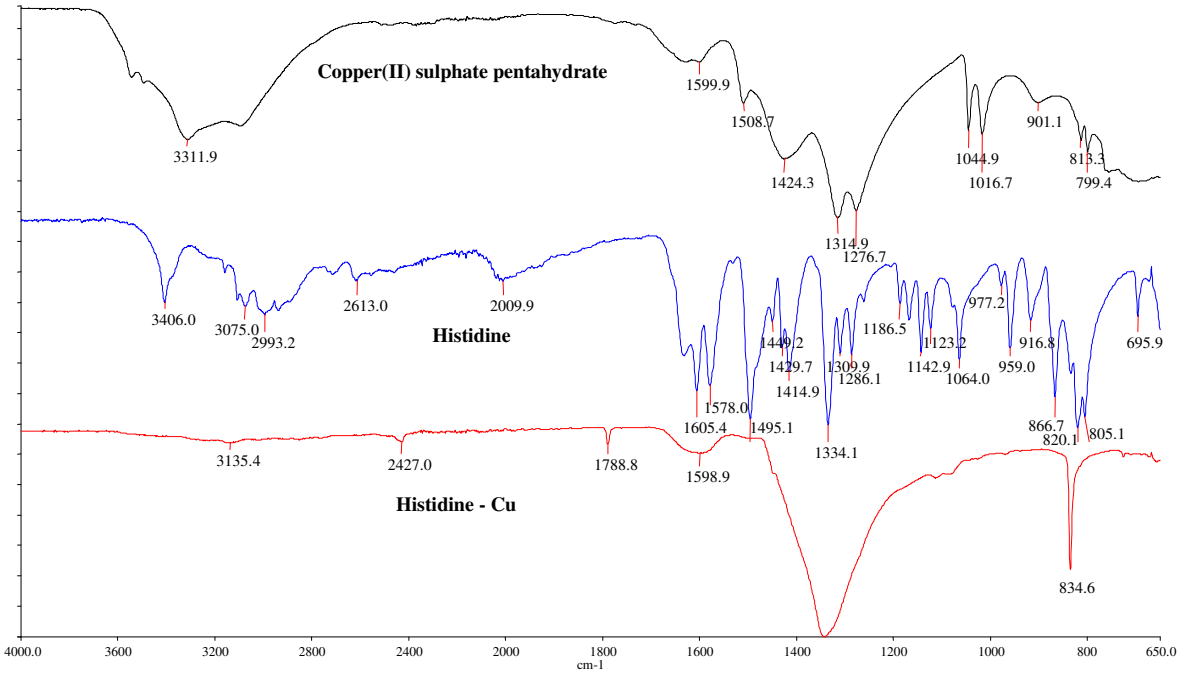

Appendix 1.2i

FTIR spectra of a copper(II) sulphate pentahydrate control, isoleucine and an isoleucine-Cu complex

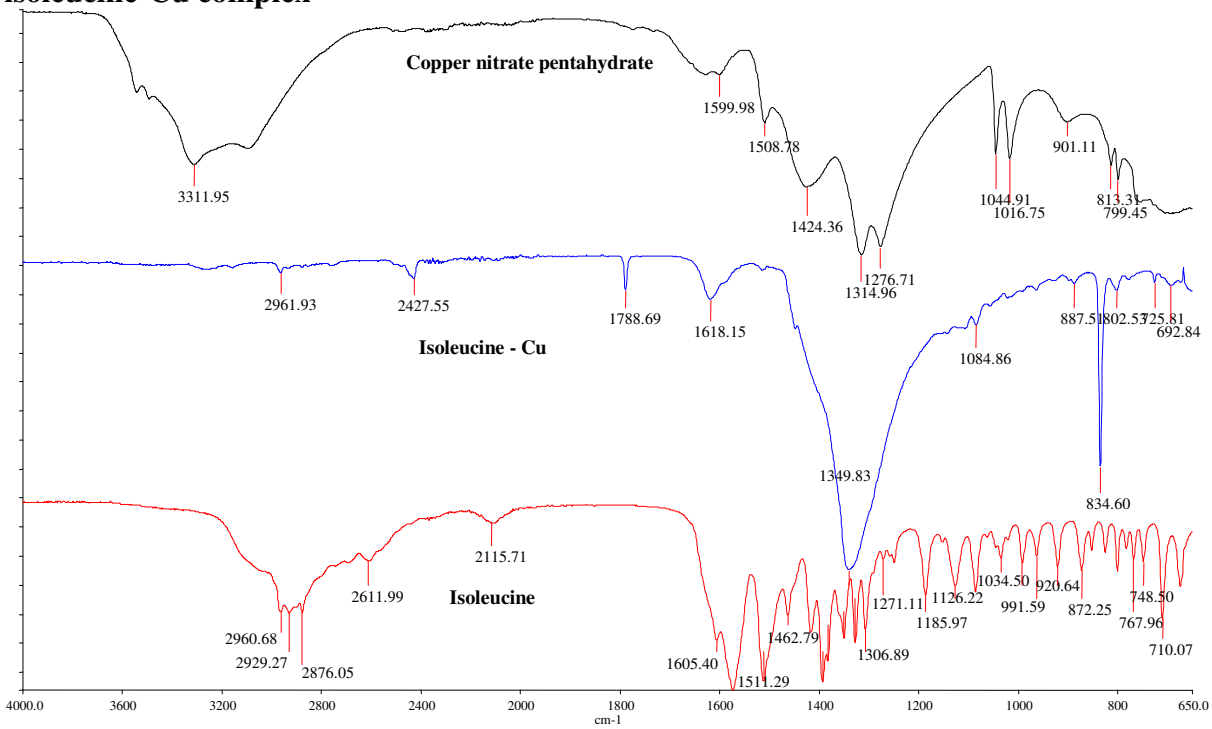

Appendix 1.2j

FTIR spectra of a copper(II) sulphate pentahydrate control, lysine and a lysine-Cu complex

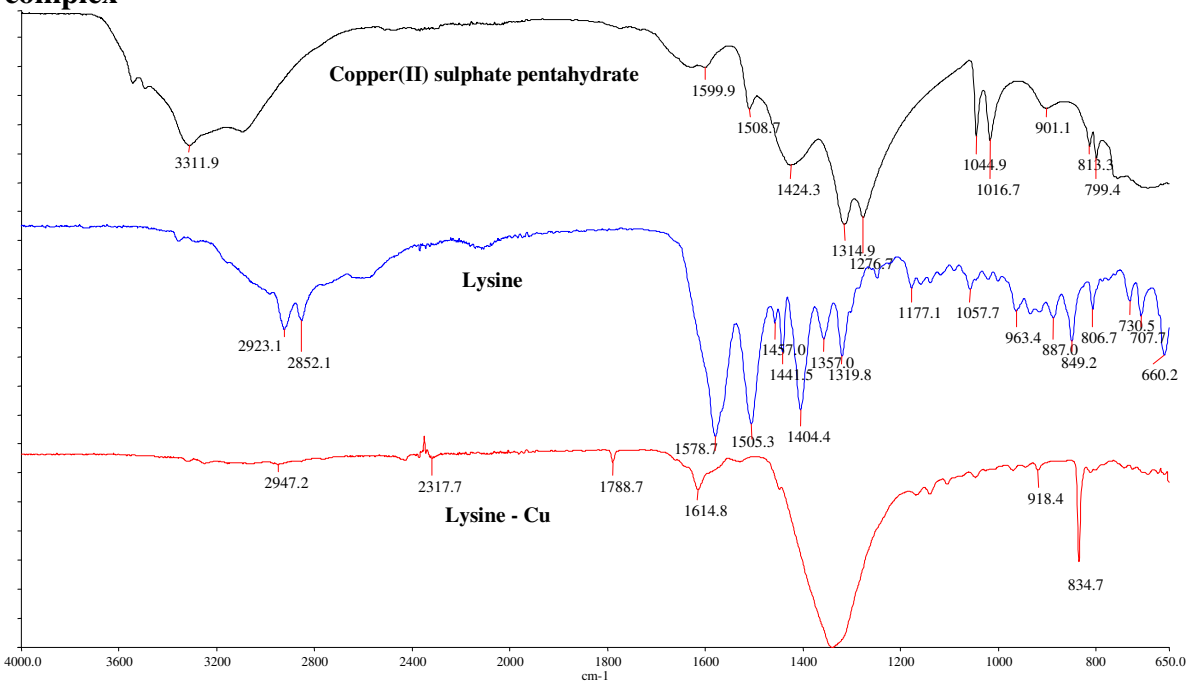

Appendix 1.2k

FTIR spectra of a copper(II) sulphate pentahydrate control, methionine and a methionine-Cu complex

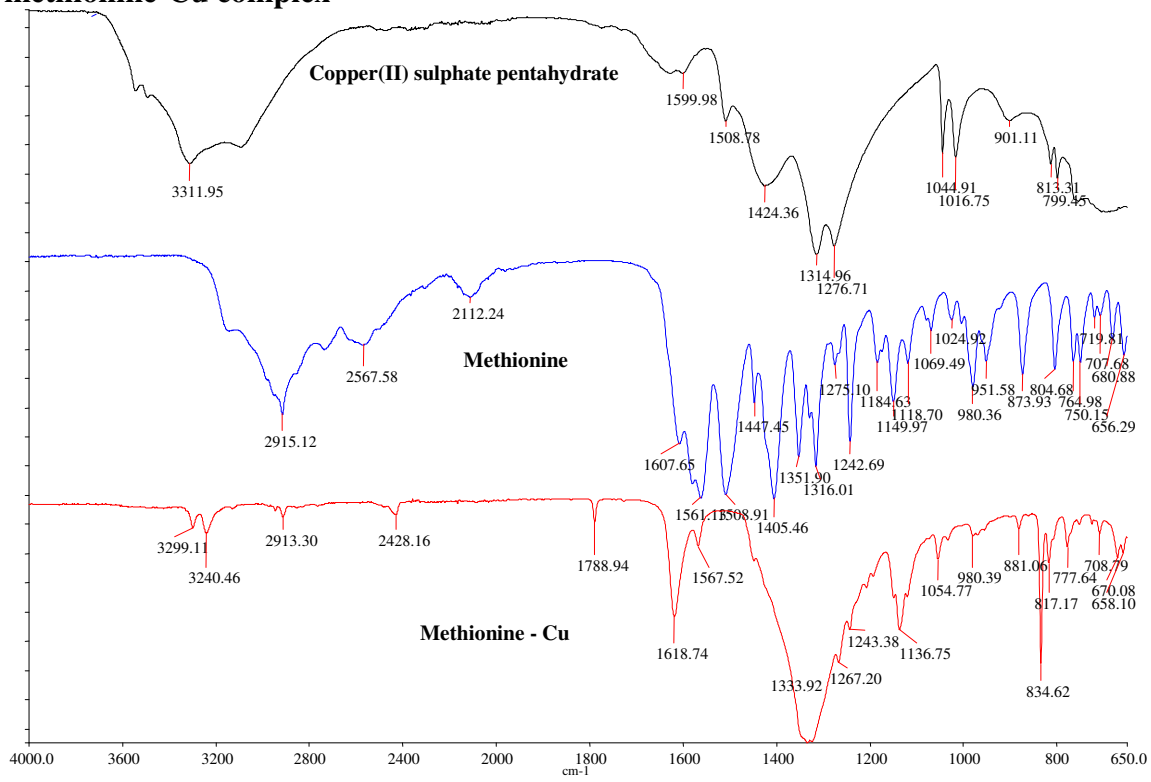

Appendix 1.2l

FTIR spectra of a copper(II) sulphate pentahydrate control, proline and a proline-Cu complex

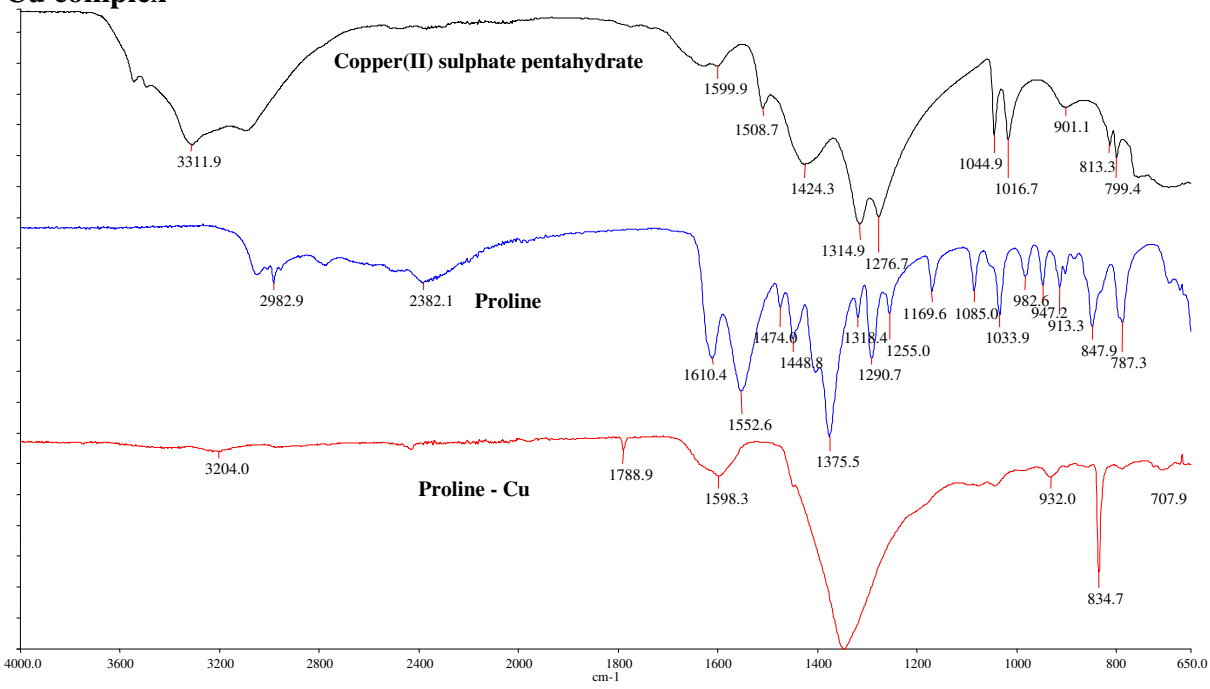

Appendix 1.2m

FTIR spectra of a copper(II) sulphate pentahydrate control, serine and a serine-Cu complex

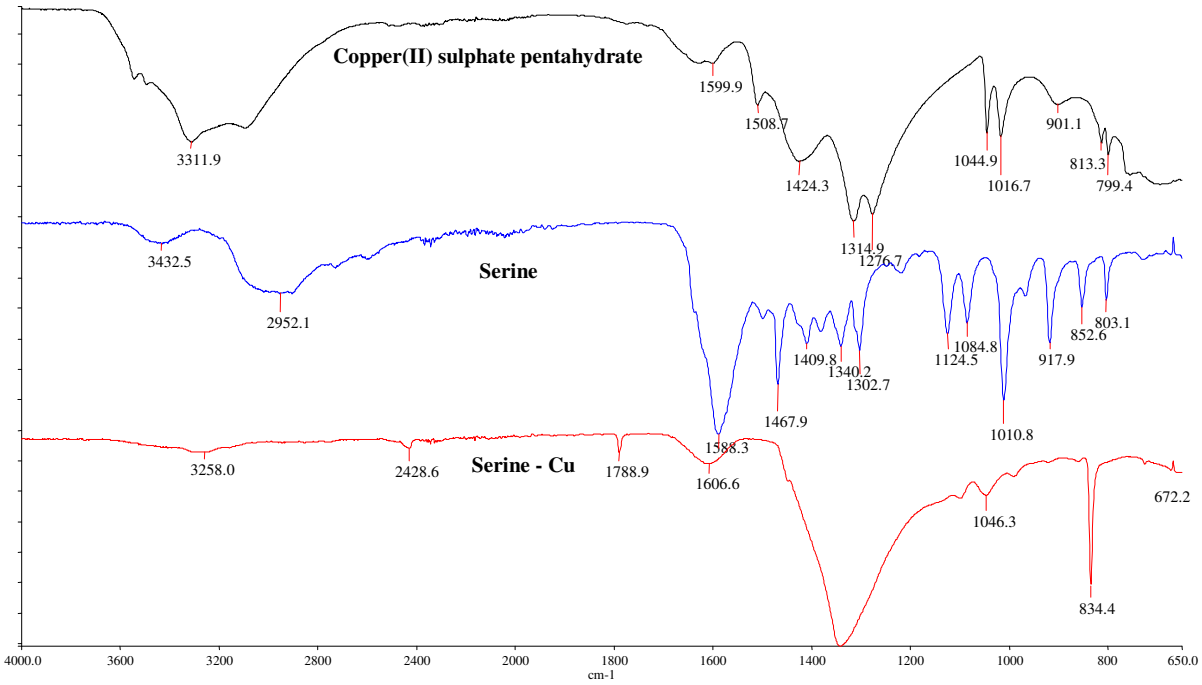

Appendix 1.2n

FTIR spectra of a copper(II) sulphate pentahydrate control, threonine and a threonine-Cu complex

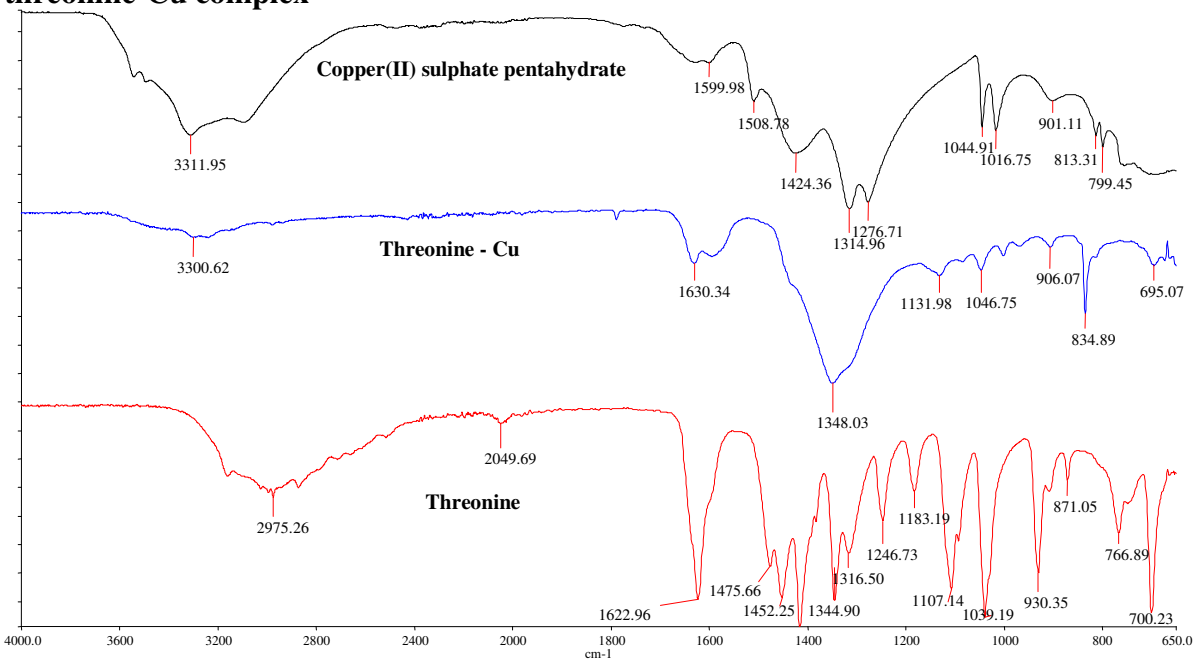

Appendix 1.2o

FTIR spectra of a copper(II) sulphate pentahydrate control, tryptophan and a tryptophan-Cu complex

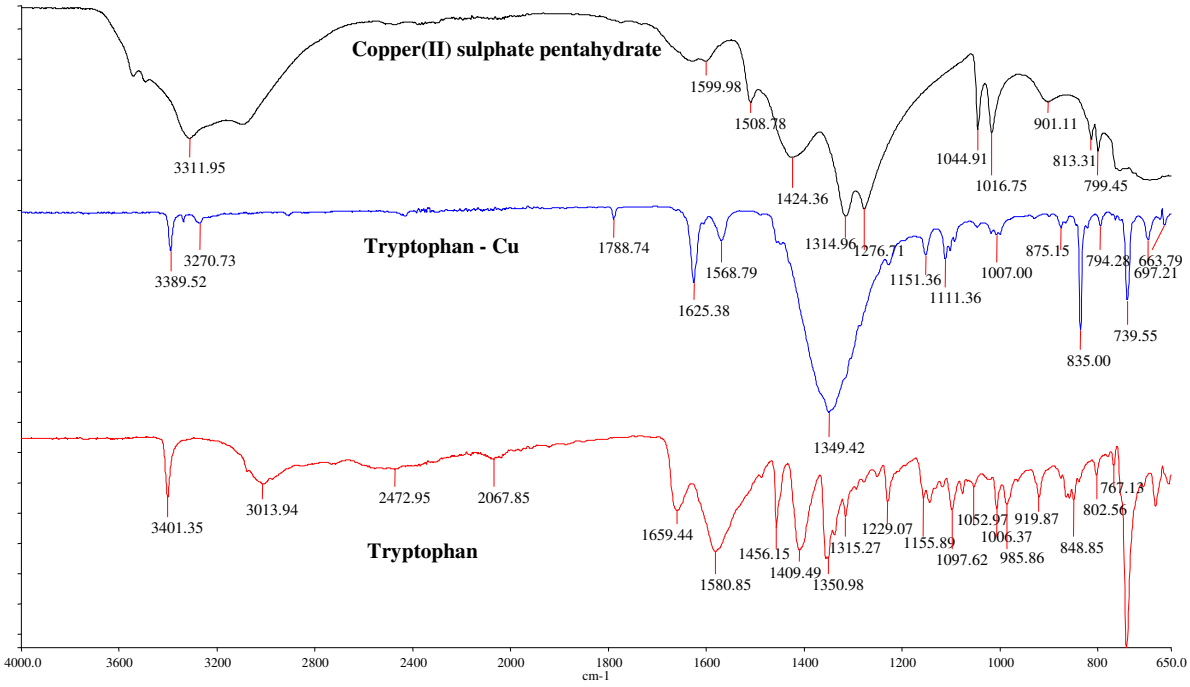

Appendix 1.2p

FTIR spectra of a copper(II) sulphate pentahydrate control, valine and a valine-Cu complex

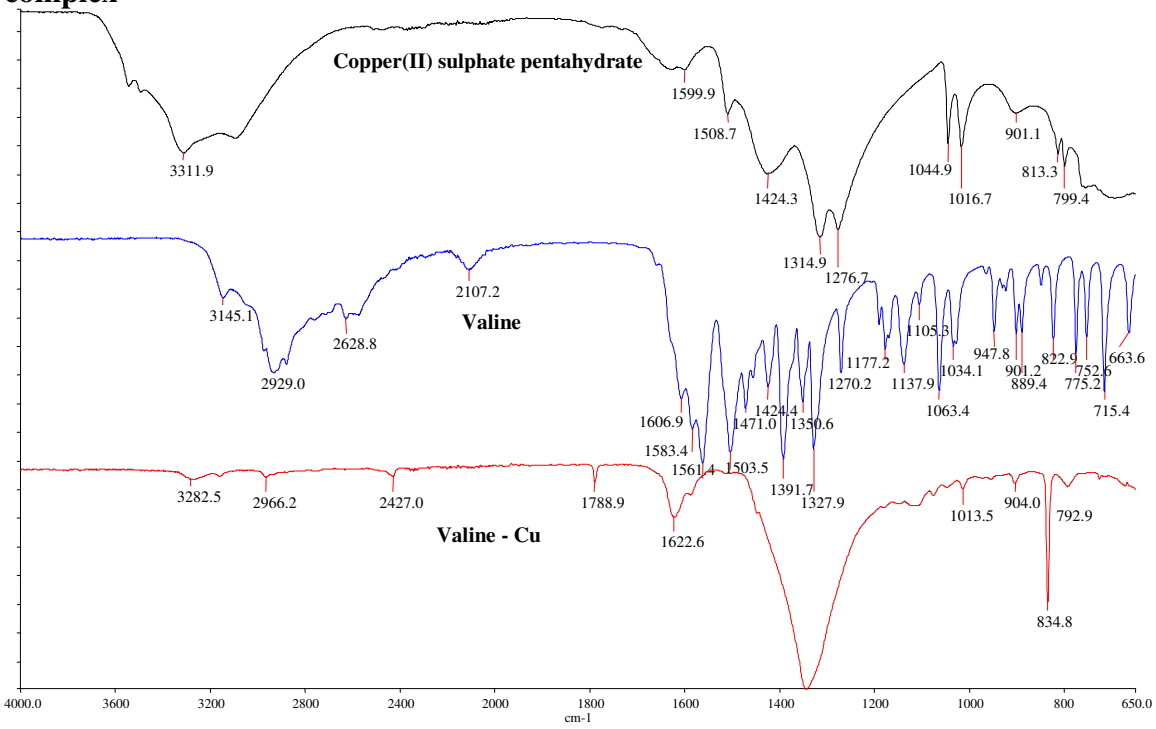

Appendix 1.3 FTIR spectra of a selection of peptide-Cu complexes and controls

Appendix 1.3a

FTIR spectra of a copper(II) sulphate pentahydrate control, dipeptide (Gly-Leu) and a Cu-Glu-Leu complex

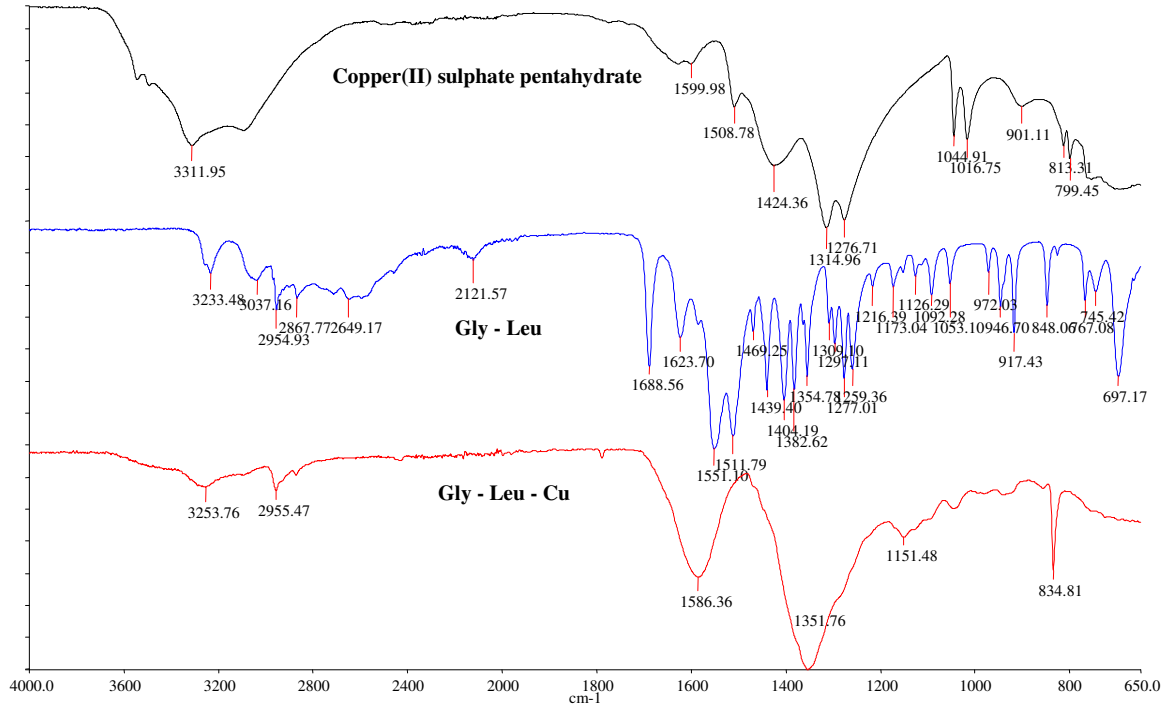

Appendix 1.3b

FTIR spectra of a copper(II) sulphate pentahydrate control, dipeptide (Gly-Phe) and a Cu-Glu-Phe complex

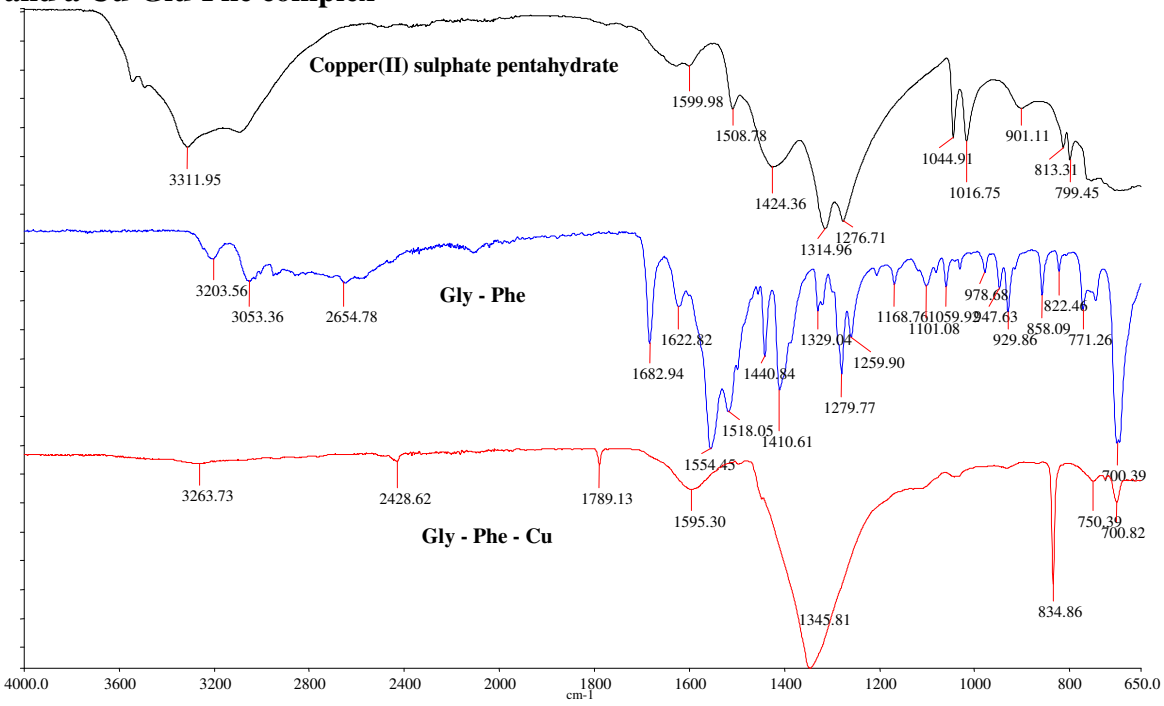

Appendix 1.3c

FTIR spectra of a copper(II) sulphate pentahydrate control, dipeptide (Gly-Pro) and a Cu-Glu-Pro complex

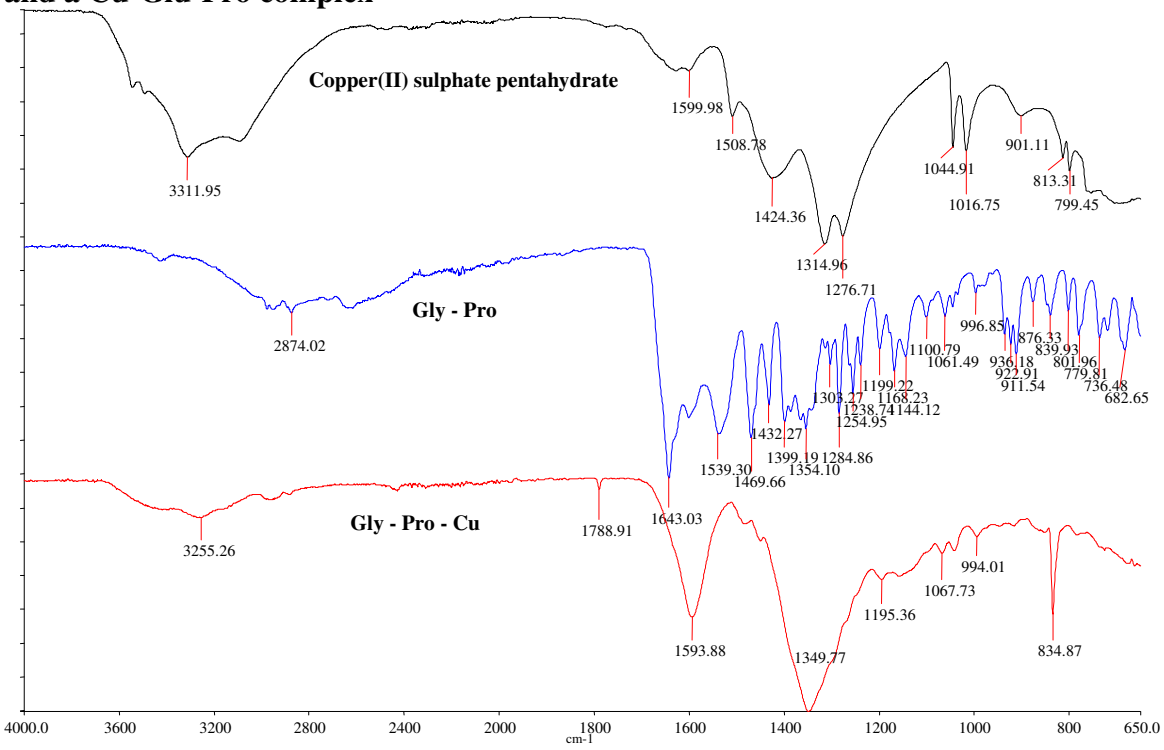

Appendix 1.3d

FTIR spectra of a copper(II) sulphate pentahydrate control, dipeptide (Gly-Ser) and a Cu-Glu-Ser complex

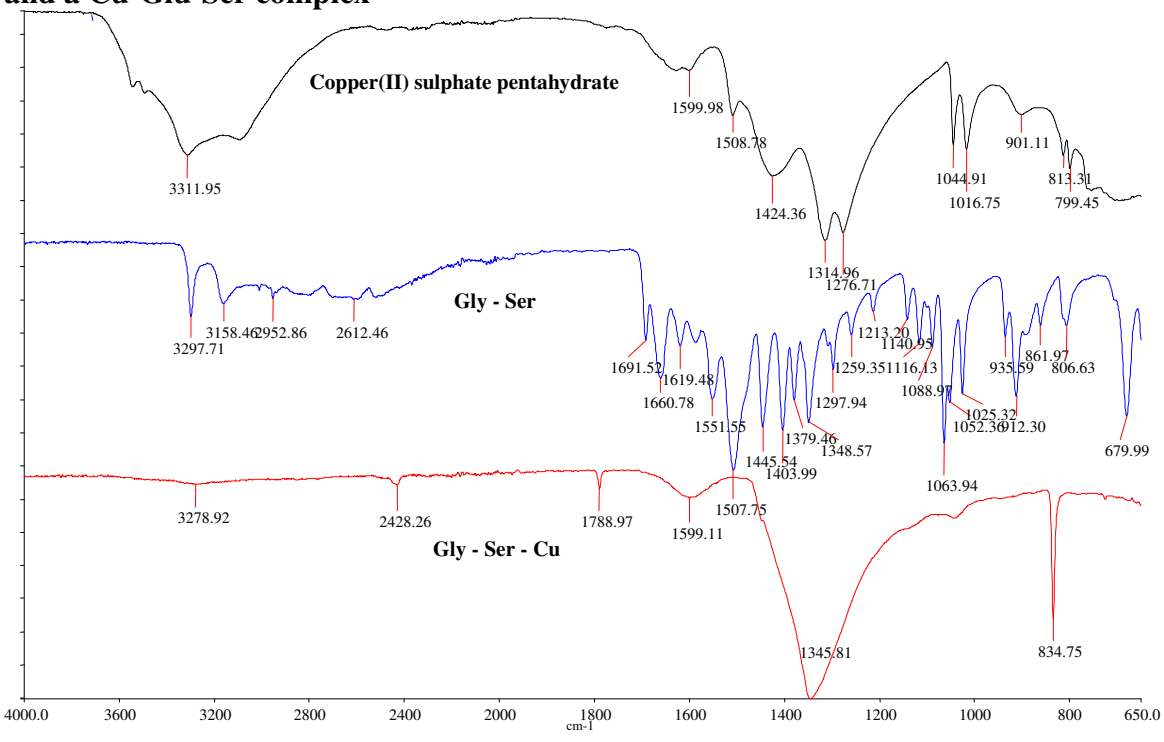

Appendix 1.3e

FTIR spectra of a copper(II) sulphate pentahydrate control, dipeptide (Gly-Val) and a Cu-Glu-Val complex

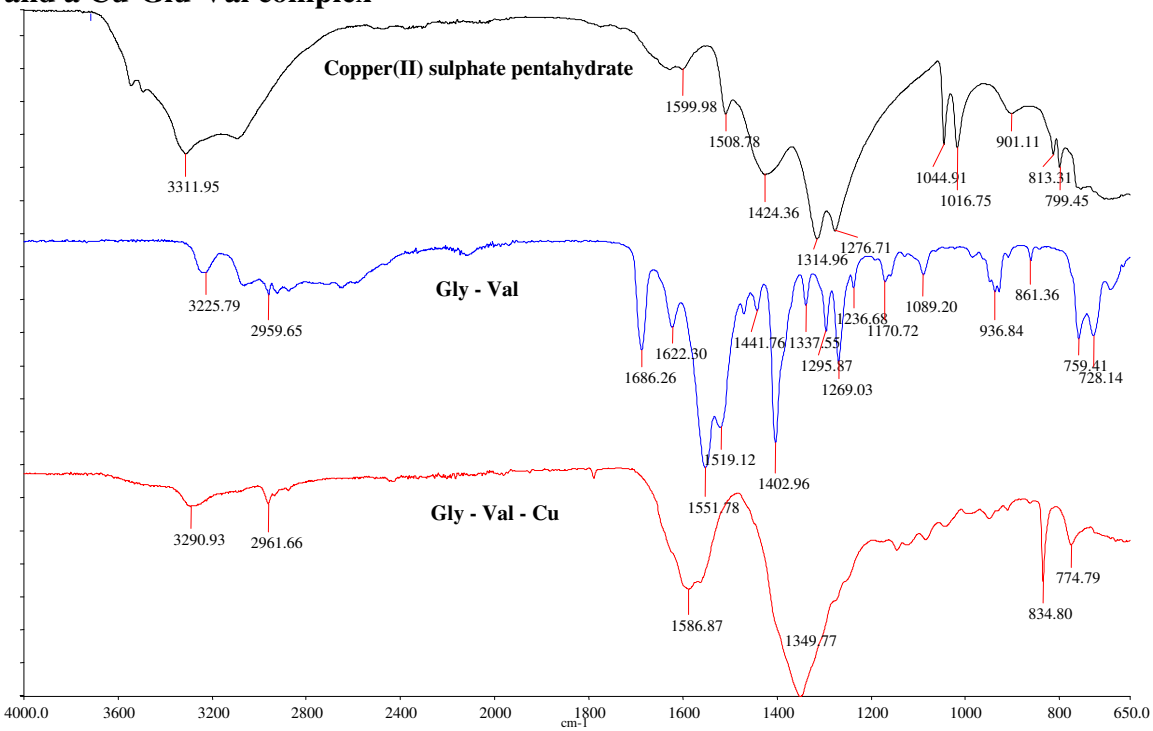

Appendix 1.3f

FTIR spectra of a copper(II) sulphate pentahydrate control, dipeptide (Gly-His) and a Cu-Gly-His complex

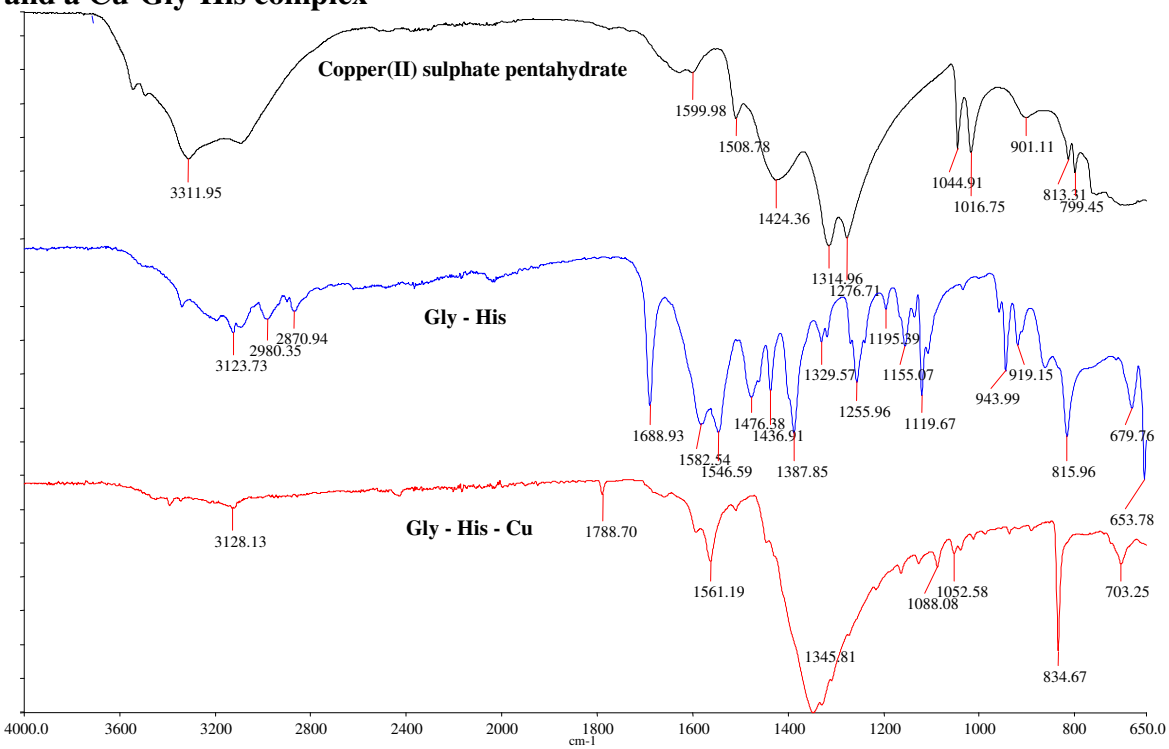

Appendix 1.3g

FTIR spectra of a copper(II) sulphate pentahydrate control, tripeptide (Gly-His-Gly) and a Cu-Gly-His-Gly complex

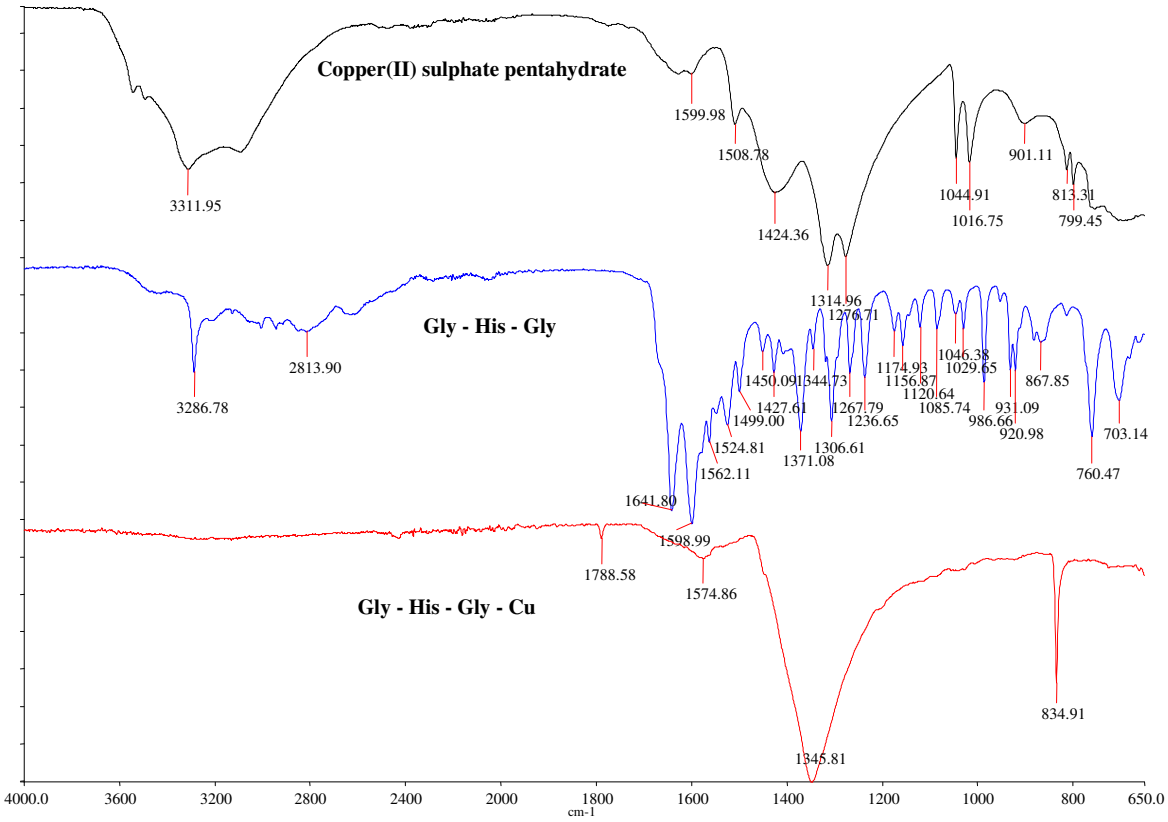

Appendix 1.4 FTIR spectra of a selection of Cu proteinates formed from various enzymatic hydrolyses and controls

Appendix 1.4a

FTIR spectra of Cu proteinate formed from a cysteine protease hydrolysis (CP1) with and without pH adjustment and a soy hydrolysate control

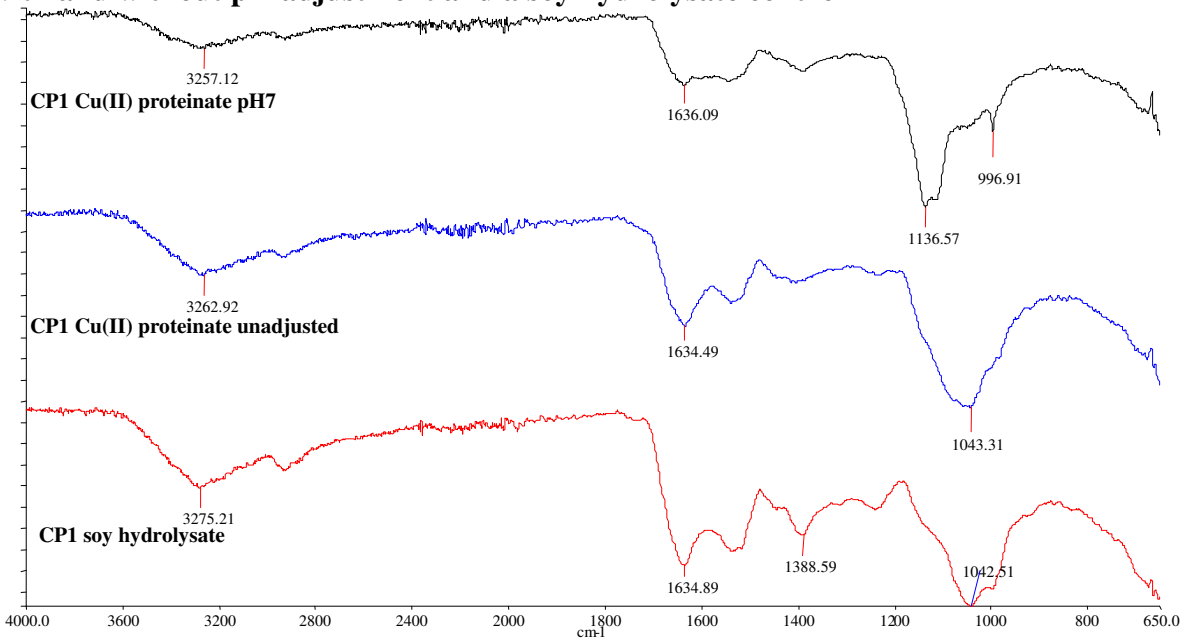

Appendix 1.4b

FTIR spectra of Cu proteinate formed from a serine protease hydrolysis (SP) with and without pH adjustment and a soy hydrolysate control

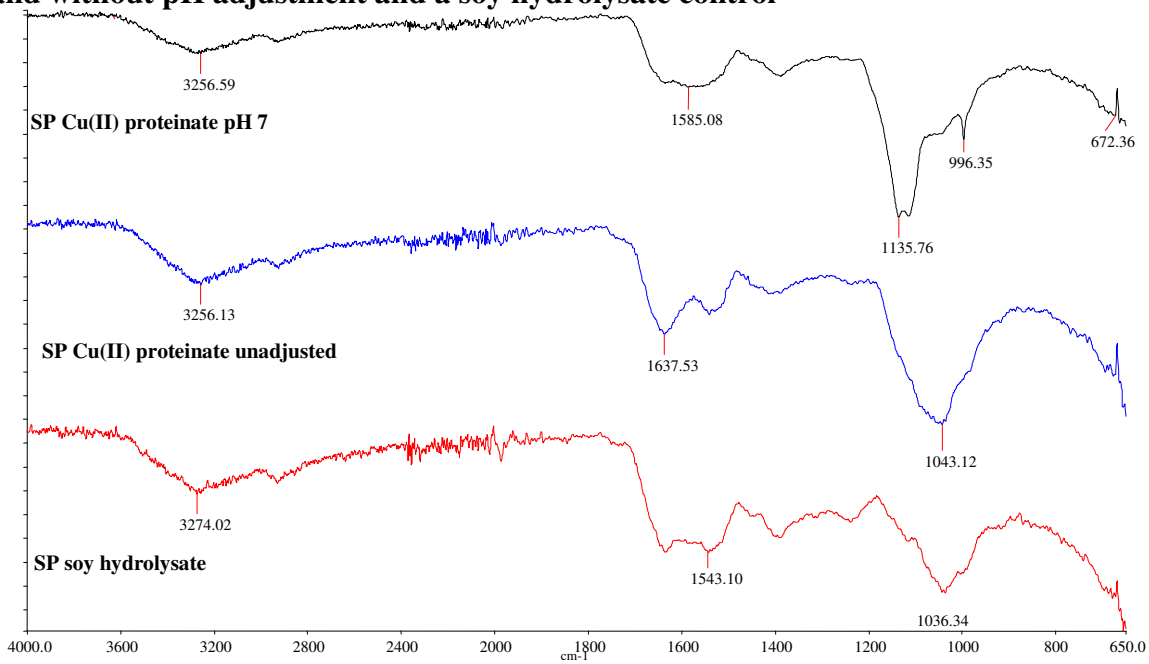

Appendix 1.4c

FTIR spectra of Cu proteinate formed from a fungal protease hydrolysis (FP) with and without pH adjustment and a soy hydrolysate control

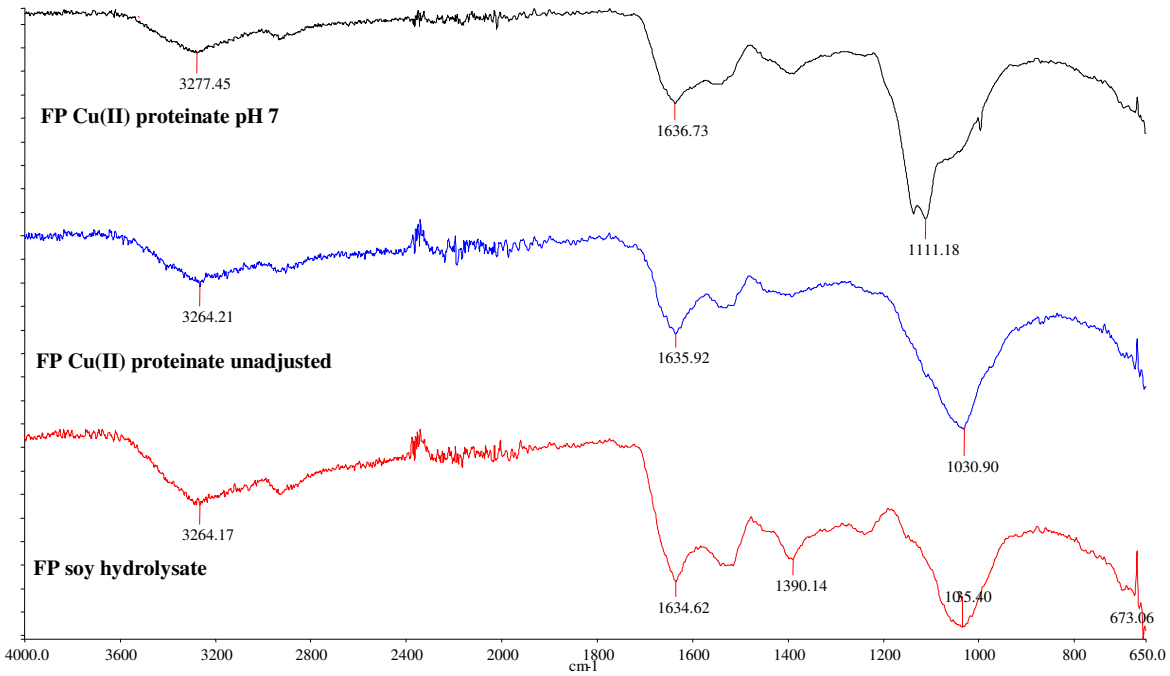

Appendix 1.4d

FTIR spectra of Cu proteinate formed from a cysteine protease hydrolysis (CP2) with and without pH adjustment and a soy hydrolysate control

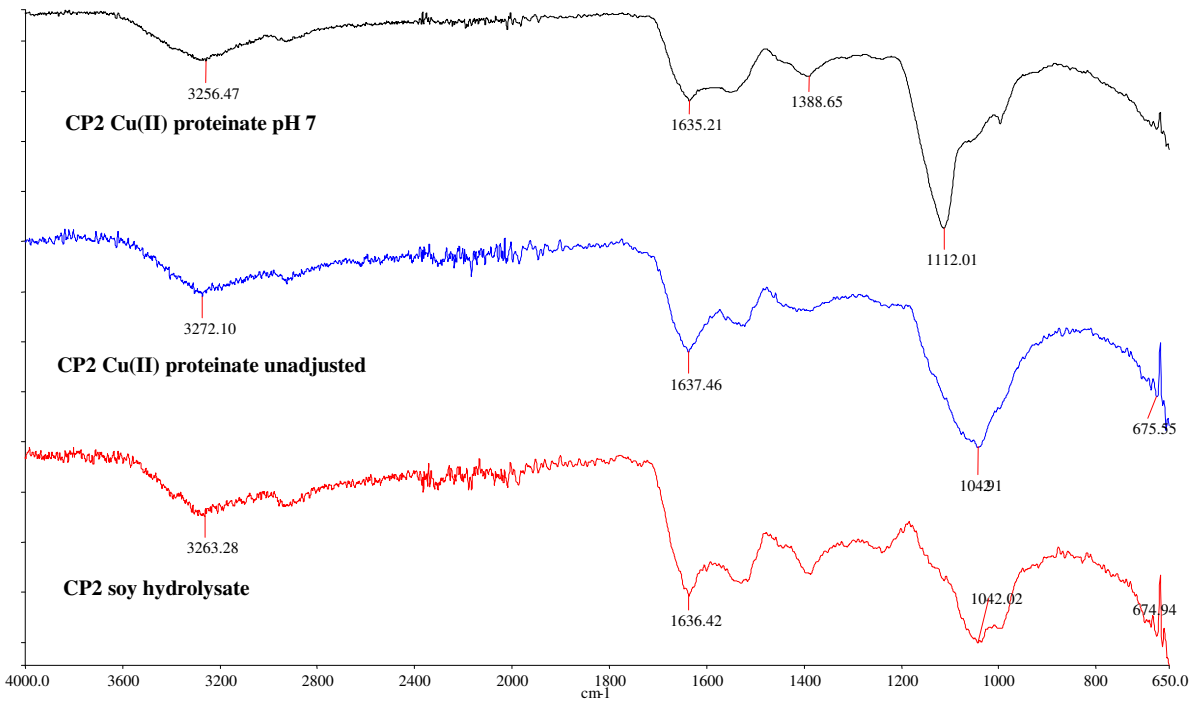

Appendix 1.4e

FTIR spectra of Cu proteinate formed from an acidic fungal protease hydrolysis (AFP) with and without pH adjustment and a soy hydrolysate control

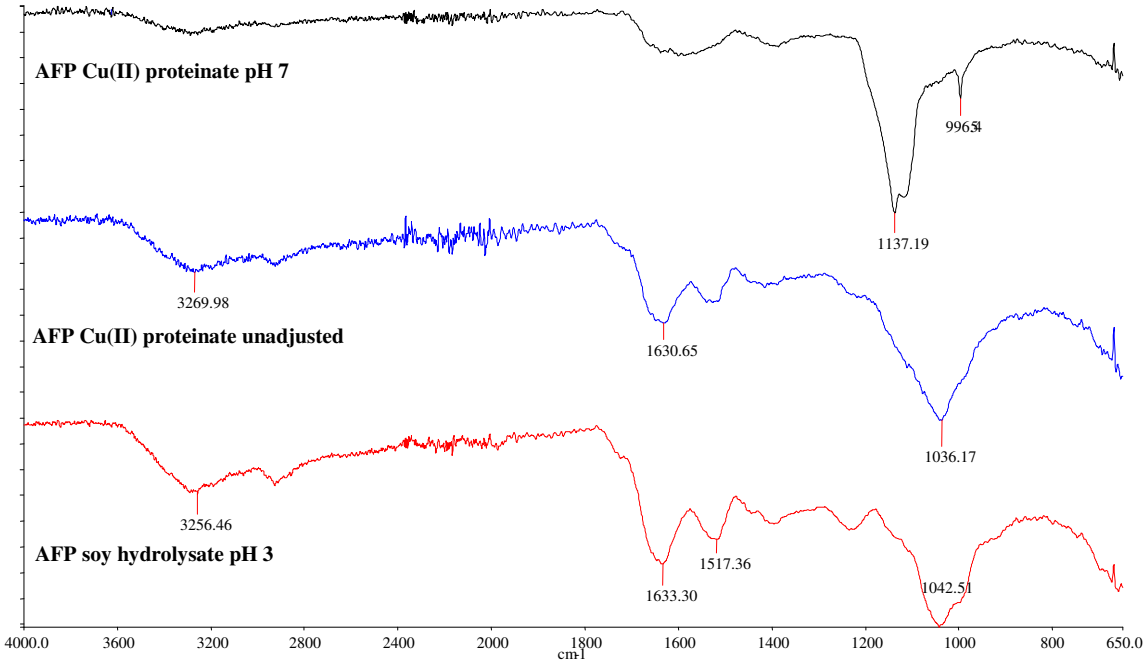

Appendix 1.4f

FTIR spectra of Cu proteinate formed from a serine protease and a fungal protease hydrolysis (SP + FP) with and without pH adjustment and a soy hydrolysate control

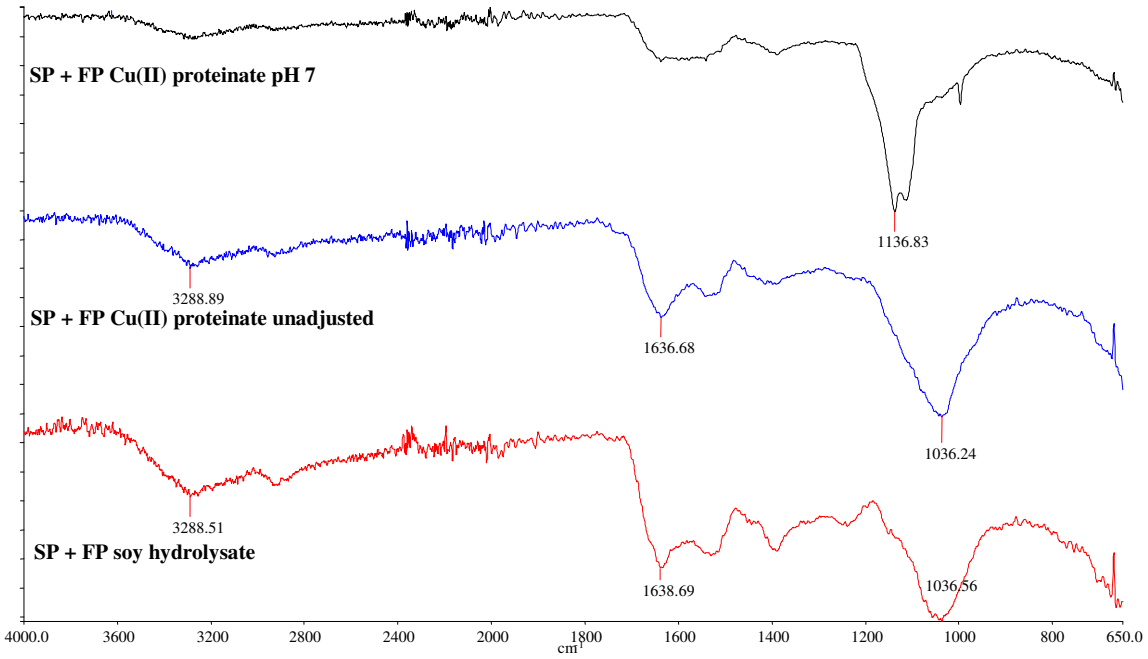

Appendix 1.4g

FTIR spectra of Cu proteinate formed from a serine protease and a cysteine protease hydrolysis (SP + CP1) with and without pH adjustment and a soy hydrolysate control

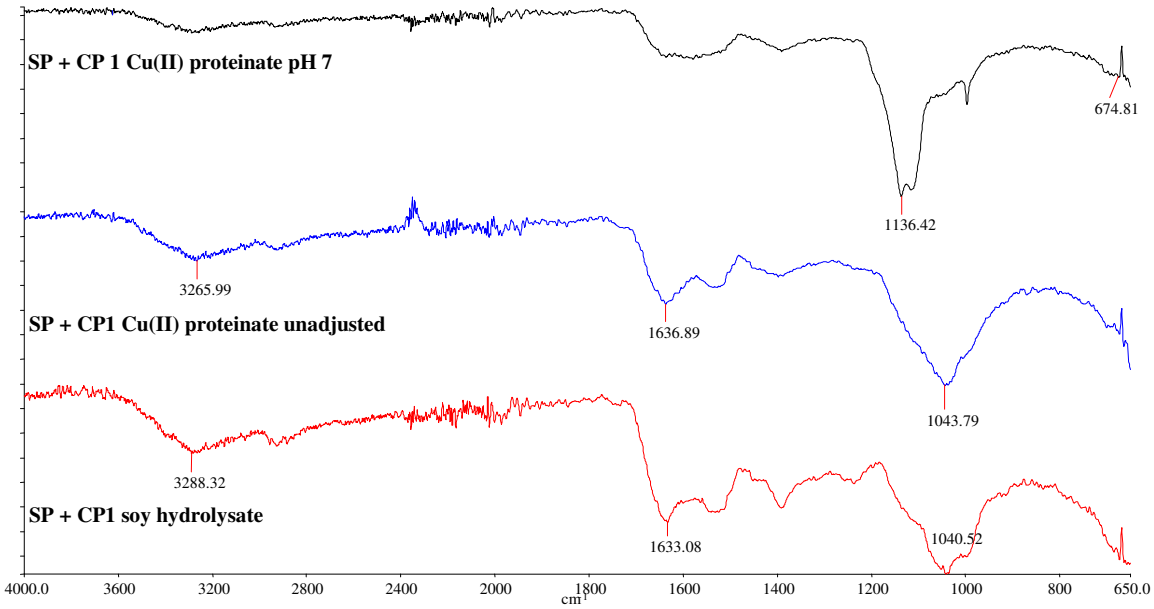

Appendix 1.4h

FTIR spectra of Cu proteinate formed from a serine protease and a cysteine protease hydrolysis (SP + CP2) with and without pH adjustment and a soy hydrolysate control

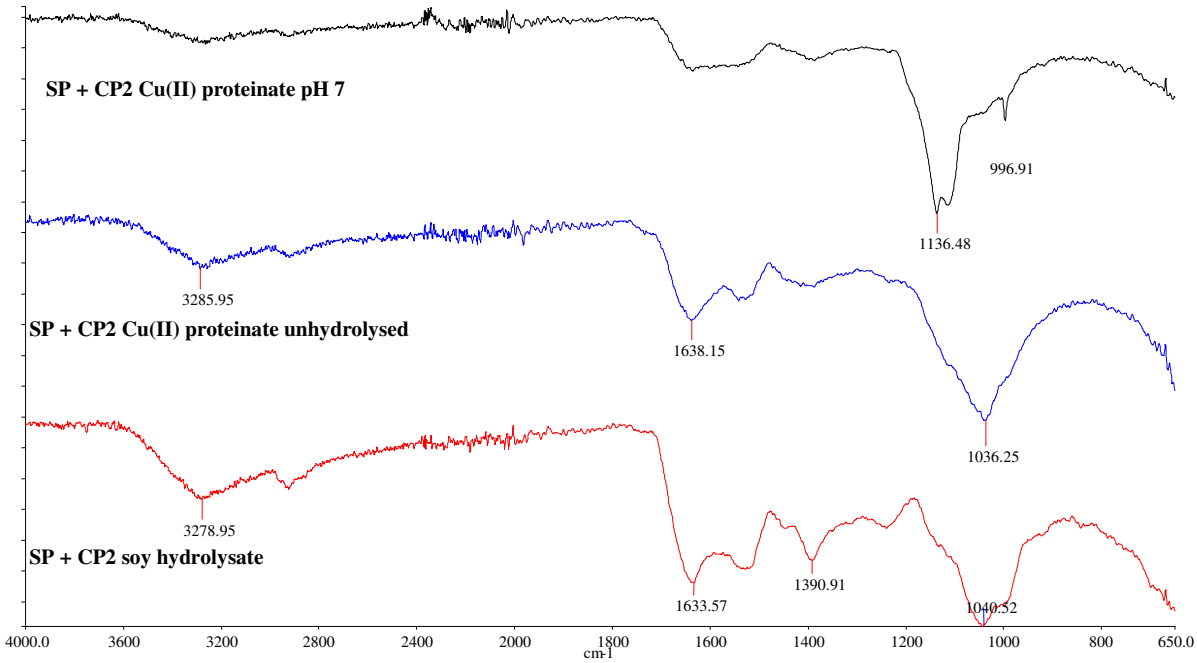

Appendix 1.4i

FTIR spectra of Cu proteinate formed from a serine protease and an acidic fungal protease hydrolysis (SP + AFP) with and without pH adjustment and a soy hydrolysate control

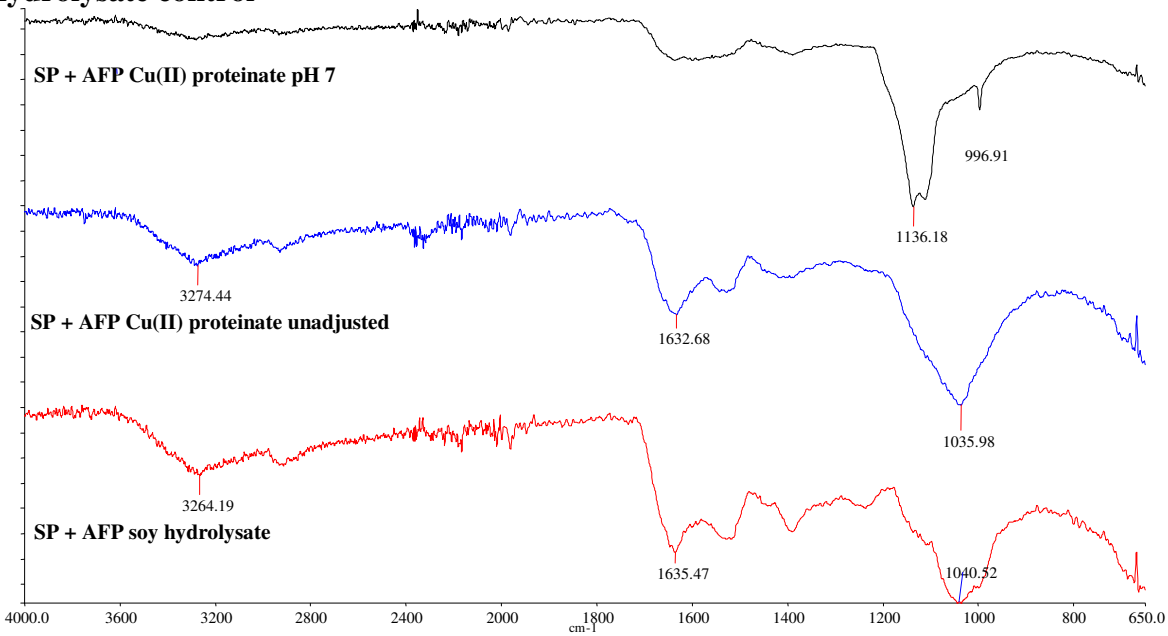

Appendix 1.4j

FTIR spectra of Cu proteinate formed from a dual hydrolysis (Dual hydrolysis 1) with and without pH adjustment and a soy hydrolysate control

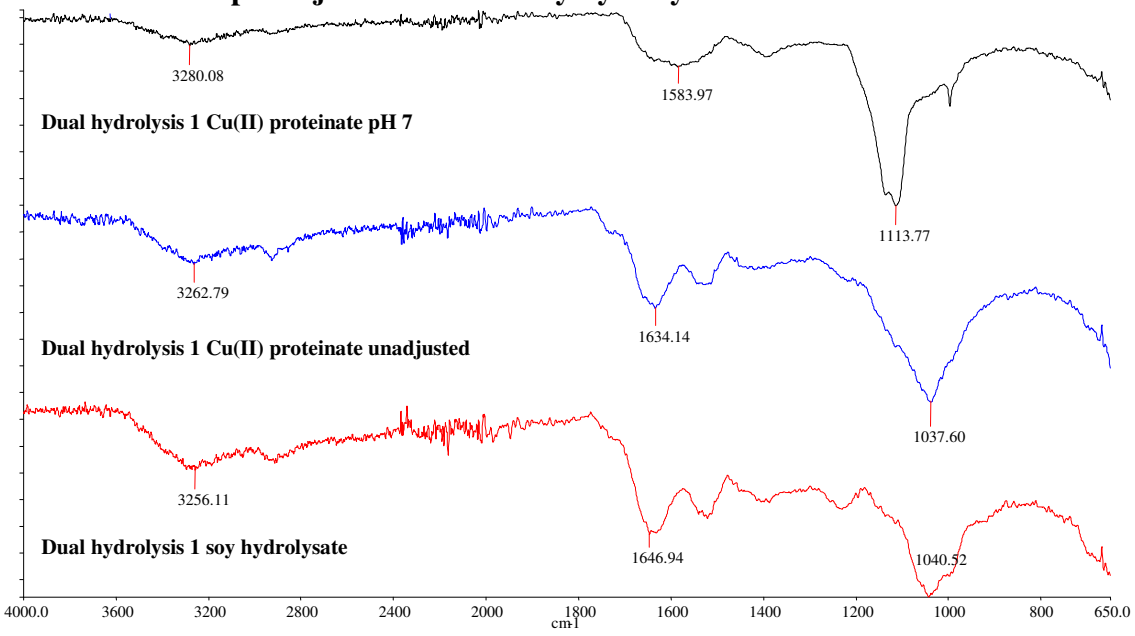

Appendix 1.4k

FTIR spectra of Cu proteinate formed from a dual hydrolysis (Dual hydrolysis 2) with and without pH adjustment and a soy hydrolysate control

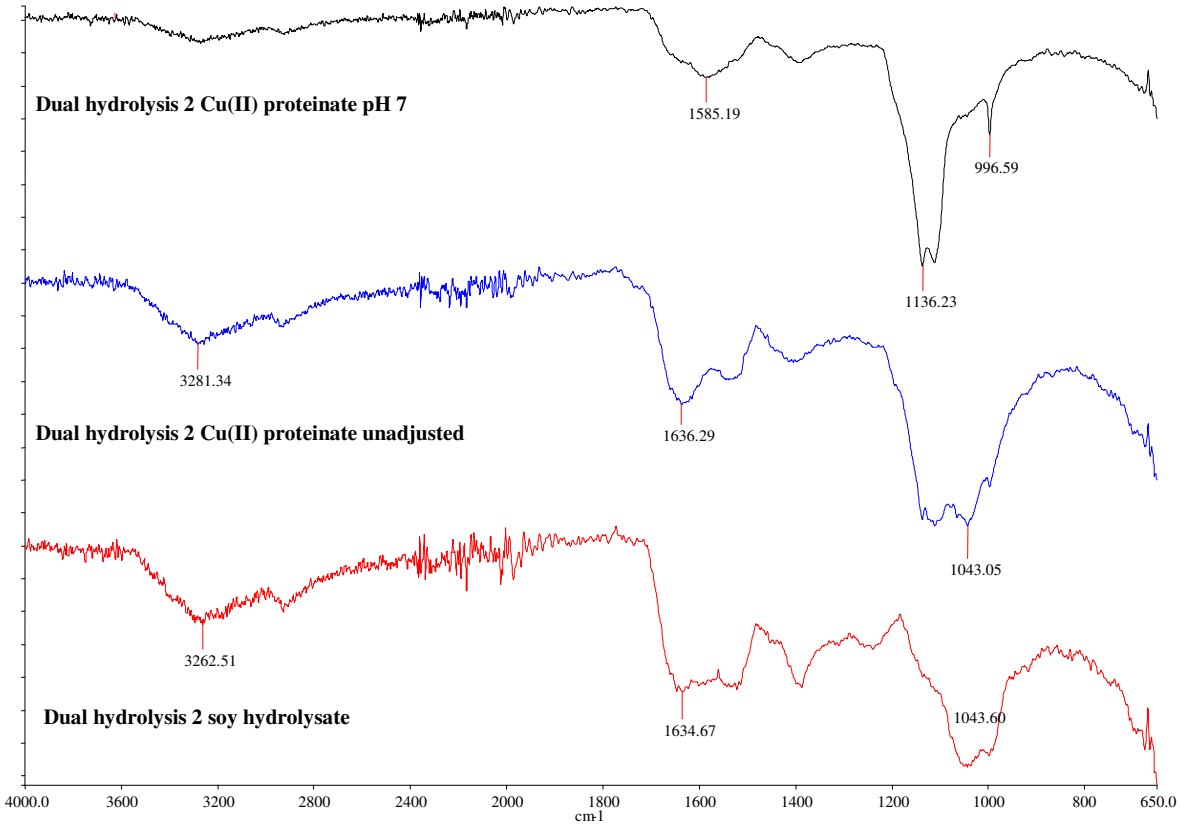

Appendix 2.1 Table of amino acid abbreviations and molecular weights

Name	3-letter symbol	1-letter symbol	Molecular weight
Alanine	Ala	A	89.10
Arginine	Arg	R	174.20
Asparagine	Asn	N	132.12
Aspartic acid	Asp	D	133.11
Cysteine	Cys	C	121.16
Glutamic acid	Glu	E	147.13
Glutamine	Gln	Q	146.15
Glycine	Gly	G	75.07
Histidine	His	H	155.16
Isoleucine	Ile	I	131.18
Leucine	Leu	L	131.18
Lysine	Lys	K	146.19
Methionine	Met	M	149.21
Phenylalanine	Phe	F	165.19
Proline	Pro	P	115.13
Serine	Ser	S	105.09
Threonine	Thr	T	119.12
Tryptophan	Trp	W	204.23
Tyrosine	Tyr	Y	181.19
Valine	Val	V	117.15

Appendix 2.2a **Acidic amino acid structures**

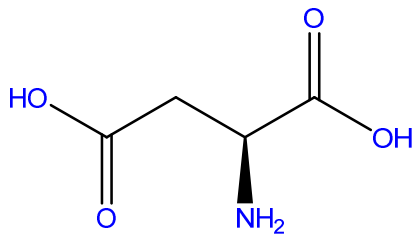

aspartic acid

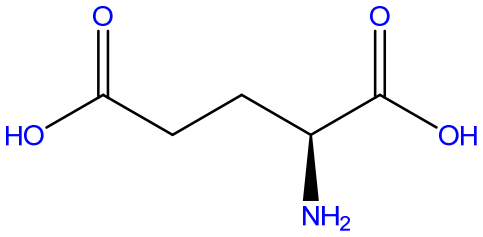

glutamic acid

Appendix 2.2b **Basic amino acid structures**

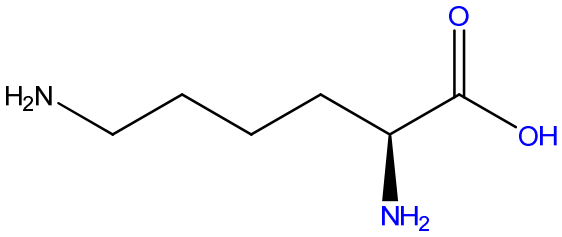

lysine

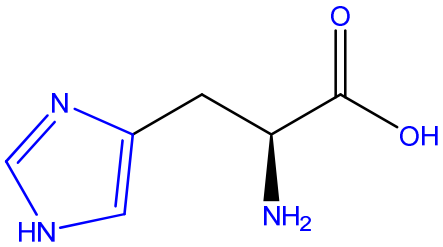

histidine

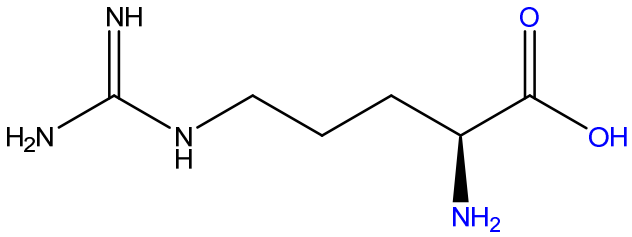

arginine

Appendix 2.2c **Neutral amino acid structures**

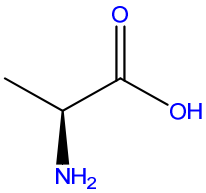

alanine

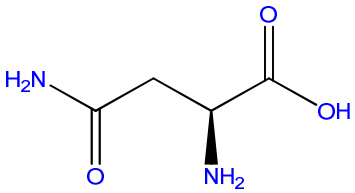

asparagine

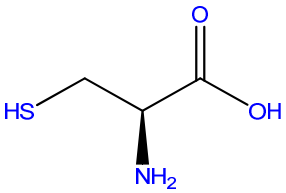

cysteine

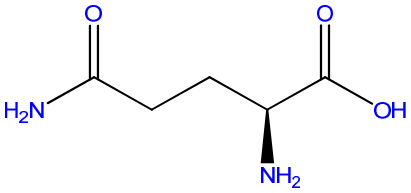

glutamine

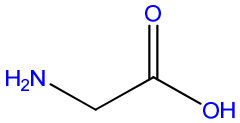

glycine

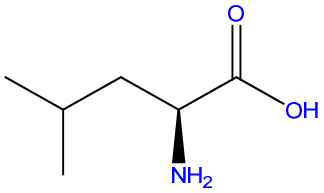

leucine

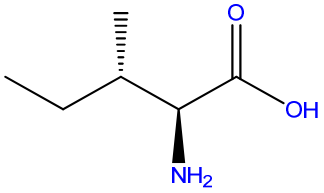

isoleucine

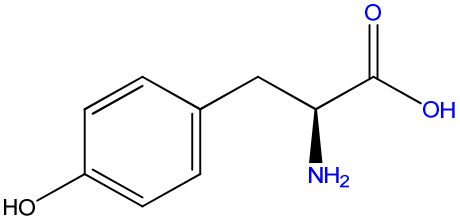

tyrosine

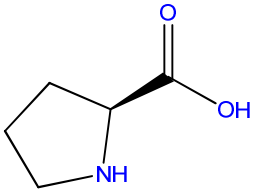

proline

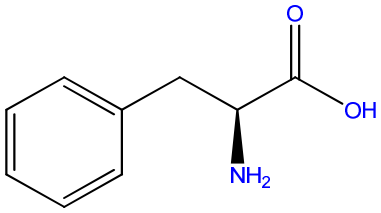

phenylalanine

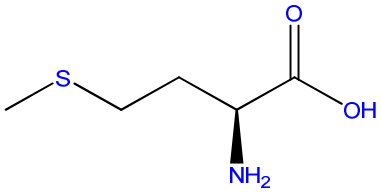

methionine

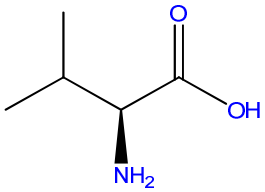

valine

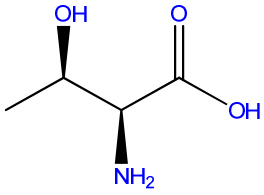

threonine

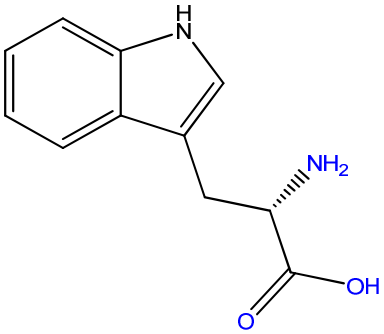

tryptophan

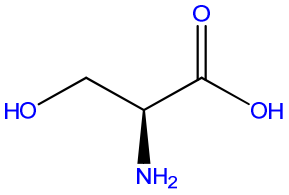

serine